PROGRESS TOWARD THE TOTAL SYNTHESIS OF CURCUSONE C AND MECHANISTIC ELUCIDATION OF AN UNEXPECTED REARRANGEMENT

Thesis by

Chung Whan Lee

In Partial Fulfillment of the Requirements for the Degree of

Doctor of Philosophy

California Institute of Technology

Pasadena, California

2015

(Defended May 29, 2015)

To my teachers

ACKNOWLEDGEMENTS

During my school life since 1993, I have met a lot of great teachers who are not only experts on teaching but are also great mentors and role model.

Foremost, I must thank my supervisor, Prof Brian Stoltz. I attended his talk in an ICOS meeting at Daejeon, Korea in 2006, and which was the first moment I dreamed to undertake doctoral studies at Caltech. Throughout my doctoral studies, Brian has been the best teacher and mentor. He has been a generous, supportive advisor who has helped me to overcome obstacles in graduate school and to be an independent researcher. He has been truly enthusiastic in science and professional in research, which has affected me a lot. He has also been respectful to his students and he has exceptional ability to motivate us without relying on his authority. He has kept priorityzed about lab safety all the time as well as doing lab work efficiently. It is truly rare to find an advisor who is talented and creative in operating a giant research lab who also cares deeply about every single student. It is impossible to thank him enough for his sacrifices over the last five years. It was truly fortunate for me to join the Stoltz group in 2010.

My committee members Prof. Sarah Reisman, Prof. Theo Agapie, and Prof. Bob Grubbs are acknowledged for their continuing advice and support. Prof. Sarah Reisman has been not only my chairwoman but also a sort of second advisor for us. I sometimes thought her guidance was too strenuous but I finally realized that her comments and directions were tremendously informative, and those hard times she gave me was an extremely valuable period for me. Prof. Theo Agapie is an out-of-

field thesis committee member, but he has offered greatly important comments from a different point of view. The final member of my committee, Prof. Bob Grubbs has been an admirable scientist for me since I learned about his catalyst during undergraduate studies. Furthermore, I was truly surprised when I attended his seminar at Seoul National University in 2009; his contents were filled with completely fresh topics, which was unusual in previous Nobel lectures in Seoul National University. I have been glad to re-meet him and have his guidance at Caltech.

I also have to thank my former academic supervisors, including Prof. Eun Lee, Prof. Chulbom Lee, and Prof. Tae-Lim Choi. Prof. Eun Lee, my M.S. thesis advisor, has been a great mentor who has always showed me the way of being a scientist. Prof. Chulbom Lee, alumni of the Eun Lee group, has also been truly supportive of me. When I visited Korea, I always stopped by his office to ask his guidance, and those meetings were always enjoyable. Prof. Tae-Lim Choi, who is a Caltech alumni, was also a great mentor at SNU.

In addition to great teachers, I have many co-workers to thank. Dr. Buck Taylor, Ashay Patel and their supervisor Prof. Ken Houk and Dr. Galina Petrova with Prof. Keiji Morokuma are wonderful theoretical chemists. It was impossible to solve ridiculous problems without collaborating with them. Also, Seo-Jung Han for collaboration on the malonates addition project is acknowledged. She has also been one of the very few Korean speakers and it has been quite comfortable to have someone that I can discuss something with in Korean.

Dr. Jimin Kim, Boram Hong are thanked for helping me settle down in the lab in the early days. It would have been frustrating without their support, but I could get use to Stoltz group life pretty quickly with them. I also want to thank Dr. Chris Henry, Dr. Kristy Tran, Dr. Doug Behenna, and Dr. Alex Goldberg for their kindness in the early days. Dr. Doug Behenna has been my hoodmate for a long time and it was pleasure to have a wonderful scientist next to me all the time. Dr. Alex Goldberg and Dr. Kristy Tran have been my baymates in the early days with Dr. Corey Reeves and Doug Duquette. I sometimes think about the early enjoyable days in the lab when our bay was completely filled every hour with great friends. Special thanks to Alex for drinking Korean liquor together in Korea town and it was fun to meet you again in Tel Aviv. With Corey and Doug, I would like to thank Dr. Rob Craig, Christopher Haley, and Dr. Yiyang Liu, who are the member of my class within the Stoltz group. It was pleasure to be with you over 5 years.

I also have to thank Kelly Eunjung Kim, Alex Sun, Steven Loskot, Elizabeth Goldstein, for being my proofreaders of the documents. Special thanks to Kelly who has never hesitated to help me for a long time. In addition, I want to thank Dr. Boger Liu, Dr. Jared Moore and again Alex and Kelly for discussion and correction of my exit proposals. Jared is my current hoodmate who reminded me the early days. I have again been surrounded by wonderful chemists with Jared and Dr. Marc Liniger, and it was truly a pleasure to be with them in my last days. I have to thank Sam Shockley for being a safety officer. It must be the most burdensome group job and I really appreciated that she was willing to take my duty. In addition to Sam, I would like to thank the Caltech safety office for focusing on lab safety.

I wish there was enough time to thank all the former and present Stoltz group members for their contributions. Every past and present post-doc, and students are great chemists and it has been my luck to be with them all including, Nick O'Connor, Beau Pritchett, Katerina Korch, Kelvin Bates, Jiaming Li, David Schuman, Austin Wright, Max Loewinger, and Drs. Kim Petersen, Koji Chiyoda, Josh Day, Christian Eldamshaus, Vinson Espejo, Michele Gatti, Christian Grünanger, Kathrin Höferl-Prantz Sandoz, Hendrik, F. T. Klare, Guillaume Lapointe, Alex N. Marziale, Kenji Negoro, Yoshitaka Numajiri, Fabian Piller, Grant Shibuya, Hideki Shimizu, Russel Smith, Yuji Sumii, Takeharu, Toyoshima, Florian Vogt, Phil Wu, Xiangyou Xing, Nathan Bennett, Chris Gilmore, Jonny Gordon, Jeff Holder, Allen Hong, Hosea Nelson, Nat Sherden, Pam Tadross, Masaki Hayashi, Kazato Inanaga, Max Klatte, and Noriko Okamoto.

Beyond the Stoltz lab, the members past and present of the Reisman and Grubbs labs are acknowledged for supporting the excellent collaborative atmosphere. I especially want to mentions Dr. Roger Nani, and Haoxuan Wang for their kindness and Lauren Chapman for discussing safety matters of 3rd floor Schlinger.

I have to thank the technical and support staff in our department. Dr. Scott Virgil has been a tremendous resource during my time here. He has never hesitated to set aside hours of his time to discuss technical or strategic problems and he has kept facility in order every moment. I also want to thank Rick Gerhart for helping repair glassware, Dr. Mike Takase and Larry Henling for X-ray crystal structure determination, Dr. Mona Shahgholi and Naseem for their help obtaining HRMS data, Tony, for his help on the third floor of Schlinger, as well as Agnes Tong, Lynne

Martinez, and Anne Penny for their help with administrative duties. Especially, Dr. Dave Vander-Velde who runs the best NMR facility and has helped me with difficult experiments. Agnes Tong is the greatest Graduate Program Administrator as well as student counselor. I have feeling at ease when I talk with her. Lynne Martinez does an incredible job of keeping the house in order, she always has answers for every question.

I want to thank every member of the Caltech Korean Graduate Student Association. I never had a chance to feel home sick with these fantastic members. Especially Dr. Chang Ho Sohn is acknowledged for important advice and support.

Beyond Caltech, it was great pleasure to have a lot of high school classmates around California. I want to thank all of them including, Dr. Hongki Kang, Dr. Yunkyung Kim, Jinwoo Lee, Kyunam Kim, Mihn-jong Lee, and Younghyun Kim.

Lastly, I would like to thank the most important people in my life. First of all, my family: Mom, and Dad. They have invested tremendously in my education, and have been truly supportive of me every step. They never pushed me too much as many other Korean parents did, but they have encouraged me to study what I want.

Thanks to all who has been a part of my life. Without their support I would not make it here.

Chung Whan

ABSTRACT

Curcusone C is tricyclic diterpenoid natural product isolated from *Jatropha curcas* that exhibits potent biological activity and features a 2,3,7,8-tetrahydroazulene-1,4-dione moiety. Herein, we describe a synthetic approach toward *ent*-curcusone C. Construction of the tricyclic scaffold of *ent*-curcusone C is achieved from a cyclopentenol boronate and a vinyl bromide, which was synthesized from (*S*)-perillaldehyde. Suzuki coupling of the two precursors furnished a dieneol, which was converted to a diazoester via transesterification followed by diazo transfer reaction. A divinylcyclopropane was synthesized from the diazoester by intramolecular cyclopropanation and subsequent Kauffmann olefination. The tricyclic core of *ent*-curcusone C was accomplished by divinylcyclopropane rearrangement, which was initiated by reduction of the lactone moiety.

We discovered an unexpected rearrangement during the course of our investigation toward the synthesis of curcusone C. Surprisingly, a silyl enol ether was converted to a complex tetracyclic compound under mild heating conditions. The transformation was elucidated as a unique reaction cascade of [3,3] Cope rearrangement, [1,5] silyl migration, Ireland–Claisen rearrangement, retro Claisen rearrangement, and [1,5] silyl migration by computational and experimental efforts.

Additionally, our work on the development of a bis(phosphine) copper catalyst for the asymmetric alkylation of 3-Bromooxindoles with α-arylated malonate esters is described. Versatile copper sources and chiral bis(phosphine) ligands were investigated.

TABLE OF CONTENTS

LIST OF FIGIRES

CHAPTER 1

Progress toward the Total Synthesis of Curcusone C

APPENDIX 3

Spectra Relevant to Chapter 1: Progress toward the Total Synthesis of Curcusone C

APPENDIX 5

Spectra Relevant to Appendix 1: Additional Studies Related to Chapter 1

CHAPTER 2

Mechanistic Elucidation of the Unexpected Rearrangement

APPENDIX 6

Spectra Relevant to Chapter 2: Mechanistic Elucidation of the Unexpected Rearrangement

LIST OF SCHEMES

CHAPTER 1

Progress toward the Total Synthesis of Curcusone C

APPENDIX 1

Additional Studies Related to Chapter 1: Progress toward the Total Synthesis of Curcusone C

APPENDIX 2

Synthetic Summary toward the Total Synthesis of Curcusone C

CHAPTER 2

Mechanistic Elucidation of the Unexpected Rearrangement

CHAPTER 3

Stereochemical Evaluation of Bis(phosphine) Copper Catalysts for the Alkylation of 3-Bromooxindoles with α-Arylated Malonate Esters

LIST OF TABLES

CHAPTER 1

Progress toward the Total Synthesis of Curcusone C

APPENDIX 4

X-ray Crystallography Reports Relevant to Chapter 1

CHAPTER 3

Stereochemical Evaluation of Bis(phosphine) Copper Catalysts for the Alkylation of 3-Bromooxindoles with α-Arylated Malonate Esters

APPENDIX 8

Notebook Cross-Reference

LIST OF ABBREVIATIONS

Å	Ångstrom
$[a]_D$	specific rotation at wavelength of sodium D line
[H]	reduction
[O]	oxidation
Ac	acetyl
acac	acethylacetonate
AFIR	artificial force induced reaction
Anal.	combustion elemental analysis
APCI	atmospheric pressure chemical ionization
app	apparent
aq	aqueous
AIBN	2,2'-azobisisobutyronitrile
Ar	aryl
atm	atmosphere
B3LYP	3-parameter hybrid Becke exchange/ Lee–Yang–Parr correlation functional
Bn	benzyl
Boc	*tert*-butyloxycarbonyl
BOX	bisoxazoline
bp	boiling point

br	broad
Bu	butyl
i-Bu	*iso*-butyl
n-Bu	butyl
t-Bu	*tert*-Butyl
Bz	benzoyl
c	concentration for specific rotation measurements
°C	degrees Celsius
ca.	about (Latin circa)
calc'd	calculated
CAN	ceric ammonium nitrate
cat	catalytic
Cbz	carbobenzyloxy
CCDC	Cambridge Crystallographic Data Centre
CDI	1,1'-carbonyldiimidazole
cf.	compare (Latin confer)
CI	chemical ionization
CID	collision-induced dissociation
cm^{-1}	wavenumber(s)
comp	complex
Cp	cyclopentadienyl
Cy	cyclohexyl
d	doublet

D	deuterium
dba	dibenzylideneacetone
DBU	1,8-diazabicyclo[5.4.0]undec-7-ene
DCC	N,N'-dicyclohexylcarbodiimide
DCE	dichloroethane
DCM	dichloromethane
DCU	dicyclohexylurea
dec	decomposition
DFT	density functional theory
DIBAL	diisobutylaluminum hydride
DIAD	diisopropyl azodicarboxylate
DMA	*N*,*N*-dimethylacetamide
DMAP	4-dimethylaminopyridine
dmdba	bis(3,5-dimethoxybenzylidene)acetone
DMF	*N*,*N*-dimethylformamide
DMSO	dimethyl sulfoxide
dppb	1,4-bis(diphenylphosphino)butane
dppf	1,1'-bis(diphenylphosphino)ferrocene
dr	diastereomeric ratio
E_A	activation energy
EC_{50}	median effective concentration (50%)
ee	enantiomeric excess
EI	electron impact

e.g.	for example (Latin exempli gratia)
equiv	equivalent
EH	ethylhexanoate
ESI	electrospray ionization
Et	ethyl
EtOAc	ethyl acetate
exp	experimental
FAB	fast atom bombardment
FID	flame ionization detector
g	gram(s)
GC	gas chromatography
gCOSY	gradient-selected correlation spectroscopy
h	hour(s)
hfacac	hexafluoroacetylacetonate
HMBC	heteronuclear multiple bond correlation
HMDS	1,1,1,3,3,3-hexamethyldisilazane
HMPA	hexamethylphosphoramide
HOBt	1-hydroxybenzotriazole
HPLC	high-performance liquid chromatography
HRMS	high-resolution mass spectroscopy
HSQC	Heteronuclear single quantum coherence
hn	light
Hz	hertz

IBX	2-iodobenzoic acid
IC_{50}	median inhibition concentration (50%)
i.e.	that is (Latin id est)
IEF	integral equation formalism
i-Pr	isopropyl
IR	infrared (spectroscopy)
IRC	intrinsic reaction coordinate
J	coupling constant
kcal	kilocalorie
KDA	potassium diisopropylamide
KHMDS	potassium hexamethyldisilazide
l	wavelength
L	liter, ligand
LDA	lithium diisopropylamide
lit.	literature value
LTQ	linear trap quadrupole
LUP	locally updated planes
m	multiplet; milli
m	meta
m/*z*	mass to charge ratio
M	metal; molar; molecular ion
m-CPBA	*meta*-chloroperoxybenzoic acid
Me	methyl

MHz	megahertz
min	minute(s)
m	micro
mwaves	microwave irradiation
M06	Minnesota functionals 06
min	minute(s)
MM	mixed method
mol	mole(s)
MOM	methoxymethyl
mp	melting point
Ms	methanesulfonyl (mesyl)
MS	molecular sieves
n	nano
N	normal
nbd	norbornadiene
NBS	*N*-bromosuccinimide
NMO	*N*-methylmorpholine *N*-oxide
NMR	nuclear magnetic resonance
NOE	nuclear Overhauser effect
NOESY	nuclear Overhauser enhancement spectroscopy
Nu	nucleophile
[O]	oxidation
o	ortho

p	para
PCC	pyridinium chlorochromate
PCM	polarizable continuum model
PDC	pyridinium dichromate
Ph	phenyl
pH	hydrogen ion concentration in aqueous solution
PhH	benzene
PhMe	toluene
PHOX	phosphinooxazoline
Pin	pinacol
Piv	pivaloyl
p*Ka*	p*K* for association of an acid
PMB	*p*-methoxybenzyl
ppm	parts per million
PPTS	pyridinium *p*-toluenesulfonate
Pr	propyl
i-Pr	isopropyl
Py	pyridine
q	quartet
ref	reference
R	generic for any atom or functional group
R_f	retention factor
rt	room temperature

s	singlet or strong or selectivity factor
sat.	saturated
Selectfluor	1-chloromethyl-4-fluoro-1,4-diazoniabicyclo[2.2.2] octane bis(tetrafluoroborate)
SFC	supercritical fluid chromatography
S_N2	second-order nucleophilic substitution
sp.	species
t	triplet
TBAF	tetrabutylammonium fluoride
TBHP	*tert*-butyl hydroperoxide
TBS	*tert*-butyldimethylsilyl
TCDI	1,1'-thiocarbonyldiimidazole
TCNE	tetracyanoethylene
TES	triethylsilyl
Tf	trifluoromethanesulfonyl (trifyl)
TFA	trifluoroacetic acid
tfacac	trifluoroacetylacetonate
TFE	2,2,2-trifluoroethanol
THF	tetrahydrofuran
TIPS	triisopropylsilyl
TLC	thin-layer chromatography
TMEDA	*N*,*N*,*N'*,*N'*-tetramethylethylenediamine
TMS	trimethylsilyl

TOF	time-of-flight
Tol	tolyl
t_R	retention time
Ts	*p*-toluenesulfonyl (tosyl)
TS	transition state
UV	ultraviolet
v/*v*	volume to volume
w	weak
w/*v*	weight to volume
X	anionic ligand or halide
Xyl	xylyl

CHAPTER 1

Progress toward the Total Synthesis of Curcusone C

1.1 INTRODUCTION AND SYNTHETIC STRATEGY

1.1.1 INTRODUCTION

Native to Central America, *Jatropha curcas* is a species of flowering plant belonging to the Euphorbiaceae family that can be found in many parts of the world. *J. curcas* has been used as a source of soap and lamp oil for hundreds of years, and recently *J. curcas* has attracted attention due to its possible use in biodiesel production.[1]

J. curcas has intrigued natural product chemists as a source of versatile diterpenoids. Diterpenes curcusones A–D (**1**-**4**), which possess novel tricyclic skeletons, were isolated by Naengchomnong and co-workers in 1986.[2a] The structures of curcusones B (**2**) and C (**3**) were confirmed by X-ray diffraction analysis. Primary NMR data indicated that curcusones A (**1**) and B (**2**), curcusones C (**3**) and D (**4**) were epimers at C(2). Recently, *J. curcas* has been further investigated and yielded more natural

products. In 2011, Taglialatela-Scafati and co-workers reported curcusone E (**5**) and spirocurcasone (**18**) as other secondary metabolites isolated from the plant and again found curcusones A–E.[2b] Furthermore, curcusones F–J (**6**-**10**) and 4-*epi*-curcusone E were discovered in 2013.[2c] In addition to the curcusones, a number of other diterpenes have been isolated from *J. curcas* (Figure 1.1.1).[2,3]

Figure 1.1.1. Curcusones A-J, Spirocurcasone and Representative Natural Products from J. curcas

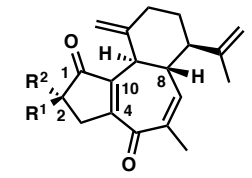

Curcusone	R_1	R_2
A (1)	Me	H
B (2)	H	Me
C (3)	Me	OH
D (4)	OH	Me

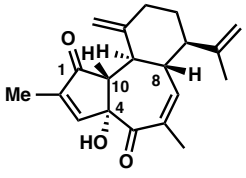

Curcusone E (5)

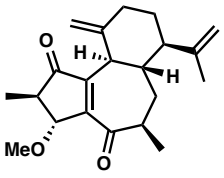

Curcusone F (6)

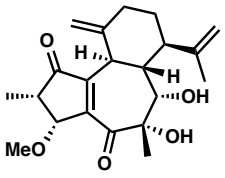

Curcusone G (7)

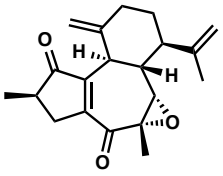

Curcusone H (8)

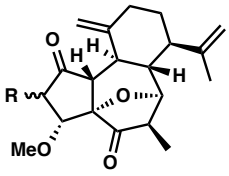

R = β-Me : Curcusone I (9)
R = α-Me : Curcusone J (10)

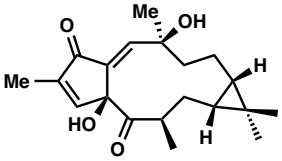

Curculathyrane A (11)

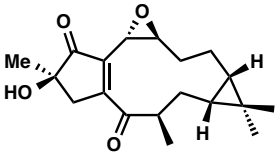

Curculathyrane B (12)

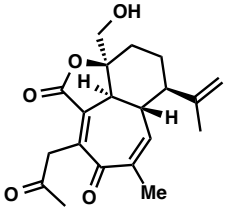

Curcusecon A (13)

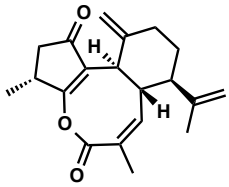

Curcusecon B (14)

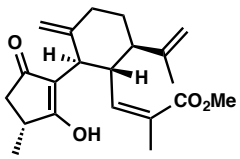

Curcusecon C (15)

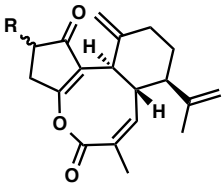

R = α-Me : Curcusecon D (16)
R = β-Me : Curcusecon E (17)

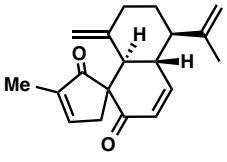

Spirocurcasone (18)

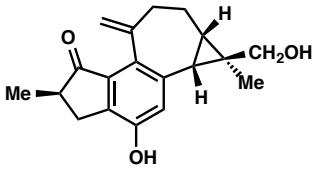

Jatrophol (19)

Among various natural products from *J. curcas*, curcusones A–D exhibited versatile cytotoxic activity. For instance, curcusone B showed an anti-invasive effect against cholangiocarcinoma cells.[4a-c] Furthermore, dose-dependent inhibitory activity of K562 (human leukemia, IC_{50} in 6 μg mL^{-1}) and H1299 (human non-small cell lung carcinoma, IC_{50} in 15 μg mL^{-1}) cell lines were discovered.[3j] Curcusones C and D, on the other hand, showed antifungal and antibacterial activity at low doses (50 μg).[4d,e] In addition, curcusones A and C show potential for anticancer activity based on their ability to enhance hyperthermic oncotherapeutics in V-79 cells (chinese hamster cells).[4a]

Inspired by these versatile biological activities, researchers have further investigated their anticancer properties. Among curcusones A–E and spirocurcasone, curcusone C has the greatest antiproliferative activity on the L5178 (mouse lymphoma, IC_{50} in 0.08 μg mL^{-1}).[2b] Furthermore, curcusone C exhibited considerable potency toward HL-60 (human promyelocytic leukemia, IC_{50} in 1.36 μM),[2c] SMMC-7221 (human heptoma, IC_{50} in 2.17 μM),[2c] A-549 (adenocarcinomic human alveolar basal epithelial, IC_{50} in 3.88 μM),[2c] MCF-7 (human breast cancer, IC_{50} in 1.61 μM),[2c] SW480 (human colon adenocarcinoma, IC_{50} in 1.99 μM),[2c] and SK-OV3 (human ovarian cancer, IC_{50} in 0.160 μM)[4f] cell lines.

Curcusones A–D (**1**-**4**) possess novel tricyclic skeletons featuring a 2,3,7,8-tetrahydroazulene-1,4-dione moiety with four stereogenic carbon centers. Since the initial isolation in 1986, a completed total synthesis has not been reported, while one methodological study for the construction of the 7-membered ring of curcusones A–D was reported in 2001 (Scheme 1.1.1).[5] These interesting biological properties and structural features make the curcusones attractive targets, inspiring us to undertake the total synthesis of curcusone C.

Scheme 1.1.1. Previous Study by Young and co-worker

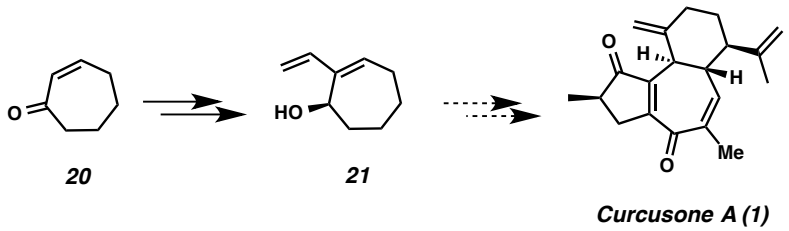

20 ***21*** ***Curcusone A (1)***

1.1.2 RETROSYNTHETIC ANALYSIS

Our retrosynthetic analysis of curcusone C **3** is outlined in Scheme 1.1.2. We envisioned that natural product **3** could be synthesized by acid cleavage, and olefin migration followed by alpha carbon functionalization of tricyclic core **22**. The tricyclic core **22** could be prepared by divinylcyclopropane rearrangement of cyclopropane **23** in a stereospecific fashion by an *endo*-boat transition state. Construction of cyclopropane **23** could be achieved via intramolecular cyclopropanation followed by lactone opening of diazo ester **24**. Cyclopropanation precursor **24** could be disconnected by transesterification followed by diazo transfer reaction of allylic alcohol, which would be assembled by cross-coupling of vinyl boronic ester **25** and vinyl triflate **27**. Vinyl boronic ester **25** would be prepared from cyclopentenone **26** according to literature precedent,[6] and vinyl triflate **27** would be prepared from triflation of a known ketone[7] derived from limonene oxide **28**.

*Scheme 1.1.2. Retrosynthetic Analysis of Curcusone C (**3**)*

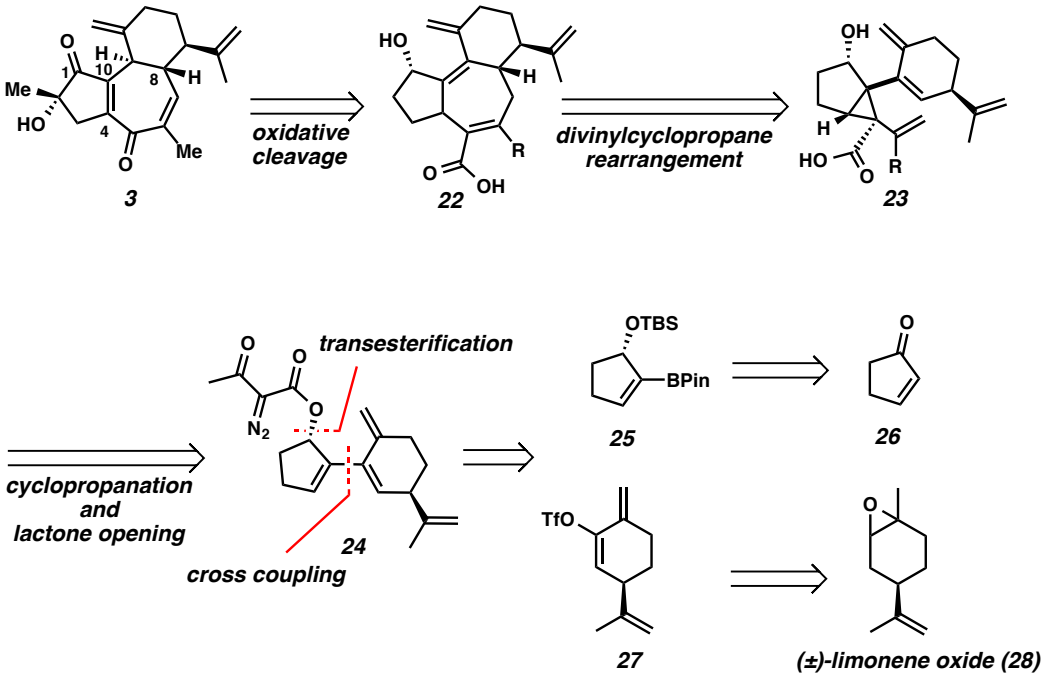

1.1.3 DIVINYLCYCLOPROPANE REARRANGEMENT

For the Cope rearrangement substrate, stereochemistry of the cyclopropane was expected to control the newly generated stereocenters by a concerted mechanism through an *endo* boat-like transition state (**29**) (Scheme 1.1.3). Thus, we expected that the cyclopropane would induce the desired stereochemistry of the ring junction position (C8). We envisioned that intramolecular cyclopropanation would be the most efficient to assemble a cyclopropane for the divinylcyclopropane rearrangement with the desired stereochemistry. In order to synthesize cyclopropane **23**, we decided to prepare diazo ester **24**, which was tethered to an allylic alcohol on the five-membered ring moiety. In this way, the allylic alcohol would control the stereochemistry of the cyclopropane and eventually estabilish the stereocenters of the whole system (Scheme 1.1.3).

Scheme 1.1.3. Proposed Divinylcyclopropane Rearrangement

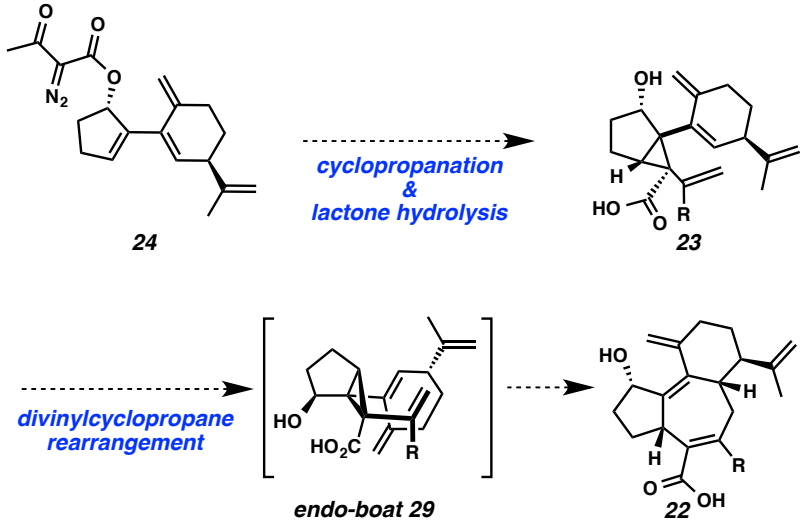

1.2 MODEL SYSTEM APPROACH

Due to the complex structure of diazo ester (**24**), we sought to first examine the cyclopropanation and divinylcyclopropane rearrangement sequence using a model substrate (**36**). Studies on this substrate could later be applied to limonene oxide (**28**) to accomplish the total synthesis.

1.2.1 PREPARATION OF MODEL CYCLOPROPANE 37

Investigation started with preparing model cyclopropanation precursor **36**. Diazo ester **36** was synthesized from allylic alcohol **33** via esterification with diketene and a diazo transfer reaction. Allylic alcohol **33** was derived by Suzuki coupling of vinyl boronate *rac*-**25** with cyclohexanone triflate **32** followed by deprotection. Vinyl boronate **31** was synthesized from known vinyl bromide **30**,[6] which was assembled by bromination, followed by Luche reduction and TBS protection from pentenone **26** (Scheme 1.2.1).

*Scheme 1.2.1. Synthesis of Diazo ester **36***

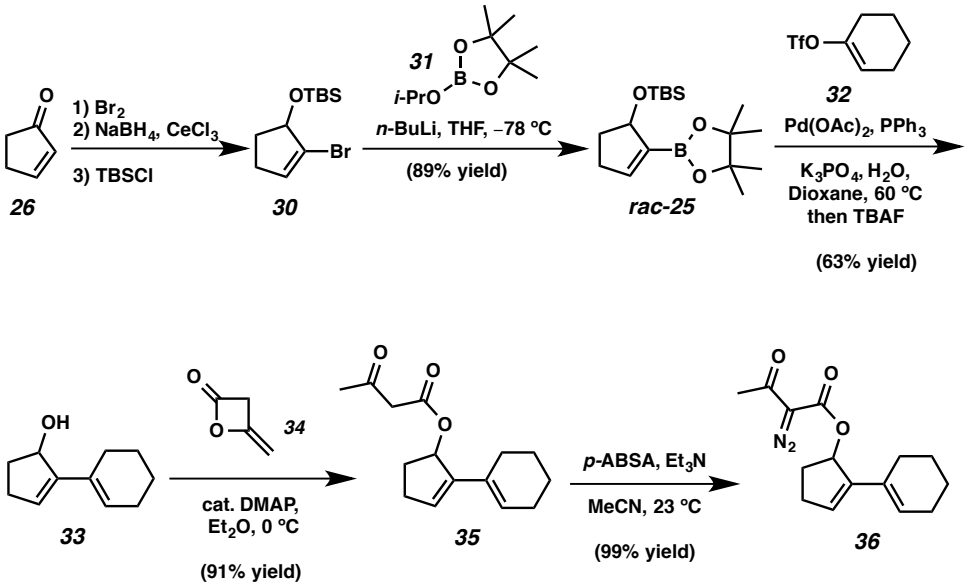

Rhodium catalysts have been used for cyclopropanation in versatile situations including intramolecular cyclopropanation of diazo esters.[8] However, we were unable to find any trace of the desired cyclopropane **37** from diazo ester **36**, despite all of our attempts with various rhodium catalysts. We were able to isolate diene **38,** interestingly (Table 1.2.1). We envisioned that rhodium carbenoid **39** would be too hindered to react with the olefin, thus it would rather abstract the allylic hydrogen via a radical mechanism. The resulting radical **40** could be cleaved to give oxidized diene **38** and reactive ketene **41** (Scheme 1.2.2).

Table 1.2.1. Intramolecular Cyclopropanation Screening of Rhodium Catalysts

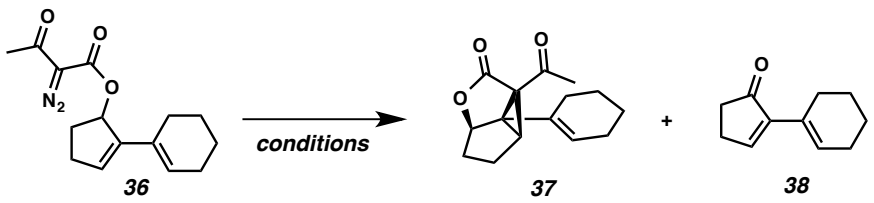

entry	catalyst[a]	solvent	temperature	result
1	$Rh_2(OAc)_4$ (3 mol %)	CH_2Cl_2	23 ºC	No Reaction
2	$Rh_2(OAc)_4$ (3 mol %)	CH_2Cl_2	reflux	**38** only
3	$Rh_2(OTfAc)_4$ (1 mol %)	CH_2Cl_2	23 ºC	No Reaction
4	$Rh_2(esp)_2$ (1 mol %)	CH_2Cl_2	0 ºC – 23 ºC	**38** only
5	$Rh_2(cap)_4$ (1 mol %)	CH_2Cl_2	reflux	**38** only (trace)
6	$Rh_2(oct)_4$ (1 mol %)	CH_2Cl_2	23 ºC	**38** only
7	$Rh_2(oct)_4$ (1 mol %)	Hexane	23 ºC	**38** only
8	$Rh_2(hfbutyrate)_4$ (1 mol %)	CH_2Cl_2	23 ºC	No Reaction

OTfAc: trifluoroacetate, esp: α,α,α',α'-tetramethyl-1,3-benzenedipropionic acid, cap: caprolactamate, oct: octanoate, hfbutyrate: heptafluorobutyrate

*Scheme 1.2.2. Possible Mechanism of **38** Formation*

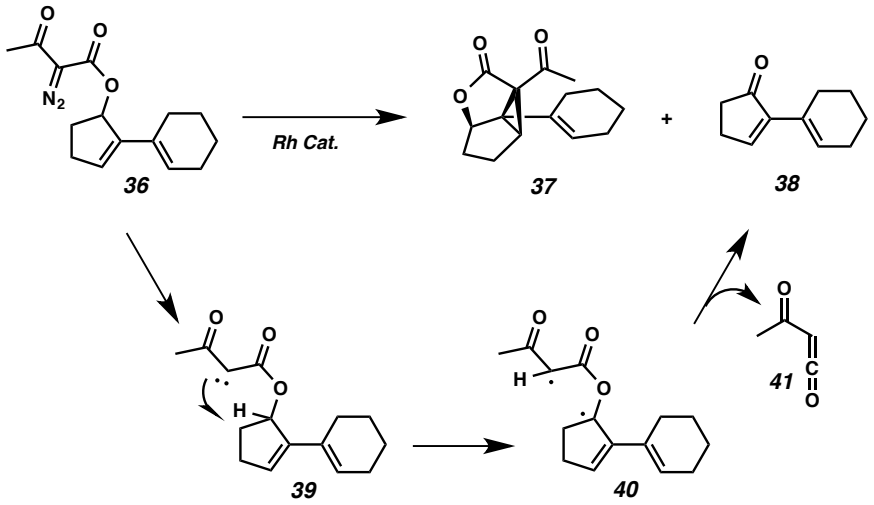

In addition to rhodium catalysts, copper[9] and ruthenium[10] catalysts have been also investigated for the intramolecular cyclopropanation of diazo esters by various researchers. A mixture of the desired cyclopropane **37** and the side product **38** was found by reaction screening under copper (II) hexafluoroacetylacetonate using μ-waves and

finally, we were able to isolate the desired cyclopropanes **37** in good yield by using copper (II) bis(salicylidene-*tert*-butylamine). We could also isolate side product **38** although the amount formed was reduced significantly (Table 1.2.2). The desired cyclopropane **37** was easily converted to hydrazone **42** of which we were able to confirm the structure by single crystal X-ray diffraction (Scheme 1.2.3).

Table 1.2.2. Intramolecular Cyclopropanation Screening of Copper Catalysts

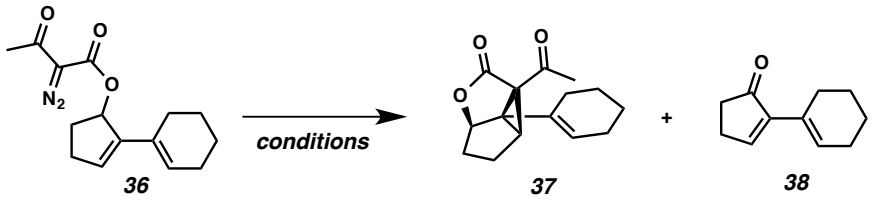

entry	catalyst	solvent	temperature	result
1	$Cu(hfacac)_2$ (10 mol %)	CH_2Cl_2	110 ºC (μ-wave)	1:1 mixture (crude NMR)
2	$Cu(TBS)_2$ (10 mol %)	toluene	reflux	**37** (65% yield) **38** (15% yield)

hfacac: hexafluoroacetylacetonate, $Cu(TBS)_2$: copper(II) bis(salicylidene-*tert*-butylamine)

*Scheme 1.2.3. Crystal Structure of Hydrazone **42***

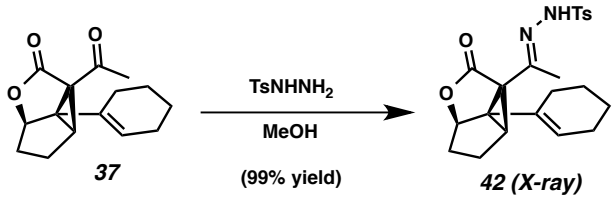

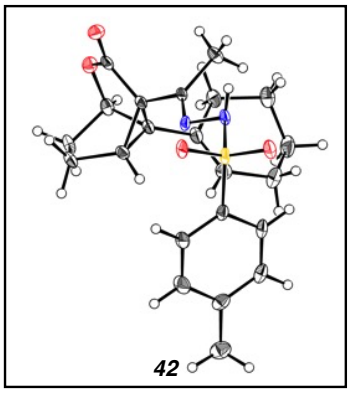

1.2.2 UNEXPECTED REARRANGEMENT

With cyclopropane **37** in hand, we directed our attention to the divinyl cyclopropane rearrangement in order to construct the tricyclic system. We first investigated silyl enol ethers as the rearrangement precursor and divinylcyclopropanes **43** and **44** were prepared by silylation of ketone **37**. Divinylcyclopropanes **43** and **44** possessed a lactone moiety and would form two anti-Bredt olefins in **45** as a result of the divinylcyclopropane rearrangement. Thus, silyl enol ethers **43** and **44** were expected to have low reactivity. Several nucleophiles (KOH, NaOMe, Morpholine-DIBAL, Weinreb amine) were applied to release the lactone in order to initiate the rearrangement reaction; however all of our attempts were unsuccessful (Scheme 1.2.4).

Scheme 1.2.4. Lactone Opening Screening

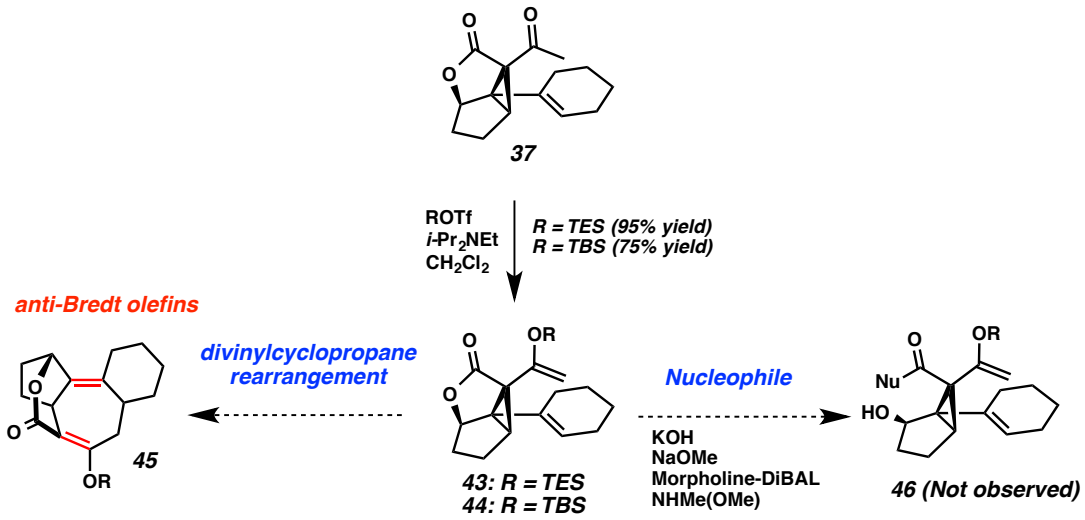

Although divinylcyclopropane **44** was expected to show low reactivity due to its lactone moiety and potential anti-Bredt outcome (**50**), surprisingly it transformed to another silyl enol ether (**47**) under mild heating. Despite significant efforts, structural determination of silyl enol ether **47** was exhibited difficult. Finally, the tetracyclic

structure of *β*-ketolactone **48**, which was furnished by removing the TBS group, was confirmed by single crystal X-ray analysis (Scheme 1.2.5). *β*-Ketolactone **48** was isolated in mixture of enol forms (**49**) in NMR solvent. Mechanistic elucidation is discussed in Chapter **2**, but the mixture was clearly from a multistep complex rearrangement.

Scheme 1.2.5. Unexpected Outcome

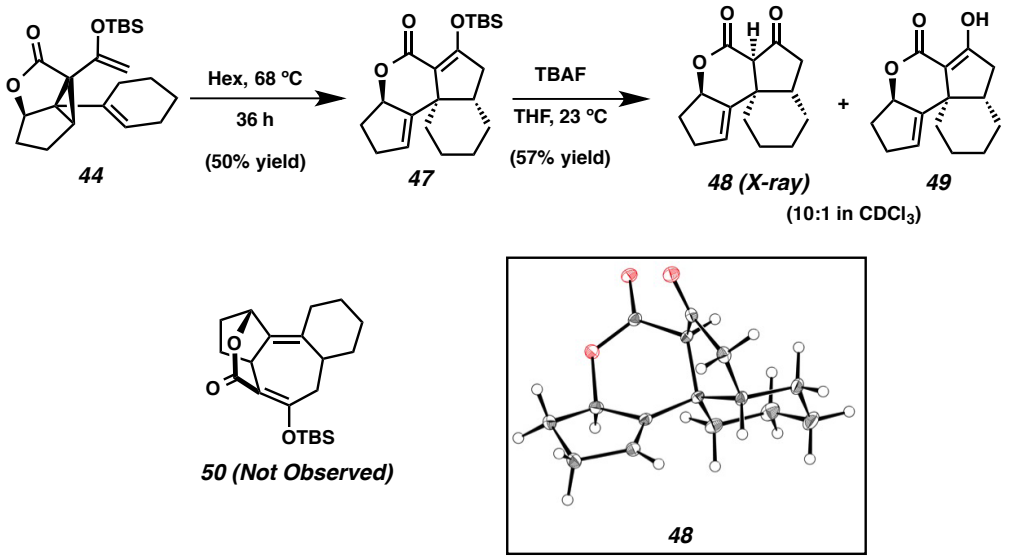

1.2.3 CONSTRUCTION OF THE TRICYCLIC CORE

We believed that ring strain from the lactone moiety prevented the formation of the desired tricyclic system. To overcome this obstacle, the lactone moiety must be ruptured. Since previous attempts with silyl enol ethers **43** and **44** were not satisfactory, we prepared divinylcyclopropane **51** via Wittig-type olefination using Wilkinson's catalyst and trimethylsilyl diazomethane as a methylene source.[11] The resulting divinylcyclopropane **51** was treated with DIBAL to reduce the lactone. Reduction

conditions also triggered the desired rearrangement, affording a tricyclic system **53**, likely via an unstable bis-aluminum alkoxide intermediate **52** (Scheme 1.2.6).

Scheme 1.2.6. Synthesis of Tricyclic Core by Reduction of the Lactone

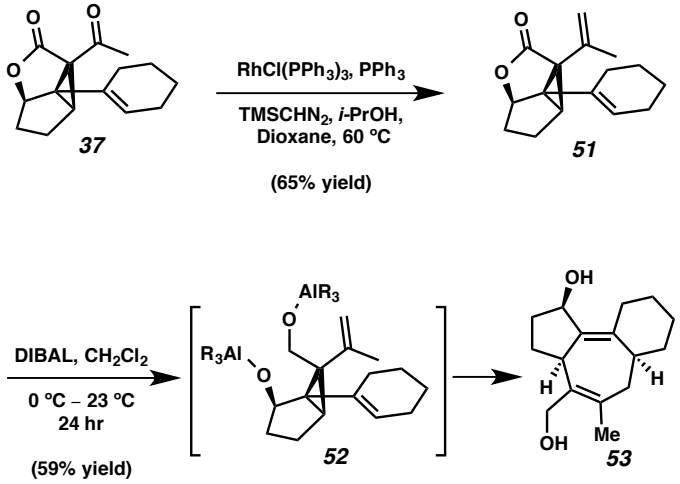

1.3 TOWARD THE TOTAL SYNTHESIS OF CURCUSONE C

1.3.1 LIMONENE OXIDE ROUTE

Based on results from model studies, we directed our attention to the total synthesis of the natural product. We expected that the cross coupling partner for assembly of the diene **24** (Scheme 1.1.2) could be synthesized from commercially available limonene oxide **28**. The α,β-unsaturated ketone **55**, accessible via epoxide opening followed by oxidation from limonene oxide **28**, is known to undergo a hetero Diels–Alder reaction to form dimer **56**. Although we were able to isolate ketone **55** as a major product using Dess–Martin periodinane, initial attempts to convert ketone **55** to vinyl triflate **27** resulted in formation of undesired dimer **56** as the major (Scheme 1.3.1). After modifications, desired triflate **27** was achieved in good yield by syringe pump addition of a diluted

solution of ketone **55** to KHMDS in THF followed by addition of Comins reagent at low temperature (Table 1.3.1).

*Scheme 1.3.1. Undesired Dimerization of Limonene Oxide-Derived Ketone **55***

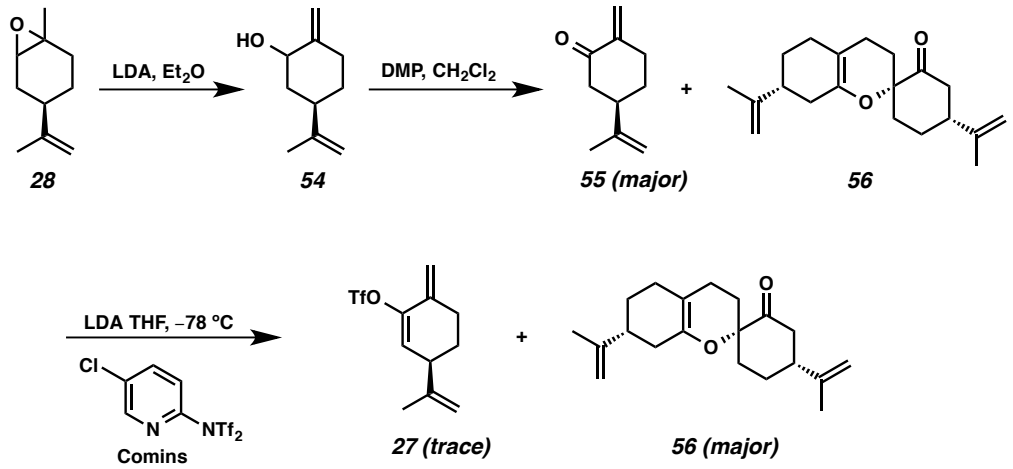

Table 1.3.1. Triflate Formation Screening

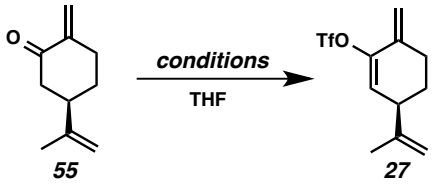

entry	base	concentration[a]	triflating reagent	addition time	yield (%)
1	KHMDS (0.02 M)	0.02 M	Comins	dropwise	42
2	KHMDS (0.01 M)	0.05 M	$PhNTf_2$	dropwise	24
3	KHMDS (0.02 M)	0.01 M	Comins	2 h	77

a: Concentration of ketone **52** in THF.

Vinyl bromide **25**, as the other cross-coupling partner, was prepared from bromo cyclopentenone **57** via CBS reduction followed by TBS protection.[6] Bromide **(*S*)-30** was then converted to pinacol boronate **25** for Suzuki coupling with vinyl triflate **27** to synthesize diene **59**. Deprotection of the alcohol followed by transesterification with

diketene **34** of diene **60** was furnished β-ketoester **61**. Finally, cyclopropanation precursor **24** was synthesized by diazo transfer reaction of ester **61** (Scheme 1.3.2).

*Scheme 1.3.2. Synthesis of Diazo ester **24***

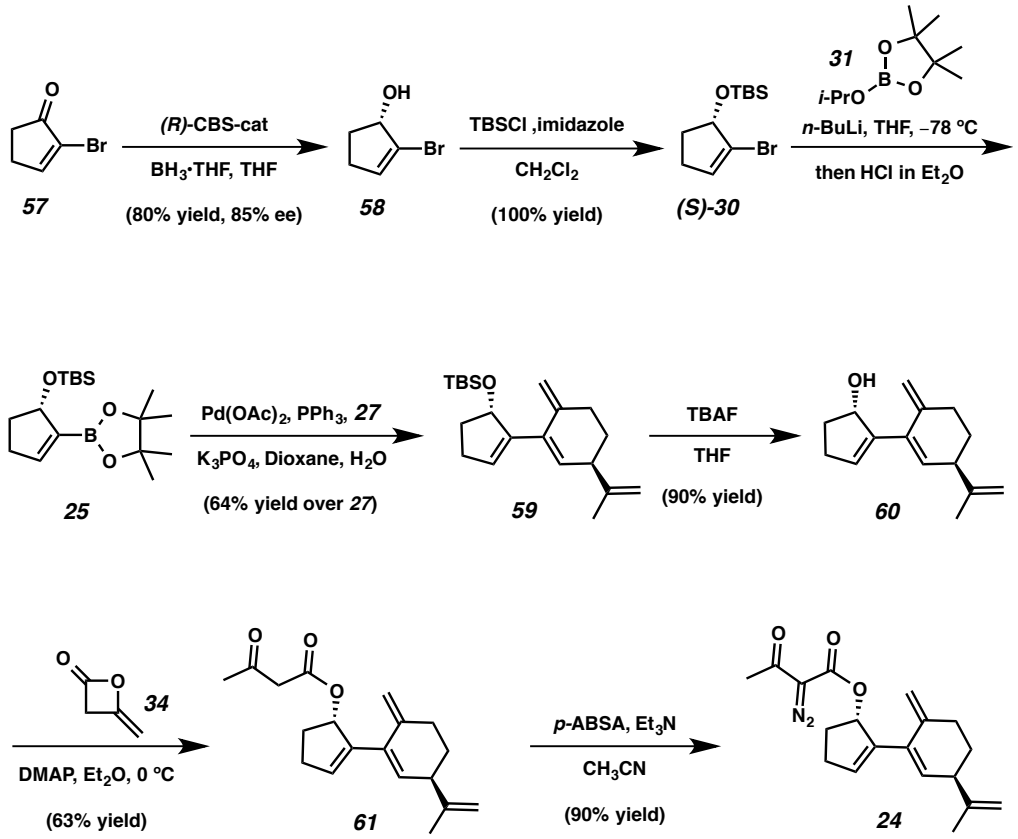

With diazo ester **24** in hand, we investigated cyclopropanation conditions. Unfortunately, despite screening various rhodium, copper, ruthenium, and palladium catalysts, we were not able to observe the desired cyclopropane (**62**) (Table 1.3.2).

Table 1.3.2. Catalyst Screening for Cyclopropanation

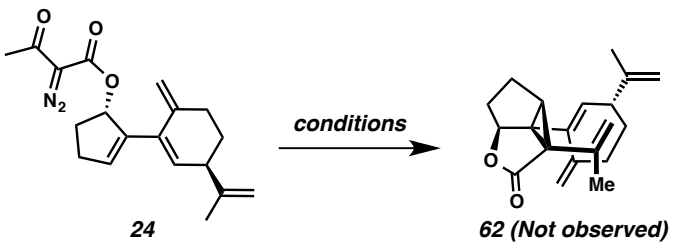

24 ***62 (Not observed)***

entry	catalyst	solvent	temperature	result
1	$Cu(TBS)_2$ (10 mol %)	toluene	reflux	decomposed
2	$Cu(hfacac)_2$ (10 mol %)	toluene	45 ºC – 75 ºC	decomposed
3	Cu(I) OTf (10 mol %)	toluene	45 ºC – 75 ºC	decomposed
4	Cu(I) OTf (10 mol %), pyr (20 mol %)	toluene	23 ºC – 80 ºC	complex mixture
5	Cu(I) OTf (10 mol %), bipyr (10 mol %)	CH_2Cl_2	reflux	no reaction
6	$[(cymen)_2RuCl_2)_2$ (3 mol %)	CH_2Cl_2	23 ºC	no reaction
7	$Rh_2(OAc)_4$ (5 mol %)	CH_2Cl_2	23 ºC	complex mixture
8	$Rh_2(OAc)_4$ (5 mol %)	CH_2Cl_2	reflux	complex mixture
9	$Rh_2(cap)_4$ (5 mol %)	CH_2Cl_2	23 ºC	complex mixture
10	$Rh_2(TfOAc)_4$ (5 mol %)	CH_2Cl_2	23 ºC	complex mixture
11	$Pd(OAc)_2$ (5 mol %)	Et_2O	0 ºC	no reaction

TfOAc: trifluoroacetate, hfacac: hexafluoroacetylacetonate, $Cu(TBS)_2$: copper (II) bis(salicylidene-*tert*-butyl-amine)

1.3.2 PERILLALDEHYDE ROUTE

Although cyclopropanation was successful with model diene **36**, the limonene oxide-derived diazo ester **24** possessing an exomethylene was not a suitable substrate for the desired cyclopropanation. The major difference between the two molecules is the exomethylene in **24** which could alter the conjugated olefins sterically and electronically; thus, modification of the limonene oxide part was required in order to synthesize the desired cyclopropane. Diazo ester **63** bearing an α,β-unsaturated carbonyl was proposed as an alternative of **24**. We expected that **63** would show better reactivity with the metal

carbenoid. Furthermore, the ketone moiety could be olefinated after cyclopropanation (Figure 1.3.1).

Figure 1.3.1. Intramolecular Cyclopropanation Precursors

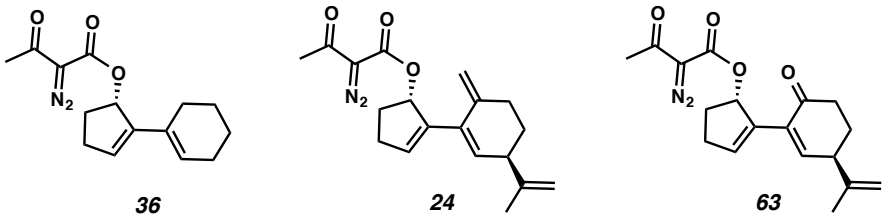

We envisioned that diazo ester **63** would be constructed by the coupling reaction of vinylboronate **25** and vinyl iodide **64** followed by the β-ketoester installation sequence we demonstrated before (Scheme 1.3.3). Although vinyl iodide **64** could be synthesized from (*R*)-perillaldehyde (*(R)*-**65**), we began with the less expensive (*S)*-perillaldehyde (**65**). Vinyl iodide *ent*-**64** was easily prepared from ketone **68**, which was synthesized from (*S)*-perillaldehyde (**65**) in a three-step known sequence (Scheme 1.3.4).[12]

Scheme 1.3.3. Synthetic Plan to Construct Diazo ester ***63***

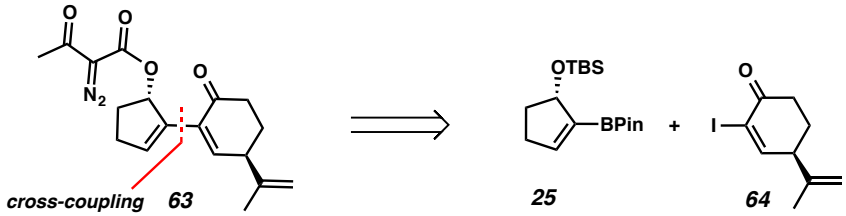

Scheme 1.3.4. Synthesis of Coupling Partner ent-***64***

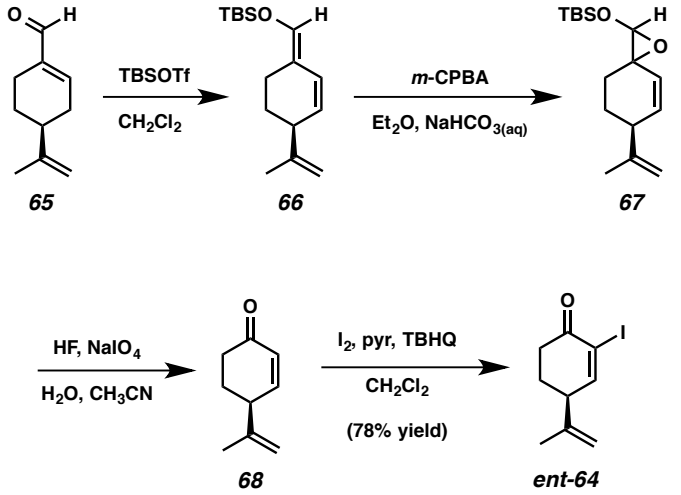

The Suzuki coupling of vinyl iodide *ent*-**64** with (*R*)-**25** which was prepared by a similar sequence as previously described, furnished diene **69**. The TBS group was removed by HF-pyridine complex to prevent deprotonation of the γ-proton of α,β-unsaturated ketone **70**. Finally, tranesterification with diketene **34** afforded β-ketoester **71** for cyclopropanation studies (Scheme 1.3.5).

Scheme 1.3.5. Synthesis of β-Ketoester ***71***

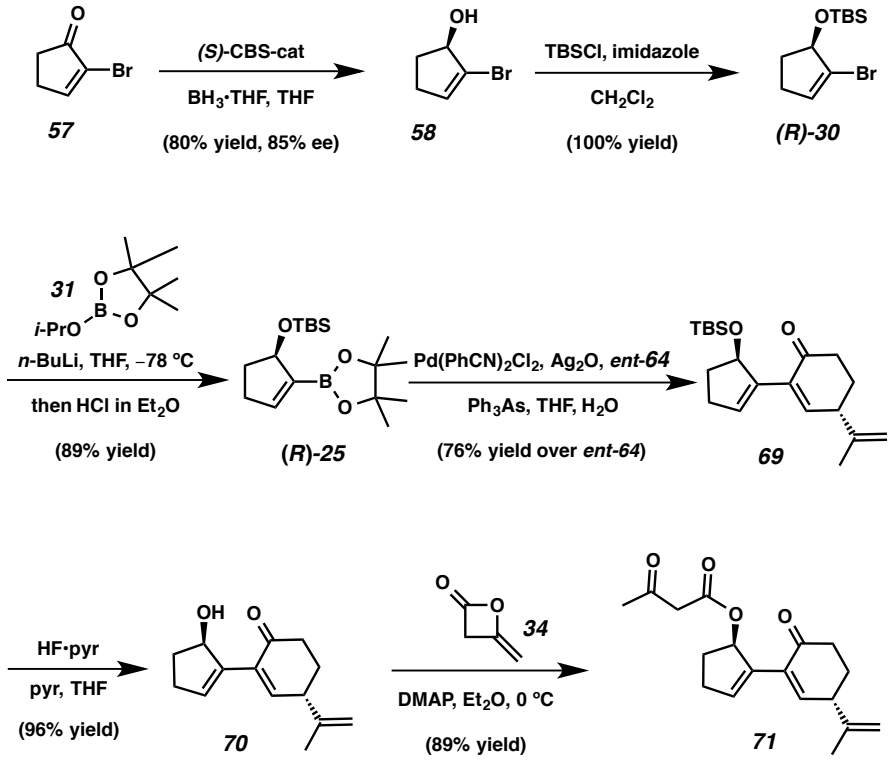

The desired cyclopropane **72** was isolated via diazo transfer reaction followed by cyclopropanation using a copper catalyst. However, cyclopropane **73**, which contains a fully-conjugated π-system as a result of olefin migration, was also isolated as a side product, lowering the yield of the desired cyclopropane was yielded lower than expected (17% yield). In addition, we observed olefin migration[13] from the purified product **72** in the presence of the copper catalyst (Scheme 1.3.6).

Scheme 1.3.6. Synthesis of Cyclopropane ***72***

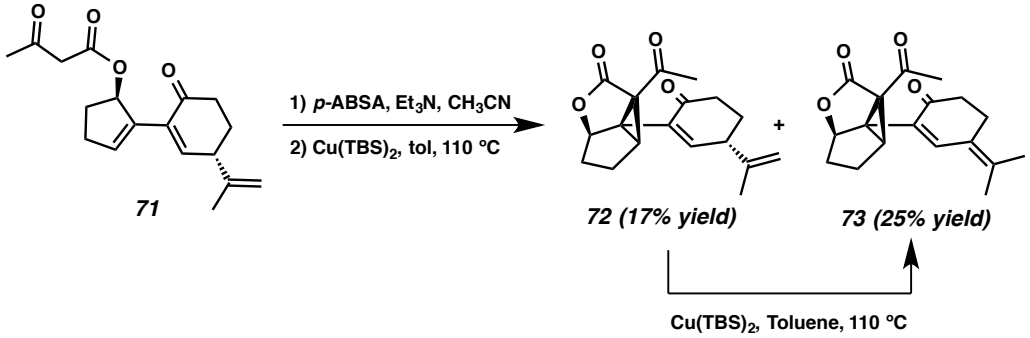

Unfortunately, efforts to doubly olefinate cyclopropane **72** failed. Attempted procedures included Wittig olefination, as well as neutral conditions with Wilkinson's catalyst (Scheme 1.3.7). Since the desired substituted product (i.e., **74**) was not observed with this substrate, we did not pursue this route further and instead shifted our focus to an alternative approach.

Scheme 1.3.7. Efforts toward Olefination of Cyclopropane ***72***

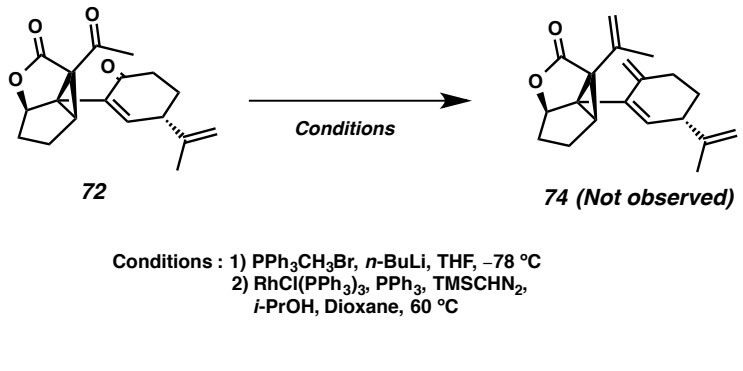

1.3.3 PROTECTED ALCOHOL ROUTE

Protected allylic alcohol **75** was proposed as an alternative to *ent*-**63**, to circumvent the obstacles caused by the acidic γ-proton in **63** (Figure 1.3.2). The exo methylene would be installed by deprotection, oxidation followed by olefination of the resulting ketone. For the preparation of diazo ester **75**, we synthesized vinyl bromide **78** from

cyclohexenone **68** by α-bromination followed by CBS reduction and TBS protection of the resulting alcohol (Scheme 1.3.8).[14]

Figure 1.3.2. Revised Cyclopropanation Precursors

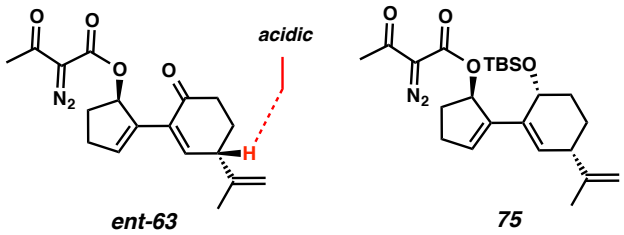

*Scheme 1.3.8. Synthesis of Protected Alcohol **78***

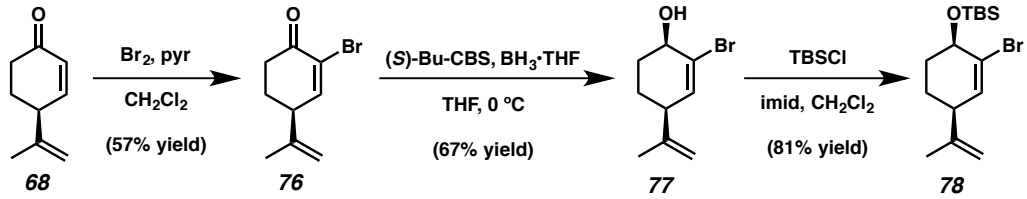

Cleavage of the TBS group from pinacol boronate ***(R)*-25** which was prepared previously (Scheme 1.3.5), furnished allylic alcohol **79**. Diene **80** was synthesized by Suzuki coupling of boronate **79** and bromide **78**. Diazo ester **75** was prepared via transesterification followed by a diazo transfer reaction of allylic alcohol **81** (Scheme 1.3.9).

*Scheme 1.3.9. Synthesis of Diazo ester **75***

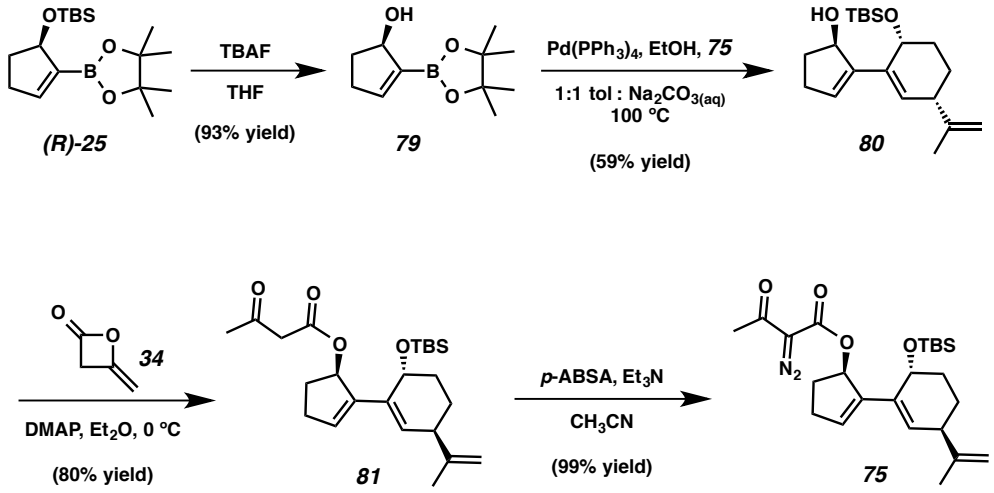

Diazo ester **75** was converted to the desired cyclopropane **82** in synthetically useful yield under copper salicylidene catalysis. Although typical Wittig-type olefination of ketone **82** did not provide the desired compound, we were able to synthesize the desired divinylcyclopropane **83** in good yield using Kauffmann olefination conditions (Scheme 1.3.10).[15,16]

*Scheme 1.3.10. Synthesis of Dinivylcyclopropane **83***

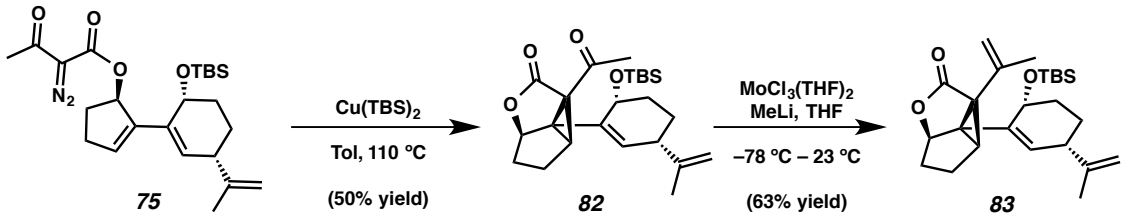

Divinylcyclopropane **83** was treated with DIBAL to reduce the lactone moiety, which was anticipated to initiate the divinylcyclopropane rearrangement. Gratifyingly, we were able to observe the desired cycloheptadiene **83** as a mixture with reduced cyclopropane **84**. Importantly, cyclopropane **84** could be transformed to the cycloheptadiene **85** in

benzene at 23 °C. Conveniently, we found that at elevated temperatures, the rearrangement could be accelerated (Scheme 1.3.11).

Scheme 1.3.11. Divinylcyclopropane Rearrangement

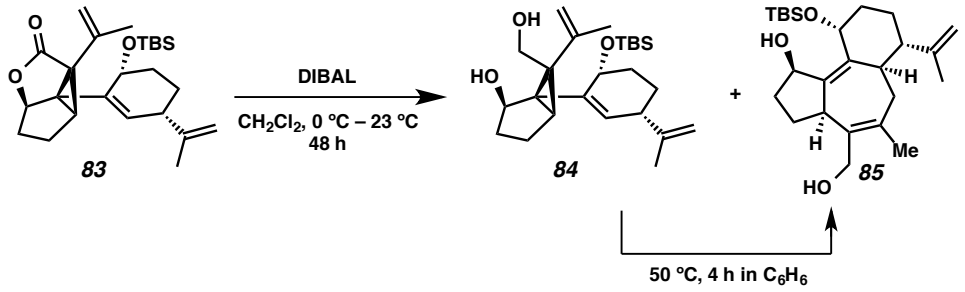

Efforts are ongoing to complete the synthesis of curcusone C by functional group modification. Unfortunately, attempts to oxidize diol **85** to hydroxyl aldehyde **86** have been unsuccessful to date, and we have not yet been able to fully elucidate the structure of the isolated undesired product of these trials. When this transformation is accomplished, addition of peroxide is expected to afford ketone **87** by oxidative cleavage of aldehyde **86** (Scheme 1.3.12).

*Scheme 1.3.12. Attempts to oxidize diol **85***

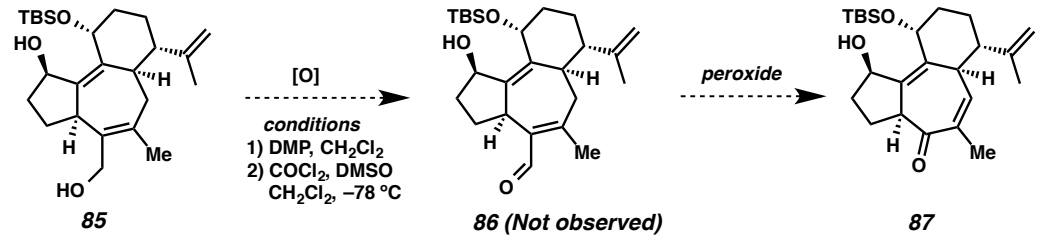

1.4 ENDGAME STRATEGY

1.4.1 ONE CARBON ELIMINATION

The remaining challenges to overcome in the synthesis of the curcusone C (**3**) include elimination of the carbon, used as tether for the synthesis of the cyclopropane with the desired stereochemistry. Bose and co-workers reported that oxidation of α,β-unsaturated aldehyde **88** using peroxide yielded formate **91** via epoxidation, Baeyer–Villiger oxidation, and subsequent rearrangement of epoxyformate **90**. Hydrolysis of formate **91** provided hydroxyl ketone **92**.[17] These transformations could be adapted to our system for the elimination of one carbon in order to construct the cycloheptadienone system (Scheme 1.4.1).

Scheme 1.4.1. Hydroxy Cyclohexanone Synthesis by Bose and co-workers

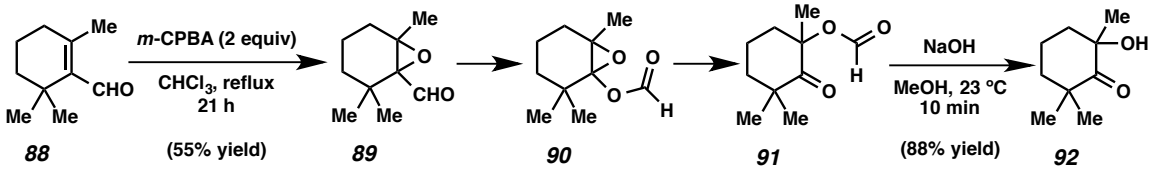

Although our initial attempts to oxidize primary alcohol **85** to aldehyde **86** for the peroxide cleavage have been unsuccessful, we are optimistic that construction of aldehyde **86** is within reach since there is an abundance of methodologies in the literature for the oxidation of primary alcohols.[18] For instance, chemoselective oxidation of a primary alcohol in the presence of a secondary alcohol would be achieved by known oxidation conditions using zirconocene[19] or TEMPO[20,21] catalysts (Scheme 1.4.2).[22]

Scheme 1.4.2. Chemoselective Oxidation of Primary Alcohol ***85***

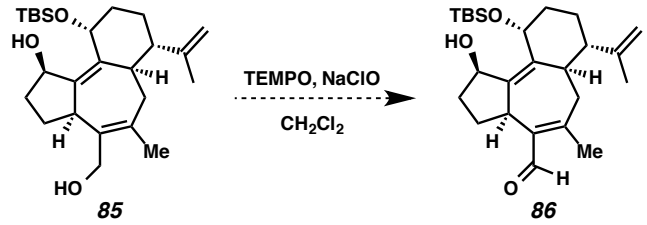

Addition of peroxide to prepared aldehyde **86** would afford epoxyformate **93** via Baeyer–Villiger oxidation and epoxidation. Hydroxy ketone **94** could be prepared by hydrolysis of formate **93**. Desired cycloheptadienone **96** will be synthesized by oxidation of secondary alcohol, followed by dehydroxylation of the α-hydroxyl group (Scheme 1.4.3).

Scheme 1.4.3. Proposed Synthesis of Cycloheptadienone ***96***

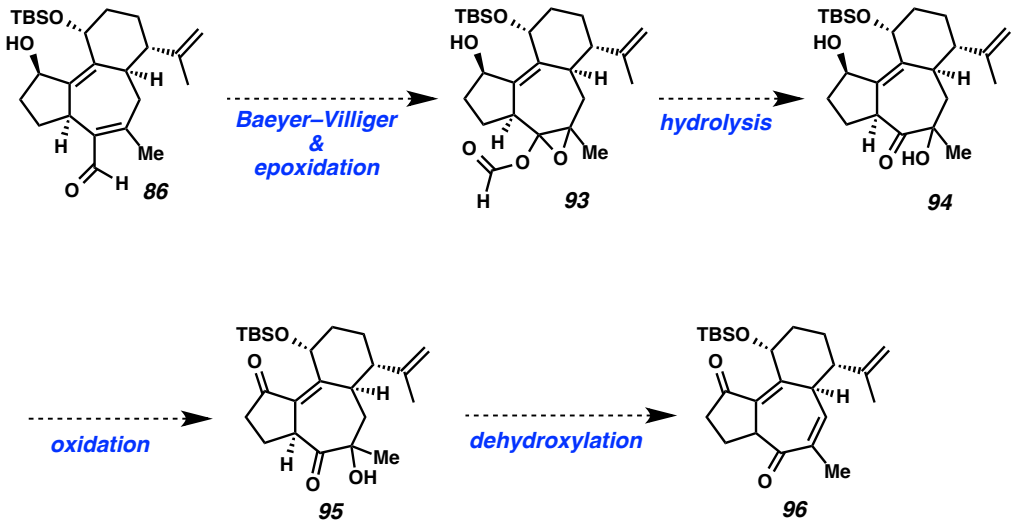

Alternatively, Baeyer–Villiger oxidation (**97**) or epoxidation (**99**) products would be formed by addition of peroxide to aldehyde **86**. Formate **97** could be converted to silyl enol ether **98** for the synthesis of cycloheptadienone **87** by Saegusa–Ito oxidation. In another pathway, epoxide **99** would be transformed to hydroxyl aldehyde **100**, which could then converted to cycloheptadienone **87** via oxidative cleavage (Scheme 1.4.4).

Scheme 1.4.4. Alternative Routes

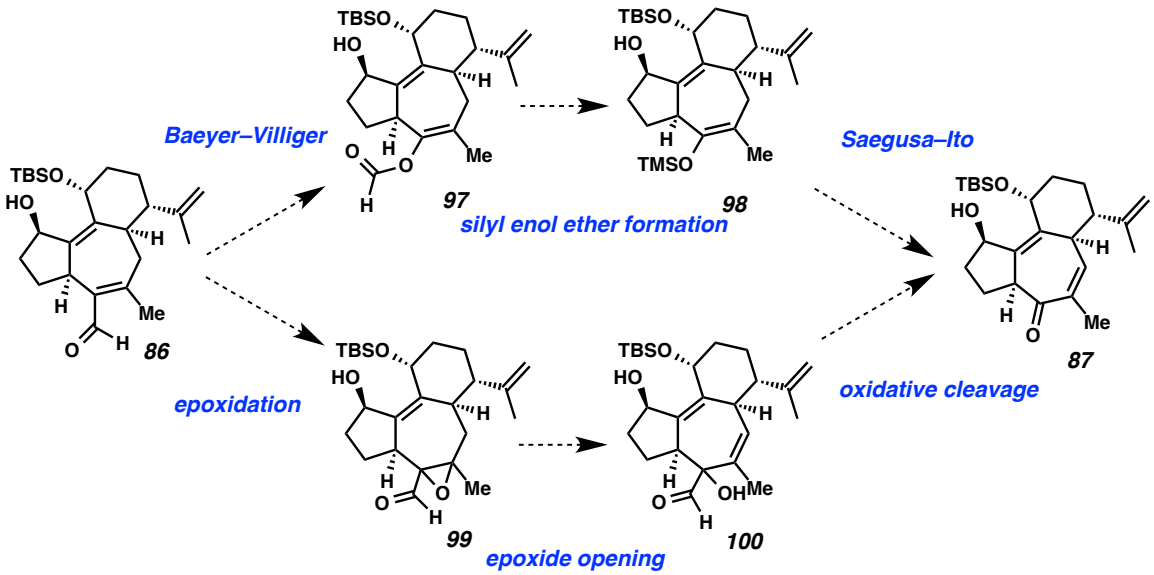

1.4.2 COMPLETION STRATEGY

With hydroxyl ketone **87** or diketone **96** (Scheme 1.4.3 and 1.4.4), total synthesis of the natural product could be accomplished in several steps. Oxidation of allylic alcohol **87** followed by olefin migration would yield cyclopentenone **101** which could be converted to α-hydroxyketone **102** by α-carbon functionalization.[23] Finally, *ent*-curcusone C could be synthesized by TBS deprotection of **102** followed by oxidation and subsequent olefination (Scheme 1.4.5).

Scheme 1.4.5. Remaining Challenges

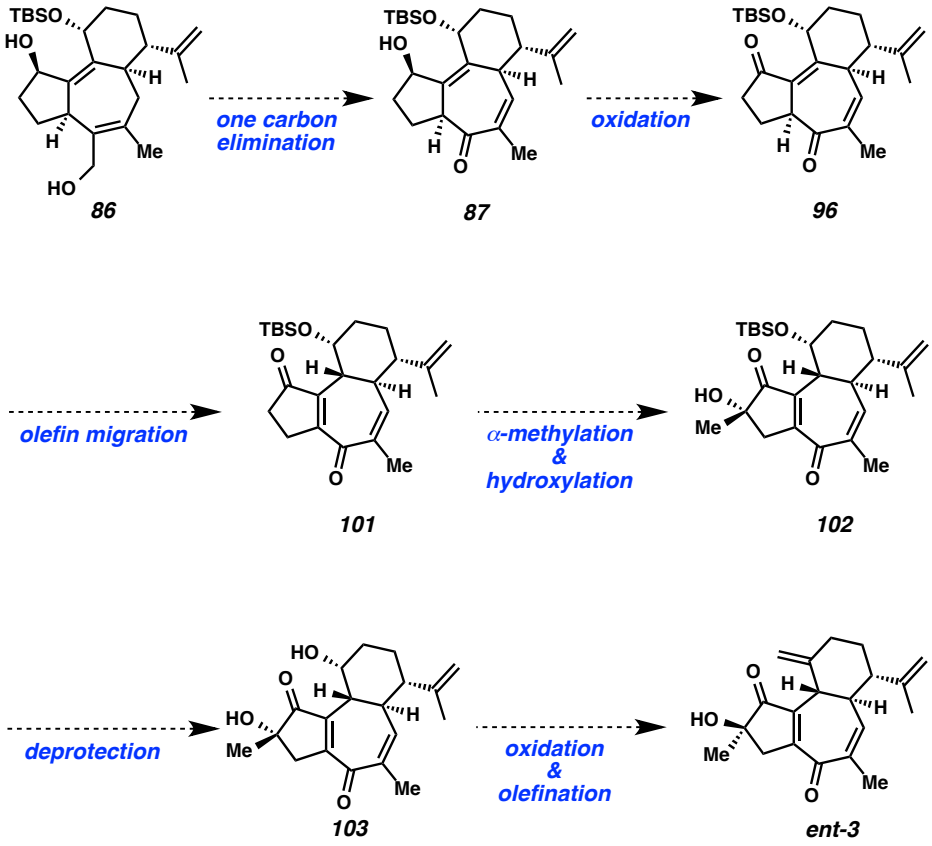

1.5 CONCLUSION

In summary, efforts to synthesize and apply a 1,1-divinylcyclopropane rearrangement toward the total synthesis of curcusone C are described. During the course of model studies, we have discovered an unexpected rearrangement of a divinylcyclopropane, which yielded a complex tetracyclic structure. Furthermore, we have synthesized a tricyclic precursor to *ent*-curcusone C (*ent*-**3**) via divinylcyclopropane rearrangement of **83**. Efforts are currently underway to complete the total synthesis by sequential oxidation and functional group modifications.

1.6 EXPERIMENTAL SECTION

1.6.1 MATERIALS AND METHODS

Unless stated otherwise, reactions were performed under an argon or nitrogen atmosphere using dry, deoxygenated solvents (distilled or passed over a column of activated alumina).[24] Et_3N, *i*-Pr_2NEt, *i*-Pr_2NH, pyridine, and *i*-PrOH were distilled from calcium hydride immediately prior to use. Commercially obtained reagents were used as received unless otherwise stated. *p*-ABSA,[25] $Cu(TBS)_2$,[26] and $MoCl_3(THF)_2$[27] were prepared by known methods. Reaction temperatures were controlled by an IKAmag temperature modulator. Microwave reactions were performed with a Biotage Initiator Eight 400 W apparatus at 2.45 GHz. Thin-layer chromatography (TLC) was performed using E. Merck silica gel 60 F254 precoated plates (0.25 mm) and visualized by UV fluorescence quenching, or potassium permanganate, iodine, or anisaldehyde staining. Silia*Flash* P60 Academic Silica gel (particle size 0.040-0.063 mm) was used for flash chromatography. ^1H and ^{13}C NMR spectra were recorded on a Varian Inova 600 (600 MHz and 151 MHz respectively), Varian Inova 500 (at 500 MHz and 126 MHz respectively), Bruker AV III HD spectrometer equipped with a Prodigy liquid nigrogen temperature cryoprobe (400 MHz and 101 MHz, respectively) and are reported relative to $CHCl_3$ (δ 7.26 & 77.16 respectively), C_6H_6 (δ 7.16 & 128.06 respectively), CH_2Cl_2 (δ 5.32 & 53.84 respectively), CH_3OH (δ 3.31 & 49.00 respectively) and $(CH_3)_2SO$ (δ 2.05 & 39.52 respectively). Data for ^1H NMR spectra are reported as follows: chemical shift (δ ppm) (multiplicity, coupling constant (Hz), integration). IR spectra were recorded on a Perkin Elmer Paragon 1000 Spectrometer and are reported in frequency of absorption

(cm^{-1}). HRMS were acquired from the Caltech Mass Spectral Facility using a JEOL JMS-600H High Resolution Mass Spectrometer in fast atom bombardment (FAB+) or electron ionization (EI+) mode or using an Agilent 6200 Series TOF with an Agilent G1978A Multimode source in electrospray ionization (ESI), atmospheric pressure chemical ionization (APCI) or mixed (MM) ionization mode. Optical rotations were measured on a Jasco P-2000 polarimeter using a 100 mm path length cell at 589 nm.

1.6.2 PREPARATIVE PROCEDURES

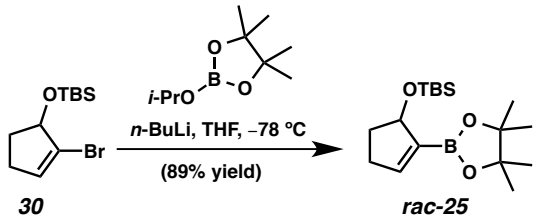

30 *rac-25*

Vinylboronate *rac*-25: To a flame-dried round-bottom flask with a magnetic stir bar were added bromide **30** (440 mg, 1.59 mmol) and THF (6 mL). The flask was cooled to –78 °C and stirred for 10 min. *n*-Butyllithium solution (2.1 M in hexanes, 0.95 mL, 2.00 mmol) was added dropwise. The reaction mixture was stirred at –78 °C for 30 min then isopropyl pinacolyl borate (0.40 mL, 1.96 mmol) was added. The reaction mixture was stirred at –78 °C for 30 min then quenched with HCl solution (2 N in Et_2O, 1.0 mL, 2.00 mmol). Following addition, the reaction mixture was diluted with Et_2O (10 mL) and warmed up to 23 °C. The reaction mixture was filtered and was concentrated under reduced pressure. The residue was purified by flash column chromatography (20:1 hexanes, EtOAc) to afford vinylboronate <u>*rac*</u>-**25** as a colorless oil (460 mg, 1.42 mmol, 89% yield); R_f = 0.60; ^{1}H NMR (500 MHz, $CDCl_3$) δ 6.62 (td, *J* = 2.4, 1.0 Hz, 1H), 5.00 (dddt, *J* = 6.1, 3.9, 2.1, 1.1 Hz, 1H), 2.56 (dddt, *J* = 17.8, 8.9, 4.6, 2.3 Hz, 1H), 2.34–2.20 (m, 1H), 2.20–2.08 (m, 1H), 1.75–1.65 (m, 1H), 1.25 (d, *J* = 1.6 Hz, 12H), 0.89 (s, 9H), 0.11 (s, 6H); ^{13}C NMR (126 MHz, $CDCl_3$) δ 149.3, 83.1, 80.0, 34.7, 33.0, 26.1, 25.1, 25.0, 18.5, 14.1, –4.6; IR (Neat Film, NaCl) 3040, 2978, 2929, 2856, 2708, 1622, 1472, 1409, 1372, 1318, 1249, 1214, 1146, 1060, 1005, 964, 952, 936, 875, 855 cm^{-1}; HRMS (FAB+) *m/z* calc'd for $C_{17}H_{32}SiO_3B$ $[M+H-H_2]^+$: 323.2214, found 323.2222.

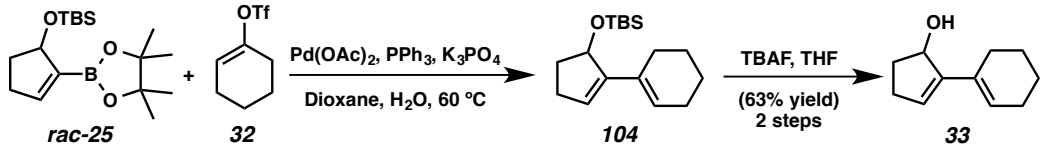

Diene 33: To a flame-dried round-bottom flask equipped with a magnetic stir bar were added boronate *rac*-**25** (2.25 g, 6.94 mmol), triflate **32** (1.71 g, 7.43 mmol), palladium acetate (70 mg, 0.311 mmol), triphenylphosphine (180 mg, 0.686 mmol), and potassium phosphate tribasic (4.43 g, 20.87 mmol). The mixture was evacuated and back filled with argon (3x). The mixture was dissolved in dioxane (35 mL) then added water (3.5 mL). The reaction was immersed in a 60 ºC oil bath. After 9 h of stirring, the reaction was cooled to ambient temperature, diluted with EtOAc (10 mL), and quenched with saturated NH_4Cl solution (10 mL). The phases were separated and the aqueous phase was extracted with EtOAc (3 x 10 mL). The combined organic phases were dried over $MgSO_4$, filtered, and concentrated under reduced pressure to afford a crude mixture of **104**. The residue was used for the next reaction without further purification.

To a round-bottom flask with a magnetic stir bar were added the crude product from former step (1.72 g, 6.18 mmol) and THF (21 mL). To the mixture was added TBAF (1.0 M in THF, 5.0 mL, 5.0 mmol) and stirred for 24 h at 23 ºC. The reaction mixture was quenched by saturated aqueous NH_4Cl (20 mL). The phases were separated and the aqueous phase was extracted with EtOAc (3 x 20 mL). The combined organic phases were dried over $MgSO_4$, filtered, and concentrated under reduced pressure. The residue was purified by flash column chromatography (4:1 hexanes:EtOAc) to afford diene allylic alcohol **33** (714 mg, 4.35 mmol, 63% yield over two steps) as a colorless oil; R_f = 0.67 (10:1, hexanes:EtOAc) ^{1}H NMR (500 MHz, $CDCl_3$) δ 6.05–5.95 (m, 1H), 5.83–5.75

(m, 1H), 5.01 (dt, *J* = 7.2, 1.9 Hz, 1H), 2.65–2.53 (m, 1H), 2.35–2.26 (m, 1H), 2.26–2.10 (m, 3H), 1.87 (ddt, *J* = 13.9, 8.0, 2.4 Hz, 1H), 1.73–1.53 (m, 5H); ^{13}C NMR (126 MHz, $CDCl_3$) δ146.39, 131.82, 127.36, 125.35, 77.16, 76.22, 33.82, 30.48, 26.39, 25.81, 22.81, 22.43; IR (Neat Film, NaCl) 3339, 3045, 2925, 2855, 1435, 1302, 1044, 986, 941, 823 cm^{-1}; HRMS (EI+) *m/z* calc'd for $C_{11}H_{16}O$ $[M\bullet]^+$: 164.1201, found 164.1170.

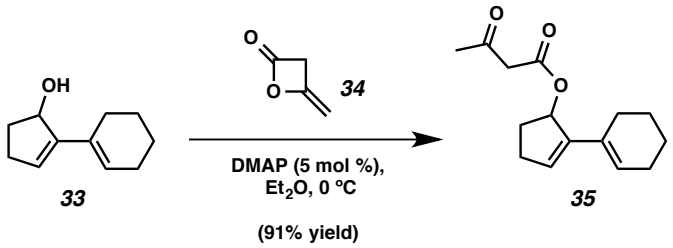

***β*-ketoester 35**: To a flame-dried round-bottom flask equipped with a magnetic stir bar were added allylic alcohol **33** (60 mg, 0.365 mmol), 4-dimethylaminopyridine (0.2 mg, 0.0016 mmol) and Et_2O (1.5 mL). The flask was cooled to 0 ºC and stirred for 10 min. Diketene (0.03 mL, 0.389 mmol) was added dropwise. The reaction mixture was stirred for 15 min at 0 ºC was then quenched by cold water (0 ºC, 1.5 mL). The mixture was extracted with Et_2O (3 x 3 mL). The combined organic layers were washed by brine (3 mL), dried over $MgSO_4$, and concentrated under reduced pressure. The crude oil was purified by flash column chromatography (4:1 hexanes, EtOAc) to afford *β*-ketoester **35** (82.7 mg, 0.333 mmol, 91% yield) as a colorless oil; R_f = 0.52 (4:1, hexanes:EtOAc); ^{1}H NMR (500 MHz, $CDCl_3$) δ 6.04 (dt, *J* = 7.2, 1.8 Hz, 1H), 5.98–5.94 (m, 1H), 5.76–5.72 (m, 1H), 3.43 (s, 2H), 2.61–2.53 (m, 1H), 2.40–2.24 (m, 2H), 2.22 (s, 3H), 2.21–2.16 (m, 2H), 2.16–2.07 (m, 2H), 1.96–1.88 (m, 2H), 1.71–1.51 (m, 4H); ^{13}C NMR (126 MHz, $CDCl_3$) δ 200.7, 167.3, 142.2, 131.1, 130.7, 125.9, 79.9, 50.7, 31.6, 30.8, 30.2, 26.6, 25.8,

22.7, 22.3; IR (Neat Film, NaCl) 2926, 2853, 1718, 1643, 1412, 1358, 1310, 1243, 1147, 1027, 977, 936, 896, 800 cm^{-1}; HRMS (MM) *m/z* calc'd for $C_{15}H_{19}O_3$ $[M-H]^-$: 247.1340, found 247.1362.

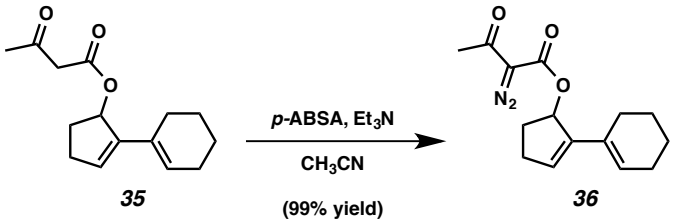

Diazo ester 36: To a round-bottom flask equipped with a magnetic stir bar were added *ß*-ketoester **35** (80 mg, 0.322 mmol), CH_3CN (3 mL), and *p*-ABSA (130 mg, 0.541 mmol). TEA (0.2 mL, 1.43 mmol) was added dropwise. The reaction mixture was stirred for 2 h at 23 ºC. The reaction mixture was filtered through a silica gel plug (pentanes:Et_2O 2:1) was then concentrated under reduced pressure to afford diazo ester **36** (88.2 mg, 0.322 mmol, 99% yield) as a yellowish oil; R_f = 0.44 (6:1, hexanes:EtOAc); ^1H NMR (500 MHz, $CDCl_3$) δ 6.08 (dt, J = 1.66 Hz, 1.66 Hz, 7.75 Hz, 1H), 5.95 (d, *J* = 2.62 Hz, 1H), 5.71 (s, 1H), 2.58–2.55 (m, 1H), 2.44 (s, 3H), 2.31–2.24 (m, 1H), 2.22 (s, 3H), 2.39-2.26 (m, 2H), 2.18–2.09 (m, 4H), 1.95–1.90 (m, 1H), 1.68–1.52 (m, 4H); ^{13}C NMR (126 MHz, $CDCl_3$) δ 190.5, 161.6, 142.1, 131.2, 130. 7, 125.5, 80.3, 31.7, 30.7, 28.4, 26.3, 25.8, 22.7, 22.3; IR (Neat Film, NaCl) 3298, 3050, 2929, 2856, 2390, 2297, 2208, 2138, 1712, 1661, 1652, 1447, 1435, 1365, 1312, 1247, 1149, 1061, 1024, 965, 926, 854, 836, 816, 800, 746 cm^{-1}; HRMS (FAB+) *m/z* calc'd for $C_{15}H_{19}O_3N_2$ $[M+H]^-$: 275.1396, found 275.1389.

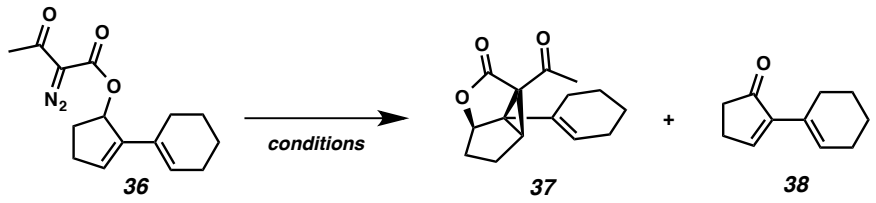

General Screening Procedure: To a flame-dried two neck round-bottom flask equipped with a magnetic stir bar was added catalyst in a nitrogen-filled glove box. The flask was sealed with rubber septums and removed from the glove box. One of the rubber septum was replaced with a reflux condenser connected to a nitrogen inlet. A solution of diazo ester **36** in solvent was added dropwise via syringe or syringe pump. The reaction was set to reaction temperature using oil or water bath. After reaction time, the mixture was set to 23 ºC and stirred for 15 min. The mixture was concentrated and crude NMR was taken.

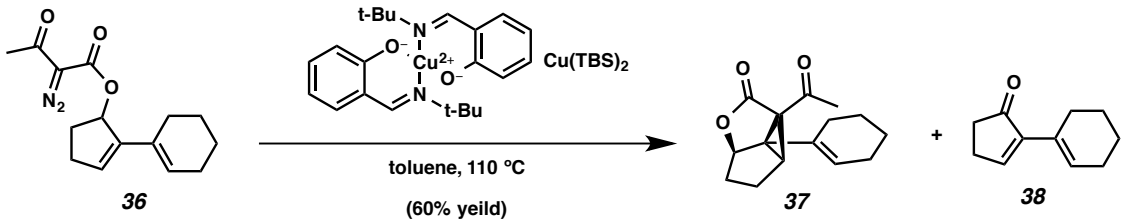

Cyclopropane 37: To a flame-dried two neck round-bottom flask equipped with a magnetic stir bar was added copper catalyst (20 mg, 0.0459 mmol) in a nitrogen-filled glove box. The flask was sealed with rubber septums and removed from the glove box. One of the rubber septum was replaced with a reflux condenser connected to a nitrogen inlet. A solution of diazo ester **36** (254.8 mg, 0.929 mmol) in toluene (46 mL) was added. The reaction was heated to reflux in a 110 ºC oil bath. After 2 h of stirring, the reaction mixture was cooled to 23 ºC and stirred for 15 min. The mixture was

concentrated and purified by flash column chromatography (15:1 hexanes, EtOAc) to afford cyclopropane **37** (148 mg, 0.601 mmol, 65% yield) as a yellowish oil; R_f = 0.36 (6:1 hexanes:EtOAc eluent); ^{1}H NMR (500 MHz, $CDCl_3$) δ 5.72–5.70 (m, 1H), 4.81 (d, *J* = 1.30 Hz, 1H), 3.10 (d, J = 6.40 Hz, 1H), 2.45 (s, 3H), 2.31–2.24 (m, 1H), 2.15–2.12 (m, 1H), 2.04–1.98 (m, 3H), 1.91–1.85 (m, 1H), 1.80–1.78 (m, 1H), 1.71–1.49 (m, 5H); ^{13}C NMR (126 MHz, $CDCl_3$) δ 197.1, 172.9, 123.0, 128.3, 85.3, 66.7, 51.6, 39.4, 38.1, 30.1, 28.3, 25.3, 24.0, 22.6, 22.0; IR (Neat Film, NaCl) 2929, 1760, 1699, 1435, 1360, 1311, 1243, 1159, 1089, 1008, 979, 956, 925, 906, 855, 799, 756 cm^{-1}; HRMS (MM+) *m/z* calc'd for $C_{15}H_{19}O_3$ $[M+H]^+$: 247.1329, found 247.1327, and dienone **38** (22 mg, 0.136 mmol, 15% yield) as a colorless oil R_f = 0.40 (6:1 hexanes:EtOAc eluent); ^{1}H NMR (500 MHz, $CDCl_3$) δ 7.39–7.33 (m, 1H), 6.91–6.85 (m, 1H), 2.60–2.54 (m, 2H), 2.51–2.43 (m, 2H), 2.21–2.15 (m, 4H), 1.74–1.67 (m, 2H), 1.65–1.55 (m, 2H); ^{13}C NMR (126 MHz, $CDCl_3$) δ 208.8, 155.2, 128.8, 128.6, 36.3, 26.8, 25.7, 25.7, 22.8, 22.1; IR (Neat Film, NaCl) 3386, 3051, 2925, 2857, 2834, 2661, 1703, 1699, 1340, 1589, 1439, 1406, 1385, 1342, 1318, 1294, 1263, 1208, 1175, 1136, 1113, 1079, 1016, 998, 976, 940, 926, 887, 840, 832, 803, 785, 762, 724 cm^{-1}; HRMS (FAB+) *m/z* calc'd for $C_{11}H_{15}O$ $[M+H]^+$: 163.1123, found 163.1128.

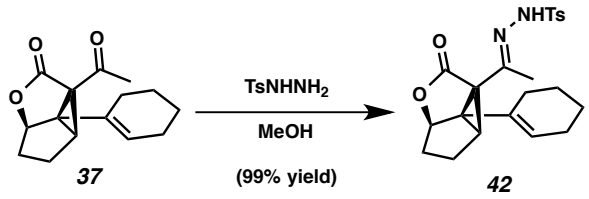

Hydrazone 42: To a round-bottom flask equipped with a magnetic stir bar were added cyclopropane **37** (54 mg, 0.219 mmol), methanol (1 mL), and *p*-toluenesulfonyl hydrazide (61 mg, 0.328 mmol). The reaction was stirred for 12 h at 23 ºC. The reaction was concentrated and purified by flash column chromatography (4:1 hexanes, EtOAc) to afford hydrazone **42** (90 mg, 0.217 mmol, 99% yield) as a white solid; R_f = 0.50 (2:1 hexanes:EtOAc); ^{1}H NMR (500 MHz, $CDCl_3$) δ 7.82–7.79 (m, 2H), 7.65 (s, 2H), 7.32–7.26 (m, 2H), 5.27 (t, *J* = 1.72 Hz, 1H), 4.91 (d, *J* = 0.95 Hz, 1H), 2.93 (d, J = 6.36 Hz, 1H), 2.43 (s, 3H), 2.28–2.22 (m, 1H), 2.04–1.96 (m, 1H), 1.88–1.79 (m, 5H), 1.76–1.67 (m, 3H), 1.52–1.38 (m, 4H); ^{13}C NMR (126 MHz, $CDCl_3$) δ 173.8, 147.6, 144.4, 135.4, 129.7, 128.5, 128.2, 127.5, 85.4, 62.2, 50.3, 38.3, 33.4, 28.1, 25.2, 23.7, 22.7, 22.0, 21.8, 16.0; IR (Neat Film, NaCl) 3214, 2926, 2360, 1748, 1339, 1168, 1094, 1057, 1002, 906, 814, 754 cm^{-1}; HRMS (MM+) *m/z* calc'd for $C_{22}H_{27}O_4N_2S$ $[M+H]^+$: 415.1686, found 415.1698.

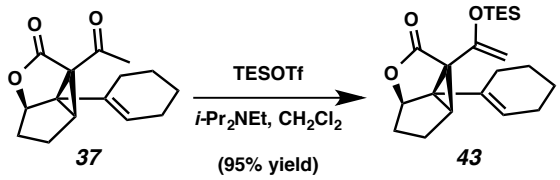

TES enol ether 43: To a flame-dried round-bottom flask equipped with a magnetic stir bar were added cyclopropane **37** (22.5 mg, 0.0913 mmol), DCM (2 mL), and *i*-Pr_2NEt (0.05 mL, 0.287 mmol). The flask was cooled to 0 ºC and stirred for 10 min. TESOTf

(0.05 mL, 0.210 mmol) was added dropwise. The reaction mixture was stirred for 30 min at 0 ºC. The reaction mixture was filtered through a silica gel plug (henxanes:EtOAc 10:1) was then concentrated under reduced pressure to afford TES enol ether **43** (28 mg, 95% yield) as colorless oil. R_f = 0.60 (6:1 hexanes:EtOAc); ^{1}H NMR (500 MHz, C_6D_6) δ 5.38 (t, *J* = 1.79 Hz, 1H), 4.53 (d, *J* = 1.68 Hz, 1H), 4.45 (dd, *J* = 0.78 Hz, 1.69, 1H), 4.37 (d, *J* = 1.68 Hz, 1H), 2.30–2.28 (m, 1H), 2.13–2.08 (m, 1H), 1.95–1.85 (m, 3H), 1.70–1.60 (m, 2H), 1.56–1.42 (m, 4H), 1.37–1.30 (m, 2H), 1.02 (t, *J* = 7.94 Hz, 9H), 0.71 (ddd, *J* = 1.34 Hz, 7.94 Hz, 9.90 Hz, 6H); ^{13}C NMR (126 MHz, C_6D_6) δ 172.8, 151.7, 131.3, 125.7, 93.7, 84.0, 58.9, 48.7, 38.9, 34.0, 27.7, 25.6, 23.6, 23.1, 22.5, 7.0, 5.2; IR (Neat Film, NaCl) 3518, 3119, 2934, 2876, 2836, 2734, 2365, 1769, 1629, 1458, 1437, 1413, 1334, 1290, 1258, 1196, 1161, 1137, 1075, 1042, 1003, 981, 933, 907, 821, 770, 747 cm^{-1}; HRMS (EI) *m/z* calc'd for $C_{21}H_{32}O_3Si$ $[M\bullet]^+$: 360.2121, found 360.2117.

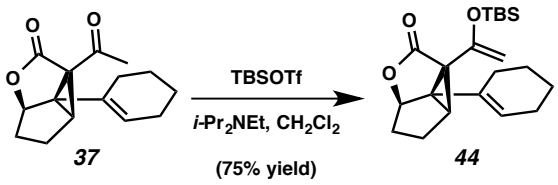

TBS enol ether 44: To a flame-dried round-bottom flask equipped with a magnetic stir bar were added cyclopropane **37** (41 mg, 0.167mmol), DCM (3.4 mL), and *i*-Pr_2NEt (0.06 mL, 0.344 mmol). The flask was cooled to 0 ºC and stirred for 10 min. TBSOTf (0.04 mL, 0.174 mmol) was added dropwise. The reaction mixture was stirred for 30 min at 0 ºC. The reaction mixture was filtered through a silica gel plug (henxanes:EtOAc 10:1) was then concentrated under reduced pressure to afford TBS enol ether **44** (45.3 mg, 75% yield) as colorless oil. R_f = 0.50 (6:1 hexanes:EtOAc); ^{1}H NMR (500 MHz,

C_6D_6) δ 5.39 (dt, *J* = 3.8, 2.0 Hz, 1H), 4.47 (dt, *J* = 2.9, 0.8 Hz, 1H), 4.44 (d, *J* = 1.6 Hz, 1H), 4.36 (d, *J* = 1.7 Hz, 1H), 2.26 (ddd, *J* = 6.7, 1.6, 0.7 Hz, 1H), 2.10 (dddt, *J* = 14.2, 6.1, 4.2, 2.0 Hz, 1H), 1.98–1.83 (m, 2H), 1.72–1.60 (m, 2H), 1.56–1.40 (m, 5H), 1.39–1.28 (m, 2H), 0.96 (s, 9H), 0.28 (s, 3H), 0.19 (s, 3H); ^{13}C NMR (126 MHz, C_6D_6) δ 167.1, 161.2, 144.2, 124.9, 113.2, 83.5, 45.5, 40.5, 38.1, 33.2, 32.1, 30.3, 25.9, 25.42, 21.6, 21.5, 18.9, –3.6, –4.50; IR (Neat Film, NaCl) 3520, 2929, 2857, 1630, 1471, 1463, 1361, 1335, 1291, 1257, 1196, 1161, 1141, 1175, 1042, 1026, 1002, 938, 907, 892, 830, 782 cm^{-1}; HRMS (FAB+) *m/z* calc'd for $C_{21}H_{33}SIO_3$ $[M+H]^+$: 361.2199, found 361.2182.

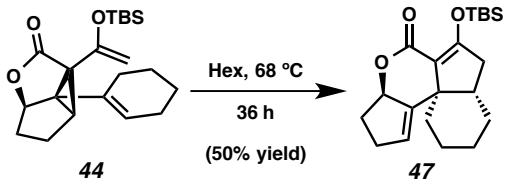

44 ***47***

Tetracycle 47: To a flame-dried two neck round-bottom flask equipped with a magnetic stir bar and a reflux condenser was added TBS enol ether **44** (15.8 mg, 0.0438 mmol) and hexane (4.4 mL). The reaction was heated to reflux in a 68 ºC oil bath. After 36 h of stirring, the reaction mixture was cooled to 23 ºC and stirred for 15 min. The mixture was concentrated and purified by flash column chromatography (15:1 hexanes, EtOAc) to afford tetracycle **47** (8 mg, 0.0222 mmol, 50% yield) as a colorless oil; R_f = 0.45 (6:1 hexanes:EtOAc); ^{1}H NMR (500 MHz, C_6D_6) δ 5.36–5.17 (m, 1H), 5.17–5.00 (m, 1H), 2.44 (dd, *J* = 16.2, 12.1 Hz, 1H), 2.25–2.16 (m, 1H), 2.11–1.99 (m, 2H), 1.96–1.85 (m, 2H), 1.75–1.61 (m, 2H), 1.45–1.34 (m, 3H), 1.27–1.20 (m, 1H), 1.20–1.11 (m, 1H), 1.04 (s, 9H), 1.01–0.79 (m, 2H), 0.42 (s, 3H), 0.31 (s, 3H); ^{13}C NMR (126 MHz, C_6D_6) δ 167.11, 161.17, 144.16, 128.06, 124.93, 113.19, 83.49, 45.48, 40.49, 38.06,

33.22, 32.11, 30.30, 25.92, 25.42, 21.55, 21.45, 18.87, –3.64, –4.50; IR (Neat Film, NaCl) 3409, 3051, 2924, 2854, 1771, 1713, 1606, 1463, 1379, 1362, 1342, 1328, 1304, 1251, 1222, 1193, 1172, 1157, 1111, 1095, 1064, 1049, 1001, 968, 939, 926, 904, 865, 839, 790, 721 cm^{-1}; HRMS (FAB+) *m/z* calc'd for $C_{21}H_{33}O_3Si$ $[M+H]^+$: 361.2199, found 361.2184.

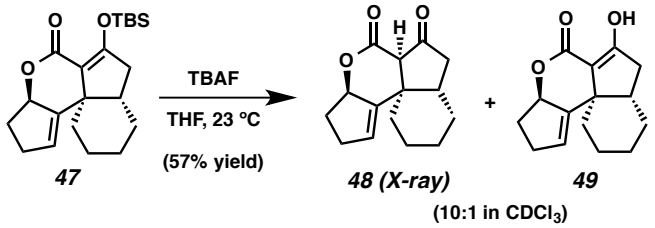

***β*-Ketolactone 48:** To a round-bottom flask with a magnetic stir bar were added tetracycle **47** (7.7 mg, 0.0214 mmol) and THF (1 mL). To the mixture was added TBAF (1.0 M in THF, 0.022 mL, 0.022 mmol) and stirred for 5 min at 23 ºC. The reaction mixture was quenched by saturated aqueous NH_4Cl (1 mL). The mixture was extracted with Et_2O (3 x 1 mL). Organic layers were combined and dried over $MgSO_4$ and concentrated under reduced pressure. The residue was purified by flash column chromatography (2:1 hexanes:EtOAc) provided *β*-ketolactone **48** (3 mg, 0.0212 mmol, 57% yield) as a colorless oil; R_f = 0.10 (6:1, hexanes:EtOAc); ^1H NMR (500 MHz, $CDCl_3$) δ5.25–5.21 (m, 1H), 4.75–4.69 (m, 1H), 2.97 (s, 1H), 2.16 (dd, J = 18.9, 8.3 Hz, 1H), 2.04–1.93 (m, 1H), 1.90–1.69 (m, 4H), 1.67–1.58 (m, 1H), 1.40–0.71 (m, 8H); ^{13}C NMR (126 MHz, $CDCl_3$) δ 208.3, 141.4, 129.1, 126.3, 85.0, 59.0, 47.7, 43.5, 42.5, 42.2, 37.0, 34.6, 33.8, 31.9, 30.9, 30.7, 30.4, 29.5, 27.7, 25.7, 22.6, 21.1; IR (Neat Film, NaCl) 3441, 2929, 2857, 1760, 1451, 1407, 1354, 1310, 1241, 1180, 1152, 1089, 1038, 949, 822,

803, 744 cm^{-1}; HRMS (MM+) *m/z* calc'd for $C_{15}H_{19}O_3$ $[M+H]^+$: 247.1329, found 247.1294.

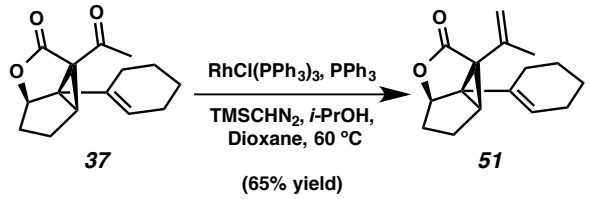

Vinyl lactone 51: To a flame-dried round-bottom flask equipped with a magnetic stir bar were added Wilkinson's catalyst (4.3 mg, 0.00465 mmol) and PPh_3 (54 mg, 0.206 mmol) in a nitrogen-filled glove box. The flask was sealed with a rubber septum, removed from the glove box and connected to a nitrogen inlet. Dioxane (2 mL) was added, and the reaction was immersed in a 60 ºC oil bath. Isopropanol (0.21 mL, 2.75 mmol) was added, followed by a solution of cyclopropane **37** (46 mg, 0.187 mmol) in dioxane (0.5 mL) to give a reddish solution. A solution of trimethylsilyldiazomethane (2 M in Et_2O, 0.22 mL, 0.44 mmol) was added to the reaction mixture. The reaction was stirred for 5 h at 60 ºC. The reaction was allowed to cool to ambient temperature and concentrated under reduced pressure. The residue was purified by flash column chromatography (15:1, hexanes:EtOAc) to afford vinyl lactone **51** (30 mg, 0.123 mmol, 65% yield) as a colorless oil. R_f = 0.40 (6:1 hexanes:EtOAc); ^{1}H NMR (500 MHz, C_6D_6) δ 5.30–5.23 (m, 1H), 4.96 (dd, *J* = 3.0, 1.5 Hz, 1H), 4.85 (dd, *J* = 1.5, 0.8 Hz, 1H), 4.53 (d, *J* = 1.0 Hz, 1H), 2.06 (dd, *J* = 4.1, 3.5 Hz, 1H), 1.83–1.77 (m, 5H), 1.75–1.60 (m, 4H), 1.58–1.45 (m, 1H), 1.46–1.25 (m, 5H); ^{13}C NMR (126 MHz, C_6D_6) δ 173.5, 138.4,

138.4, 125.5, 116.5, 83.9, 58.9, 50.2, 38.9, 33.3, 28.0, 25.5, 23.6, 23.0, 22.3, 22.0; IR (Neat Film, NaCl), 3498, 2918, 2850, 1960, 1645, 1539, 1436, 1373, 1335, 1302, 1289, 1262, 1212, 1161, 1137, 1093, 1077, 1044, 1012, 997, 906, 841, 802, 751 cm^{-1}; HRMS (MM+) *m/z* calc'd for $C_{16}H_{21}O_2$ $[M+H]^+$: 245.1536, found 245.1555.

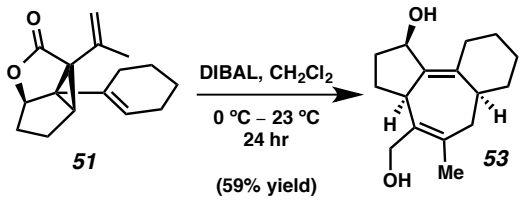

Diol 53: To a flame-dried round-bottom flask equipped with a magnetic stir bar were added vinyl lactone **51** (10 mg, 0.0403 mmol) and DCM (1 mL). The flask was cooled to 0 ºC and stirred for 10 min. A solution of DIBAL (1 M in DCM, 0.4 mL, 0.4 mmol) was added dropwise. The reaction mixture was slowly warmed up to 23 ºC and remained stirring for 24 h. The reaction was quenched by methanol (0.4 mL). Saturated aqueous potassium sodium tartarate solution (1 mL) was added to the mixture. The phases were separated and the aqueous phases were extracted with DCM (5 x 2 mL). The combined organic phases were dried over $MgSO_4$, filtered, and concentrated under reduced pressure. The residue was purified by flash column chromatography (2:1, hexanes:EtOAc) to afford diol **53** as a white solid (6 mg, 0.024 mmol, 59% yield); R_f = 0.08 (2:1 hexanes:EtOAc); ^{1}H NMR (500 MHz, C_6D_6) δ 4.61 (d, *J* = 4.2 Hz, 1H), 4.20 (d, *J* = 11.3 Hz, 1H), 3.96 (d, *J* = 11.3 Hz, 1H), 3.58–3.49 (m, 1H), 3.04 (dd, *J* = 13.6, 4.1 Hz, 1H), 2.75 (dd, *J* = 12.8, 3.5 Hz, 1H), 2.41 (qd, *J* = 12.4, 6.1 Hz, 1H), 1.95–1.83 (m, 2H), 1.76–1.67 (m, 5H), 1.64–1.57 (m, 1H), 1.52 (dd, *J* = 13.6, 3.6 Hz, 1H), 1.43–1.27

(m, 6H); ^{13}C NMR (126 MHz, C_6D_6) δ 138.9, 138.7, 138.3, 134.2, 73.2, 60.1, 41.6, 40.5, 38.5, 34.8, 34.6, 34.2, 30.2, 29.4, 27.6, 26.5, 21.9; IR (Neat Film, NaCl) 3338, 2927, 2853, 1740, 1447, 1373, 1242, 1177, 1043, 965, 913 cm^{-1}; HRMS (FAB+) *m/z* calc'd for $C_{16}H_{23}O_2$ $[M+H-H_2]^+$: 247.1698, found 247.1692.

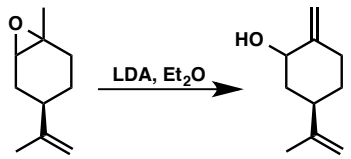

28 ***54***

Alcohol 54: To a flame-dried round-bottom flask with a magnetic stir bar were added diisopropyl amine (1.75 mL, 13.3 mmol) and Et_2O (35 mL). A solution of *n*-butyllithium (2.12 M in hexane, 6.84 mL, 14.5 mmol) was added dropwise over a period of 30 min. A solution of epoxide **28** (2 mL, 12.1 mmol) in Et_2O (7 mL) was added dropwise over a period of 30 min. The resulting mixture was allowed to warm up to 23 ºC and then stirred for 7 h. The reaction mixture was cooled in ice bath and water was added. The organic phase was separated and washed with 2 M aqueous HCl (10 mL), water (10 mL), saturated aqueous $NaHCO_3$ (10 mL) and brine (10 mL). The Et_2O extracts are combined, dried over $MgSO_4$, and evaporated to afford crude mixture. The residue was used for the next reaction without further purification.

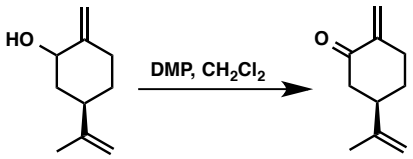

54 ***55***

Ketone 55: To a round-bottom flask equipped with a magnetic stir bar were added alcohol **54** (124 mg, 0.815 mmol) and DCM (10 mL). Dess-Martin periodinane (440 mg, 1.06 mmol) was added to the mixture. The reaction was stirred for 3 h at 23 ºC. The reaction mixture was diluted with Et_2O (10 mL) and then a 1:1:1 mixture of saturated aqueous $Na_2S_2O_3$ (10 mL), saturated aqueous $NaHCO_3$ (10 mL), and water (10 mL) was added slowly. The resulting mixture was stirred for 20 min resulting in two clear layers. The organic layer was gathered and the aqueous layer was extracted with Et_2O (30 mL x 3). The organic layers were combined and dried over Na_2SO_4, and evaporated to afford crude mixture (Caution, the solvent was partially removed. ***55*** can be dimerized easily). The mixture was filtered silica gel 8:1 pentanes:Et_2O) and used in the next reaction without further purification. The characterization data matched those reported in the literature.[7]

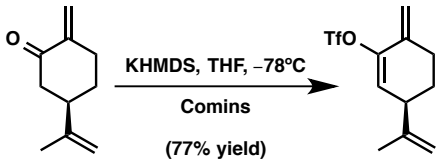

55 ***27***

Triflate 27: To a flame-dried round-bottom flask equipped with a magnetic stir bar was added potassium bis(trimethylsilyl)amide (310 mg, 1.55 mmol) in a nitrogen filled glove box. The flask was sealed with rubber septum and removed from the glove box, connected to a nitrogen inlet, and cooled to –78 ºC. A solution of ketone **55** (150 mg, 1

mmol) in THF (10 mL) was added dropwise by syringe pump over 2 h. After addition of ketone **55** was completed, comins' reagent (652 mg, 1.66 mmol) in THF (10 mL) was added dropwisely. The mixture was stirred for 4 hr at –78 ºC. The reaction mixture was added saturated aqeous $NaHCO_3$ (50 mL), and then allowed to warm up to 23 ºC. The mixture was extracted with Et_2O (30 x 3 mL). The combined organic layers were washed by brine (100 mL), dried over $MgSO_4$, and concentrated under reduced pressure. The residue was purified by flash column chromatography (25:1 hexanes:EtOAc) to afford triflate **27** (218 mg, 0.77 mmol, 77% yield); R_f = 0.52 (4:1, hexanes:EtOAc); ^{1}H NMR (500 MHz, $CDCl_3$) δ 5.82 (dd, *J* = 4.0, 1.7 Hz, 1H), 5.28 (s, 1H), 5.06–4.99 (m, 1H), 4.88 (t, *J* = 1.5 Hz, 1H), 4.77 (dt, *J* = 1.7, 0.9 Hz, 1H), 3.14–3.06 (m, 1H), 2.63–2.49 (m, 1H), 2.48–2.37 (m, 1H), 1.95–1.83 (m, 1H), 1.77 (s, 3H), 1.72–1.60 (m, 1H); ^{13}C NMR (126 MHz, $CDCl_3$) δ 149.5, 147.1, 145.8, 144.0, 139.5, 136.5, 136.0, 126.3, 123.9, 120.7, 119.9, 117.4, 112.8, 112.0, 111.1, 1102, 43.4, 29.6, 27.0, 21.3; IR (Neat Film, NaCl) 3084, 2947, 2869, 1648, 1608, 1447, 1436, 1422, 1428, 1373, 1245, 1214, 1143, 1129, 1066, 1045, 1017, 998, 978, 948, 755, 737 cm^{-1}; HRMS (FAB+) *m/z* calc'd for $C_{11}H_{12}F_3O_3S$ $[M+H-H_2]^+$: 281.0459, found 281.0473; $[\alpha]_D^{25.0}$ 61.1° (*c* 0.25, $CHCl_3$).

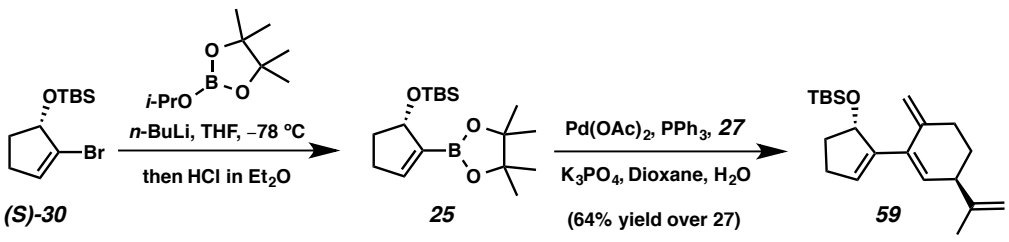

Diene 59: To a flame-dried round-bottom flask with a magnetic stir bar were added bromide (*S*)**-30** (6 g, 21.6 mmol) and THF (70 mL). The flask was cooled to –78 ºC and

stirred for 10 min. *n*-Butyllithium solution (2.5 M in hexanes, 13 mL, 32.5 mmol) was added dropwise. The reaction mixture was stirred at −78 ºC for 30 min then isopropyl pinacolyl borate (6.9 mL, 33.8 mmol) was added. The reaction mixture was stirred at −78 ºC for 30 min then quenched with HCl solution (2 N in Et_2O, 16.3 mL, 32.5 mmol). Following addition, the reaction mixture was diluted with Et_2O (70 mL) and warmed up to 23 ºC. The reaction mixture was filtered and was concentrated under reduced pressure, and the residue was used in the next reaction without further purification.

To a flame-dried round-bottom flask equipped with a magnetic stir bar were added boronate **25** (2.65 g, 7.74 mmol), triflate **27** (1.987 g, 7.04 mmol), palladium acetate (82 mg, 0.35 mmol), triphenylphosphine (199 mg, 0.70 mmol), potassium phosphate tribasic (4.5 g, 21 mmol). The mixture was evacuated and back filled with argon (3x). The mixture was dissolved in dioxane (25 mL) then added water (2.5 mL). The reaction mixture was stirred at 23 ºC for 40 hr. The resulting mixture was then diluted with EtOAc (25 mL), washed by saturated aqueous NH_4Cl (25 mL), and then dried over $MgSO_4$. The mixture was filtered and concentrated under reduced pressure to afford crude mixture of **25** as a colorless oil. The residue was purified by flash column chromatography (25:1 hexanes:EtOAc) to afford diene **59** (1.5 g, 4.54 mmol, 64% yield over triflate **27**); R_f = 0.95 (10:1, hexanes:EtOAc); ^{1}H NMR (400 MHz, C_6D_6) δ 5.88–5.84 (m, 1H), 5.70–5.68 (m, 1H), 5.02–4.93 (m, 2H), 4.93–4.88 (m, 2H), 4.85–4.81 (m, 1H), 2.97–2.91 (m, 1H), 2.51–2.30 (m, 4H), 2.16–2.02 (m, 2H), 1.80 (tt, *J* = 8.3, 4.0 Hz, 2H), 1.72–1.56 (m, 2H), 1.00 (s, 9H), 0.09 (s, 6H); ^{13}C NMR (101 MHz, C_6D_6) δ 148.5, 146.7, 143.4, 135.9, 132.7, 130.9, 111.0, 110.7, 78.7, 45.1, 34.8, 32.1, 29.3, 26.2, 26.0, 20.9, 18.4, –4.3, –4.5; IR (Neat Film, NaCl) 3435, 3080, 2956, 2929, 2856, 2360, 1725,

1645, 1472, 1463, 1362, 1258, 1095, 1020, 947, 865, 836, 801, 776 cm^{-1}; HRMS (FAB+) *m/z* calc'd for $C_{21}H_{33}OSi$ $[M+H-H_2]^+$: 329.2301, found 329.2297; $[\alpha]_D^{25.0}$ –38.3° (*c* 0.150, $CHCl_3$).

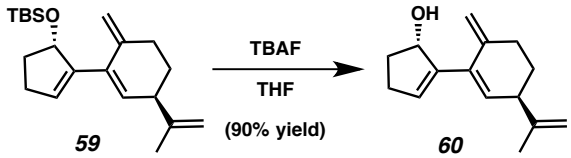

Allylic alcohol 60: To a round-bottom flask with a magnetic stir bar were added diene **59** (1.5 g, 4.54 mmol) and THF (23 mL). To the mixture was added TBAF (1.0 M in THF, 7.7 mL, 7.7 mmol) and stirred for 24 h at 23 ºC. The reaction mixture was quenched by saturated aqueous NH_4Cl (20 mL). The mixture was extracted with Et_2O (3 x 10 mL). Organic layers were combined and dried over $MgSO_4$ and concentrated under reduced pressure. The residue was purified by flash column chromatography (3:1 hexanes:EtOAc) to afford allylic alcohol **60** (1.23 g, 5.69 mmol, 90% yield) as a colorless oil; R_f = 0.10 (10:1, hexanes:EtOAc); ^1H NMR (400 MHz, C_6D_6) δ5.84–5.79 (m, 1H), 5.76–5.71 (m, 1H), 5.11–5.05 (m, 1H), 4.95–4.86 (m, 3H), 4.85–4.80 (m, 1H), 2.92–2.81 (m, 1H), 2.43–2.21 (m, 3H), 2.19–1.98 (m, 2H), 1.85–1.68 (m, 2H), 1.66–1.45 (m, 4H), 1.21 (d, *J* = 5.8 Hz, 1H); ^{13}C NMR (101 MHz, C_6D_6) δ 148.6, 146.0, 143.4, 135.1, 132.2, 131.2, 128.4, 128.3, 128.2, 128.1, 127.9, 127.8, 111.2, 111.1, 78.0, 45.0, 33.9, 32. 5, 30.3, 29.5, 20.7; IR (Neat Film, NaCl) 3774, 3659, 3078, 3042, 2935, 2852, 2112, 1644, 1442, 1373, 1311, 1166, 1047, 930, 889, 843 cm^{-1}; HRMS (FAB+) *m/z* calc'd for $C_{15}H_{19}O_3$ $[M+H-H_2]^+$: 215.1436, found 215.1441; $[\alpha]_D^{25.0}$ –16.2° (*c* 0.150, $CHCl_3$).

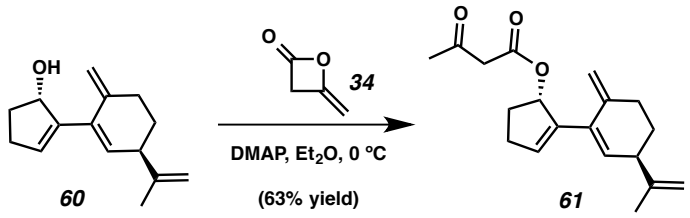

***β*-ketoester 61:** To a flame-dried round-bottom flask with a magnetic stir bar were added allylic alcohol **60** (1.23 g, 5.69 mmol), 4-dimethylaminopyridine (35 mg, 0.29 mmol) and Et_2O (20 mL). The flask was cooled to 0 ºC and stirred for 10 min. Diketene (0.5 mL, 6.48 mmol) was added dropwise. The reaction mixture was stirred 15 min at 0 ºC was then quenched by cold water (0 ºC, 10 mL). The mixture was extracted with Et_2O (3 x 15 mL). The combined organic layers were washed by brine (15 mL), dried over $MgSO_4$, and concentrated under reduced pressure. The crude oil was purified by flash column chromatography (10:1 hexanes, EtOAc) to afford *β*-ketoester **61** (1.07 g, 3.56 mmol, 63% yield) as a colorless oil; R_f = 0.40 (3:1, hexanes:Et_2O); ^{1}H NMR (400 MHz, C_6D_6) δ 6.23–6.15 (m, 1H), 5.82–5.80 (m, 1H), 5.80–5.77 (m, 1H), 5.05 (d, *J* = 2.1 Hz, 1H), 4.97–4.81 (m, 3H), 2.94 (s, 2H), 2.92–2.83 (m, 1H), 2.43–2.23 (m, 3H), 2.23–2.11 (m, 1H), 2.08–1.92 (m, 1H), 1.92–1.83 (m, 1H), 1.82–1.73 (m, 1H), 1.68 (s, 3H), 1.65 (s, 3H), 1.62–1.50 (m, 1H); ^{13}C NMR (101 MHz, C_6D_6) δ 199.0, 169.0, 166.9, 148.5, 143.2, 141.6, 134.9, 132.1, 111.2, 111.1, 81.3, 50.1, 45.0, 32.4, 31.1, 30.8, 29.54, 29.47, 20.8; IR (Neat Film, NaCl) 3629, 3078, 2935, 2855, 1727, 1644, 1440, 1360, 1315, 1238, 1149, 1029, 934, 895, 847, 802, 739 cm^{-1}; HRMS (FAB+) *m/z* calc'd for $C_{19}H_{25}O_3$ $[M+H]^+$: 301.1804, found 301.1814; $[\alpha]_D^{25.0}$ –41.8° (*c* 0.150, $CHCl_3$).

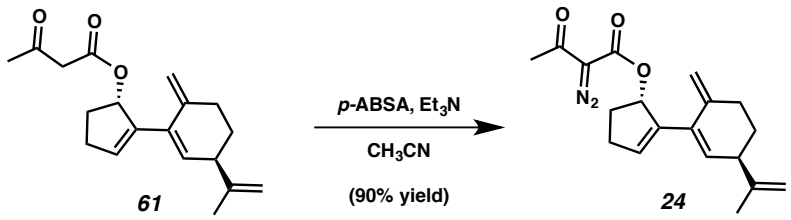

Diazo ester 24: To a round-bottom flask equipped with a magnetic stir bar were added *ß*-ketoester **61** (1.07 g, 3.56 mmol), CH_3CN (36 mL), and *p*-ABSA (1.3 g, 5.41 mmol). TEA (1.5 mL, 10.75 mmol) was added dropwise. The reaction mixture was stirred for 2 h at 23 ºC. The reaction mixture was filtered through a silica gel plug (pentanes:Et_2O 2:1) was then concentrated under reduced pressure to afford diazo ester **24** (1.04 g, 3.19 mmol, 90% yield) as a yellowish oil; R_f = 0.44 (4:1, hexanes:EtOAc); ^{1}H NMR (500 MHz, $CDCl_3$) δ 6.06–5.98 (m, 2H), 5.61 (dd, *J* = 2.9, 1.5 Hz, 1H), 4.91–4.87 (m, 2H), 4.76 (dd, *J* = 2.0, 1.4 Hz, 1H), 4.74–4.69 (m, 1H), 2.93 (ddd, *J* = 9.1, 5.4, 3.2 Hz, 1H), 2.65–2.54 (m, 1H), 2.51–2.40 (m, 6H), 2.36–2.27 (m, 1H), 2.00–1.88 (m, 2H), 1.71 (dd, *J* = 1.4, 0.8 Hz, 3H), 1.60–1.52 (m, 1H); ^{13}C NMR (126 MHz, $CDCl_3$) δ 190.5, 161.4, 148.3, 142.9, 140.8, 135.2, 134.1, 132.1, 132.1, 110.9, 110.9, 82.2, 44.6, 31.9, 31.0, 30.7, 29.1, 28.4, 20.8; IR (Neat Film, NaCl) 3794, 3417, 3301, 3078, 2932, 2855, 2617, 2486, 2391, 2301, 2210, 2135, 1953, 1713, 1659, 1441, 1361, 1307, 1247, 1151, 1063, 1025, 965, 895, 847 cm^{-1}; HRMS (FAB+) *m/z* calc'd for $C_{19}H_{23}O_3N_2$ $[M+H]^+$: 327.1709, found 327.1725; $[\alpha]_D^{25.0}$ –6.7° (*c* 0.250, $CHCl_3$).

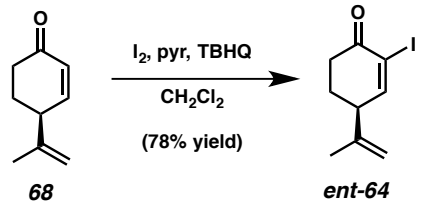

Iodide *ent*-64: To a round-bottom flask equipped with a magnetic stir bar were added ketone **68**[7] (200 mg, 1.47 mmol), DCM (35 mL), and *tert*-butylhydroquinone (5 mg, 0.03 mmol). A solution of iodine (700 mg, 2.76 mmol) in pyridine (1.5 mL, 10.75 mmol) was added. The reaction mixture was stirred for 2 h at 23 ºC. The reaction was diluted with Et_2O (20 mL) and water (20 mL) and quenched by saturated aqueous $Na_2S_2O_3$ (20 mL). The phases were separated and the aqueous phases were extracted with DCM (3 x 20 mL). The combined organic phases were dried over $MgSO_4$, filtered and concentrated under reduced pressure. The crude product was purified by flash column chromatography (15:1, hexanes:EtOAc) to afford iodide *ent*-**64** (300 mg, 1.14 mmol, 78% yield) as a yellowish oil; R_f = 0.40 (6:1, hexanes:EtOAc); ^{1}H NMR (400 MHz, C_6D_6)) δ 7.17 (d, *J* = 1.1 Hz, 1H), 4.62–4.55 (m, 1H), 4.47–4.43 (m, 1H), 2.36–2.22 (m, 2H), 1.92 (ddd, *J* = 16.2, 11.2, 4.8 Hz, 1H), 1.40–1.31 (m, 1H), 1.31–1.20 (m, 4H); ^{13}C NMR (101 MHz, C_6D_6) δ 190.5, 160.2, 144.5, 128.4, 128.3, 128.1, 127.9, 127.8, 112.8, 105.1, 47.5, 35.4, 27.7, 20.9; IR (Neat Film, NaCl) 3357, 3077, 2951, 2867, 1683, 1645, 1585, 1450, 1414, 1376, 1325, 1278, 1217, 1170, 1151, 1128, 1081, 1036, 971, 952, 89, 805, 713, 644 cm^{-1}; HRMS (FAB+) *m/z* calc'd for $C_9H_{12}OI$ $[M+H]^+$: 262.9933, found 262.9936; $[\alpha]_D^{25.0}$ –40.1° (*c* 0.44, $CHCl_3$).

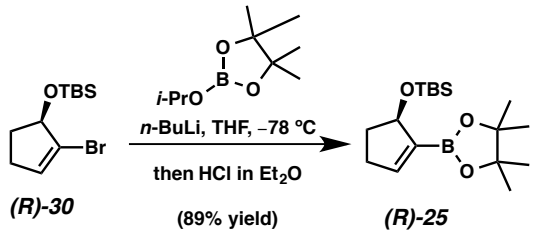

Boronate (*R*)-30: To a round-bottom flask equipped with a magnetic stir bar were added bromide (*R*)-**30** (1.04 g, 3.82 mmol) and THF (15 mL). The flask was cooled to –78 ºC and stirred for 10 min. *n*-Butyllithium solution (2.5 M in hexanes, 2.3 mL, 5.75 mmol) was added dropwise. The reaction mixture was stirred at –78 ºC for 30 min then isopropyl pinacolyl borate (1.2 mL, 5.88 mmol) was added. The reaction mixture was stirred at –78 ºC for 30 min then quenched with HCl solution (2 N in Et_2O, 2.9 mL, 5.8 mmol). Following addition, the reaction mixture was diluted with diethyl ether (15 mL) and warmed up to 23 ºC. The reaction mixture was filtered and was concentrated under reduced pressure to afford boronate (*R*)-**25** (1.1 g, 3.39 mmol, 89% yield) as a colorless oil. The characterization data matched those of **25**, racemic mixture. $[\alpha]_D^{25.0}$ 9.8° (*c* 1.35, $CHCl_3$).

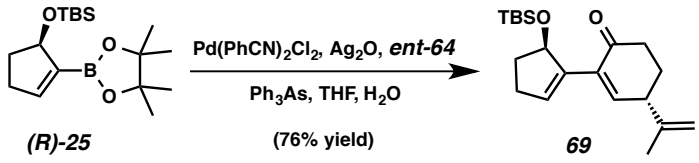

To a flame-dried round-bottom flask equipped with a magnetic stir bar were added boronate (*R*)-**25** (92 mg, 0.28 mmol), triflate *ent*-**64** (50 mg, 0.19 mmol), silver oxide (70 mg, 0.30 mmol), triphenylarsine (6 mg, 0.02 mmol). The mixture was evacuated and back filled with argon (3x). The mixture was dissolved in dioxane (25 mL) then added

water (2.5 mL). The mixture was added bis(benzonitrile)palladium chloride (4 mg, 0.01 mmol). The reaction was stirred at 23 ºC for 6 hr. The resulting mixture was filtered through celite with EtOAc and the solvent was removed under reduced pressure. The crude product was purified by flash column chromatography (20:1, hexanes:EtOAc) to afford diene **69** (48 mg, 0.144 mmol, 76% yield over *ent*-**64**) as a white solid; R_f = 0.54 (6:1, hexanes:EtOAc); ^{1}H NMR (400 MHz, C_6D_6) δ 6.72 (dd, *J* = 3.4, 1.3 Hz, 1H), 6.26–6.17 (m, 1H), 5.33–5.25 (m, 1H), 4.76–4.74 (m, 1H), 4.72–4.70 (m, 1H), 2.72 (dt, *J* = 8.5, 4.1 Hz, 1H), 2.51–2.29 (m, 2H), 2.26–1.99 (m, 3H), 1.79–1.62 (m, 2H), 1.62–1.45 (m, 4H), 0.96 (s, 9H), 0.11 (s, 3H), 0.09 (s, 3H); ^{13}C NMR (101 MHz, C_6D_6) δ 197.0, 147.9, 146.2, 143.0, 135.7, 132.4, 128.3, 128.2, 128.1, 127.9, 127.8, 112.3, 78.5, 44.4, 38.1, 34.6, 30.6, 27.9, 26.2, 21.2, 18.3, −3.9, –4.4; IR (Neat Film, NaCl) 3348, 3078, 3042, 2929, 2893, 2855, 2737, 2708, 1687, 1683, 1649, 1472, 1463, 1451, 1388, 1375, 1360, 1314, 1287, 1251, 1218, 1189, 1157, 1141, 1064, 1006, 980, 941, 868, 836, 775, 735, 677 cm^{-1}; HRMS (FAB+) *m/z* calc'd for $C_{15}H_{19}O_3N_2$ $[M+H-H_2]^+$: 331.2093, found 331.2096; $[\alpha]_D^{25.0}$ –60.8° (*c* 0.44, $CHCl_3$).

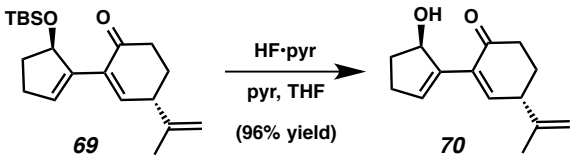

Allylic alcohol 70: To a round-bottom plastic coated flask equipped with a magnetic stir bar were added diene **69** (30 mg, 0.090 mmol), THF (4 mL), and pyridine (0.05 mL, 0.62 mmol). A solution of hydrogen fluoride pyridine (pyridine 30%, hydrogen fluoride 70%, 0.1 mL) was added dropwise. The reaction mixture was stirred for 18 h at 23 ºC.

The reaction was diluted with Et_2O (4 mL) and neutralized by saturated aqueous $NaHCO_3$ (10 mL). The phases were separated and the aqueous phases were extracted with EtOAc (3 x 10 mL). The combined organic phases were dried over $MgSO_4$, filtered and concentrated under reduced pressure. The crude product was purified by flash column chromatography (5:1, hexanes:EtOAc) to afford allylic alcohol **70** (19 mg, 0.087 mmol, 96% yield) as a colorless oil; R_f = 0.25 (2:1, hexanes:EtOAc); ^{1}H NMR (400 MHz, C_6D_6) δ 6.86–6.76 (m, 1H), 6.44–6.35 (m, 1H), 4.99–4.90 (m, 1H), 4.82–4.74 (m, 1H), 4.74–4.69 (m, 1H), 2.96 (s, 1H), 2.58 (dt, *J* = 8.7, 4.2 Hz, 1H), 2.54–2.43 (m, 1H), 2.36 (ddd, *J* = 16.3, 6.2, 4.3 Hz, 1H), 2.14–1.96 (m, 3H), 1.93–1.78 (m, 1H), 1.63–1.42 (m, 5H); ^{13}C NMR (101 MHz, C_6D_6) δ 198.9, 149.3, 146.2, 142.2, 135.2, 134.0, 112.4, 77.5, 44.3, 37.9, 34.0, 30.9, 27.8, 21.1; IR (Neat Film, NaCl) 3418, 3077, 3040, 2938, 2848, 1674, 1586, 1451, 1377, 1309, 1086, 1047, 990, 935, 895 cm^{-1}; HRMS (FAB+) *m/z* calc'd for $C_{14}H_{17}O_2$ $[M+H-H_2]^+$: 217.1229, found 217.1235; $[\alpha]_D^{25.0}$ –120.4° (*c* 0.33, $CHCl_3$).

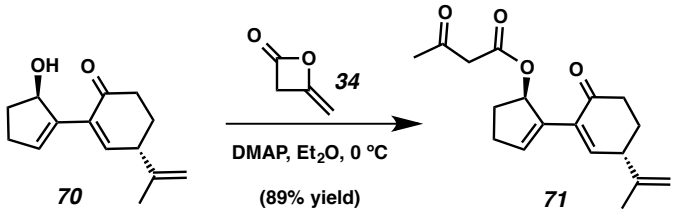

***β*-ketoester 71**: To a flame-dried round-bottom flask equipped with a magnetic stir bar were added allylic alcohol **70** (870 mg, 3.99 mmol), 4-dimethylaminopyridine (50 mg, 0.41 mmol) and Et_2O (20 mL). The flask was cooled to 0 ºC and stirred for 10 min. Diketene **34** (0.36 mL, 4.67 mmol) was added dropwise. The reaction mixture stirred for 15 min at 0 ºC was then quenched by cold water (0 ºC, 20 mL). The mixture was

extracted with Et_2O (3 x 20 mL). The combined organic layers were washed by brine (15 mL), dried over $MgSO_4$, and concentrated under reduced pressure. The crude oil was purified by flash column chromatography (4:1 hexanes, EtOAc) to afford *β*-ketoester **71** (1.07 g, 3.54 mmol, 89% yield) as a colorless oil; R_f = 0.40 (2:1, hexanes:Et_2O); ^{1}H NMR (400 MHz, CD_2Cl_2) δ 6.74–6.72 (m, 1H), 6.70–6.68 (m, 1H), 6.05 (dt, *J* = 7.5, 2.4 Hz, 1H), 4.89 (t, *J* = 1.5 Hz, 1H), 4.76–4.73 (m, 1H), 3.40–3.33 (m, 2H), 3.15 (dt, *J* = 8.7, 4.4 Hz, 1H), 2.65–2.27 (m, 5H), 2.18 (s, 3H), 2.17–2.09 (m, 1H), 1.98–1.81 (m, 2H), 1.79 (t, *J* = 1.2 Hz, 3H); ^{13}C NMR (101 MHz, CD_2Cl_2) δ 200.7, 198.5, 167.3, 148.8, 146.5, 138.1, 136.2, 133.1, 112.3, 81.4, 50.6, 44.4, 38.1, 31.7, 30.8, 30.3, 28.0, 21.4; IR (Neat Film, NaCl) 3655, 3643, 3080, 2943, 2850, 1726, 1640, 1554, 1450, 1356, 1315, 1256, 1146, 1088, 1029, 995, 900, 854, 778, 706, 634, 617 cm^{-1}; HRMS (FAB+) *m/z* calc'd for $C_{18}H_{23}O_4$ $[M+H]^+$: 303.1596, found 303.1594; $[\alpha]_D^{25.0}$ –30.6° (*c* 0.13, $CHCl_3$). Enol ether form of *β*-ketoester **71** was existed in CD_2Cl_2.

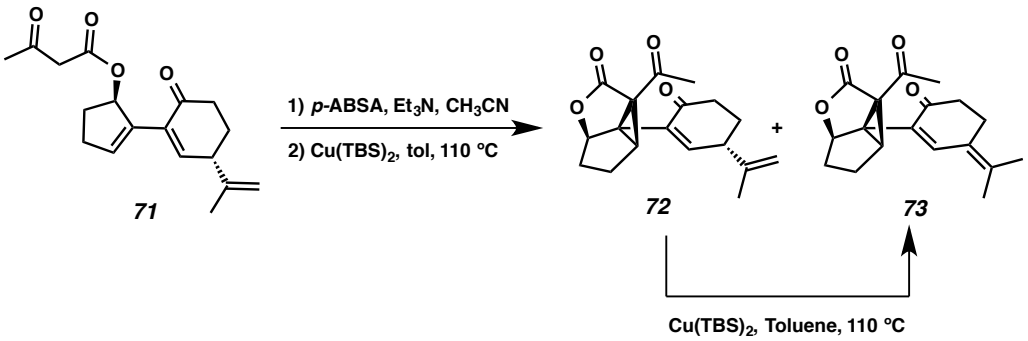

Cyclopropane 72: To a round-bottom flask equipped with a magnetic stir bar were added *β*-ketoester **71** (95 mg, 0.314mmol), CH_3CN (3 mL), and *p*-ABSA (113 mg, 0.47 mmol). TEA (0.1 mL, 0.717 mmol) was added dropwise. The reaction mixture was remained to stir 2 h at 23 ºC. The reaction mixture was filtered through a Florisil (2:1,

pentanes:Et_2O) was then concentrated under reduced pressure. The residue was used in the next reaction without further purification.

To a flame-dried two neck round-bottom flask equipped with a magnetic stir bar was added copper catalyst (8 mg, 0.019 mmol) in a nitrogen-filled glove box. The flask was sealed with rubber septums and removed from the glove box. One of the rubber septum was replaced with a reflux condenser connected to a nitrogen inlet. A solution of diazo ester from the previous step (60mg, 0.198 mmol) in toluene (40 mL) was added. The reaction was heated to reflux in a 110 ºC oil bath. After 3 h of stirring, the reaction mixture was cooled to 23 ºC and stirred for 15 min. The mixture was concentrated and purified by flash column chromatography (10:1 hexanes, EtOAc) to afford cyclopropane **72** (10 mg, 0.033 mmol, 17% yield) as a colorless oil; R_f = 0.40 (2:1 hexanes:EtOAc); ^{1}H NMR (400 MHz, $CDCl_3$) δ 6.79 (dd, *J* = 3.2, 1.1 Hz, 1H), 4.96–4.89 (m, 1H), 4.75–4.73 (m, 1H), 4.73–4.71 (m, 1H), 3.13 (dt, *J* = 8.3, 4.2 Hz, 1H), 2.96 (dd, *J* = 6.5, 1.0 Hz, 1H), 2.56 (ddd, *J* = 16.8, 6.5, 4.4 Hz, 1H), 2.44 (s, 3H), 2.40–2.26 (m, 2H), 2.21–2.00 (m, 2H), 2.00–1.78 (m, 6H); ^{13}C NMR (101 MHz, $CDCl_3$) δ 198.5, 198.2, 172.3, 153.8, 145.2, 131.7, 112.9, 85.7, 77.2, 59.2, 50.7, 43.7, 38.9, 38.6, 36.5, 29.9, 27.7, 23.9, 21.7; IR (Neat Film, NaCl) 3371, 3077, 2939, 1760, 182, 1651, 1488, 1439, 1362, 1339, 1309, 1242, 1223, 1190, 1160, 1136, 1085, 1067, 1006, 957, 912, 850, 817, 727, 703, 622, 612 cm^{-1}; HRMS (MM+) *m/z* calc'd for $C_{15}H_{19}O_3$ $[M+H]^+$: 301.1440, found 301.1450; $[\alpha]_D^{25.0}$ – 56.8° (*c* 0.30, $CHCl_3$), and side product **73** (15 mg, 0.050 mmol, 25% yield) as a colorless oil; R_f = 0.05 (2:1 hexanes:EtOAc); ^{1}H NMR (400 MHz, $CDCl_3$) δ 7.32 (s, 1H), 4.75 (dd, *J* = 2.0, 1.1 Hz, 1H), 3.03 (dt, *J* = 6.5, 1.1 Hz, 1H), 2.75–2.60 (m, 2H), 2.54–2.35 (m, 6H), 2.10–2.01 (m, 1H), 2.01–1.96 (m, 3H), 1.96–1.84 (m, 5H); ^{13}C NMR (101 MHz,

$CDCl_3$) δ 198.6, 198.2, 172.5, 144.5, 142.3, 126.3, 126.1, 85.8, 77.2, 60.1, 51.5, 38.5, 38.4, 37.1, 29.8, 25.6, 23.9, 22.2, 21.3; IR (Neat Film, NaCl) 3484, 3369, 3051, 2928, 2853, 2435, 2305, 2143, 1755, 1679, 1615, 1434, 1361, 1348, 1311, 1297, 1257, 1242, 1216, 1199, 1164, 1131, 1090, 1064, 1037, 1004, 966, 918, 888, 851, 822, 798, 753, 719, 667, 655, 633, 614 cm^{-1}; HRMS(FAB+) *m/z* calc'd for $C_{18}H_{21}O_4$ $[M+H]^+$: 301.1440, found 301.1434; $[\alpha]_D^{25.0}$ 53.1° (*c* 0.10, $CHCl_3$)

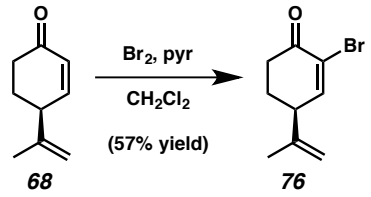

Bromide 76: To a flame-dried round-bottom flask equipped with a magnetic stir bar were added ketone **68** (553 mg, 4.06 mmol) and DCM (35 mL). The flask was cooled to 0 ºC and stirred for 10 min. A solution of bromine (0.24 mL, 4.66 mmol) in DCM (5 mL) was added dropwise with vigorous stirring at 0 ºC. After reaction became a reddish-brown color, TEA (0.6 mL, 4.30 mmol) was added at 0 ºC. The cooling bath was removed and the flask was allowed to warm to 23 ºC. After 30 min of stirring, the reaction was washed with water (40 mL). The aqueous phase was extracted with DCM (3 x 40 mL). The combined organic phases were dried over $MgSO_4$, filtered and concentrated under reduced pressure. The crude product was purified by flash column chromatography (20:1 hexanes, EtOAc) to afford bromide **76** as a colorless oil (500 mg, 2.32 mmol, 57% yield); R_f = 0.45 (6:1 hexanes:EtOAc); ^{1}H NMR (500 MHz, $CDCl_3$) δ 7.29 (dd, *J* = 3.6, 0.9 Hz, 1H), 4.96–4.88 (m, 1H), 4.87–4.72 (m, 1H), 3.19–3.08 (m, 1H), 2.70 (ddd, *J* = 16.6, 7.0, 4.3 Hz, 1H), 2.51 (ddd, *J* = 16.6, 10.7, 4.5 Hz, 1H), 2.19 (ddtd, *J*

= 12.8, 7.0, 4.7, 1.0 Hz, 1H), 1.99 (dddd, *J* = 13.5, 10.7, 8.2, 4.4 Hz, 1H), 1.79 (dd, *J* = 1.1 Hz, 3H); ^{13}C NMR (126 MHz, $CDCl_3$) δ 191.2, 153.1, 144.2, 124.0, 113.4, 46.1, 36.5, 27.6, 21.4.; IR (Neat Film, NaCl) 3853, 3650, 3371, 3035, 2953, 2869, 2360, 1694, 1646, 1595, 1451, 1417, 1377, 1327, 1278, 1218, 1172, 1153, 1132, 1085, 1037, 984, 958, 899, 816, 798, 786, 749, 716, 668, 650, 611 cm^{-1}; HRMS (FAB+) *m/z* calc'd for $C_9H_{12}OBr$ $[M+H]^+$: 215.0072, found 215.0071; $[\alpha]_D^{25.0}$ 52.9° (*c* 0.30, $CHCl_3$).

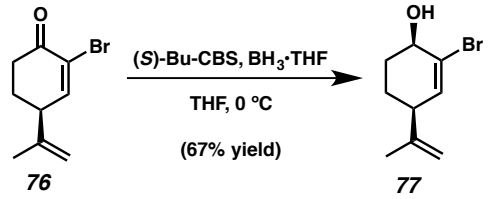

Alcohol 77: To a flame-dried round-bottom flask equipped with a magnetic stir bar were added bromide **76** (76 mg, 0.353 mmol) and THF (4 mL). The flask was cooled to 0 ºC and stirred for 10 min. A solution of (*S*)-(–)-2-Butyl-CBS-oxazaborolidine (0.04 mL, 1 M in toluene, 0.004 mmol) was added. A solution of BH3•THF (0.4 mL, 1 M in THF, 0.4 mmol) was added dropwise by syringe pump over 2 h at 0 ºC. The cooling bath was removed and the flask was allowed to warm to 23 ºC. After 2 h of stirring, methanol (0.4 mL) and the reaction was stirred for 10 min. 2 M aqueous HCl (5 mL) was added and the reaction mixture was stirred for 10 min. The phases were separated and the aqueous phase was extracted with Et_2O (3 x 5 mL). The combined organic phases were dried over $MgSO_4$, filtered, and concentrated under reduced pressure. The crude product was purified by flash column chromatography (20:1 hexanes, EtOAc) to afford alcohol **77** as a white solid (51 mg, 0.235 mmol, 67% yield); R_f = 0.45 (6:1 hexanes:EtOAc); ^{1}H NMR (500 MHz, $CDCl_3$) δ 6.12 (dd, *J* = 3.0, 0.6 Hz, 1H), 4.85–4.80 (m, 1H), 4.76 (dt, *J*

= 1.7, 0.8 Hz, 1H), 4.19 (ddd, *J* = 5.0, 4.0, 1.3 Hz, 1H), 2.76 (dddd, *J* = 7.2, 4.2, 2.9, 1.5 Hz, 1H), 2.25 (s, 1H), 1.99 (ddt, *J* = 13.4, 6.2, 3.5 Hz, 1H), 1.90–1.82 (m, 1H), 1.78–1.70 (m, 5H), 1.65 (dddd, *J* = 13.4, 11.8, 8.8, 3.1 Hz, 1H); ^{13}C NMR (126 MHz, $CDCl_3$) δ 146.6, 135.5, 126.2, 111.9, 69.9, 46.4, 30.7, 22.6, 21.0; IR (Neat Film, NaCl) 3392, 3077, 2943, 2864, 2361, 1648, 1437, 1375, 1260, 1198, 1165, 1121, 1050, 1018, 976, 955, 893, 800, 759 cm^{-1}; HRMS (FAB+) *m/z* calc'd for $C_9H_{12}OBr$ $[M+H-H_2]^+$: 215.0072, found, 215.0078; $[\alpha]_D^{25.0}$ 2.0° (*c* 0.10, $CHCl_3$).

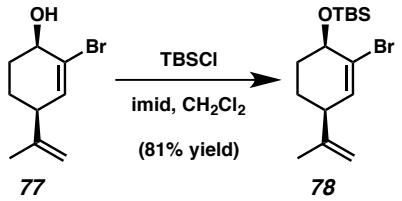

TBS protected alcohol 78: To a round-bottom flask equipped with a magnetic stir bar were added alcohol **77** (84 mg, 0.387 mmol), DCM (10 mL), imidazole (60 mg, 0.881 mmol) and TBSCl (100 mg, 0.663 mmol). The reaction mixture stirred for 9 h at 23 ºC. The reaction was washed with water (10 mL). The aqueous phase were extracted with DCM (3 x 10 mL). The combined organic phases were dried over $MgSO_4$, filtered and concentrated under reduced pressure. The crude product was purified by flash column chromatography (20:1 hexanes, EtOAc) to afford bromide **78** as a colorless oil (100 mg, 0.302mmol, 81% yield); R_f = 0.90 (6:1 hexanes:EtOAc); ^{1}H NMR (500 MHz, $CDCl_3$) δ 6.03 (dd, *J* = 2.9, 0.8 Hz, 1H), 4.81–4.75 (m, 2H), 4.18 (td, *J* = 3.7, 1.2 Hz, 1H), 2.79–2.70 (m, 1H), 1.88–1.83 (m, 1H), 1.79–1.73 (m, 1H), 1.73–1.71 (m, 4H), 1.68–1.62 (m, 1H), 0.91 (s, 9H), 0.16 (s, 3H), 0.10 (s, 3H); ^{13}C NMR (126 MHz, $CDCl_3$) δ 147.1, 134.5,

126.3, 111.5, 70.6, 46.7, 32.7, 26.0, 22.2, 20.6, 18.3, –4.3, –4.5; IR (Neat Film, NaCl) 3077, 2950, 2929, 2885, 2856, 2738, 2709, 2360, 1918, 1793, 2738, 2709, 2360, 1918, 1793, 1684, 1648, 1472, 1462, 1448, 1436, 1407, 1388, 1375, 1361, 1300, 1280, 1251, 1219, 1194, 1171, 1126, 1084, 1064, 1025, 1006, 987, 960, 939, 914, 894, 880, 834, 814, 775, 729, 669, 639 cm^{-1}; HRMS (MM+) *m/z* calc'd for $C_{15}H_{19}O_3$ $[M+H-H_2]^+$: 331.0916, found 331.0902; $[\alpha]_D^{25.0}$ –22.6° (*c* 0.30, $CHCl_3$).

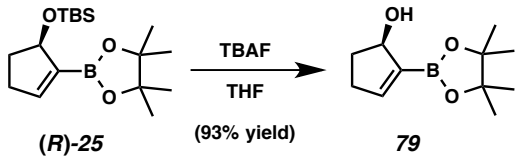

(*R*)-*25* *79*

Allylic alcohol 79: To a round-bottom plastic coated flask equipped with a magnetic stir bar were added vinylboronate (*R*)-***25*** (1 g, 3.08 mmol), and THF (30 mL). A solution of TBAF (1M in THF, 8 mL, 8 mmol) was added. The reaction mixture was stirred for 24 h at 23 ºC. The reaction was diluted with Et_2O (30 mL) and washed with saturated aqueous NH_4Cl (30 mL). The phases were separated and the aqueous phases were extracted with EtOAc (3 x 30 mL). The combined organic phases were dried over $MgSO_4$, filtered and concentrated under reduced pressure. The crude product was purified by flash column chromatography (4:1, hexanes:EtOAc) to afford allylic alcohol **79** (600 mg, 2.86 mmol, 93% yield) as a white solid; R_f = 0.10 (6:1, hexanes:EtOAc); ^1H NMR (400 MHz, $CDCl_3$) δ 6.70–6.63 (m, 1H), 5.05–4.95 (m, 1H), 2.64–2.51 (m, 1H), 2.41–2.18 (m, 2H), 1.71 (dddd, *J* = 13.7, 9.1, 5.5, 4.5 Hz, 1H), 1.28 (s, 12H); ^{13}C NMR (126 MHz, $CDCl_3$) δ 150.1, 83.6, 79.8, 33.2, 33.0, 26.0, 25.0; IR (Neat Film, NaCl) 3478, 3038, 2978, 2931, 2731, 2219, 1995, 1887, 1622, 1615, 1372, 1214, 1144, 1111, 1046,

1020, 964, 925, 854, 832, 759, 710 cm^{-1}; HRMS (FAB+) *m/z* calc'd for $C_{15}H_{19}O_3N_2$ $[M+H–H_2]^-$: 209.1349, found 209.1344; $[\alpha]_D^{25.0}$ –59.6° (*c* 0.80, $CHCl_3$).

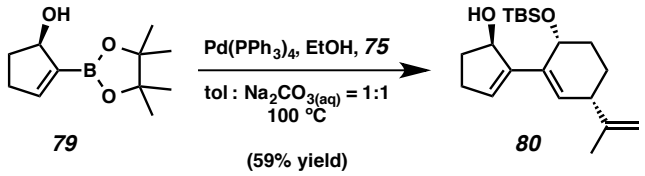

Diene 80: To a two neck round-bottom flask equipped with reflux condenser and a magnetic stir bar were added boronate **79** (200 mg, 0.952 mmol), and bromide **78** (200 mg, 0.605 mmol). The mixture was evacuated and back filled with argon (3x). Toluene (6 mL), ethanol (1.2 mL) tetrakis(triphenylphosphine)palladium(0) (21 mg, 0.018 mmol), and 2 M aqueous Na_2CO_3 (6 mL) were added. The reaction was heated to reflux in a 110 ºC oil bath. After 12 h of stirring, the reaction mixture was cooled to 23 ºC and stirred for 15 min. The phases were separated and the aqueous phases were extracted with EtOAc (3 x 10 mL). The combined organic phases were washed with brine (10 mL), dried over $MgSO_4$, filtered and concentrated under reduced pressure. The crude product was purified by flash column chromatography (20:1, hexanes:EtOAc) to afford diene **80** (120 mg, 0.359 mmol, 59.3% yield) as a colorless oil; R_f = 0.40 (6:1, hexanes:EtOAc); ^1H NMR (500 MHz, $CDCl_3$) δ 5.85–5.81 (m, 2H), 4.95 (dt, *J* = 7.2, 2.5 Hz, 1H), 4.80–4.78 (m, 1H), 4.77 (dd, *J* = 2.0, 1.4 Hz, 1H), 4.43 (ddd, *J* = 3.6, 2.8, 1.3 Hz, 1H), 2.85–2.78 (m, 1H), 2.62–2.50 (m, 1H), 2.38–2.28 (m, 1H), 2.26–2.16 (m, 1H), 1.93–1.80 (m, 2H), 1.80–1.74 (m, 1H), 1.72 (dd, *J* = 1.5, 0.8 Hz, 3H), 1.68–1.58 (m, 2H), 0.85 (s, 9H), 0.09 (s, 3H), 0.05 (s, 3H); ^{13}C NMR (126 MHz, $CDCl_3$) δ 149.0, 145.1, 135.0, 130.7, 128.7, 110.9, 76.8, 65.1, 44.9, 33.7, 31.8, 30.7, 26.0, 22.4, 20.5, 18.3, –3.9, –4.2; IR (Neat Film,

NaCl) 3601, 3412, 3072, 2929, 2855, 2737, 2708, 1924, 1647, 1472, 1463, 1436, 1407, 1389, 1375, 1360, 1334, 1305, 1252, 1218, 1024, 959, 934, 889, 835, 773, 723, 676 cm^{-1}; HRMS (MM+) *m/z* calc'd for $C_{20}H_{34}O_2NSiNa$ $[M+Na]^+$: 356.2220, found 357.2237; $[\alpha]_D^{25.0}$ –21.1° (*c* 0.10, $CHCl_3$).

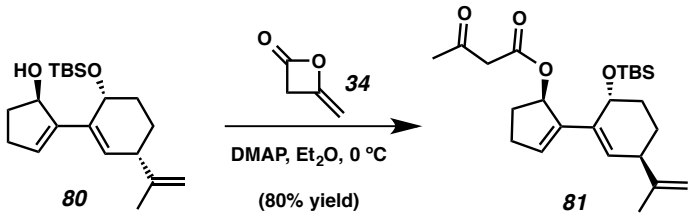

***β*-ketoester 81**: To a two neck round-bottom flask with a magnetic stir bar and were added allylic alcohol **80** (20 mg, 0.060 mmol), 4-dimethylaminopyridine (1 mg, 0.0082 mmol) and Et_2O (1.5 mL). The flask was cooled to 0 ºC and stirred for 10 min. Diketene (0.07 mL, 0.907 mmol) was added dropwise. The reaction mixture was stirred for 15 min at 0 ºC was then quenched by cold water (0 ºC, 2 mL). The mixture was extracted with Et_2O (3 x 3 mL). The combined organic layers were washed by brine (3 mL), dried over $MgSO_4$, and concentrated under reduced pressure. The crude oil was purified by flash column chromatography (4:1 hexanes, EtOAc) to afford *β*-ketoester **81** (20 mg, 0.048 mmol, 80% yield) as a colorless oil; R_f = 0.45 (6:1, hexanes:Et_2O); ^1H NMR (500 MHz, $CDCl_3$) δ 6.18–5.98 (m, 2H), 5.62 (d, *J* = 2.8 Hz, 1H), 4.85–4.67 (m, 2H), 4.44 (t, *J* = 3.2 Hz, 1H), 3.36 (s, 2H), 2.77 (t, *J* = 8.6 Hz, 1H), 2.62–2.53 (m, 1H), 2.44–2.27 (m, 2H), 2.22 (s, 3H), 1.96–1.83 (m, 2H), 1.79–1.72 (m, 1H), 1.73–1.54 (m, 5H), 0.84 (s, 9H), 0.08 (s, 3H), 0.05 (s, 3H); ^{13}C NMR (126 MHz, $CDCl_3$) δ 200.8, 167.3, 148.8, 140.9, 134.4, 131.8, 130.4, 110.6, 79.8, 64.7, 50.4, 44.7, 31.7, 31.1, 30.8, 30.3, 25.9, 22.3, 20.4,

18.2, –3.8, –4.4; IR (Neat Film, NaCl) 2976, 2926, 2854, 1876, 1659, 1612, 1584, 1512, 1464, 1410, 1388, 1379, 1370, 1315, 1246, 1175, 1166, 1145, 1113, 1039, 967, 862, 819, 750, 688, 671 cm^{-1}; HRMS (MM+) *m/z* calc'd for $C_{24}H_{38}O_4SiNa$ $[M+Na]^+$: 441.2432, found 441.2441; $[\alpha]_D^{25.0}$ 4.4° (*c* 0.34, $CHCl_3$).

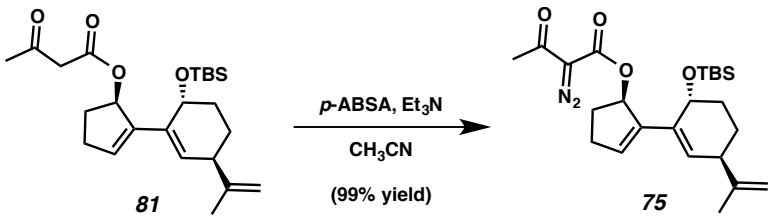

Diazo ester 75: To a round-bottom flask equipped with a magnetic stir bar were added *β*-ketoester **81** (20 mg, 0.048 mmol), CH_3CN (2.5 mL), and *p*-ABSA (40 mg, 0.167 mmol). TEA (0.03 mL, 0.215 mmol) was added dropwise. The reaction mixture was stirred for 1 h min at 23 ºC. The reaction mixture was filtered through a silica gel plug (pentanes:Et_2O 4:1) was then concentrated under reduced pressure to afford diazo ester **75** (21 mg, 0.047 mmol, 99% yield) as a yellowish oil; R_f = 0.44 (4:1, hexanes:EtOAc); ^1H NMR (500 MHz, $CDCl_3$) δ 6.08 (dt, J = 1.66 Hz, 1.66 Hz, 7.75 Hz, 1H; ^{13}C NMR (126 MHz, $CDCl_3$) δ 190.47; IR (Neat Film, NaCl) 3408, 3073, 2929, 2855, 2362, 2139, 1713, 1661, 1652, 1472, 1464, 1366, 1312, 1250, 1195, 1150, 1086, 1064, 1025, 1006, 963, 938, 921, 895, 850, 834, 808, 773, 742, 676, 635 cm^{-1}; HRMS (MM+) *m/z* calc'd for $C_{24}H_{36}O_4N_2SiNa$ $[M+Na]^+$: 467.2337, found 467.2354; $[\alpha]_D^{25.0}$ –11.4° (*c* 0.31, $CHCl_3$).

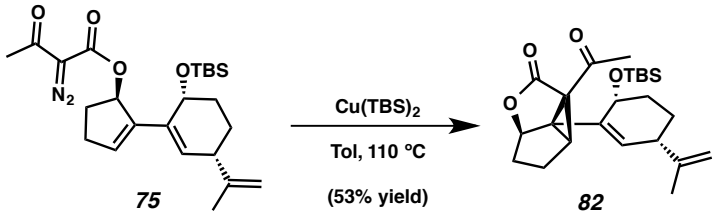

Cyclopropane 82: To a flame-dried two neck round-bottom flask equipped with a magnetic stir bar was added copper catalyst (3 mg, 0.0072 mmol) in a nitrogen-filled glove box. The flask was sealed with rubber septums and removed from the glove box. One of the rubber septum was replaced with a reflux condenser connected to a nitrogen inlet. A solution of diazo ester **75** (20 mg, 0.045 mmol) in toluene (15 mL) was added. The reaction was heated to reflux in a 110 ºC oil bath. After 3 h of stirring, the reaction mixture was cooled to 23 ºC and stirred for 15 min. The mixture was concentrated and purified by flash column chromatography (10:1 hexanes, EtOAc) to afford cyclopropane **82** (10 mg, 0.024 mmol, 53% yield) as a white solid; R_f = 0.40 (6:1 hexanes:EtOAc); ^{1}H NMR (500 MHz, $CDCl_3$) δ 5.69 (d, J = 3.0 Hz, 1H), 5.09–5.00 (m, 1H), 4.81 (t, *J* = 1.7 Hz, 1H), 4.75–4.67 (m, 1H), 3.84–3.74 (m, 1H), 2.96 (dt, *J* = 6.3, 1.1 Hz, 1H), 2.76 (d, *J* = 7.6 Hz, 1H), 2.55 (s, 3H), 2.36–2.26 (m, 1H), 2.02 (dd, *J* = 13.0, 5.8 Hz, 1H), 1.96–1.85 (m, 1H), 1.82–1.70 (m, 5H), 1.69–1.52 (m, 3H), 0.90 (s, 9H), 0.09 (s, 6H); ^{13}C NMR (126 MHz, $CDCl_3$) δ198.4, 172.7, 147.7, 136.2, 132.9, 111.5, 86.4, 68.9, 65.1, 50.6, 43.7, 42.7, 38.3, 31.0, 30.4, 26.1, 23.9, 22.8, 21.0, 18.1, –3.8, –4.3; IR (Neat Film, NaCl) 2930, 2857, 1760, 1964, 1436, 1360, 1346, 1312, 1259, 1157, 1084, 1055, 1027, 1005, 983, 935, 896, 863, 832, 802, 774 cm^{-1}; HRMS (EI+) *m/z* calc'd for $C_{24}H_{36}O_4Si$ $[M\bullet]^+$: 416.2383, found, 416.2379; $[\alpha]_D^{25.0}$ –68.1° (*c* 0.10, $CHCl_3$).

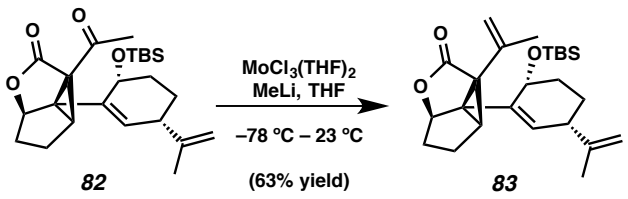

82 ***83***

Vinyl lactone 83: To a flame-dried round-bottom flask equipped with a magnetic stir bar was added trichlorobis(THF) molybdenum (III) (750 mg, 2.08 mmol) in a nitrogen-filled glove box. The flask was sealed with a rubber septum, removed from the glove box and connected to a nitrogen inlet. THF (3 mL) was added to the flask to generate a bright green solution. The flask was cooled to –78 ºC and stirred for 10 min. A solution of methyllithium (1.6 M in Et_2O, 1.2 mL, 1.92 mmol) was added dropwise to the reaction transforming the reaction mixture to a dark red solution. After 1 h of stirring at –78 ºC, a solution of cyclopropane **82** (48 mg, 0.115 mmol) in THF (1 mL) was added dropwise. The reaction was slowly warm up to ambient temperature and remained to stir for 6 h. The reaction was quenched by water (4 mL). The phases were separated and the aqueous phase was extracted with Et_2O (3 x 4 mL). The combined organic phases were dried over $MgSO_4$, filtered, and concentrated under reduced pressure. The residue was purified by flash column chromatography (15:1 hexanes, EtOAc) to afford vinyl lactone **83** (30 mg, 0.0723 mmol, 63% yield) as a colorless oil; R_f = 0.50 (6:1 hexanes:EtOAc); ^{1}H NMR (500 MHz, $CDCl_3$) δ 5.51 (dd, *J* = 2.8, 0.9 Hz, 1H), 5.18–5.15 (m, 1H), 5.12–5.07 (m, 1H), 5.00–4.96 (m, 1H), 4.79 (dd, *J* = 2.0, 1.4 Hz, 1H), 4.73 (dt, *J* = 2.0, 0.9 Hz, 1H), 4.23–4.20 (m, 1H), 2.70 (ddd, *J* = 9.1, 5.9, 2.7 Hz, 1H), 2.44 (dt, *J* = 6.7, 1.3 Hz, 1H), 2.27–2.16 (m, 1H), 2.08–1.97 (m, 1H), 1.93–1.81 (m, 2H), 1.78–1.66 (m, 8H), 1.64–1.58 (m, 1H), 1.55–1.48 (m, 1H), 0.90 (s, 9H), 0.12 (s, 3H), 0.11 (s, 3H); ^{13}C NMR (126 MHz, $CDCl_3$) δ 174.9, 148.2, 136.5, 133.6, 133.5, 117.0, 111.2, 85.8, 67.5, 58.6, 49.1, 44.3,

38.9, 34.7, 31.5, 26.1, 23.5, 22.4, 22.3, 20.5, 18.1, –3.6, –4.4; IR (Neat Film, NaCl) 2953, 2857, 1766, 1645, 1463, 1343, 1254, 1197, 1159, 1079, 1057, 1024, 891, 864, 833, 775, 673 cm^{-1}; HRMS (MM+) *m/z* calc'd for $C_{25}H_{39}O_3Si$ $[M+H]^+$: 415.2663, found, 415.2697; $[\alpha]_D^{25.0}$ –35.4° (*c* 0.10, $CHCl_3$).

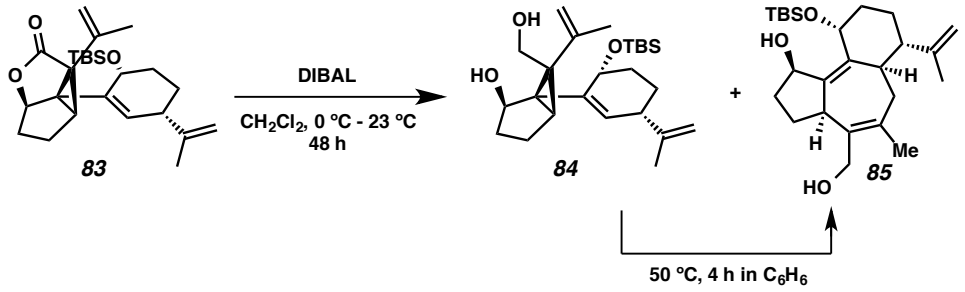

Diol 85: To a flame-dried round-bottom flask equipped with a magnetic stir bar were added vinyl lactone **83** (29 mg, 0.0699 mmol) and DCM (14 mL). The flask was cooled to 0 ºC and stirred for 10 min. A solution of DIBAL (1 M in DCM, 0.35 mL, 0.35 mmol) was added dropwise. The reaction mixture was slowly warmed up to 23 ºC and remained to stir for 24 h. The reaction was quenched by methanol (0.35 mL). Saturated aqueous potassium sodium tartarate solution (3 mL) was added to the mixture. The phases were separated and the aqueous phases were extracted with DCM (5 x 10 mL). The combined organic phases were dried over $MgSO_4$, filtered, and transferred to round-bottom flask. The mixture was concentrated under reduced pressure and dissolved in benzene. The flask was immersed in a 50 ºC oil bath. After 4 h of stirring, the reaction was cooled to ambient temperature and concentrated under reduced pressure. The residue was purified by flash column chromatography (1:1, hexanes:EtOAc) to afford diol **85** as a white solid (9 mg, 0.215 mmol, 31% yield); R_f = 0.08 (3:1 hexanes:EtOAc); ^{1}H NMR (600 MHz,

C_6D_6) 5.00 (dd, *J* = 4.1, 1.9 Hz, 1H), 4.92–4.89 (m, 1H), 4.87 (d, *J* = 2.2 Hz, 1H), 4.83 (d, *J* = 4.2 Hz, 1H), 4.16 (d, *J* = 11.3 Hz, 1H), 3.91 (d, *J* = 11.3 Hz, 1H), 3.56–3.49 (m, 1H), 3.06–3.00 (m, 1H), 2.85 (dd, *J* = 13.8, 4.5 Hz, 1H), 2.38 (dtd, *J* = 13.7, 11.8, 6.1 Hz, 1H), 2.28–2.13 (m, 2H), 2.04 (dd, *J* = 14.7, 11.4 Hz, 1H), 1.92–1.84 (m, 2H), 1.81 (d, *J* = 1.7 Hz, 3H), 1.77 (d, *J* = 1.2 Hz, 3H), 1.76–1.70 (m, 1H), 1.54 (tdd, *J* = 13.0, 4.3, 2.0 Hz, 1H), 1.51–1.37 (m, 2H), 1.01 (s, 9H), 0.08 (s, 3H), 0.08 (s, 3H); δ ^{13}C NMR (101 MHz, DMSO-*d6*) 148.5, 140.1, 138.8, 137.8, 132.4, 111.9, 71. 3, 68.8, 57.9, 49.1, 42.1, 34.4, 34.0, 33.8, 29.3, 26.7, 26.6, 25.8, 25.7, 21.5, 17.7, –4.5, –4.7; IR (Neat Film, NaCl) 3342, 2929, 2856, 1645, 1451, 1254, 1163, 1079, 1033, 890, 836, 773, 739, 702 cm^{-1}; HRMS (FAB+) *m/z* calc'd for $C_{25}H_{41}O_3Si$ $[M+H-H_2]^+$: 417.2825, found 417.2833; $[\alpha]_D^{25.0}$ –27.6° (*c* 0.10, CH_3OH).

1.7 NOTES AND REFERENCES

(1) (a) Bernauer, K.; Englert, G.; Vetter, W. *Experientia* **1965**, *21*, 374–375. (b) Bernauer, K.; Englert, G.; Vetter, W.; Weiss, E. *Helv. Chim. Acta*. **1969**, *52*, 1886–1905. (c) Cannon, J. R.; Croft, K. D.; Matsuki, Y.; Patrick, V. A.; Toia, R. F.; White, A. H. *Aust. J. Chem*. **1982**, *35*, 1655–1664. (d) Openshaw, K. *Biomass Bioenergy* **2000**, *19*, 1-15. (e) Szabó, L. F. *ARKIVOC* **2007**, 280–290. (f) Fairless, D. *Nature* **2007**, *449*, 652.

(2) (a) Naengchomnong, W.; Thebtaranonth, Y.; Wiriyachitra, P.; Okamoto, K. T.; Clardy, J. *Tetrahedron Lett*. **1986**, *27*, 2439–2442. (b) Chianese, G.; Fattorusso, E.; Aiyelaagbe, O. O.; Luciano, P.; Schröder, H. C.; Müller, W. E. G.; Taglialatela-Scafati, O. *Org. Lett*. **2011**, *13*, 316–319. (c) Liu, J.-Q.; Yang, Y.-F.; Li, X.-Y.; Liu, E.-Q.; Li, Z.-R.; Zhou, L.; Li, Y.; Qiu, M.-H. *Phytochemistry* **2013**, *96*, 265–272.

(3) (a) Naengchomnong, W.; Thebtaranonth, Y.; Wiriyachitra, P.; Okamoto, K. T.; Clardy, J. *Tetrahedron Lett*. **1986**, *27*, 5675–5678. (b) Kimbu, S. F.; Keumedjio, F.; Sondengam, L. B.; Connolly, J. D. *Phytochemistry* **1991**, *30*, 619–621. (c) Naengchomnong, W. T., B.; Thebtaranonth, Y. *J. Sci. Soc. Thailand* **1994**, *20*, 73–83. (d) Haas, W.; Sterk, H.; Mittelbach, M. *J. Nat. Prod*. **2002**, *65*, 1434–1440. (e) Ravindranath, N.; Ramesh, C.; Das, B. *Biochem. Syst. and Ecol*. **2003**, *31*, 431–432. (f) Ravindranath, N.; Ravinder Reddy, M.; Mahender, G.; Ramu, R.; Ravi Kumar, K.; Das, B. *Phytochemistry* **2004**, *65*, 2387–2390. (g) Ravindranath, N. R., M. R.; Ramesh, C.; Ramu, R.; Prabhakar, A.; Jagadeesh, B.; Das, B. *Chem. Pharm. Bull*. **2004**, *52*, 608–611. (h) Jing, L. F., Y.; Ying, X.; Wenxing, H.; Meng, X.; Syed, M. N.; Mang, C. *J. Appl. Entomol*. **2005**, *129*, 98–104. (i) Goel, G. M., H. P. S.; Francis, G.; Becker, K. *Int. J. Toxicol*. **2007**, *26*,

279–288. (j) Wang, X.-C.; Zheng, Z.-P.; Gan, X.-W.; Hu, L.-H. *Org. Lett.* **2009**, *11*, 5522–5524. (k) Devappa, R.; Maes, J.; Makkar, H.; De Greyt, W.; Becker, K. *J. Am. Oil Chem. Soc.* **2010**, *87*, 697–704. (l) Devappa, R. K. M., H. P. S.; Becker, K. *J. Toxicol. Environ. Health* **2010**, *13*, 476–507. (m) Li, C.-Y.; Devappa, R. K.; Liu, J.-X.; Lv, J.-M.; Makkar, H. P. S.; Becker, K. *Food Chem. Toxicol.* **2010**, *48*, 620–625. (n) Zhang, X.-Q.; Li, F.; Zhao, Z.-G.; Liu, X.-L.; Tang, Y.-X.; Wang, M.-K. *Phytochemistry Lett.* **2012**, *5*, 721–724. Review: Devappa, R.; Makkar, H.; Becker, K. *J. Am. Oil Chem. Soc.* **2011**, *88*, 301-322.

(4) (a) Picha, P. N., W.; Promratanapongse, P.; Kano, E.; Hayashi, S.; Ohtsubo,; T.; Zhang, S. W. S., H.; Kitai, R. *J. Exp. Clin. Cancer Res.* **1996**, *15*, 177–183. (b) Muangman, S. T., M.; Tohtong, R. *In Vivo* **2005**, *19*, 265–268. (c) Aiyelaagbe, O. O. H., A. A.; Fattorusso, E.; Taglialatela-Scafati, O.; Schroder, H. C.; Muller, W. E. G. *Evid-Based Compl. Alt.* **2011**, *Article ID 134954*, 7 pages. (d) Achenbach, H.; Benirschke, G. *Phytochemistry* **1997**, *45*, 149–157. (e) Thippornwong, M.; Tohtong, R. *AACR Meeting Abstracts* **2006**, A112. (f) Zhu, Q. A., J.; Li, F.; Wang, M.; Wu, J.; Tang, Y. *Chin. J. Appl. Environ. Biol.* **2013**, *19*, 956–959.

(5) Mayasundari, A.; Young, D. G. J. *Tetrahedron Lett.* **2001**, *42*, 203-206.

(6) Khan, S.; Nobuki, K.; Masahiro, H. *Synlett* **2000**, 1494–1496.

(7) Wang, Q.; Fan, S. Y.; Wong, H. N. C. *Tetrahedron* **1993**, *49*, 619–638.

(8) (a) Doyle, M. P.; Dyatkin, A. B.; Kalinin, A. V.; Ruppar, D. A. *J. Am. Chem. Soc.* **1995**, *117*, 11021–11022. (b) Doyle, M. P.; Dyatkin, A. B.; Autry, C. L. *J. Chem.*

Soc. Perkin Trans. **1995**, 619–621. (c) Müller, P.; Bernardinelli, G.; Nury, P. *Tetrahedron Asymmetry* **2002**, *13*, 551–558.

(9) (a) Clive, D. L.; Daigneault, S. *K. Chem. Soc., Chem. Commun.* **1989**, 332–335. (b) Fukuyama, T.; Chen, X. *J. Am. Chem. Soc.* 1994, *116*, 3125–3126. (c) Meyer, M. E.; Phillips, J. H.; Ferreira, E. M.; Stoltz B. M. *Tetrahedron* **2003**, *69*, 7626–7635. (d) Min, S.-J.; Danishefsky, S. J. *Tetrahedron Lett.* **2008**, *49*, 3496–2399. (e) Newhouse, T. R.; Kaib, P. S. J.; Gross, A. W.; Corey, E. J. *Org. Lett.* **2013**, *15*, 1591–1593.

(10) Zhang, J. L; Che, C.-M. *Org. Lett.* **2002**, *4*, 1911–1914.

(11) Lebel, H.; Paquet. V. *J. Am. Chem. Soc.* **2004**, *126*, 320–326.

(12) Abe, H.; Sato, A.; Kobayashi, T.; Ito, H. *Org. Lett.* **2013**, *15*, 1298–1301.

(13) Please see A1.2 for additional studies.

(14) Stereochemistry of **74** was confirmed by generating Mosher esters. See A1.3

(15) (a) Kauffmann, T.; Ennen, B.; Sander, J.; Wieschollek, R. *Angew. Chem.* **1983**, *95*, 237–238; *Angew. Chem., Int. Ed. Engl.* **1983**, *22*, 244–245. b) Kauffmann, T.; Fiegenbaum, P.; Wieschollek, R. *Angew. Chem.* **1984**, *96*, 500–501; *Angew. Chem., Int. Ed. Engl.* **1984**, *23*, 531–532. c) Kauffmann, T.; Mçller, T.; Rennefeld, H.; Welke, S.; Wieschollek, R. *Angew. Chem.* **1985**, *97*, 351 –352; *Angew. Chem., Int. Ed. Engl.* **1985**, *24*, 348–350. d) Kauffmann, T.; Abel, T.; Beirich, C.; Kieper, G.; Pahde, C.; Schreer, M.; Toliopoulos, E.; Wiescholiek, R. *Tetrahedron Lett.* **1986**, *27*, 5355–5358.

(16) Synthetic study using Kauffmann olefination: Bennett, N. B.; Stoltz. B. M. *Chem. Eur. J.* **2013**, *52*, 17745.

(17) Subbaraju, G. V.; Manhas, M. S.; Bose, A. K. *Synthesis* **1991**, 816–818.

(18) Smith, M. B.; March, J. March's *Advanced Organic Chemistry: Reactions, Mechanisms, and Structure,* 5th ed.; Wiley-Interscience: New York, 2001; pp 1514–1517.

(19) Nakano, T. T., T.; Ishii, Y.; Ogawa, M. *Synthesis* **1986**, 774–776.

(20) Lucio Anelli, P.; Biffi, C.; Montanari, F.; Quici, S. *J. Org. Chem.* **1987**, *52*, 2559–2562.

(21) (a) De Luca, L.; Giacomelli, G.; Porcheddu, A. *Org. Lett.* **2001**, *3*, 3041–3043. (b) Hoover, J. M.; Stahl, S. S. *J. Am. Chem. Soc.* **2011**, *133*, 16901–16910.

(22) Selected total synthesis examples: (a) Matsumoto, K.; Koyachi, K.; Shindo, M. *Tetrahedron* **2013**, *69*, 1043–1049. (b) Yadav, J. S.; Mallikarjuna Reddy, N.; Ataur Rahman, M.; Mallikarjuna Reddy, A.; Prasad, A. R. *Helv. Chim. Acta* **2014**, *97*, 491–498. (c) Matthies, S.; Stallforth, P.; Seeberger, P. H. *J. Am. Chem. Soc.* **2015**, *137*, 2848–2851.

(23) Chen, B.-C.; Zhou, P.; Davis, F. A.; Ciganek, E. *Org. React.* **2003**, *62*, 1–356.

(24) Pangborn, A. B.; Giardello, M. A.; Grubbs, R. H.; Rosen, R. K.; Timmers, F. J. *Organometallics* **1996**, *15*, 1518–1520.

(25) Davies, M. L. H.; Cantrell, R. W.; Jr.; Romines, R. K.; and Baum, S. J.; *Org. Synth.* **1992**, 70, 93-100; *Coll. Vol. IX* **1998**, 422-426.

(26) Charles, R. G. *J. Org. Chem.* **1957**, *22*, 677–679.

(27) McUliffe, C. A.; Hosseiny, A.; McCullough, F. P. *Inorg. Chim. Acta* **1979,** *33*, 5–10.

APPENDIX 1

Additional Studies Related to Chapter 1:

Progress toward the Total Synthesis of Curcusone C

A1.1 INITIAL STUDIES

A1.1.1 RETROSYNTHETIC ANALYSIS

Firstly, we expected that curcusone C could be synthesized from tricyclic system **105** by α-methylation followed by hydroxylation. In order to synthesize the tertiary alcohol, chiral oxaziridine would be applicable for hydroxylation if desired selectivity is not observed with substrate controllable. The tricycle core **105** was then disconnected by a (4+3) cycloaddition type reaction from diene **107** and vinyl aldehyde **108**. However, the diene **107** and aldehyde **108** do not exhibit the appropriate eletron character for a normal (4+3) cycloaddition reaction; inversion via Stetter reaction or radical cyclization would be necessary for tandem umpolung Michael and another Michael reaction. Diene **107** could be achieved from cross-coupling of vinyl bromide **109** and vinyl triflate **27**. Vinyl

bromide **109** could be synthesized from cyclopentenone **26**, which is commercially available (Scheme A1.1.1).

Scheme A1.1.1. Retrosynthetic Analysis

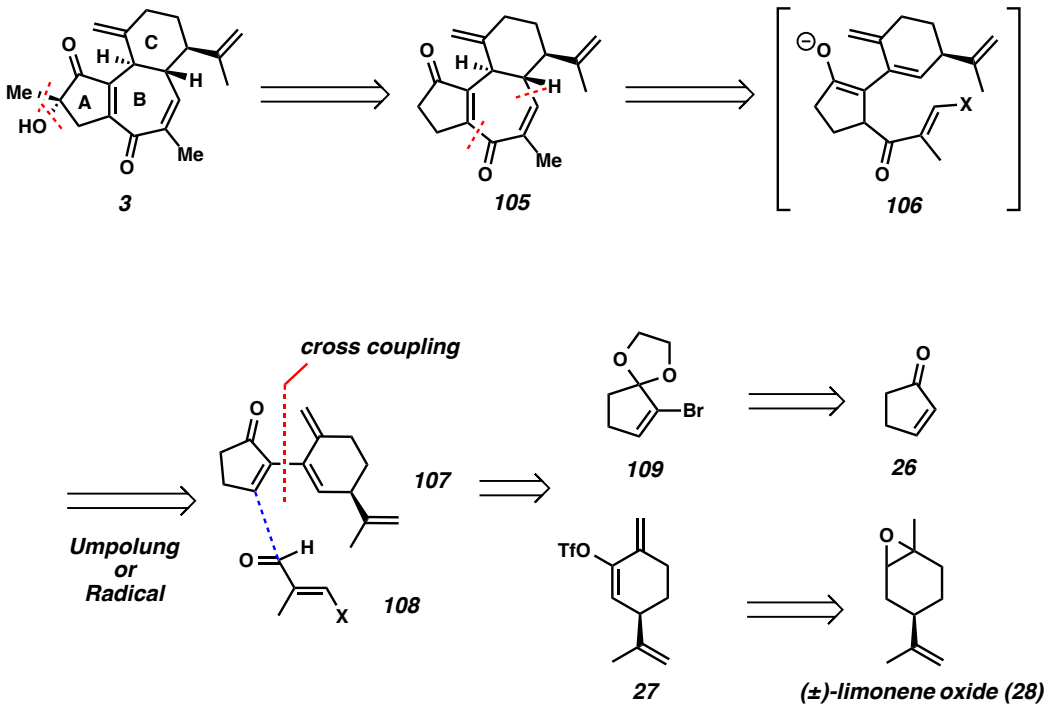

A1.1.2 SYNTHESIS OF SIMPLIFIED DIENE

Initial studies on the [4+3] type reaction were performed on a model system **38** lacking side chains of ring **C**. In order to synthesize the model diene **38**, we prepared cyclohexanone triflate **32** and vinyl bromide **109** by a known procedure.[1] Construction of model diene **38** was accomplished by Suzuki coupling of vinyl boronate **110,** which was quantitatively prepared from vinyl bromide **109,** and vinyl triflate **32** (Scheme A1.1.2).

Scheme A1.1.2. Synthesis of Simplified Diene ***38***

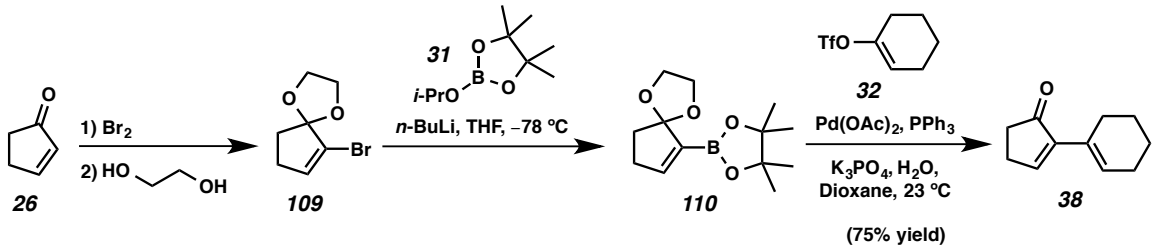

A1.1.3 RADICAL APPROACH

First, we investigated radical conditions to construct the 1,4-dione moiety. Thiol is known to selectively generate radicals on aldehydes, which can attack radical acceptors such as α,β-unsaturated carbonyls to initiate intramolecular acyl radical cyclization of alkenals.[2,3] Although all previous examples are intramolecular reactions, model diene **38** was thought to act as an appropriate radical acceptor so some intermolecular reactions were attempted with isobutyraldehyde and methacrylaldehyde. However we were not able to find the desired product using *t*-BuSH and AIBN or triethylborane radical initiator (Scheme A1.1.3).

Scheme A1.1.3. Intermolecula Radical Reaction Approach

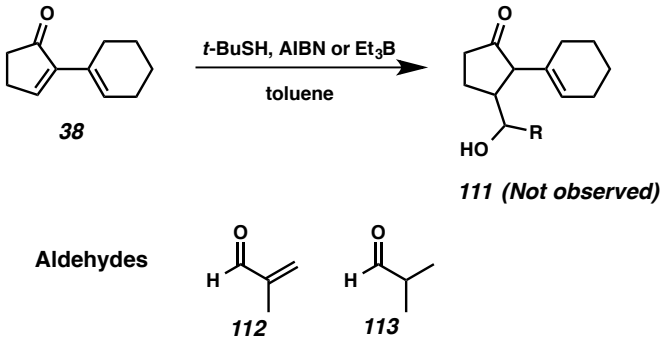

A1.1.4 UMPOLUNG APPROACH

Umpolung reactivity of aldehyde or ketone groups can provide access to distinct bond disconnections. One such reaction is the benzoin reaction, which is an addition reaction of an aldehyde or imine by a nucleophile catalyzed aldehyde.[4] The Stetter reaction is an extension of this reaction to give 1,4-dicarbonyl compounds. A number of thiazolium salts have proven to be useful nucleophilic catalysts for this purpose, accessing 1,4-dicarbonyl compounds by either intermolecular or intramolecular Stetter reaction.[5] Unfortunately, we were unable to isolate the desired product **115** by the Stetter condition. Diene **38** was recovered mostly, and only aldehyde was consumed. We concluded that diene **38** was not a good Michael acceptor, and then examined approaches using transition metal chemistry (Scheme A1.1.4).

Scheme A1.1.4. Stetter Reaction Approach

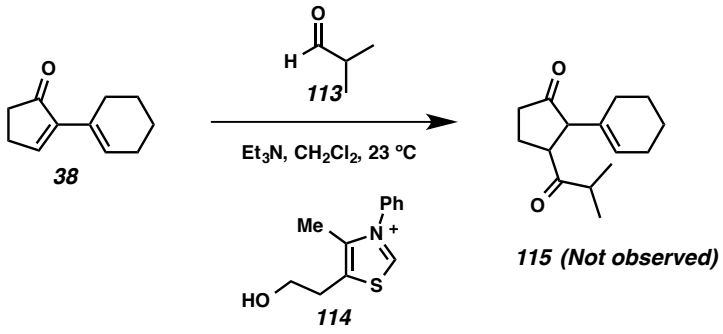

A1.1.5 ACYL METAL SPECIES

The acyl metal species [RC(O)M] reacts as an 'unmasked' acyl anion donor. The acyl metal species with a main group metal (Li, Zn, etc.) has been studied as well as several transition metal species (Co, Fe, Ni).[6] However, acyl metal species with main group metals have limited applications due to their lack of stability and extensive reaction

condition. In addition, starting materials for acyl transition metal species have severe limitations due to toxicity of metal carbonyls. In 2002, Taguchi and co-workers reported palladium-catalyzed regioselective acylation of an α,β-unsaturated ketone by acylzirconocene chloride, which was conveniently prepared by Schwartz's reagent (Scheme A1.1.5).[7]

Scheme A1.1.5. Regioselective Acylation of α,β-Unsaturated Ketones by Acylzirconocene Chloride by Taguchi and co-workers

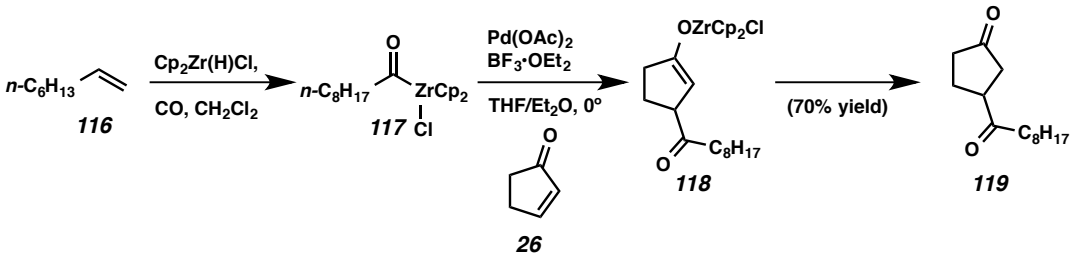

They were able to selectively construct 1,4-dicarbonyl **119** from cyclopentenone and acylzirconocene chloride **117** in 70% yield. Thus we envisioned that diene **38** could react with an acylzirconocene chloride to produce 1,4-dicarbonyl compound **121**, which could be advanced to tricyclic core **122** via a Michael reaction. We decided to use trimethylsilyl propyne **120** to prepare acylzirconocene chloride which would provide a 3-carbon insertion to diene **38**. However, the desired diketone **121** was not obtained. Even though we screened a number of different catalyst alternatives to palladium acetate with cyclopentenone **26**, the desired product **123** was not obserbed. All of these results led us to attempt different acyl metal species altogether (Scheme A1.1.6).

Scheme A1.1.6. Acylation Studies using Acylzirconocene Chloride

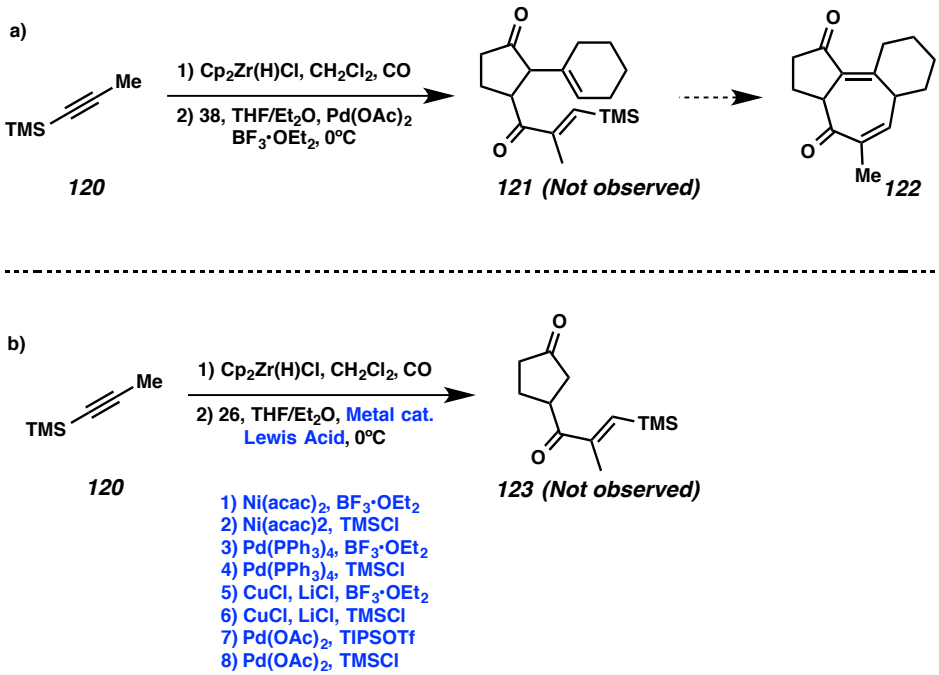

Next, we examined the palladium-catalyzed carbonylative Heck reaction. We envisioned that acylpalladium species could be generated by insertion of carbon monoxide to a simple triflate **124**, which could react with diene **38** to afford a 1,4-dicarbonyl product **125**. However, we were not able to observe desired product **125** or any analogous structure with vinyl triflate **125** (Scheme A1.1.7).

Scheme A1.1.7. Carbonylative Heck Reaction

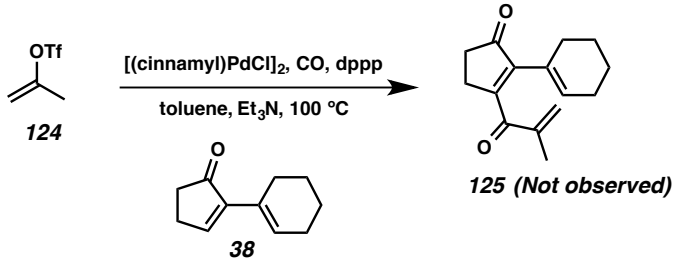

A1.1.6 REVISED SYNTHETIC PLAN

Previously, we had failed to insert a 3-carbon unit into diene by various ways. Therefore, we decided to establish the 5-7-6 ring fused system first, followed by functional group modification to elaborate the core system **126** later. We envisioned that the desired 5-7-6 fused ring system could be accessed by Diels–Alder reaction followed by one carbon insertion sequence on diene **127** (Scheme A1.1.8).

Scheme A1.1.8. Revised Retrosynthesis

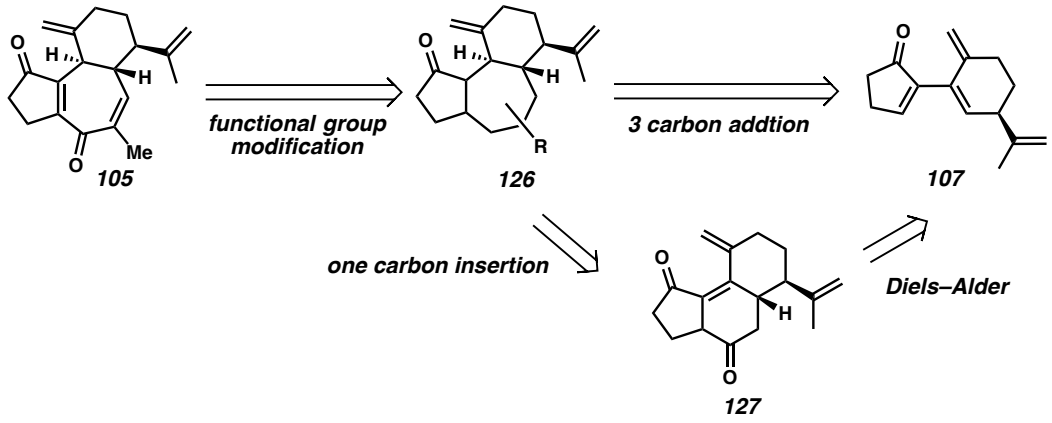

A1.1.7 DIELS–ALDER REACTION AND RING EXPANSION APPROACH

A number of ketene derivatives such as nitroethylene and chloroacrylonitrile have been applied in the synthesis of cyclohexenone type products for many years.[8] Furthermore, we expected that cyclohexanones could be expanded to 7-membered rings via one-carbon insertion reaction (Scheme A1.1.9).[9]

Scheme A1.1.9. Diels–Alder Reaction and One Carbon Insertion Strategy

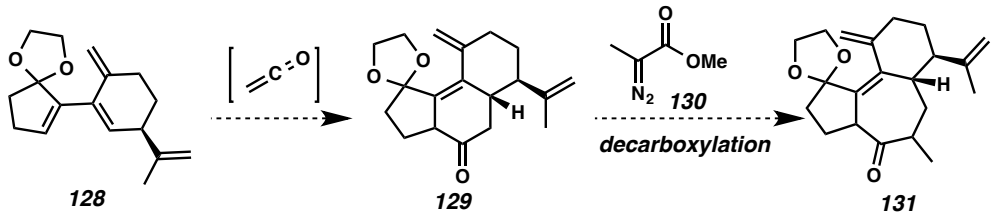

Initially, we attempted phenyl vinyl sulfone, 2-chloro acrylonitrile and nitroethylene as dienophiles. A number of conditions were attempted, and nitroethylene showed reactivity with diene **38**, but afforded an inseparable mixture. Aromatized product **132** was isolated as a result of Nef reaction product from the mixture (Scheme A1.1.10a). Since the carbonyl group could cause aromatization under Nef conditions, we decided to change diene moiety for the Diels–Alder reaction screening. Thus, we examined protected diene **104** for the Diels–Alder reaction with nitroethylene. However, we were only able to observe complex mixtures from the reaction conditions (Scheme A1.1.10b).

Scheme A1.1.10. Diels–Alder and Nef Reaction Studies

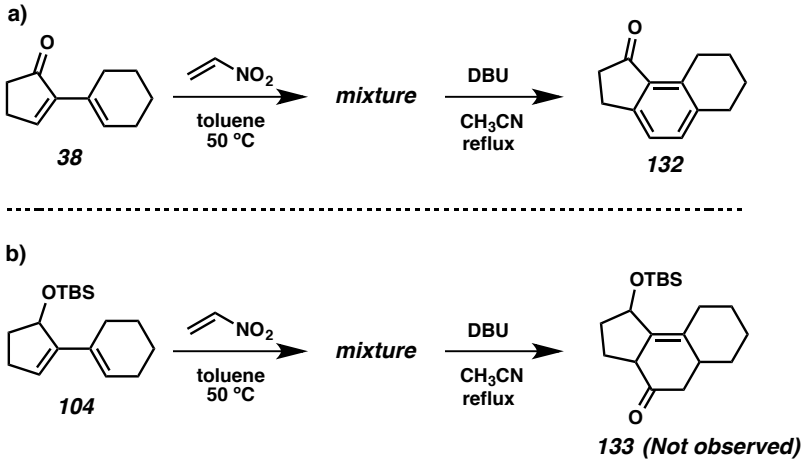

A1.2 ADDITIONAL STUDIES REALATED TO PERILALDEHYDE ROUTE (Chapter 1.3.2)

During the synthesis of the cyclopropane from perillaldehyde, we encountered olefin migration issues, which yielded products with fully conjugated olefin systems. Addition of TBAF to silylated allylic alcohol **69** furnished **134** instead of the deprotection product (Scheme A1.2.1a). Next we examined Suzuki coupling of deprotected allylic alcohol **79**

with iodide *ent*-**64** to avoid late stage deprotection, however another olefin migrated product **135** was formed (Scheme A1.2.1b). Thus, we concluded that treatment of base would cause olefin migration due to its labile γ-proton. Since the allylic C-O bond could be epimerized by acidic conditions, we applied extra pyridine in addition to hydrogen fluoride-pyridine complex, and allowing us to prepare deprotected allylic alcohol **70** successfully (Scheme A1.2.1c).

*Scheme A1.2.1. Deprotection Screening of **69***

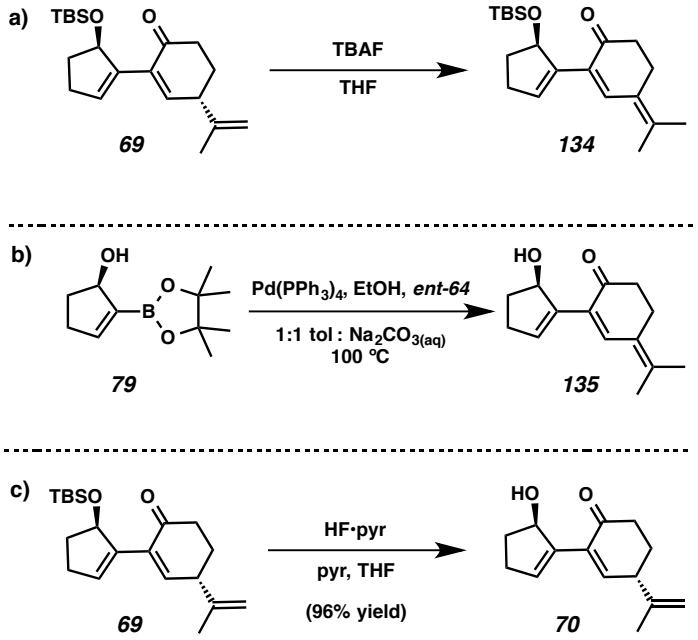

As stated before (Schemes 1.3.5 and 1.3.6) allylic alcohol **70** was transformed to β-ketoester **71**, which was then transformed to an inseparable mixture of diazo esters **136** and **137**. Although the desired diazo ester **136** existed as a major component, cyclopropanation condition induced more olefin migration to afford a mixture of cyclopropanes **72** and **73**, which contains undesired **73** as a major compound. Despite screening of versatile catalysts, we were not able to find proper cyclopropanation conditions to synthesize **72** selectively (Scheme A1.2.2).

Scheme A1.2.2. Cyclopropanation Screening

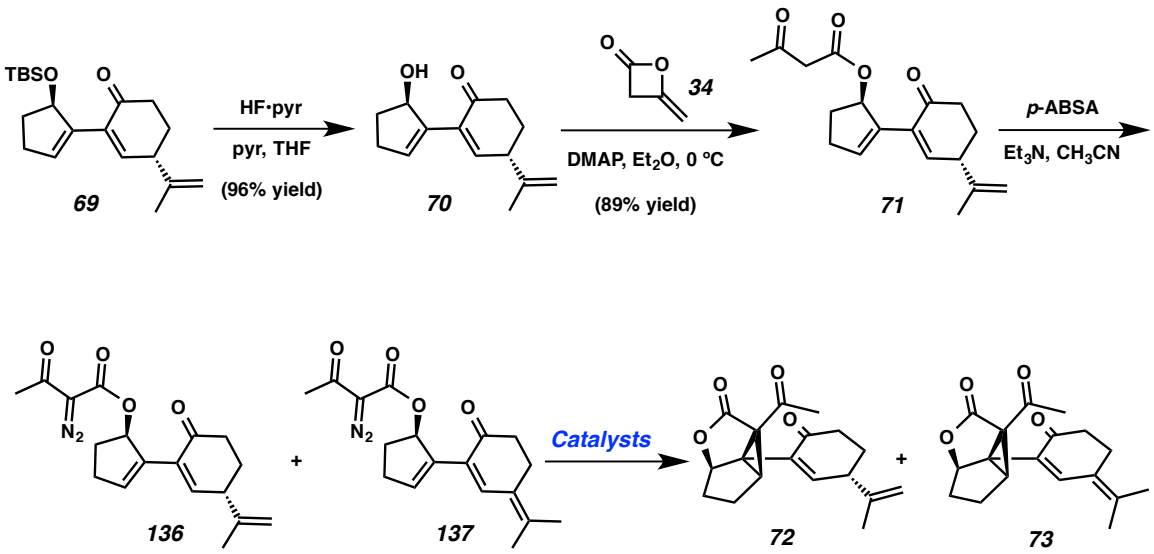

Catalysts: $Cu(TBS)_2$, Cu alloy, $Cu(hfacac)_2$, Cu(II)OTf, Cu(I)OTf·tol, CuI, $Cu(I)(CH_3CN)_4PF_6$ $Rh_2(OAc)_4$, $Rh_2(esp)_2$, Rh_2(heptafluorobutyrate)$_4$, $Rh_2(OPiv)_4$, $[Rh(nbd)Cl]_2$, Rh_2cap_4

A1.3 STEREOCHEMICAL ELUCIDATION OF ALLYLIC ALCOHOL 77

In order to confirm the stereochemistry of allylic alcohol **77**, we utilized Mosher ester analysis.[10] Both α-methoxy-α-trifluoromethylphenylacetic acid (MTPA) esters were prepared by addition of (*R*) and (*S*)-MTPA to allylic alcohol **77** and comparative analysis (δ^{SR}) of ^{1}H NMR spectral data was performed. Result showed matched stereochemistry with the desired compound **77** (Scheme A1.3.1).

Scheme A1.3.1. Preparation of Mosher Esters

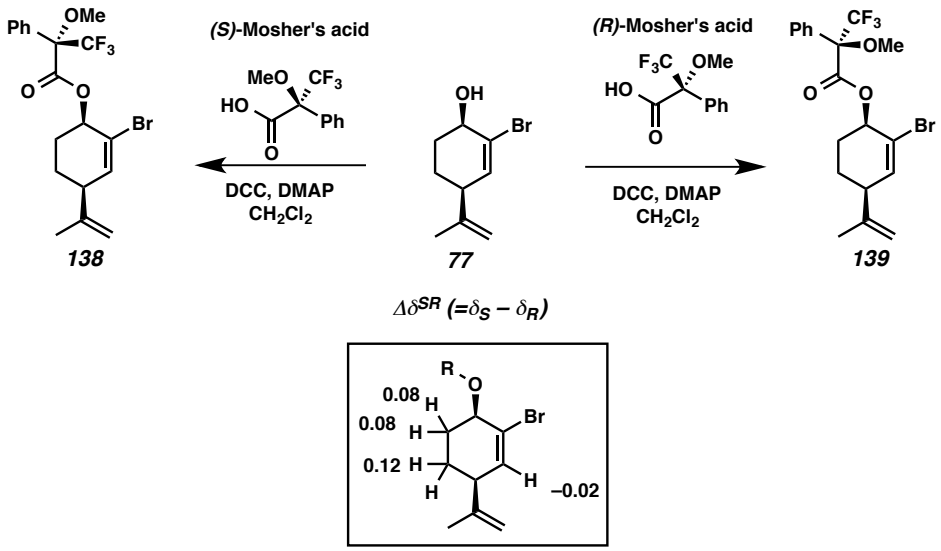

A1.4 EXPERIMENTAL SECTION

A1.4.1 MATERIALS AND METHODS

Unless stated otherwise, reactions were performed under an argon or nitrogen atmosphere using dry, deoxygenated solvents (distilled or passed over a column of activated alumina).[11] Et_3N was distilled from calcium hydride immediately prior to use. Commercially obtained reagents were used as received unless otherwise stated. Reaction temperatures were controlled by an IKAmag temperature modulator. Thin-layer chromatography (TLC) was performed using E. Merck silica gel 60 F254 precoated plates (0.25 mm) and visualized by UV fluorescence quenching, or potassium permanganate, iodine, or anisaldehyde staining. Silia*Flash* P60 Academic Silica gel (particle size 0.040-0.063 mm) was used for flash chromatography. ^{1}H and ^{13}C NMR spectra were recorded on a Varian Inova 500 (at 500 MHz and 126 MHz respectively), Bruker AV III HD spectrometer equipped with a Prodigy liquid nigrogen temperature cryoprobe (400 MHz and 101 MHz, respectively) and are reported relative to $CHCl_3$ (δ 7.26 & 77.16 respectively) and C_6H_6 (δ 7.16 & 128.06 respectively. Data for ^{1}H NMR spectra are reported as follows: chemical shift (δ ppm) (multiplicity, coupling constant (Hz), integration).

A1.4.2 PREPARATIVE PROCEDURES

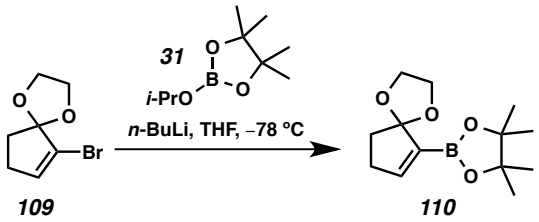

Boronate 110: To a flame-dried round-bottom flask with a magnetic stir bar were added bromide **109** (328 mg, 1.60 mmol) and THF (8 mL). The flask was cooled to –78 ºC and stirred for 10 min. *n*-Butyllithium solution (2.4 M in hexanes, 0.67 mL, 1.61 mmol) was added dropwise. The reaction mixture was stirred at –78 ºC for 30 min then isopropyl pinacolyl borate (0.33 mL, 1.62 mmol) was added. The reaction mixture was stirred at –78 ºC for 30 min then quenched with HCl solution (2 N in Et_2O, 0.8 mL, 1.60 mmol). Following addition, the reaction mixture was diluted with Et_2O (10 mL) and warmed up to 23 ºC. The reaction mixture was filtered and was concentrated under reduced pressure, and the residue was used in the next reaction without further purification.

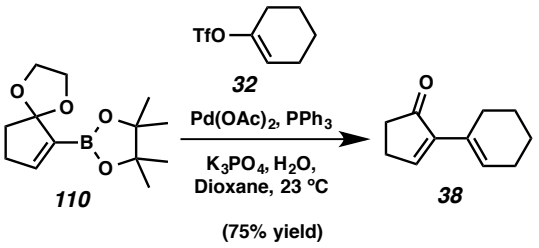

Diene 38: To a flame-dried round-bottom flask equipped with a magnetic stir bar were added a crude mixture of boronate **110** from the previous step, triflate **32** (280 mg, 1.26 mmol), palladium acetate (18 mg, 0.080 mmol), triphenylphosphine (42 mg, 0.160

mmol), potassium phosphate tribasic (1 g, 4.71 mmol). The mixture was evacuated and back filled with argon (3x). The mixture was dissolved in dioxane (8 mL) then added water (0.8 mL). The reaction mixture was stirred at 23 ºC for 6 hr. The resulting mixture was then diluted with EtOAc (10 mL), washed by saturated aqueous NH_4Cl (10 mL), and then dried over $MgSO_4$. The mixture was filtered and concentrated under reduced pressure to afford crude mixture of **38** as a colorless oil. The residue was purified by flash column chromatography (20:1 hexanes:EtOAc) to afford diene **38** (148 mg, 0.914 mmol, 73% yield over triflate **32**).

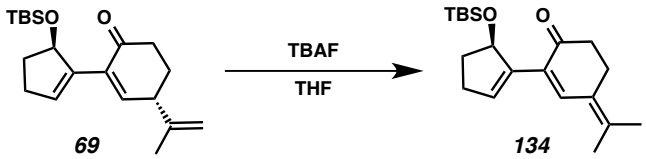

Triene 134: To a round-bottom flask with a magnetic stir bar were added diene **69** (50 mg, 0.15 mmol) and THF (2 mL). To the mixture was added TBAF (1.0 M in THF, 0.23 mL, 0.23 mmol) and stirred for 5 min at 23 ºC. The reaction mixture was diluted with Et_2O (2 mL) and quenched by saturated aqueous NH_4Cl (2 mL). The phases were separated and the aqueous phase was extracted with EtOAc (3 x 2 mL). The combined organic phases were dried over $MgSO_4$, filtered, and concentrated under reduced pressure. The residue was purified by flash column chromatography (4:1 hexanes:EtOAc) to afford olefin migrated product **134** (24 mg, 0.072 mmol, 48% yield) as a colorless oil; R_f = 0.45 (6:1, hexanes:EtOAc) ^{1}H NMR (500 MHz, $CDCl_3$) δ 7.47 (s, 1H), 6.52 (d, *J* = 0.8 Hz, 1H), 5.5–5.28 (m, 1H), 2.53–2.30 (m, 4H), 2.27–2.12 (m, 1H), 2.08 (dddd, *J* = 13.2, 8.6, 7.2, 4.5 Hz, 1H), 1.78 (dddd, *J* = 13.1, 9.0, 5.0, 4.0 Hz, 1H),

1.63 (s, 3H), 1.43 (s, 3H), 0.97 (s, 9H), 0.15 (s, 3H), 0.12 (s, 3H); ^{13}C NMR (126 MHz, $CDCl_3$) δ 197.6, 143.4, 139.6, 136.8, 133.0, 130.7, 78.5, 38.7, 34.4, 31.0, 26.2, 26.0, 21.5, 20.6, 18.4, –3.7, –4.3.

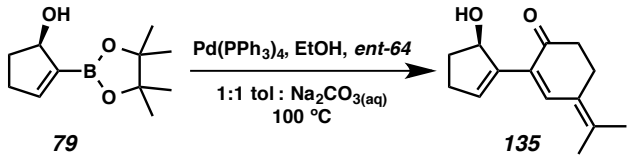

Alcohol 135: To a two neck round-bottom flask equipped with reflux condenser and a magnetic stir bar were added boronate **79** (34 mg, 0.103 mmol), and iodide *ent*-**64** (27 mg, 0.103 mmol). The mixture was evacuated and back filled with argon (3x). Toluene (2 mL), ethanol (0.4 mL) tetrakis(triphenylphosphine)palladium(0) (5 mg, 0.0043 mmol), and 2 M aqueous Na_2CO_3 (2 mL) were added. The reaction was heated to reflux in a 110 ºC oil bath. After 12 h of stirring, the reaction mixture was cooled to 23 ºC and stirred for 15 min. The phases were separated and the aqueous phases were extracted with EtOAc (3 x 5 mL). The combined organic phases were washed with brine (5 mL), dried over $MgSO_4$, filtered and concentrated under reduced pressure. The crude product was purified by flash column chromatography (20:1, hexanes:EtOAc) to afford diene **135** (5 mg, 0.023 mmol, 22.2% yield) as a colorless oil; R_f = 0.10 (6:1, hexanes:EtOAc); ^{1}H NMR (500 MHz, $CDCl_3$) δ 7.57 (s, 1H), 6.53 (s, 1H), 5.06–4.99 (m, 1H), 2.96 (d, J = 5.1 Hz, 1H), 2.67–2.43 (m, 1H), 2.33–2.26 (m, 2H), 2.24–2.11 (m, 2H), 2.10–1.99 (m, 1H), 1.98–1.80 (m, 1H), 1.58 (s, 3H), 1.40 (s, 3H).

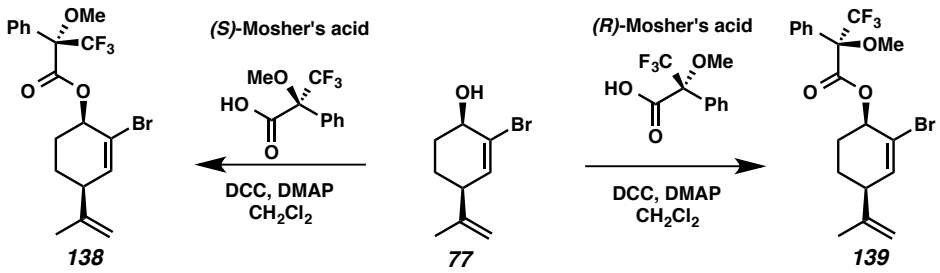

(*S*)-Mosher ester 138: To a flame-dried round-bottom flask with a magnetic stir bar were added alcohol **77** (15 mg, 0.069 mmol) and DCM (2 mL). To a reaction, *(S)*-Mosher's acid (40 mg, 0.171 mmol), DCC (42 mg, 0.204 mmol) and DMAP (1 mg, 0.0082 mmol) were added sequentially. The reaction mixture was stirred at 23 ºC for 30 min. The reaction mixture was concentrated under reduced pressure. The mixture was purified by preparatory TLC (10:1 hexanes, EtOAc). A mixture of DCU and the desired product **138** was isolated and ^{1}H NMR was taken.

(*R*)-Mosher ester 139: To a flame-dried round-bottom flask with a magnetic stir bar were added alcohol **77** (6.5 mg, 0.030 mmol) and DCM (1 mL). To a reaction, *(R)*-Mosher's acid (14 mg, 0.060 mmol), DCC (15 mg, 0.073 mmol) and DMAP (0.5 mg, 0.0041 mmol) were added sequentially. The reaction mixture was stirred at 23 ºC for 30 min. The reaction mixture was concentrated under reduced pressure. The mixture was purified by preparatory TLC (10:1 hexanes, EtOAc). A mixture of DCU and the desired product **139** was isolated and ^{1}H NMR was taken.

A1.5 NOTES AND REFERENCES

(1) Branca, S. J.; Smith, A. B. III *J. Am. Chem. Soc.* **1978**, *100*, 7767–7768.

(2) Enquist. J. A.l Stoltz, B. M. *Nature* **2008,** *453*, 1228–1231.

(3) Yoshikai, K.; Hayama, T.; Nishimura, K.; Yamada, K.; Tomioka, K. *J. Org. Chem.* **2005,** *70*, 681–683.

(4) Ide, W. S.; Buck, J. S. *In Organic Reactions*; Adams, R., Ed.; Wiley: New York, **1948**, 4, 269.

(5) (a) Stetter, H.; Kuhlmann, H. *In Organic Reactions*; Paquette, L. A., Ed.; Wiley: New York, **1991**, *40*, 407. (b) Stetter, H.; Kuhlmann, H. *Chem. Ber.* **1976**, *109*, 2890–2896. (c) Stetter, H. *Angew. Chem., Int. Ed. Engl.* **1976**, *15*, 639–647.

(6) (a) Corey, E. J.; Hegedus, L. S. *J. Am. Chem. Soc.* **1969**, *91*, 4926–4928. (b) Sawa, Y.; Hashimoto, I.; Ryang, M.; Tsutsumi, S. *J. Org. Chem.* **1968**, *33*, 2159–2161. (c) Hermanson, J. R.; Hershberger, J. W.; Pinhas, A. R. *Organometallics* **1995**, *14*, 5426–5437. (d) Hegedus, L. S.; Tamura, R. *Organometallics* **1982**, 1, 1188–1194. (e) Collman, J. P.; Winter, S. R.; Clark, D. R. *J. Am. Chem. Soc.* **1972**, *94*, 1788–1789. (f) McMurry, J. E.; Andrus, A. *Tetrahedron Lett.* **1980**, *21*, 4687–4690. (g) Cooke, M. P., Jr.; Parlman, R. M. *J. Am. Chem. Soc.* **1977**, *99*, 5222–5224. (h) Hegedus, L. S.; Inoue, Y. *J. Am. Chem. Soc.* **1982**, *104*, 4917–4921. (i) Hegedus, L. S.; Perry, R. J. *J. Org. Chem.* **1985**, *50*, 4955–4960.

(7) (a) Hanzawa, Y.; Narita, K.; Yabe, M.; Taguchi, T.; *Tetrahedron* **2002,** *58*, 10429–10435. (b) Hanzawa, Y.; Tabuchi, N.; Narita, K.; Kakuuchi, A.; Yabe M.; Taguchi, T.; *Tetrahedron* **2002**, *58*, 7559–7571.

(8) Examples of different ketene derivatives (a) Li, P.; Yamamoto, H. *J. Am. Chem. Soc.* **2009**, *131*, 16628–16629. (b) Ochoa, M. E.; Arias, M. S.; Aguilar, R.; Delagade, F.; Tamariz, J. *Tetrahedron* **1999**, *55*, 14535–14546. (c) Plettner, E. Mohle, A.; Mwangi, M. T.; Griscti, J.; Patrick, B. O.; Nair, R.; Batchelor, R. J.; Einstein, F. *Tetrahedron Aymmetry* **2005**, *16*, 2754–2763.

(9) Hashimoto, T.; Naganawa, Y.; Maruoka, K.; *J. Am. Chem. Soc.* **2011**, *133*, 8834–8837.

(10) For protocol see; Hoye, T. R.; Jefferey, C. S.; Shao, F. *Nat. Protoc.* **2007**, *2*, 2451–2458.

(11) Pangborn, A. B.; Giardello, M. A.; Grubbs, R. H.; Rosen, R. K.; Timmers, F. J. *Organometallics* **1996**, *15*, 1518–1520.

APPENDIX 2

Synthetic Summary toward the Total Synthesis of Curcusone C

*Scheme A2.1. Retrosynthetic analysis of curcusone C (**3**)*

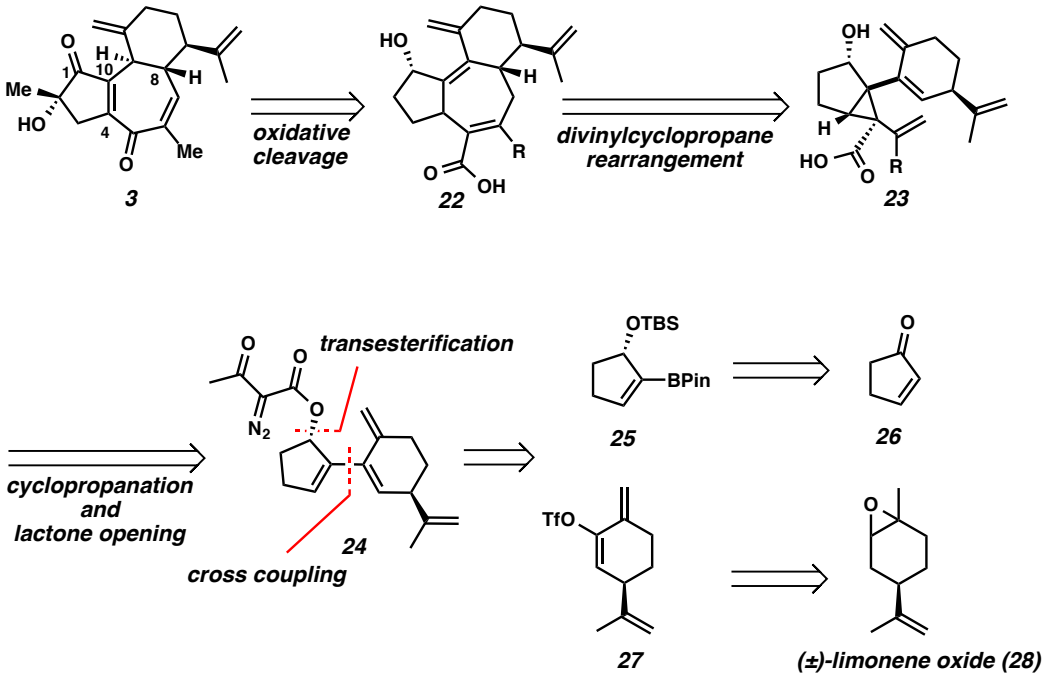

*Scheme A2.2. Synthesis of diazo ester **36** for model studies*

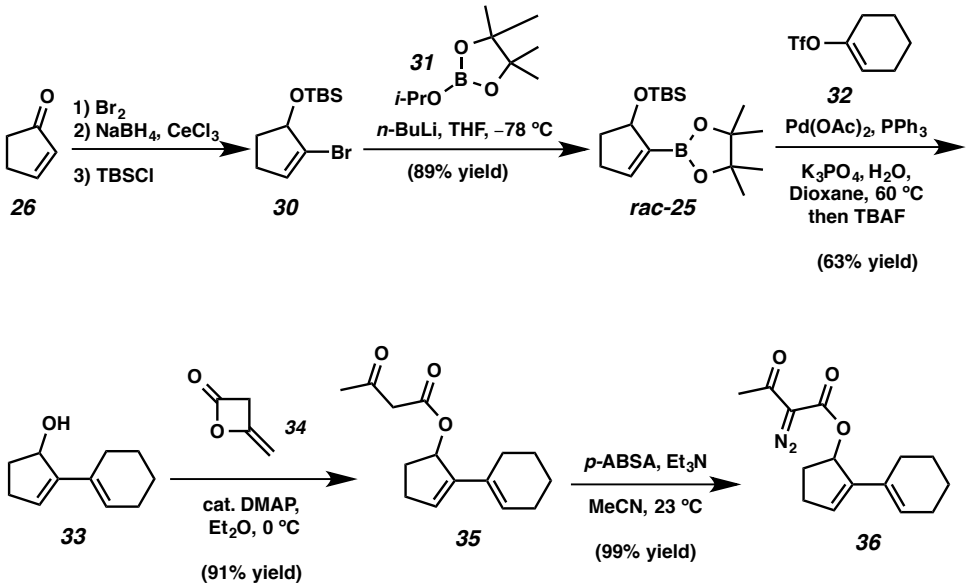

*Scheme A2.3. Syntheses cyclopropane **37** and hydrazone **42***

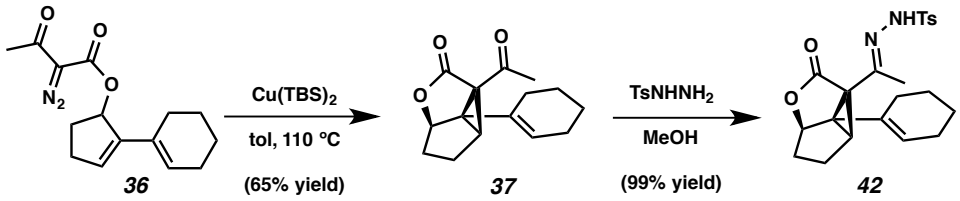

Scheme A2.4. Unexpected rearrangement

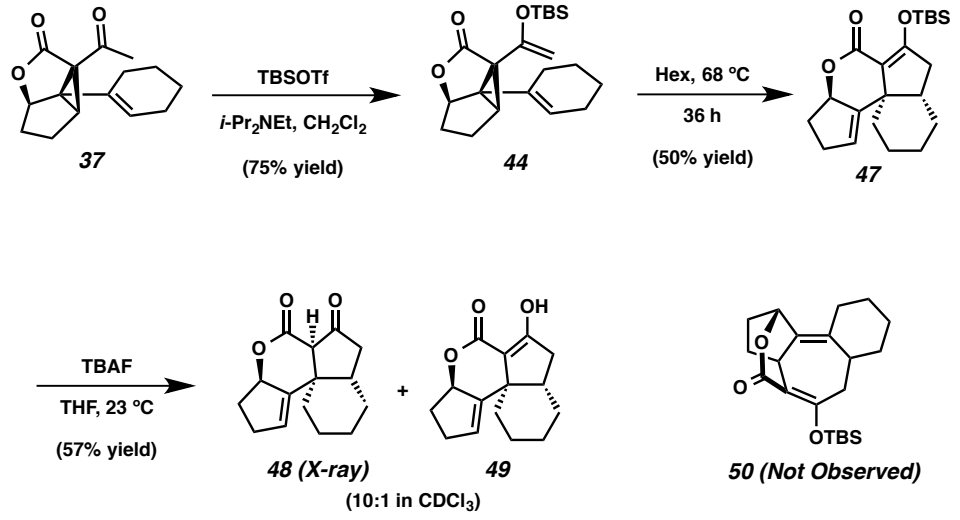

*Scheme A2.5. Synthesis of tricyclic core **53***

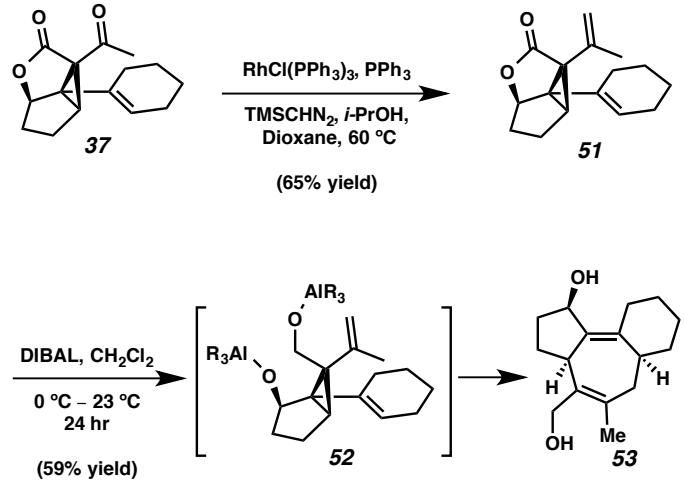

Scheme A2.6. Synthesis of vinyltriflate ***27***

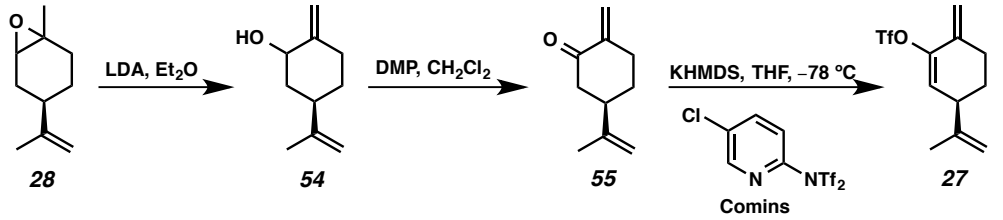

Scheme A2.7. Synthesis of diazo ester ***24***

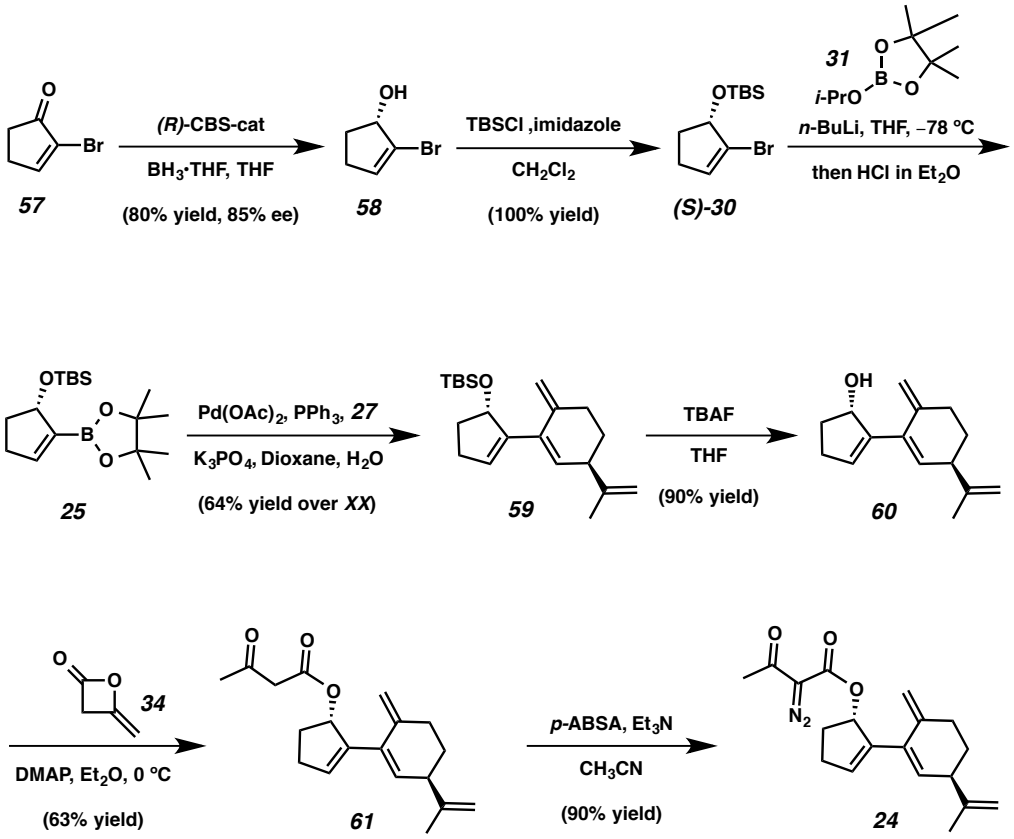

Scheme A2.8. Synthesis of iodide ent-***64***

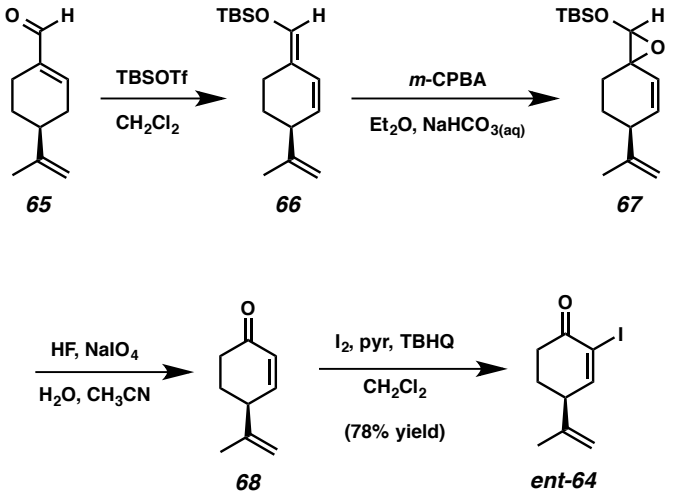

Scheme A2.9. Synthesis of β-ketoester ***71***

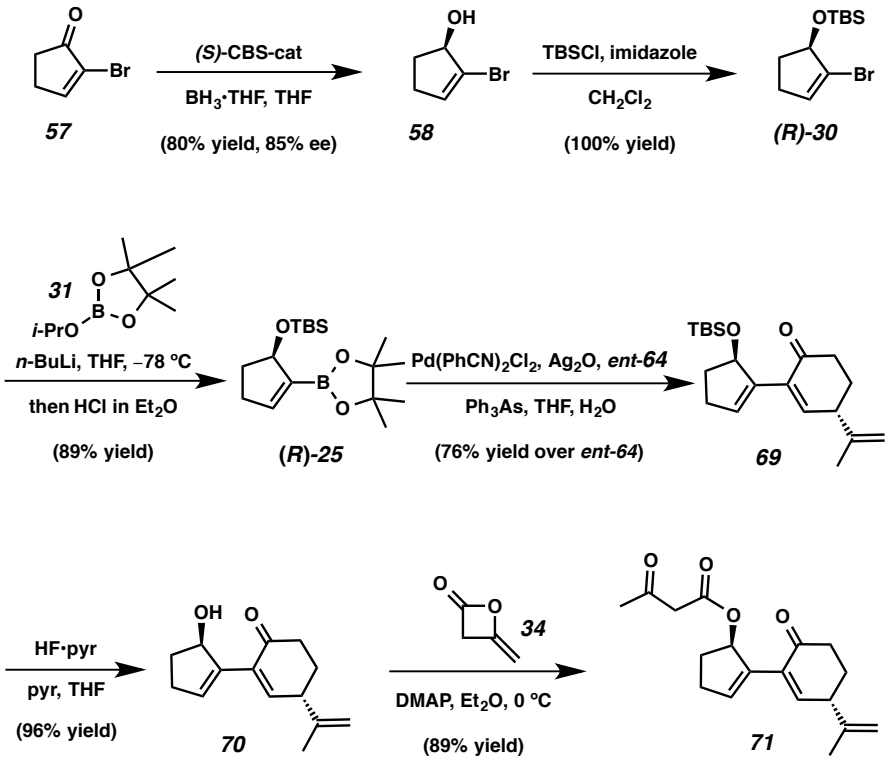

Scheme A2.10. Synthesis of cyclopropane ***72***

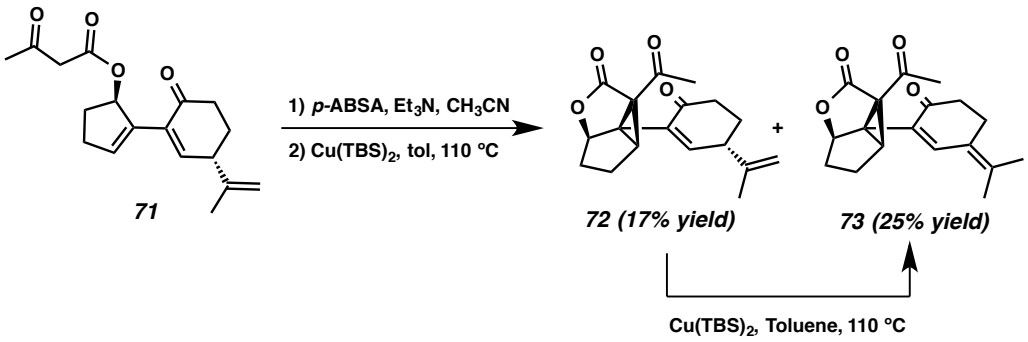

Scheme A2.11. Synthesis of protected alcohol ***78***

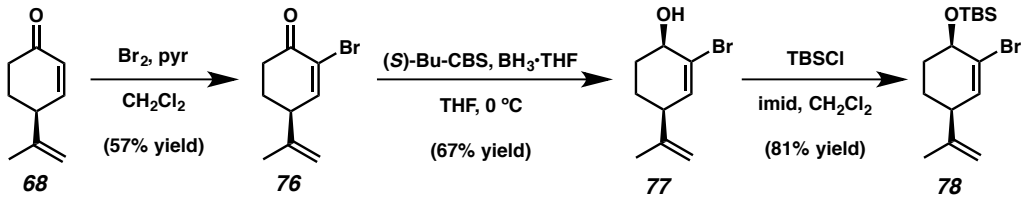

Scheme A2.12. Synthesis of diazo ester ***75***

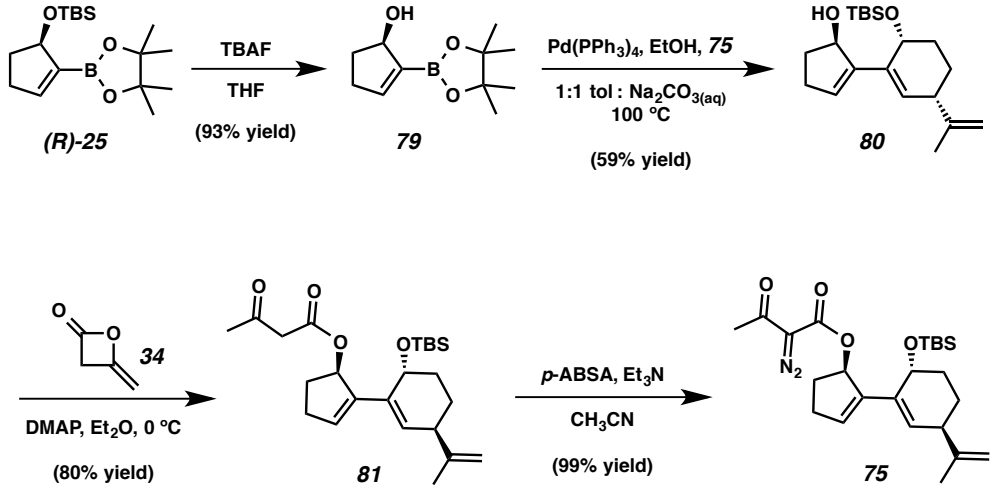

Scheme A2.13. Synthesis of divinylcyclopropane ***83***

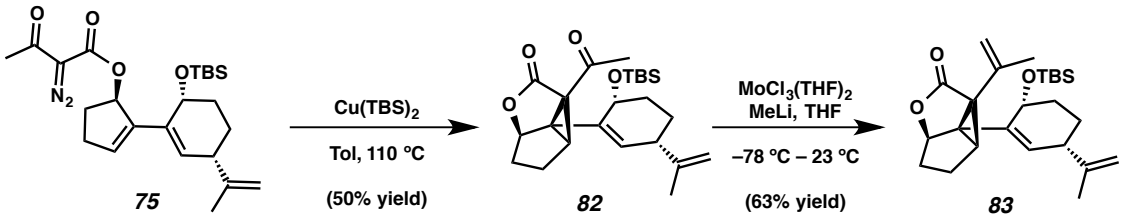

Scheme A2.14. Synthesis of tricyclic core ***85***

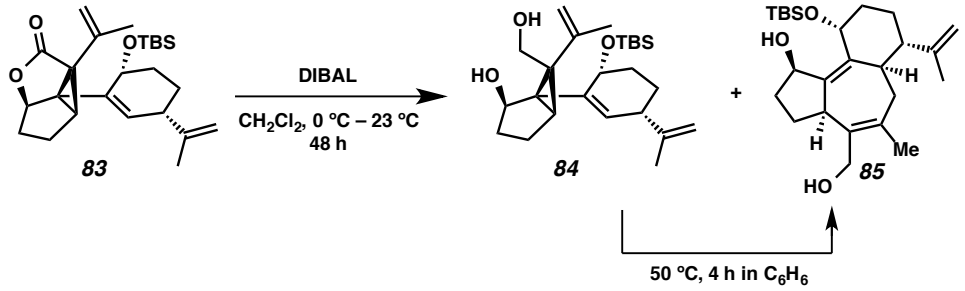

Scheme A2.15. Proposed chemoselective oxidation of diol ***85***

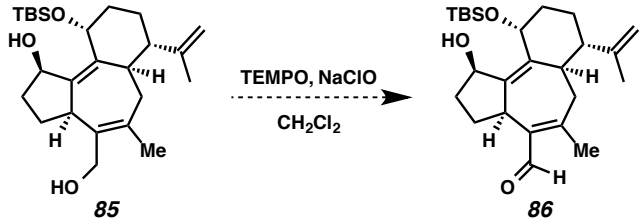

Scheme A2.16. Proposed synthesis of cycloheptadienone ***96***

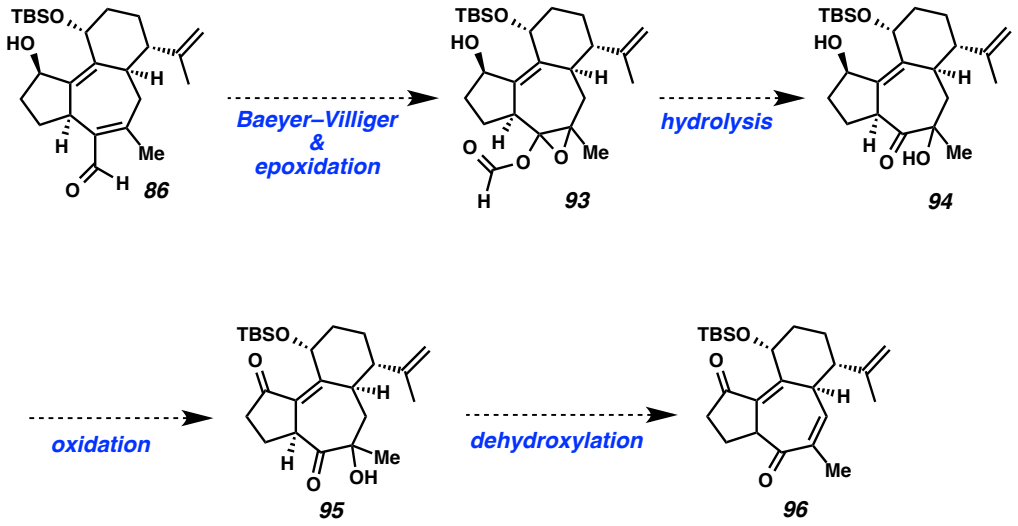

Scheme A2.17. Alternative routes

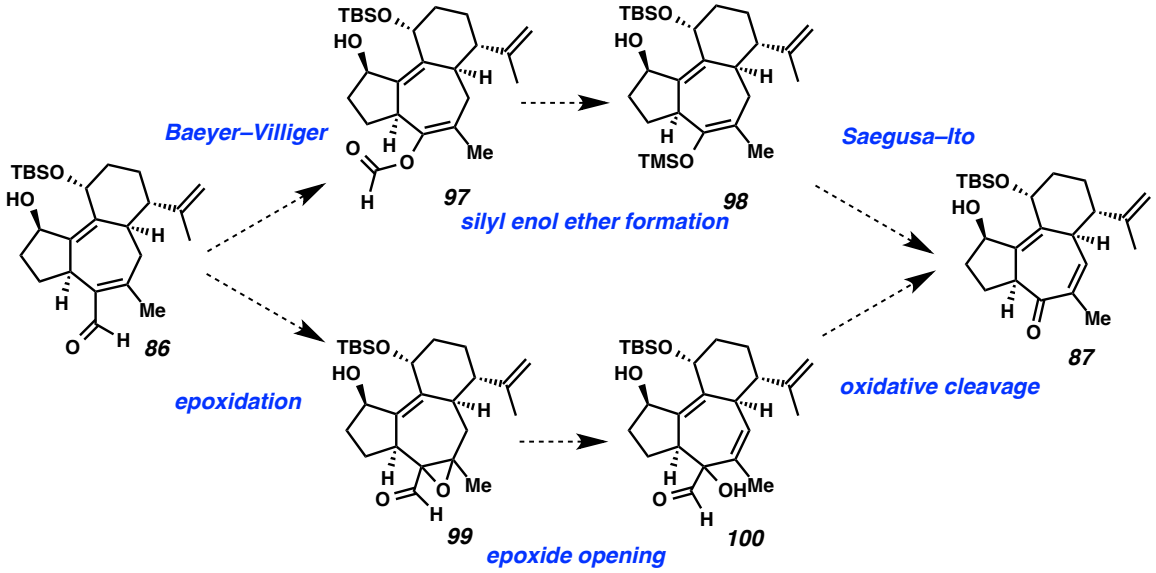

Scheme A2.18. Proposed synthesis of ent-*curcusone C*

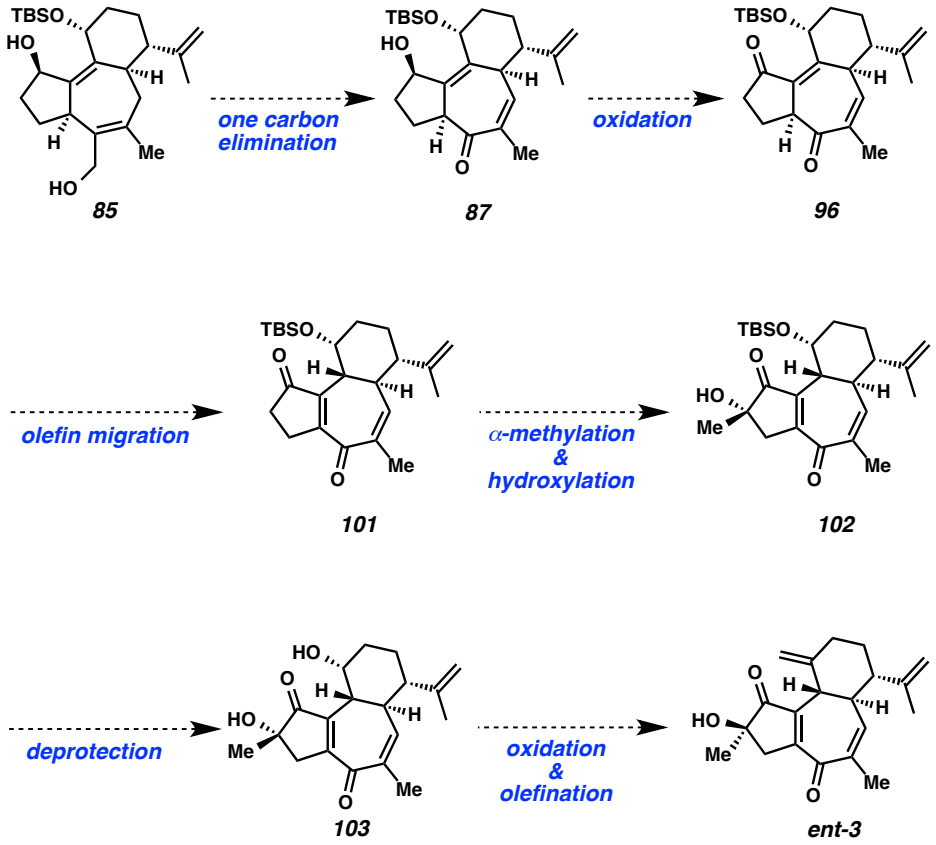

APPENDIX 3

Spectra Relevant to Chapter 1:

Progress toward the Total Synthesis of Curcusone C

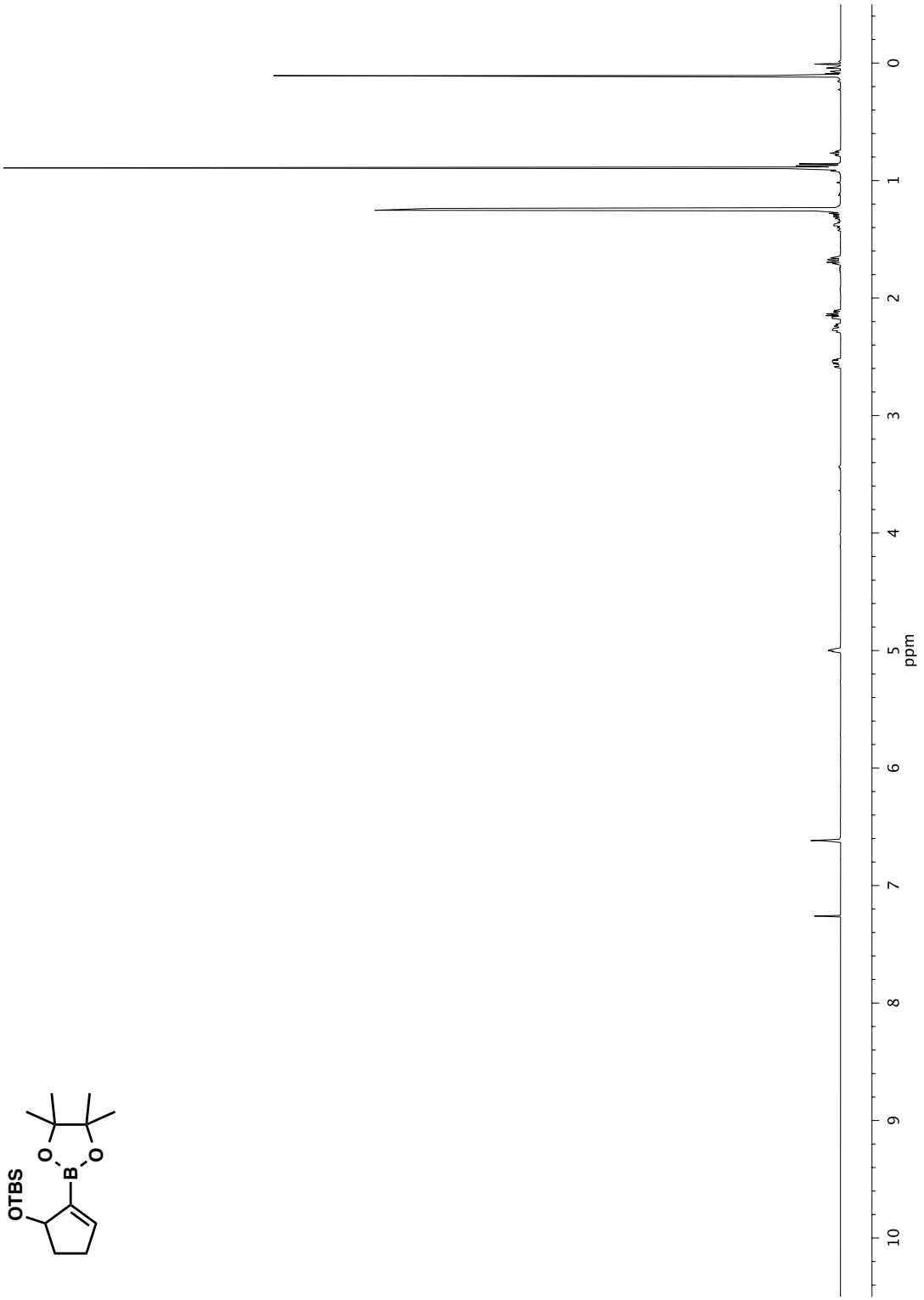

Figure A3.1 ^{1}H NMR (500 MHz, $CDCl_3$) of compound *rac*-**25**

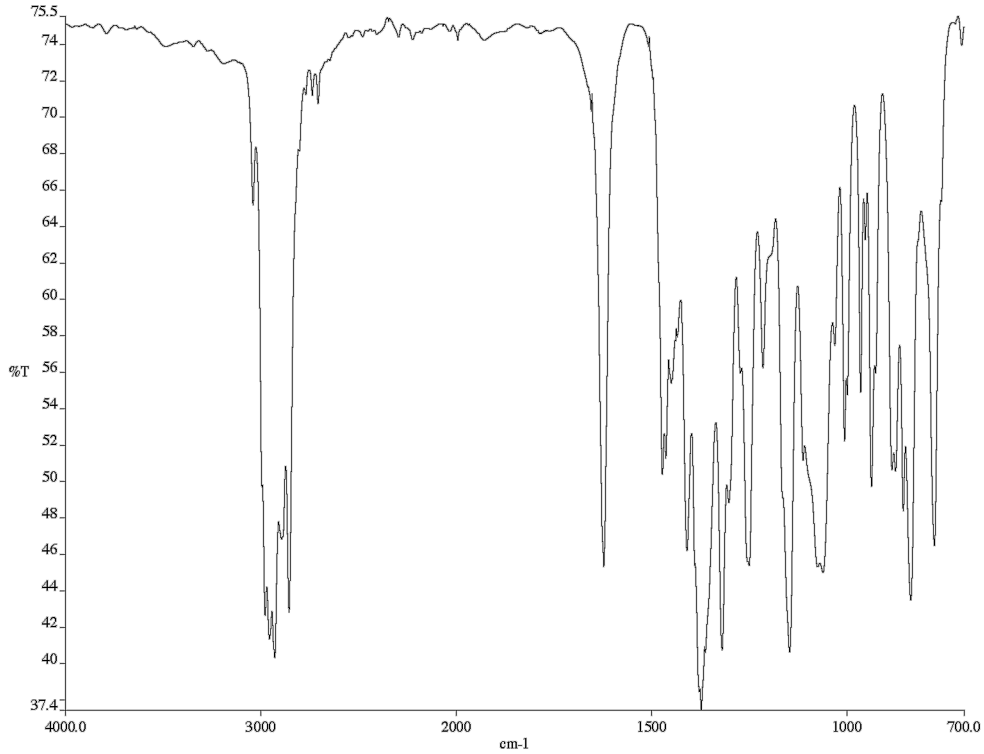

Figure A3.2 Infrared spectrum (thin film/NaCl) of compound *rac*-**25**

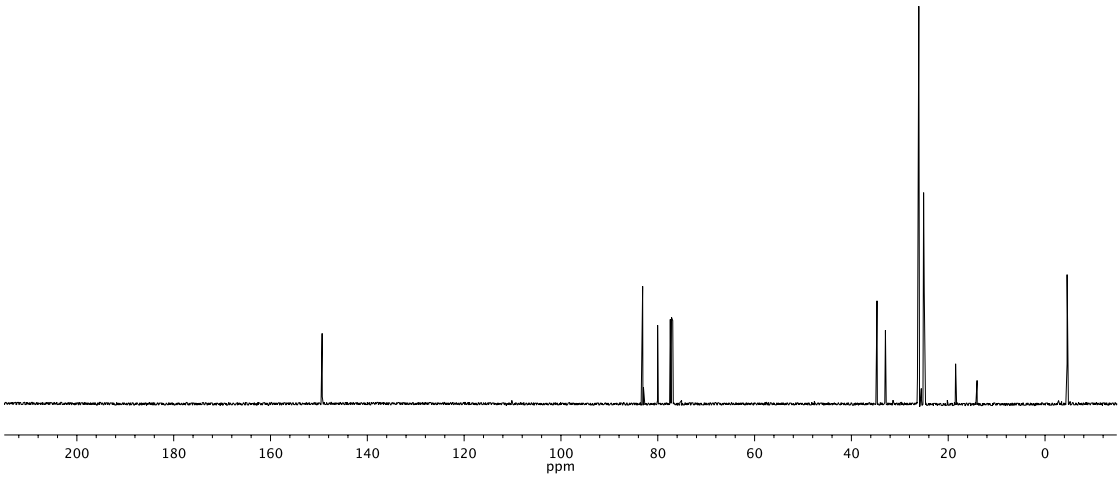

Figure A3.3 ^{13}C NMR (126 MHz, $CDCl_3$) of compound *rac*-**25**

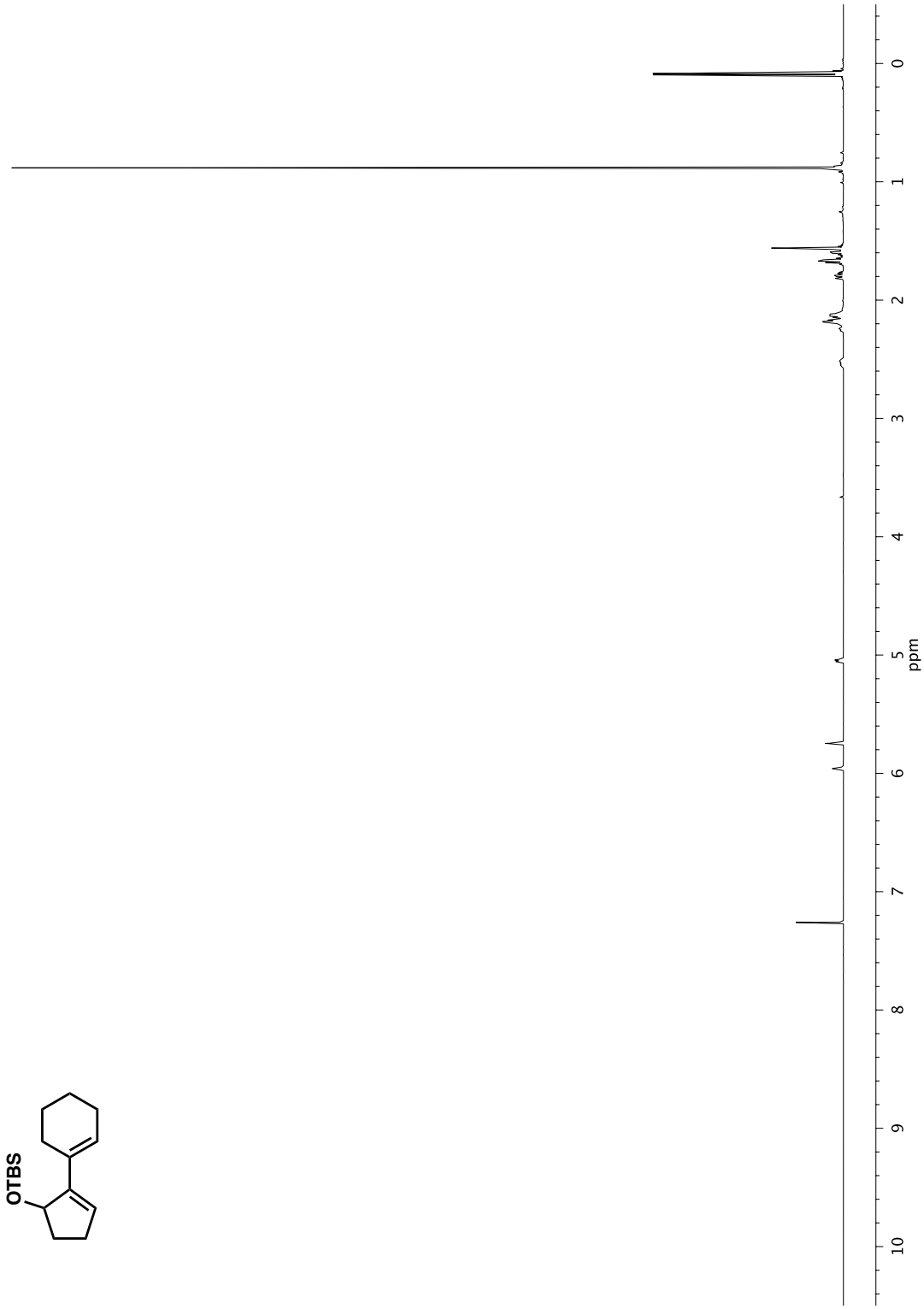

Figure A3.4 ^{1}H NMR (500 MHz, $CDCl_3$) of compound **104**

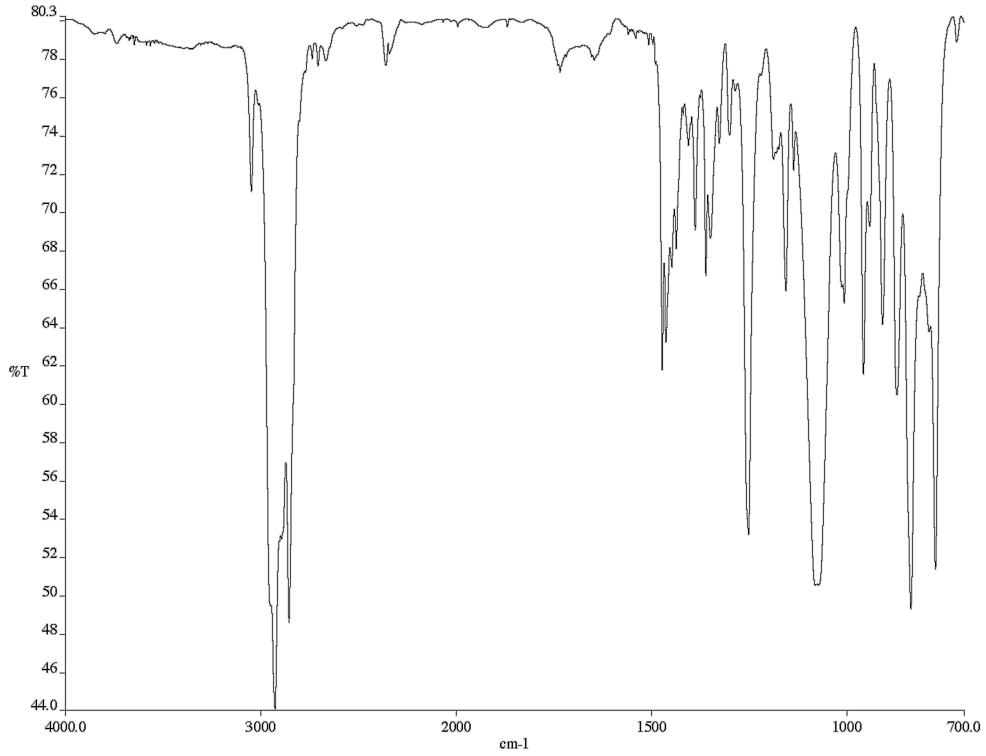

Figure A3.5 Infrared spectrum (thin film/NaCl) of compound **104**

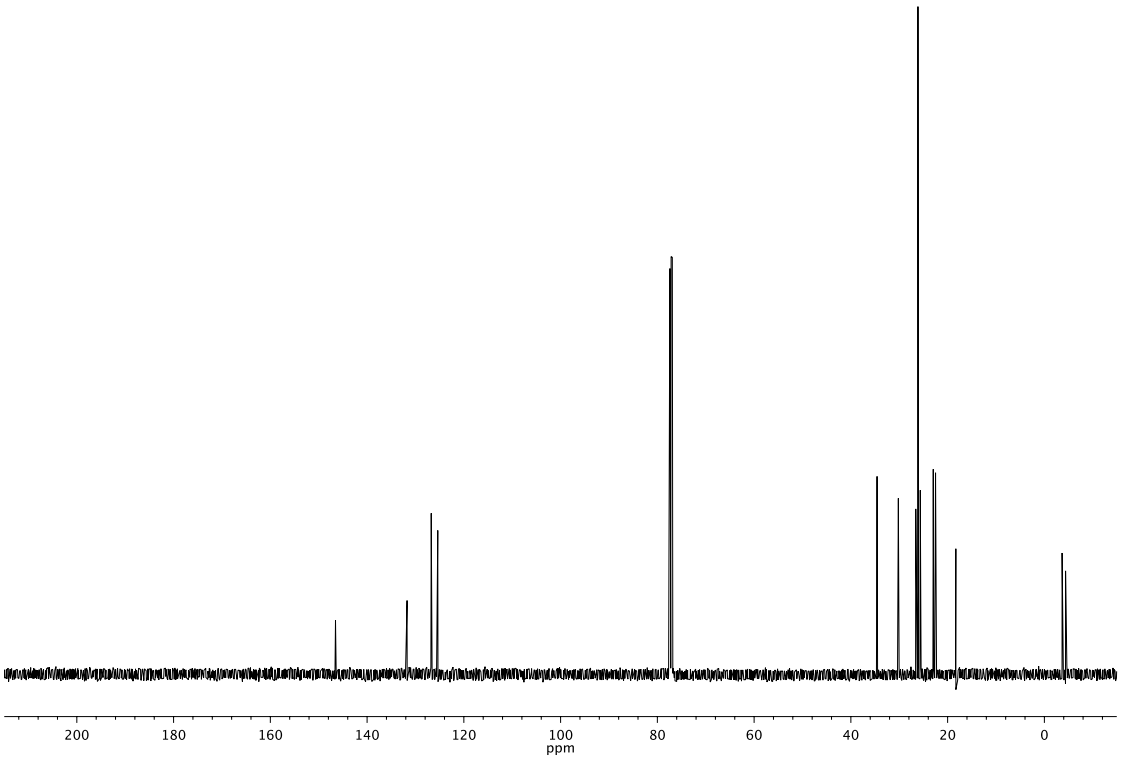

Figure A3.6 ^{13}C NMR (126 MHz, $CDCl_3$) of compound **104**

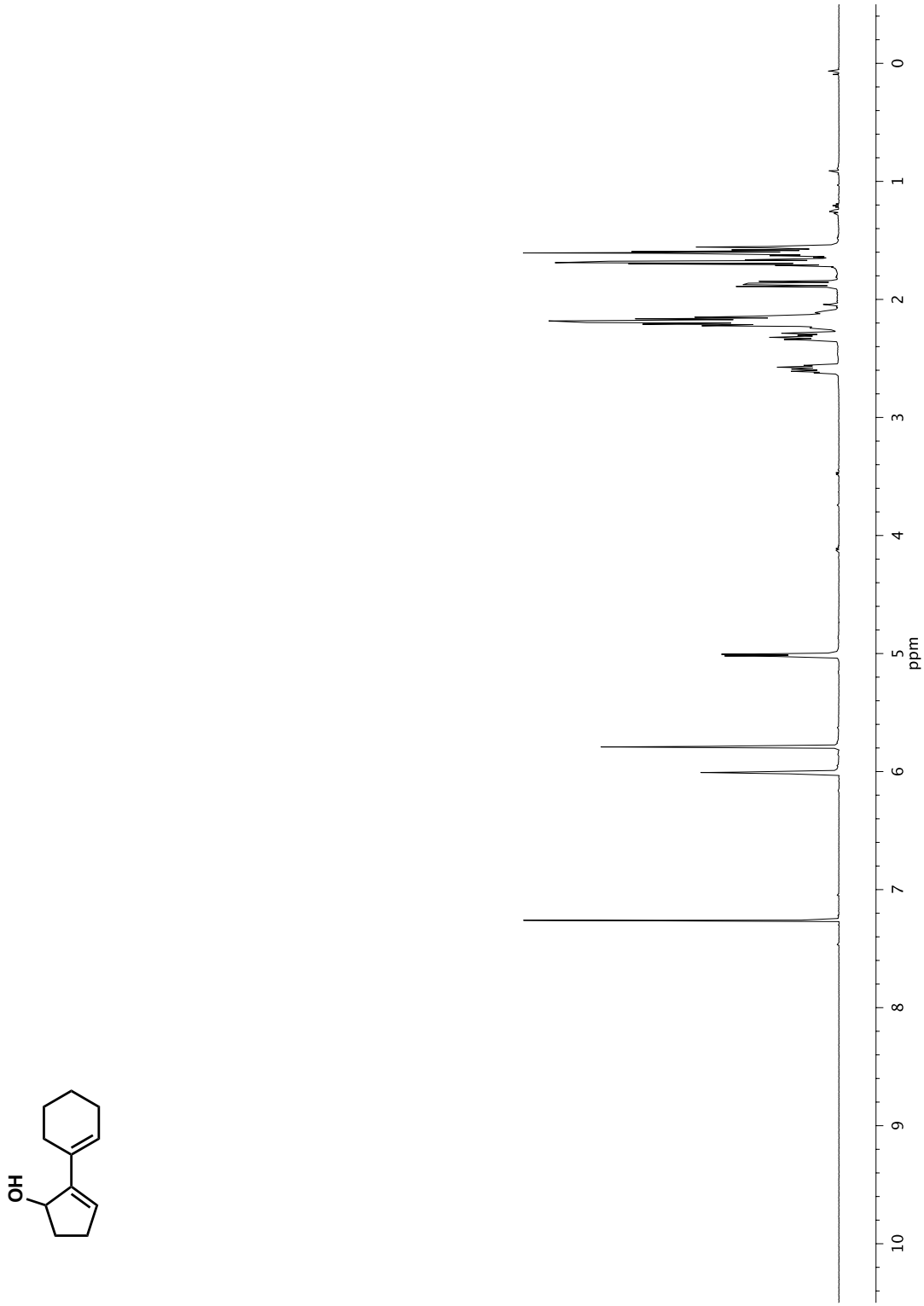

Figure A3.7 ^{1}H NMR (500 MHz, $CDCl_3$) of compound **33**

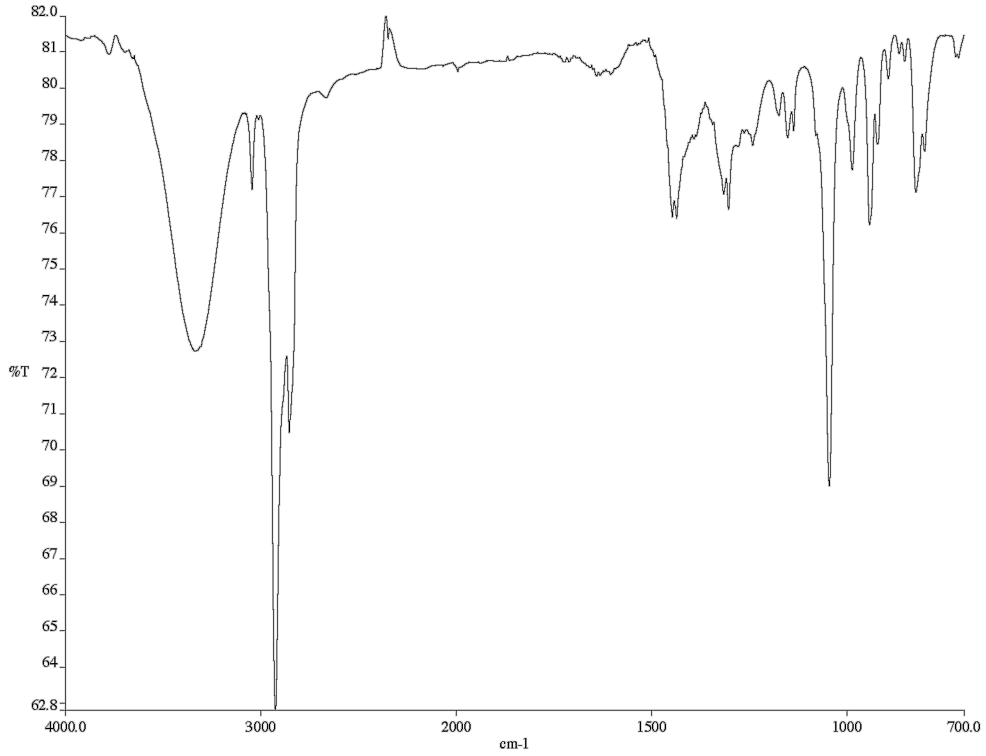

Figure A3.8 Infrared spectrum (thin film/NaCl) of compound **33**

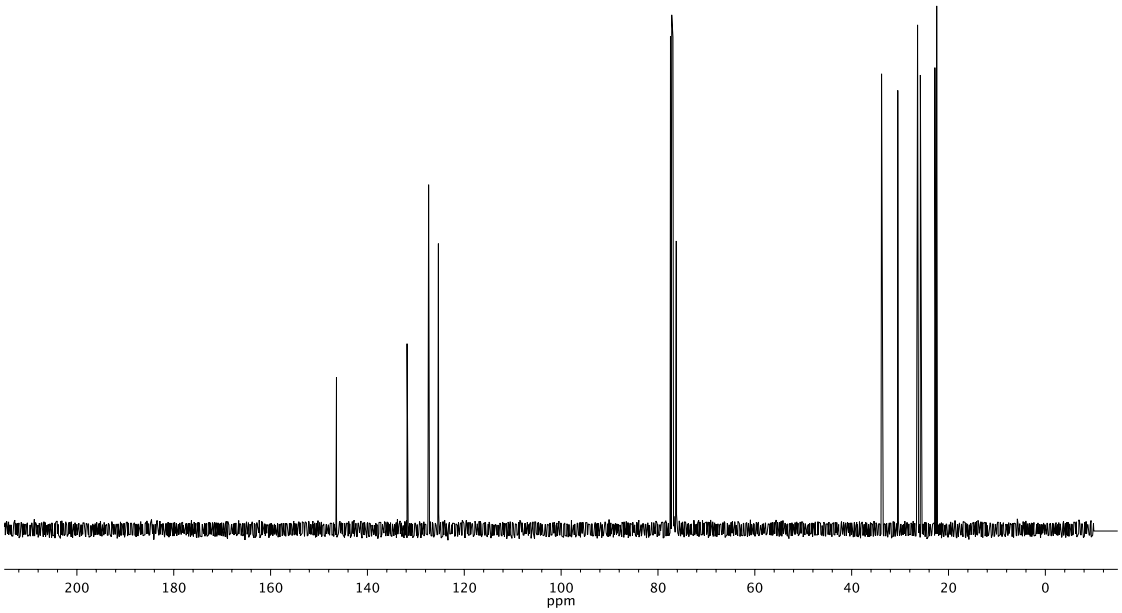

Figure A3.9 ^{13}C NMR (126 MHz, $CDCl_3$) of compound **33**

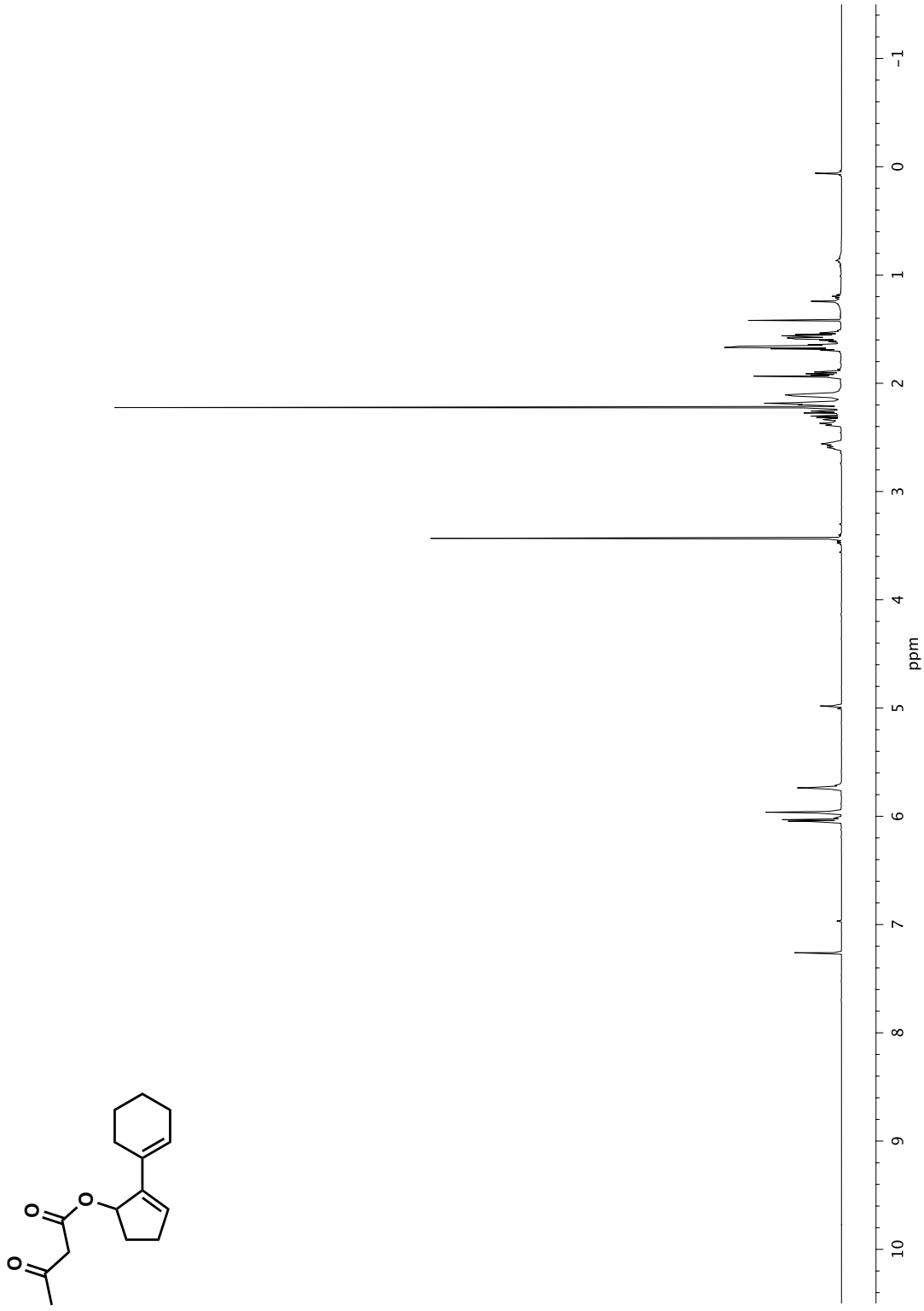

Figure A3.10 ^{1}H NMR (500 MHz, $CDCl_3$) of compound **35**

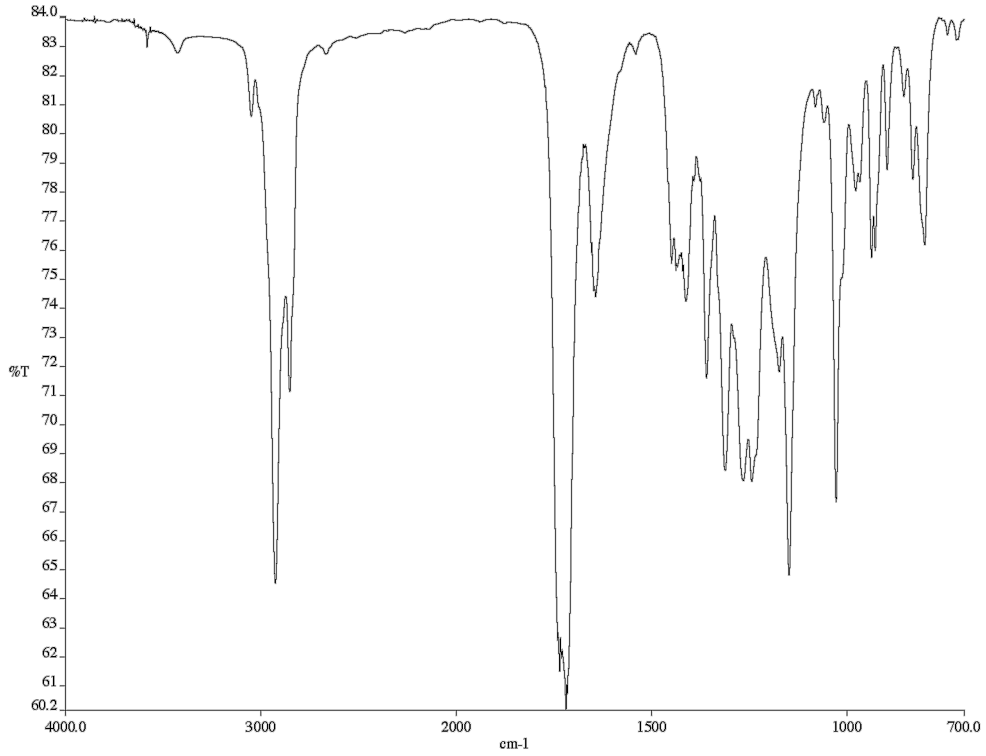

Figure A3.11 Infrared spectrum (thin film/NaCl) of compound **35**

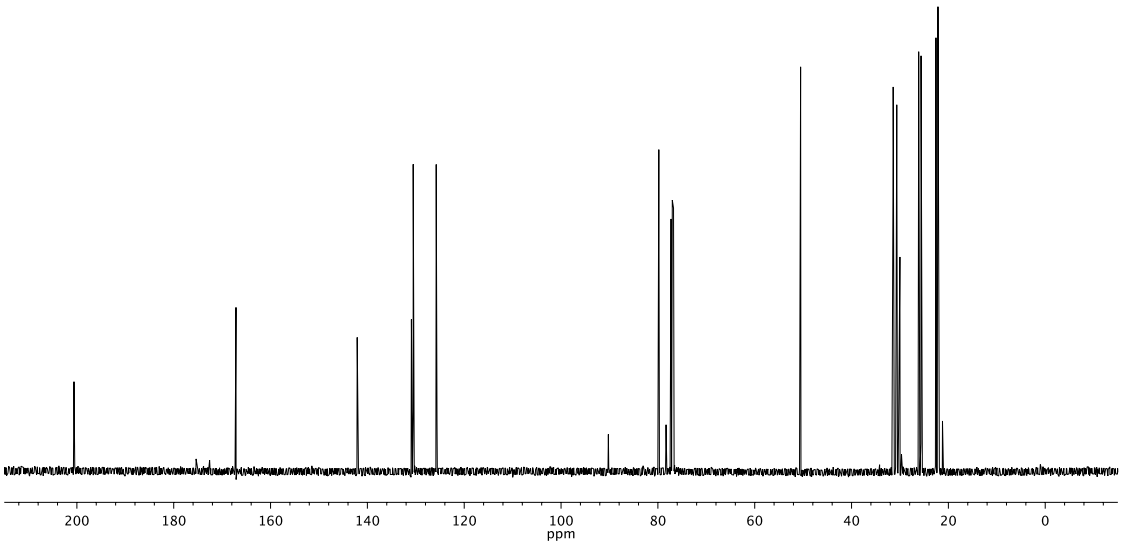

Figure A3.12 ^{13}C NMR (126 MHz, $CDCl_3$) of compound **35**

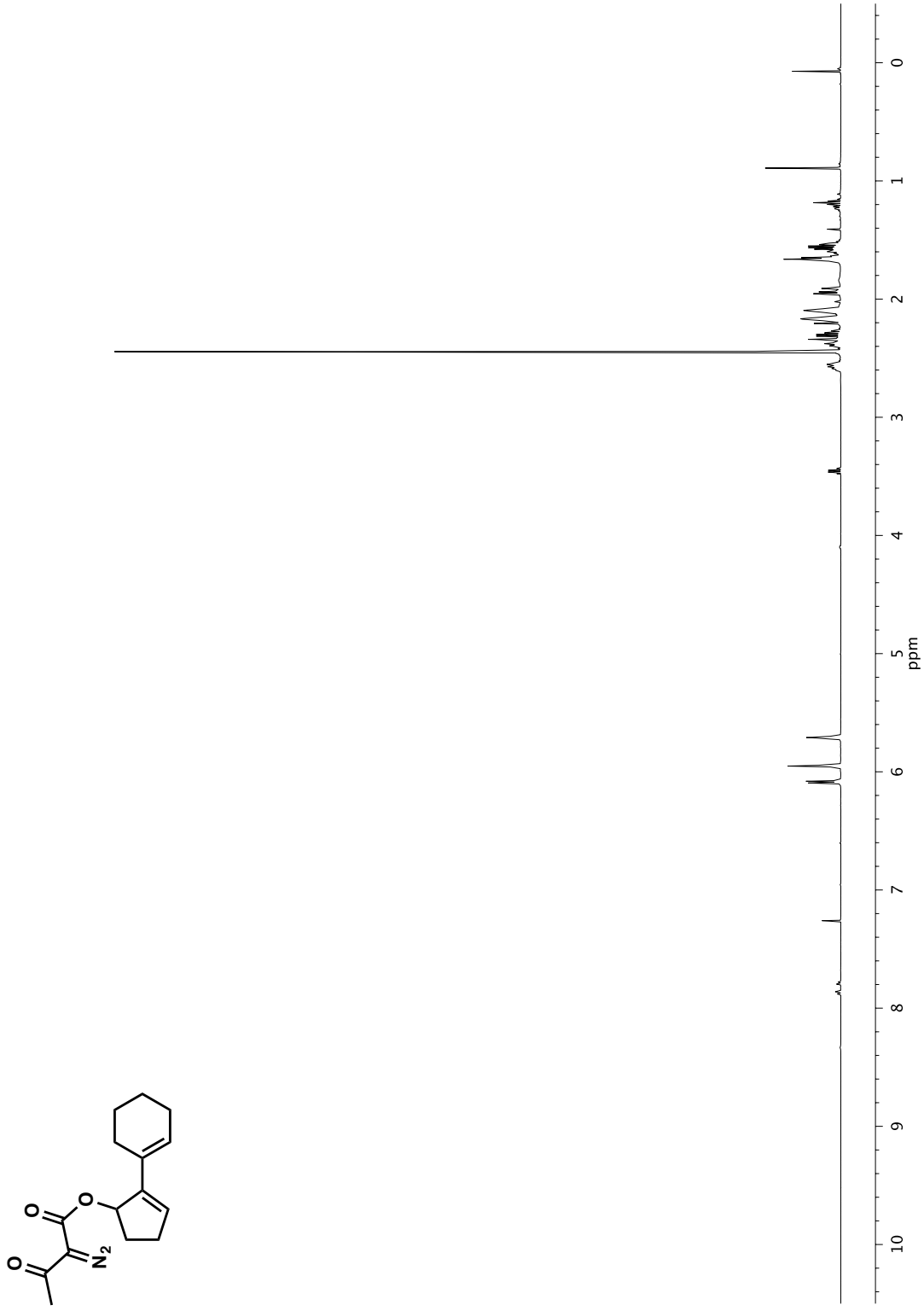

Figure A3.13 ^{1}H NMR (500 MHz, $CDCl_3$) of compound **36**

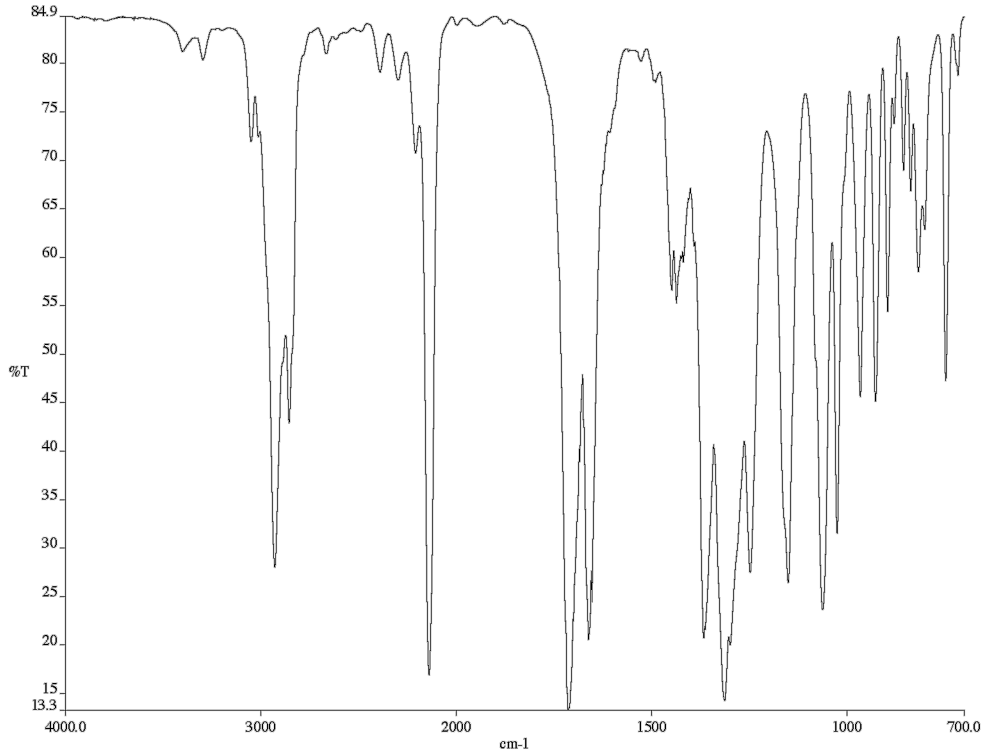

Figure A3.14 Infrared spectrum (thin film/NaCl) of compound **36**

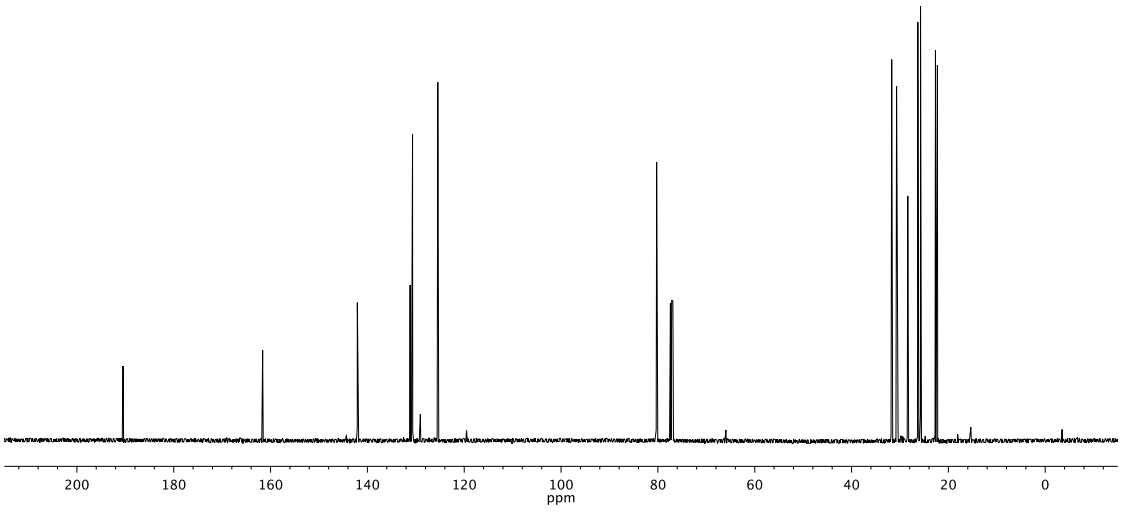

Figure A3.15 ^{13}C NMR (126 MHz, $CDCl_3$) of compound **36**

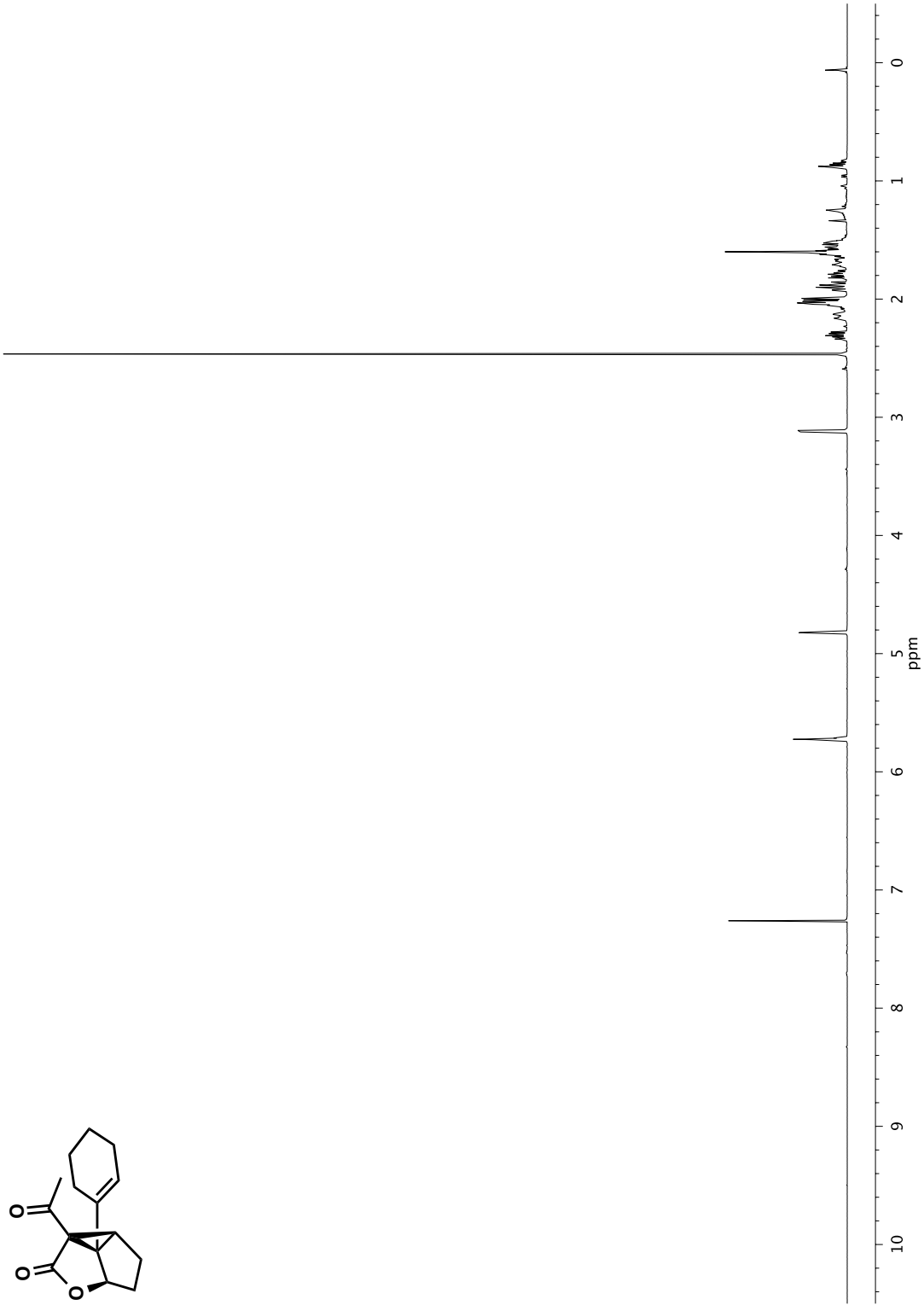

Figure A3.16 ^{1}H NMR (500 MHz, $CDCl_3$) of compound **37**

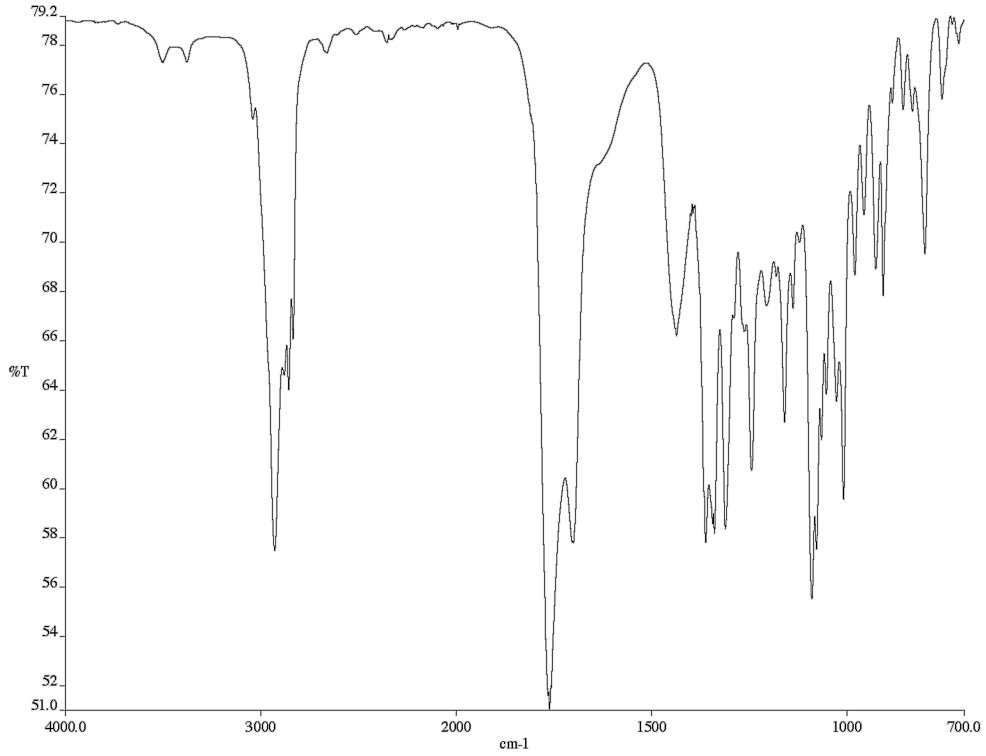

Figure A3.17 Infrared spectrum (thin film/NaCl) of compound **37**

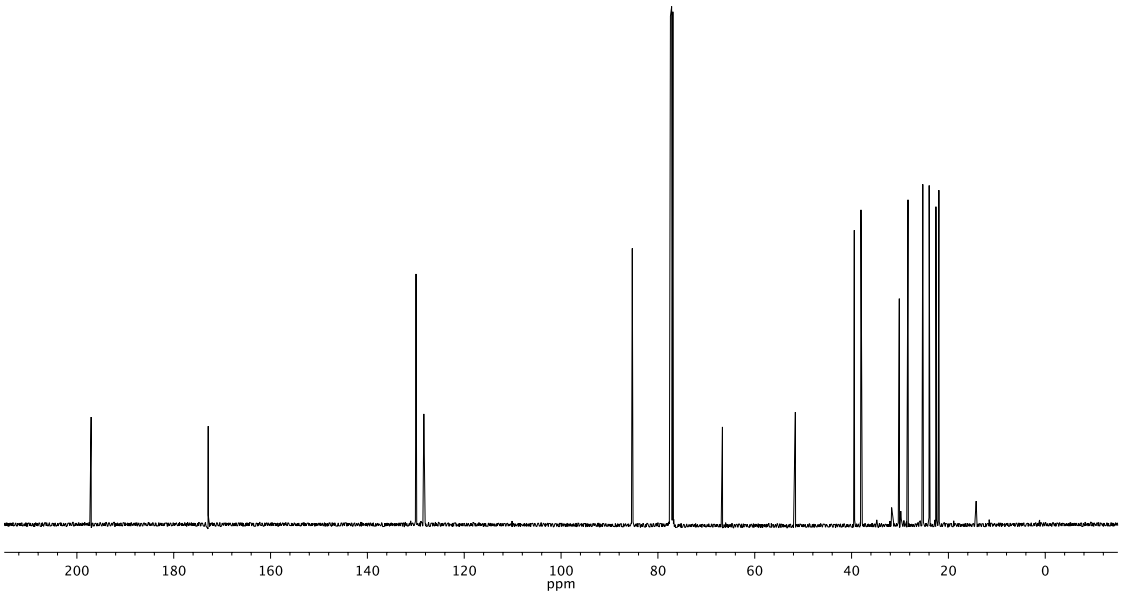

Figure A3.18 ^{13}C NMR (126 MHz, $CDCl_3$) of compound **37**

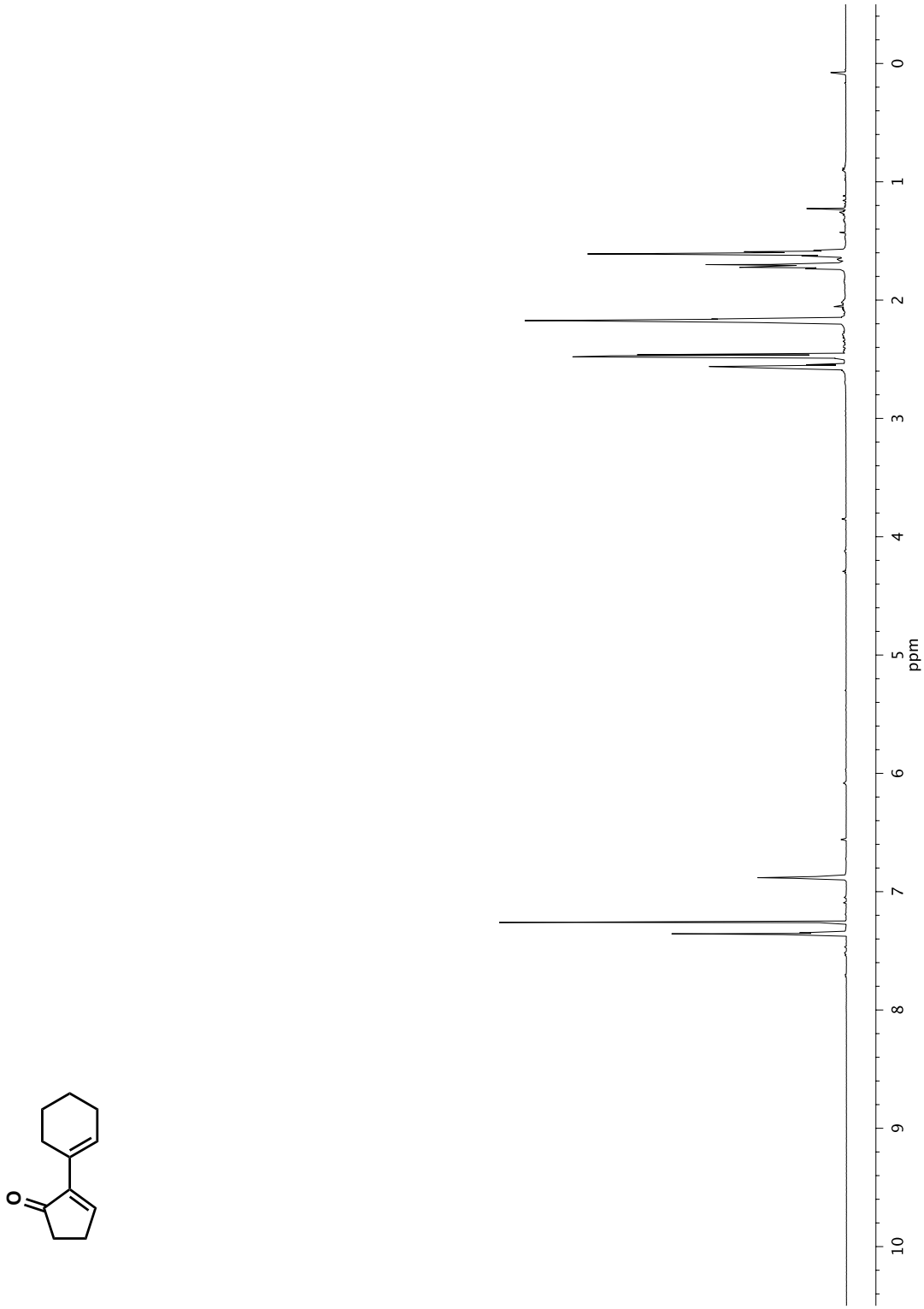

Figure A3.19. ^{1}H NMR (500 MHz, $CDCl_3$) of compound **38**

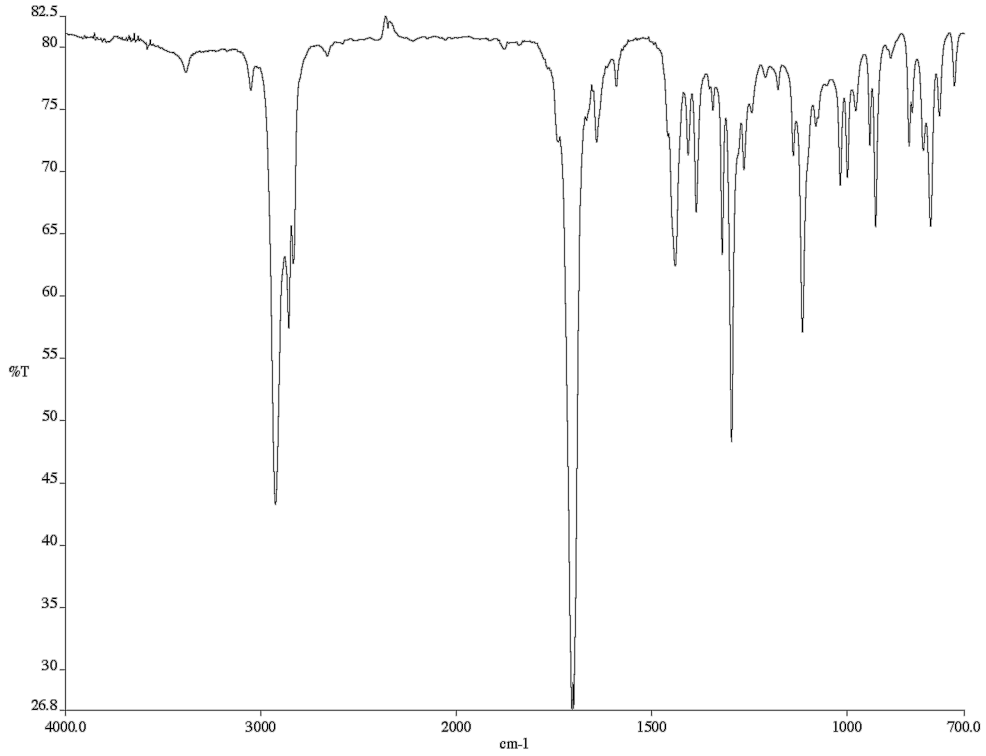

Figure A3.20 Infrared spectrum (thin film/NaCl) of compound **38**

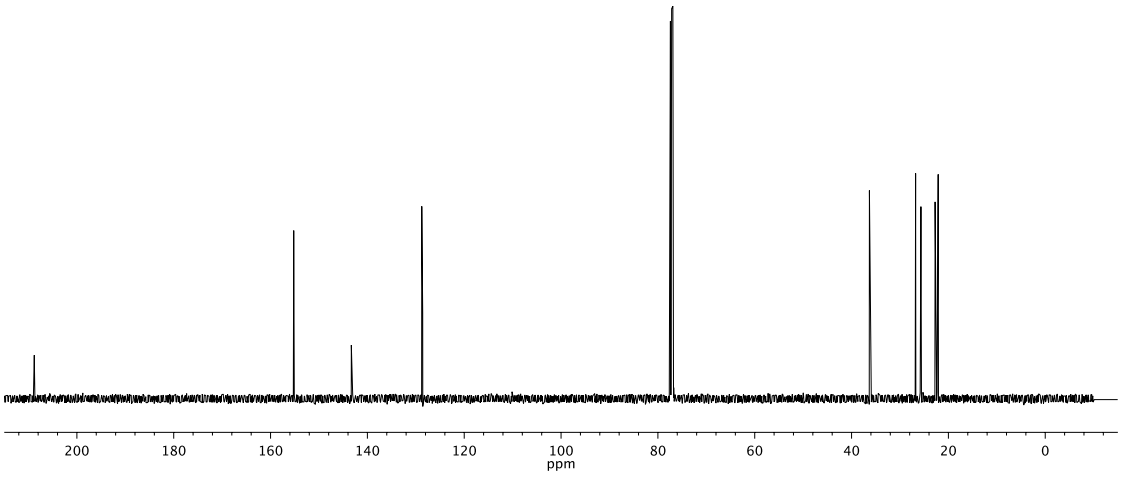

Figure A3.21 ^{13}C NMR (126 MHz, $CDCl_3$) of compound **38**

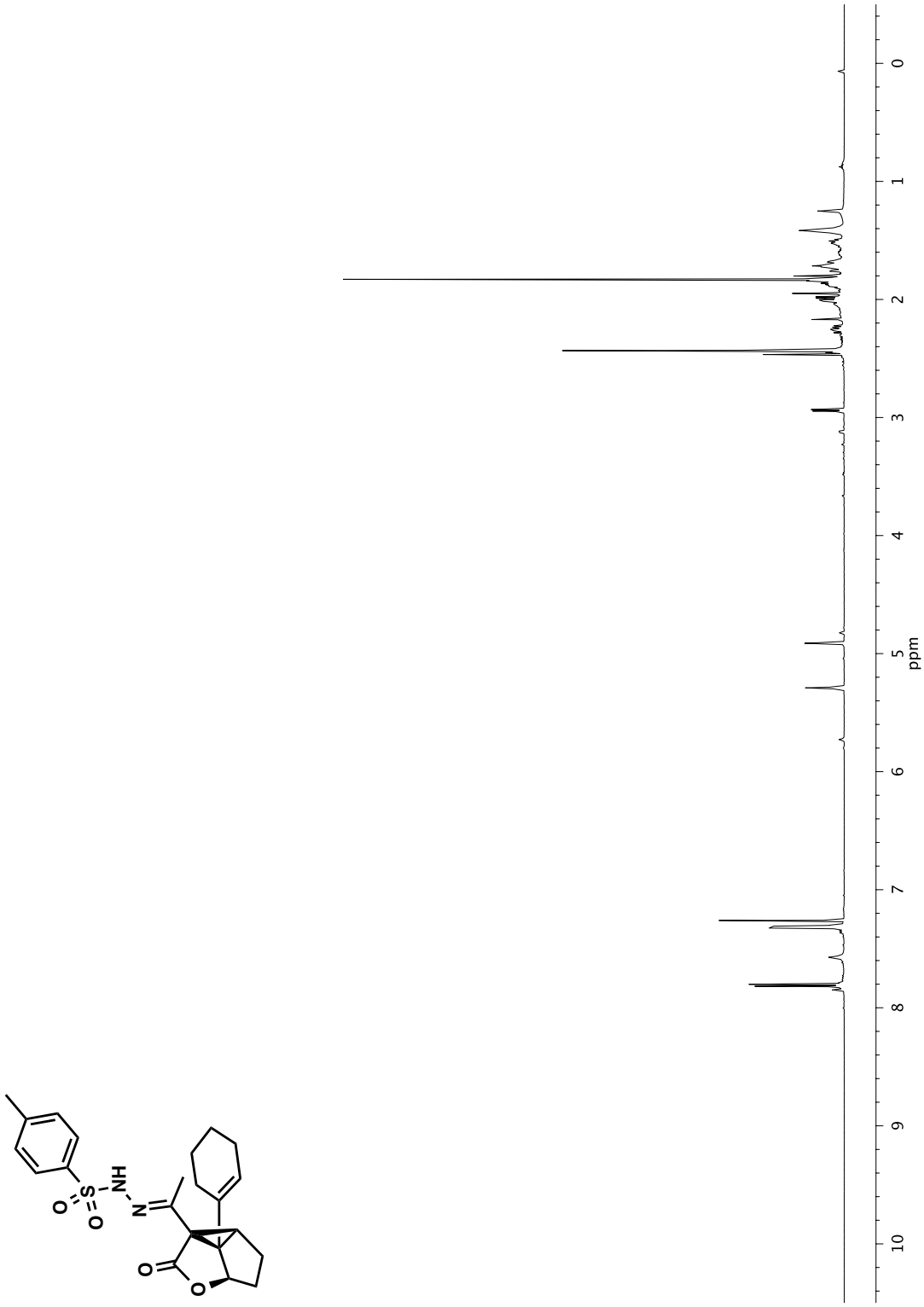

Figure A3.22 ^{1}H NMR (500 MHz, $CDCl_3$) of compound **42**

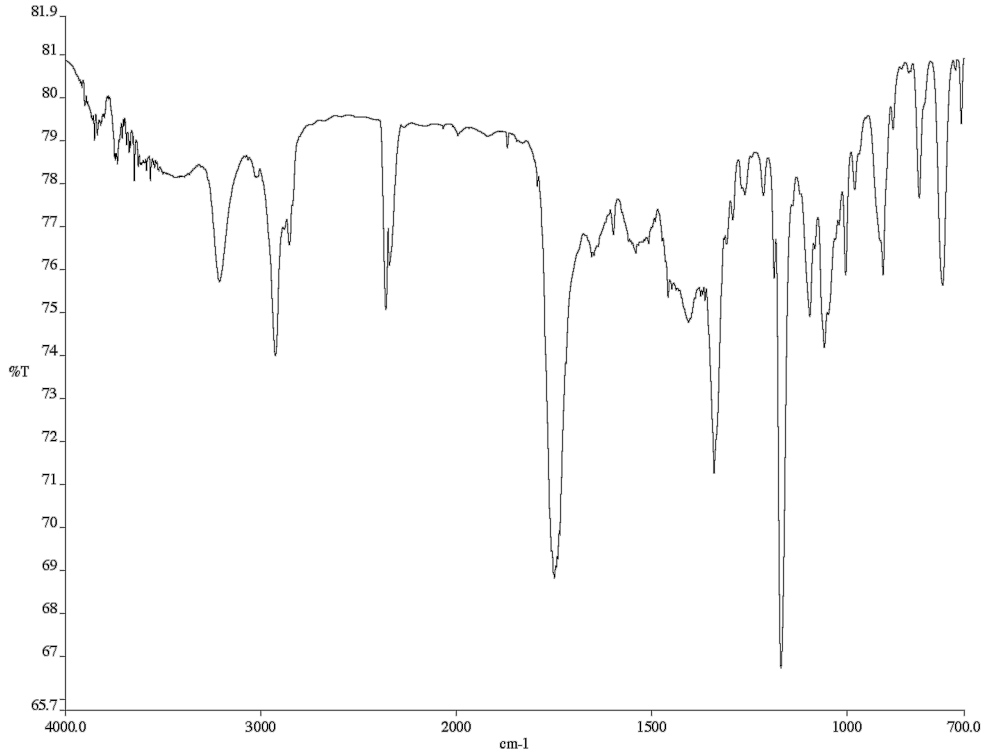

Figure A3.23 Infrared spectrum (thin film/NaCl) of compound **42**

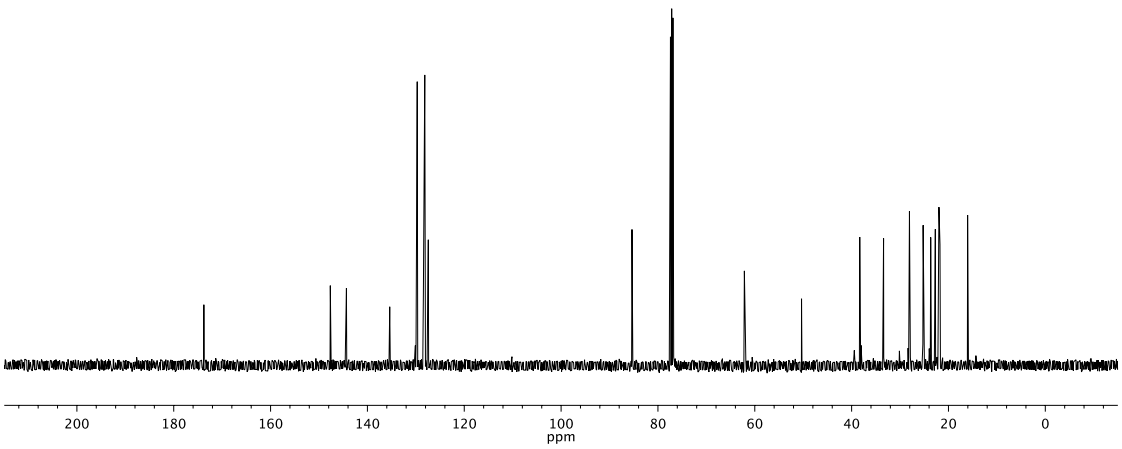

Figure A3.24 ^{13}C NMR (126 MHz, $CDCl_3$) of compound **42**

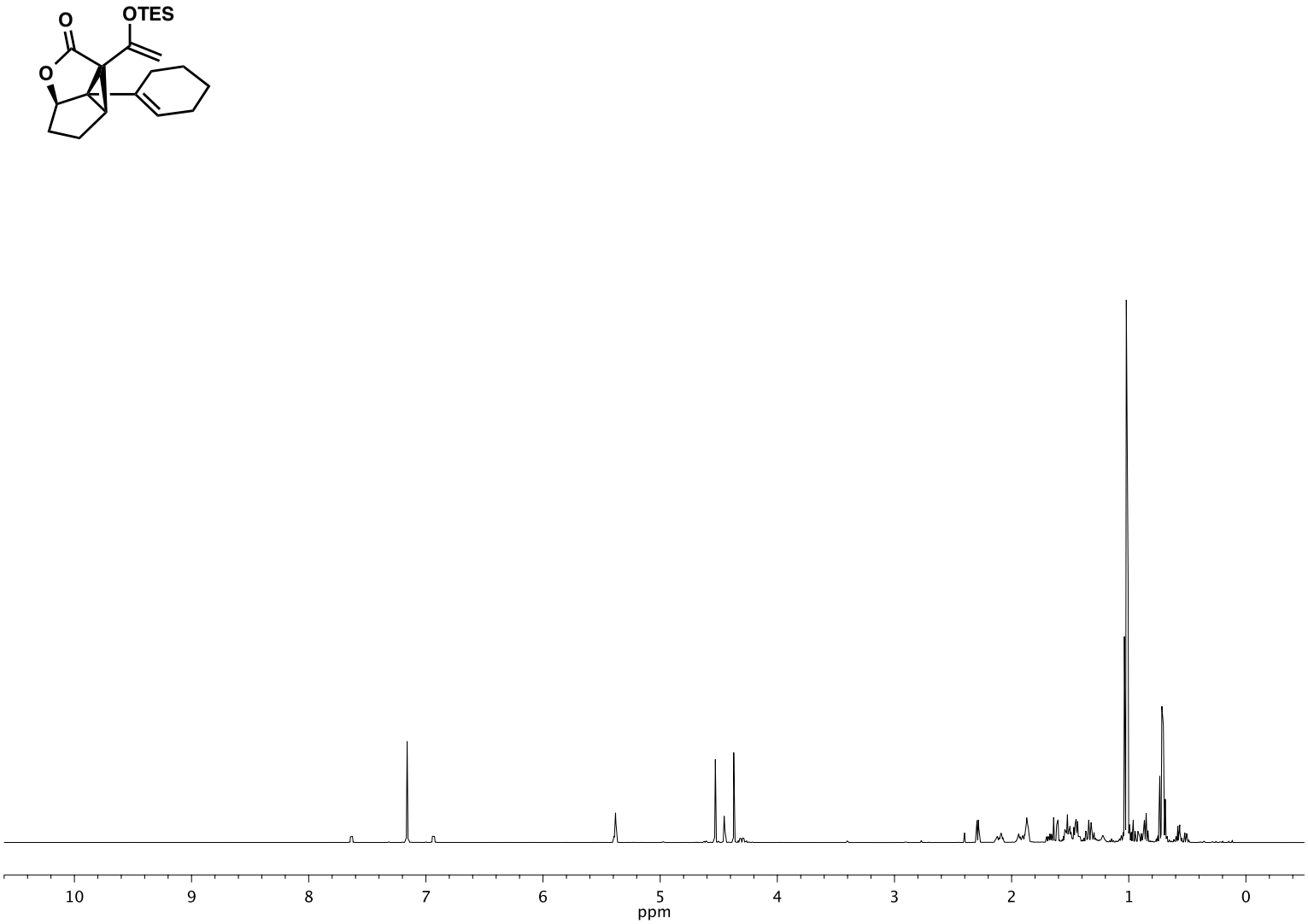

Figure A3.25 ^{1}H NMR (500 MHz, C_6D_6) of compound **43**

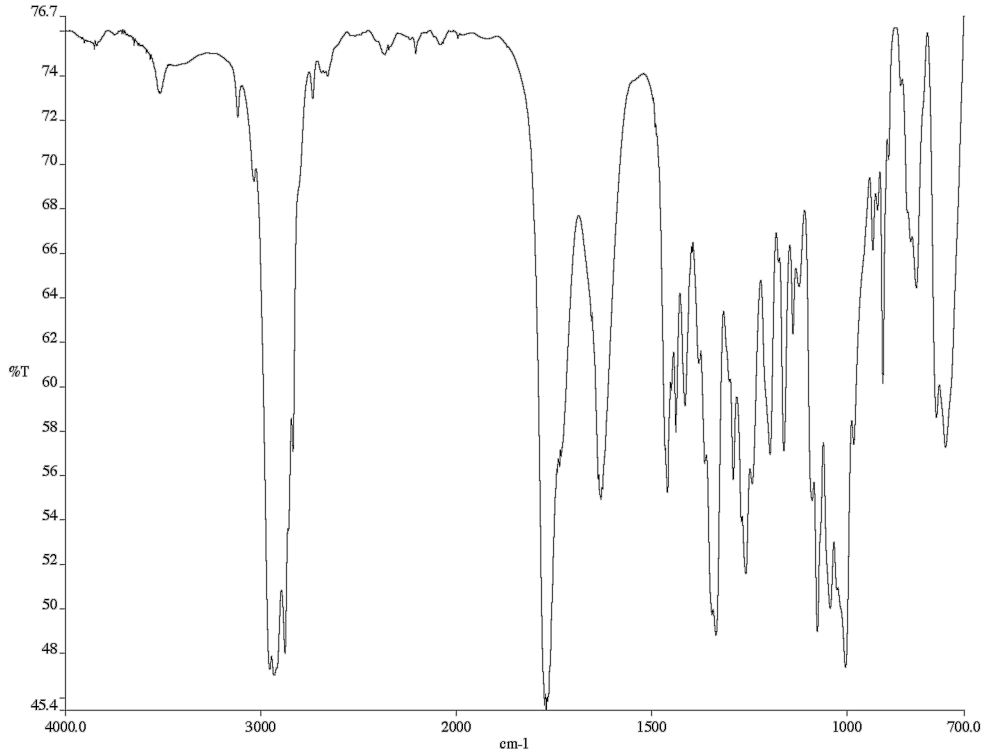

Figure A3.26 Infrared spectrum (thin film/NaCl) of compound **43**

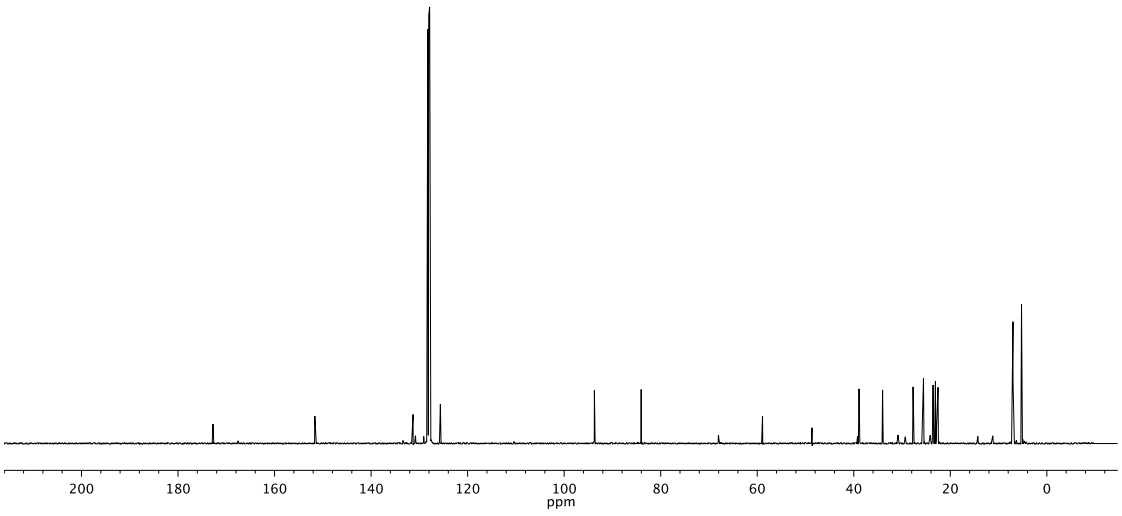

Figure A3.27 ^{13}C NMR (126 MHz, C_6D_6) of compound **43**

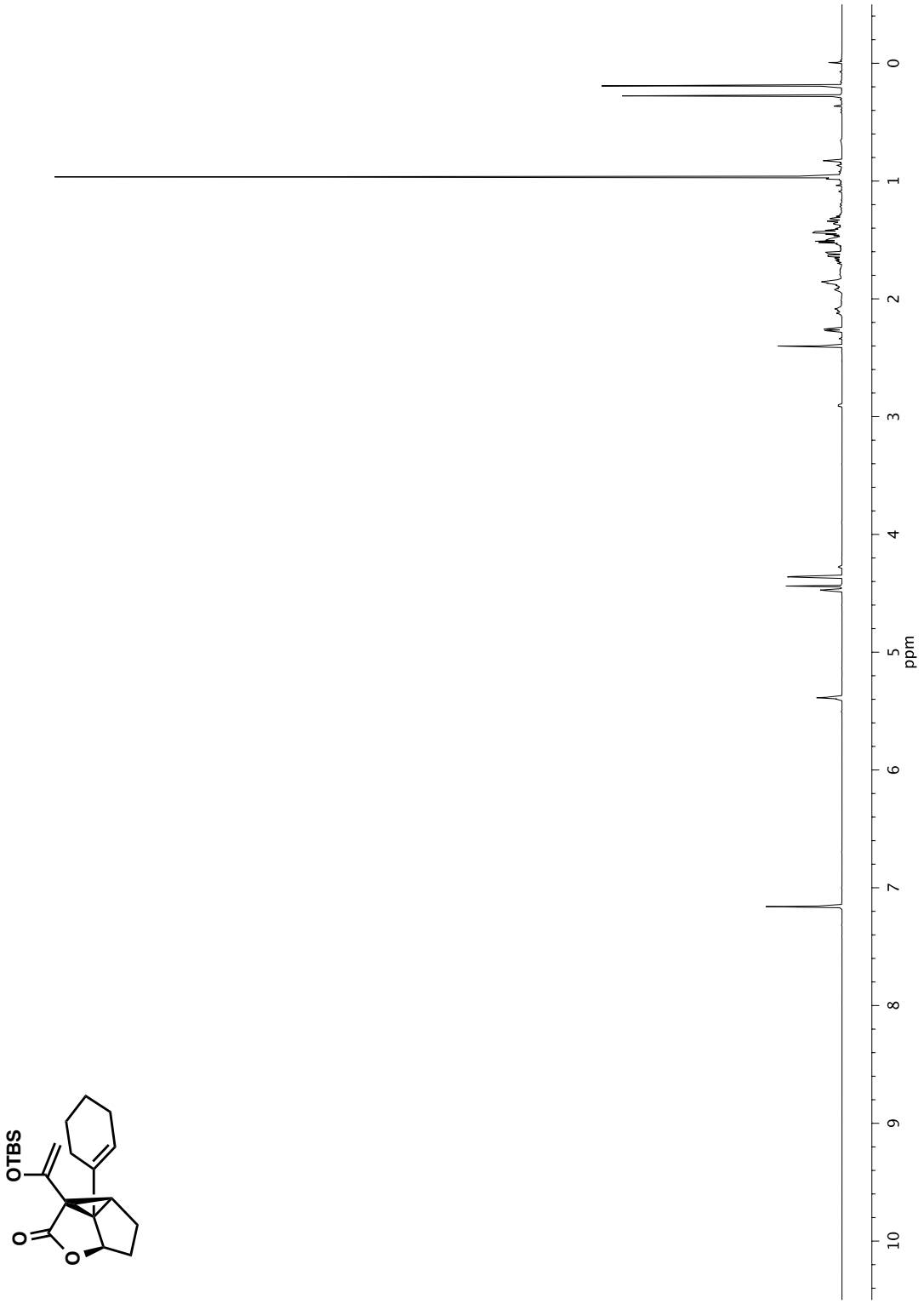

Figure A3.28 ^{1}H NMR (500 MHz, C_6D_6) of compound **44**

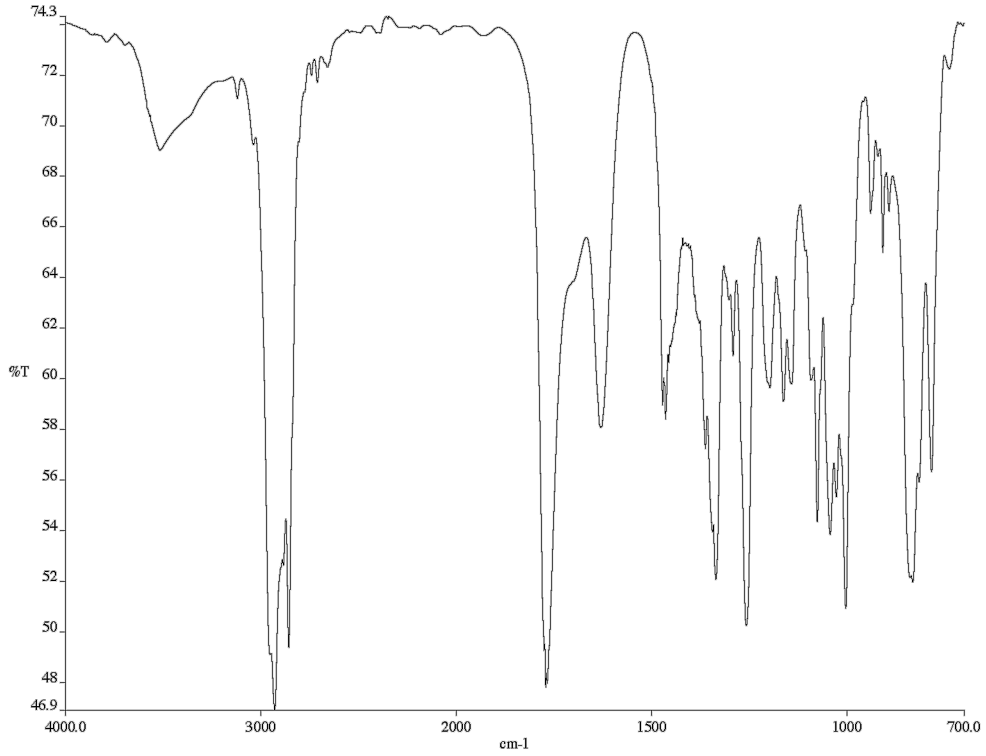

Figure A3.29 Infrared spectrum (thin film/NaCl) of compound **44**

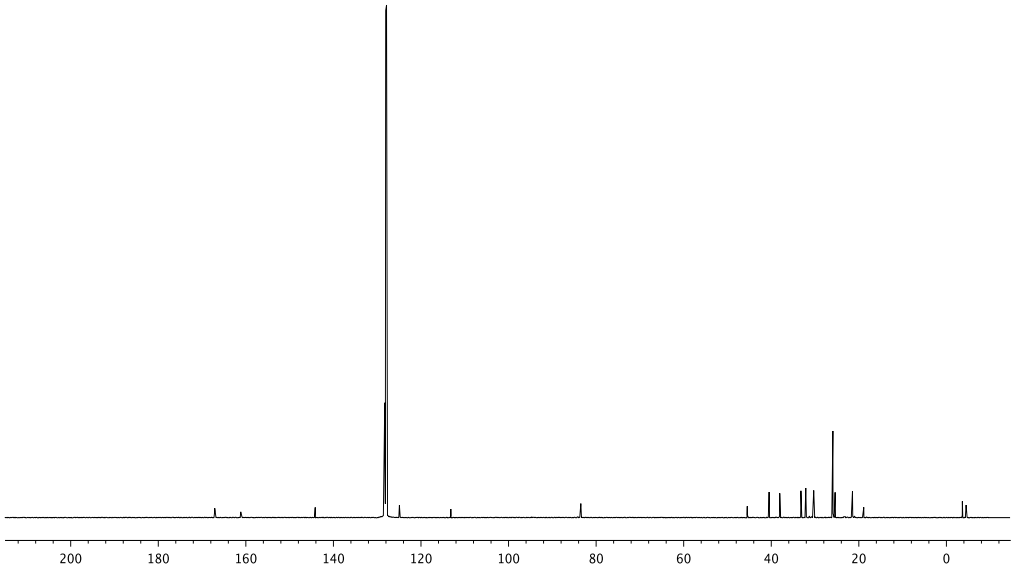

Figure A3.30 ^{13}C NMR (126 MHz, C_6D_6) of compound **44**

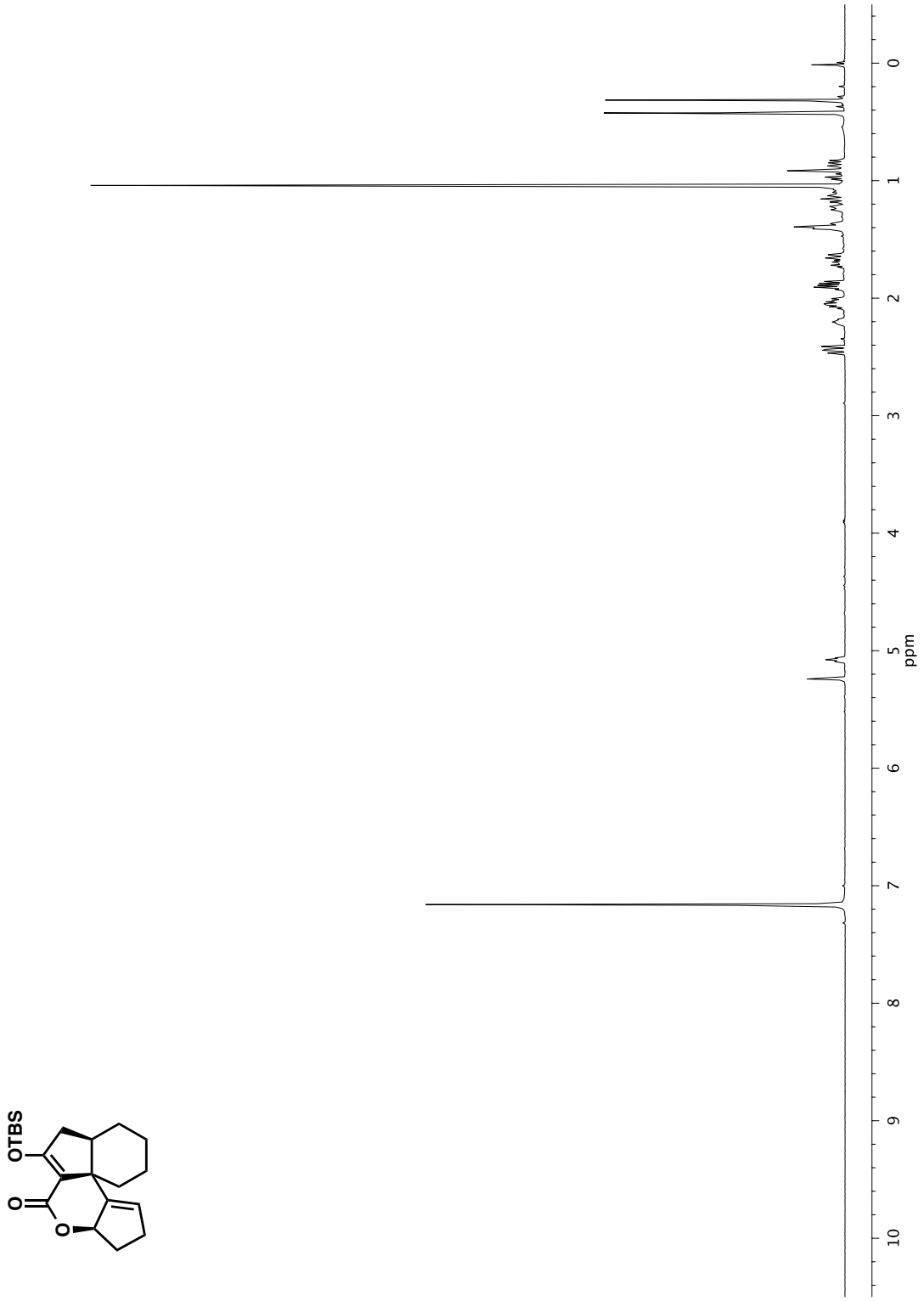

Figure A3.31 ^{1}H NMR (500 MHz, C_6D_6) of compound **47**

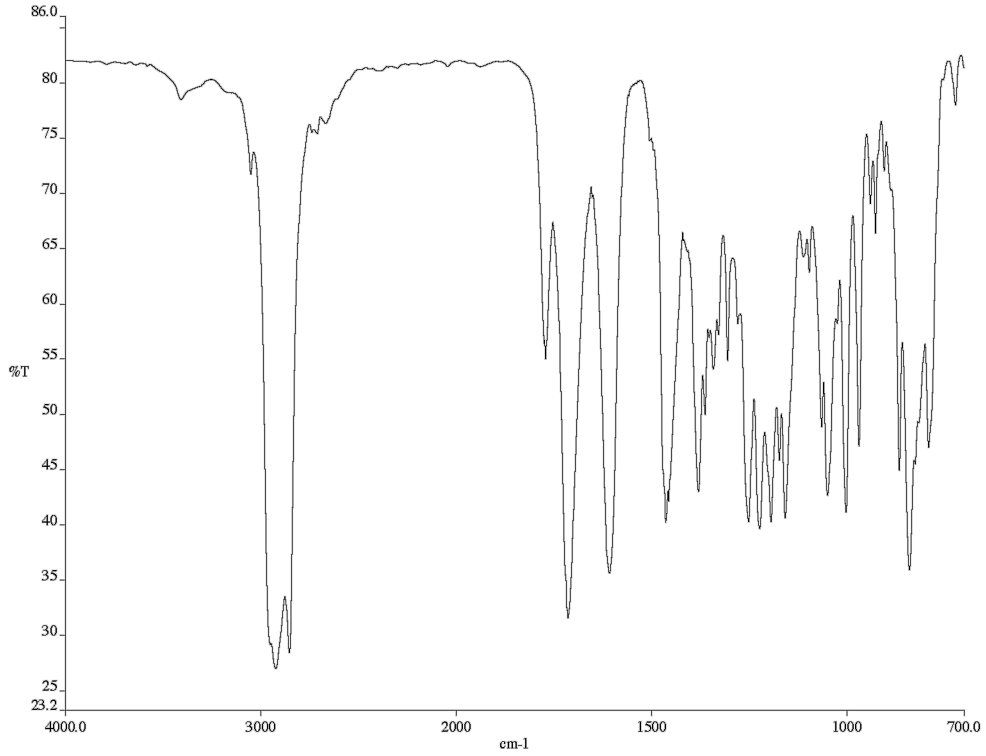

Figure A3.32 Infrared spectrum (thin film/NaCl) of compound **47**

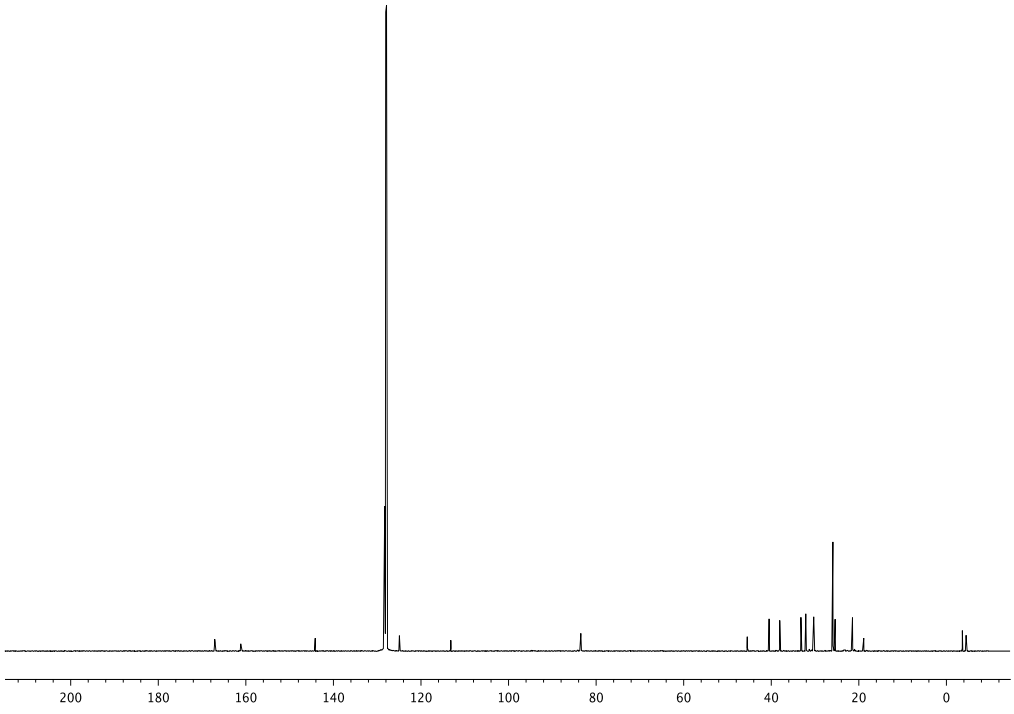

Figure A3.33 ^{13}C NMR (126 MHz, C_6D_6) of compound **47**

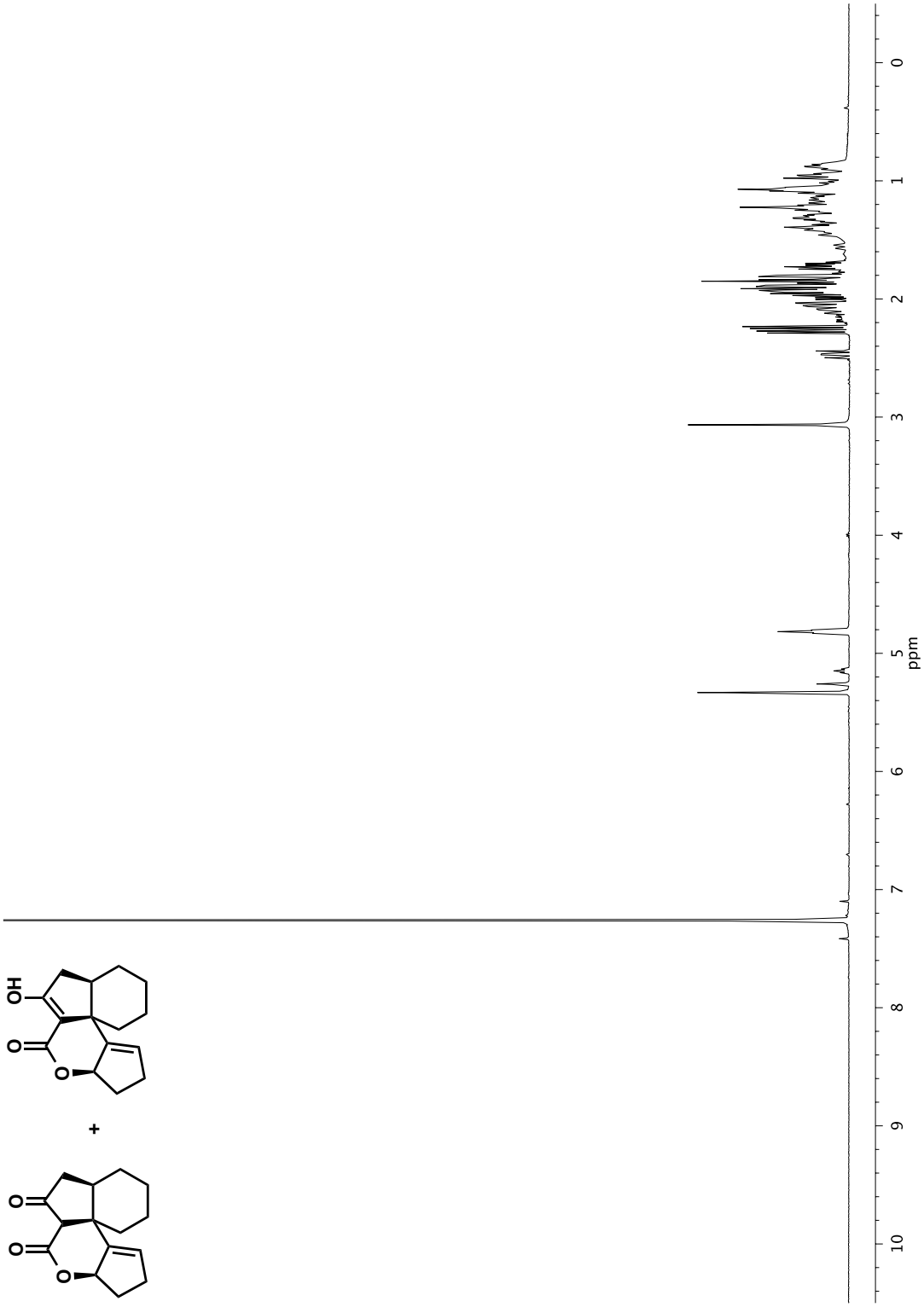

Figure A3.34 ^{1}H NMR (500 MHz, $CDCl_3$) of compound **48**

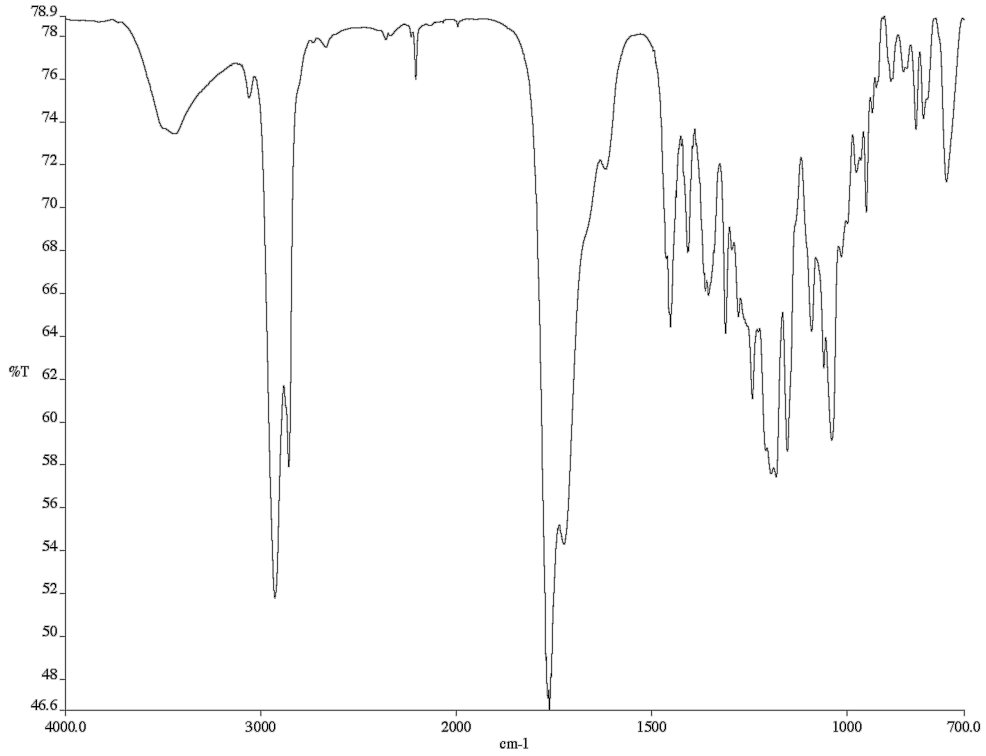

Figure A3.35 Infrared spectrum (thin film/NaCl) of compound **48**

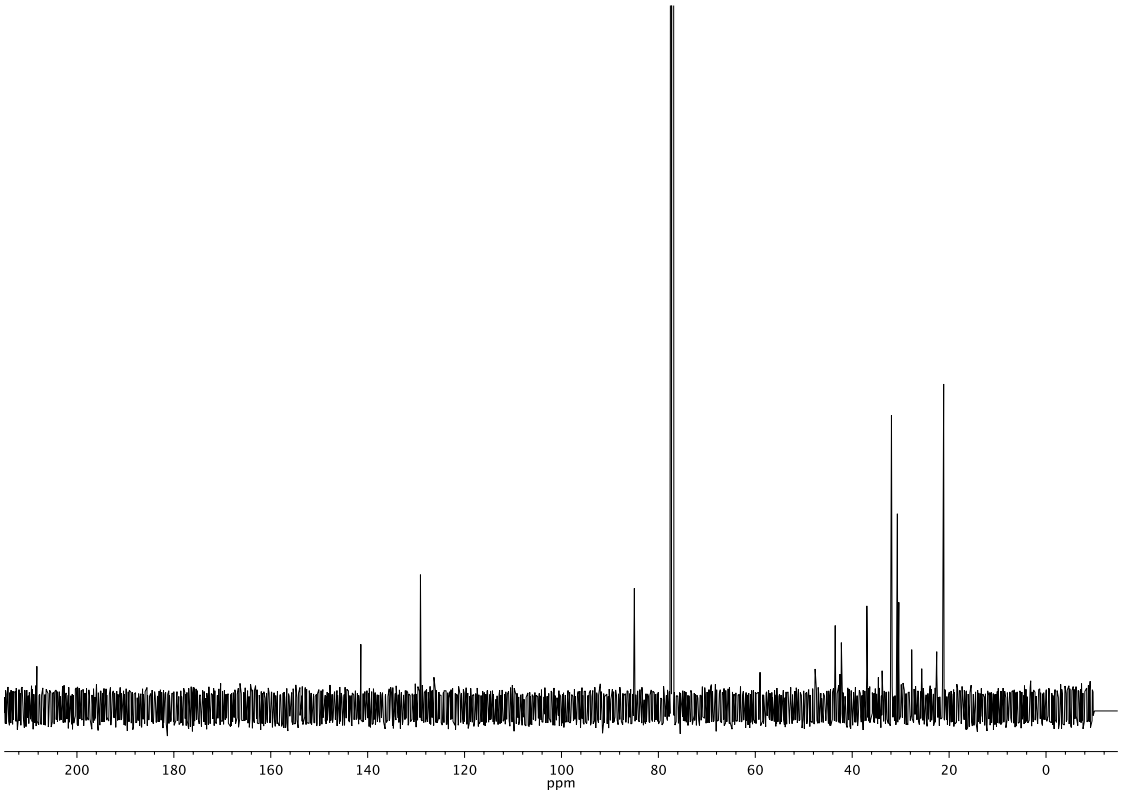

Figure A3.36 ^{13}C NMR (126 MHz, $CDCl_3$) of compound **48**

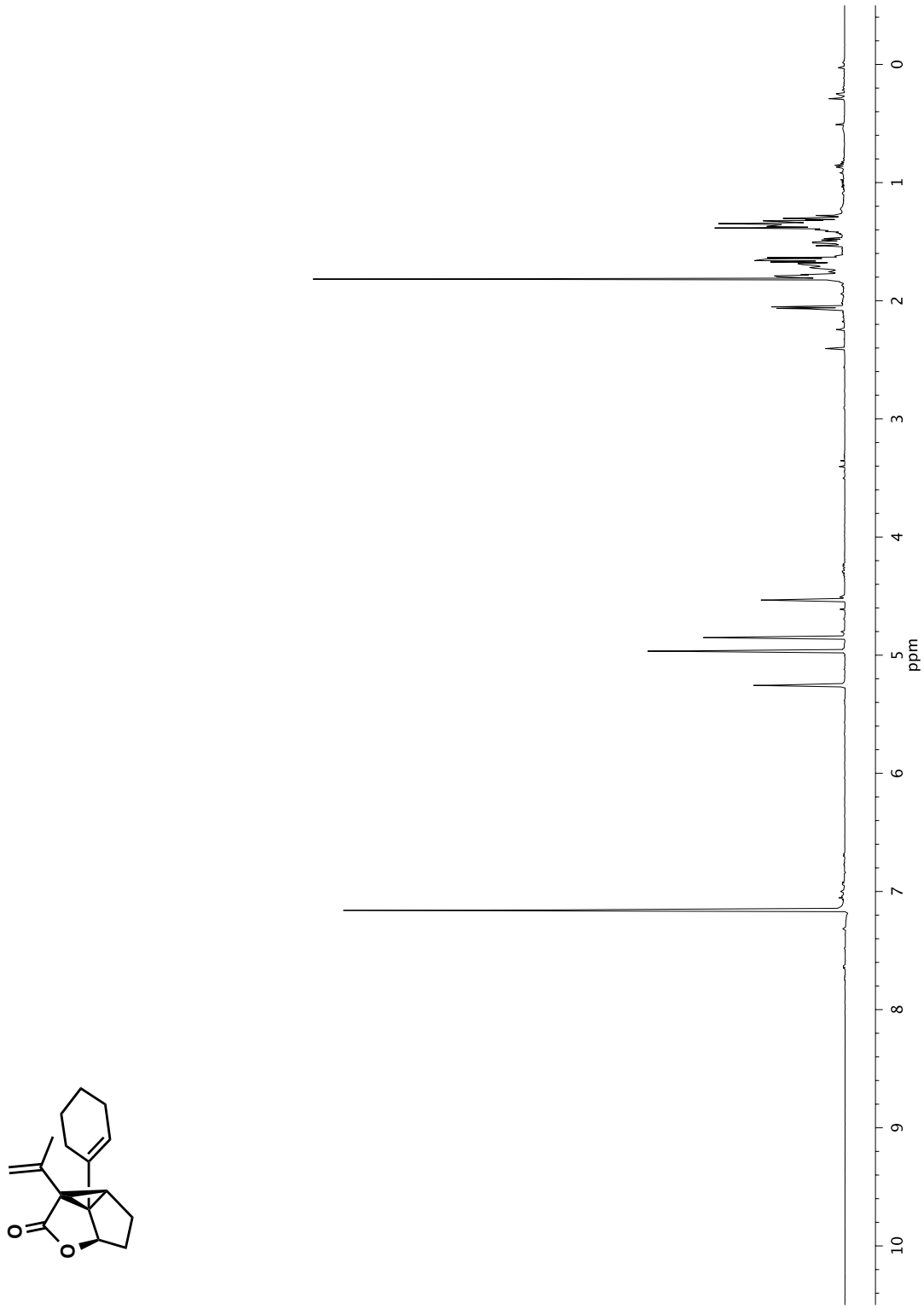

Figure A3.37 ^{1}H NMR (500 MHz, C_6D_6) of compound **51**

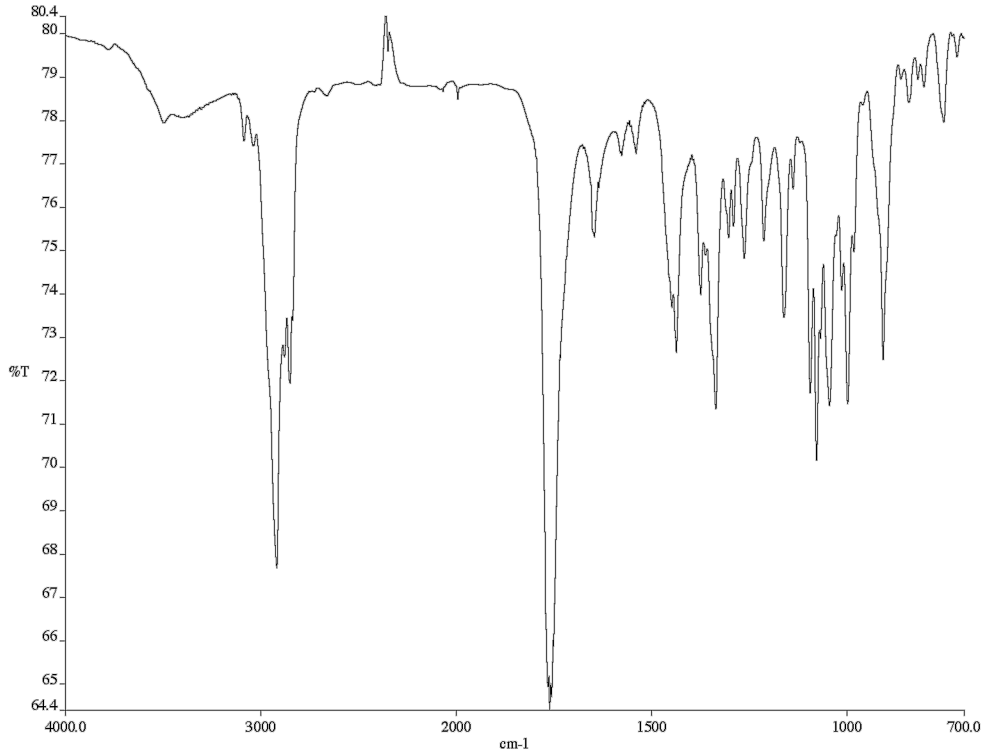

Figure A3.38 Infrared spectrum (thin film/NaCl) of compound **51**

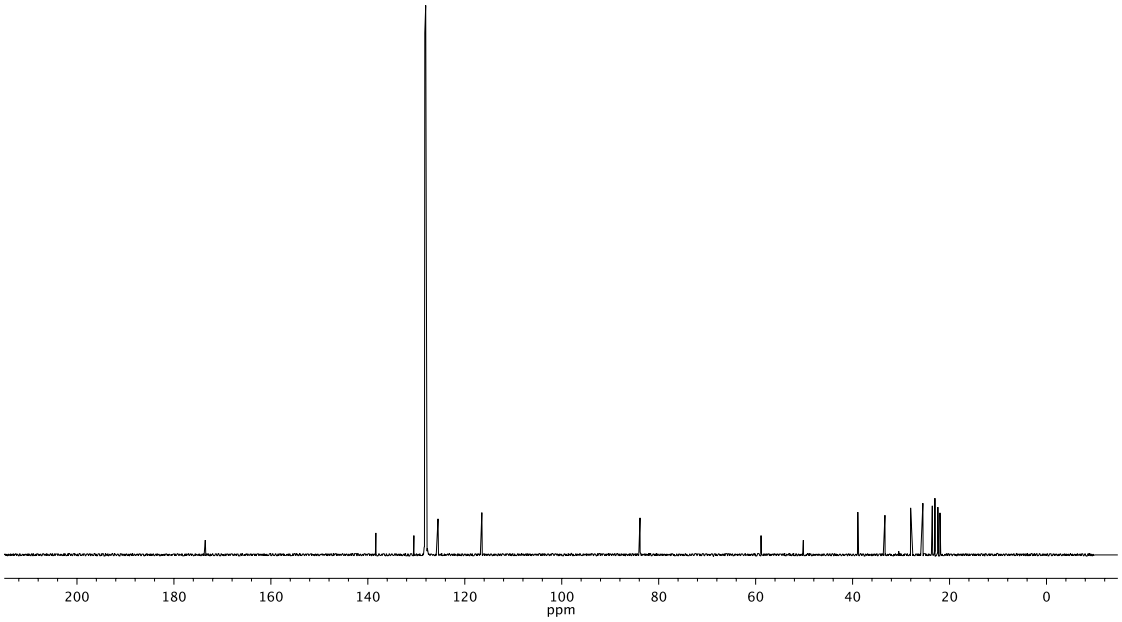

Figure A3.39 ^{13}C NMR (126 MHz, C_6D_6) of compound **51**

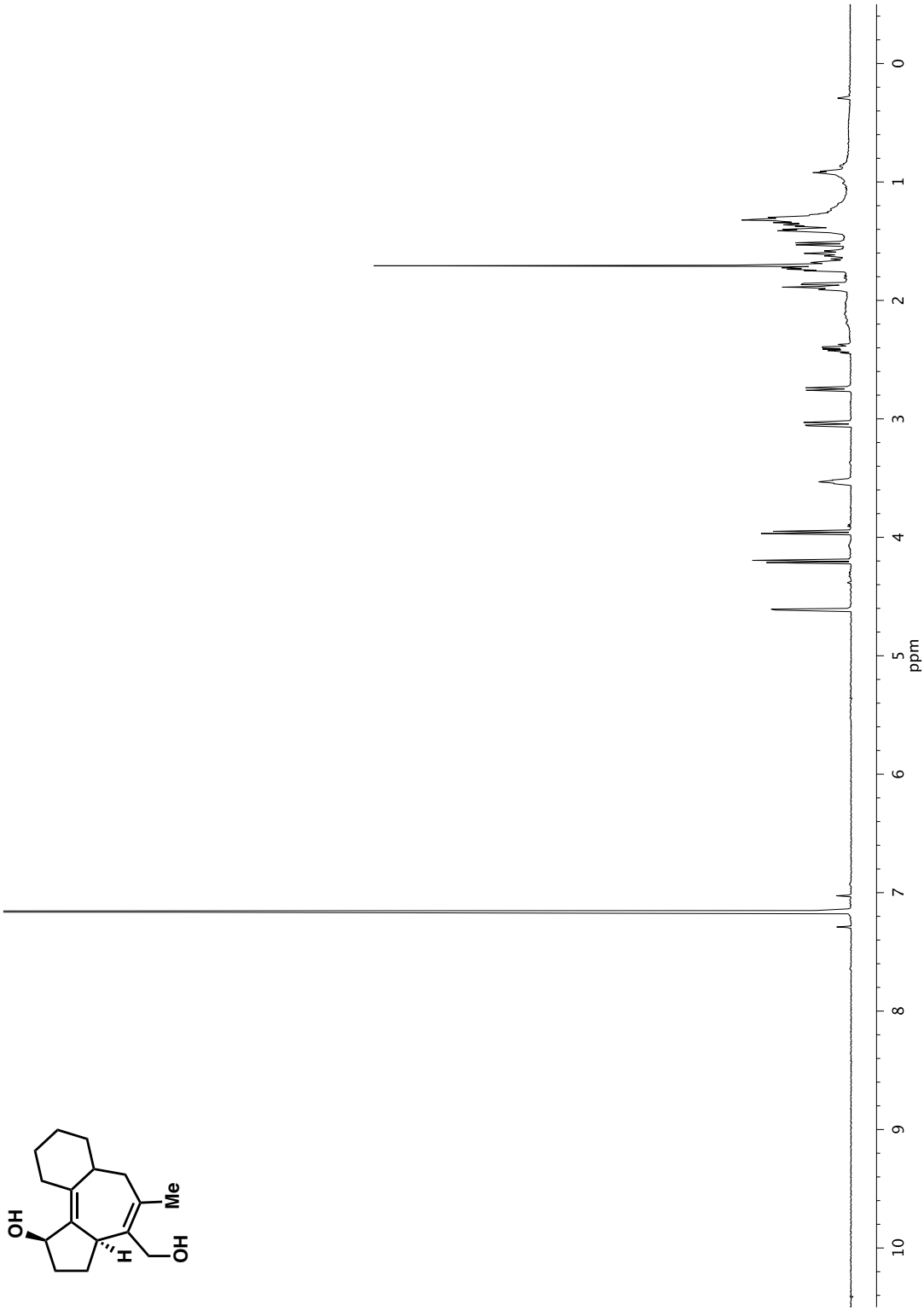

Figure A3.40 ^{1}H NMR (500 MHz, C_6D_6) of compound **53**

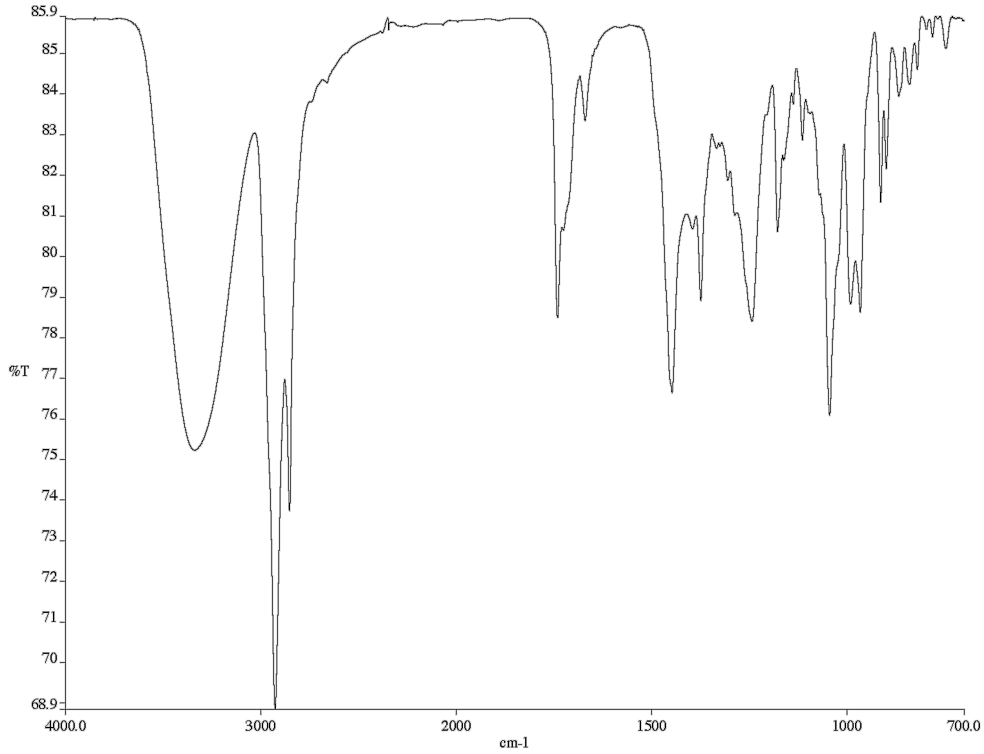

Figure A3.41 Infrared spectrum (thin film/NaCl) of compound **53**

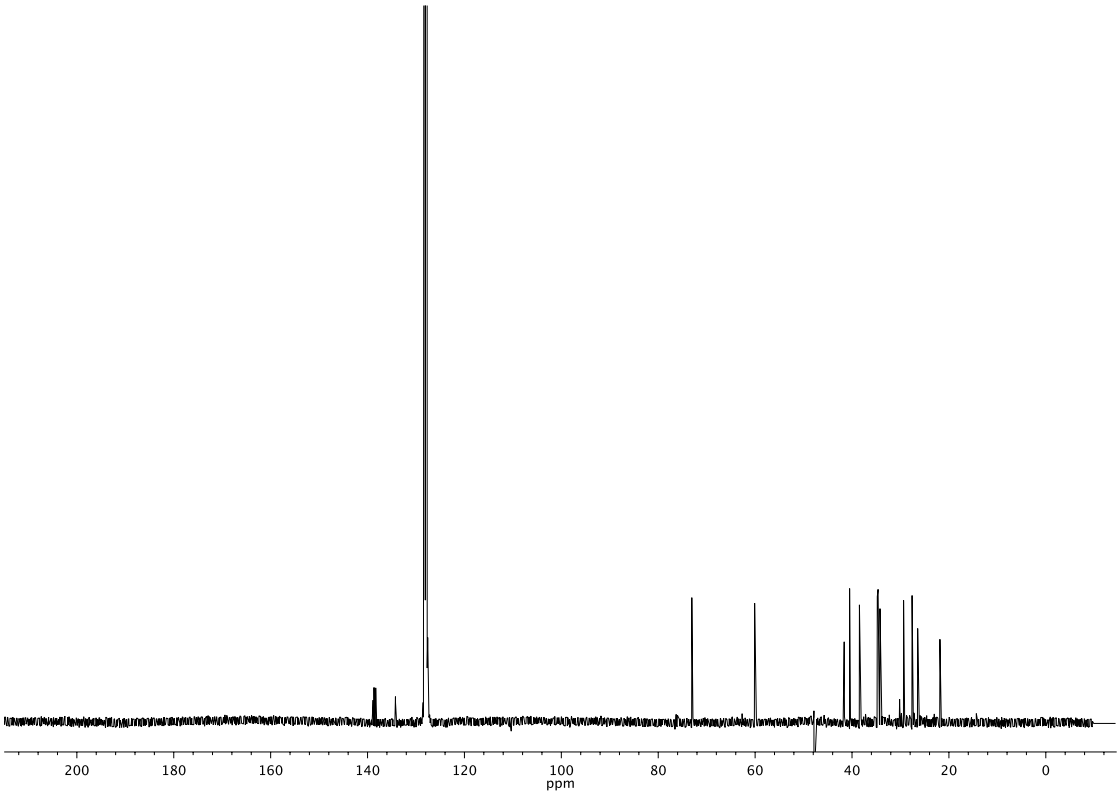

Figure A3.42 ^{13}C NMR (126 MHz, C_6D_6) of compound **53**

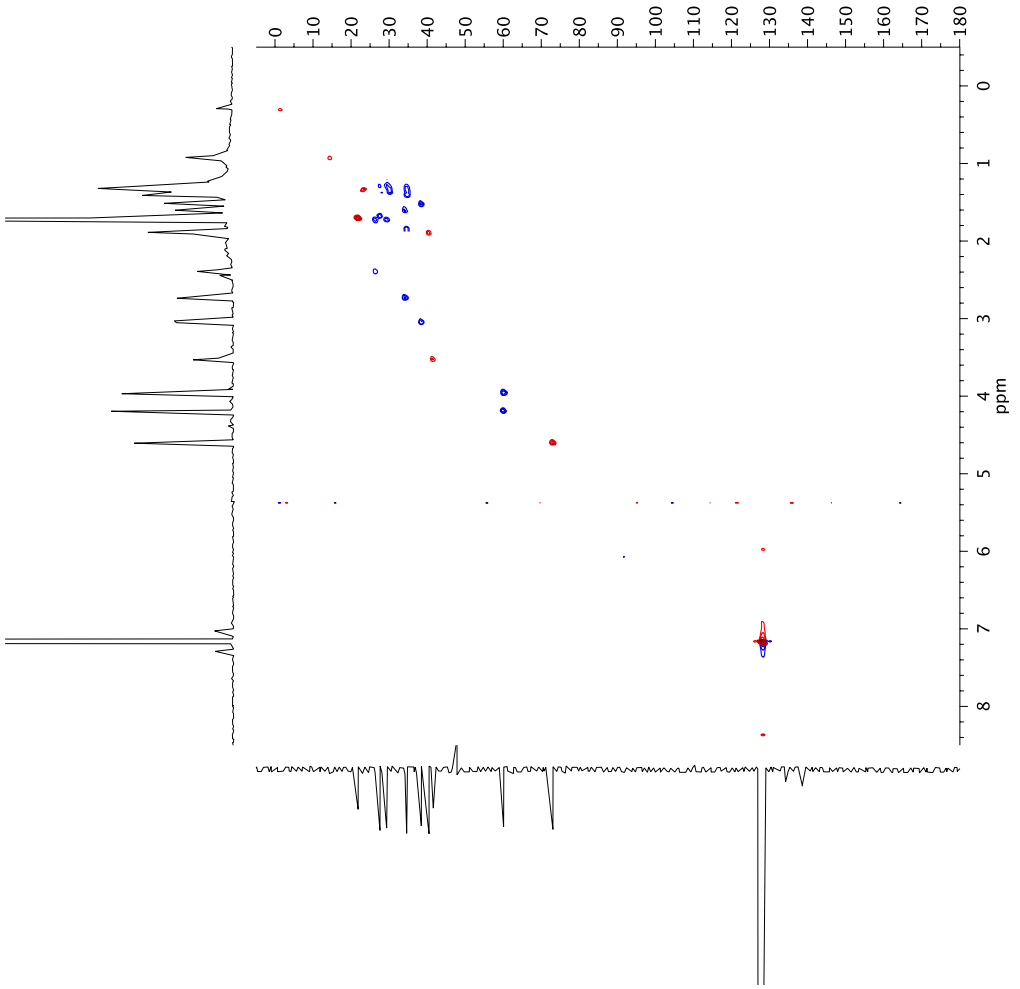

Figure A3.43 ^{1}H-^{13}C HSQC (600 MHz, C_6D_6) of compound **53**

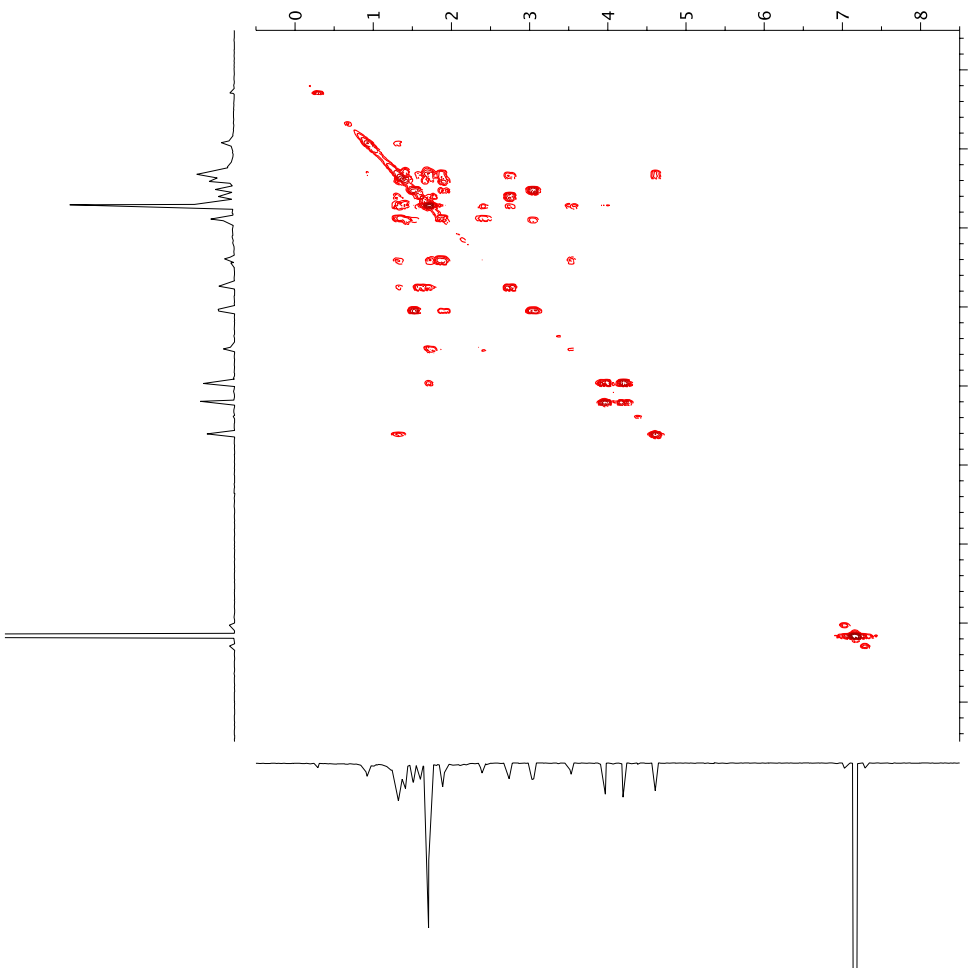

Figure A3.44 gCOSY (600 MHz, C_6D_6) of compound **53**

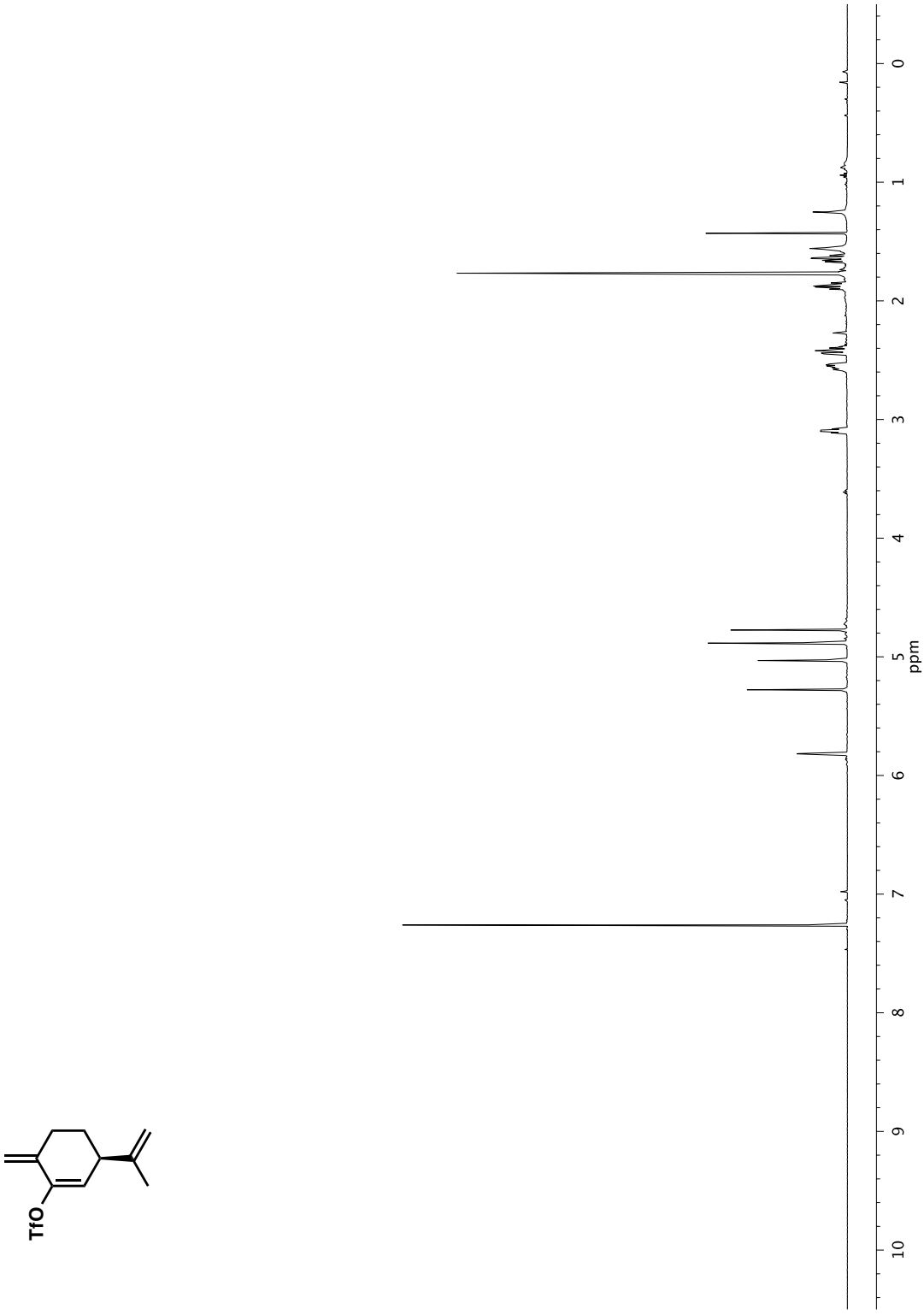

Figure A3.45 ^{1}H NMR (500 MHz, $CDCl_3$) of compound **27**

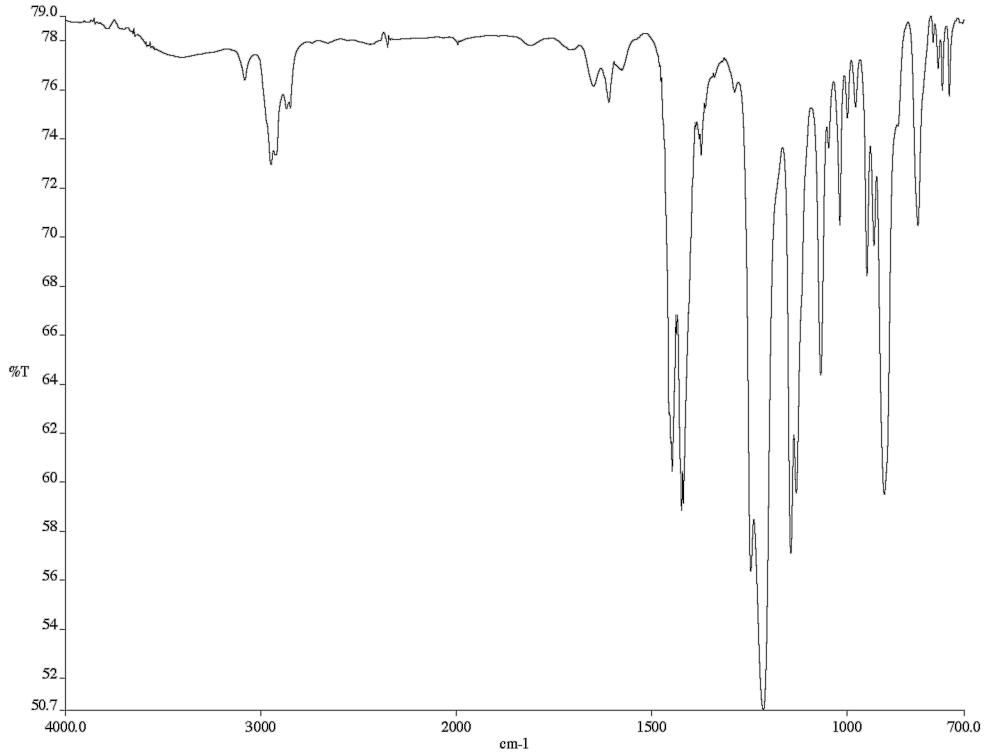

Figure A3.46 Infrared spectrum (thin film/NaCl) of compound **27**

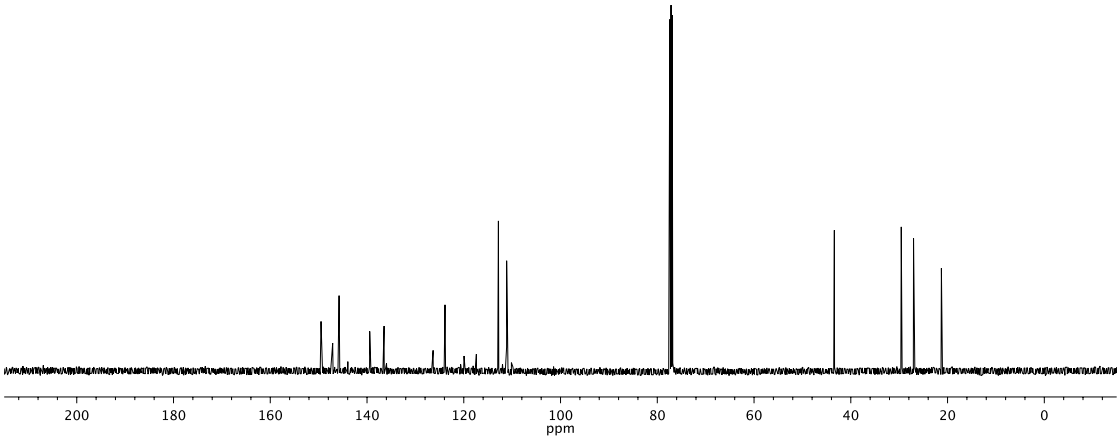

Figure A3.47 ^{13}C NMR (126 MHz, $CDCl_3$) of compound **27**

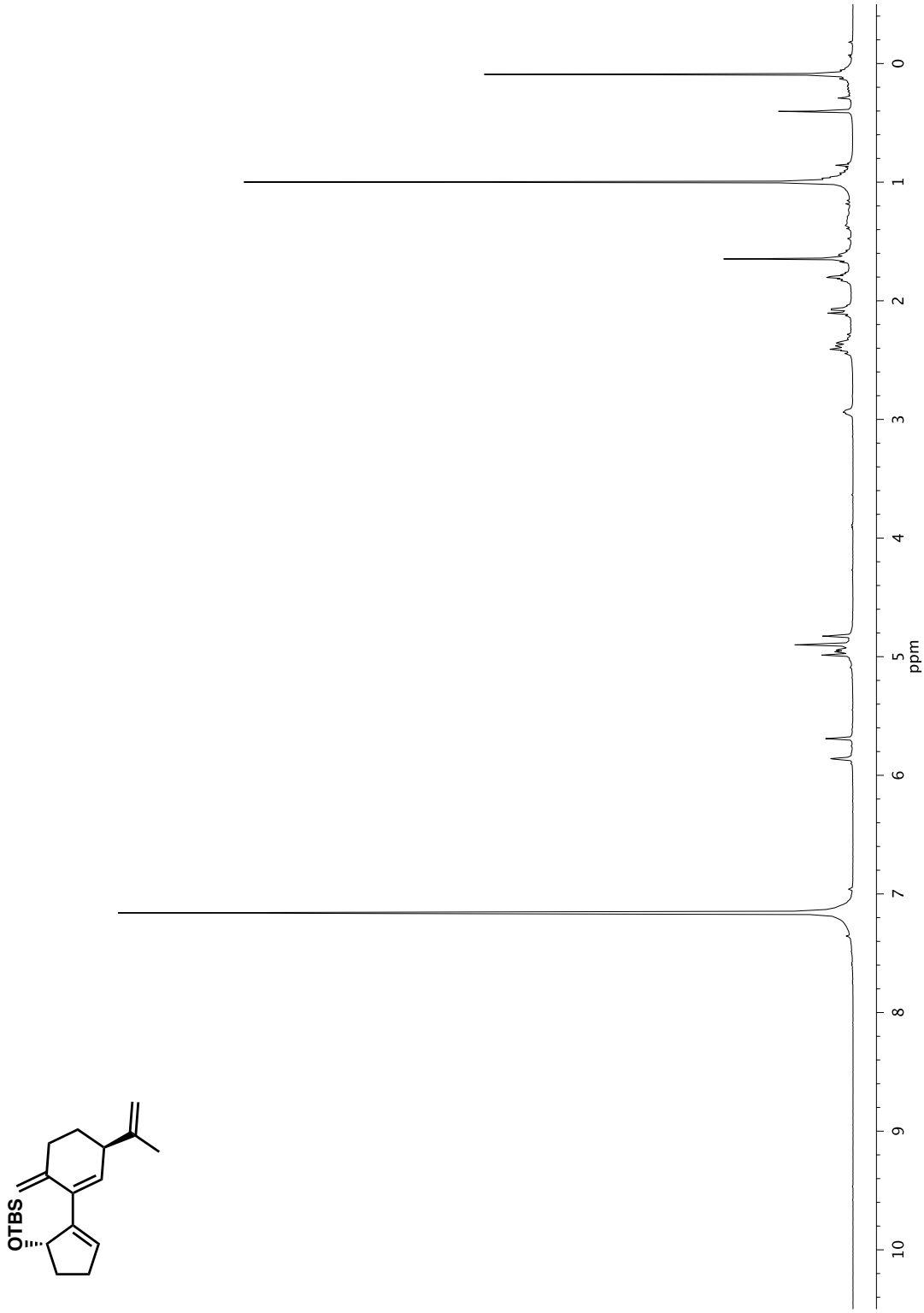

Figure A3.48 ^{1}H NMR (400 MHz, C_6D_6) of compound **59**

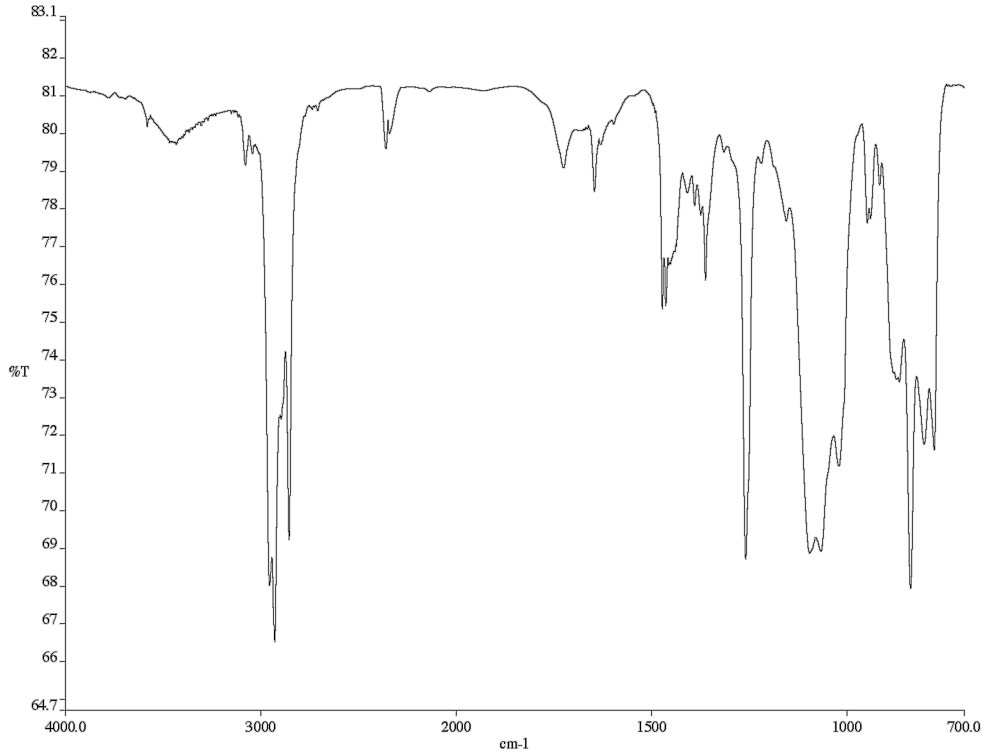

Figure A3.49 Infrared spectrum (thin film/NaCl) of compound **59**

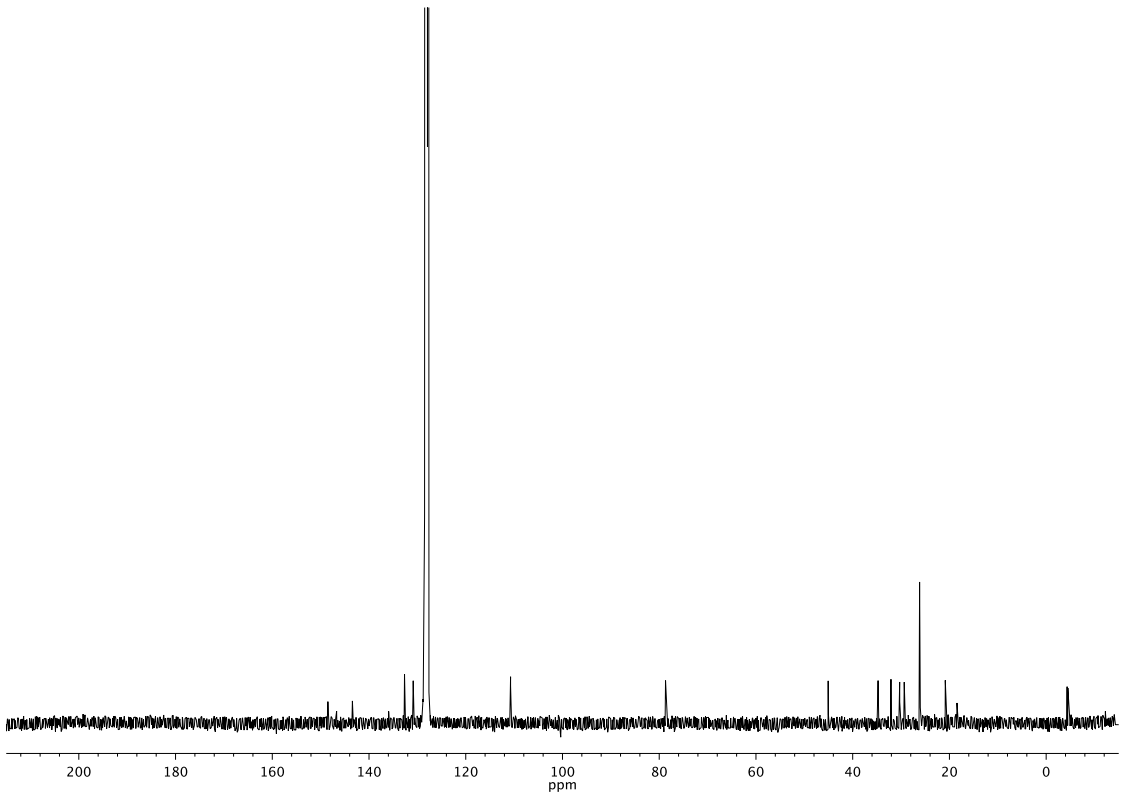

Figure A3.50 ^{13}C NMR (101 MHz, C_6D_6) of compound **59**

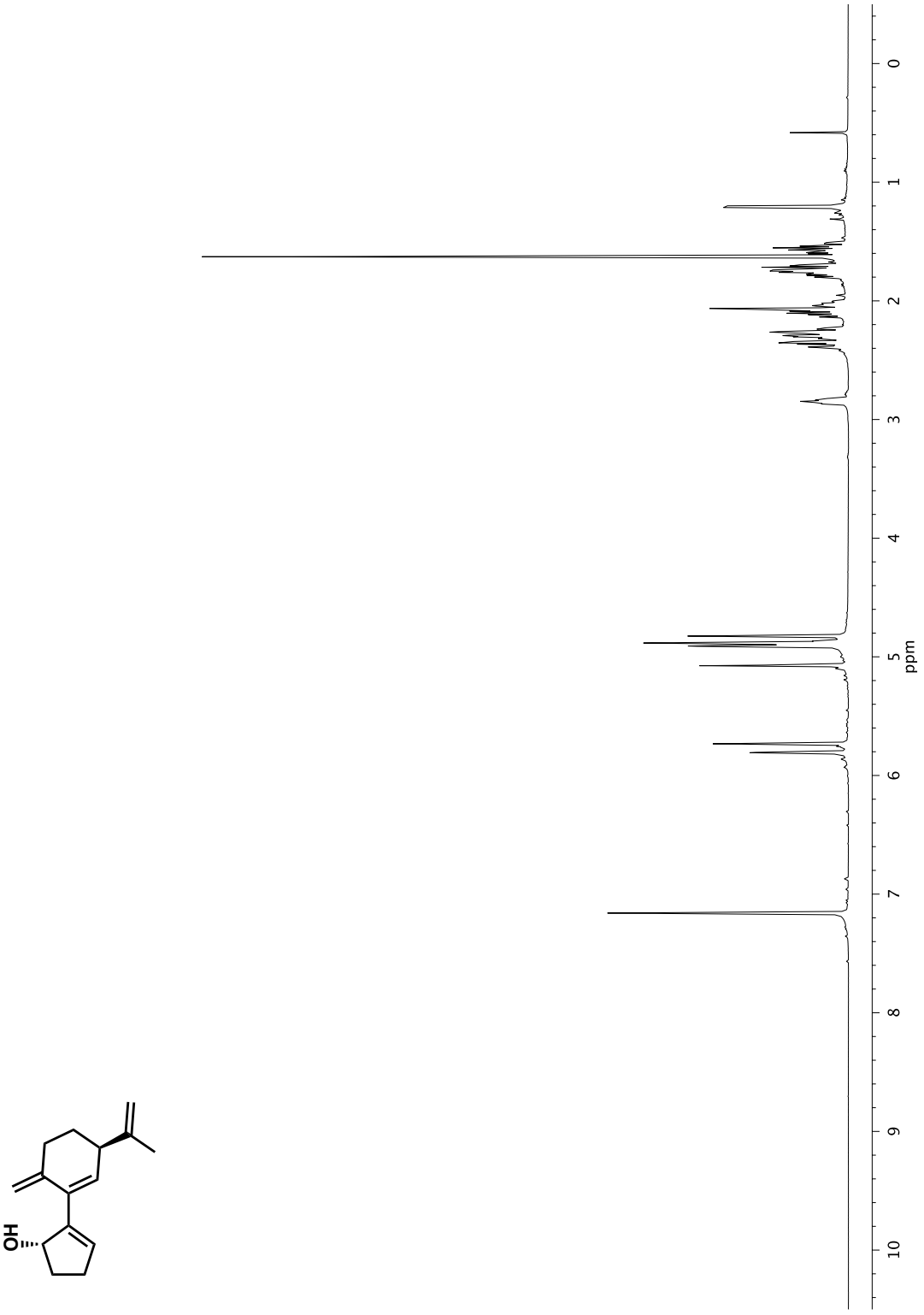

Figure A3.51 ^{1}H NMR (400 MHz, C_6D_6) of compound **60**

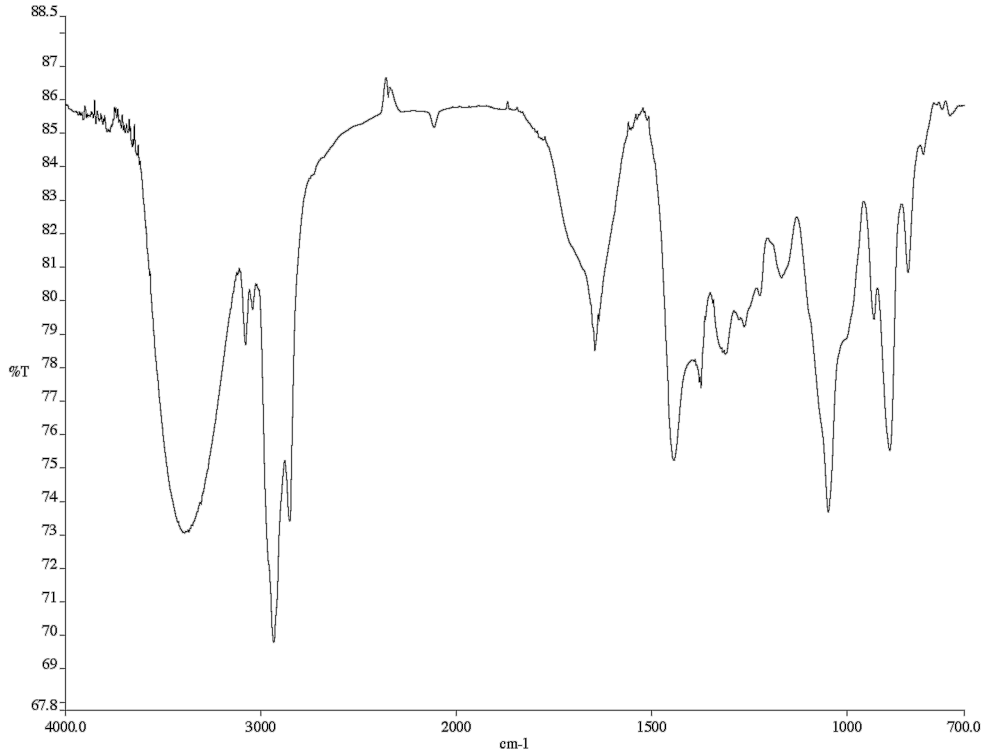

Figure A3.52 Infrared spectrum (thin film/NaCl) of compound **60**

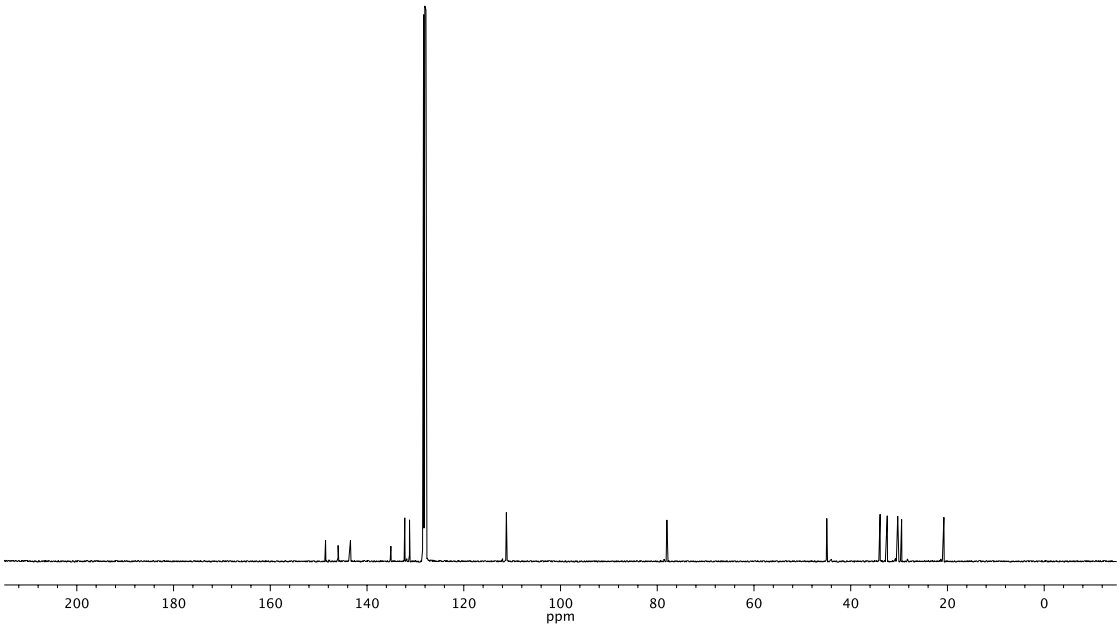

Figure A3.53 ^{13}C NMR (101 MHz, C_6D_{63}) of compound **60**

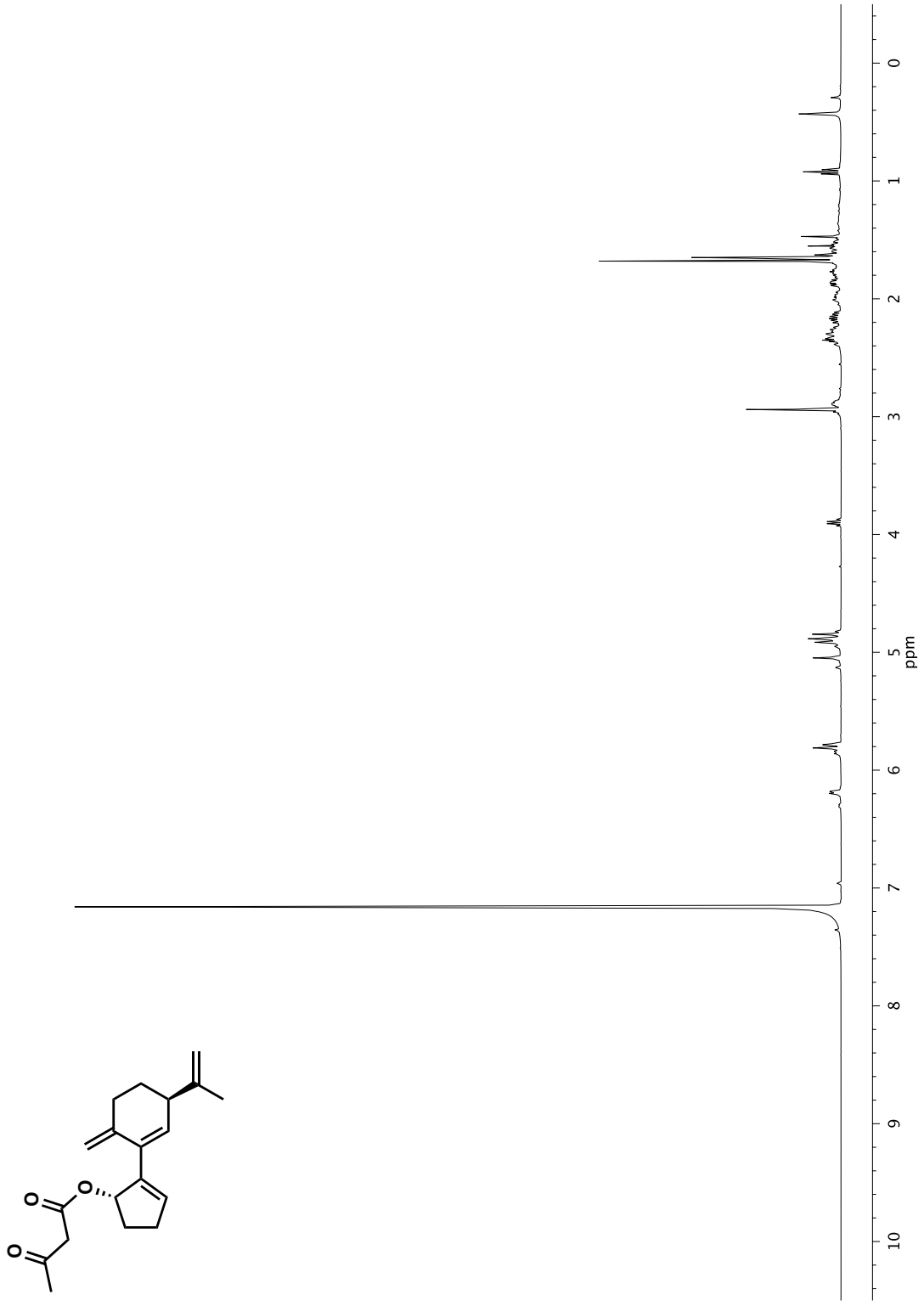

Figure A3.54 ^{1}H NMR (400 MHz, C_6D_6) of compound **61**

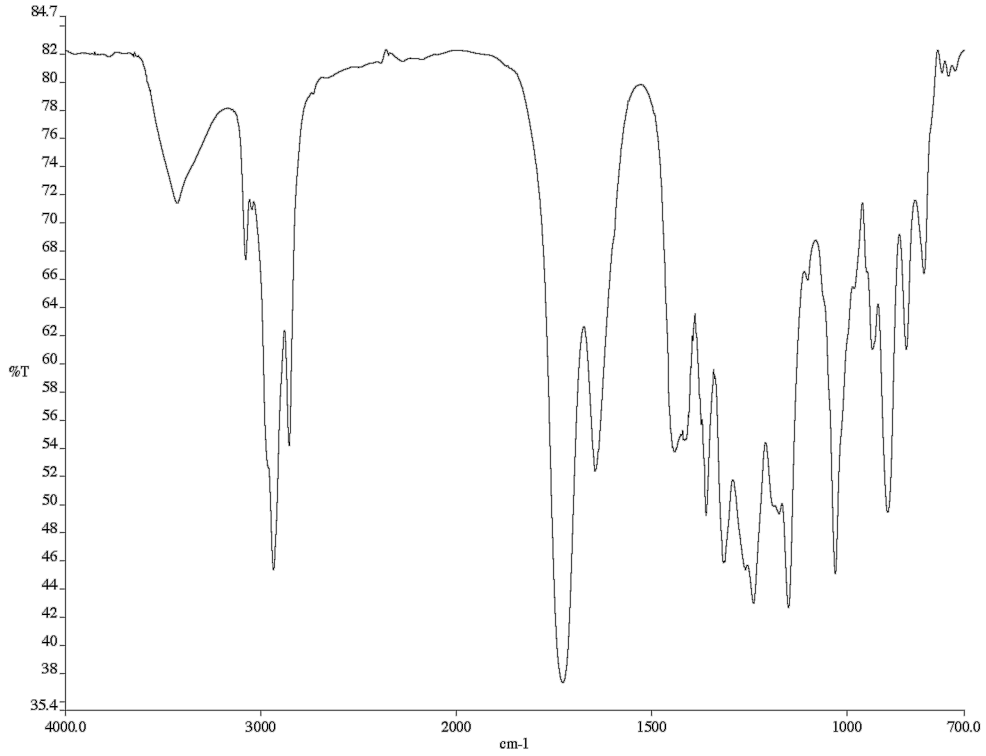

Figure A3.55 Infrared spectrum (thin film/NaCl) of compound **61**

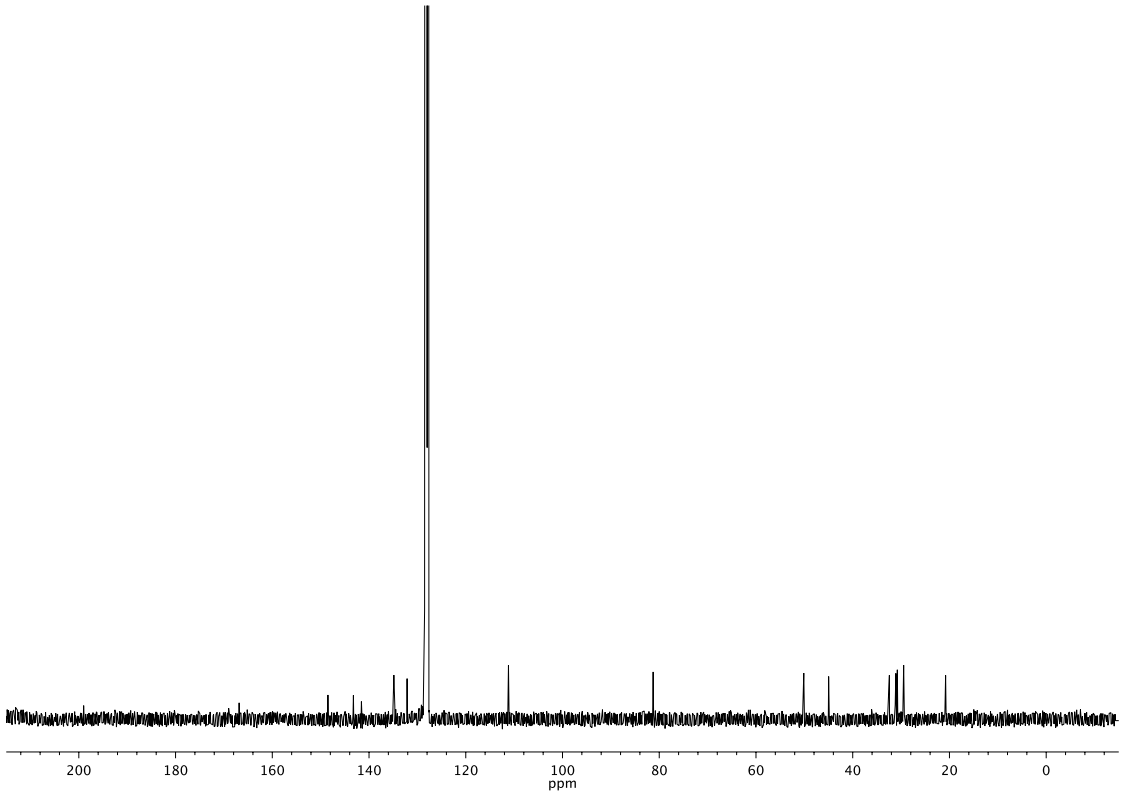

Figure A3.56 ^{13}C NMR (101 MHz, C_6D_6) of compound **61**

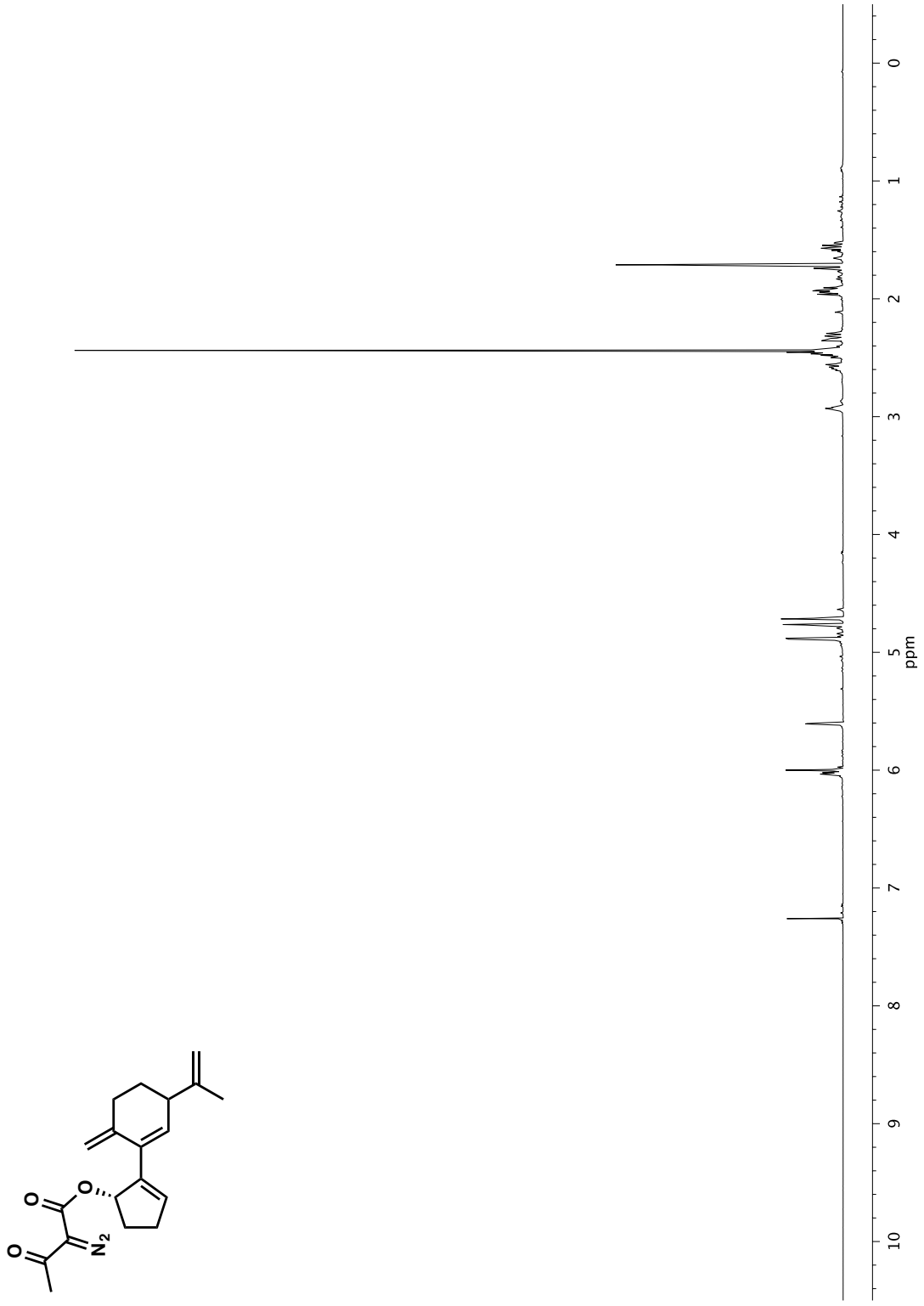

Figure A3.57 ^{1}H NMR (500 MHz, $CDCl_3$) of compound **24**

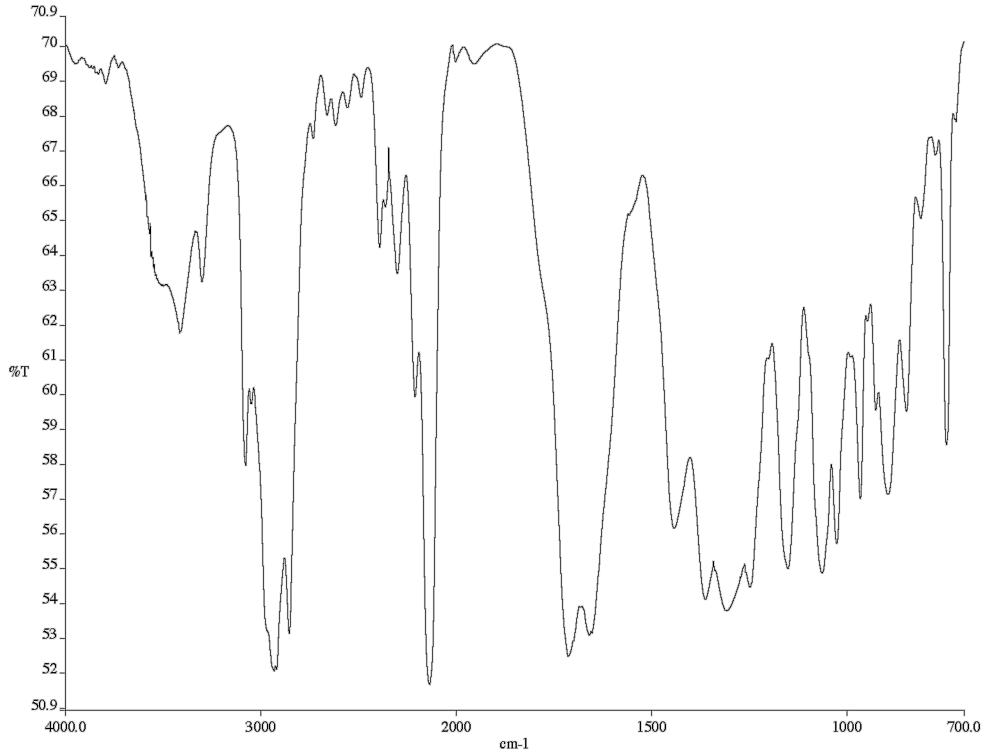

Figure A3.58 Infrared spectrum (thin film/NaCl) of compound **24**

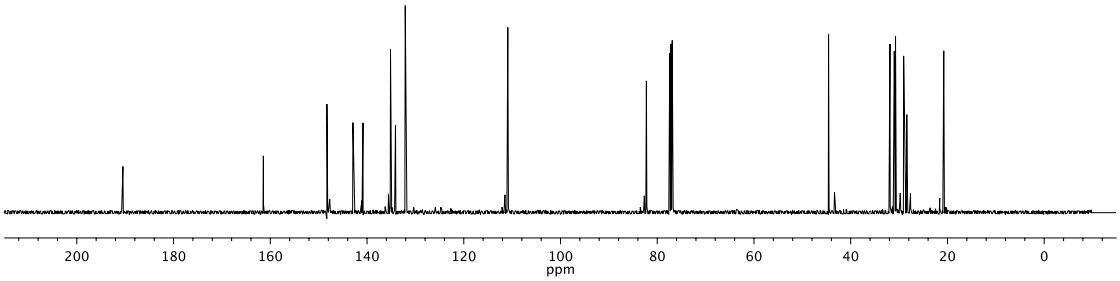

Figure A3.59 ^{13}C NMR (126 MHz, $CDCl_3$) of compound **24**

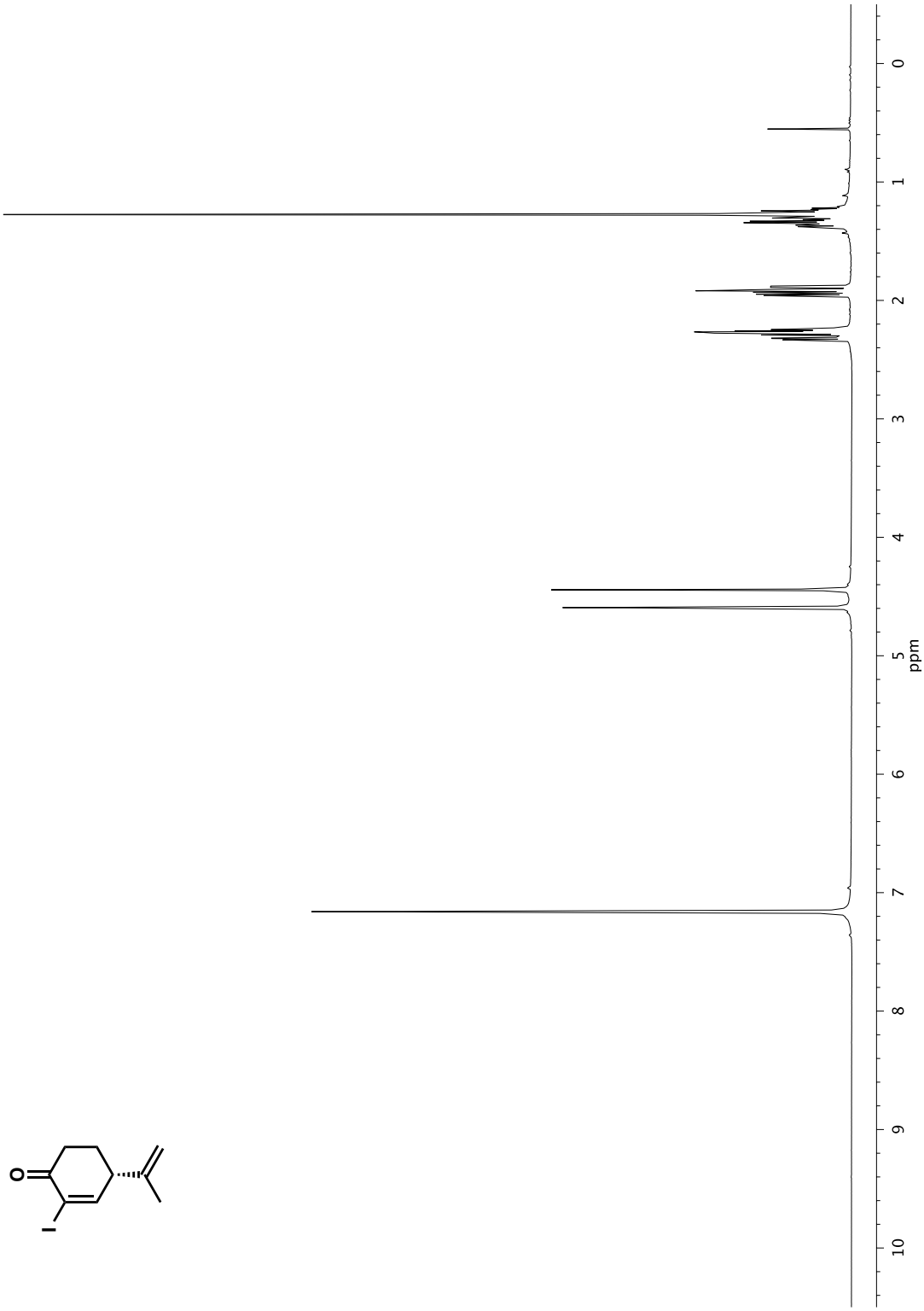

Figure A3.60 ^{1}H NMR (400 MHz, C_6D_6) of compound *ent*-**64**

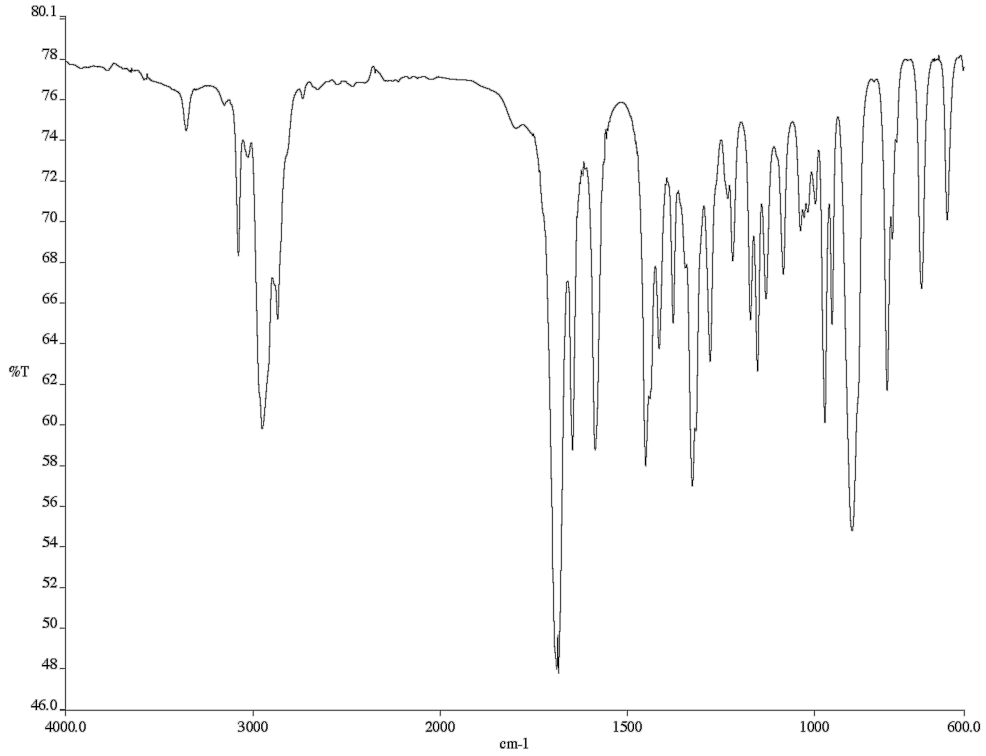

Figure A3.61 Infrared spectrum (thin film/NaCl) of compound *ent*-**64**

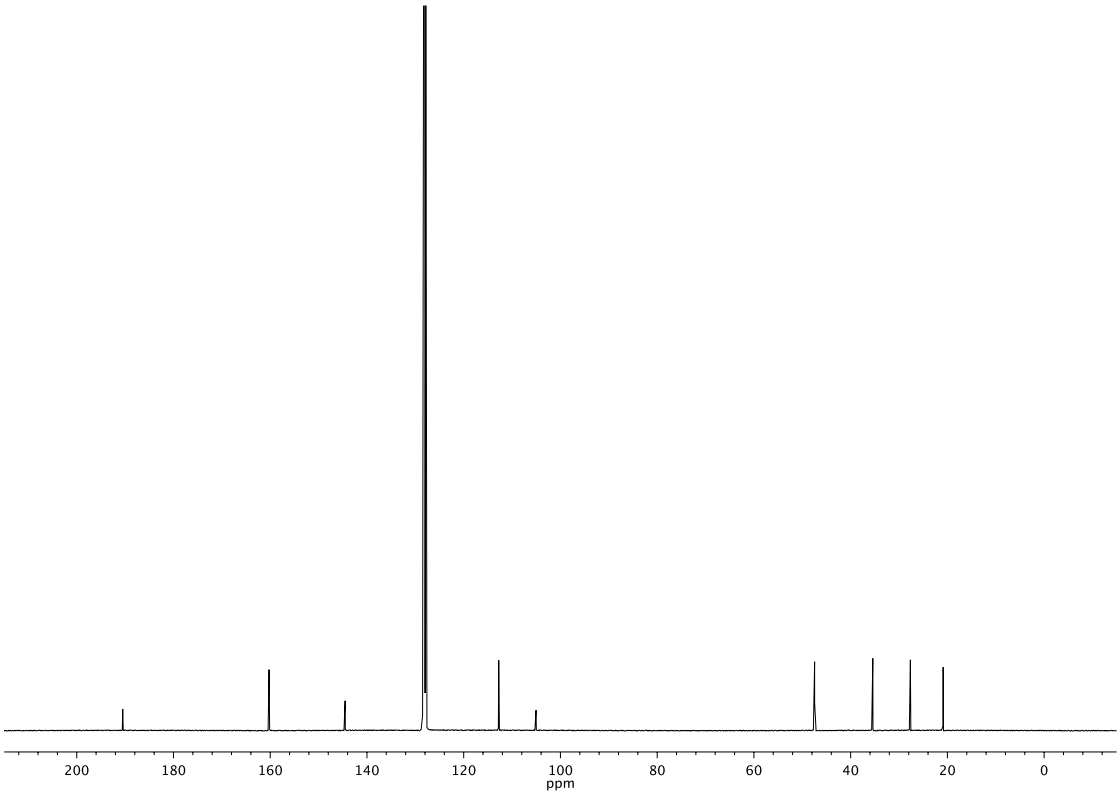

Figure A3.62 ^{13}C NMR (101 MHz, C_6D_6) of compound *ent*-**64**

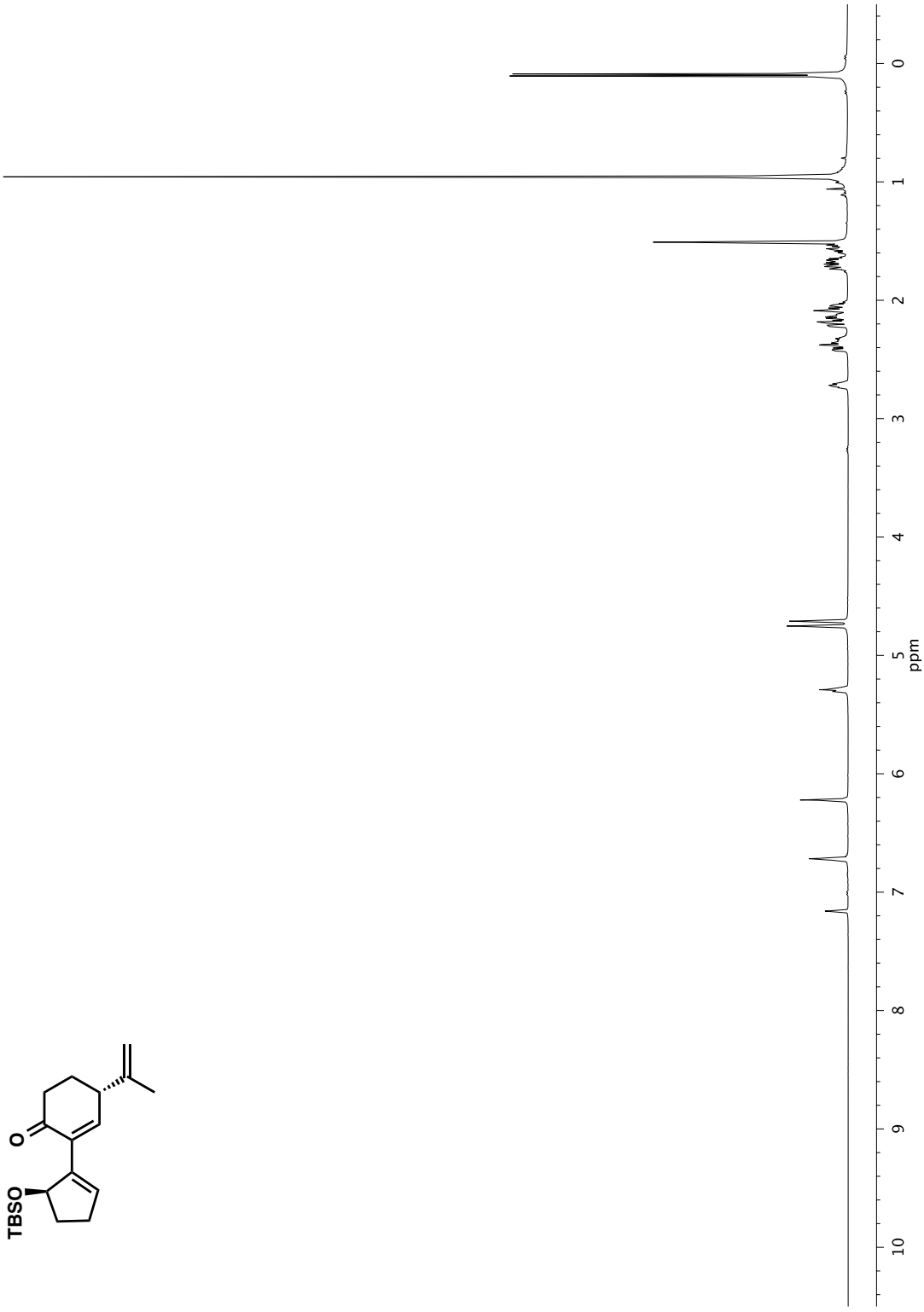

Figure A3.63 ^{1}H NMR (400 MHz, C_6D_6) of compound **69**

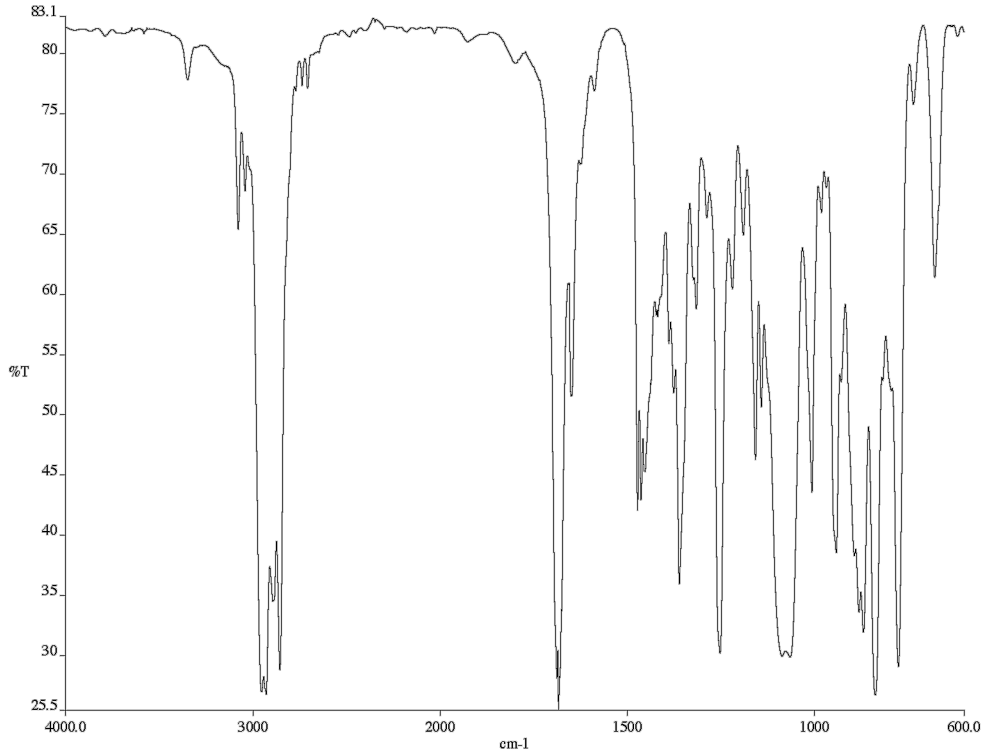

Figure A3.64 Infrared spectrum (thin film/NaCl) of compound **69**

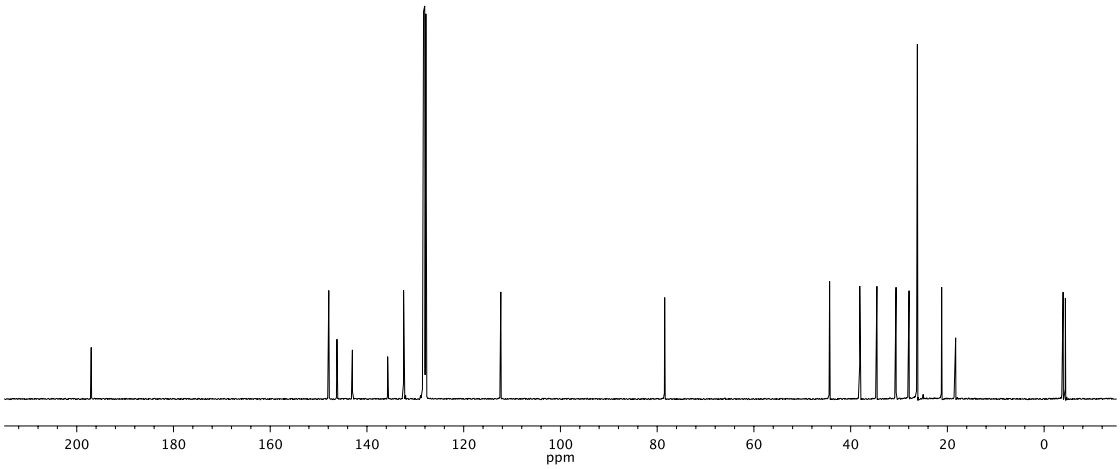

Figure A3.65 ^{13}C NMR (101 MHz, C_6D_6) of compound **69**

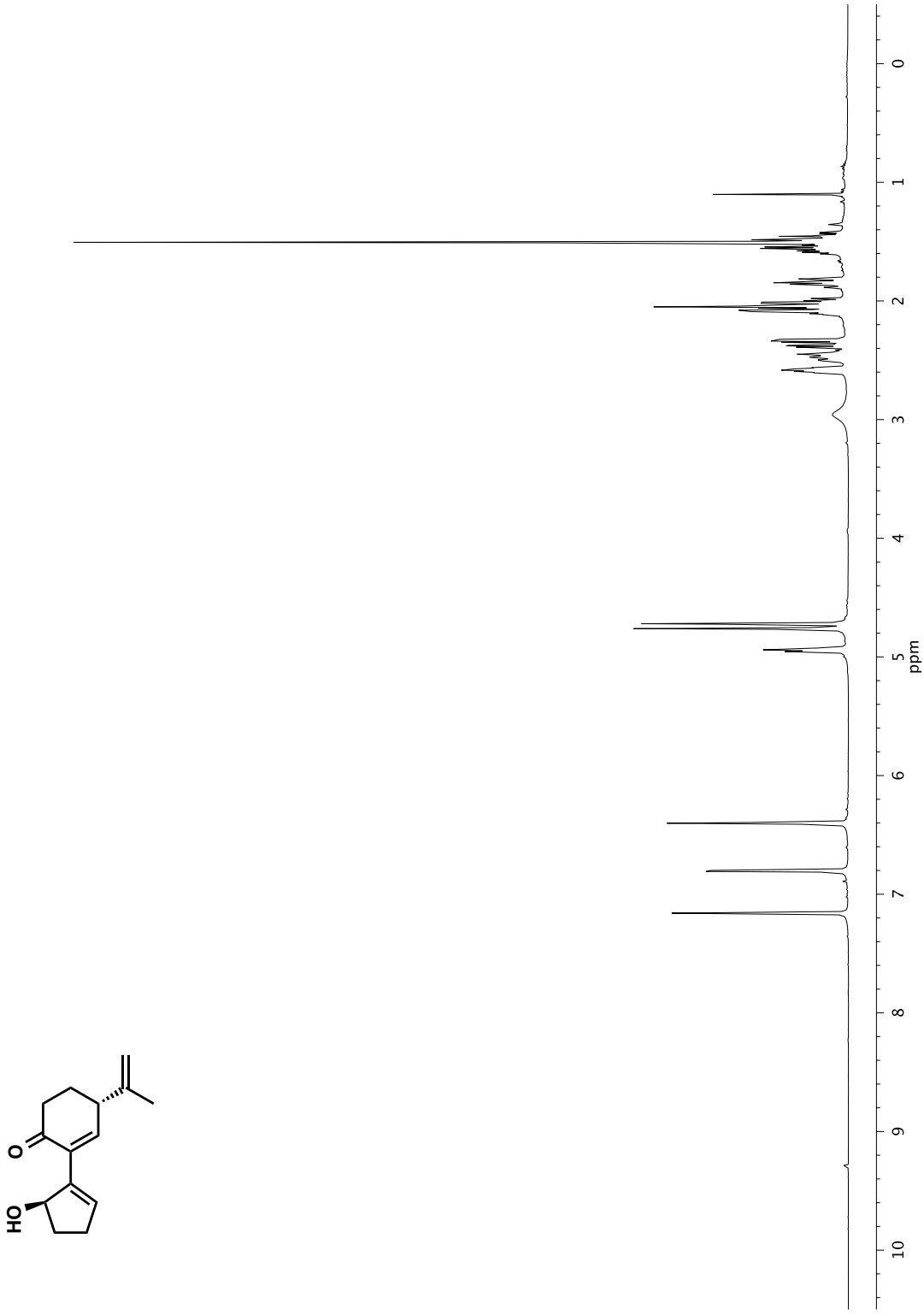

Figure A3.66 ^{1}H NMR (400 MHz, C_6D_6) of compound **70**

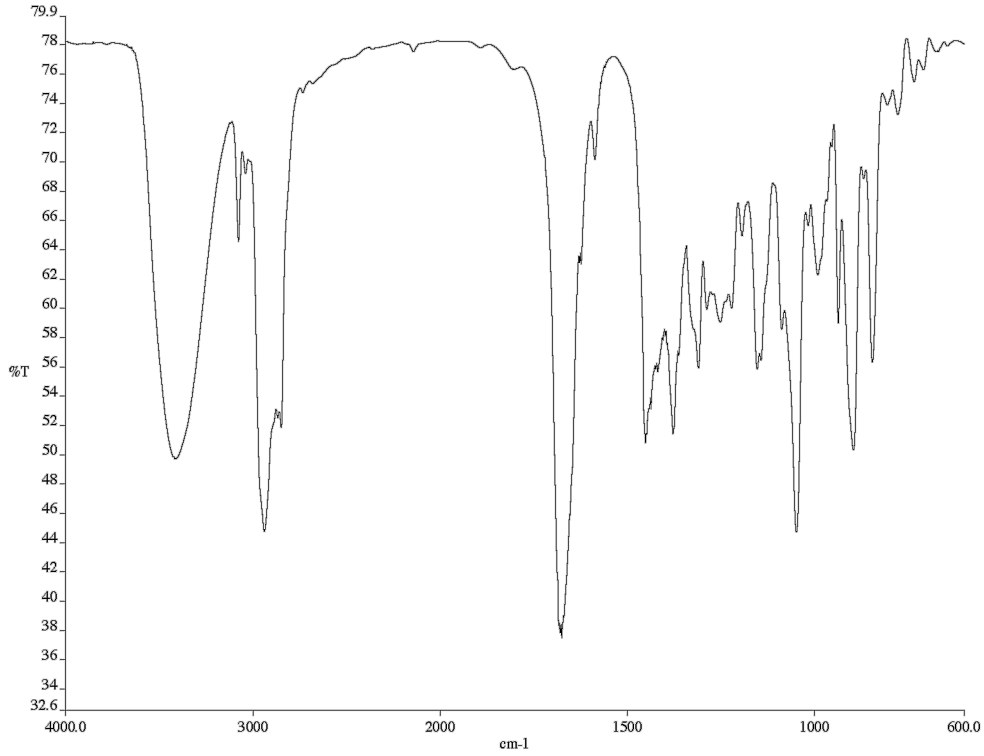

Figure A3.67 Infrared spectrum (thin film/NaCl) of compound **70**

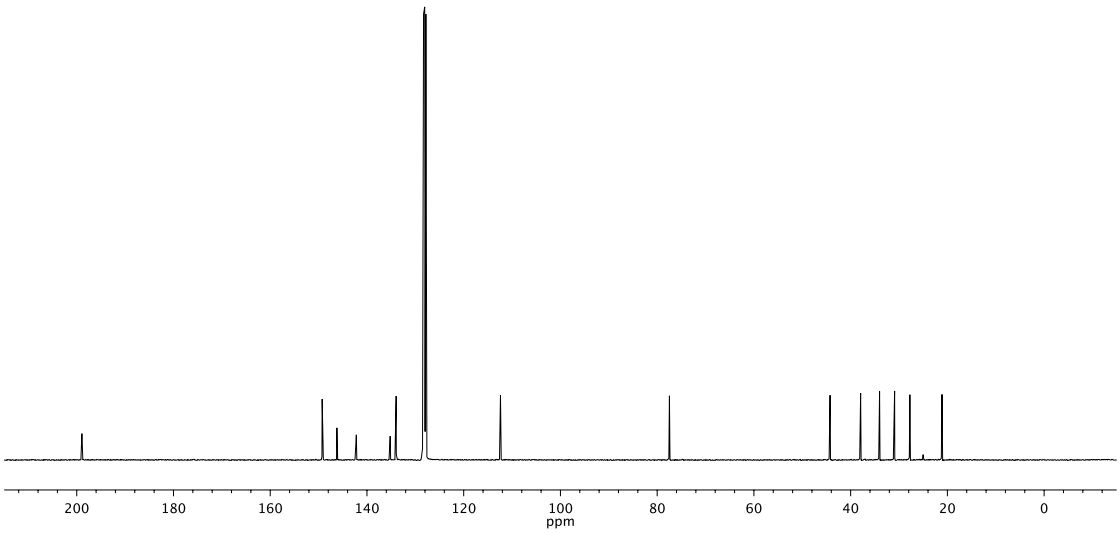

Figure A3.68 ^{13}C NMR (101 MHz, C_6D_6) of compound **70**

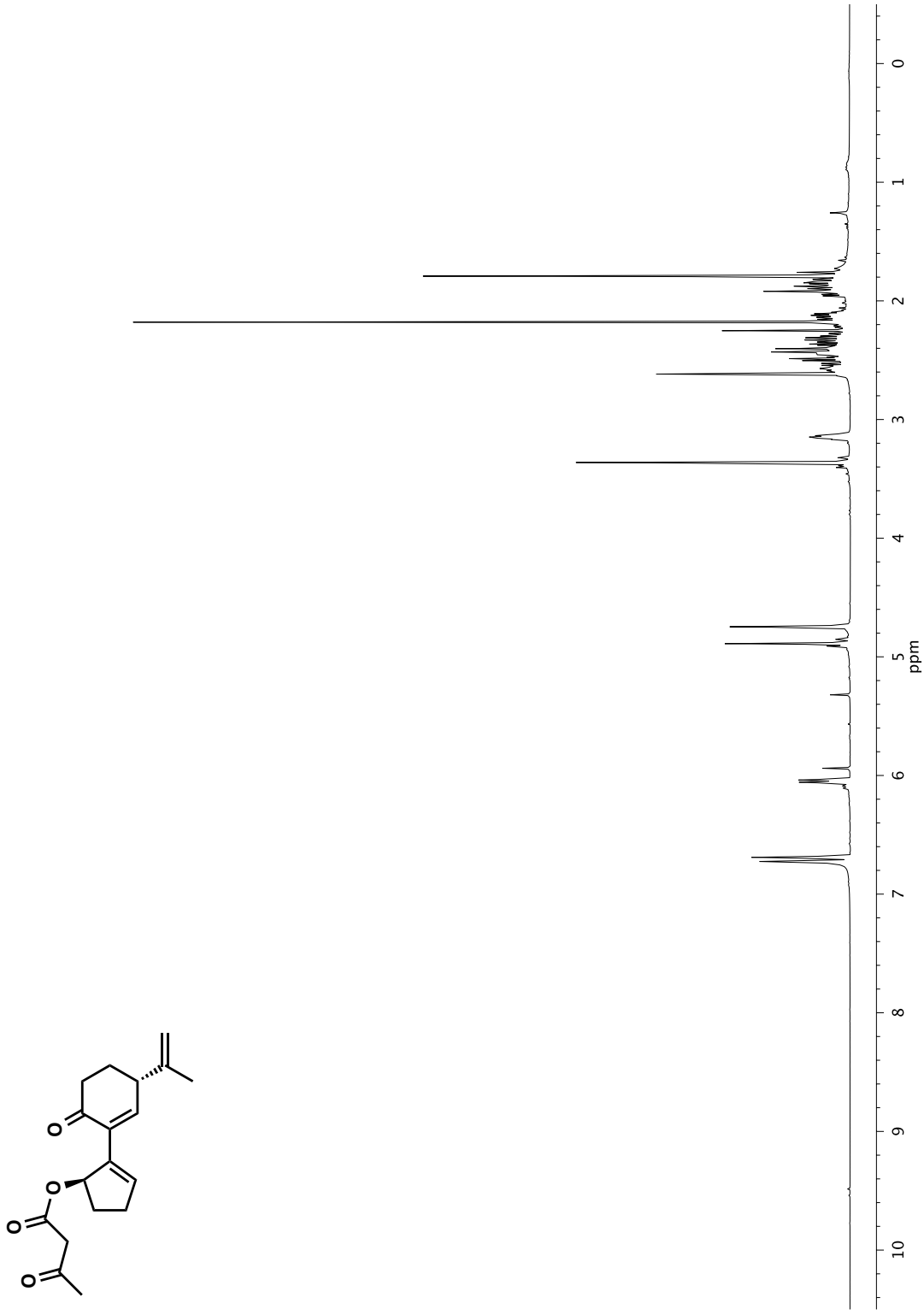

Figure A3.69 ^{1}H NMR (400 MHz, CD_2Cl_2) of compound **71**

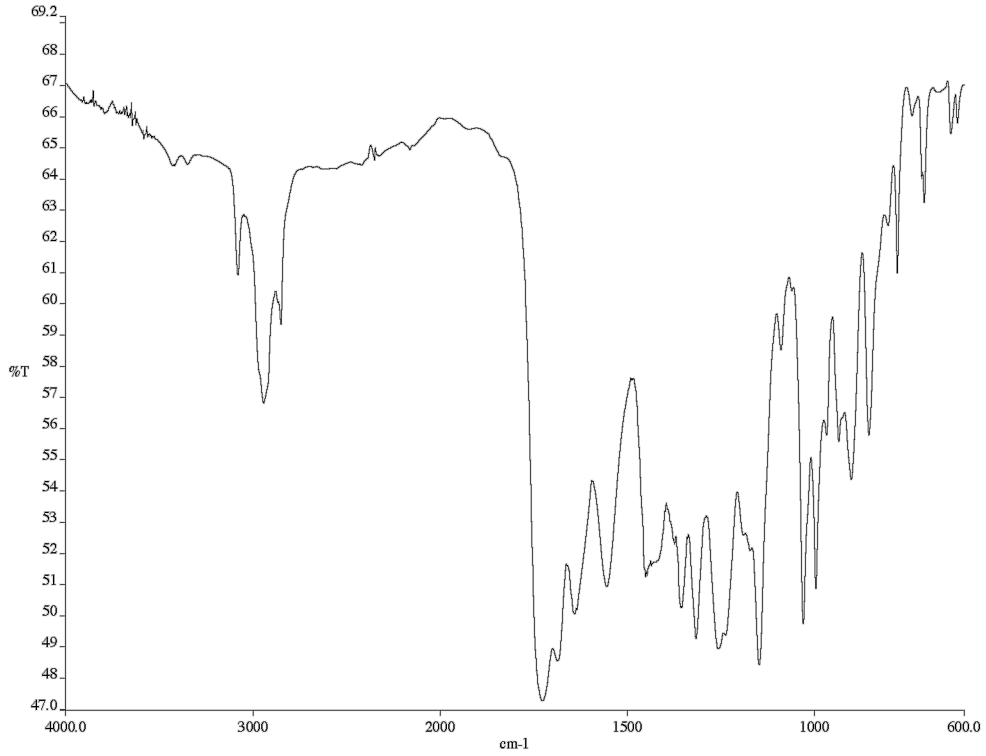

Figure A3.70 Infrared spectrum (thin film/NaCl) of compound **71**

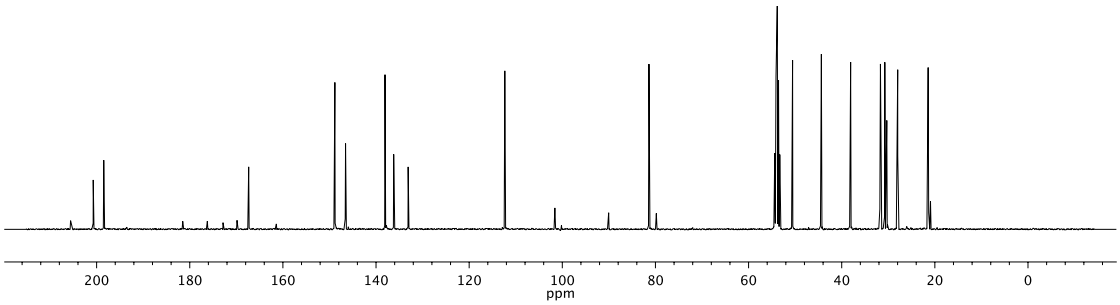

Figure A3.71 ^{13}C NMR (101 MHz, CD_2Cl_2) of compound **71**

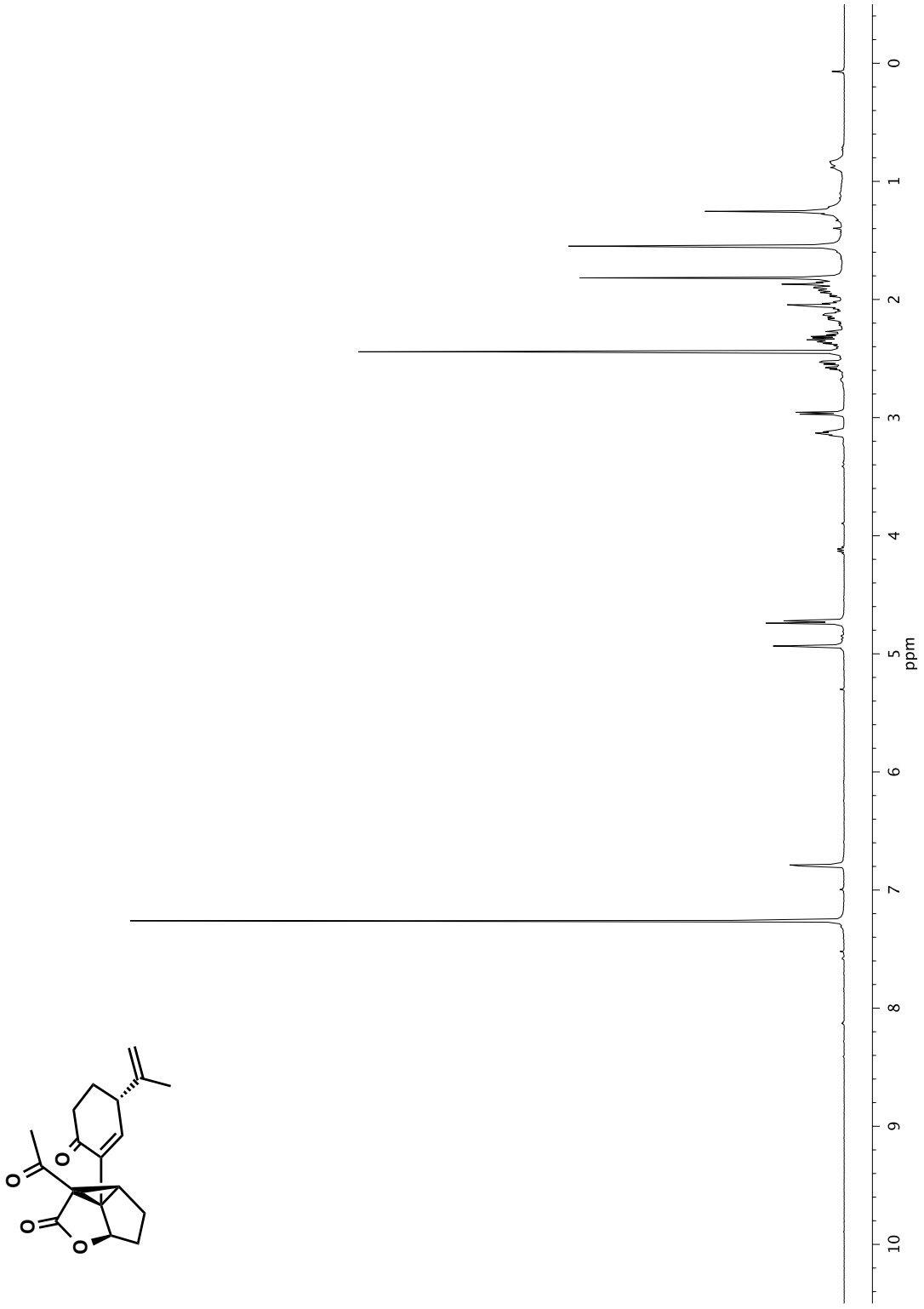

Figure A3.72 ^{1}H NMR (400 MHz, $CDCl_3$) of compound **72**

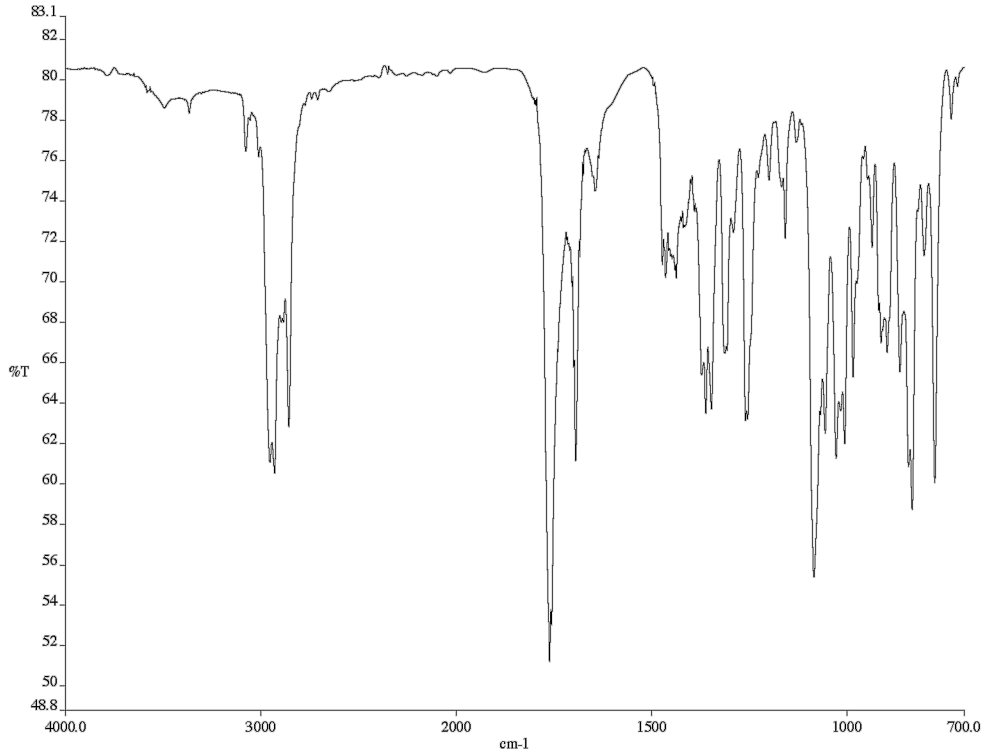

Figure A3.73 Infrared spectrum (thin film/NaCl) of compound **72**

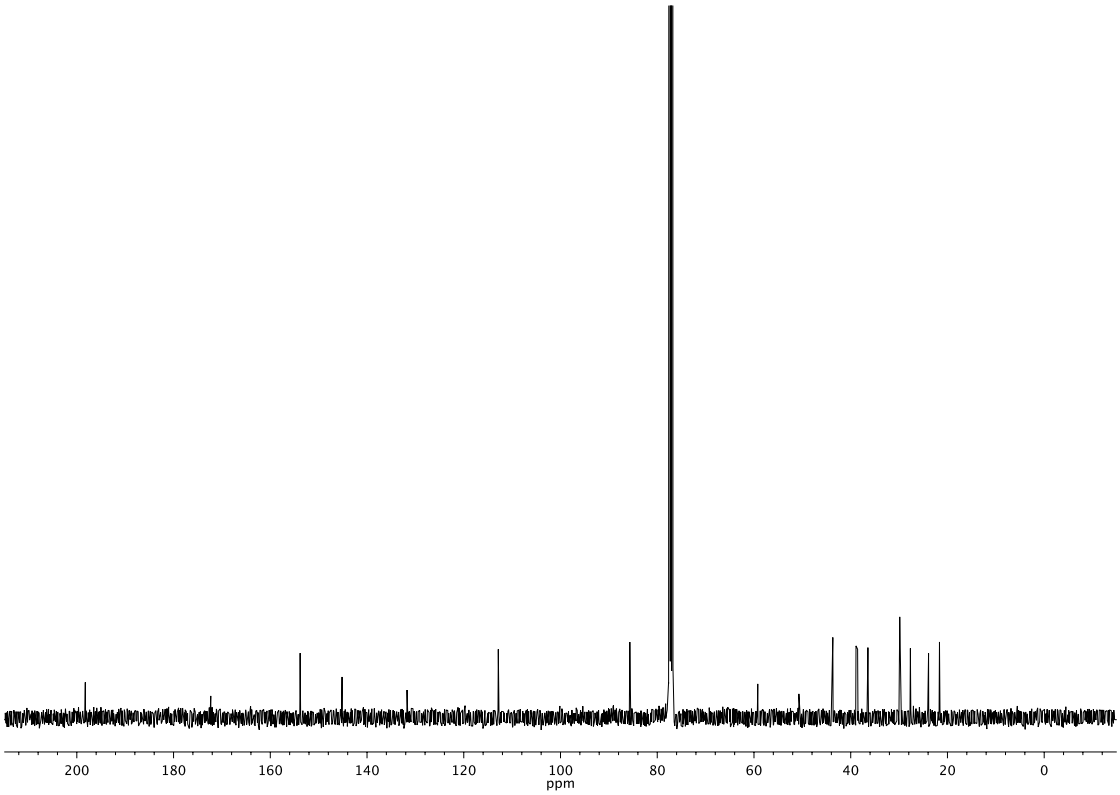

Figure A3.74 ^{13}C NMR (101 MHz, $CDCl_3$) of compound **72**

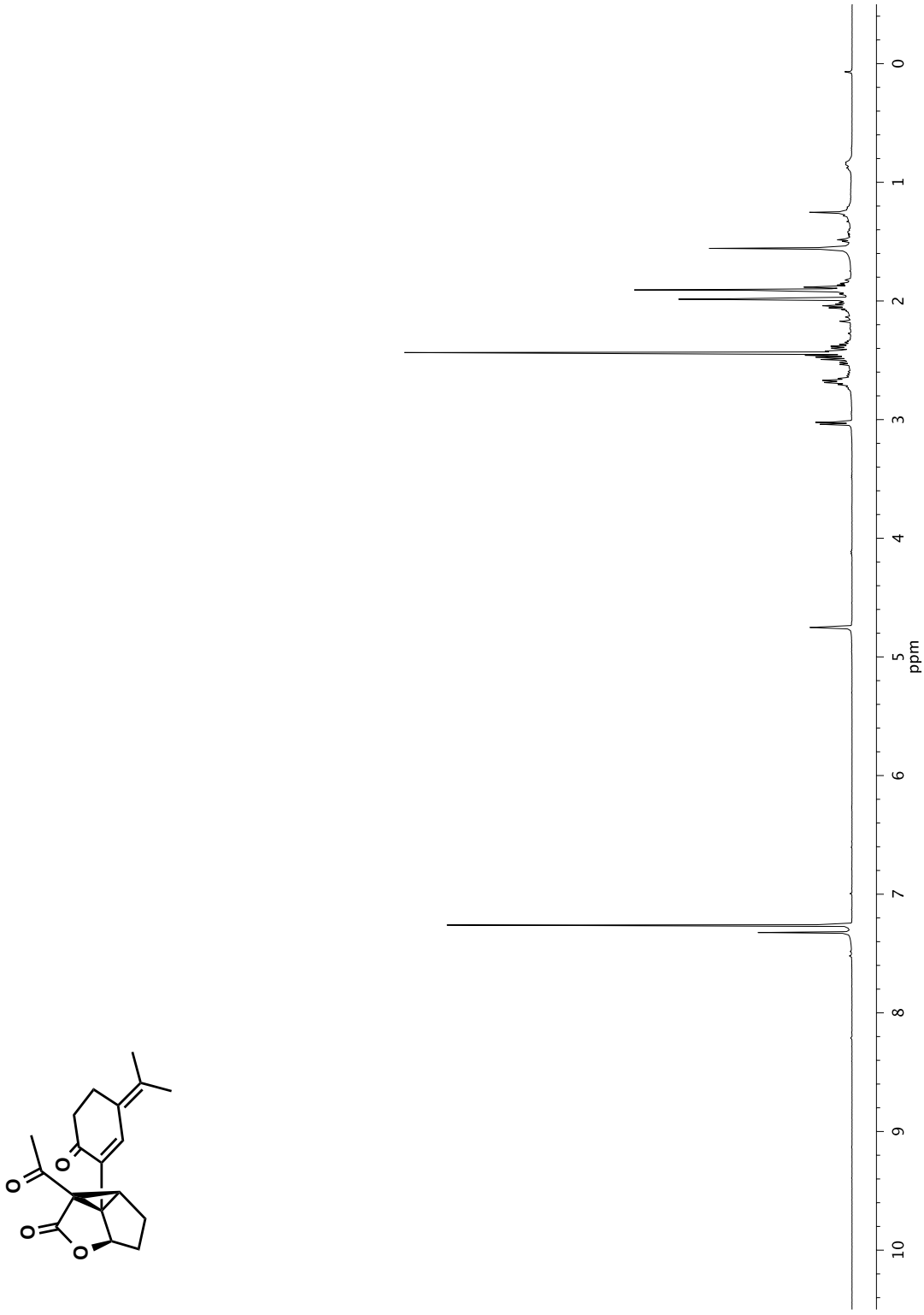

Figure A3.75 ^{1}H NMR (400 MHz, $CDCl_3$) of compound **73**

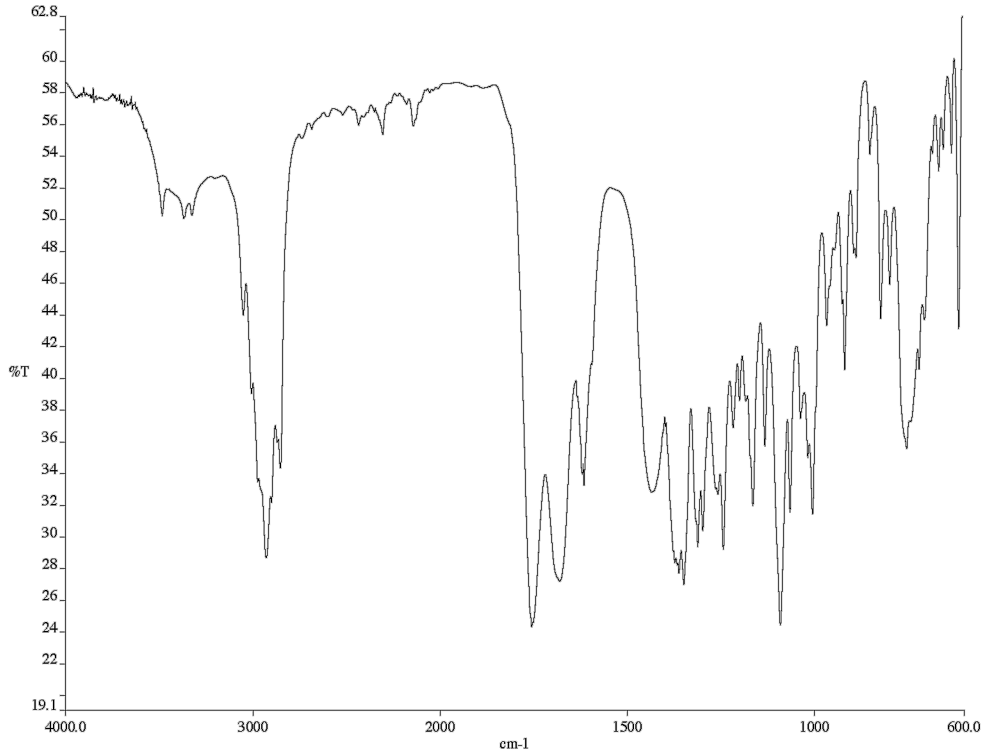

Figure A3.76 Infrared spectrum (thin film/NaCl) of compound **73**

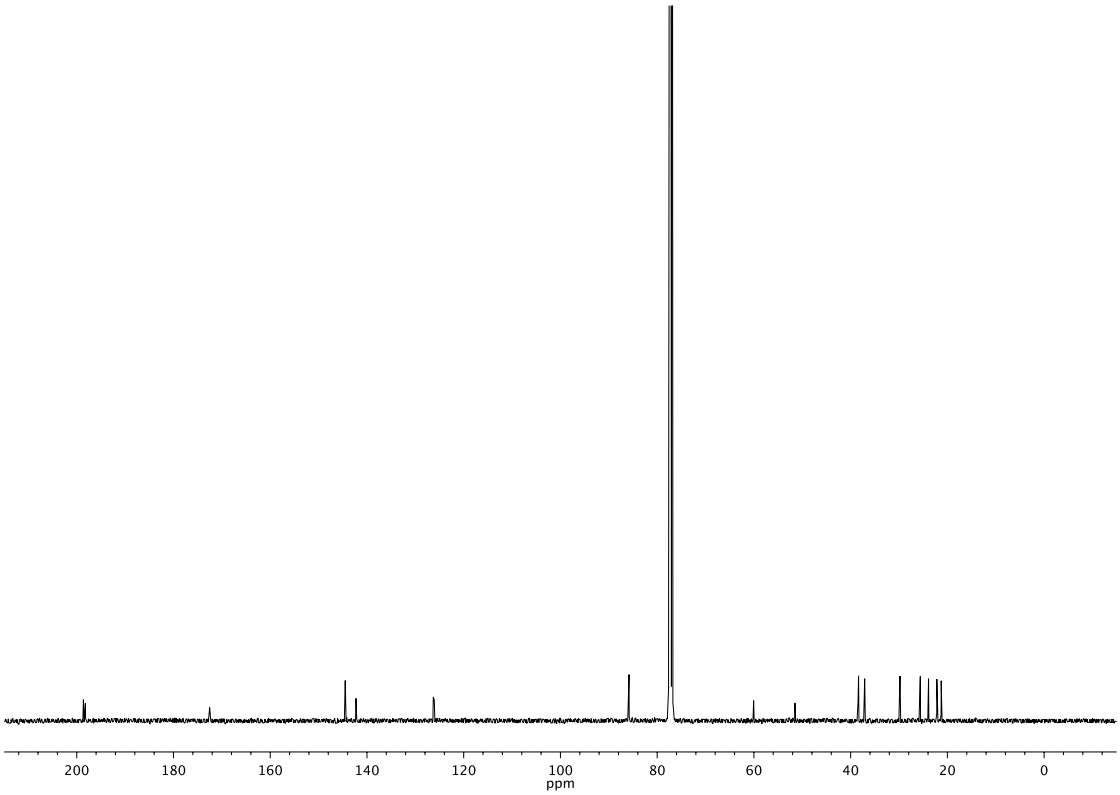

Figure A3.77 ^{13}C NMR (101 MHz, $CDCl_3$) of compound **73**

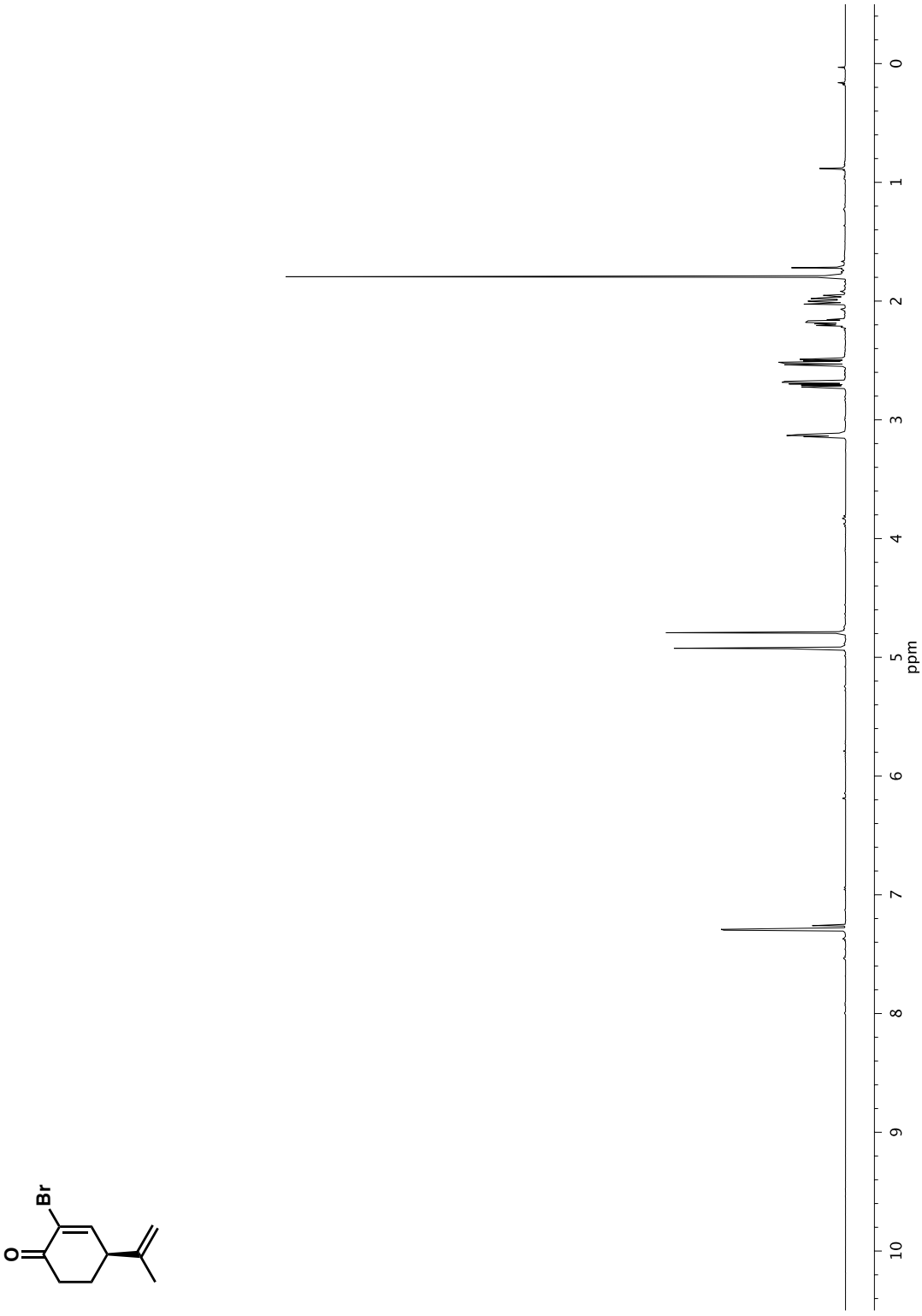

Figure A3.78 ^{1}H NMR (500 MHz, $CDCl_3$) of compound **76**

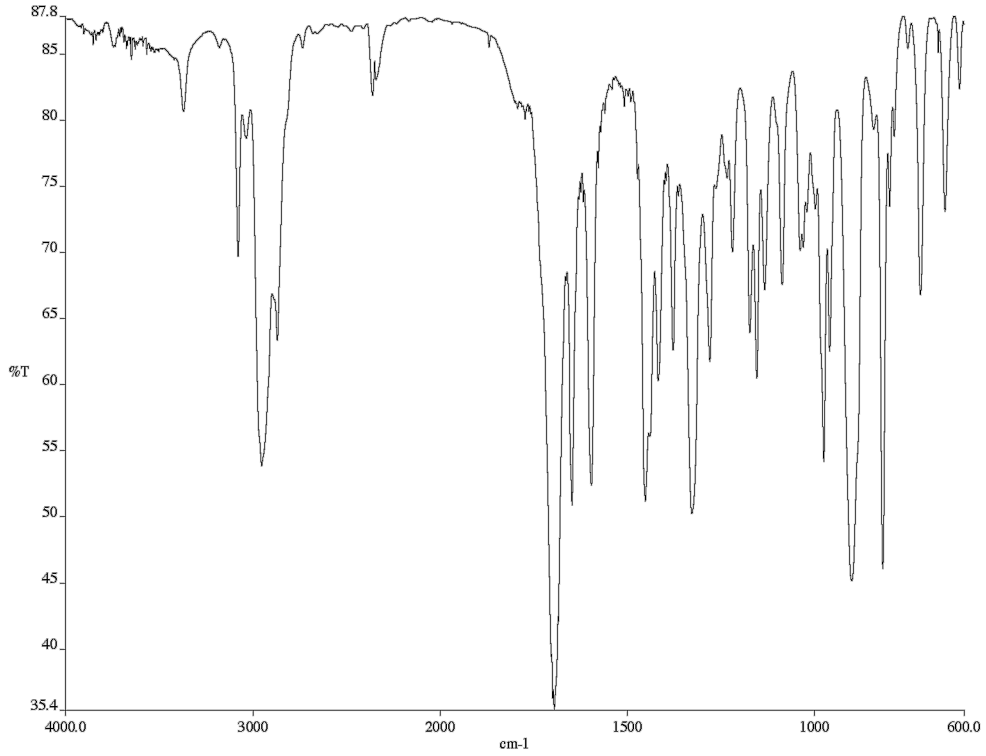

Figure A3.79 Infrared spectrum (thin film/NaCl) of compound **76**

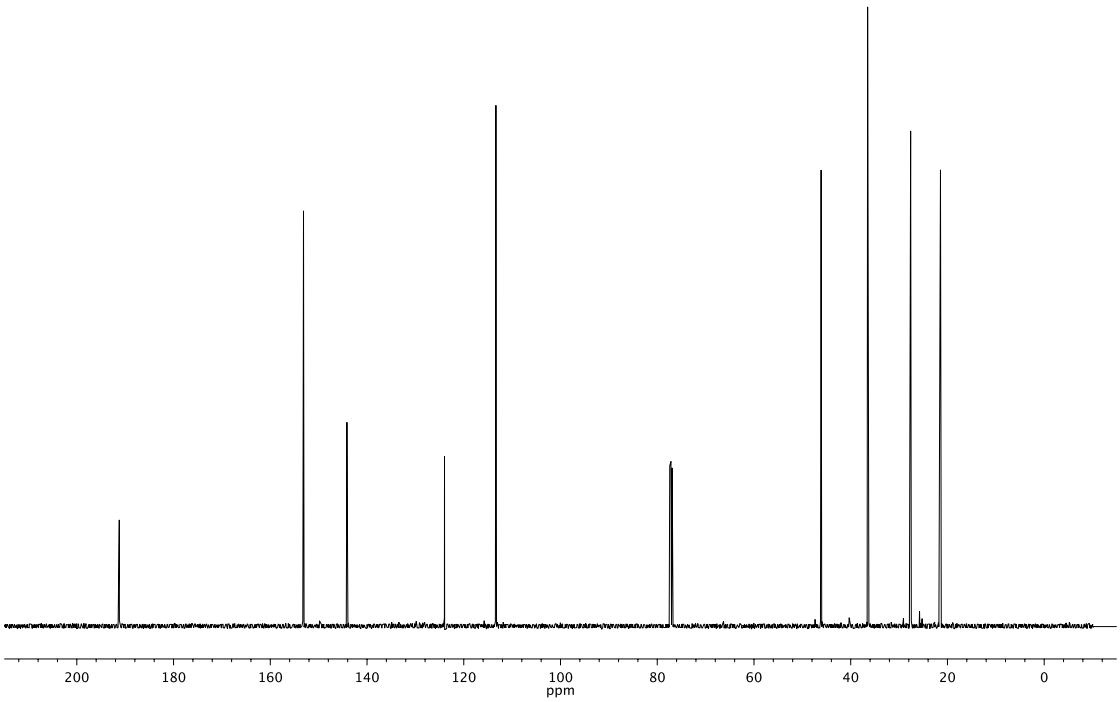

Figure A3.80 ^{13}C NMR (126 MHz, $CDCl_3$) of compound **76**

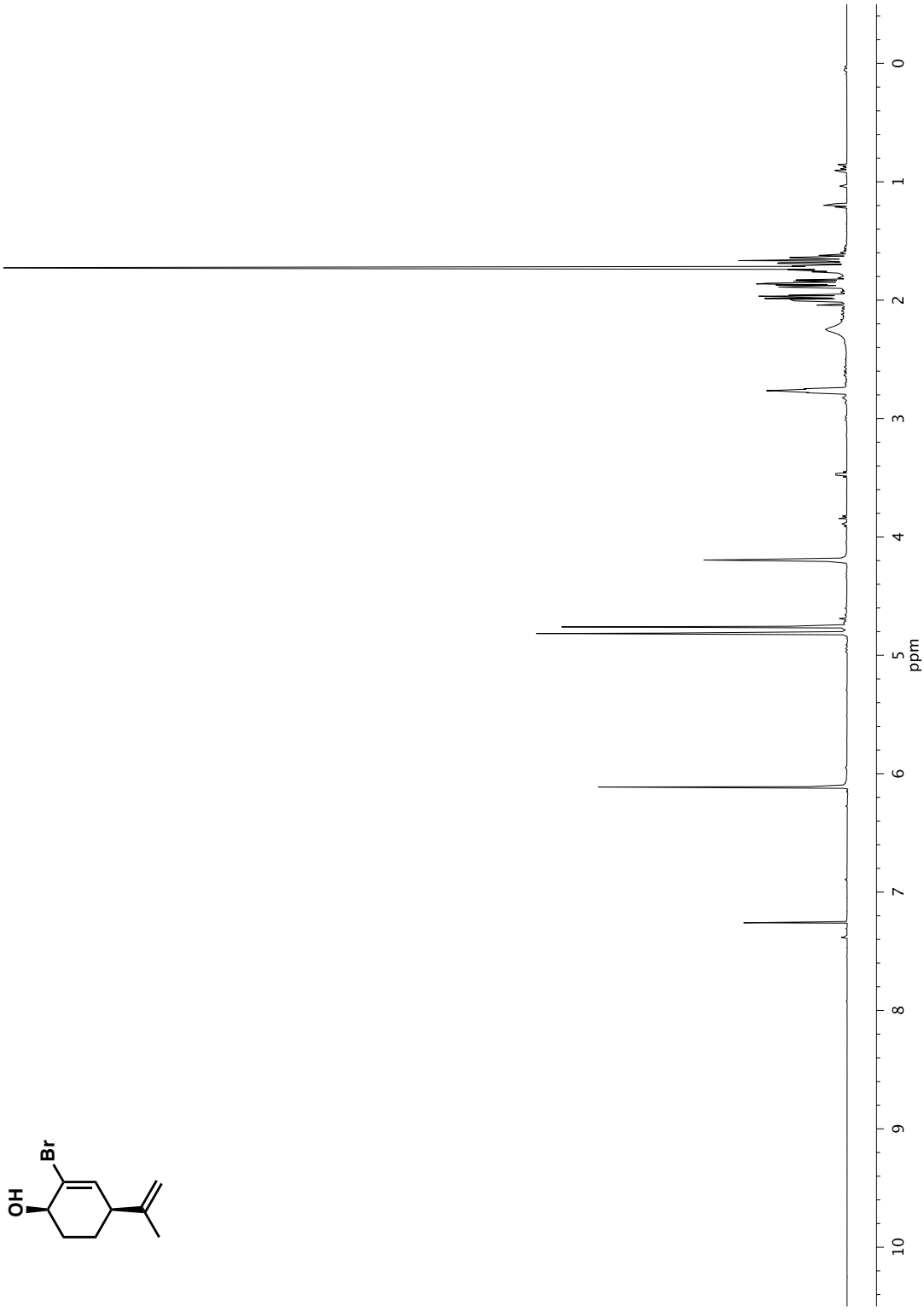

Figure A3.81 ^{1}H NMR (500 MHz, $CDCl_3$) of compound **77**

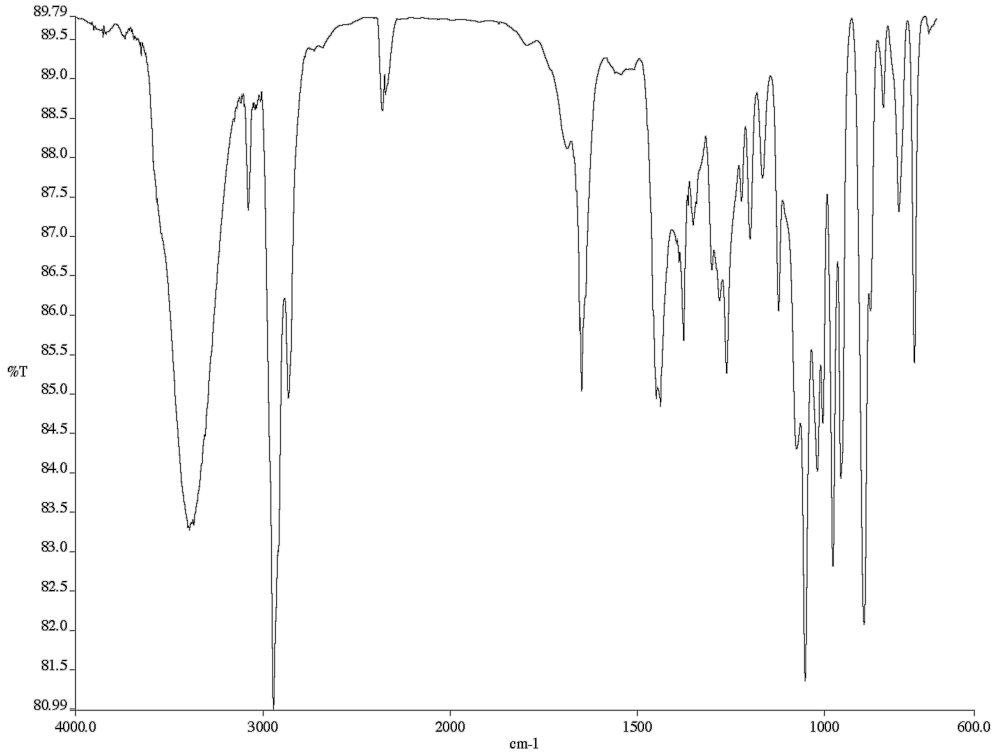

Figure A3.82 Infrared spectrum (thin film/NaCl) of compound **77**

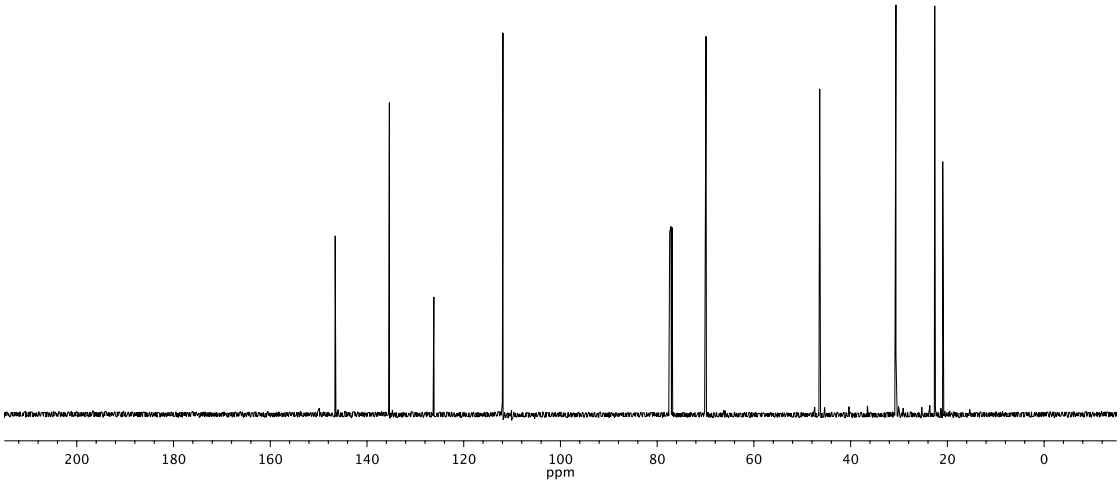

Figure A3.83 ^{13}C NMR (126 MHz, $CDCl_3$) of compound **77**

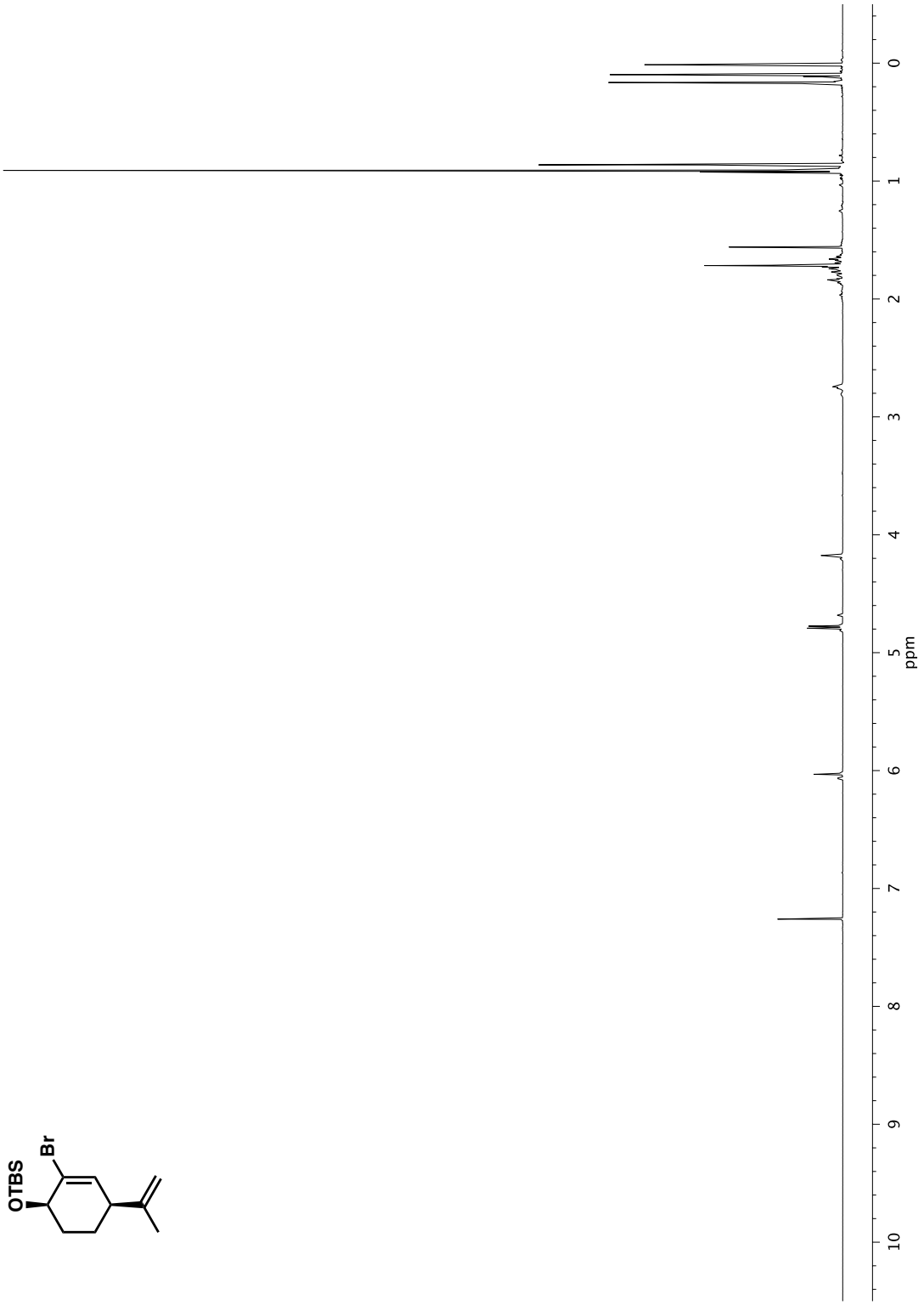

Figure A3.84 ^{1}H NMR (500 MHz, $CDCl_3$) of compound **78**

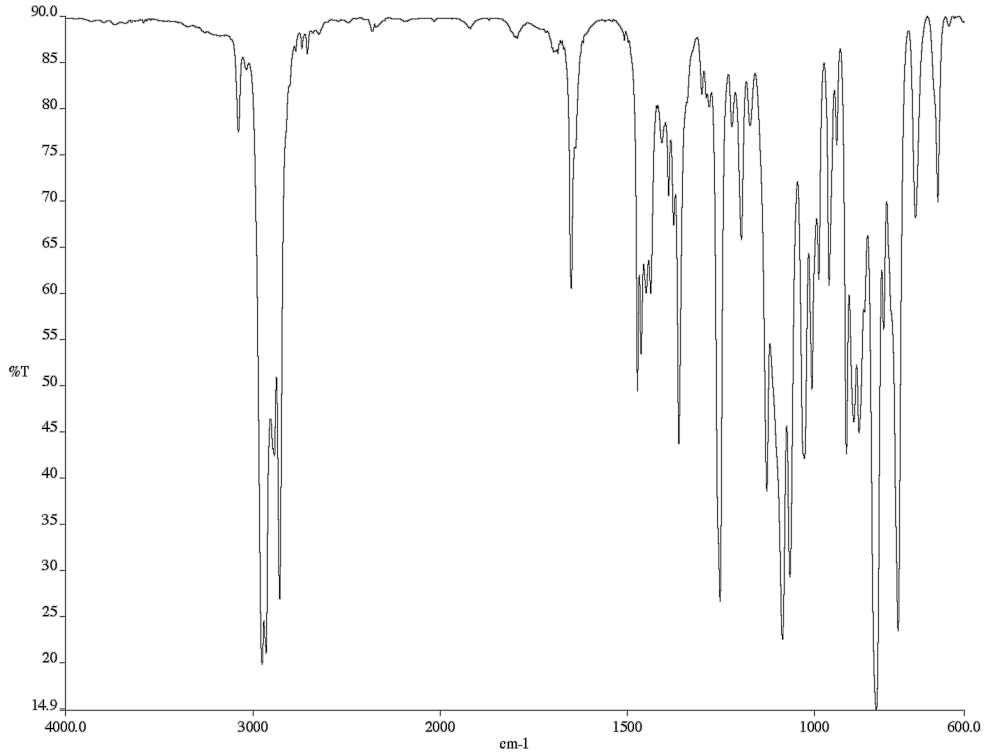

Figure A3.85 Infrared spectrum (thin film/NaCl) of compound **78**

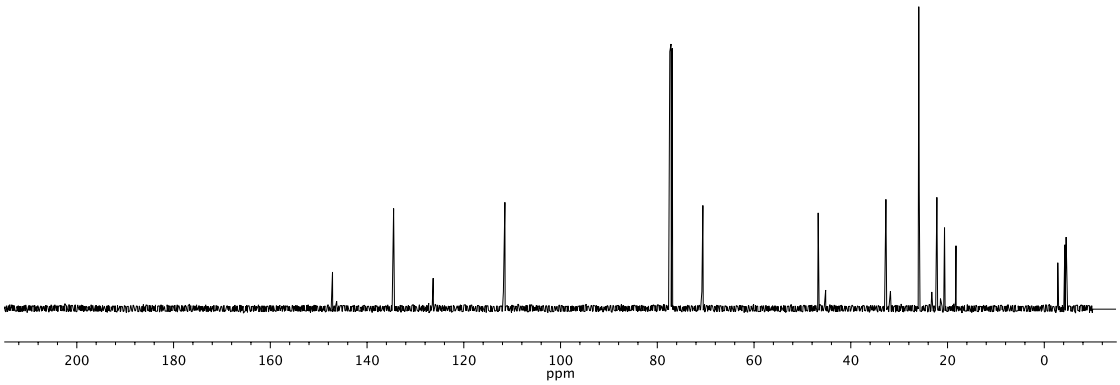

Figure A3.86 ^{13}C NMR (126 MHz, $CDCl_3$) of compound **78**

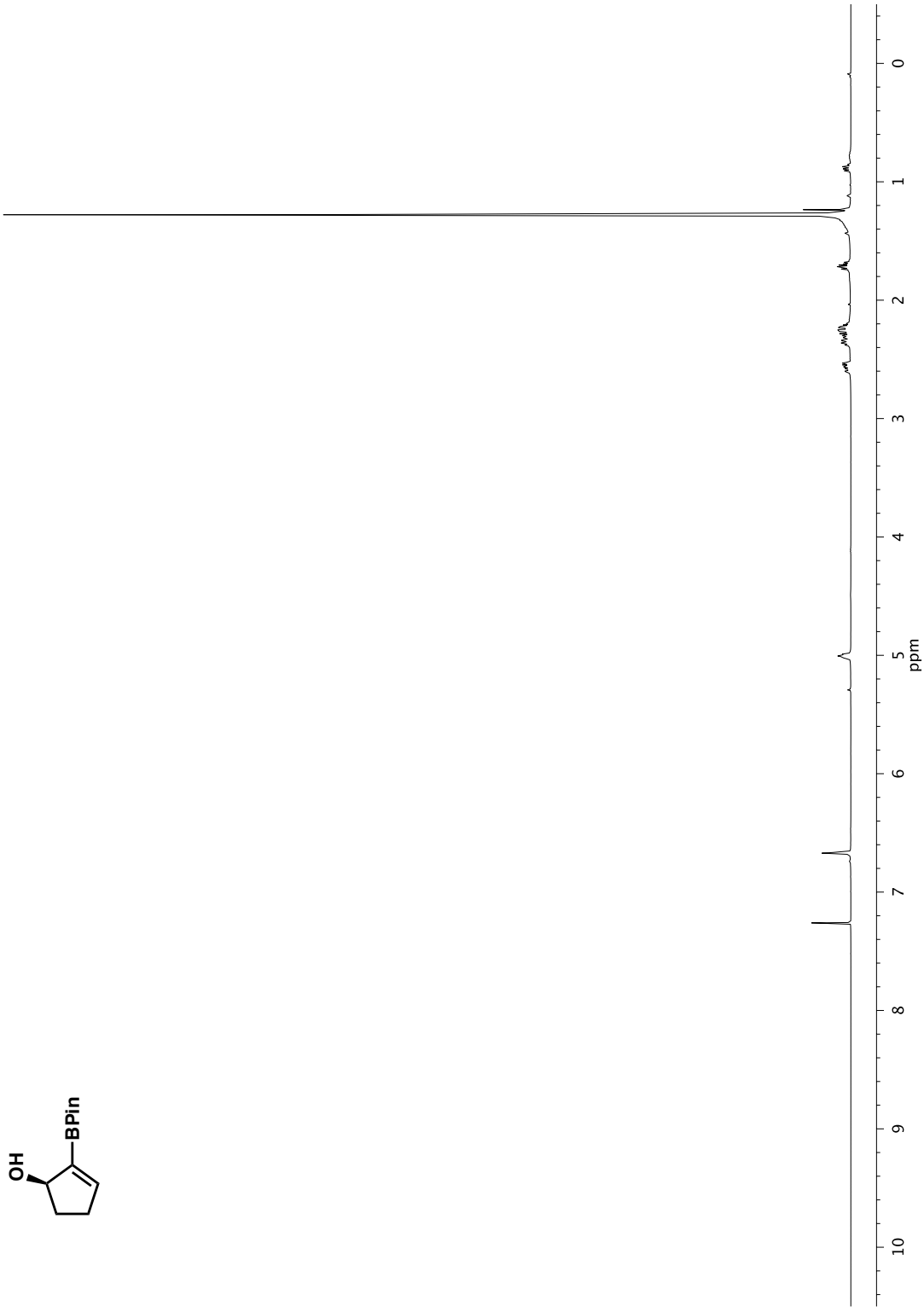

Figure A3.87 ^{1}H NMR (400 MHz, $CDCl_3$) of compound **79**

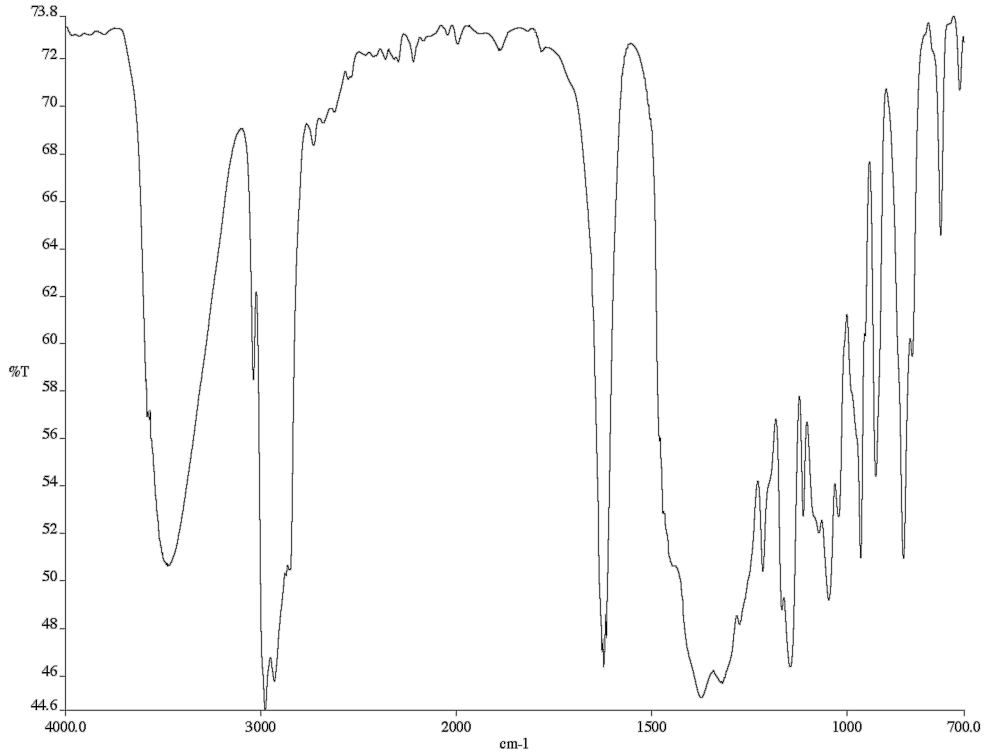

Figure A3.88 Infrared spectrum (thin film/NaCl) of compound **79**

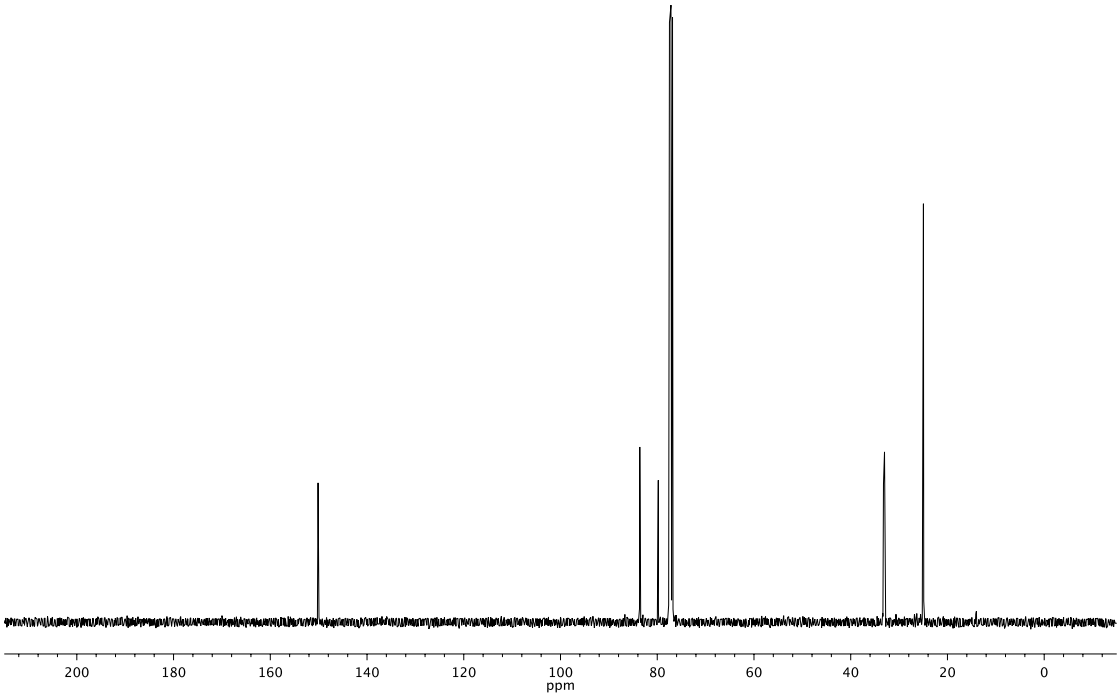

Figure A3.89 ^{13}C NMR (101 MHz, $CDCl_3$) of compound **79**

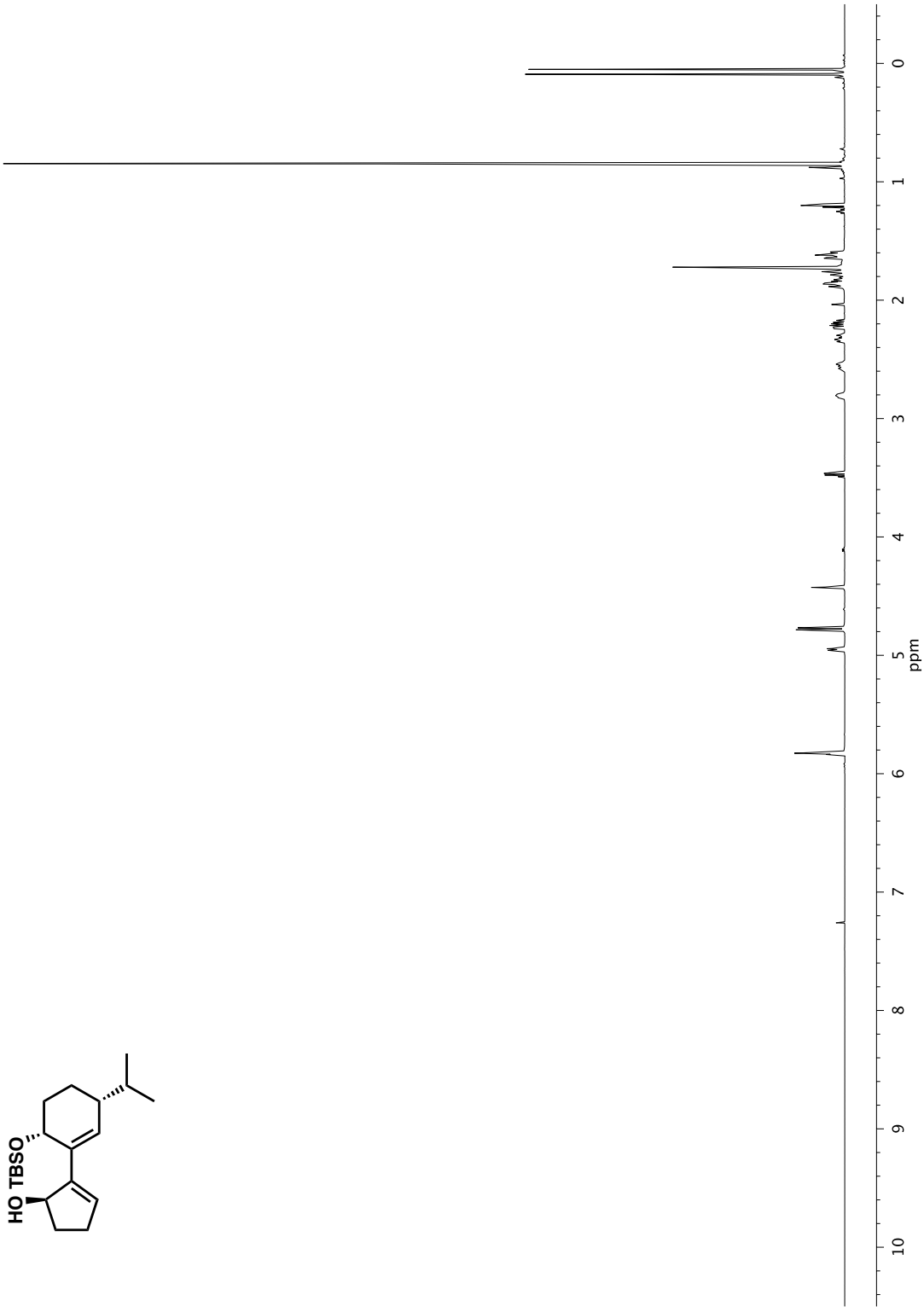

Figure A3.90 ^{1}H NMR (500 MHz, $CDCl_3$) of compound **80**

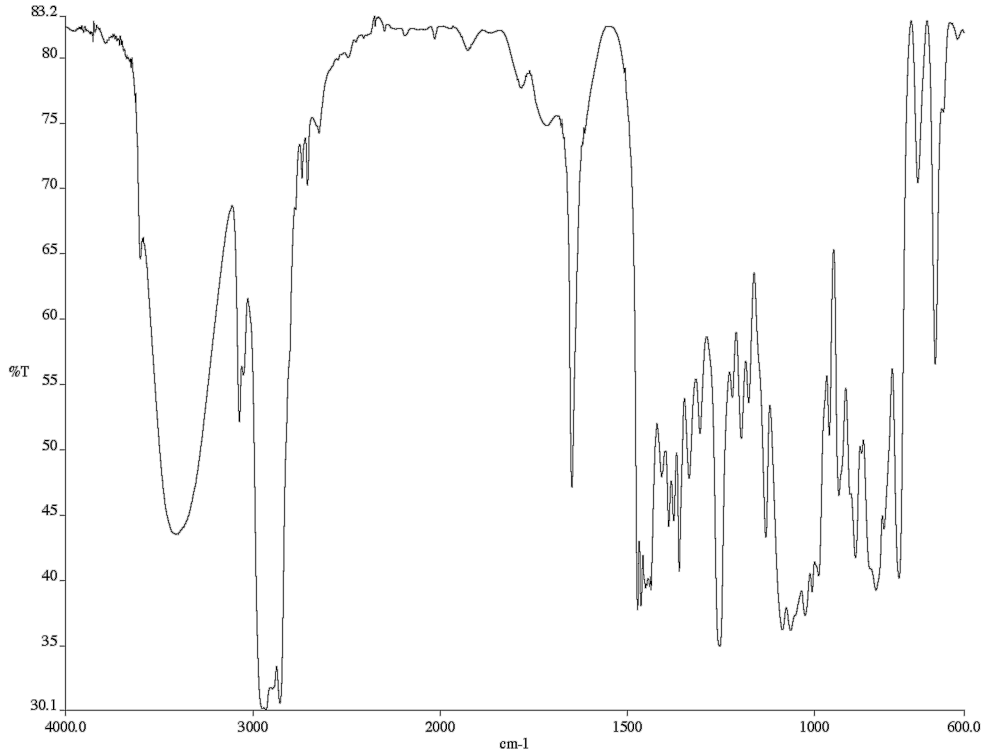

Figure A3.91 Infrared spectrum (thin film/NaCl) of compound **80**

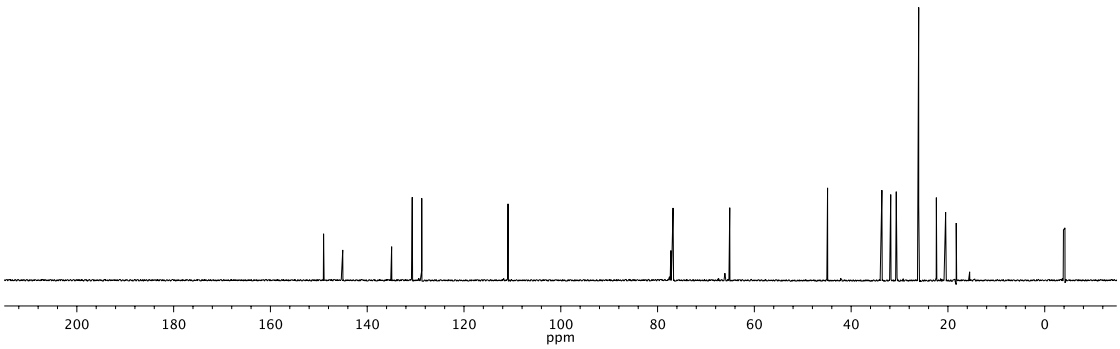

Figure A3.92 ^{13}C NMR (126 MHz, $CDCl_3$) of compound **80**

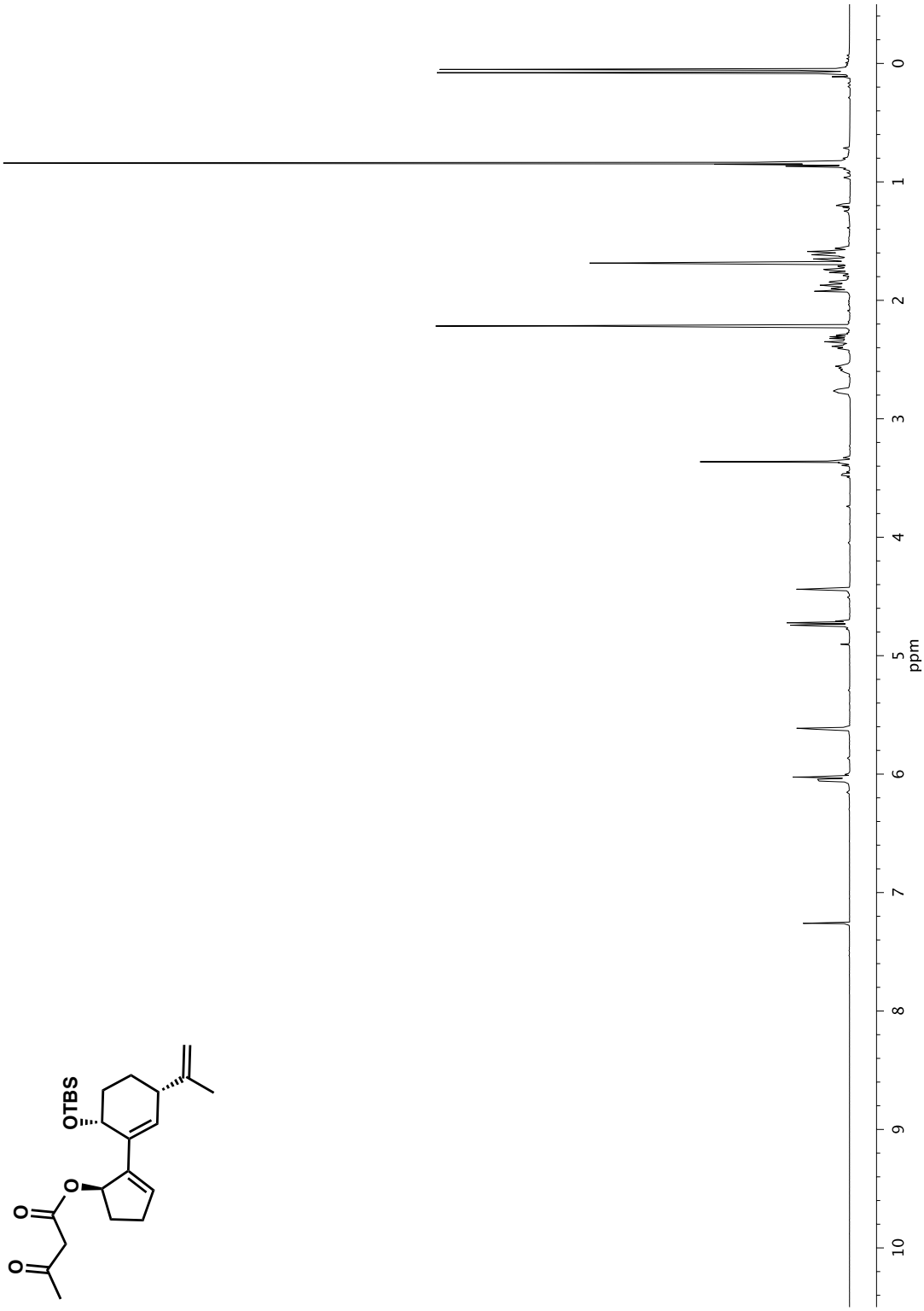

Figure A3.93 ^{1}H NMR (500 MHz, $CDCl_3$) of compound **81**

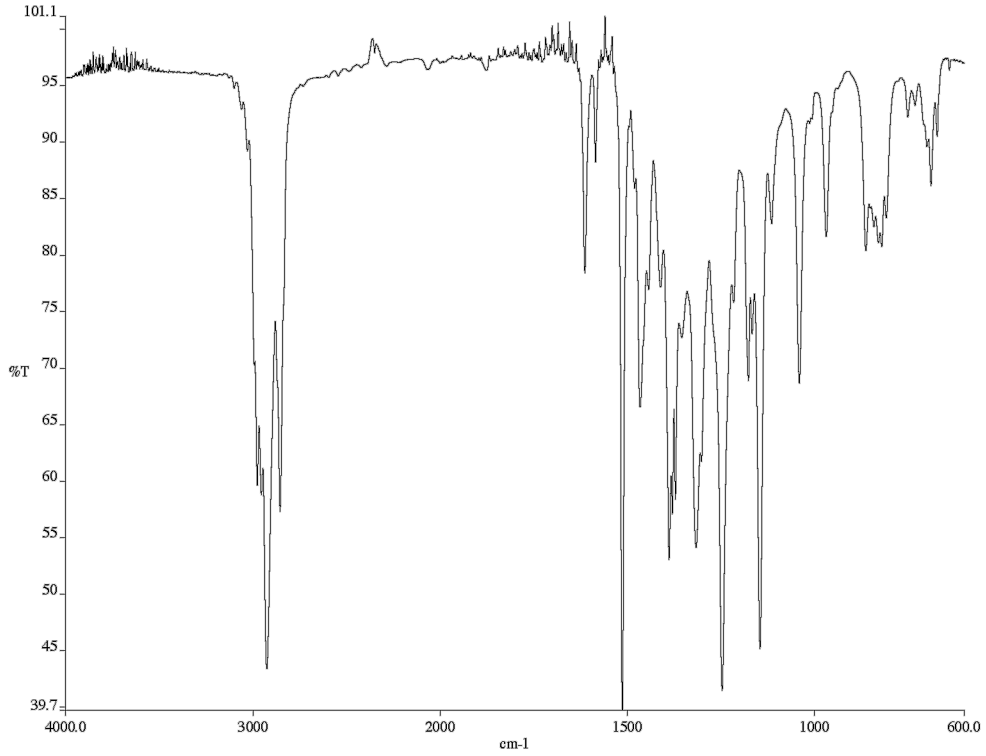

Figure A3.94 Infrared spectrum (thin film/NaCl) of compound **81**

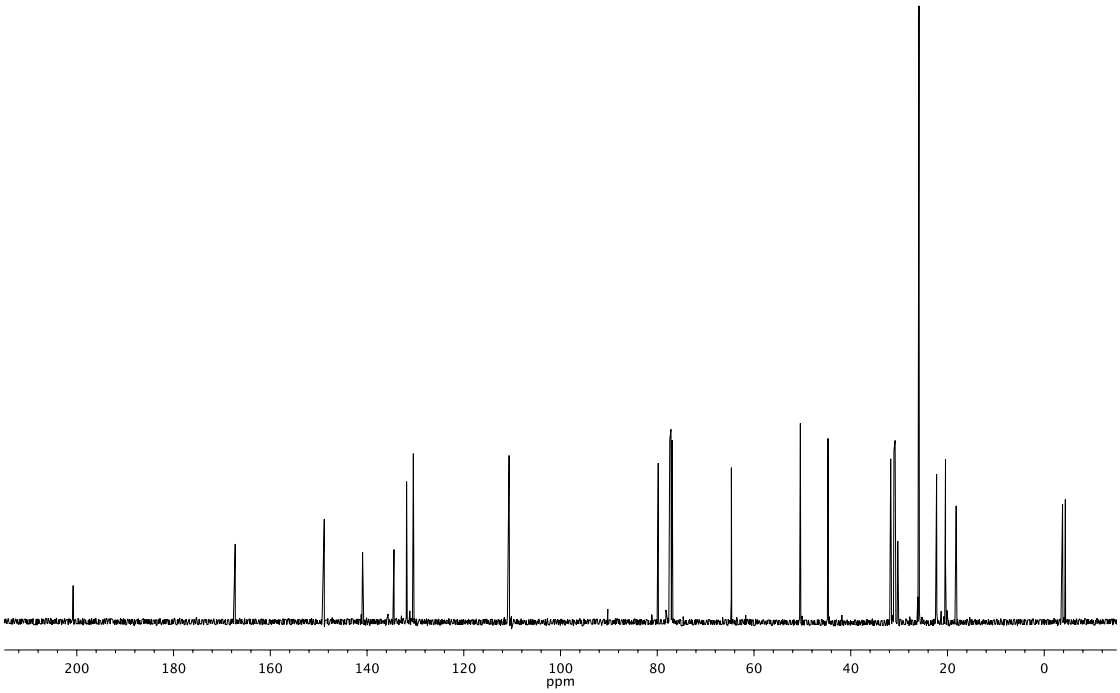

Figure A3.95 ^{13}C NMR (126 MHz, $CDCl_3$) of compound **81**

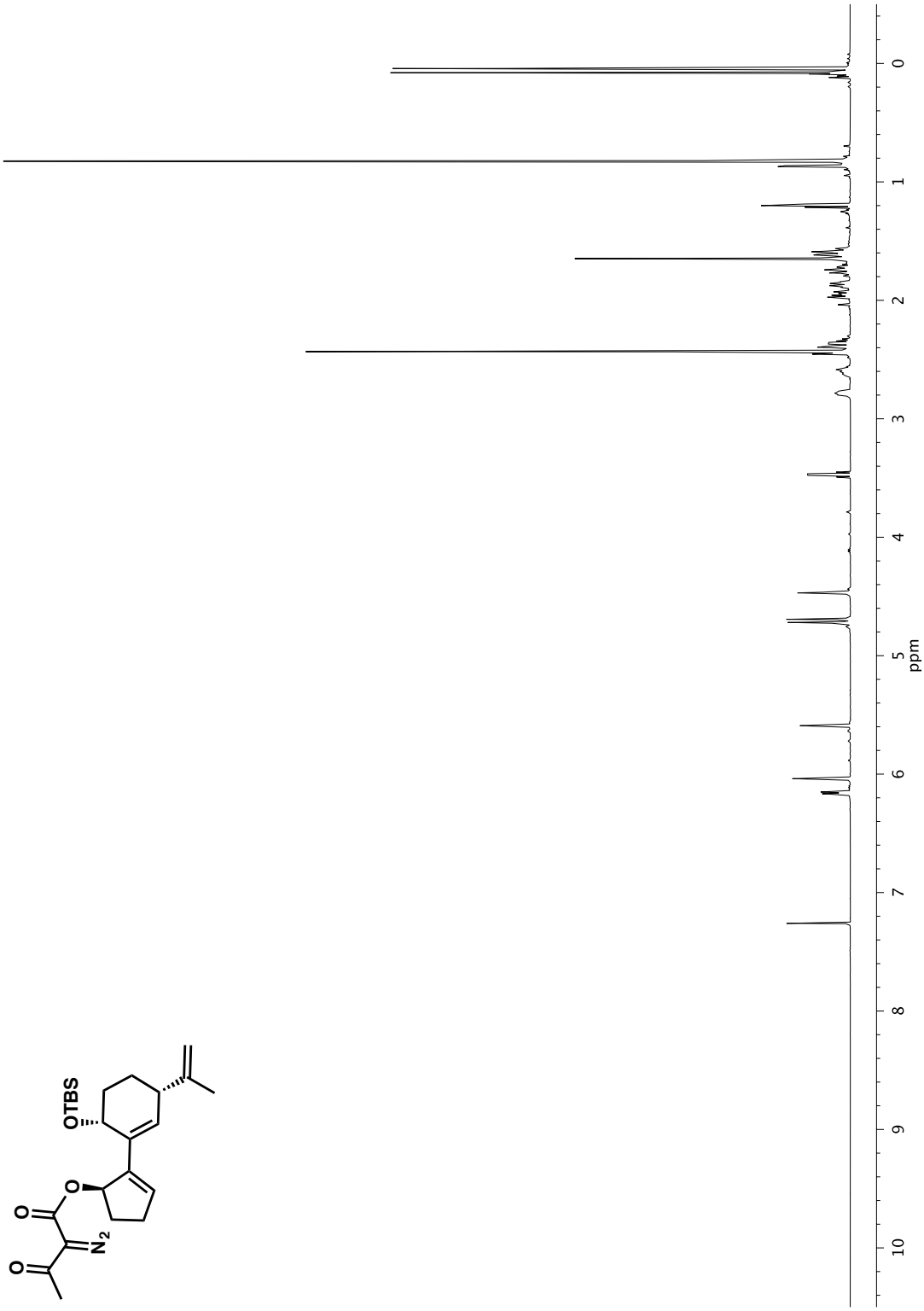

Figure A3.96 ^{1}H NMR (500 MHz, $CDCl_3$) of compound **75**

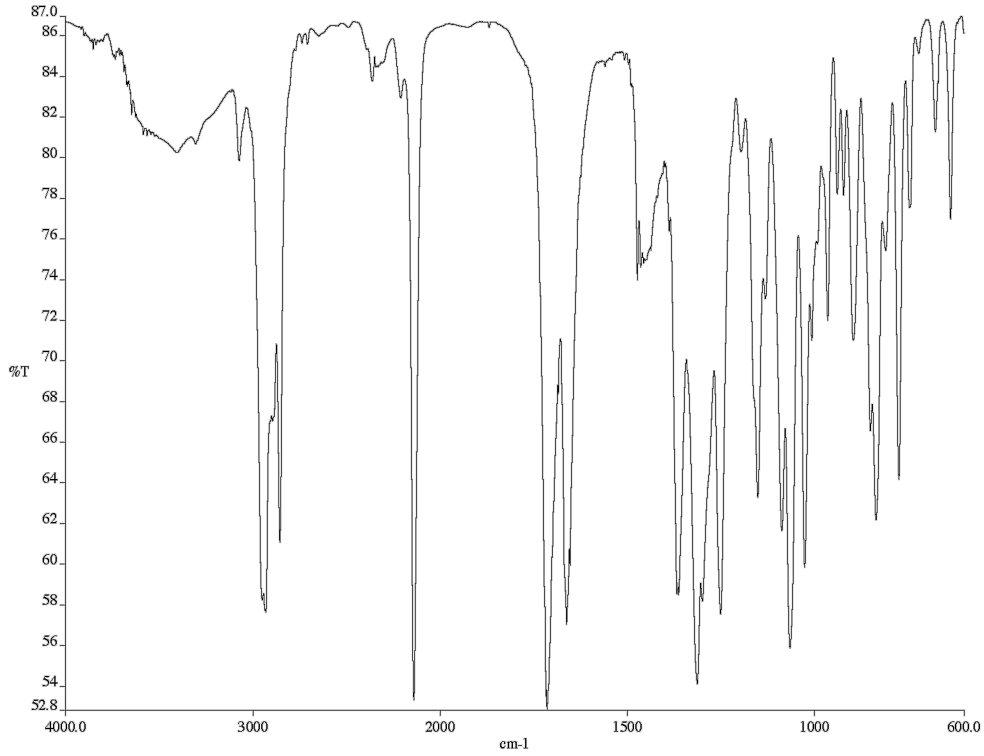

Figure A3.97 Infrared spectrum (thin film/NaCl) of compound **75**

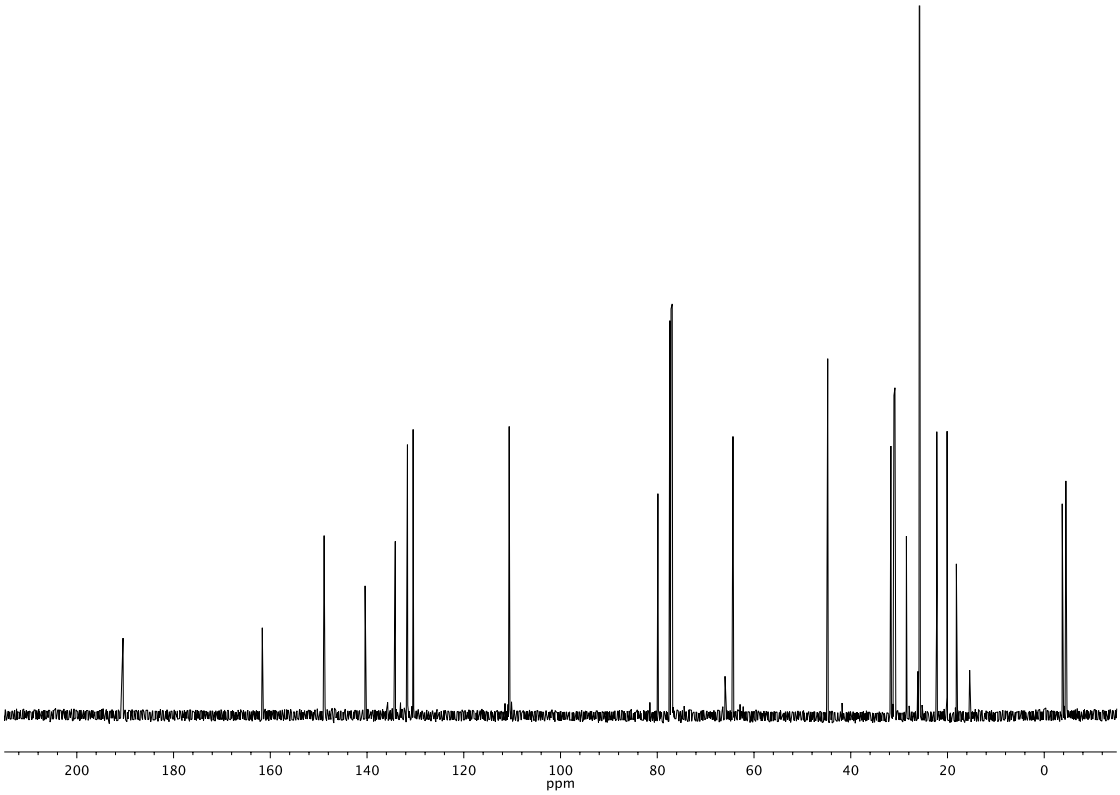

Figure A3.98 ^{13}C NMR (126 MHz, $CDCl_3$) of compound **75**

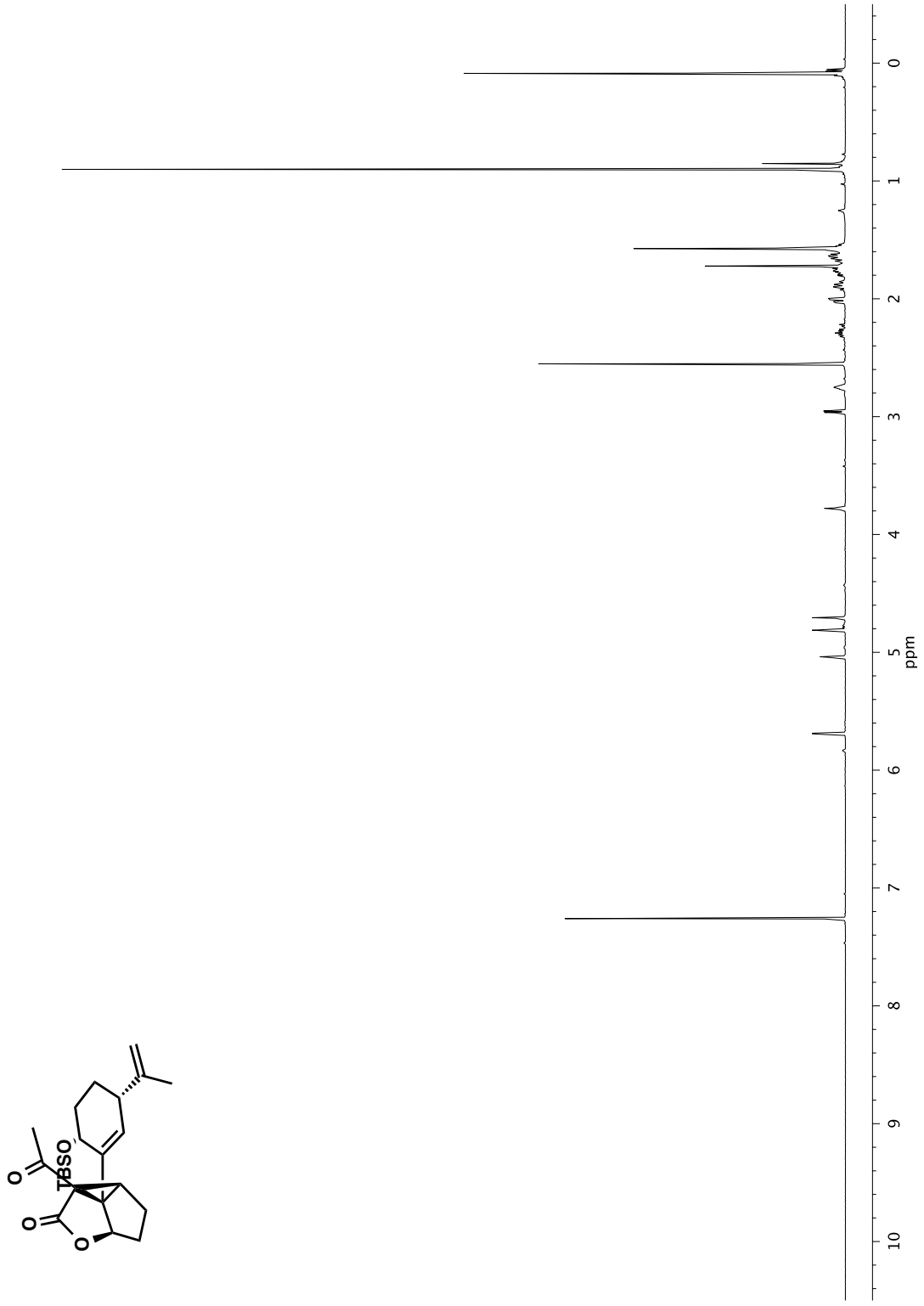

Figure A3.99 ^{1}H NMR (500 MHz, $CDCl_3$) of compound **82**

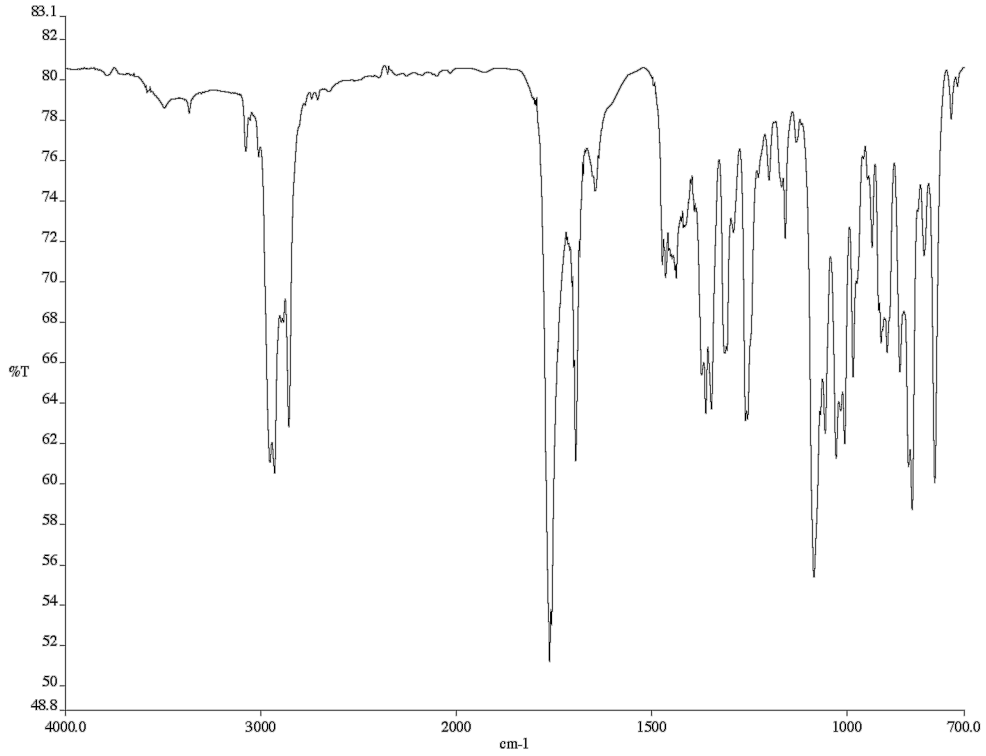

Figure A3.100 Infrared spectrum (thin film/NaCl) of compound **82**

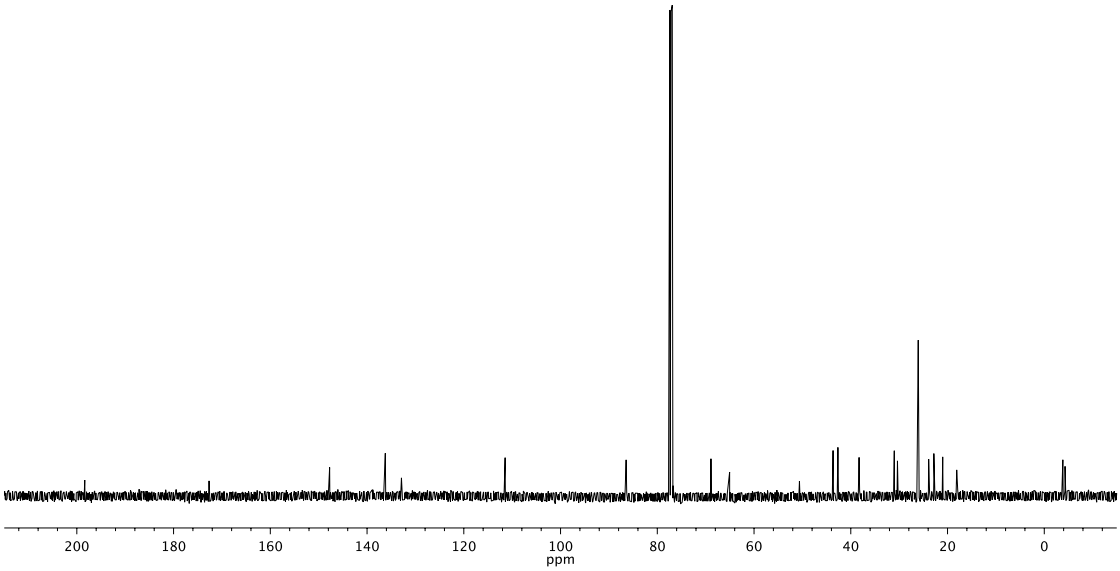

Figure A3.101 ^{13}C NMR (126 MHz, $CDCl_3$) of compound **82**

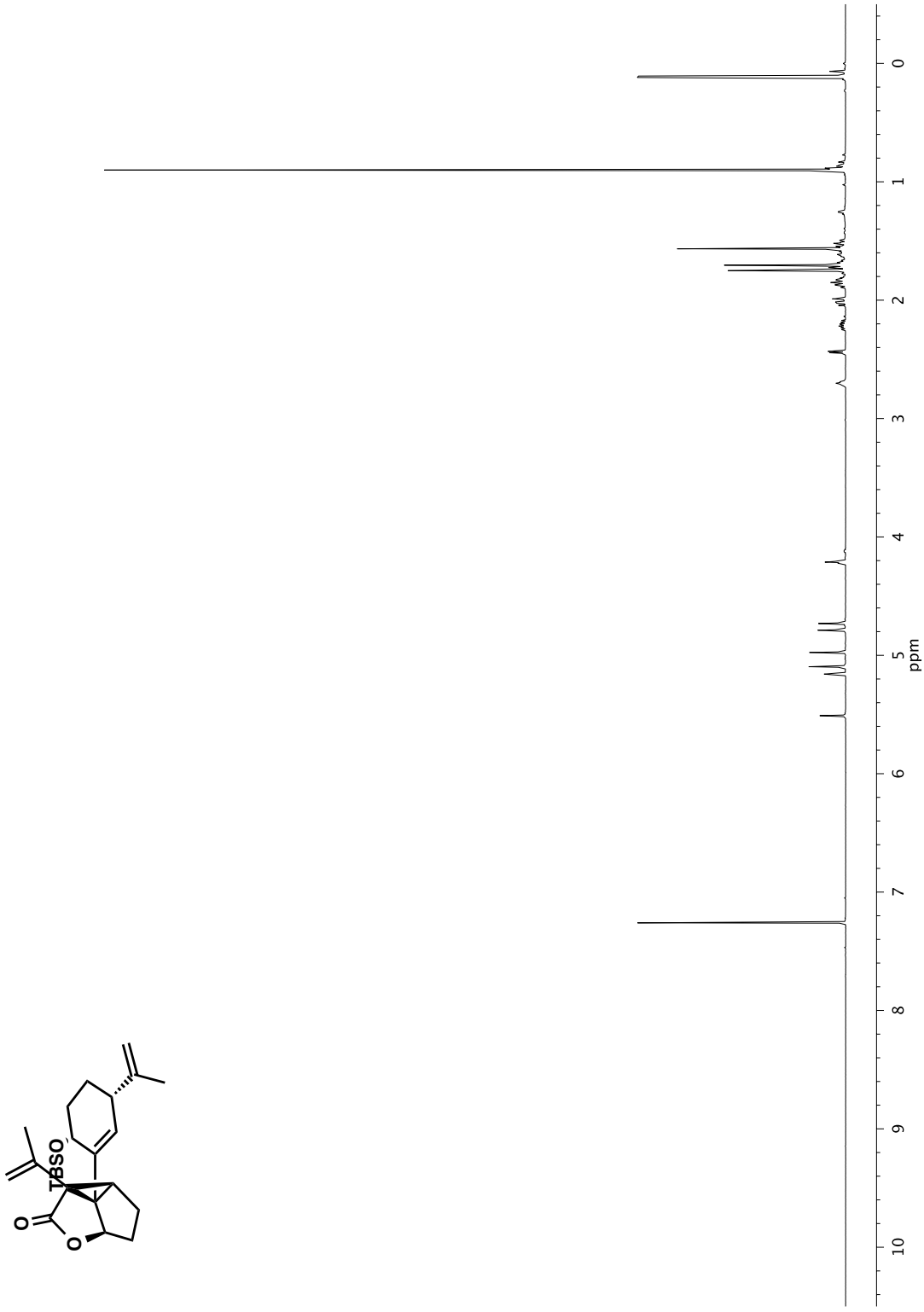

Figure A3.102 ^{1}H NMR (500 MHz, $CDCl_3$) of compound **83**

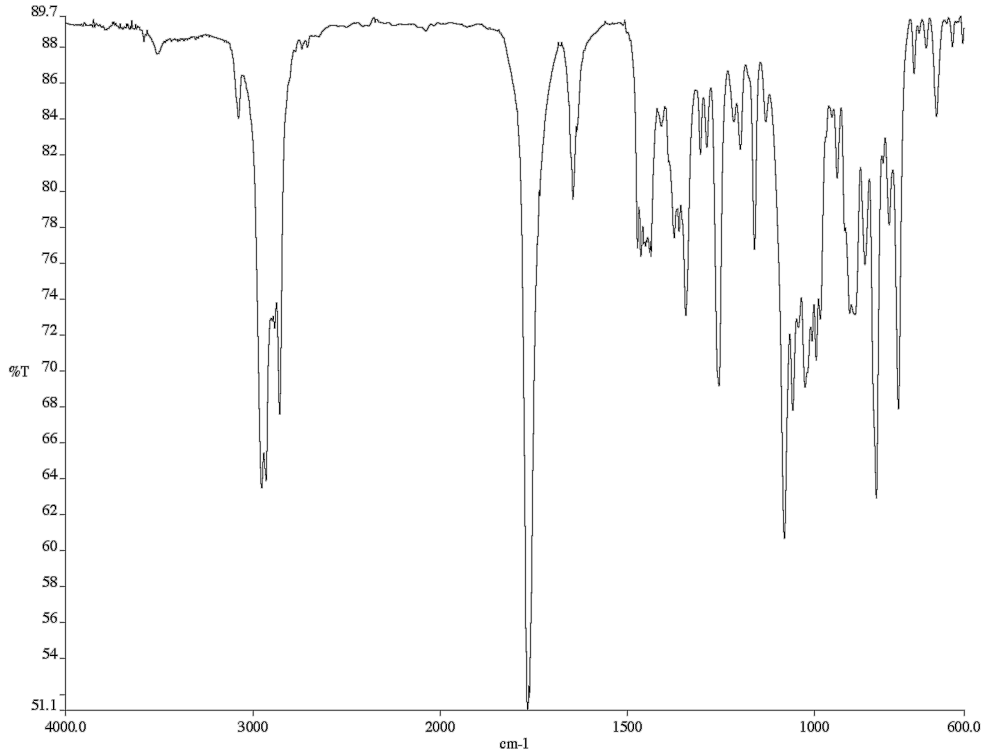

Figure A3.103 Infrared spectrum (thin film/NaCl) of compound **83**

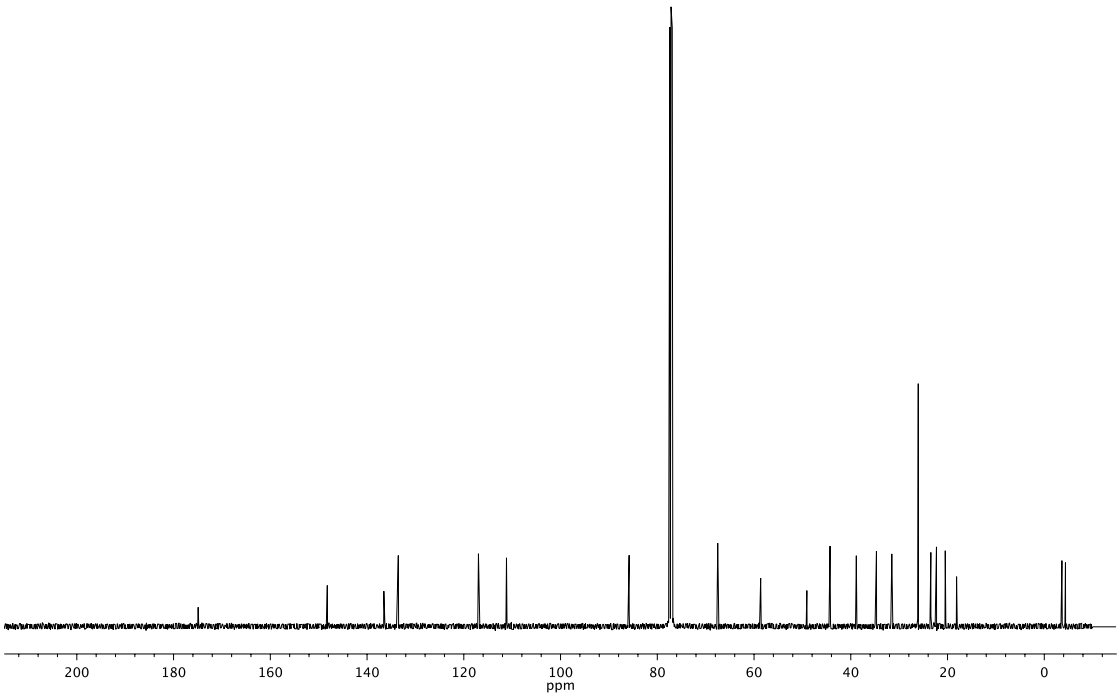

Figure A3.104 ^{13}C NMR (126 MHz, $CDCl_3$) of compound **83**

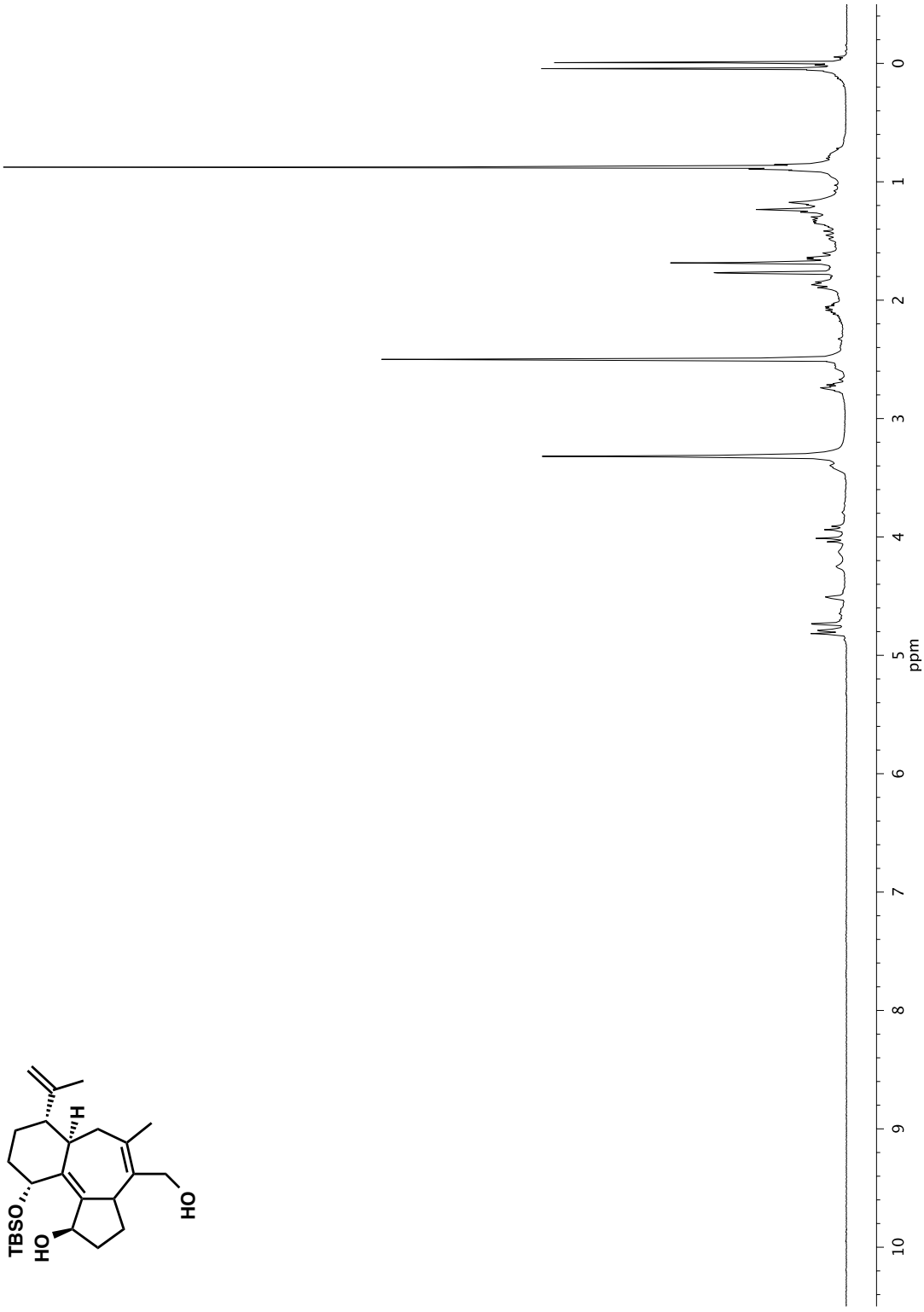

Figure A3.105 ^{1}H NMR (400 MHz, DMSO-*d6*) of compound **85**

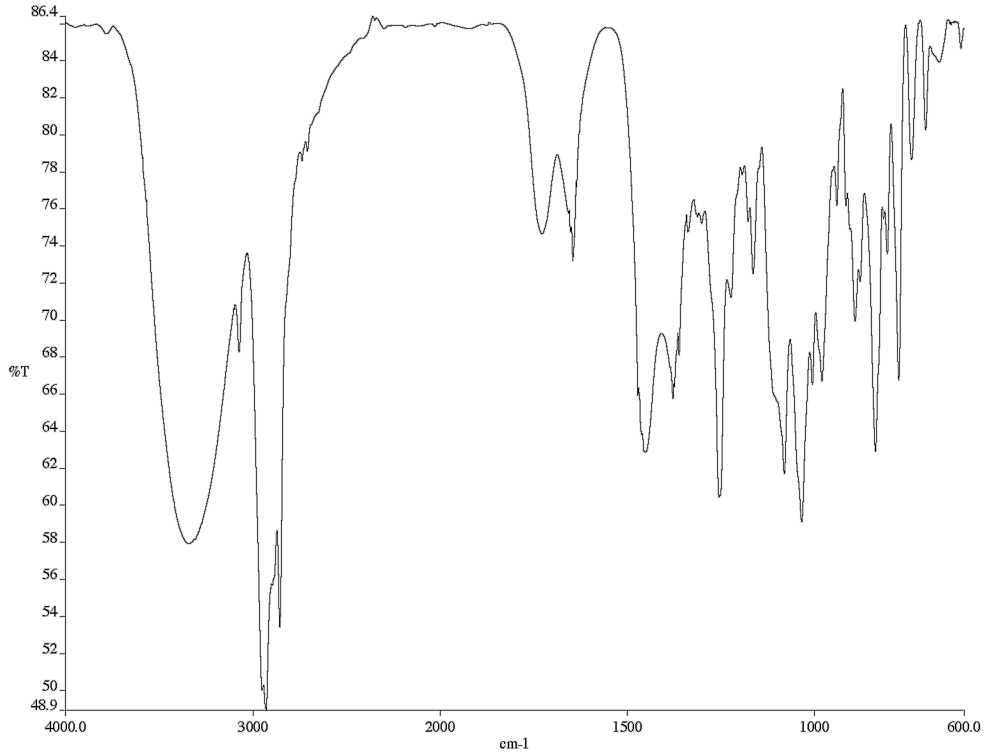

Figure A3.106 Infrared spectrum (thin film/NaCl) of compound **85**

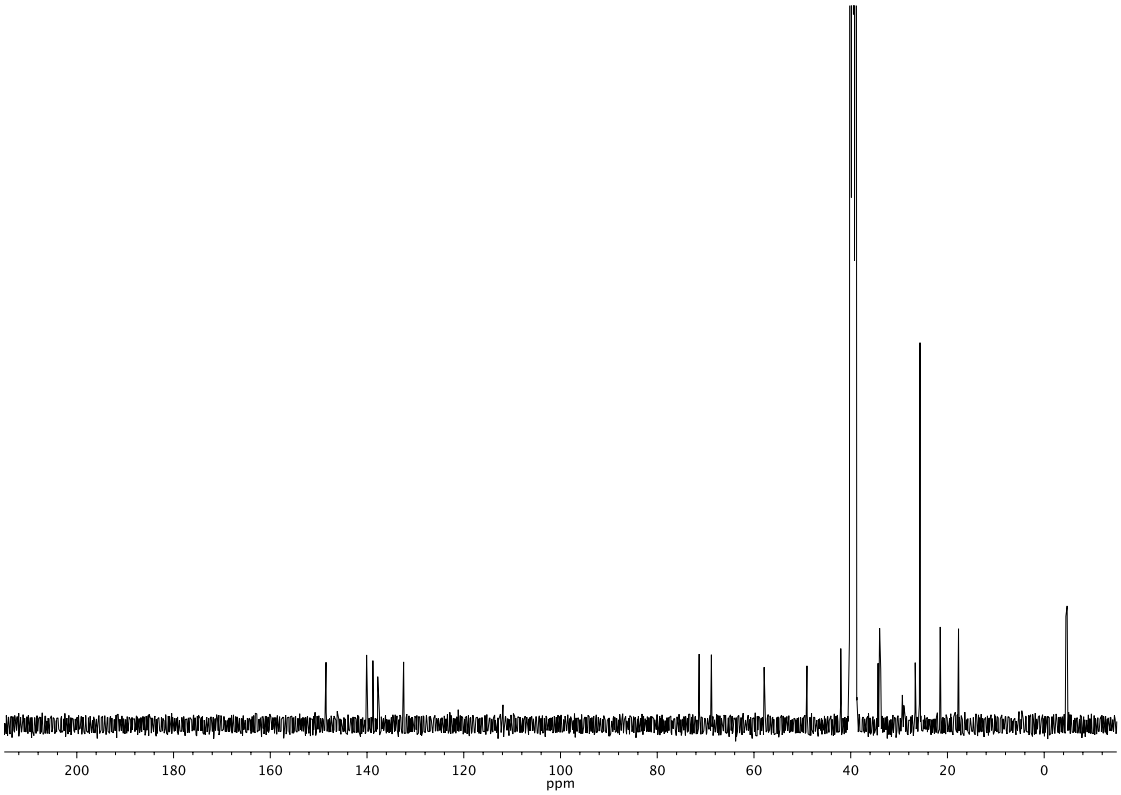

Figure A3.107 ^{13}C NMR (101 MHz, DMSO-*d6*) of compound **85**

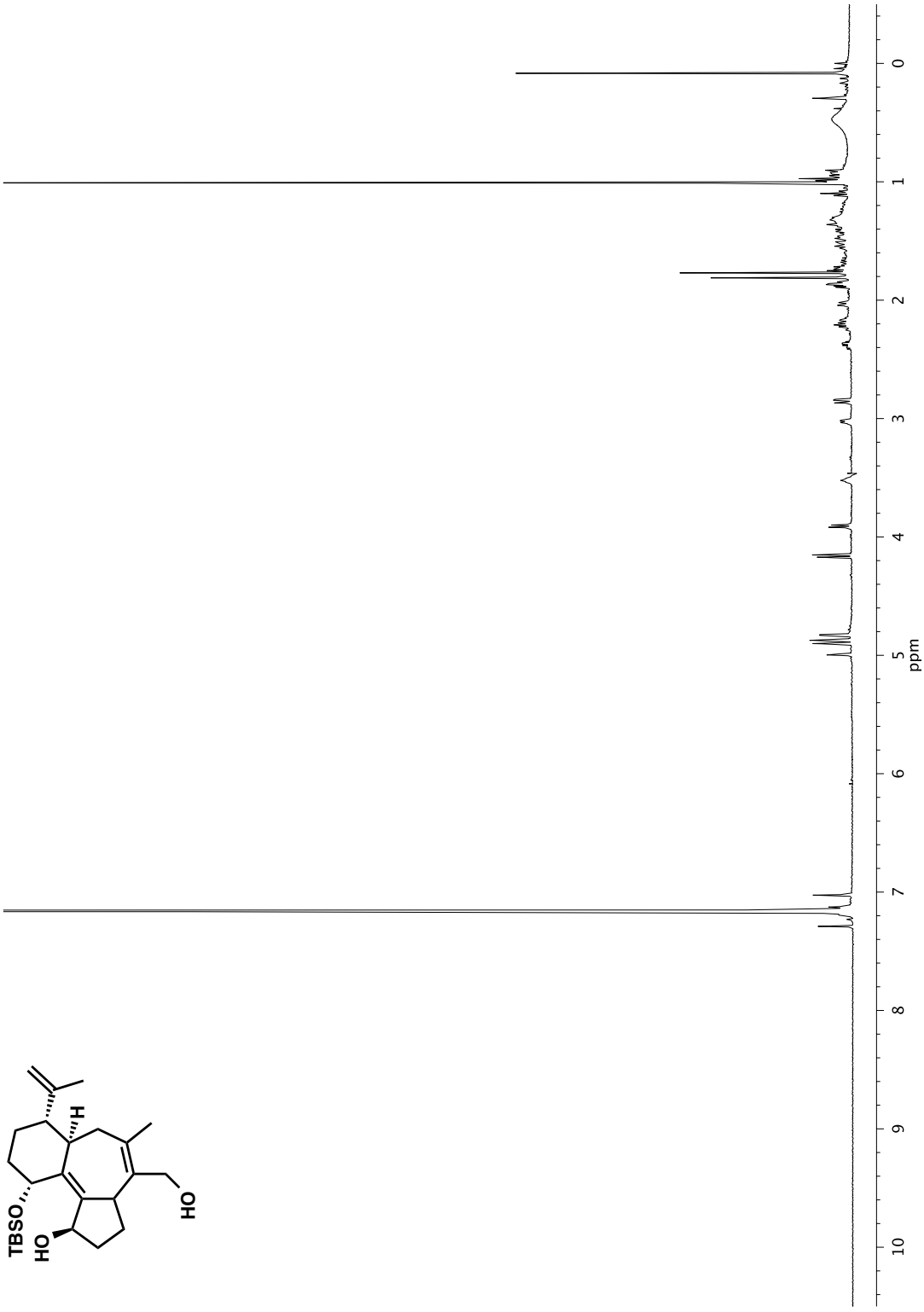

Figure A3.108 ^{1}H NMR (600 MHz, C_6D_6) of compound **85**

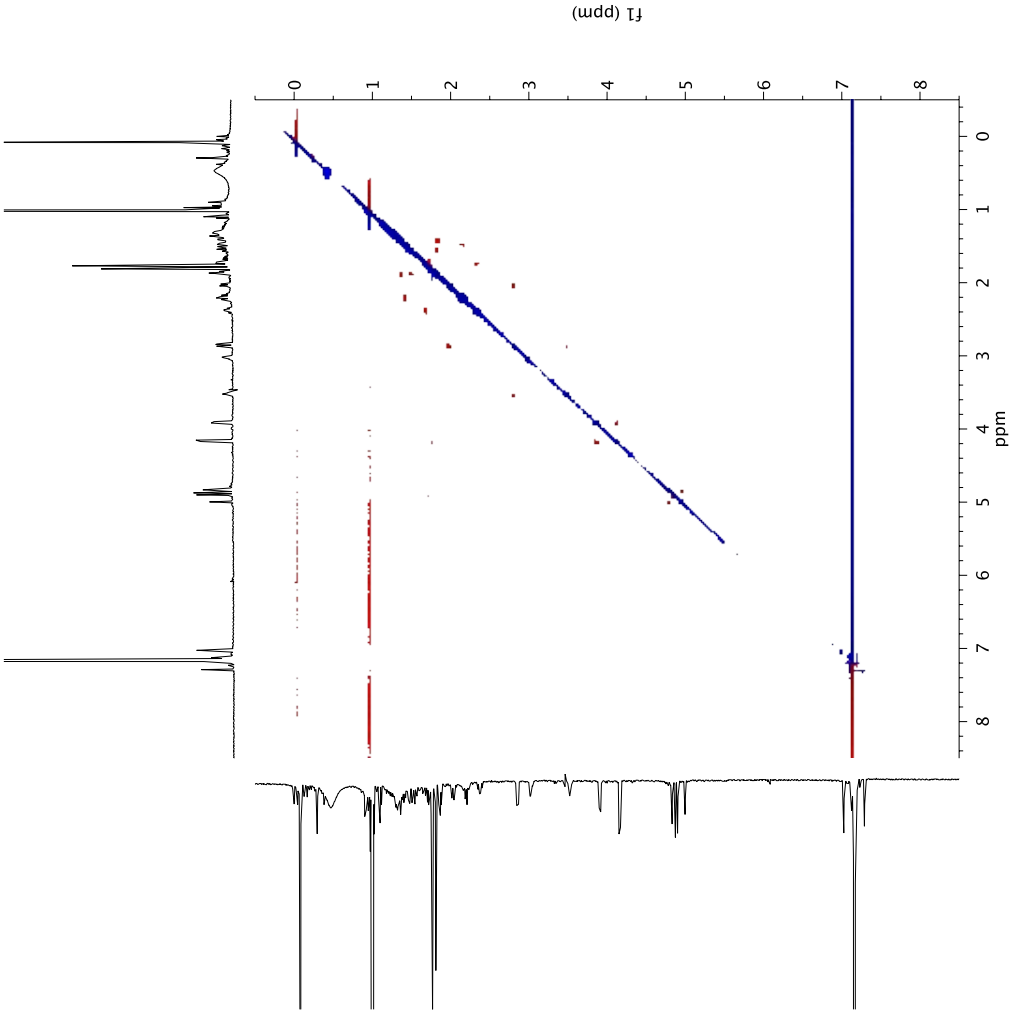

Figure A3.109 NOESY (600 MHz, C_6D_6) of compound **85**

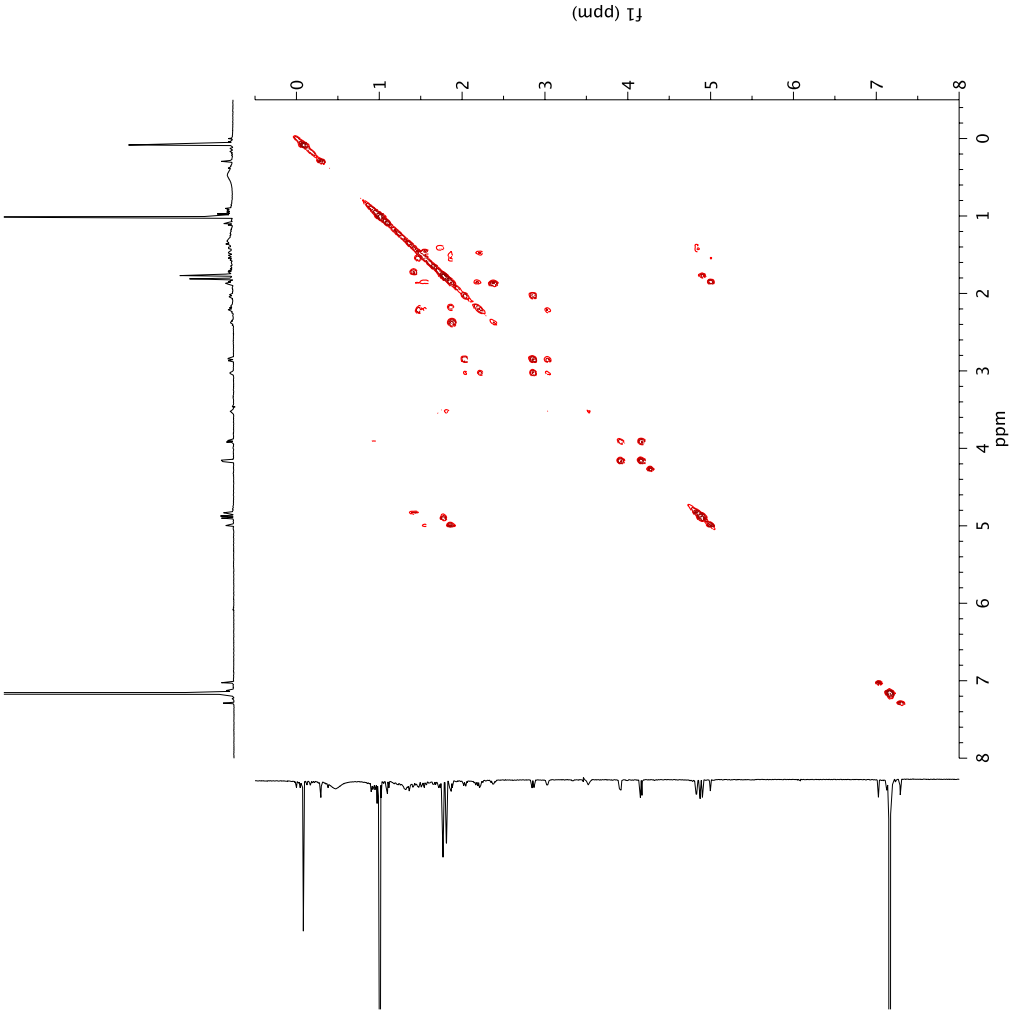

Figure A3.110 gCOSY (600 MHz, C_6D_6) of compound **85**

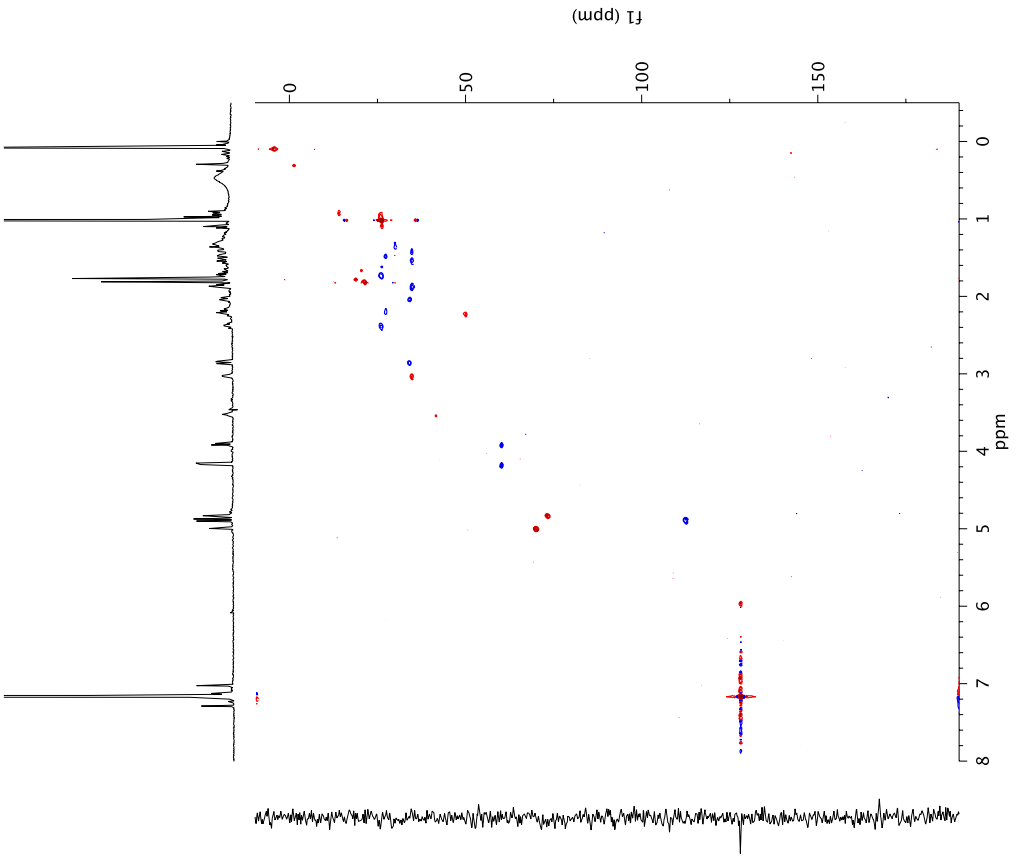

Figure A3.111 ^{1}H-^{13}C HSQC (600 MHz, C_6D_6) of compound **85**

APPENDIX 4

X-ray Crystallography Reports

Relevant to Chapter 1

A4.1 CRYSTAL STRUCTURE ANALYSIS OF 42

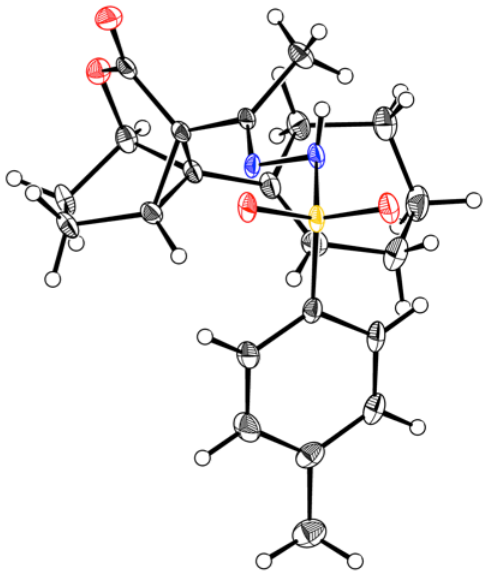

42

*Table A4.1.1. Crystal data and structure refinement for **42**.*

Empirical formula	$C_{22}H_{26}N_2O_4S$	
Formula weight	414.51	
Temperature	100 K	
Wavelength	0.71073 Å	
Crystal system	Triclinic	
Space group	P-1	
Unit cell dimensions	a = 19.3346(10) Å	α= 90.199(3)°
	b = 21.5305(11) Å	β= 93.729(3)°
	c = 9.9784(5) Å	γ = 90.810(3)°
Volume	4144.6(4) $Å^3$	
Z	8	
Density (calculated)	1.329 Mg/m^3	
Absorption coefficient	0.187 mm^{-1}	
F(000)	1760	
Crystal size	0.35 x 0.33 x 0.10 mm^3	
Theta range for data collection	2.045 to 32.962°.	
Index ranges	-28<=h<=29, -32<=k<=32, -15<=l<=15	
Reflections collected	272986	
Independent reflections	29250 [R(int) = 0.0867]	
Completeness to theta = 25.000°	100.0 %	
Absorption correction	Semi-empirical from equivalents	
Max. and min. transmission	1.0000 and 0.8821	
Refinement method	Full-matrix least-squares on F^2	
Data / restraints / parameters	29250 / 0 / 1054	
Goodness-of-fit on F^2	1.037	
Final R indices [I>2sigma(I)]	R1 = 0.0907, wR2 = 0.2272	
R indices (all data)	R1 = 0.1406, wR2 = 0.2638	

Extinction coefficient	n/a
Largest diff. peak and hole	3.274 and -1.435 e.Å^{-3}

Table A4.1.2. Atomic coordinates (x 10^5) and equivalent isotropic displacement parameters (Å^{2}x 10^4) for ***42****. U(eq) is defined as one third of the trace of the orthogonalized U^{ij} tensor.*

	x	y	z	U(eq)
S(1)	13320(4)	13122(4)	9576(7)	150(2)
O(1)	49133(12)	21574(12)	19580(20)	194(5)
O(2)	44907(13)	12484(11)	11420(30)	211(5)
O(3)	15151(13)	11293(12)	-3620(20)	190(5)
O(4)	8084(12)	9653(12)	15920(20)	212(5)
N(1)	25759(13)	16229(13)	15610(20)	141(5)
N(2)	20329(13)	12431(13)	19710(20)	154(5)
C(1)	37110(16)	20221(14)	18900(30)	131(5)
C(2)	35319(17)	26494(15)	12570(30)	162(6)
C(3)	40319(18)	29526(16)	3160(30)	201(6)
C(4)	46367(19)	31992(17)	12740(30)	220(7)
C(5)	46470(17)	27472(16)	24340(30)	182(6)
C(6)	38727(16)	26291(14)	26600(30)	149(5)
C(7)	43909(16)	17536(15)	16040(30)	150(5)
C(8)	31453(16)	15936(14)	22810(30)	131(5)
C(9)	32779(18)	11975(16)	34940(30)	204(6)
C(10)	11225(16)	21054(16)	9060(30)	162(6)
C(11)	8810(18)	23791(18)	20540(30)	225(7)
C(12)	7000(19)	29940(18)	20140(40)	240(7)
C(13)	7617(17)	33456(17)	8660(40)	217(7)
C(14)	10150(20)	30670(18)	-2540(30)	270(8)
C(15)	11900(20)	24434(17)	-2480(30)	229(7)
C(16)	5700(20)	40190(19)	8610(40)	289(8)
C(17)	35745(18)	27620(15)	39590(30)	181(6)
C(18)	29230(20)	29568(17)	40370(40)	245(7)
C(19)	25920(20)	30390(20)	53470(40)	324(9)
C(20)	30980(20)	30028(19)	65620(40)	299(8)

C(21)	36180(20)	24935(19)	64100(40)	268(7)
C(22)	40298(19)	26011(17)	51900(30)	209(6)
S(1B)	13258(4)	12852(4)	59543(7)	158(2)
O(1B)	48049(13)	2551(12)	71500(30)	235(5)
O(2B)	45243(13)	11942(12)	63860(30)	240(5)
O(3B)	8386(13)	16497(12)	66270(20)	224(5)
O(4B)	15006(13)	14527(13)	46240(20)	214(5)
N(1B)	25455(14)	9277(12)	65110(20)	142(5)
N(2B)	20429(13)	13340(13)	69390(20)	140(5)
C(1B)	36234(16)	4545(14)	69050(30)	135(5)
C(2B)	34054(17)	-1502(15)	61640(30)	172(6)
C(3B)	39125(19)	-4647(16)	52690(40)	224(7)
C(4B)	44500(20)	-7532(17)	62690(40)	258(7)
C(5B)	44493(18)	-3253(16)	74870(40)	217(7)
C(6B)	36840(17)	-1734(14)	76100(30)	161(6)
C(7B)	43437(16)	6938(15)	67610(30)	174(6)
C(8B)	30958(16)	9018(14)	72880(30)	135(5)
C(9B)	32315(18)	12629(16)	85720(30)	184(6)
C(10B)	10660(16)	5029(16)	59400(30)	170(6)
C(11B)	10420(20)	1525(19)	47510(30)	251(7)
C(12B)	8420(20)	-4650(19)	47970(30)	261(7)
C(13B)	6617(17)	-7465(18)	59790(30)	225(7)
C(14B)	6810(20)	-3817(19)	71390(30)	262(7)
C(15B)	8802(19)	2314(18)	71350(30)	235(7)
C(16B)	4430(20)	-14150(20)	60160(40)	292(8)
C(17B)	32930(20)	-3298(15)	88040(30)	215(7)
C(18B)	26310(20)	-5250(20)	86790(40)	306(8)
C(19B)	22050(30)	-6570(30)	98570(50)	441(11)
C(20B)	26640(40)	-6770(30)	111880(50)	574(17)
C(21B)	32030(30)	-1710(20)	112750(50)	507(14)
C(22B)	36780(20)	-2140(20)	101310(40)	319(9)
S(1C)	12001(4)	59892(4)	58426(7)	159(2)
O(1C)	47966(11)	53435(11)	70150(20)	166(4)
O(2C)	43592(13)	62294(11)	62170(20)	189(5)
O(3C)	13902(13)	61910(12)	45460(20)	206(5)
O(4C)	6620(13)	63038(13)	64810(20)	235(5)

N(1C)	24509(13)	57423(14)	64920(20)	157(5)
N(2C)	18921(14)	60905(14)	68850(20)	163(5)
C(1C)	35919(15)	54088(14)	68830(30)	119(5)
C(2C)	34398(16)	47727(14)	62260(30)	139(5)
C(3C)	39586(17)	44999(16)	52950(30)	173(6)
C(4C)	45639(17)	42921(16)	62630(30)	188(6)
C(5C)	45393(16)	47354(14)	74430(30)	151(5)
C(6C)	37624(15)	48043(14)	76390(30)	125(5)
C(7C)	42663(15)	57166(14)	66440(30)	132(5)
C(8C)	30100(15)	58024(15)	72500(30)	133(5)
C(9C)	31215(18)	62083(17)	84720(30)	211(6)
C(10C)	10190(16)	51853(16)	57500(30)	171(6)
C(11C)	6450(20)	49013(19)	67320(40)	253(7)
C(12C)	5370(20)	42627(19)	66860(40)	280(8)
C(13C)	7957(17)	39030(17)	56930(30)	209(6)
C(14C)	11720(20)	41909(18)	47140(30)	251(7)
C(15C)	12810(20)	48307(18)	47320(30)	239(7)
C(16C)	6650(20)	32119(18)	56590(40)	271(7)
C(17C)	34480(17)	46447(15)	89070(30)	169(6)
C(18C)	28090(20)	43981(18)	89350(40)	273(8)
C(19C)	24650(30)	42670(20)	102160(50)	404(11)
C(20C)	29590(30)	43440(20)	114700(40)	408(11)
C(21C)	34510(20)	48930(20)	113750(40)	326(9)
C(22C)	38780(20)	48217(18)	101720(30)	249(7)
S(1D)	12549(4)	60151(4)	8655(7)	163(2)
O(1D)	47108(12)	72046(12)	21250(30)	221(5)
O(2D)	44078(13)	62556(11)	13520(30)	213(5)
O(3D)	7684(13)	56290(12)	15030(20)	217(5)
O(4D)	14494(13)	58580(13)	-4550(20)	225(5)
N(1D)	24626(13)	64383(13)	14950(20)	150(5)
N(2D)	19606(13)	60038(13)	18830(20)	150(5)
C(1D)	35252(16)	69711(14)	19390(30)	141(5)
C(2D)	33047(17)	75661(16)	12120(30)	178(6)
C(3D)	37996(19)	78934(17)	3020(30)	225(7)
C(4D)	43560(20)	82021(17)	12880(40)	249(7)
C(5D)	43667(19)	77748(16)	25010(30)	214(6)

C(6D)	35989(18)	76021(15)	26490(30)	174(6)
C(7D)	42440(17)	67559(15)	17510(30)	171(6)
C(8D)	30004(16)	64977(15)	23020(30)	136(5)
C(9D)	31320(18)	61505(17)	35780(30)	203(6)
C(10D)	9991(16)	67894(15)	8530(30)	152(5)
C(11D)	10280(20)	71519(19)	-2880(30)	272(8)
C(12D)	8490(20)	77700(20)	-2210(40)	292(8)
C(13D)	6363(17)	80359(18)	9490(30)	216(6)
C(14D)	5960(20)	76578(19)	20710(40)	255(7)
C(15D)	7735(19)	70414(18)	20390(30)	232(7)
C(16D)	4490(20)	87097(19)	10090(40)	282(8)
C(17D)	32200(20)	77514(16)	38530(30)	229(7)
C(18D)	25620(20)	79330(20)	37590(40)	348(9)
C(19D)	21470(30)	80520(30)	49430(50)	526(14)
C(20D)	25560(60)	79880(60)	62300(70)	1440(60)
C(21D)	31590(40)	76930(60)	63360(50)	1140(40)
C(22D)	36090(30)	76440(20)	51850(40)	356(10)

Table A4.1.3. Bond lengths [Å] and angles [°] for ***42****.*

S(1)-O(3)	1.440(2)
S(1)-O(4)	1.431(2)
S(1)-N(2)	1.646(3)
S(1)-C(10)	1.761(3)
O(1)-C(5)	1.466(4)
O(1)-C(7)	1.352(4)
O(2)-C(7)	1.203(4)
N(1)-N(2)	1.404(4)
N(1)-C(8)	1.277(4)
N(2)-H(2)	0.8603
C(1)-C(2)	1.528(4)
C(1)-C(6)	1.532(4)
C(1)-C(7)	1.488(4)
C(1)-C(8)	1.493(4)
C(2)-H(2A)	1.0000
C(2)-C(3)	1.532(4)
C(2)-C(6)	1.509(4)
C(3)-H(3A)	0.9900
C(3)-H(3B)	0.9900
C(3)-C(4)	1.548(5)
C(4)-H(4A)	0.9900
C(4)-H(4B)	0.9900
C(4)-C(5)	1.513(4)
C(5)-H(5)	1.0000
C(5)-C(6)	1.546(4)
C(6)-C(17)	1.481(4)
C(8)-C(9)	1.494(4)
C(9)-H(9A)	0.9800
C(9)-H(9B)	0.9800
C(9)-H(9C)	0.9800
C(10)-C(11)	1.396(4)
C(10)-C(15)	1.376(4)

C(11)-H(11)	0.9500
C(11)-C(12)	1.374(5)
C(12)-H(12)	0.9500
C(12)-C(13)	1.385(5)
C(13)-C(14)	1.386(5)
C(13)-C(16)	1.501(5)
C(14)-H(14)	0.9500
C(14)-C(15)	1.389(5)
C(15)-H(15)	0.9500
C(16)-H(16A)	0.9800
C(16)-H(16B)	0.9800
C(16)-H(16C)	0.9800
C(17)-C(18)	1.340(5)
C(17)-C(22)	1.509(5)
C(18)-H(18)	0.9500
C(18)-C(19)	1.504(5)
C(19)-H(19A)	0.9900
C(19)-H(19B)	0.9900
C(19)-C(20)	1.511(6)
C(20)-H(20A)	0.9900
C(20)-H(20B)	0.9900
C(20)-C(21)	1.512(6)
C(21)-H(21A)	0.9900
C(21)-H(21B)	0.9900
C(21)-C(22)	1.513(5)
C(22)-H(22A)	0.9900
C(22)-H(22B)	0.9900
S(1B)-O(3B)	1.433(2)
S(1B)-O(4B)	1.437(2)
S(1B)-N(2B)	1.648(3)
S(1B)-C(10B)	1.751(4)
O(1B)-C(5B)	1.468(5)
O(1B)-C(7B)	1.349(4)
O(2B)-C(7B)	1.197(4)
N(1B)-N(2B)	1.403(3)
N(1B)-C(8B)	1.277(4)

N(2B)-H(2B)	0.8596
C(1B)-C(2B)	1.535(4)
C(1B)-C(6B)	1.529(4)
C(1B)-C(7B)	1.494(4)
C(1B)-C(8B)	1.480(4)
C(2B)-H(2BA)	1.0000
C(2B)-C(3B)	1.531(5)
C(2B)-C(6B)	1.508(4)
C(3B)-H(3BA)	0.9900
C(3B)-H(3BB)	0.9900
C(3B)-C(4B)	1.532(5)
C(4B)-H(4BA)	0.9900
C(4B)-H(4BB)	0.9900
C(4B)-C(5B)	1.522(5)
C(5B)-H(5B)	1.0000
C(5B)-C(6B)	1.532(5)
C(6B)-C(17B)	1.488(5)
C(8B)-C(9B)	1.502(4)
C(9B)-H(9BA)	0.9800
C(9B)-H(9BB)	0.9800
C(9B)-H(9BC)	0.9800
C(10B)-C(11B)	1.402(5)
C(10B)-C(15B)	1.396(4)
C(11B)-H(11B)	0.9500
C(11B)-C(12B)	1.381(6)
C(12B)-H(12B)	0.9500
C(12B)-C(13B)	1.390(5)
C(13B)-C(14B)	1.394(5)
C(13B)-C(16B)	1.495(6)
C(14B)-H(14B)	0.9500
C(14B)-C(15B)	1.370(6)
C(15B)-H(15B)	0.9500
C(16B)-H(16D)	0.9800
C(16B)-H(16E)	0.9800
C(16B)-H(16F)	0.9800
C(17B)-C(18B)	1.340(6)

C(17B)-C(22B)	1.496(5)
C(18B)-H(18B)	0.9500
C(18B)-C(19B)	1.504(6)
C(19B)-H(19C)	0.9900
C(19B)-H(19D)	0.9900
C(19B)-C(20B)	1.550(8)
C(20B)-H(20C)	0.9900
C(20B)-H(20D)	0.9900
C(20B)-C(21B)	1.496(9)
C(21B)-H(21C)	0.9900
C(21B)-H(21D)	0.9900
C(21B)-C(22B)	1.514(6)
C(22B)-H(22C)	0.9900
C(22B)-H(22D)	0.9900
S(1C)-O(3C)	1.435(2)
S(1C)-O(4C)	1.432(2)
S(1C)-N(2C)	1.652(3)
S(1C)-C(10C)	1.762(4)
O(1C)-C(5C)	1.468(4)
O(1C)-C(7C)	1.345(4)
O(2C)-C(7C)	1.200(4)
N(1C)-N(2C)	1.400(4)
N(1C)-C(8C)	1.283(4)
N(2C)-H(2C)	0.8602
C(1C)-C(2C)	1.533(4)
C(1C)-C(6C)	1.536(4)
C(1C)-C(7C)	1.488(4)
C(1C)-C(8C)	1.482(4)
C(2C)-H(2CA)	1.0000
C(2C)-C(3C)	1.532(4)
C(2C)-C(6C)	1.505(4)
C(3C)-H(3CA)	0.9900
C(3C)-H(3CB)	0.9900
C(3C)-C(4C)	1.541(5)
C(4C)-H(4CA)	0.9900
C(4C)-H(4CB)	0.9900

C(4C)-C(5C)	1.516(4)
C(5C)-H(5C)	1.0000
C(5C)-C(6C)	1.537(4)
C(6C)-C(17C)	1.478(4)
C(8C)-C(9C)	1.500(4)
C(9C)-H(9CA)	0.9800
C(9C)-H(9CB)	0.9800
C(9C)-H(9CC)	0.9800
C(10C)-C(11C)	1.393(4)
C(10C)-C(15C)	1.394(4)
C(11C)-H(11C)	0.9500
C(11C)-C(12C)	1.388(6)
C(12C)-H(12C)	0.9500
C(12C)-C(13C)	1.379(5)
C(13C)-C(14C)	1.397(5)
C(13C)-C(16C)	1.505(5)
C(14C)-H(14C)	0.9500
C(14C)-C(15C)	1.390(5)
C(15C)-H(15C)	0.9500
C(16C)-H(16G)	0.9800
C(16C)-H(16H)	0.9800
C(16C)-H(16I)	0.9800
C(17C)-C(18C)	1.340(5)
C(17C)-C(22C)	1.511(5)
C(18C)-H(18C)	0.9500
C(18C)-C(19C)	1.505(5)
C(19C)-H(19E)	0.9900
C(19C)-H(19F)	0.9900
C(19C)-C(20C)	1.531(7)
C(20C)-H(20E)	0.9900
C(20C)-H(20F)	0.9900
C(20C)-C(21C)	1.515(7)
C(21C)-H(21E)	0.9900
C(21C)-H(21F)	0.9900
C(21C)-C(22C)	1.508(5)
C(22C)-H(22E)	0.9900

C(22C)-H(22F)	0.9900
S(1D)-O(3D)	1.428(2)
S(1D)-O(4D)	1.434(2)
S(1D)-N(2D)	1.647(3)
S(1D)-C(10D)	1.746(3)
O(1D)-C(5D)	1.464(4)
O(1D)-C(7D)	1.348(4)
O(2D)-C(7D)	1.201(4)
N(1D)-N(2D)	1.411(4)
N(1D)-C(8D)	1.277(4)
N(2D)-H(2D)	0.8599
C(1D)-C(2D)	1.527(4)
C(1D)-C(6D)	1.531(4)
C(1D)-C(7D)	1.494(4)
C(1D)-C(8D)	1.490(4)
C(2D)-H(2DA)	1.0000
C(2D)-C(3D)	1.528(5)
C(2D)-C(6D)	1.509(4)
C(3D)-H(3DA)	0.9900
C(3D)-H(3DB)	0.9900
C(3D)-C(4D)	1.551(5)
C(4D)-H(4DA)	0.9900
C(4D)-H(4DB)	0.9900
C(4D)-C(5D)	1.521(5)
C(5D)-H(5D)	1.0000
C(5D)-C(6D)	1.542(5)
C(6D)-C(17D)	1.484(5)
C(8D)-C(9D)	1.488(4)
C(9D)-H(9DA)	0.9800
C(9D)-H(9DB)	0.9800
C(9D)-H(9DC)	0.9800
C(10D)-C(11D)	1.387(4)
C(10D)-C(15D)	1.397(4)
C(11D)-H(11D)	0.9500
C(11D)-C(12D)	1.383(6)
C(12D)-H(12D)	0.9500

C(12D)-C(13D)	1.387(5)
C(13D)-C(14D)	1.392(5)
C(13D)-C(16D)	1.502(5)
C(14D)-H(14D)	0.9500
C(14D)-C(15D)	1.376(5)
C(15D)-H(15D)	0.9500
C(16D)-H(16J)	0.9800
C(16D)-H(16K)	0.9800
C(16D)-H(16L)	0.9800
C(17D)-C(18D)	1.333(6)
C(17D)-C(22D)	1.504(5)
C(18D)-H(18D)	0.9500
C(18D)-C(19D)	1.495(6)
C(19D)-H(19G)	0.9900
C(19D)-H(19H)	0.9900
C(19D)-C(20D)	1.472(10)
C(20D)-H(20G)	0.9900
C(20D)-H(20H)	0.9900
C(20D)-C(21D)	1.334(12)
C(21D)-H(21G)	0.9900
C(21D)-H(21H)	0.9900
C(21D)-C(22D)	1.490(8)
C(22D)-H(22G)	0.9900
C(22D)-H(22H)	0.9900

O(3)-S(1)-N(2)	106.95(14)
O(3)-S(1)-C(10)	108.01(15)
O(4)-S(1)-O(3)	119.12(15)
O(4)-S(1)-N(2)	104.63(14)
O(4)-S(1)-C(10)	110.16(15)
N(2)-S(1)-C(10)	107.33(15)
C(7)-O(1)-C(5)	111.2(2)
C(8)-N(1)-N(2)	115.7(2)
S(1)-N(2)-H(2)	113.2
N(1)-N(2)-S(1)	111.25(19)
N(1)-N(2)-H(2)	113.3

C(2)-C(1)-C(6)	59.1(2)
C(7)-C(1)-C(2)	117.1(3)
C(7)-C(1)-C(6)	106.4(3)
C(7)-C(1)-C(8)	118.5(3)
C(8)-C(1)-C(2)	119.9(3)
C(8)-C(1)-C(6)	120.9(2)
C(1)-C(2)-H(2A)	117.9
C(1)-C(2)-C(3)	119.4(3)
C(3)-C(2)-H(2A)	117.9
C(6)-C(2)-C(1)	60.6(2)
C(6)-C(2)-H(2A)	117.9
C(6)-C(2)-C(3)	109.3(3)
C(2)-C(3)-H(3A)	111.0
C(2)-C(3)-H(3B)	111.0
C(2)-C(3)-C(4)	103.9(2)
H(3A)-C(3)-H(3B)	109.0
C(4)-C(3)-H(3A)	111.0
C(4)-C(3)-H(3B)	111.0
C(3)-C(4)-H(4A)	111.1
C(3)-C(4)-H(4B)	111.1
H(4A)-C(4)-H(4B)	109.1
C(5)-C(4)-C(3)	103.4(3)
C(5)-C(4)-H(4A)	111.1
C(5)-C(4)-H(4B)	111.1
O(1)-C(5)-C(4)	107.6(3)
O(1)-C(5)-H(5)	112.8
O(1)-C(5)-C(6)	106.2(3)
C(4)-C(5)-H(5)	112.8
C(4)-C(5)-C(6)	104.2(3)
C(6)-C(5)-H(5)	112.8
C(1)-C(6)-C(5)	102.9(2)
C(2)-C(6)-C(1)	60.3(2)
C(2)-C(6)-C(5)	103.1(2)
C(17)-C(6)-C(1)	121.8(3)
C(17)-C(6)-C(2)	129.3(3)
C(17)-C(6)-C(5)	122.3(3)

O(1)-C(7)-C(1)	110.6(3)
O(2)-C(7)-O(1)	122.4(3)
O(2)-C(7)-C(1)	127.0(3)
N(1)-C(8)-C(1)	115.7(3)
N(1)-C(8)-C(9)	126.0(3)
C(1)-C(8)-C(9)	118.2(3)
C(8)-C(9)-H(9A)	109.5
C(8)-C(9)-H(9B)	109.5
C(8)-C(9)-H(9C)	109.5
H(9A)-C(9)-H(9B)	109.5
H(9A)-C(9)-H(9C)	109.5
H(9B)-C(9)-H(9C)	109.5
C(11)-C(10)-S(1)	118.5(3)
C(15)-C(10)-S(1)	120.4(2)
C(15)-C(10)-C(11)	121.1(3)
C(10)-C(11)-H(11)	120.5
C(12)-C(11)-C(10)	119.0(3)
C(12)-C(11)-H(11)	120.5
C(11)-C(12)-H(12)	119.4
C(11)-C(12)-C(13)	121.2(3)
C(13)-C(12)-H(12)	119.4
C(12)-C(13)-C(14)	118.8(3)
C(12)-C(13)-C(16)	120.0(3)
C(14)-C(13)-C(16)	121.2(3)
C(13)-C(14)-H(14)	119.4
C(13)-C(14)-C(15)	121.1(3)
C(15)-C(14)-H(14)	119.4
C(10)-C(15)-C(14)	118.8(3)
C(10)-C(15)-H(15)	120.6
C(14)-C(15)-H(15)	120.6
C(13)-C(16)-H(16A)	109.5
C(13)-C(16)-H(16B)	109.5
C(13)-C(16)-H(16C)	109.5
H(16A)-C(16)-H(16B)	109.5
H(16A)-C(16)-H(16C)	109.5
H(16B)-C(16)-H(16C)	109.5

C(6)-C(17)-C(22)	115.2(3)
C(18)-C(17)-C(6)	122.4(3)
C(18)-C(17)-C(22)	122.1(3)
C(17)-C(18)-H(18)	118.5
C(17)-C(18)-C(19)	123.0(3)
C(19)-C(18)-H(18)	118.5
C(18)-C(19)-H(19A)	108.9
C(18)-C(19)-H(19B)	108.9
C(18)-C(19)-C(20)	113.6(3)
H(19A)-C(19)-H(19B)	107.7
C(20)-C(19)-H(19A)	108.9
C(20)-C(19)-H(19B)	108.9
C(19)-C(20)-H(20A)	109.3
C(19)-C(20)-H(20B)	109.3
C(19)-C(20)-C(21)	111.5(3)
H(20A)-C(20)-H(20B)	108.0
C(21)-C(20)-H(20A)	109.3
C(21)-C(20)-H(20B)	109.3
C(20)-C(21)-H(21A)	109.4
C(20)-C(21)-H(21B)	109.4
C(20)-C(21)-C(22)	111.1(3)
H(21A)-C(21)-H(21B)	108.0
C(22)-C(21)-H(21A)	109.4
C(22)-C(21)-H(21B)	109.4
C(17)-C(22)-C(21)	112.4(3)
C(17)-C(22)-H(22A)	109.1
C(17)-C(22)-H(22B)	109.1
C(21)-C(22)-H(22A)	109.1
C(21)-C(22)-H(22B)	109.1
H(22A)-C(22)-H(22B)	107.9
O(3B)-S(1B)-O(4B)	119.67(15)
O(3B)-S(1B)-N(2B)	104.24(14)
O(3B)-S(1B)-C(10B)	109.80(16)
O(4B)-S(1B)-N(2B)	107.40(14)
O(4B)-S(1B)-C(10B)	108.51(15)
N(2B)-S(1B)-C(10B)	106.40(15)

C(7B)-O(1B)-C(5B)	110.8(3)
C(8B)-N(1B)-N(2B)	114.7(3)
S(1B)-N(2B)-H(2B)	113.6
N(1B)-N(2B)-S(1B)	111.1(2)
N(1B)-N(2B)-H(2B)	113.7
C(6B)-C(1B)-C(2B)	59.0(2)
C(7B)-C(1B)-C(2B)	117.5(3)
C(7B)-C(1B)-C(6B)	107.1(3)
C(8B)-C(1B)-C(2B)	120.5(3)
C(8B)-C(1B)-C(6B)	120.0(3)
C(8B)-C(1B)-C(7B)	117.9(3)
C(1B)-C(2B)-H(2BA)	117.9
C(3B)-C(2B)-C(1B)	119.6(3)
C(3B)-C(2B)-H(2BA)	117.9
C(6B)-C(2B)-C(1B)	60.3(2)
C(6B)-C(2B)-H(2BA)	117.9
C(6B)-C(2B)-C(3B)	109.7(3)
C(2B)-C(3B)-H(3BA)	111.0
C(2B)-C(3B)-H(3BB)	111.0
C(2B)-C(3B)-C(4B)	103.9(3)
H(3BA)-C(3B)-H(3BB)	109.0
C(4B)-C(3B)-H(3BA)	111.0
C(4B)-C(3B)-H(3BB)	111.0
C(3B)-C(4B)-H(4BA)	111.1
C(3B)-C(4B)-H(4BB)	111.1
H(4BA)-C(4B)-H(4BB)	109.0
C(5B)-C(4B)-C(3B)	103.5(3)
C(5B)-C(4B)-H(4BA)	111.1
C(5B)-C(4B)-H(4BB)	111.1
O(1B)-C(5B)-C(4B)	107.6(3)
O(1B)-C(5B)-H(5B)	112.3
O(1B)-C(5B)-C(6B)	107.2(3)
C(4B)-C(5B)-H(5B)	112.3
C(4B)-C(5B)-C(6B)	104.6(3)
C(6B)-C(5B)-H(5B)	112.3
C(1B)-C(6B)-C(5B)	102.1(3)

C(2B)-C(6B)-C(1B)	60.7(2)
C(2B)-C(6B)-C(5B)	102.6(3)
C(17B)-C(6B)-C(1B)	122.5(3)
C(17B)-C(6B)-C(2B)	127.3(3)
C(17B)-C(6B)-C(5B)	123.9(3)
O(1B)-C(7B)-C(1B)	109.8(3)
O(2B)-C(7B)-O(1B)	121.8(3)
O(2B)-C(7B)-C(1B)	128.4(3)
N(1B)-C(8B)-C(1B)	116.2(3)
N(1B)-C(8B)-C(9B)	125.5(3)
C(1B)-C(8B)-C(9B)	118.2(3)
C(8B)-C(9B)-H(9BA)	109.5
C(8B)-C(9B)-H(9BB)	109.5
C(8B)-C(9B)-H(9BC)	109.5
H(9BA)-C(9B)-H(9BB)	109.5
H(9BA)-C(9B)-H(9BC)	109.5
H(9BB)-C(9B)-H(9BC)	109.5
C(11B)-C(10B)-S(1B)	120.8(3)
C(15B)-C(10B)-S(1B)	118.9(3)
C(15B)-C(10B)-C(11B)	120.2(3)
C(10B)-C(11B)-H(11B)	120.7
C(12B)-C(11B)-C(10B)	118.6(3)
C(12B)-C(11B)-H(11B)	120.7
C(11B)-C(12B)-H(12B)	118.9
C(11B)-C(12B)-C(13B)	122.1(3)
C(13B)-C(12B)-H(12B)	118.9
C(12B)-C(13B)-C(14B)	117.8(4)
C(12B)-C(13B)-C(16B)	121.7(3)
C(14B)-C(13B)-C(16B)	120.6(3)
C(13B)-C(14B)-H(14B)	119.1
C(15B)-C(14B)-C(13B)	121.8(3)
C(15B)-C(14B)-H(14B)	119.1
C(10B)-C(15B)-H(15B)	120.3
C(14B)-C(15B)-C(10B)	119.4(3)
C(14B)-C(15B)-H(15B)	120.3
C(13B)-C(16B)-H(16D)	109.5

C(13B)-C(16B)-H(16E)	109.5
C(13B)-C(16B)-H(16F)	109.5
H(16D)-C(16B)-H(16E)	109.5
H(16D)-C(16B)-H(16F)	109.5
H(16E)-C(16B)-H(16F)	109.5
C(6B)-C(17B)-C(22B)	115.1(3)
C(18B)-C(17B)-C(6B)	121.6(3)
C(18B)-C(17B)-C(22B)	123.2(3)
C(17B)-C(18B)-H(18B)	118.3
C(17B)-C(18B)-C(19B)	123.4(4)
C(19B)-C(18B)-H(18B)	118.3
C(18B)-C(19B)-H(19C)	109.4
C(18B)-C(19B)-H(19D)	109.4
C(18B)-C(19B)-C(20B)	111.4(4)
H(19C)-C(19B)-H(19D)	108.0
C(20B)-C(19B)-H(19C)	109.4
C(20B)-C(19B)-H(19D)	109.4
C(19B)-C(20B)-H(20C)	109.1
C(19B)-C(20B)-H(20D)	109.1
H(20C)-C(20B)-H(20D)	107.9
C(21B)-C(20B)-C(19B)	112.3(4)
C(21B)-C(20B)-H(20C)	109.1
C(21B)-C(20B)-H(20D)	109.1
C(20B)-C(21B)-H(21C)	109.4
C(20B)-C(21B)-H(21D)	109.4
C(20B)-C(21B)-C(22B)	111.2(4)
H(21C)-C(21B)-H(21D)	108.0
C(22B)-C(21B)-H(21C)	109.4
C(22B)-C(21B)-H(21D)	109.4
C(17B)-C(22B)-C(21B)	112.8(4)
C(17B)-C(22B)-H(22C)	109.0
C(17B)-C(22B)-H(22D)	109.0
C(21B)-C(22B)-H(22C)	109.0
C(21B)-C(22B)-H(22D)	109.0
H(22C)-C(22B)-H(22D)	107.8
O(3C)-S(1C)-N(2C)	106.71(14)

O(3C)-S(1C)-C(10C)	108.08(15)
O(4C)-S(1C)-O(3C)	119.43(15)
O(4C)-S(1C)-N(2C)	104.18(14)
O(4C)-S(1C)-C(10C)	110.35(16)
N(2C)-S(1C)-C(10C)	107.40(15)
C(7C)-O(1C)-C(5C)	110.7(2)
C(8C)-N(1C)-N(2C)	115.1(3)
S(1C)-N(2C)-H(2C)	113.3
N(1C)-N(2C)-S(1C)	111.5(2)
N(1C)-N(2C)-H(2C)	113.5
C(2C)-C(1C)-C(6C)	58.74(19)
C(7C)-C(1C)-C(2C)	117.6(2)
C(7C)-C(1C)-C(6C)	106.6(2)
C(8C)-C(1C)-C(2C)	119.7(3)
C(8C)-C(1C)-C(6C)	121.1(2)
C(8C)-C(1C)-C(7C)	118.3(3)
C(1C)-C(2C)-H(2CA)	117.9
C(3C)-C(2C)-C(1C)	119.4(3)
C(3C)-C(2C)-H(2CA)	117.9
C(6C)-C(2C)-C(1C)	60.72(19)
C(6C)-C(2C)-H(2CA)	117.9
C(6C)-C(2C)-C(3C)	109.5(2)
C(2C)-C(3C)-H(3CA)	111.0
C(2C)-C(3C)-H(3CB)	111.0
C(2C)-C(3C)-C(4C)	103.8(2)
H(3CA)-C(3C)-H(3CB)	109.0
C(4C)-C(3C)-H(3CA)	111.0
C(4C)-C(3C)-H(3CB)	111.0
C(3C)-C(4C)-H(4CA)	111.0
C(3C)-C(4C)-H(4CB)	111.0
H(4CA)-C(4C)-H(4CB)	109.0
C(5C)-C(4C)-C(3C)	103.6(2)
C(5C)-C(4C)-H(4CA)	111.0
C(5C)-C(4C)-H(4CB)	111.0
O(1C)-C(5C)-C(4C)	107.6(2)
O(1C)-C(5C)-H(5C)	112.4

O(1C)-C(5C)-C(6C)	107.0(2)
C(4C)-C(5C)-H(5C)	112.4
C(4C)-C(5C)-C(6C)	104.4(3)
C(6C)-C(5C)-H(5C)	112.4
C(1C)-C(6C)-C(5C)	102.2(2)
C(2C)-C(6C)-C(1C)	60.54(19)
C(2C)-C(6C)-C(5C)	103.0(2)
C(17C)-C(6C)-C(1C)	121.9(2)
C(17C)-C(6C)-C(2C)	128.7(3)
C(17C)-C(6C)-C(5C)	122.9(3)
O(1C)-C(7C)-C(1C)	110.6(3)
O(2C)-C(7C)-O(1C)	121.9(3)
O(2C)-C(7C)-C(1C)	127.5(3)
N(1C)-C(8C)-C(1C)	115.4(3)
N(1C)-C(8C)-C(9C)	126.9(3)
C(1C)-C(8C)-C(9C)	117.7(3)
C(8C)-C(9C)-H(9CA)	109.5
C(8C)-C(9C)-H(9CB)	109.5
C(8C)-C(9C)-H(9CC)	109.5
H(9CA)-C(9C)-H(9CB)	109.5
H(9CA)-C(9C)-H(9CC)	109.5
H(9CB)-C(9C)-H(9CC)	109.5
C(11C)-C(10C)-S(1C)	119.9(3)
C(11C)-C(10C)-C(15C)	120.2(3)
C(15C)-C(10C)-S(1C)	119.8(3)
C(10C)-C(11C)-H(11C)	120.4
C(12C)-C(11C)-C(10C)	119.3(3)
C(12C)-C(11C)-H(11C)	120.4
C(11C)-C(12C)-H(12C)	119.3
C(13C)-C(12C)-C(11C)	121.4(3)
C(13C)-C(12C)-H(12C)	119.3
C(12C)-C(13C)-C(14C)	119.0(3)
C(12C)-C(13C)-C(16C)	120.3(3)
C(14C)-C(13C)-C(16C)	120.7(3)
C(13C)-C(14C)-H(14C)	119.7
C(15C)-C(14C)-C(13C)	120.7(3)

C(15C)-C(14C)-H(14C)	119.7
C(10C)-C(15C)-H(15C)	120.3
C(14C)-C(15C)-C(10C)	119.4(3)
C(14C)-C(15C)-H(15C)	120.3
C(13C)-C(16C)-H(16G)	109.5
C(13C)-C(16C)-H(16H)	109.5
C(13C)-C(16C)-H(16I)	109.5
H(16G)-C(16C)-H(16H)	109.5
H(16G)-C(16C)-H(16I)	109.5
H(16H)-C(16C)-H(16I)	109.5
C(6C)-C(17C)-C(22C)	115.2(3)
C(18C)-C(17C)-C(6C)	122.5(3)
C(18C)-C(17C)-C(22C)	122.2(3)
C(17C)-C(18C)-H(18C)	118.4
C(17C)-C(18C)-C(19C)	123.2(4)
C(19C)-C(18C)-H(18C)	118.4
C(18C)-C(19C)-H(19E)	109.0
C(18C)-C(19C)-H(19F)	109.0
C(18C)-C(19C)-C(20C)	112.9(4)
H(19E)-C(19C)-H(19F)	107.8
C(20C)-C(19C)-H(19E)	109.0
C(20C)-C(19C)-H(19F)	109.0
C(19C)-C(20C)-H(20E)	109.1
C(19C)-C(20C)-H(20F)	109.1
H(20E)-C(20C)-H(20F)	107.8
C(21C)-C(20C)-C(19C)	112.6(4)
C(21C)-C(20C)-H(20E)	109.1
C(21C)-C(20C)-H(20F)	109.1
C(20C)-C(21C)-H(21E)	109.6
C(20C)-C(21C)-H(21F)	109.6
H(21E)-C(21C)-H(21F)	108.1
C(22C)-C(21C)-C(20C)	110.2(3)
C(22C)-C(21C)-H(21E)	109.6
C(22C)-C(21C)-H(21F)	109.6
C(17C)-C(22C)-H(22E)	109.0
C(17C)-C(22C)-H(22F)	109.0

C(21C)-C(22C)-C(17C)	113.1(3)
C(21C)-C(22C)-H(22E)	109.0
C(21C)-C(22C)-H(22F)	109.0
H(22E)-C(22C)-H(22F)	107.8
O(3D)-S(1D)-O(4D)	119.56(16)
O(3D)-S(1D)-N(2D)	104.59(14)
O(3D)-S(1D)-C(10D)	111.06(15)
O(4D)-S(1D)-N(2D)	107.65(14)
O(4D)-S(1D)-C(10D)	108.15(15)
N(2D)-S(1D)-C(10D)	104.75(15)
C(7D)-O(1D)-C(5D)	111.1(3)
C(8D)-N(1D)-N(2D)	115.5(2)
S(1D)-N(2D)-H(2D)	113.3
N(1D)-N(2D)-S(1D)	111.66(19)
N(1D)-N(2D)-H(2D)	113.2
C(2D)-C(1D)-C(6D)	59.1(2)
C(7D)-C(1D)-C(2D)	116.5(3)
C(7D)-C(1D)-C(6D)	106.5(3)
C(8D)-C(1D)-C(2D)	120.8(3)
C(8D)-C(1D)-C(6D)	121.9(3)
C(8D)-C(1D)-C(7D)	117.8(3)
C(1D)-C(2D)-H(2DA)	117.7
C(1D)-C(2D)-C(3D)	120.0(3)
C(3D)-C(2D)-H(2DA)	117.7
C(6D)-C(2D)-C(1D)	60.6(2)
C(6D)-C(2D)-H(2DA)	117.7
C(6D)-C(2D)-C(3D)	109.5(3)
C(2D)-C(3D)-H(3DA)	110.9
C(2D)-C(3D)-H(3DB)	110.9
C(2D)-C(3D)-C(4D)	104.3(3)
H(3DA)-C(3D)-H(3DB)	108.9
C(4D)-C(3D)-H(3DA)	110.9
C(4D)-C(3D)-H(3DB)	110.9
C(3D)-C(4D)-H(4DA)	111.2
C(3D)-C(4D)-H(4DB)	111.2
H(4DA)-C(4D)-H(4DB)	109.1

C(5D)-C(4D)-C(3D)	103.0(3)
C(5D)-C(4D)-H(4DA)	111.2
C(5D)-C(4D)-H(4DB)	111.2
O(1D)-C(5D)-C(4D)	107.0(3)
O(1D)-C(5D)-H(5D)	112.6
O(1D)-C(5D)-C(6D)	106.8(3)
C(4D)-C(5D)-H(5D)	112.6
C(4D)-C(5D)-C(6D)	104.6(3)
C(6D)-C(5D)-H(5D)	112.6
C(1D)-C(6D)-C(5D)	102.6(3)
C(2D)-C(6D)-C(1D)	60.3(2)
C(2D)-C(6D)-C(5D)	103.0(3)
C(17D)-C(6D)-C(1D)	122.3(3)
C(17D)-C(6D)-C(2D)	127.1(3)
C(17D)-C(6D)-C(5D)	123.8(3)
O(1D)-C(7D)-C(1D)	110.4(3)
O(2D)-C(7D)-O(1D)	122.8(3)
O(2D)-C(7D)-C(1D)	126.8(3)
N(1D)-C(8D)-C(1D)	116.4(3)
N(1D)-C(8D)-C(9D)	125.6(3)
C(9D)-C(8D)-C(1D)	118.0(3)
C(8D)-C(9D)-H(9DA)	109.5
C(8D)-C(9D)-H(9DB)	109.5
C(8D)-C(9D)-H(9DC)	109.5
H(9DA)-C(9D)-H(9DB)	109.5
H(9DA)-C(9D)-H(9DC)	109.5
H(9DB)-C(9D)-H(9DC)	109.5
C(11D)-C(10D)-S(1D)	121.4(3)
C(11D)-C(10D)-C(15D)	120.4(3)
C(15D)-C(10D)-S(1D)	118.2(2)
C(10D)-C(11D)-H(11D)	120.6
C(12D)-C(11D)-C(10D)	118.8(3)
C(12D)-C(11D)-H(11D)	120.6
C(11D)-C(12D)-H(12D)	119.0
C(11D)-C(12D)-C(13D)	121.9(3)
C(13D)-C(12D)-H(12D)	119.0

C(12D)-C(13D)-C(14D)	118.0(4)
C(12D)-C(13D)-C(16D)	121.3(3)
C(14D)-C(13D)-C(16D)	120.7(3)
C(13D)-C(14D)-H(14D)	119.3
C(15D)-C(14D)-C(13D)	121.4(3)
C(15D)-C(14D)-H(14D)	119.3
C(10D)-C(15D)-H(15D)	120.4
C(14D)-C(15D)-C(10D)	119.3(3)
C(14D)-C(15D)-H(15D)	120.4
C(13D)-C(16D)-H(16J)	109.5
C(13D)-C(16D)-H(16K)	109.5
C(13D)-C(16D)-H(16L)	109.5
H(16J)-C(16D)-H(16K)	109.5
H(16J)-C(16D)-H(16L)	109.5
H(16K)-C(16D)-H(16L)	109.5
C(6D)-C(17D)-C(22D)	115.7(3)
C(18D)-C(17D)-C(6D)	122.0(3)
C(18D)-C(17D)-C(22D)	122.2(4)
C(17D)-C(18D)-H(18D)	118.0
C(17D)-C(18D)-C(19D)	123.9(4)
C(19D)-C(18D)-H(18D)	118.0
C(18D)-C(19D)-H(19G)	109.1
C(18D)-C(19D)-H(19H)	109.1
H(19G)-C(19D)-H(19H)	107.8
C(20D)-C(19D)-C(18D)	112.7(5)
C(20D)-C(19D)-H(19G)	109.1
C(20D)-C(19D)-H(19H)	109.1
C(19D)-C(20D)-H(20G)	106.7
C(19D)-C(20D)-H(20H)	106.7
H(20G)-C(20D)-H(20H)	106.6
C(21D)-C(20D)-C(19D)	122.5(6)
C(21D)-C(20D)-H(20G)	106.7
C(21D)-C(20D)-H(20H)	106.7
C(20D)-C(21D)-H(21G)	106.9
C(20D)-C(21D)-H(21H)	106.9
C(20D)-C(21D)-C(22D)	121.8(6)

H(21G)-C(21D)-H(21H)	106.7
C(22D)-C(21D)-H(21G)	106.9
C(22D)-C(21D)-H(21H)	106.9
C(17D)-C(22D)-H(22G)	109.1
C(17D)-C(22D)-H(22H)	109.1
C(21D)-C(22D)-C(17D)	112.7(5)
C(21D)-C(22D)-H(22G)	109.1
C(21D)-C(22D)-H(22H)	109.1
H(22G)-C(22D)-H(22H)	107.8

Symmetry transformations used to generate equivalent atoms:

Table A4.1.4. Anisotropic displacement parameters ($Å^2 x\ 10^4$) for ***42****. The anisotropic displacement factor exponent takes the form: $-2\pi^2[h^2 a^{*2} U^{11} + ... + 2 h k a^* b^* U^{12}]$*

	U^{11}	U^{22}	U^{33}	U^{23}	U^{13}	U^{12}
S(1)	133(3)	254(4)	66(3)	3(3)	22(2)	-17(3)
O(1)	151(10)	238(12)	190(11)	9(9)	3(8)	-10(9)
O(2)	222(12)	188(11)	224(12)	-5(9)	21(9)	41(9)
O(3)	224(11)	294(12)	55(9)	-20(8)	28(8)	-9(9)
O(4)	185(11)	310(13)	141(10)	45(9)	23(8)	-45(10)
N(1)	136(11)	208(12)	84(10)	3(9)	40(9)	8(9)
N(2)	140(11)	239(13)	86(10)	37(9)	19(9)	-9(10)
C(1)	176(13)	137(13)	78(11)	13(9)	4(10)	1(10)
C(2)	192(14)	168(14)	124(13)	29(10)	1(10)	13(11)
C(3)	272(16)	211(15)	122(13)	61(11)	19(12)	-11(13)
C(4)	280(17)	236(16)	147(14)	57(12)	49(12)	-71(13)
C(5)	203(15)	211(15)	132(13)	7(11)	8(11)	-42(12)
C(6)	188(14)	152(13)	107(12)	21(10)	20(10)	-9(11)
C(7)	167(13)	179(14)	104(12)	55(10)	-9(10)	-5(11)
C(8)	172(13)	148(13)	76(11)	10(10)	23(10)	14(10)
C(9)	220(15)	229(16)	158(14)	64(12)	-35(12)	-28(12)
C(10)	135(13)	242(15)	110(12)	-11(11)	18(10)	9(11)
C(11)	231(16)	301(18)	153(14)	-9(13)	99(12)	0(13)
C(12)	219(16)	311(18)	199(15)	-51(13)	86(13)	11(14)
C(13)	143(14)	293(17)	209(15)	-45(13)	-36(12)	42(12)
C(14)	400(20)	291(18)	116(14)	14(13)	19(13)	46(16)
C(15)	335(19)	276(17)	82(13)	7(12)	46(12)	74(14)
C(16)	253(17)	330(20)	279(18)	-45(15)	-47(14)	56(15)
C(17)	266(16)	146(13)	136(13)	-2(11)	54(11)	-26(12)
C(18)	317(18)	211(16)	212(16)	10(13)	50(14)	32(14)
C(19)	290(19)	390(20)	310(20)	-10(17)	151(16)	44(16)
C(20)	400(20)	299(19)	213(17)	-54(14)	147(15)	-23(16)

C(21)	307(19)	342(19)	157(15)	-6(14)	48(13)	-26(15)
C(22)	275(17)	242(16)	108(13)	-7(11)	14(12)	-20(13)
S(1B)	152(3)	264(4)	64(3)	30(3)	25(2)	61(3)
O(1B)	150(11)	249(12)	303(13)	-28(10)	-14(9)	44(9)
O(2B)	212(12)	212(12)	299(13)	-30(10)	54(10)	-37(9)
O(3B)	216(12)	326(13)	139(10)	10(9)	49(9)	112(10)
O(4B)	230(12)	362(14)	55(9)	64(9)	37(8)	61(10)
N(1B)	157(11)	174(12)	101(10)	15(9)	37(9)	45(9)
N(2B)	141(11)	200(12)	82(10)	8(9)	16(8)	46(9)
C(1B)	151(13)	144(13)	110(12)	7(10)	2(10)	18(10)
C(2B)	203(14)	154(13)	158(13)	-29(11)	23(11)	-6(11)
C(3B)	284(17)	194(15)	200(15)	-36(12)	49(13)	23(13)
C(4B)	294(18)	209(16)	278(18)	-44(13)	44(14)	98(14)
C(5B)	205(15)	218(16)	226(16)	-14(12)	-23(12)	81(12)
C(6B)	203(14)	144(13)	136(13)	2(10)	-3(11)	33(11)
C(7B)	150(13)	203(15)	168(14)	-52(11)	10(11)	-3(11)
C(8B)	155(13)	145(13)	110(12)	3(10)	27(10)	19(10)
C(9B)	216(15)	221(15)	112(13)	-33(11)	-15(11)	26(12)
C(10B)	144(13)	277(16)	91(12)	18(11)	18(10)	29(12)
C(11B)	328(19)	342(19)	90(13)	-4(13)	63(12)	25(15)
C(12B)	304(19)	350(20)	131(14)	-48(13)	19(13)	12(15)
C(13B)	137(14)	348(19)	188(15)	-16(13)	9(11)	-17(13)
C(14B)	269(18)	390(20)	133(14)	12(14)	64(13)	-59(15)
C(15B)	273(17)	340(19)	95(13)	-12(12)	51(12)	-22(14)
C(16B)	273(18)	350(20)	256(18)	-52(15)	74(14)	-79(15)
C(17B)	357(19)	154(14)	139(14)	10(11)	53(13)	38(13)
C(18B)	390(20)	330(20)	219(17)	-4(15)	153(15)	-23(17)
C(19B)	480(30)	520(30)	350(20)	40(20)	230(20)	0(20)
C(20B)	980(50)	440(30)	350(20)	160(20)	370(30)	220(30)
C(21B)	890(40)	430(30)	210(20)	9(18)	100(20)	190(30)
C(22B)	520(30)	284(19)	156(15)	41(14)	-10(16)	79(18)
S(1C)	139(3)	267(4)	73(3)	28(3)	19(2)	57(3)
O(1C)	99(9)	207(11)	193(11)	-16(9)	21(8)	-7(8)
O(2C)	210(11)	191(11)	169(11)	16(8)	36(9)	-34(9)
O(3C)	224(11)	314(13)	83(9)	45(9)	25(8)	51(10)
O(4C)	181(11)	369(14)	162(11)	11(10)	26(9)	118(10)

N(1C)	124(11)	270(14)	83(10)	12(10)	26(8)	46(10)
N(2C)	161(12)	249(13)	82(10)	9(9)	19(9)	57(10)
C(1C)	117(12)	152(13)	87(11)	13(10)	2(9)	-13(10)
C(2C)	131(12)	179(13)	105(12)	-4(10)	4(10)	-24(10)
C(3C)	191(14)	212(15)	119(13)	-34(11)	33(11)	9(12)
C(4C)	195(15)	191(15)	181(14)	-21(11)	36(11)	41(12)
C(5C)	135(13)	163(13)	154(13)	5(11)	3(10)	21(10)
C(6C)	137(12)	136(13)	104(12)	-17(10)	21(10)	7(10)
C(7C)	117(12)	168(13)	111(12)	-30(10)	4(9)	-16(10)
C(8C)	136(12)	194(14)	72(11)	27(10)	16(9)	15(10)
C(9C)	220(15)	276(17)	137(13)	-68(12)	13(11)	42(13)
C(10C)	128(13)	283(16)	106(12)	33(11)	21(10)	49(11)
C(11C)	263(17)	338(19)	174(15)	40(13)	119(13)	77(14)
C(12C)	251(17)	370(20)	238(17)	106(15)	132(14)	30(15)
C(13C)	151(14)	300(17)	172(14)	73(13)	-10(11)	-24(12)
C(14C)	294(18)	317(19)	147(14)	-6(13)	52(13)	12(14)
C(15C)	294(18)	318(18)	116(13)	15(12)	89(12)	7(14)
C(16C)	243(17)	306(19)	266(18)	81(15)	25(14)	-13(14)
C(17C)	231(15)	155(13)	128(13)	4(10)	55(11)	21(11)
C(18C)	311(19)	276(18)	242(17)	5(14)	119(14)	-65(15)
C(19C)	410(20)	420(20)	410(20)	36(19)	260(20)	-50(19)
C(20C)	590(30)	390(20)	270(20)	68(17)	240(20)	60(20)
C(21C)	450(20)	370(20)	174(16)	16(15)	73(16)	67(18)
C(22C)	349(19)	272(17)	127(14)	25(12)	7(13)	82(15)
S(1D)	142(3)	273(4)	75(3)	-2(3)	25(2)	-10(3)
O(1D)	155(11)	219(12)	284(13)	34(10)	-19(9)	-33(9)
O(2D)	211(11)	179(11)	254(12)	44(9)	45(9)	25(9)
O(3D)	174(11)	306(13)	172(11)	15(9)	39(9)	-39(10)
O(4D)	232(12)	362(14)	84(9)	-36(9)	53(8)	-12(10)
N(1D)	130(11)	235(13)	88(10)	28(9)	38(9)	5(10)
N(2D)	147(11)	226(13)	78(10)	16(9)	23(8)	-9(10)
C(1D)	169(13)	152(13)	101(12)	27(10)	3(10)	17(11)
C(2D)	203(15)	227(15)	106(12)	61(11)	7(11)	47(12)
C(3D)	286(17)	241(16)	154(14)	73(12)	49(12)	34(13)
C(4D)	327(19)	214(16)	205(16)	54(13)	11(14)	-26(14)
C(5D)	241(16)	201(15)	196(15)	34(12)	-11(12)	-37(12)

C(6D)	236(15)	167(14)	118(13)	32(11)	-2(11)	12(12)
C(7D)	171(14)	182(14)	156(13)	73(11)	-10(11)	-9(11)
C(8D)	146(13)	189(14)	77(11)	6(10)	24(10)	9(11)
C(9D)	208(15)	271(16)	125(13)	53(12)	-28(11)	-12(13)
C(10D)	138(13)	247(15)	70(11)	22(10)	-7(10)	26(11)
C(11D)	380(20)	360(20)	88(13)	32(13)	60(13)	9(16)
C(12D)	390(20)	360(20)	130(15)	68(14)	58(14)	16(17)
C(13D)	154(14)	320(18)	173(14)	25(13)	6(11)	12(13)
C(14D)	264(17)	350(20)	160(15)	36(13)	84(13)	68(15)
C(15D)	268(17)	337(19)	99(13)	49(12)	58(12)	61(14)
C(16D)	265(18)	360(20)	227(17)	82(15)	67(14)	64(15)
C(17D)	370(19)	170(15)	150(14)	20(11)	46(13)	-1(13)
C(18D)	450(20)	400(20)	211(17)	42(16)	135(16)	141(19)
C(19D)	680(40)	590(30)	350(20)	0(20)	280(20)	140(30)
C(20D)	1780(100)	2350(130)	280(30)	100(50)	410(50)	1470(100)
C(21D)	790(50)	2530(130)	110(20)	270(40)	50(30)	-420(70)
C(22D)	570(30)	320(20)	159(16)	-24(14)	-60(17)	-61(19)

Table A4.1.5. Hydrogen coordinates (x 10^4) and isotropic displacement parameters (Å^{2}x 10^3) for ***42***.

	x	y	z	U(eq)
H(2)	2151	864	2106	19
H(2A)	3032	2765	1151	19
H(3A)	3806	3296	-195	24
H(3B)	4198	2645	-325	24
H(4A)	5080	3196	832	26
H(4B)	4548	3627	1581	26
H(5)	4915	2910	3254	22
H(9A)	3044	794	3349	31
H(9B)	3099	1403	4276	31
H(9C)	3778	1136	3654	31
H(11)	843	2144	2850	27
H(12)	529	3181	2787	29
H(14)	1069	3307	-1038	32
H(15)	1353	2254	-1026	28
H(16A)	906	4254	1448	43
H(16B)	106	4062	1187	43
H(16C)	574	4180	-56	43
H(18)	2658	3047	3227	29
H(19A)	2229	2714	5419	39
H(19B)	2363	3447	5347	39
H(20A)	2841	2923	7371	36
H(20B)	3347	3406	6689	36
H(21A)	3371	2088	6320	32
H(21B)	3938	2480	7224	32
H(22A)	4369	2943	5385	25
H(22B)	4292	2222	5007	25
H(2B)	2194	1708	7071	17
H(2BA)	2899	-233	5965	21

H(3BA)	4133	-157	4690	27
H(3BB)	3674	-788	4694	27
H(4BA)	4312	-1182	6502	31
H(4BB)	4913	-760	5901	31
H(5B)	4663	-522	8318	26
H(9BA)	3020	1044	9305	28
H(9BB)	3031	1677	8469	28
H(9BC)	3733	1304	8779	28
H(11B)	1162	336	3931	30
H(12B)	826	-705	3994	31
H(14B)	553	-563	7954	31
H(15B)	892	470	7940	28
H(16D)	831	-1663	6385	44
H(16E)	304	-1558	5104	44
H(16F)	51	-1461	6585	44
H(18B)	2420	-584	7800	37
H(19C)	1959	-1060	9716	53
H(19D)	1853	-331	9919	53
H(20C)	2366	-638	11953	69
H(20D)	2895	-1084	11261	69
H(21C)	3481	-201	12141	61
H(21D)	2974	238	11248	61
H(22C)	3949	178	10086	38
H(22D)	4009	-554	10317	38
H(2C)	1995	6475	7039	20
H(2CA)	2945	4632	6096	17
H(3CA)	4115	4817	4661	21
H(3CB)	3752	4143	4778	21
H(4CA)	4497	3857	6549	23
H(4CB)	5011	4330	5839	23
H(5C)	4802	4580	8267	18
H(9CA)	2869	6596	8327	32
H(9CB)	3617	6301	8637	32
H(9CC)	2951	5992	9250	32
H(11C)	466	5142	7426	30
H(12C)	280	4069	7352	34

H(14C)	1354	3947	4028	30
H(15C)	1532	5024	4056	29
H(16G)	675	3053	6579	41
H(16H)	1026	3010	5173	41
H(16I)	210	3123	5203	41
H(18C)	2561	4301	8105	33
H(19E)	2276	3837	10184	48
H(19F)	2071	4552	10284	48
H(20E)	2684	4398	12264	49
H(20F)	3232	3961	11602	49
H(21E)	3184	5282	11293	39
H(21F)	3762	4922	12202	39
H(22E)	4229	4499	10366	30
H(22F)	4126	5218	10021	30
H(2D)	2123	5637	2009	18
H(2DA)	2797	7637	1036	21
H(3DA)	3554	8210	-259	27
H(3DB)	4013	7591	-292	27
H(4DA)	4814	8218	898	30
H(4DB)	4223	8628	1531	30
H(5D)	4591	7973	3329	26
H(9DA)	2900	6357	4297	30
H(9DB)	3632	6141	3812	30
H(9DC)	2951	5725	3464	30
H(11D)	1168	6978	-1103	33
H(12D)	872	8021	-999	35
H(14D)	442	7829	2877	31
H(15D)	743	6790	2814	28
H(16J)	854	8955	1347	42
H(16K)	73	8761	1612	42
H(16L)	296	8852	108	42
H(18D)	2345	7990	2887	42
H(19G)	1960	8478	4879	63
H(19H)	1749	7757	4920	63
H(20G)	2647	8414	6583	173
H(20H)	2250	7781	6855	173

H(21G)	3058	7264	6626	137
H(21H)	3442	7894	7082	137
H(22G)	3815	7226	5183	43
H(22H)	3992	7952	5305	43

Table A4.1.6. Torsion angles [°] for ***42****.*

S(1)-C(10)-C(11)-C(12)	-178.4(3)
S(1)-C(10)-C(15)-C(14)	179.5(3)
O(1)-C(5)-C(6)-C(1)	-16.3(3)
O(1)-C(5)-C(6)-C(2)	-78.3(3)
O(1)-C(5)-C(6)-C(17)	125.3(3)
O(3)-S(1)-N(2)-N(1)	59.8(2)
O(3)-S(1)-C(10)-C(11)	175.7(3)
O(3)-S(1)-C(10)-C(15)	-3.7(3)
O(4)-S(1)-N(2)-N(1)	-172.9(2)
O(4)-S(1)-C(10)-C(11)	44.0(3)
O(4)-S(1)-C(10)-C(15)	-135.3(3)
N(2)-S(1)-C(10)-C(11)	-69.3(3)
N(2)-S(1)-C(10)-C(15)	111.3(3)
N(2)-N(1)-C(8)-C(1)	-176.8(2)
N(2)-N(1)-C(8)-C(9)	0.0(4)
C(1)-C(2)-C(3)-C(4)	-74.8(4)
C(1)-C(2)-C(6)-C(5)	97.5(3)
C(1)-C(2)-C(6)-C(17)	-108.5(4)
C(1)-C(6)-C(17)-C(18)	-78.9(4)
C(1)-C(6)-C(17)-C(22)	95.2(4)
C(2)-C(1)-C(6)-C(5)	-97.9(3)
C(2)-C(1)-C(6)-C(17)	120.2(3)
C(2)-C(1)-C(7)-O(1)	55.8(3)
C(2)-C(1)-C(7)-O(2)	-125.2(3)
C(2)-C(1)-C(8)-N(1)	31.1(4)
C(2)-C(1)-C(8)-C(9)	-146.0(3)
C(2)-C(3)-C(4)-C(5)	30.1(3)
C(2)-C(6)-C(17)-C(18)	-3.2(5)
C(2)-C(6)-C(17)-C(22)	170.9(3)
C(3)-C(2)-C(6)-C(1)	-113.6(3)
C(3)-C(2)-C(6)-C(5)	-16.1(3)
C(3)-C(2)-C(6)-C(17)	138.0(3)

C(3)-C(4)-C(5)-O(1)	71.8(3)
C(3)-C(4)-C(5)-C(6)	-40.7(3)
C(4)-C(5)-C(6)-C(1)	97.2(3)
C(4)-C(5)-C(6)-C(2)	35.1(3)
C(4)-C(5)-C(6)-C(17)	-121.2(3)
C(5)-O(1)-C(7)-O(2)	177.4(3)
C(5)-O(1)-C(7)-C(1)	-3.6(3)
C(5)-C(6)-C(17)-C(18)	146.5(3)
C(5)-C(6)-C(17)-C(22)	-39.4(4)
C(6)-C(1)-C(2)-C(3)	96.7(3)
C(6)-C(1)-C(7)-O(1)	-7.4(3)
C(6)-C(1)-C(7)-O(2)	171.6(3)
C(6)-C(1)-C(8)-N(1)	100.8(3)
C(6)-C(1)-C(8)-C(9)	-76.3(4)
C(6)-C(2)-C(3)-C(4)	-8.4(3)
C(6)-C(17)-C(18)-C(19)	174.4(3)
C(6)-C(17)-C(22)-C(21)	-156.5(3)
C(7)-O(1)-C(5)-C(4)	-98.2(3)
C(7)-O(1)-C(5)-C(6)	12.9(3)
C(7)-C(1)-C(2)-C(3)	3.1(4)
C(7)-C(1)-C(2)-C(6)	-93.6(3)
C(7)-C(1)-C(6)-C(2)	112.2(3)
C(7)-C(1)-C(6)-C(5)	14.3(3)
C(7)-C(1)-C(6)-C(17)	-127.6(3)
C(7)-C(1)-C(8)-N(1)	-124.7(3)
C(7)-C(1)-C(8)-C(9)	58.2(4)
C(8)-N(1)-N(2)-S(1)	-179.1(2)
C(8)-C(1)-C(2)-C(3)	-153.0(3)
C(8)-C(1)-C(2)-C(6)	110.3(3)
C(8)-C(1)-C(6)-C(2)	-108.6(3)
C(8)-C(1)-C(6)-C(5)	153.5(3)
C(8)-C(1)-C(6)-C(17)	11.7(4)
C(8)-C(1)-C(7)-O(1)	-147.8(3)
C(8)-C(1)-C(7)-O(2)	31.2(4)
C(10)-S(1)-N(2)-N(1)	-55.9(2)
C(10)-C(11)-C(12)-C(13)	-0.9(6)

C(11)-C(10)-C(15)-C(14)	0.2(5)
C(11)-C(12)-C(13)-C(14)	-0.3(6)
C(11)-C(12)-C(13)-C(16)	-179.0(3)
C(12)-C(13)-C(14)-C(15)	1.5(6)
C(13)-C(14)-C(15)-C(10)	-1.4(6)
C(15)-C(10)-C(11)-C(12)	0.9(5)
C(16)-C(13)-C(14)-C(15)	-179.8(4)
C(17)-C(18)-C(19)-C(20)	11.2(6)
C(18)-C(17)-C(22)-C(21)	17.6(5)
C(18)-C(19)-C(20)-C(21)	-40.8(5)
C(19)-C(20)-C(21)-C(22)	59.6(4)
C(20)-C(21)-C(22)-C(17)	-47.0(4)
C(22)-C(17)-C(18)-C(19)	0.7(6)
S(1B)-C(10B)-C(11B)-C(12B)	179.2(3)
S(1B)-C(10B)-C(15B)-C(14B)	-179.5(3)
O(1B)-C(5B)-C(6B)-C(1B)	16.8(3)
O(1B)-C(5B)-C(6B)-C(2B)	79.2(3)
O(1B)-C(5B)-C(6B)-C(17B)	-126.8(3)
O(3B)-S(1B)-N(2B)-N(1B)	171.6(2)
O(3B)-S(1B)-C(10B)-C(11B)	131.4(3)
O(3B)-S(1B)-C(10B)-C(15B)	-48.5(3)
O(4B)-S(1B)-N(2B)-N(1B)	-60.4(2)
O(4B)-S(1B)-C(10B)-C(11B)	-1.1(3)
O(4B)-S(1B)-C(10B)-C(15B)	179.0(3)
N(2B)-S(1B)-C(10B)-C(11B)	-116.4(3)
N(2B)-S(1B)-C(10B)-C(15B)	63.7(3)
N(2B)-N(1B)-C(8B)-C(1B)	177.0(2)
N(2B)-N(1B)-C(8B)-C(9B)	0.0(4)
C(1B)-C(2B)-C(3B)-C(4B)	73.9(4)
C(1B)-C(2B)-C(6B)-C(5B)	-96.9(3)
C(1B)-C(2B)-C(6B)-C(17B)	110.3(4)
C(1B)-C(6B)-C(17B)-C(18B)	81.9(4)
C(1B)-C(6B)-C(17B)-C(22B)	-94.4(4)
C(2B)-C(1B)-C(6B)-C(5B)	97.8(3)
C(2B)-C(1B)-C(6B)-C(17B)	-117.9(4)
C(2B)-C(1B)-C(7B)-O(1B)	-56.5(4)

C(2B)-C(1B)-C(7B)-O(2B)	124.7(4)
C(2B)-C(1B)-C(8B)-N(1B)	-31.3(4)
C(2B)-C(1B)-C(8B)-C(9B)	146.0(3)
C(2B)-C(3B)-C(4B)-C(5B)	-29.0(4)
C(2B)-C(6B)-C(17B)-C(18B)	5.9(5)
C(2B)-C(6B)-C(17B)-C(22B)	-170.4(3)
C(3B)-C(2B)-C(6B)-C(1B)	113.5(3)
C(3B)-C(2B)-C(6B)-C(5B)	16.6(3)
C(3B)-C(2B)-C(6B)-C(17B)	-136.2(3)
C(3B)-C(4B)-C(5B)-O(1B)	-73.4(3)
C(3B)-C(4B)-C(5B)-C(6B)	40.3(4)
C(4B)-C(5B)-C(6B)-C(1B)	-97.2(3)
C(4B)-C(5B)-C(6B)-C(2B)	-34.9(3)
C(4B)-C(5B)-C(6B)-C(17B)	119.2(3)
C(5B)-O(1B)-C(7B)-O(2B)	-176.7(3)
C(5B)-O(1B)-C(7B)-C(1B)	4.3(4)
C(5B)-C(6B)-C(17B)-C(18B)	-141.5(4)
C(5B)-C(6B)-C(17B)-C(22B)	42.2(4)
C(6B)-C(1B)-C(2B)-C(3B)	-97.0(3)
C(6B)-C(1B)-C(7B)-O(1B)	6.9(3)
C(6B)-C(1B)-C(7B)-O(2B)	-171.9(3)
C(6B)-C(1B)-C(8B)-N(1B)	-100.8(3)
C(6B)-C(1B)-C(8B)-C(9B)	76.5(4)
C(6B)-C(2B)-C(3B)-C(4B)	7.6(4)
C(6B)-C(17B)-C(18B)-C(19B)	-176.7(4)
C(6B)-C(17B)-C(22B)-C(21B)	160.8(3)
C(7B)-O(1B)-C(5B)-C(4B)	98.1(3)
C(7B)-O(1B)-C(5B)-C(6B)	-13.9(4)
C(7B)-C(1B)-C(2B)-C(3B)	-2.7(4)
C(7B)-C(1B)-C(2B)-C(6B)	94.3(3)
C(7B)-C(1B)-C(6B)-C(2B)	-112.2(3)
C(7B)-C(1B)-C(6B)-C(5B)	-14.4(3)
C(7B)-C(1B)-C(6B)-C(17B)	129.9(3)
C(7B)-C(1B)-C(8B)-N(1B)	125.5(3)
C(7B)-C(1B)-C(8B)-C(9B)	-57.2(4)
C(8B)-N(1B)-N(2B)-S(1B)	-174.5(2)

C(8B)-C(1B)-C(2B)-C(3B)	154.2(3)
C(8B)-C(1B)-C(2B)-C(6B)	-108.8(3)
C(8B)-C(1B)-C(6B)-C(2B)	109.7(3)
C(8B)-C(1B)-C(6B)-C(5B)	-152.4(3)
C(8B)-C(1B)-C(6B)-C(17B)	-8.1(5)
C(8B)-C(1B)-C(7B)-O(1B)	146.0(3)
C(8B)-C(1B)-C(7B)-O(2B)	-32.8(5)
C(10B)-S(1B)-N(2B)-N(1B)	55.6(2)
C(10B)-C(11B)-C(12B)-C(13B)	0.2(6)
C(11B)-C(10B)-C(15B)-C(14B)	0.6(5)
C(11B)-C(12B)-C(13B)-C(14B)	0.7(6)
C(11B)-C(12B)-C(13B)-C(16B)	179.8(4)
C(12B)-C(13B)-C(14B)-C(15B)	-1.0(6)
C(13B)-C(14B)-C(15B)-C(10B)	0.4(6)
C(15B)-C(10B)-C(11B)-C(12B)	-0.9(5)
C(16B)-C(13B)-C(14B)-C(15B)	179.9(4)
C(17B)-C(18B)-C(19B)-C(20B)	-12.3(7)
C(18B)-C(17B)-C(22B)-C(21B)	-15.5(6)
C(18B)-C(19B)-C(20B)-C(21B)	42.1(6)
C(19B)-C(20B)-C(21B)-C(22B)	-59.4(6)
C(20B)-C(21B)-C(22B)-C(17B)	44.9(5)
C(22B)-C(17B)-C(18B)-C(19B)	-0.7(6)
S(1C)-C(10C)-C(11C)-C(12C)	-176.7(3)
S(1C)-C(10C)-C(15C)-C(14C)	176.1(3)
O(1C)-C(5C)-C(6C)-C(1C)	16.8(3)
O(1C)-C(5C)-C(6C)-C(2C)	79.0(3)
O(1C)-C(5C)-C(6C)-C(17C)	-124.9(3)
O(3C)-S(1C)-N(2C)-N(1C)	-60.3(2)
O(3C)-S(1C)-C(10C)-C(11C)	-162.5(3)
O(3C)-S(1C)-C(10C)-C(15C)	20.8(3)
O(4C)-S(1C)-N(2C)-N(1C)	172.4(2)
O(4C)-S(1C)-C(10C)-C(11C)	-30.2(3)
O(4C)-S(1C)-C(10C)-C(15C)	153.0(3)
N(2C)-S(1C)-C(10C)-C(11C)	82.7(3)
N(2C)-S(1C)-C(10C)-C(15C)	-94.0(3)
N(2C)-N(1C)-C(8C)-C(1C)	176.7(2)

N(2C)-N(1C)-C(8C)-C(9C)	-1.1(5)
C(1C)-C(2C)-C(3C)-C(4C)	74.0(3)
C(1C)-C(2C)-C(6C)-C(5C)	-96.8(2)
C(1C)-C(2C)-C(6C)-C(17C)	109.0(3)
C(1C)-C(6C)-C(17C)-C(18C)	80.7(4)
C(1C)-C(6C)-C(17C)-C(22C)	-95.1(4)
C(2C)-C(1C)-C(6C)-C(5C)	98.2(2)
C(2C)-C(1C)-C(6C)-C(17C)	-119.6(3)
C(2C)-C(1C)-C(7C)-O(1C)	-55.9(3)
C(2C)-C(1C)-C(7C)-O(2C)	125.9(3)
C(2C)-C(1C)-C(8C)-N(1C)	-31.1(4)
C(2C)-C(1C)-C(8C)-C(9C)	146.9(3)
C(2C)-C(3C)-C(4C)-C(5C)	-28.9(3)
C(2C)-C(6C)-C(17C)-C(18C)	4.8(5)
C(2C)-C(6C)-C(17C)-C(22C)	-171.0(3)
C(3C)-C(2C)-C(6C)-C(1C)	113.5(3)
C(3C)-C(2C)-C(6C)-C(5C)	16.7(3)
C(3C)-C(2C)-C(6C)-C(17C)	-137.5(3)
C(3C)-C(4C)-C(5C)-O(1C)	-73.4(3)
C(3C)-C(4C)-C(5C)-C(6C)	40.1(3)
C(4C)-C(5C)-C(6C)-C(1C)	-97.1(3)
C(4C)-C(5C)-C(6C)-C(2C)	-34.9(3)
C(4C)-C(5C)-C(6C)-C(17C)	121.1(3)
C(5C)-O(1C)-C(7C)-O(2C)	-177.5(3)
C(5C)-O(1C)-C(7C)-C(1C)	4.3(3)
C(5C)-C(6C)-C(17C)-C(18C)	-144.8(3)
C(5C)-C(6C)-C(17C)-C(22C)	39.4(4)
C(6C)-C(1C)-C(2C)-C(3C)	-97.1(3)
C(6C)-C(1C)-C(7C)-O(1C)	7.0(3)
C(6C)-C(1C)-C(7C)-O(2C)	-171.1(3)
C(6C)-C(1C)-C(8C)-N(1C)	-100.4(3)
C(6C)-C(1C)-C(8C)-C(9C)	77.6(4)
C(6C)-C(2C)-C(3C)-C(4C)	7.4(3)
C(6C)-C(17C)-C(18C)-C(19C)	-176.3(4)
C(6C)-C(17C)-C(22C)-C(21C)	156.9(3)
C(7C)-O(1C)-C(5C)-C(4C)	97.9(3)

C(7C)-O(1C)-C(5C)-C(6C)	-13.8(3)
C(7C)-C(1C)-C(2C)-C(3C)	-3.6(4)
C(7C)-C(1C)-C(2C)-C(6C)	93.5(3)
C(7C)-C(1C)-C(6C)-C(2C)	-112.5(3)
C(7C)-C(1C)-C(6C)-C(5C)	-14.3(3)
C(7C)-C(1C)-C(6C)-C(17C)	127.9(3)
C(7C)-C(1C)-C(8C)-N(1C)	124.7(3)
C(7C)-C(1C)-C(8C)-C(9C)	-57.2(4)
C(8C)-N(1C)-N(2C)-S(1C)	179.4(2)
C(8C)-C(1C)-C(2C)-C(3C)	152.4(3)
C(8C)-C(1C)-C(2C)-C(6C)	-110.5(3)
C(8C)-C(1C)-C(6C)-C(2C)	108.1(3)
C(8C)-C(1C)-C(6C)-C(5C)	-153.7(3)
C(8C)-C(1C)-C(6C)-C(17C)	-11.5(4)
C(8C)-C(1C)-C(7C)-O(1C)	147.7(3)
C(8C)-C(1C)-C(7C)-O(2C)	-30.4(4)
C(10C)-S(1C)-N(2C)-N(1C)	55.4(2)
C(10C)-C(11C)-C(12C)-C(13C)	0.4(6)
C(11C)-C(10C)-C(15C)-C(14C)	-0.7(5)
C(11C)-C(12C)-C(13C)-C(14C)	-0.2(6)
C(11C)-C(12C)-C(13C)-C(16C)	-179.4(4)
C(12C)-C(13C)-C(14C)-C(15C)	-0.4(6)
C(13C)-C(14C)-C(15C)-C(10C)	0.8(6)
C(15C)-C(10C)-C(11C)-C(12C)	0.1(5)
C(16C)-C(13C)-C(14C)-C(15C)	178.8(3)
C(17C)-C(18C)-C(19C)-C(20C)	-9.4(6)
C(18C)-C(17C)-C(22C)-C(21C)	-18.9(5)
C(18C)-C(19C)-C(20C)-C(21C)	39.2(5)
C(19C)-C(20C)-C(21C)-C(22C)	-58.8(5)
C(20C)-C(21C)-C(22C)-C(17C)	47.5(5)
C(22C)-C(17C)-C(18C)-C(19C)	-0.8(6)
S(1D)-C(10D)-C(11D)-C(12D)	-177.0(3)
S(1D)-C(10D)-C(15D)-C(14D)	177.4(3)
O(1D)-C(5D)-C(6D)-C(1D)	-16.0(3)
O(1D)-C(5D)-C(6D)-C(2D)	-78.0(3)
O(1D)-C(5D)-C(6D)-C(17D)	128.0(3)

O(3D)-S(1D)-N(2D)-N(1D)	-171.3(2)
O(3D)-S(1D)-C(10D)-C(11D)	-135.3(3)
O(3D)-S(1D)-C(10D)-C(15D)	45.8(3)
O(4D)-S(1D)-N(2D)-N(1D)	60.6(2)
O(4D)-S(1D)-C(10D)-C(11D)	-2.3(3)
O(4D)-S(1D)-C(10D)-C(15D)	178.8(3)
N(2D)-S(1D)-C(10D)-C(11D)	112.3(3)
N(2D)-S(1D)-C(10D)-C(15D)	-66.6(3)
N(2D)-N(1D)-C(8D)-C(1D)	-177.8(3)
N(2D)-N(1D)-C(8D)-C(9D)	0.2(5)
C(1D)-C(2D)-C(3D)-C(4D)	-73.8(4)
C(1D)-C(2D)-C(6D)-C(5D)	97.3(3)
C(1D)-C(2D)-C(6D)-C(17D)	-109.8(4)
C(1D)-C(6D)-C(17D)-C(18D)	-81.7(5)
C(1D)-C(6D)-C(17D)-C(22D)	94.4(4)
C(2D)-C(1D)-C(6D)-C(5D)	-97.9(3)
C(2D)-C(1D)-C(6D)-C(17D)	117.4(4)
C(2D)-C(1D)-C(7D)-O(1D)	56.8(4)
C(2D)-C(1D)-C(7D)-O(2D)	-124.6(4)
C(2D)-C(1D)-C(8D)-N(1D)	33.1(4)
C(2D)-C(1D)-C(8D)-C(9D)	-145.1(3)
C(2D)-C(3D)-C(4D)-C(5D)	28.8(4)
C(2D)-C(6D)-C(17D)-C(18D)	-6.6(6)
C(2D)-C(6D)-C(17D)-C(22D)	169.5(3)
C(3D)-C(2D)-C(6D)-C(1D)	-114.1(3)
C(3D)-C(2D)-C(6D)-C(5D)	-16.9(3)
C(3D)-C(2D)-C(6D)-C(17D)	136.0(3)
C(3D)-C(4D)-C(5D)-O(1D)	73.0(3)
C(3D)-C(4D)-C(5D)-C(6D)	-40.0(3)
C(4D)-C(5D)-C(6D)-C(1D)	97.2(3)
C(4D)-C(5D)-C(6D)-C(2D)	35.2(3)
C(4D)-C(5D)-C(6D)-C(17D)	-118.8(3)
C(5D)-O(1D)-C(7D)-O(2D)	177.0(3)
C(5D)-O(1D)-C(7D)-C(1D)	-4.2(3)
C(5D)-C(6D)-C(17D)-C(18D)	141.0(4)
C(5D)-C(6D)-C(17D)-C(22D)	-42.8(5)

C(6D)-C(1D)-C(2D)-C(3D)	96.7(3)
C(6D)-C(1D)-C(7D)-O(1D)	-6.5(3)
C(6D)-C(1D)-C(7D)-O(2D)	172.2(3)
C(6D)-C(1D)-C(8D)-N(1D)	103.7(3)
C(6D)-C(1D)-C(8D)-C(9D)	-74.5(4)
C(6D)-C(2D)-C(3D)-C(4D)	-7.3(4)
C(6D)-C(17D)-C(18D)-C(19D)	176.3(4)
C(6D)-C(17D)-C(22D)-C(21D)	-169.7(6)
C(7D)-O(1D)-C(5D)-C(4D)	-98.4(3)
C(7D)-O(1D)-C(5D)-C(6D)	13.2(3)
C(7D)-C(1D)-C(2D)-C(3D)	2.6(4)
C(7D)-C(1D)-C(2D)-C(6D)	-94.1(3)
C(7D)-C(1D)-C(6D)-C(2D)	111.4(3)
C(7D)-C(1D)-C(6D)-C(5D)	13.5(3)
C(7D)-C(1D)-C(6D)-C(17D)	-131.1(3)
C(7D)-C(1D)-C(8D)-N(1D)	-121.3(3)
C(7D)-C(1D)-C(8D)-C(9D)	60.5(4)
C(8D)-N(1D)-N(2D)-S(1D)	174.0(2)
C(8D)-C(1D)-C(2D)-C(3D)	-152.1(3)
C(8D)-C(1D)-C(2D)-C(6D)	111.2(3)
C(8D)-C(1D)-C(6D)-C(2D)	-109.3(3)
C(8D)-C(1D)-C(6D)-C(5D)	152.8(3)
C(8D)-C(1D)-C(6D)-C(17D)	8.1(5)
C(8D)-C(1D)-C(7D)-O(1D)	-147.8(3)
C(8D)-C(1D)-C(7D)-O(2D)	30.9(5)
C(10D)-S(1D)-N(2D)-N(1D)	-54.4(2)
C(10D)-C(11D)-C(12D)-C(13D)	-0.6(6)
C(11D)-C(10D)-C(15D)-C(14D)	-1.5(5)
C(11D)-C(12D)-C(13D)-C(14D)	-1.0(6)
C(11D)-C(12D)-C(13D)-C(16D)	179.5(4)
C(12D)-C(13D)-C(14D)-C(15D)	1.3(6)
C(13D)-C(14D)-C(15D)-C(10D)	-0.1(6)
C(15D)-C(10D)-C(11D)-C(12D)	1.8(6)
C(16D)-C(13D)-C(14D)-C(15D)	-179.2(4)
C(17D)-C(18D)-C(19D)-C(20D)	3.8(10)
C(18D)-C(17D)-C(22D)-C(21D)	6.4(8)

C(18D)-C(19D)-C(20D)-C(21D)	-17.4(16)
C(19D)-C(20D)-C(21D)-C(22D)	27(2)
C(20D)-C(21D)-C(22D)-C(17D)	-19.8(14)
C(22D)-C(17D)-C(18D)-C(19D)	0.4(7)

Symmetry transformations used to generate equivalent atoms:

A4.2 CRYSTAL STRUCTURE ANALYSIS OF 48

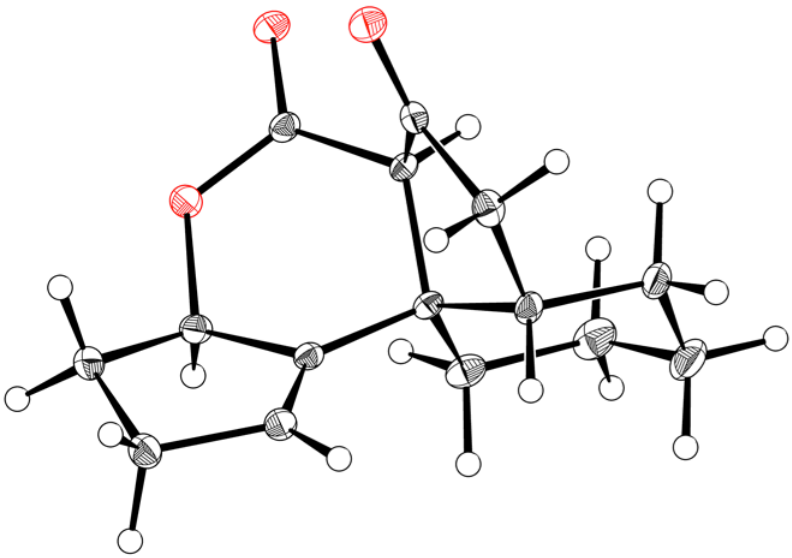

48

*Table A4.2.1. Crystal data and structure refinement for **48**.*

Empirical formula	$C_{15}H_{18}O_3$
Formula weight	246.29
Crystallization solvent	Dichloromethane/hexane
Crystal shape	slab
Crystal color	colorless
Crystal size	0.12 x 0.37 x 0.44 mm

Data Collection

Preliminary photograph(s)	rotation	
Type of diffractometer	Bruker APEX-II CCD	
Wavelength	0.71073 Å MoK	
Data collection temperature	100 K	
Theta range for 9118 reflections used		
in lattice determination	2.42 to 41.03°	
Unit cell dimensions	a = 8.0015(4) Å	α= 90°
	b = 10.2072(6) Å	β= 90.669(3)°
	c = 14.8838(8) Å	γ = 90°
Volume	1215.52(11) Å3	
Z	4	
Crystal system	monoclinic	
Space group	P 1 21/c 1 (# 14)	
Density (calculated)	1.346 g/cm3	
F(000)	528	
Theta range for data collection	2.4 to 41.6°	
Completeness to theta = 25.000°	100.0%	
Index ranges	-14 £ h £ 14, -18 £ k £ 18, -27 £ l £ 27	
Data collection scan type	and scans	
Reflections collected	83376	

Independent reflections	8050 [Rint= 0.0411]
Reflections > 2s(I)	6562
Average s(I)/(net I)	0.0218
Absorption coefficient	0.09 mm-1
Absorption correction	Semi-empirical from equivalents
Max. and min. transmission	1.0000 and 0.9532

Structure Solution and Refinement

Primary solution method	dual
Secondary solution method	?
Hydrogen placement	difmap
Refinement method	Full-matrix least-squares on F2
Data / restraints / parameters	8050 / 0 / 235
Treatment of hydrogen atoms	refall
Goodness-of-fit on F^2	1.76
Final R indices [I>2s(I), 6562 reflections]	R1 = 0.0379, wR2 = 0.1076
R indices (all data)	R1 = 0.0511, wR2 = 0.1117
Type of weighting scheme used	calc
Weighting scheme used	
Max shift/error	0.001
Average shift/error	0.000
Extinction coefficient	n/a
Largest diff. peak and hole	0.73 and -0.25 e·Å-3

Programs Used

Cell refinement	SAINT V8.27B (Bruker-AXS, 2007)
Data collection	APEX2 2012.4-3 (Bruker-AXS, 2007)
Data reduction	SAINT V8.27B (Bruker-AXS, 2007)
Structure solution	SHELXT (Sheldrick, 2012)
Structure refinement	SHELXL-2012/7 (Sheldrick, 2012)
Graphics	DIAMOND 3 (Crystal Impact, 1999)

Table A4.2.2. Atomic coordinates (x 10^4) and equivalent isotropic displacement parameters ($Å^2$x 10^3) for ***48****. U(eq) is defined as one third of the trace of the orthogonalized U^{ij} tensor.*

	x	y	z	U_{eq}
C(1)	2582(1)	2999(1)	3879(1)	10(1)
C(2)	2552(1)	1559(1)	4084(1)	11(1)
C(3)	2217(1)	517(1)	3570(1)	13(1)
C(4)	2307(1)	-752(1)	4089(1)	16(1)
C(5)	2394(1)	-289(1)	5078(1)	15(1)
C(6)	2960(1)	1140(1)	5028(1)	13(1)
C(7)	1538(1)	3132(1)	5540(1)	12(1)
C(8)	1423(1)	3615(1)	4585(1)	10(1)
C(9)	-338(1)	3348(1)	4189(1)	11(1)
C(10)	-176(1)	3116(1)	3187(1)	14(1)
C(11)	1677(1)	3328(1)	2979(1)	12(1)
C(12)	1995(1)	4738(1)	2671(1)	17(1)
C(13)	3846(1)	5080(1)	2663(1)	23(1)
C(14)	4600(1)	4910(1)	3603(1)	21(1)
C(15)	4396(1)	3498(1)	3924(1)	16(1)
O(1)	2128(1)	1920(1)	5713(1)	17(1)
O(2)	1036(1)	3773(1)	6164(1)	17(1)
O(3)	-1608(1)	3301(1)	4617(1)	17(1)

Table A4.2.3. Bond lengths [Å] and angles [°] for ***48***

C(1)-C(2)	1.5015(7)
C(1)-C(8)	1.5433(6)
C(1)-C(11)	1.5520(6)
C(1)-C(15)	1.5386(6)
C(2)-C(3)	1.3351(6)
C(2)-C(6)	1.5009(6)
C(3)-H(3)	0.986(9)
C(3)-C(4)	1.5094(7)
C(4)-H(4A)	1.025(10)
C(4)-H(4B)	1.012(8)
C(4)-C(5)	1.5463(7)
C(5)-H(5A)	0.984(9)
C(5)-H(5B)	1.011(10)
C(5)-C(6)	1.5301(7)
C(6)-H(6)	0.983(8)
C(6)-O(1)	1.4605(6)
C(7)-C(8)	1.5062(6)
C(7)-O(1)	1.3487(6)
C(7)-O(2)	1.2096(6)
C(8)-H(8)	0.972(8)
C(8)-C(9)	1.5450(6)
C(9)-C(10)	1.5172(7)
C(9)-O(3)	1.2065(6)
C(10)-H(10A)	0.999(10)
C(10)-H(10B)	0.983(9)
C(10)-C(11)	1.5338(7)
C(11)-H(11)	0.994(9)
C(11)-C(12)	1.5322(7)
C(12)-H(12A)	0.996(11)
C(12)-H(12B)	1.003(9)
C(12)-C(13)	1.5221(9)
C(13)-H(13A)	1.038(10)
C(13)-H(13B)	0.998(10)
C(13)-C(14)	1.5271(9)
C(14)-H(14A)	1.028(10)
C(14)-H(14B)	0.982(10)
C(14)-C(15)	1.5271(8)
C(15)-H(15A)	0.998(8)
C(15)-H(15B)	1.032(9)
C(2)-C(1)-C(8)	104.44(4)
C(2)-C(1)-C(11)	112.23(4)
C(2)-C(1)-C(15)	109.42(4)
C(8)-C(1)-C(11)	102.78(4)
C(15)-C(1)-C(8)	114.19(4)
C(15)-C(1)-C(11)	113.36(4)
C(3)-C(2)-C(1)	131.88(4)
C(3)-C(2)-C(6)	110.41(4)
C(6)-C(2)-C(1)	117.72(4)

C(2)-C(3)-H(3)	125.9(5)
C(2)-C(3)-C(4)	112.54(4)
C(4)-C(3)-H(3)	121.5(5)
C(3)-C(4)-H(4A)	109.0(5)
C(3)-C(4)-H(4B)	112.7(5)
C(3)-C(4)-C(5)	103.04(4)
H(4A)-C(4)-H(4B)	108.8(7)
C(5)-C(4)-H(4A)	112.1(5)
C(5)-C(4)-H(4B)	111.2(5)
C(4)-C(5)-H(5A)	110.5(5)
C(4)-C(5)-H(5B)	114.0(5)
H(5A)-C(5)-H(5B)	107.3(7)
C(6)-C(5)-C(4)	104.79(4)
C(6)-C(5)-H(5A)	107.5(5)
C(6)-C(5)-H(5B)	112.6(5)
C(2)-C(6)-C(5)	104.83(4)
C(2)-C(6)-H(6)	112.5(5)
C(5)-C(6)-H(6)	111.2(5)
O(1)-C(6)-C(2)	113.77(4)
O(1)-C(6)-C(5)	110.34(4)
O(1)-C(6)-H(6)	104.4(5)
O(1)-C(7)-C(8)	119.93(4)
O(2)-C(7)-C(8)	122.09(4)
O(2)-C(7)-O(1)	117.88(4)
C(1)-C(8)-H(8)	112.0(5)
C(1)-C(8)-C(9)	102.82(3)
C(7)-C(8)-C(1)	118.57(4)
C(7)-C(8)-H(8)	106.2(5)
C(7)-C(8)-C(9)	110.30(4)
C(9)-C(8)-H(8)	106.4(5)
C(10)-C(9)-C(8)	108.29(4)
O(3)-C(9)-C(8)	125.18(4)
O(3)-C(9)-C(10)	126.50(4)
C(9)-C(10)-H(10A)	107.2(6)
C(9)-C(10)-H(10B)	108.3(5)
C(9)-C(10)-C(11)	105.70(4)
H(10A)-C(10)-H(10B)	107.2(8)
C(11)-C(10)-H(10A)	115.1(6)
C(11)-C(10)-H(10B)	113.0(5)
C(1)-C(11)-H(11)	109.4(5)
C(10)-C(11)-C(1)	103.75(4)
C(10)-C(11)-H(11)	112.0(5)
C(12)-C(11)-C(1)	112.54(4)
C(12)-C(11)-C(10)	110.90(4)
C(12)-C(11)-H(11)	108.2(5)
C(11)-C(12)-H(12A)	107.2(6)
C(11)-C(12)-H(12B)	108.4(5)
H(12A)-C(12)-H(12B)	106.6(8)
C(13)-C(12)-C(11)	112.52(5)
C(13)-C(12)-H(12A)	111.7(6)
C(13)-C(12)-H(12B)	110.2(5)
C(12)-C(13)-H(13A)	109.8(5)
C(12)-C(13)-H(13B)	108.7(5)
C(12)-C(13)-C(14)	109.89(4)

H(13A)-C(13)-H(13B)	109.2(8)
C(14)-C(13)-H(13A)	110.4(5)
C(14)-C(13)-H(13B)	108.9(6)
C(13)-C(14)-H(14A)	109.3(6)
C(13)-C(14)-H(14B)	112.7(6)
H(14A)-C(14)-H(14B)	106.0(8)
C(15)-C(14)-C(13)	110.59(5)
C(15)-C(14)-H(14A)	110.5(6)
C(15)-C(14)-H(14B)	107.8(6)
C(1)-C(15)-H(15A)	105.7(5)
C(1)-C(15)-H(15B)	108.2(5)
C(14)-C(15)-C(1)	113.75(4)
C(14)-C(15)-H(15A)	113.1(5)
C(14)-C(15)-H(15B)	105.2(5)
H(15A)-C(15)-H(15B)	110.9(7)
C(7)-O(1)-C(6)	121.80(4)

Symmetry transformations used to generate equivalent atoms:

Table A4.2.4. Anisotropic displacement parameters (Å2x 104) for ***48****. The anisotropic displacement factor exponent takes the form: -2p2 [h2 a*2U 11 + ... + 2 h k a* b* U12]*

	U^{11}	U^{22}	U^{33}	U^{23}	U^{13}	U^{12}
C(1)	111(2)	121(2)	78(2)	-12(1)	10(1)	-10(1)
C(2)	100(2)	129(2)	87(2)	-3(1)	4(1)	9(1)
C(3)	150(2)	131(2)	109(2)	-10(1)	0(1)	3(1)
C(4)	193(2)	127(2)	148(2)	0(2)	5(2)	15(2)
C(5)	181(2)	147(2)	126(2)	23(2)	8(1)	39(2)
C(6)	134(2)	157(2)	94(2)	-3(1)	-7(1)	37(1)
C(7)	132(2)	141(2)	82(2)	-3(1)	6(1)	5(1)
C(8)	111(2)	118(2)	73(2)	-2(1)	5(1)	-3(1)
C(9)	116(2)	104(2)	122(2)	15(1)	-10(1)	2(1)
C(10)	159(2)	146(2)	113(2)	3(1)	-42(1)	2(2)
C(11)	175(2)	123(2)	71(2)	-1(1)	4(1)	-2(1)
C(12)	253(2)	138(2)	113(2)	18(2)	44(2)	-6(2)
C(13)	275(3)	202(2)	206(2)	24(2)	108(2)	-53(2)
C(14)	207(2)	200(2)	236(2)	-28(2)	57(2)	-88(2)
C(15)	119(2)	193(2)	163(2)	-27(2)	26(1)	-37(2)
O(1)	266(2)	168(2)	78(1)	4(1)	11(1)	79(1)
O(2)	242(2)	183(2)	90(1)	-18(1)	31(1)	43(1)
O(3)	122(1)	192(2)	201(2)	20(1)	28(1)	-7(1)

Table A4.2.5. Hydrogen coordinates (x 10^3) and isotropic displacement parameters ($Å^2$x 10^3) for ***48****.*

	x	y	z	U_{iso}
H(3)	199(1)	53(1)	292(1)	24(2)
H(4A)	336(1)	-125(1)	391(1)	26(2)
H(4B)	130(1)	-133(1)	398(1)	24(2)
H(5A)	128(1)	-30(1)	535(1)	23(2)
H(5B)	315(1)	-84(1)	548(1)	31(2)
H(6)	416(1)	123(1)	517(1)	18(2)
H(8)	154(1)	456(1)	461(1)	15(2)
H(10A)	-96(1)	373(1)	288(1)	35(3)
H(10B)	-56(1)	222(1)	305(1)	27(2)
H(11)	207(1)	273(1)	250(1)	22(2)
H(12A)	147(1)	484(1)	207(1)	33(2)
H(12B)	138(1)	535(1)	308(1)	22(2)
H(13A)	400(1)	604(1)	244(1)	37(3)
H(13B)	442(1)	447(1)	224(1)	32(2)
H(14A)	403(1)	555(1)	404(1)	33(2)
H(14B)	580(1)	512(1)	363(1)	35(3)
H(15A)	477(1)	337(1)	456(1)	20(2)
H(15B)	510(1)	294(1)	349(1)	24(2)

Table A4.2.6. Torsion angles [°] for ***48****.*

C(1)-C(2)-C(3)-C(4)	-178.62(5)
C(1)-C(2)-C(6)-C(5)	165.91(4)
C(1)-C(2)-C(6)-O(1)	45.28(6)
C(1)-C(8)-C(9)-C(10)	-21.53(5)
C(1)-C(8)-C(9)-O(3)	156.69(5)
C(1)-C(11)-C(12)-C(13)	51.22(6)
C(2)-C(1)-C(8)-C(7)	42.15(5)
C(2)-C(1)-C(8)-C(9)	-79.79(4)
C(2)-C(1)-C(11)-C(10)	71.42(5)
C(2)-C(1)-C(11)-C(12)	-168.64(4)
C(2)-C(1)-C(15)-C(14)	172.17(4)
C(2)-C(3)-C(4)-C(5)	11.74(6)
C(2)-C(6)-O(1)-C(7)	-21.18(6)
C(3)-C(2)-C(6)-C(5)	-14.01(5)
C(3)-C(2)-C(6)-O(1)	-134.65(4)
C(3)-C(4)-C(5)-C(6)	-19.35(5)
C(4)-C(5)-C(6)-C(2)	20.41(5)
C(4)-C(5)-C(6)-O(1)	143.29(4)
C(5)-C(6)-O(1)-C(7)	-138.67(5)
C(6)-C(2)-C(3)-C(4)	1.30(6)
C(7)-C(8)-C(9)-C(10)	-148.91(4)
C(7)-C(8)-C(9)-O(3)	29.31(6)
C(8)-C(1)-C(2)-C(3)	126.52(5)
C(8)-C(1)-C(2)-C(6)	-53.39(5)
C(8)-C(1)-C(11)-C(10)	-40.24(4)
C(8)-C(1)-C(11)-C(12)	79.71(5)
C(8)-C(1)-C(15)-C(14)	-71.20(5)
C(8)-C(7)-O(1)-C(6)	11.90(7)
C(8)-C(9)-C(10)-C(11)	-3.29(5)
C(9)-C(10)-C(11)-C(1)	26.79(5)
C(9)-C(10)-C(11)-C(12)	-94.27(4)
C(10)-C(11)-C(12)-C(13)	166.94(4)
C(11)-C(1)-C(2)-C(3)	15.90(7)
C(11)-C(1)-C(2)-C(6)	-164.01(4)
C(11)-C(1)-C(8)-C(7)	159.47(4)
C(11)-C(1)-C(8)-C(9)	37.53(4)
C(11)-C(1)-C(15)-C(14)	46.07(6)
C(11)-C(12)-C(13)-C(14)	-59.11(6)
C(12)-C(13)-C(14)-C(15)	59.53(6)
C(13)-C(14)-C(15)-C(1)	-53.81(6)
C(15)-C(1)-C(2)-C(3)	-110.84(6)
C(15)-C(1)-C(2)-C(6)	69.25(5)
C(15)-C(1)-C(8)-C(7)	-77.33(5)
C(15)-C(1)-C(8)-C(9)	160.73(4)
C(15)-C(1)-C(11)-C(10)	-163.99(4)
C(15)-C(1)-C(11)-C(12)	-44.05(5)
O(1)-C(7)-C(8)-C(1)	-24.29(6)
O(1)-C(7)-C(8)-C(9)	93.79(5)
O(2)-C(7)-C(8)-C(1)	159.53(4)
O(2)-C(7)-C(8)-C(9)	-82.38(6)

O(2)-C(7)-O(1)-C(6)	-171.76(4)
O(3)-C(9)-C(10)-C(11)	178.52(5)

Symmetry transformations used to generate equivalent atoms:

APPENDIX 5

Spectra Relevant to Appendix 1:

Additional Studies Related to Chapter 1

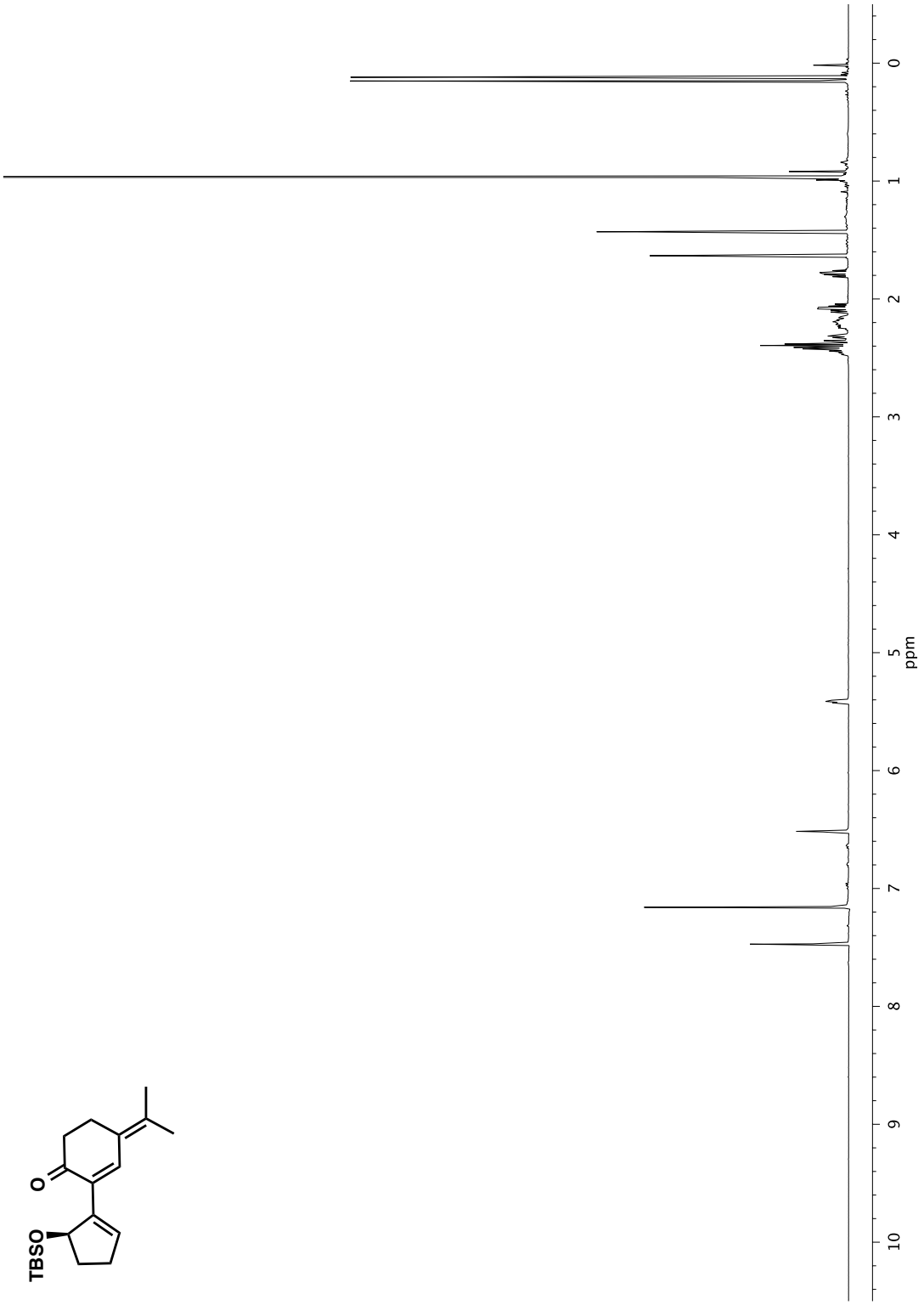

Figure A5.1 ^{1}H NMR (500 MHz, $CDCl_3$) of compound **134**

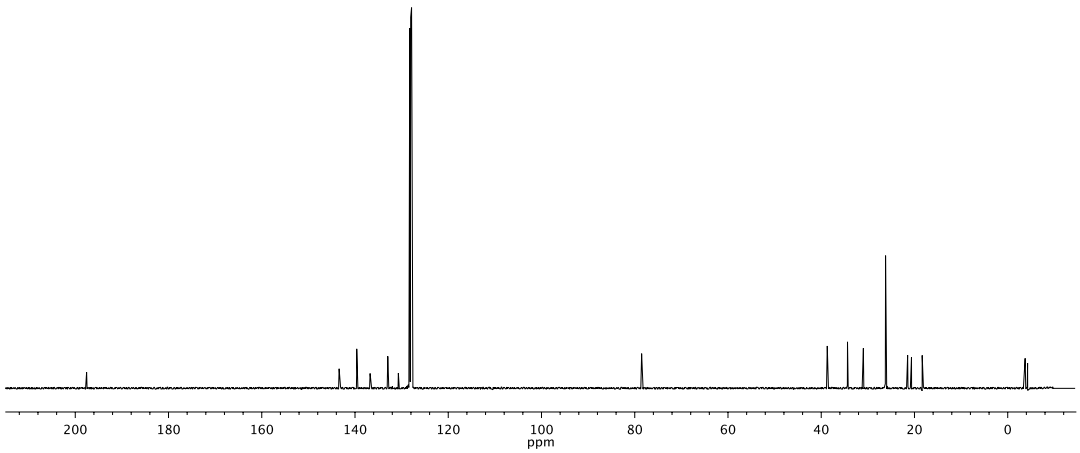

Figure A5.2 ^{13}C NMR (126 MHz, $CDCl_3$) of compound **134**

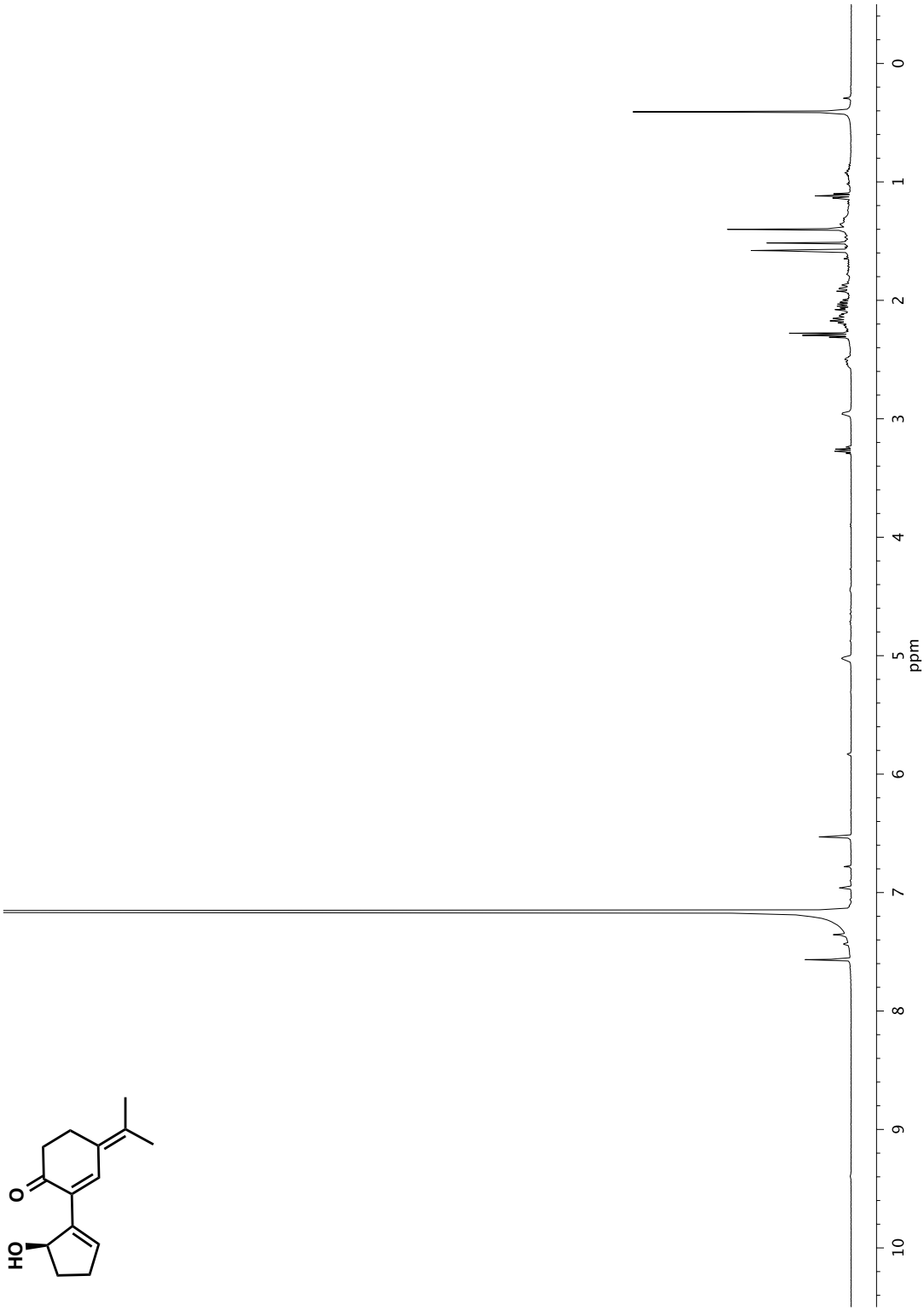

Figure A5.3 ^{1}H NMR (400 MHz, C_6D_6) of compound **135**

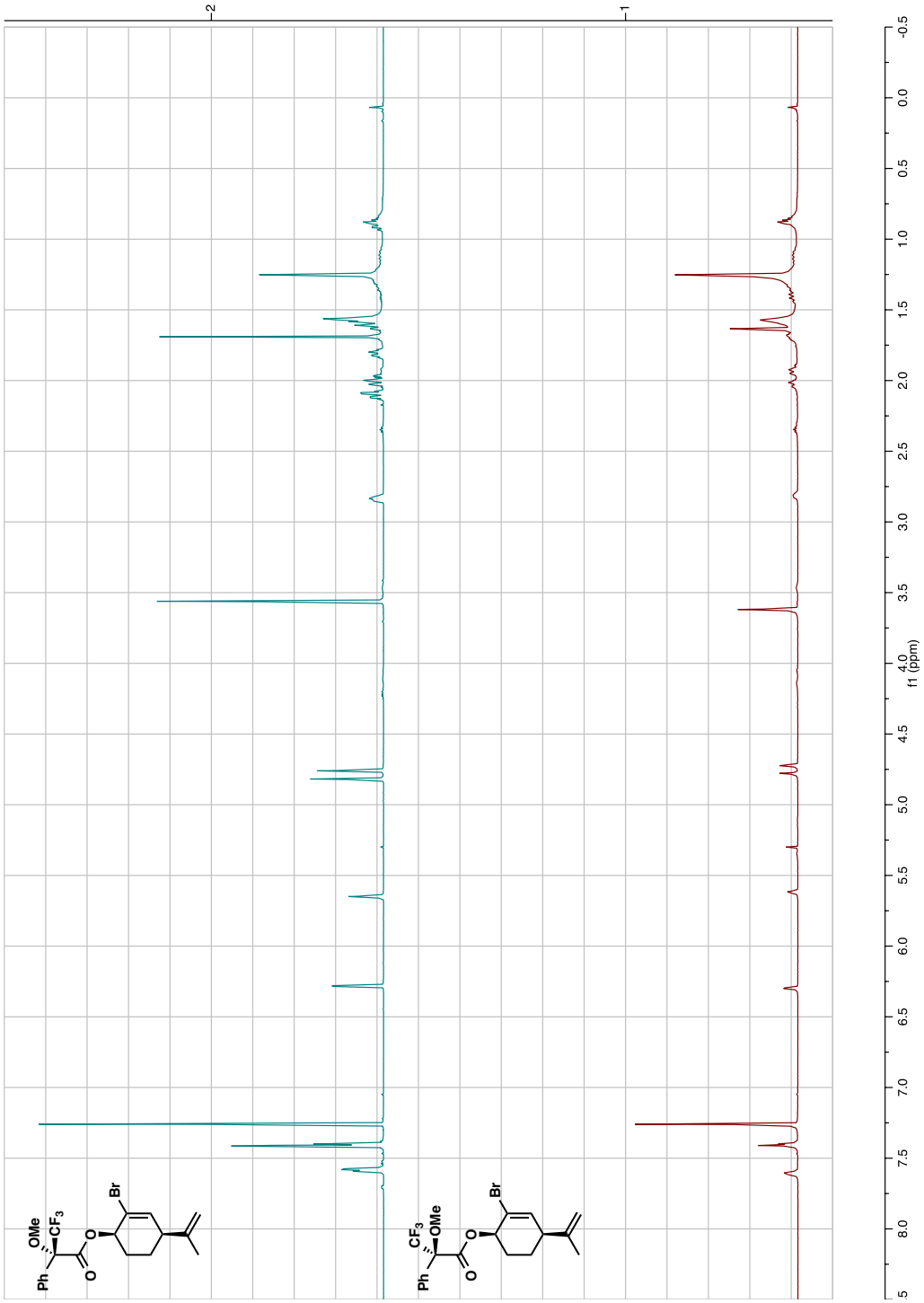

Figure A5.4 ^{1}H NMR (500 MHz, $CDCl_3$) of compound **138** and **139**

CHAPTER 2

Mechanistic Elucidation of the Unexpected Rearrangement†

2.1 INTRODUCTION

During the course of the total synthesis of a complex molecule, organic chemists sometimes discover unexpected structures that arise from unknown rearrangement cascades. In most cases, it is difficult to determinate correct structure and it requires enormous effort to rationalize reaction mechanism. However, unexpected transformations later revealed as general methodology for certain moieties sometimes offer new possibilities to access complex structures. Therefore, it is important to investigate an unexpected reaction and elucidate its mechanism to expand its potential.

† This work was performed in collaboration with Buck L. H. Taylor and Ashay Patel in the Houk group (University of California, Los Angeles) and Galina P. Petrova in the Morokuma group (Kyoto University, Japan).

2.1.1 THE UNEXPECTED REARRANGEMENT

We discovered an unexpected rearrangement of divinylcyclopropane **44** during investigations toward the total synthesis of curcusone C (Ch. 1.2.2). The desired divinylcyclopropane rearrangement product was synthesized by reduction of lactone **51** (Scheme 2.1.1a), however unexpected tetracycle **47** was isolated from silyl enol ether **44** (Scheme 2.1.1b).

Scheme 2.1.1. Unexpected Rearrangement

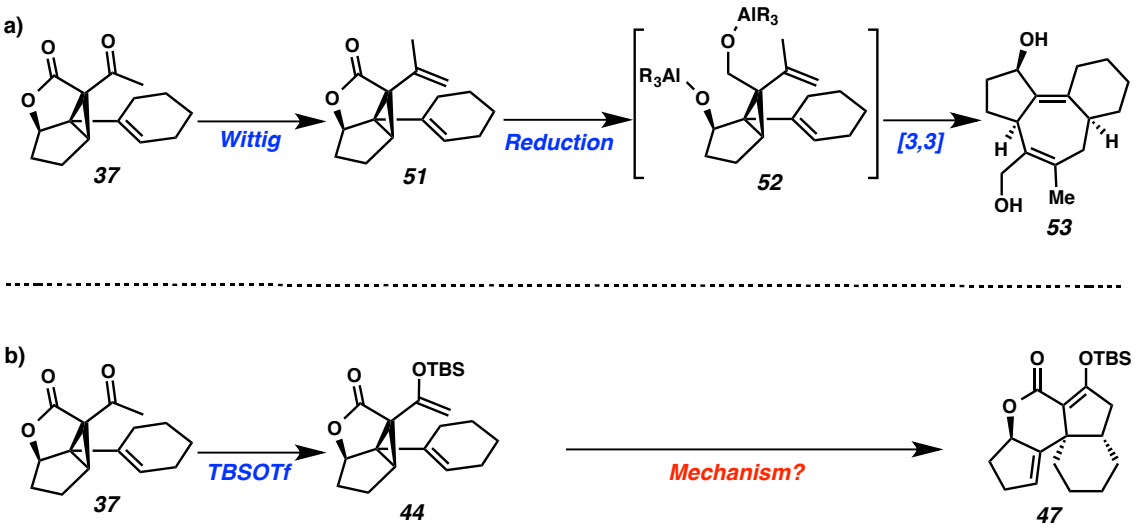

Rearrangements involving the migration of an allyl group in 1,5-dienes are some of the most studied reactions in organic synthesis since 1940.[1] However, the transformation of 1,5-dienes to tetracyclic compounds such as **47** are completely unknown. Suspecting that this could be another variant of the Cope rearrangement, thus we turned our attention to understanding the mechanism of the unexpected rearrangement.

2.2 MECHANISTIC ELUCIDATION

2.2.1 ADDITIONAL REACTION SCREENINGS

First, we investigated the rearrangement of several silyl enol ethers. In addition to the TBS and TES enol ethers (**44** and **43**), which were previously synthesized, we also prepared the TIPS enol ether **140** for screening. In a previous chapter (1.2.2), we described the rearrangement of TBS enol ether **44** to tetracycle **47**, which proceeded in 50% yield. In addition, TES enol ether **43** was transformed to desilylated tetracycle **48** directly in higher yield (57%). However, TIPS enol ether **140** was observed as a less efficient substrate for the rearrangement (Scheme 2.2.1).

Scheme 2.2.1. Rearrangements of Silyl Enol Ethers

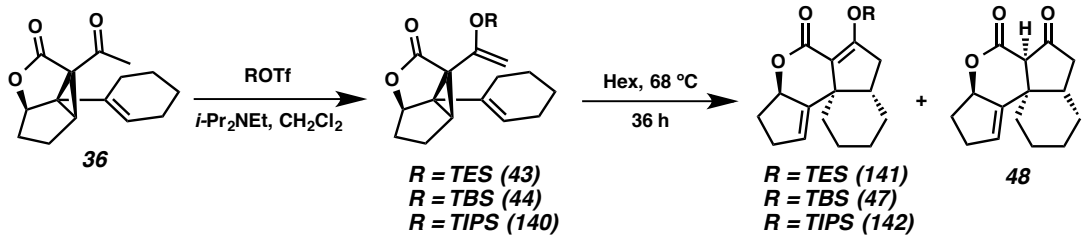

R	result
TES	**48** (57% yield)
TBS	**47** (50% yield)
TIPS	**142** (39% yield), **140** (20% recovered)

In contrast, vinyl lactone **51** did not undergo the rearrangement to afford tetracycle **143** (Scheme 2.2.2). Based on these results, we envisioned that the silyl enol ether moiety strongly affects or even participates in the transformation.

*Scheme 2.2.2. Rearrangement Attempt of Vinyl Lactone **51***

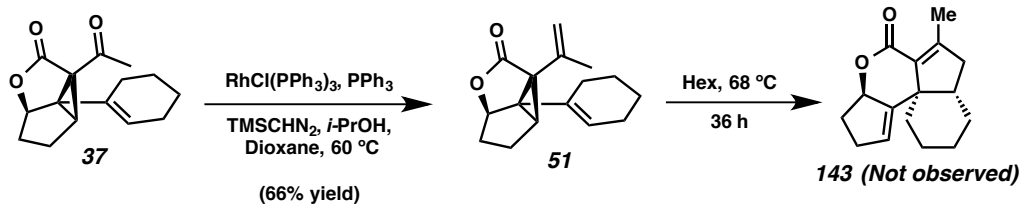

The rearrangement of TBS enol ether **44** was repeated in toluene-*d8* and monitored by ^{1}H NMR and ^{1}H-^{13}C HMBC (Scheme 2.2.3). The NMR data showed smooth conversion to the rearranged product **48**, and no discernible intermediates were observed.[2]

Scheme 2.2.3. NMR Study

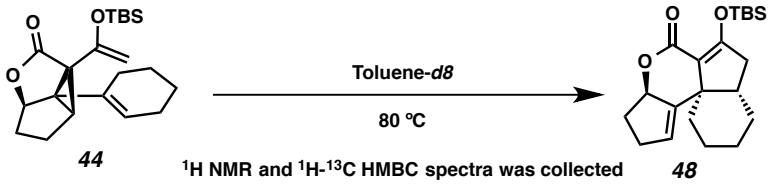

2.2.2 COMPUTATIONAL STUDIES

We undertook a computational study of the mechanism of the rearrangement using two approaches: standard transition state search algorithms as implemented in Gaussian 09, and automatic reaction path searches using artificial force induced reaction (AFIR) simulations.[3] In the latter method, possible reactive atoms are defined and reaction paths are explored automatically by applying an artificial force between pairs of reactive atoms. Details on this method are given in the Experimental section (2.5.3 and 2.5.4). Here we describe how both methods identified the same mechanism for the rearrangement to form **47**.

Density functional theory (DFT) calculations were performed in Gaussian 09. Geometries were optimized using B3LYP/6-31G(d) in the gas phase. Single-point energy calculations were performed with both B3LYP-D3 and M06-2X functional using the larger 6-311++G(2d,2p) basis set and the IEF-PCM solvation model for *n*-hexane. The M06-2X functional has been shown to give more accurate barriers and thermodynamics for pericyclic reactions.[4] However, UM06-2X has also been found to give unreliable (overestimated) energies for diradical processes,[5] so we emphasize UB3LYP-D3 energies for open-shell species.

Our hypothesis was that the desired Cope rearrangement of **44** occurs, but cycloheptadiene **50** is unstable due to the presence of two anti-Bredt (bridgehead) alkenes (Scheme 2.2.4). Further rearrangement occurs to alleviate strain, forming observed product **47** (along with desilylation to **48**). This rearrangement is formally a suprafacial 1,3-shift of the enol silane **50**, which is disallowed by Woodward-Hoffmann rules. We therefore expected that a stepwise rearrangement would be the favored pathway, through either diradical intermediates or a series of pericyclic reactions. Although zwitterionic intermediates could also be proposed, these should be disfavored in nonpolar solvents.

Scheme 2.2.4. Mechanistic hypothesis

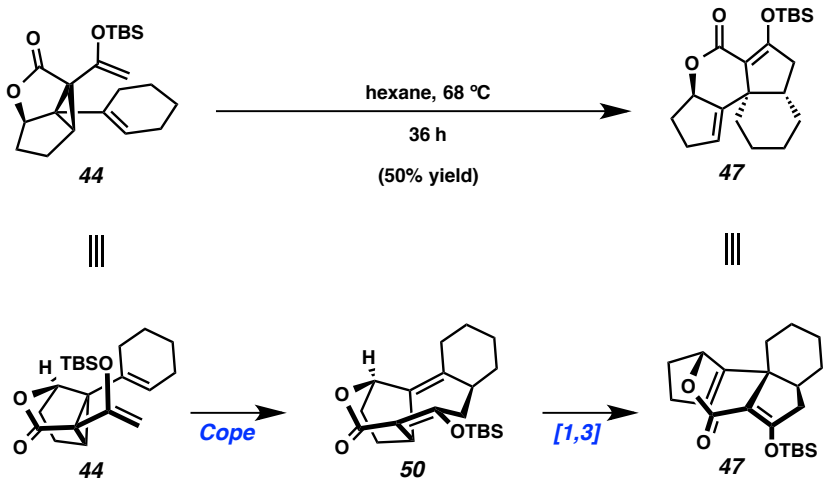

Our computational study began by examining the Cope rearrangement of model compound **144**, in which the TBS group is replaced by TMS (Figure 2.2.1). The free-energy barrier to form **145** is 25.9 kcal/mol, which is reasonable under the reaction conditions. The reaction is endergonic by 7 kcal/mol, despite the release of strain in the cyclopropane ring of **144**. A structural analysis of **145** shows the strain incurred by the two bridgehead alkenes leading. The alkenes are bent out of planarity, with C–C=C–C dihedral angles of 141 and 150 degrees, to accommodate the bicyclic system. The calculations predict that the Cope rearrangement can occur, but intermediate **145** is unstable and will either revert to **144** or undergo further rearrangement.

*Figure 2.2.1. Cope Rearrangement of Divinylcyclopropane **144***

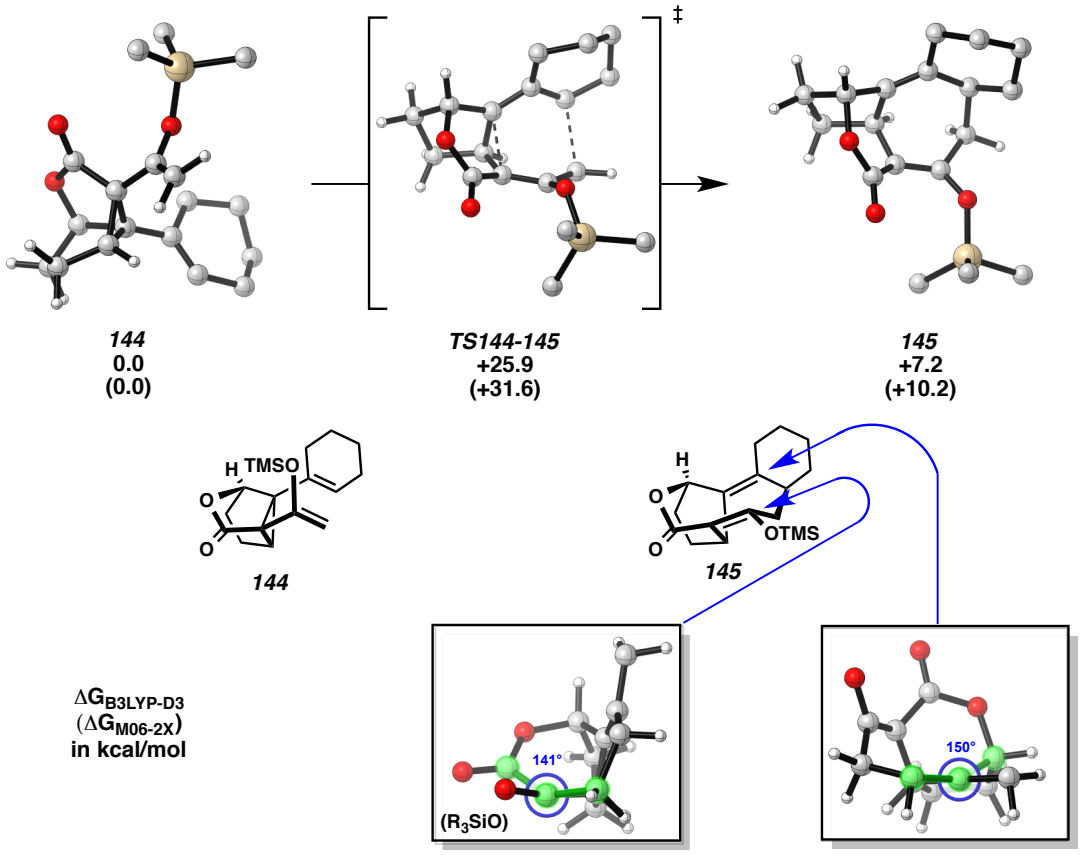

Experimentally, reduction of the ester in divinylcyclopropane **51** with DIBAL leads to spontaneous Cope rearrangement to cycloheptadiene **53**. Our calculations indicate that Cope rearrangement of diol **146** is exergonic by about 10 kcal/mol, with a free-energy barrier of 26 kcal/mol (Figure 2.2.2). The stability of cycloheptadiene **53** relative to **145** highlights the torsional strain incurred by the two anti-Bredt alkenes in **145**. Overall, these calculations are consistent with the hypothesis that bridging ester must be removed in order to forge the tricyclic core via a divinylcyclopropane rearrangement.

Figure 2.2.2. Computed Structures for Cope Rearrangement of ***146***

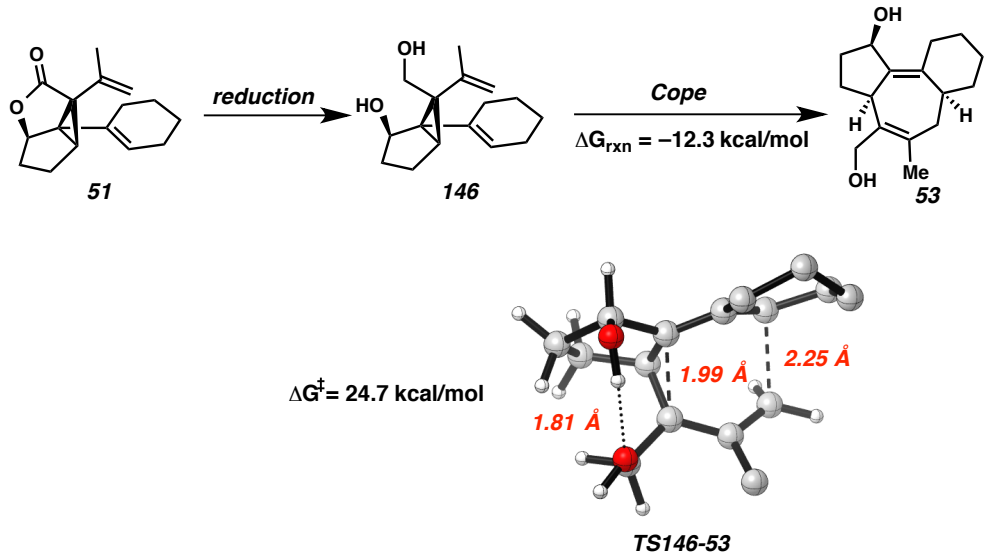

We next considered the possibility of a formal [1,3]-shift of the enol silane in **145** to form **149**, including three limiting cases of concerted, dissociative, and associative processes (Scheme 2.2.5). We could not locate a transition state for the concerted process, which would violate Woodward-Hoffmann rules. The dissociative process involves C–C bond homolysis to generate the allylic/vinylic diradical **147**, while the associative process involves first C–C bond-formation to give the cyclobutylcarbinyl diradical **148**. Neither diradical could be located as a minimum using unrestricted DFT calculations.

Scheme 2.2.5. Possible Mechanisms for Formal 1,3-Shift.

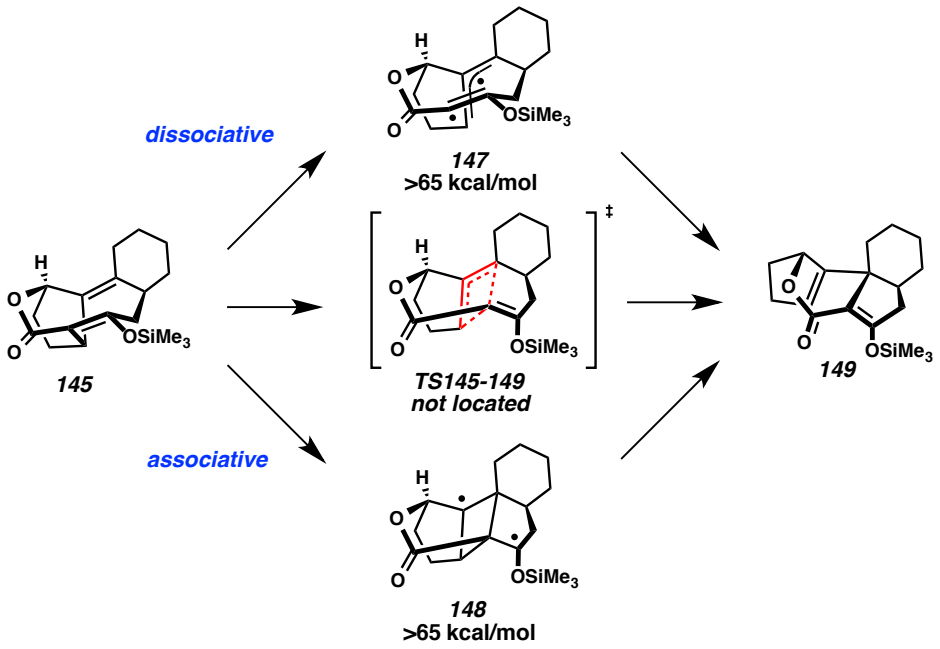

To conclusively rule out diradical processes, we calculated the potential energy for surface breaking of C–C bond **a** and formation of C–C bond **b** (Figure 2.2.3). This analysis shows that a 70 kcal/mol barrier separates intermediate **145** from product **149**. Associative and dissociative processes are also ruled out from this analysis, as the diradical intermediates **147** and **148** both appear on the potential energy surface at about 70 kcal/mol.

*Figure 2.2.3. Potential Energy Surface Connecting Intermediates **145** and **149** Calculated with UB3LYP/6-31G(d)*

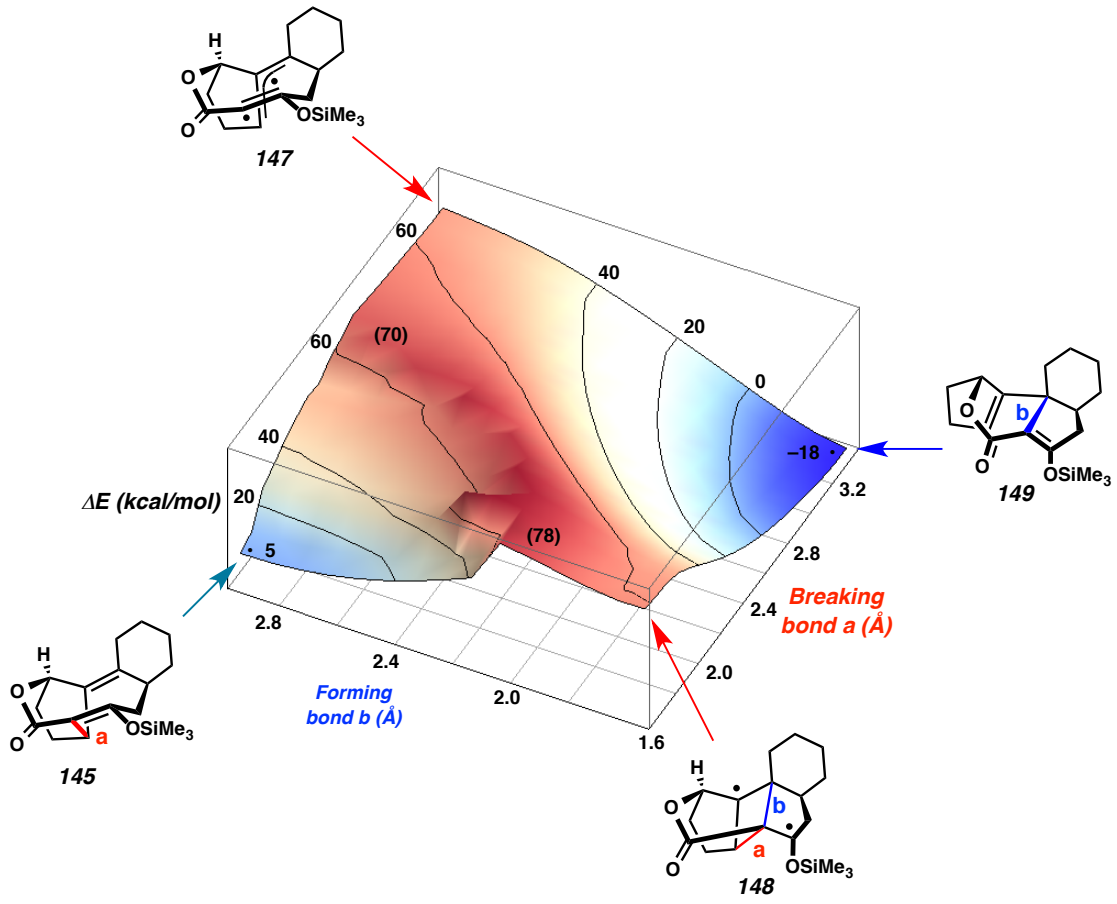

2.2.3 IRELAND–CLAISEN/RETRO-CLAISEN SEQUENCE

While the silyl protecting group remains intact in the observed product **149**, we considered the possibility that it participates in the rearrangement. The 1,5-migration of silyl groups in protected 1,3-dicarbonyls has been reported to be rapid. Our calculations indicate that 1,5-silyl migration in **145** occurs in a concerted manner via distorted square pyramidal transition state **TS145-150** (Figure 2.2.4). The formation of silyl ketene acetal

150 is endergonic with a barrier of 25.7 kcal/mol, making it competitive with the Cope rearrangement.

*Figure 2.2.4. 1,5-Silyl Shift of **145***

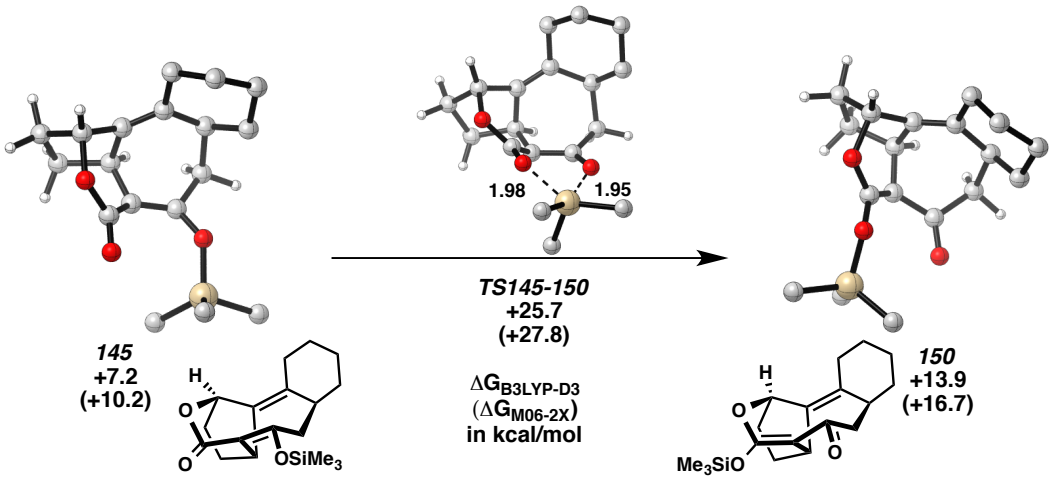

Silyl ketene acetal **150** is poised to undergo an Ireland-Claisen rearrangement to form the required C–C bond (b) in observed product **149**. The Claisen rearrangement occurs with a relatively low barrier of 21.7 kcal/mol (UB3LYP) to form the alkylidene cyclobutane **151** (Figure 2.2.5). Although the process is concerted, the transition state **TS150-151** has significant diradical character and is characterized by a long breaking C–O bond. We have computed the barrier for this process with several density functionals, including UM06 (24.7 kcal/mol) and UM06-2X (34.2 kcal/mol). We believe the latter functional significantly overestimates the energy of this open-shell transition state.

*Figure 2.2.5. Formation and Ring-Opening of Alkylidene Cyclobutane **151***

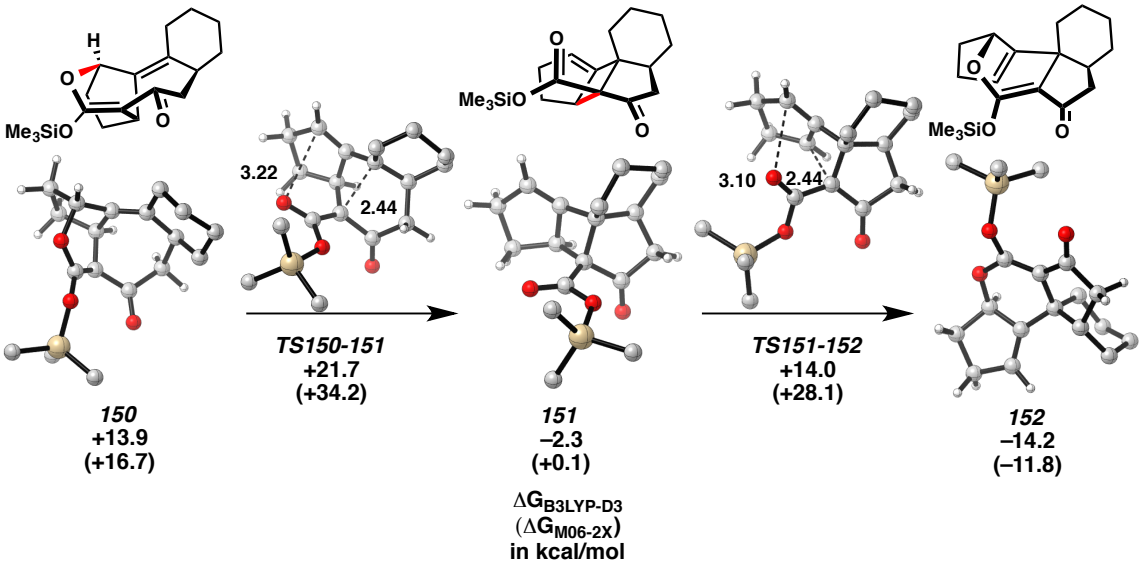

While alkylidene cyclobutane **151** is a relatively stable intermediate, it undergoes an unusually facile retro-Claisen rearrangement via **TS151-152** (14.0 kcal/mol). The formation of **152** is exergonic due to release of the significant strain associated with fused bicyclo[3.2.0]heptene system in **151**. Importantly, the Claisen/retro-Claisen sequence **150**→**152** represents a formal suprafacial 1,3-shift of the enol silane. A second 1,5 migration of the silyl group affords the observed product **149**. The free energy profile for the overall rearrangement of divinylcyclopropane **144** to give **149** is shown in Figure 2.2.6. The initial Cope rearrangement and 1,5-silyl migration have similar barriers of about 26 kcal/mol, while the Claisen/retro-Claisen steps are predicted to be rapid.

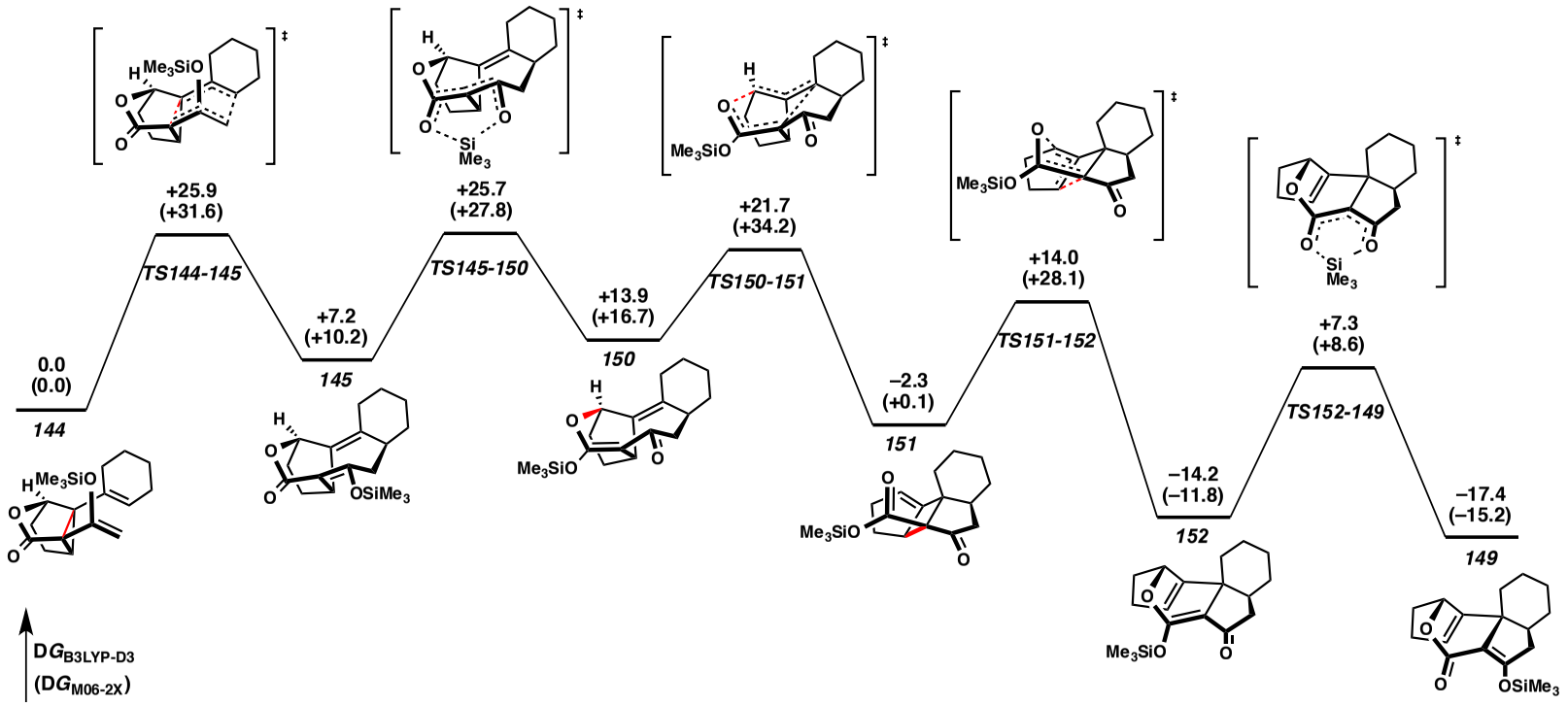

Figure 2.2.6. Free-energy Profile for Formation of **149** by a Silyl-Shift/Claisen Rearrangement

The alkylidene cyclobutane **151** represents a key intermediate in the Claisen/retro-Claisen squence predicted by our DFT studies, and we have studied the stability of this intermediate in detail. As shown in Figure 2.2.7, the trisubstituted alkene in **151** (the experimental system) is distorted from planarity with a C–C=C–C dihedral angle of 146 degrees. Several derivatives are shown in Figure 2.2.7 along with their energy with respect to the corresponding cyclopropanes. While removal of the fused cyclohexane portion makes a small impact (**153**), the intermediate is much more stable when the two methylenes of the cyclopentene ring are removed (**154** and **155**). This modification removes the strain associated with the alkene, allowing C–C=C–C dihedral angles near 180 degrees.

Figure 2.2.7. Stability of Alkylidene Cyclybutanes ***151-155*** *Respect to the Corresoponding Cyclopropanes*

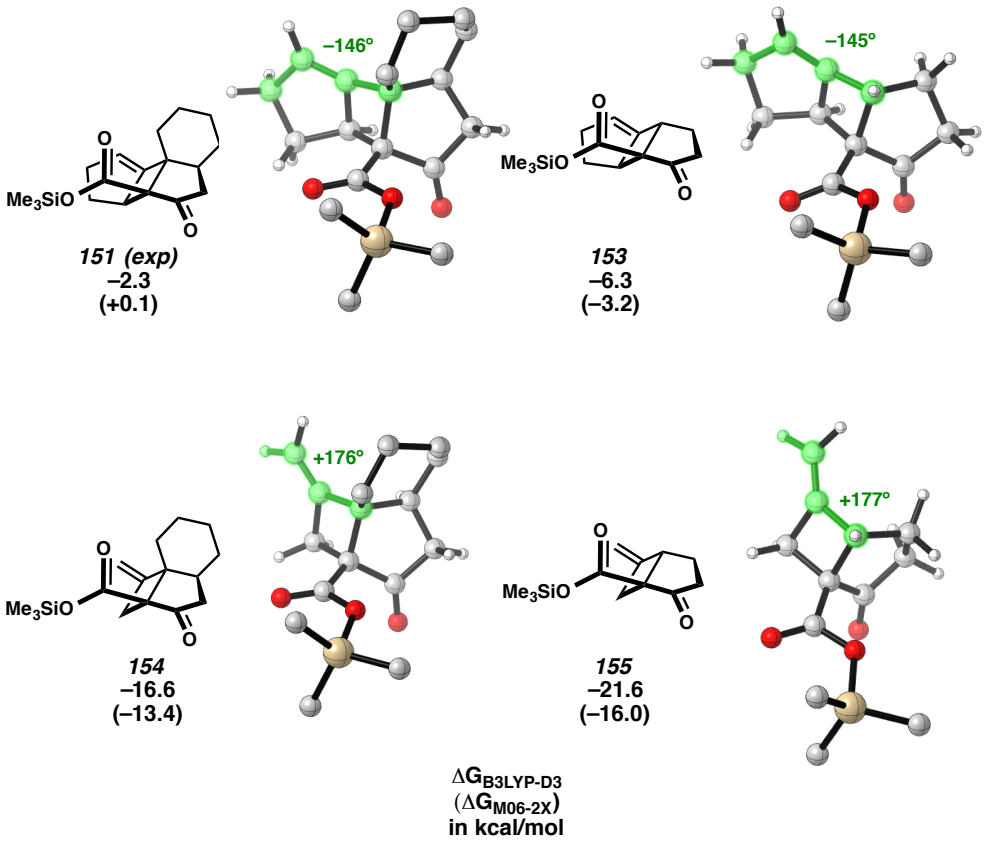

We have studied the formation and reaction of the most stable derivative, **155**, in greater detail (Figure 2.2.8). The formation of **155** from divinylcyclopropane **156** is predicted to be exergonic and irreversible. This is attributed to release of the strain associated with anti-Bredt alkenes in **157** and **158** to form the relatively unstrained alkene in **155**. Importantly, **155** is predicted to be unreactive toward retro-Claisen rearrangement (**TS155-159**), with a barrier of over 40 kcal/mol. Therefore, Cope rearrangement of **156**, or other derivatives lacking the fused cyclopentane, is predicted to give **155** as an observable product. In fact, as a result of our investigations, we uncovered a report of this precise rearrangement by Davies from 1997 (Scheme 2.2.6).[6]

Though the mechanism and the stereochemistry of the rearrangement was not known at the time, it was proposed to involve a Cope rearrangement to the desired but unobserved [4.3.1]-bicycle **162**, followed by further rearrangement.

Scheme 2.2.6. Rearrangement Reported by Davies and Co-Workers

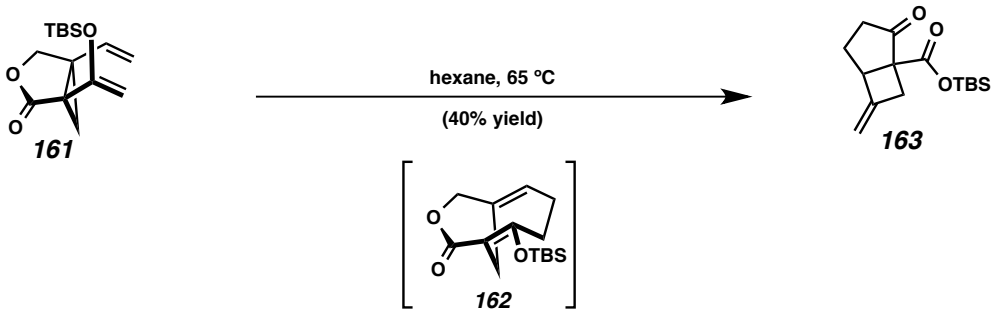

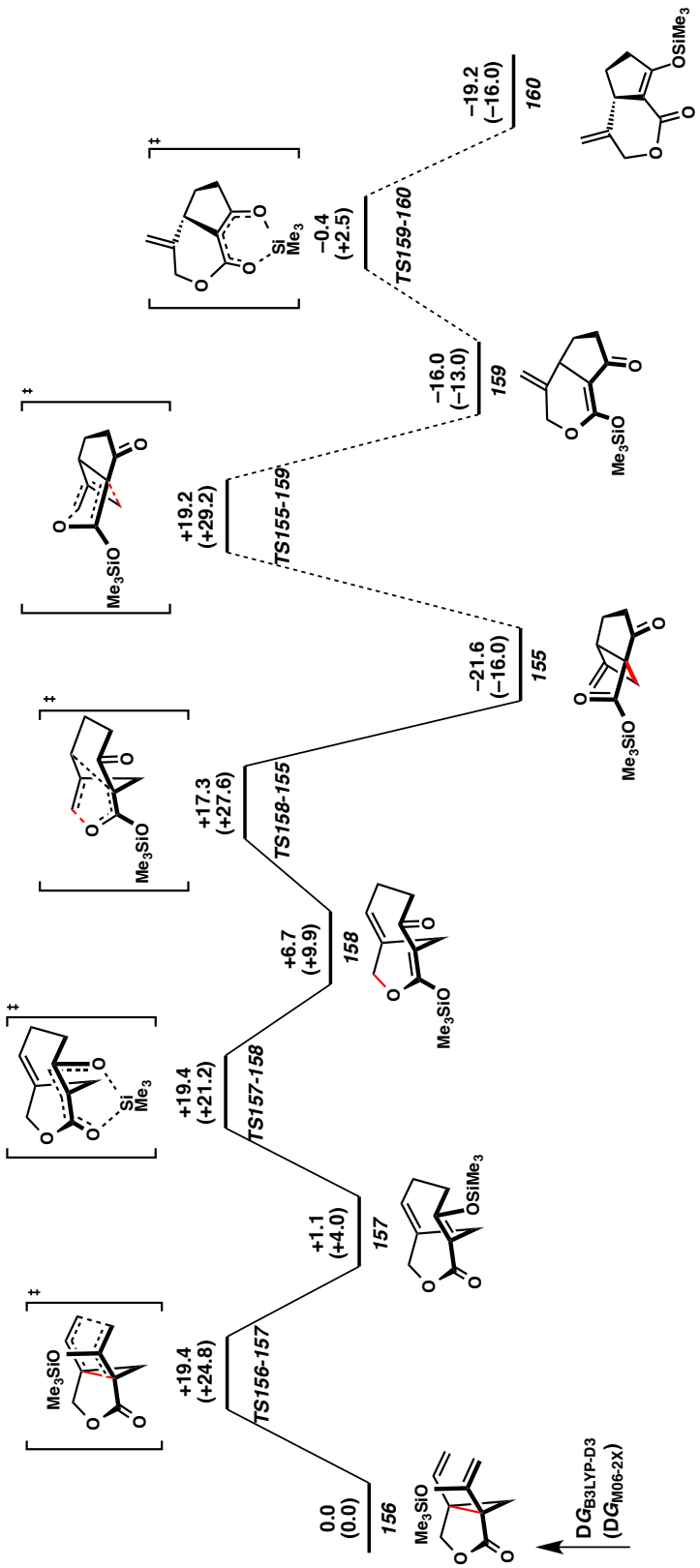

Figure 2.2.8. Free-Energy Surface for Formation of Alkylidene Cyclobutane **155** Predicted to be stable

2.3 FUTURE STUDIES RELATED TO THE REACTION CASCADE

Based on the computational studies above, the fused cyclobutane without the strained exomethylene is predicted to be highly unreactive toward retro-Claisen rearrangement. Therefore rearrangement cascade of **161** or other derivatives without a fused carbocycle is expected to give a fused cyclobutane as the isolated product. This reaction cascade could be expanded as a general methodology to assemble a fused 5-4 membered ring moiety.

The stereogenic center including the carbons at the ring junction of the product would be determined by the transition state of the Cope rearrangement. Among four possible transition states, the exo/endo chair-like and exo/endo boat-like transition states afford the *trans* enol ether olefin (**166c** and **166d**) as the Cope rearrangement products. The 1,5-silyl migration is expected to be a concerted process; consequently, this transformation is forbidden for those two compounds. In addition, an endo/exo chair-like transition state (**167b–168b**) would result in a *trans* fused cyclobutane **168b** with a sp^2 carbon center, which is unlikely to exist due to its highly strained linkage. Therefore, the only possible reaction cascade for cyclopropane **164** is expected to afford fused cyclobutane **168a** as a single diastereomer through an endo/endo-boat like transition state, with formation of the stereogenic centers controlled by the stereochemistry of cyclopropane **164** (Scheme 2.3.1).

Scheme 2.3.1. Proposed Cascade of Divinylcyclopropane ***164***

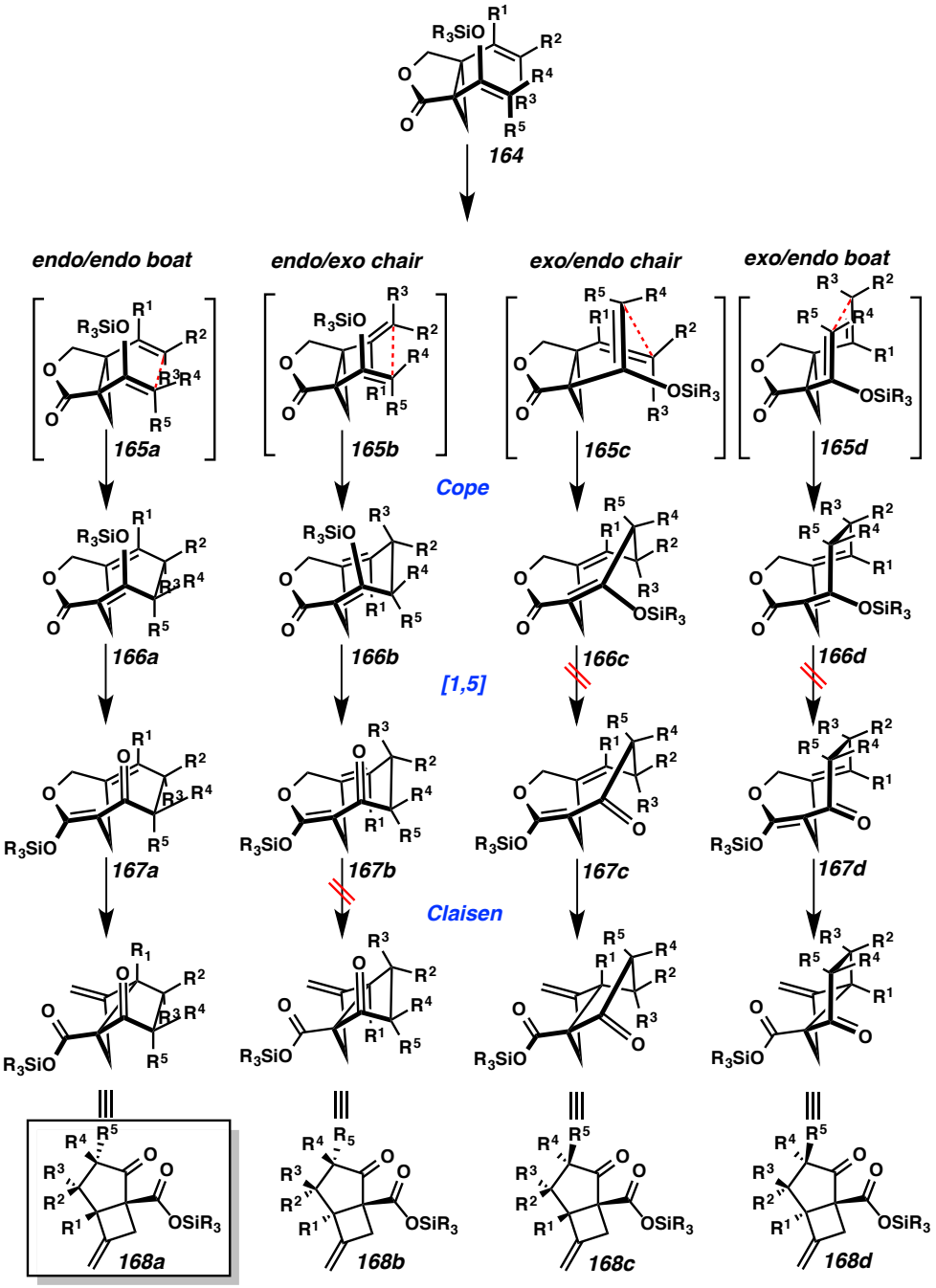

We expect this reaction cascade can be implemented with R^1 and R^2 alkyl substituents, based on the previous case with cyclohexene ring as R^1 and R^2 for the rearrangement (Scheme 2.1.1b). In order to expand the substrate scope, divinylcyclopropanes with various substituted olefins must be tested. This reaction cascade can be applied to the preparation of a highly functionalized fused cyclopentane combined with post modification of the cyclobutane moiety for the total synthesis of complex natural products. For example, following oxidative cleavage of the exomethylene, decarbonylation conditions[7] would afford cyclopropane **172**, and Baeyer–Villiger oxidation[8] would provide lactone **173** from cyclobutanone **169**. In addition, various methods[9] are known for the preparation of [3.3.0] bicyclic compounds such as **174** and **175**, and several ring expansion methods to afford medium-sized rings[10] such as **171** and **177** can be applied (Scheme 2.3.2).

Scheme 2.3.2. Modification of ***168***

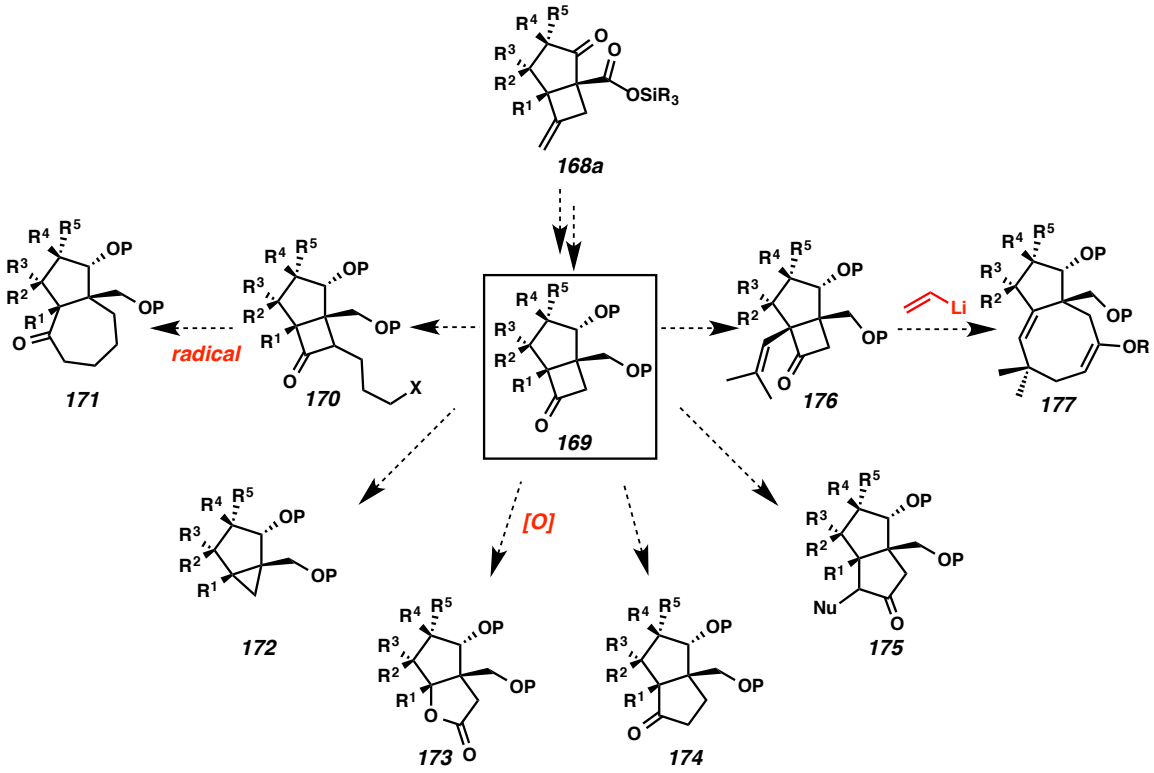

2.4 CONCLUSION

In summary, a unique reaction cascade of divinylcyclopropanes containing silyloxy groups was elucidated. Surprisingly, the cascade was found to include a cycloheptadiene intermediate with two anti-Bredt olefins via a [3,3]-Cope. The intermediate was converted to the fused cyclobutane intermediate via a [1,5]-silyl migration followed by an Ireland–Claisen rearrangement. Finally, the tetracyclic compound was formed via a retro Claisen rearrangement of the cyclobutane intermediate and subsequent [1,5]-silyl migration. Based on the mechanism and free-energy analysis, divinylcyclopropanes with a small-sized ring would result in unstable strained cyclobutane intermediates which should undergo retro-Claisen and [1,5]-silyl migration sequence to afford tetracycles. In

contrast, the rearrangement cascade of divinylcyclopropanes without fused carbocycles is expected to give a fused cyclobutane as an isolated product. Additional studies are required to expand the applications of the reaction cascade.

2.5 EXPERIMENTAL SECTION

2.5.1 MATERIALS AND METHODS

Unless stated otherwise, reactions were performed under an argon or nitrogen atmosphere using dry, deoxygenated solvents (distilled or passed over a column of activated alumina).[11] *i*-Pr_2NEt was distilled from calcium hydride immediately prior to use. Commercially obtained reagents were used as received unless otherwise stated. Reaction temperatures were controlled by an IKAmag temperature modulator. Microwave reactions were performed with a Biotage Initiator Eight 400 W apparatus at 2.45 GHz. Thin-layer chromatography (TLC) was performed using E. Merck silica gel 60 F254 precoated plates (0.25 mm) and visualized by UV fluorescence quenching, or potassium permanganate, iodine, or anisaldehyde staining. Silia*Flash* P60 Academic Silica gel (particle size 0.040-0.063 mm) was used for flash chromatography. ^{1}H and ^{13}C NMR spectra were recorded on a Varian Inova 600 (600 MHz and 151 MHz respectively), Varian Inova 500 (at 500 MHz and 126 MHz respectively), Bruker AV III HD spectrometer equipped with a Prodigy liquid nigrogen temperature cryoprobe (400 MHz and 101 MHz, respectively) and are reported relative to $CHCl_3$ (δ 7.26 & 77.16 respectively), C_6H_6 (δ 7.16 & 128.06 respectively), and toluene (δ 7.98 & 137.48 respectively). Data for ^{1}H NMR spectra are reported as follows: chemical shift (δ ppm) (multiplicity, coupling constant (Hz), integration). IR spectra were recorded on a Perkin Elmer Paragon 1000 Spectrometer and are reported in frequency of absorption (cm^{-1}). HRMS were acquired from the Caltech Mass Spectral Facility using a JEOL JMS-600H

High Resolution Mass Spectrometer in fast atom bombardment (FAB+) or electron ionization (EI+) mode or using an Agilent 6200 Series TOF with an Agilent G1978A Multimode source in electrospray ionization (ESI), atmospheric pressure chemical ionization (APCI) or mixed (MM) ionization mode.

2.5.2 PREPARATIVE PROCEDURES

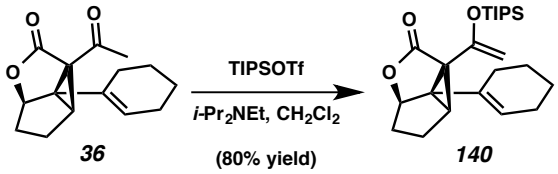

TIPS enol ether 140: To a flame-dried round-bottom flask equipped with a magnetic stir bar were added cyclopropane **36** (23 mg, 0.0934 mmol), DCM (2 mL), and *i*-Pr_2NEt (0.05 mL, 0.287 mmol). The flask was cooled to 0 ºC and stirred for 10 min. TBSOTf (0.04 mL, 0.148 mmol) was added dropwise. The reaction mixture was stirred for 30 min at 0 ºC. The reaction mixture was filtered through a silica gel plug (henxanes:EtOAc 10:1) was then concentrated under reduced pressure to afford TIPS enol ether **140** (30 mg, 0.0745 mmol, 80% yield) as colorless oil. R_f = 0.50 (6:1 hexanes:EtOAc); ^{1}H NMR (500 MHz, C_6D_6) δ 5.45–5.37 (m, 1H), 4.52–4.46 (m, 1H), 4.41 (d, *J* = 1.7 Hz, 1H), 4.37 (d, *J* = 1.7 Hz, 1H), 2.28 (dt, *J* = 6.5, 1.2 Hz, 1H), 2.17–2.08 (m, 1H), 2.01–1.84 (m, 3H), 1.74–1.61 (m, 2H), 1.61–1.43 (m, 4H), 1.40–1.10 (m, 21H); ^{13}C NMR (126 MHz, C_6D_6) δ 172.7, 151.7, 131.0, 125.8, 93.9, 84.1, 58.9, 49.3, 39.0, 33.6, 27.6, 25.5, 23.5, 23.0, 22.4, 18.5, 18.4, 13.0; IR (Neat Film, NaCl) 3521, 3121, 2929, 2866, 2717, 2233, 2077, 1770, 1626, 1463, 1383, 1362, 1335, 1302, 1290, 1258, 1197, 1161, 1138, 1075, 1043, 1003, 920, 907, 883, 821, 769, 740, 709 cm^{-1}; HRMS (FAB+) *m/z* calc'd for $C_{24}H_{39}SIO_3$ $[M+H]^+$: 403.2669, found 403.2688.

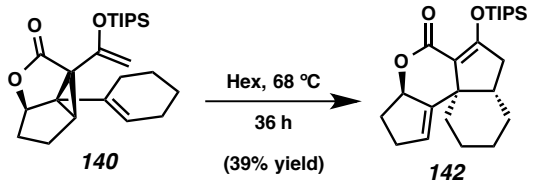

140 *142*

Tetracycle 142: To a flame-dried two neck round-bottom flask equipped with a magnetic stir bar and a reflux condenser was added TIPS enol ether **140** (28 mg, 0.0695 mmol) and hexane (8 mL). The reaction was heated to reflux in a 68 ºC oil bath. After 36 h of stirring, the reaction mixture was cooled to 23 ºC and stirred for 15 min. The mixture was concentrated and purified by flash column chromatography (15:1 hexanes, EtOAc) to afford tetracycle **142** (10.9 mg, 0.0271 mmol, 39% yield) as a colorless oil; R_f = 0.45 (6:1 hexanes:EtOAc); ^{1}H NMR (400 MHz, C_6D_6) δ 5.25 (dt, *J* = 3.1, 1.8 Hz, 1H), 5.12–5.05 (m, 1H), 2.56 (dd, *J* = 16.1, 12.0 Hz, 1H), 2.28 (ddt, *J* = 11.9, 7.5, 3.6 Hz, 1H), 2.15–1.83 (m, 4H), 1.79–1.67 (m, 1H), 1.51–1.11 (m, 28H); ^{13}C NMR (101 MHz, C_6D_6) δ 166.8, 160.9, 144.4, 124.8, 112.8, 83.4, 45.3, 40.7, 38.1, 33.0, 32.2, 30.3, 25.5, 21.7, 21.5, 18.2, 13.6; IR (Neat Film, NaCl) 3416, 3051, 2928, 2864, 2719, 2243, 1768, 1712, 1605, 1463, 1450, 1430, 1382, 1363, 1342, 1328, 1304, 1279, 1240, 1223, 1193, 1172, 1155, 1132, 1112, 1096, 1063, 1048, 1000, 967, 926, 903, 882, 864, 835, 805, 781, 768 cm^{-1}; HRMS (EI+) *m/z* calc'd for $C_{24}H_{38}O_3Si$ $[M\bullet]^+$: 402.2590, found 402.2602. TIPS enol ether **140** (5.6 mg, 0.0139 mmol, 20% yield) was recovered.

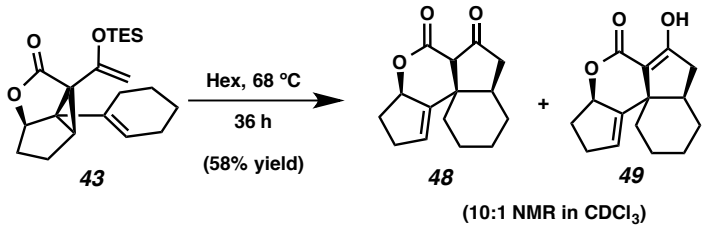

***β*-ketolactone 48**: To a flask equipped with reflux condenser were added TES enol ether **43** (70 mg, 0.194 mmol) and hexane (20 mL, 0.01 M). The reaction was then heated to 110 ºC and stirred for 36 h. The mixture was cooled down to ambient temperature, concentrated and purified by flash column chromatography (8:1 hexanes, EtOAc) to afford tetracycle **48** (28 mg, 0.114 mmol, 58% yield).

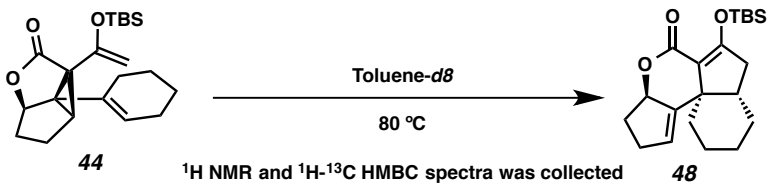

NMR Screening: To a NMR tube was added a solution of silyl enol ether **44** (39.1 mg, 0.108 mmol) in toluene-*d8* (0.5 mL). The NMR tube was inserted to Varian Inova 600 and the reaction temperature was set to 80 ºC. ^{1}H NMR and ^{1}H-^{13}C HMBC spectra was collected to monitor reaction.

2.5.3 COMPUTATIONAL METHODS

All quantum chemical calculations were performed with Gaussian 09.[12] Structural representations were generated with CYLview.[13]

Geometry optimization and frequency calculations were performed with the B3LYP[14] functional in the gas phase, using the 6-31G(d) basis set. The nature of stationary points were confirmed by frequency analysis. Thermal corrections were calculated from unscaled vibrational frequencies at the same level of theory for a standard state of 1 atm and 298.15 K. Entropies were corrected for the breakdown of the harmonic oscillator approximation at low frequencies by raising all harmonic frequencies below 100 cm^{-1} to 100 cm^{-1}.[15] Intrinsic Reaction Coordinate (IRC)[16] calculations were performed to confirm that transition states properly connected reactants and products. This was essential for the Claisen and retro-Claisen steps, for which both concerted and stepwise diradical transition states were located.

Electronic energies were obtained from single-point energy calculations performed with a larger 6-311++G(2d,2p) basis set and the IEF-PCM[17] solvation model for n-hexane. We tested the following density functionals for single-point energy calculations: B3LYP-D3(BJ) [including the Becke–Johnson damping function],[18] M06-2X,[19] M06L,[20] M11L,[21] and ωB97X-D.[22] We found B3LYP-D3 and M06-2X results to be representative, and these are included in the main text.

Unrestricted calculations (UB3LYP, UM06-2X, etc) were performed for diradical intermediates and transition states leading to diradicals. This involves HOMO-LUMO mixing in the initial guess leading to unrestricted wave functions using the keyword

`guess=(mix,always)`. Some diradical intermediates were initially located as triplets, followed by re-optimization as an unrestricted singlet.

2.5.4 AFIR SIMULATION METHODS

Systematic transition-state searches were performed using artificial force induced reaction (AFIR) simulations,[3a-c] and single-component AFIR for intramolecular paths starting from local minima (SC-AFIR).[3d,e] The computational procedure included AFIR search of reaction pathways, followed by optimization of the reaction pathways by applying the locally updated planes (LUP) method.[23] Once a TS structure was located and optimized, an intrinsic reaction coordinate simulation (IRC)[16] was performed to locate the corresponding local minima conformations of the reactant and product. AFIR and IRC simulations and the following full optimization of the structures were performed at the relatively low HF/3-21G level in gas phase by applying GRRM program[24] and Gaussian09.[12]

2.6 NOTES AND REFERENCES

(1) Cope A. C.; Hardy, E. M. *J. Am. Chem. Soc.* **1940**, *62*, 441–444.

(2) 1H NMR and 1H 13C HMBC spectra were taken sequentially. Check Appendix 6 Figures 6.7 – 6.20 for detail.

(3) (a) Maeda, S., Saito, R., Morokuma, K. *J. Chem. Phys.* **2010**, *24*, 241102/1–4. (b) Maeda, S., Morokuma, K. *J. Chem. Theo. Comp.* **2011**, *7*, 2335–2345. (c) Maeda, S., Ohno, K., Morokuma, K. *Phys. Chem. Chem. Phys.* **2013**, *15*, 3683–3701. (d) Maeda, S., Taketsugu, T., Morokuma, K. *J. Comp. Chem.* **2014**, *35*, 166–173. (e) Isegawa, M., Maeda, S., Tantillo, D. J., Morokuma, K. *Chem. Sci.* **2014**, *5*, 1555–1560.

(4) Pieniazek, S. N.; Clemente, F. R.; Houk, K. N. *Angew. Chem. Int. Ed.* **2008**, *47*, 7746–7749.

(5) James, N. C.; Um, J. M.; Padias, A. B.; Hall Jr., H. K.; Houk, K. N. *J. Org. Chem.* **2013**, *78*, 6582–6592.

(6) Davies, H. M. L.; Calvo, R.; Ahmed, G. *Tetrahedron Lett.* **1997**, *38*, 1737–1740. (b) Davies, H. M. L.; Calvo, R.; Townsend, R. J.; Ren, P.; Churchill, R. M. *J. Org. Chem.* **2000**, *65*, 4261–4268.

(7) Murakami, M.; Amii, H.; Shigeto, K.; Ito, Y. *J. Am. Chem. Soc.* **1996**, *118*, 8285–8290.

(8) (a) Herrmann, W. A.; Fischer, R. W.; Correia, J. D. G. *J. Mol. Catal.* **1994**, *94*, 213–223. (b) Phillips, A. M. F.; Romao, C. *Eur. J. Org. Chem.* **1999**, 1767–1770.

(9) (a) Reeder, L. M.; Hegedus, L. S. *J. Org. Chem.* **1999**, *64*, 3306–3311. (b) Wen, X.; Norling, H.; Hegedus, L. S. *J. Org. Chem.* **2000**, *65*, 2096–2103. (c) Greene, A. E.; Luche, M. J.; Serra, A. A. *J. Org. Chem.* **1985**, *50*, 3957–3962. (d) Trost, B. M.; Mikhail, G. K. *J. Am. Chem. Soc.* **1987**, *109,* 4124–4127.

(10) (a) Ziegler, F. E.; Kover, R. X.; Yee, N. N. K. *Tetrahedron Lett.* **2000**, *41,* 5155–5159. (b) MacDougall, J. M.; Santora, V. J.; Verma, S. K.; Turnbull, P.; Hernandez, C. R.; Moore, H. W. *J. Org. Chem.* **1998**, *63*, 6905–6913.

(11) Pangborn, A. B.; Giardello, M. A.; Grubbs, R. H.; Rosen, R. K.; Timmers, F. J. *Organometallics* **1996**, *15*, 1518–1520.

(12) Gaussian 09, Revision B.01, Frisch, M. J.; Trucks, G. W.; Schlegel, H. B.; Scuseria, G. E.; Robb, M. A.; Cheeseman, J. R.; Scalmani, G.; Barone, V.; Mennucci, B.; Petersson, G. A.; Nakatsuji, H.; Caricato, M.; Li, X.; Hratchian, H. P.; Izmaylov, A. F.; Bloino, J.; Zheng, G.; Sonnenberg, J. L.; Hada, M.; Ehara, M.; Toyota, K.; Fukuda, R.; Hasegawa, J.; Ishida, M.; Nakajima, T.; Honda, Y.; Kitao, O.; Nakai, H.; Vreven, T.; Montgomery, J. A.; Peralta, J. E.; Ogliaro, F.; Bearpark, M.; Heyd, J. J.; Brothers, E.; Kudin, K. N.; Staroverov, V. N.; Kobayashi, R.; Normand, J.; Raghavachari, K.; Rendell, A.; Burant, J. C.; Iyengar, S. S.; Tomasi, J.; Cossi, M.; Rega, N.; Millam, J. M.; Klene, M.; Knox, J. E.; Cross, J. B.; Bakken, V.; Adamo, C.; Jaramillo, J.; Gomperts, R.; Stratmann, R. E.; Yazyev, O.; Austin, A. J.; Cammi, R.; Pomelli, C.; Ochterski, J. W.; Martin, R. L.; Morokuma, K.; Zakrzewski, V. G.; Voth, G. A.; Salvador, P.; Dannenberg, J. J.; Dapprich, S.; Daniels, A. D.; Farkas; Foresman, J. B.; Ortiz, J. V.; Cioslowski, J.; Fox, D. J. Gaussian, Inc., Wallingford CT, **2010**.

(13) Legault, C. Y. CYLView, version 1.0b, Université de Sherbrooke, 2009.

(14) (a) Becke, A. D. *J. Chem. Phys.* **1993**, *98*, 5648. (b) Lee, C.; Yang, W.; Parr, R. G. *Phys. Rev. B* **1988**, *37*, 785.

(15) (a) Ribeiro, R. F.; Marenich, A. V.; Cramer, C. J.; Truhlar, D. G. *J. Phys. Chem. B* **2011**, *115*, 14556. (b) Zhao, Y.; Truhlar, D. G. *Phys. Chem. Chem. Phys.* **2008**, *10*, 2813.

(16) (a) Fukui, K. *Acc. Chem. Res.* **1981**, *14*, 363. (b) Hratchian, H. P.; Schlegel, H. B. *J. Chem. Theory Comput.* **2005**, *1*, 61.

(17) Cances, E.; Mennucci, B.; Tomasi, J. *J. Chem. Phys.* **1997**, *107*, 3032.

(18) Grimme, S.; Ehrlich S.; Goerigk, L. *J. Comput. Chem.* **2011**, *32*, 1456.

(19) Zhao, Y.; Truhlar, D. *Theor. Chem. Acc.* **2008**, *120*, 215.

(20) Zhao, Y.; Truhlar, D. G. *J. Chem. Phys.* **2006**, *125*, 194101.

(21) Peverati, R.; Truhlar, D. G. *J. Phys. Chem. Lett.* **2011**, *3*, 117.

(22) Chai, J.-D.; Head-Gordon, M. *Phys. Chem. Chem. Phys.* **2008**, *10*, 6615.

(23) (a) Ulitsky, A.; Elber, R. *J. Chem. Phys.* **1990**, *92*, 1510. (b) Choi, C.; Elber, R. *J. Chem. Phys.* **1991**, *94*, 751.

(24) Maeda, S.; Osada, Y.; Morokuma, K.; Ohno, K. GRRM, a developmental version at Kyoto University.

APPENDIX 6

Spectra Relevant to Chapter 2:

Mechanistic Elucidation of the Unexpected Rearrangement

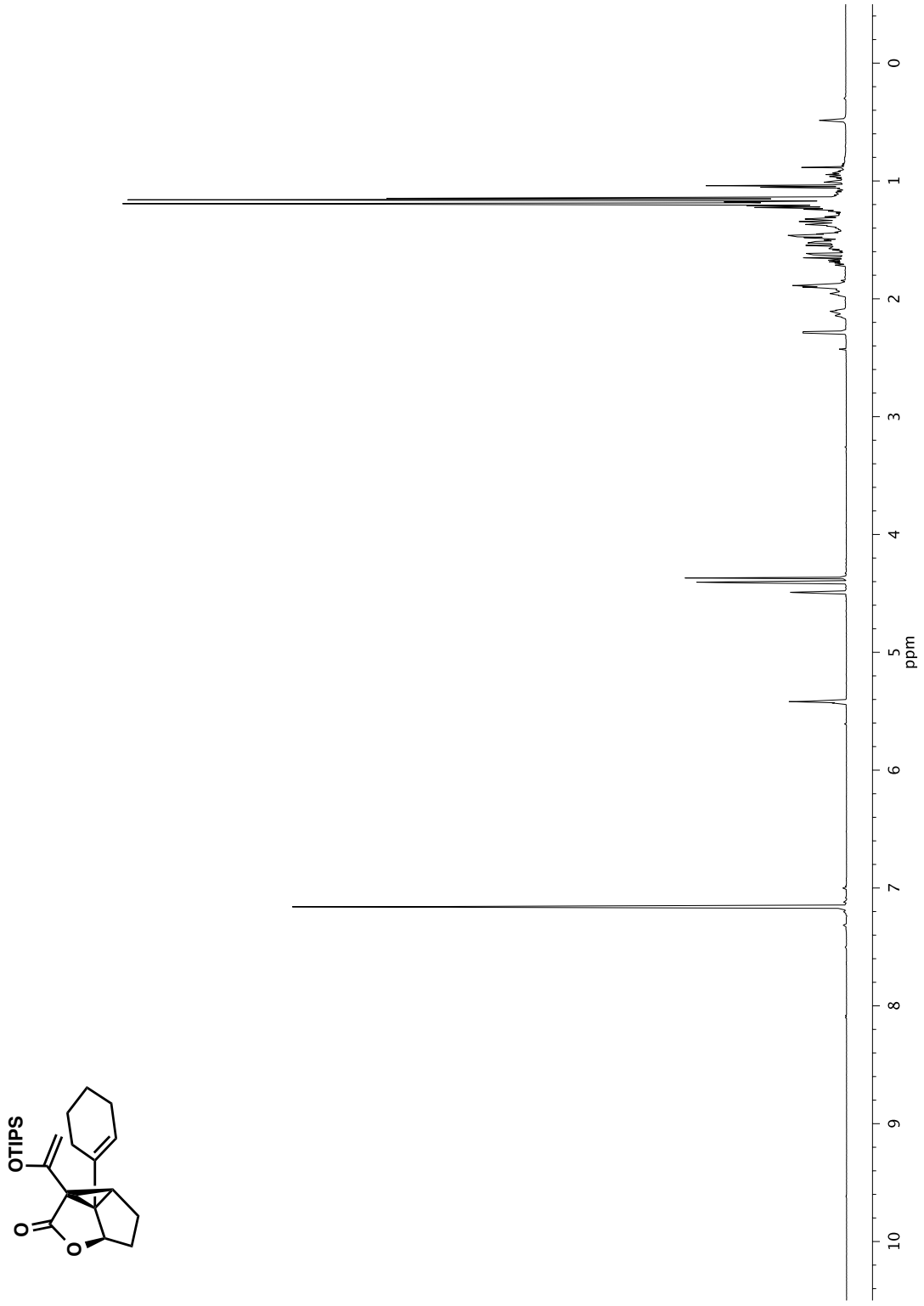

Figure A6.1 ^{1}H NMR (500 MHz, C_6D_6) of compound **140**

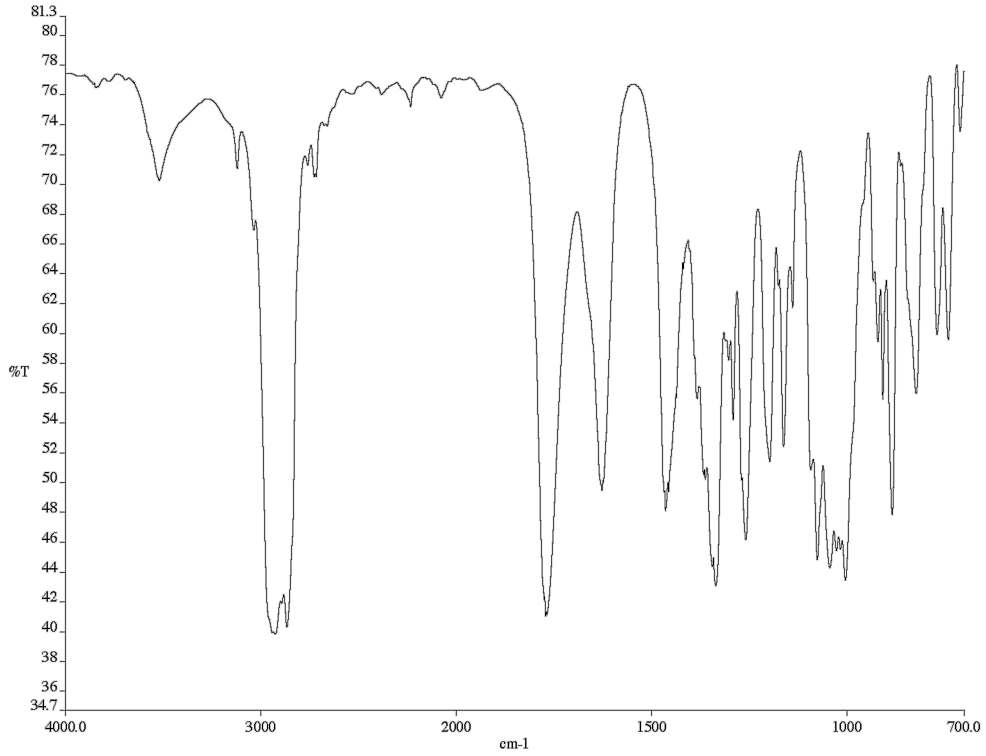

Figure A6.2 Infrared spectrum (thin film/NaCl) of compound **140**

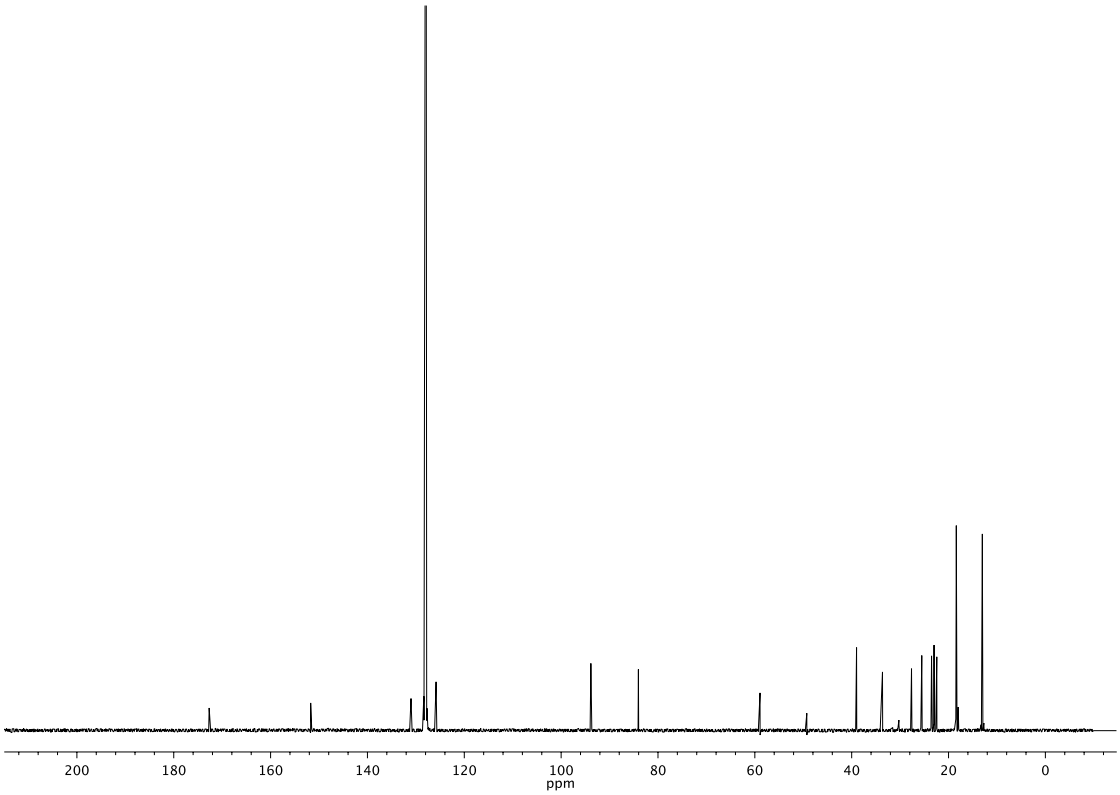

Figure A6.3 ^{13}C NMR (126 MHz, C_6D_6) of compound **140**

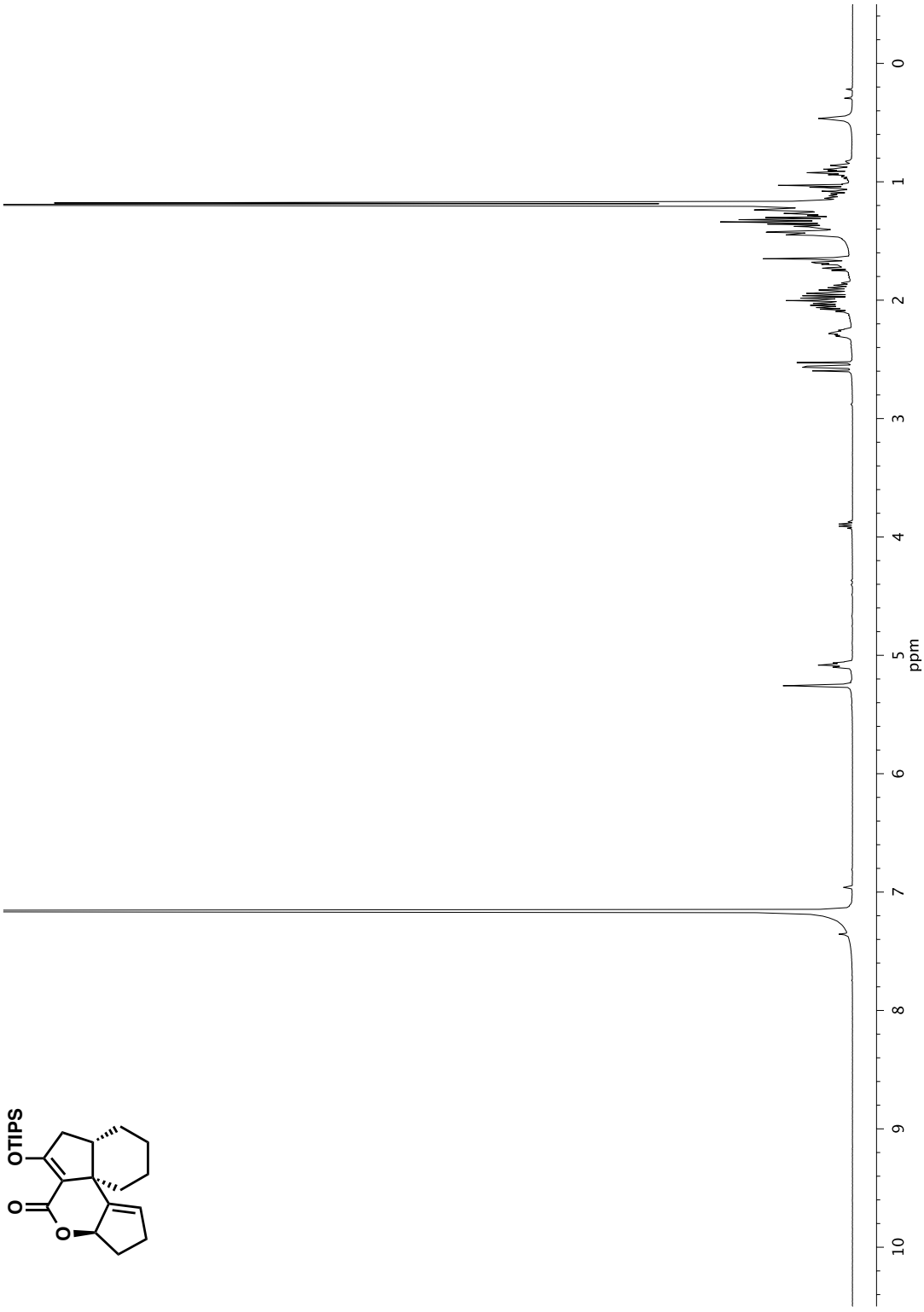

Figure A6.4 ^{1}H NMR (400 MHz, C_6D_6) of compound **142**

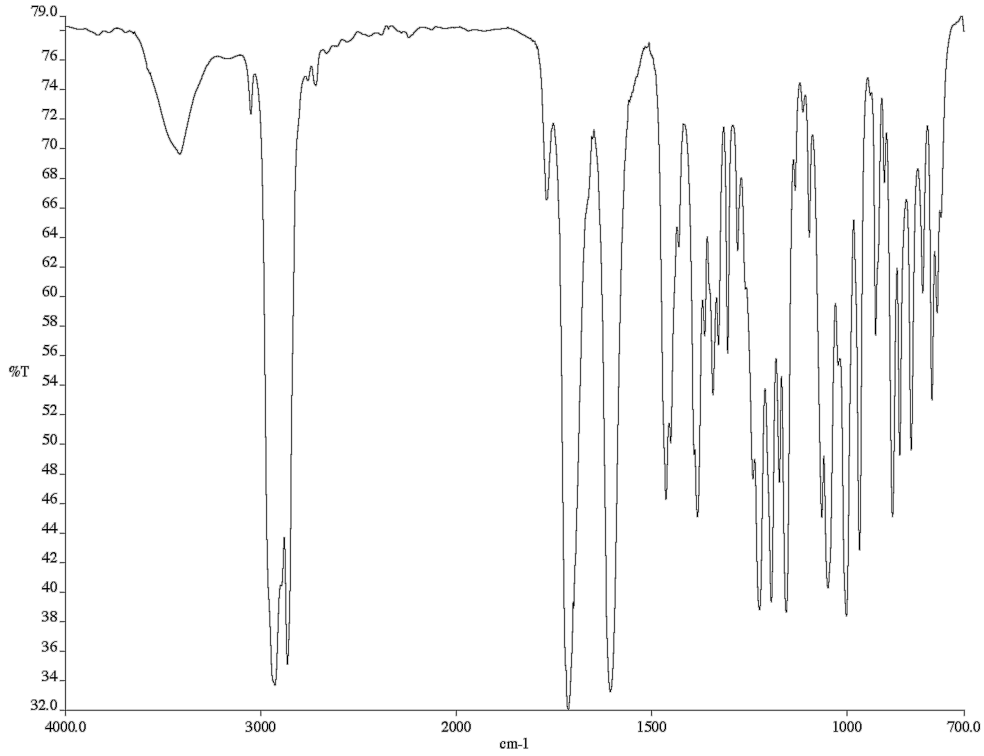

Figure A6.5 Infrared spectrum (thin film/NaCl) of compound **142**

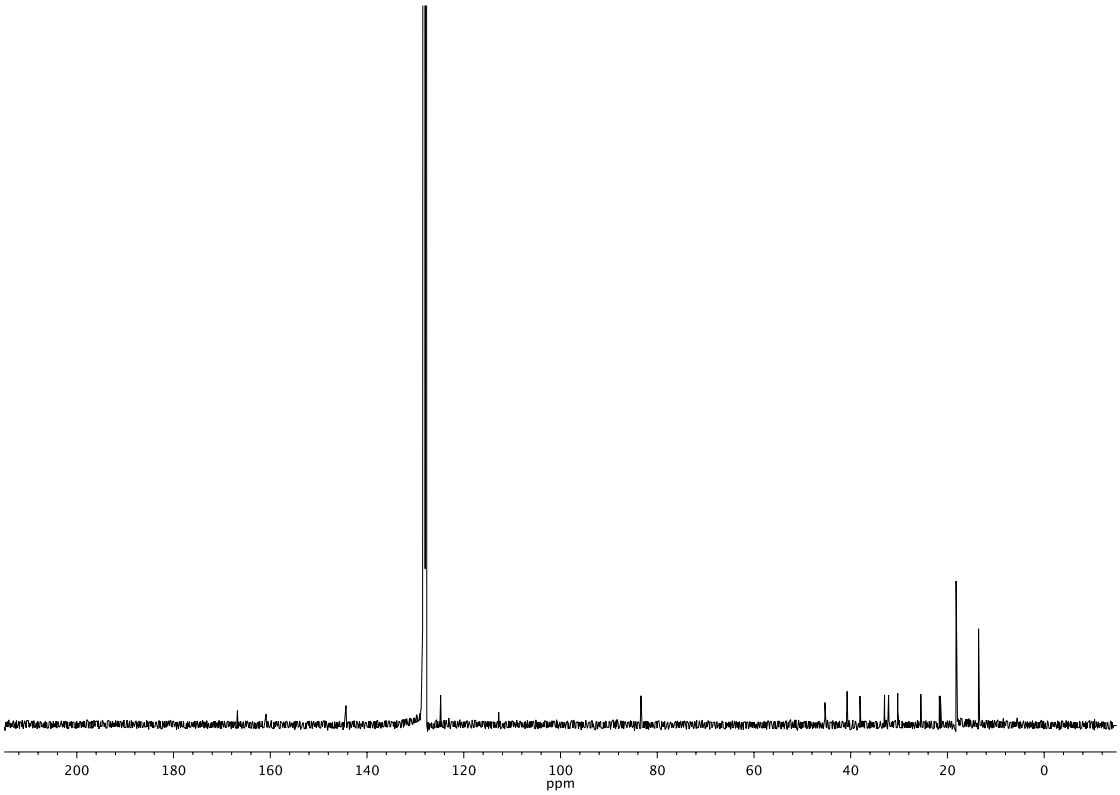

Figure A6.6 ^{13}C NMR (101 MHz, C_6D_6) of compound **142**

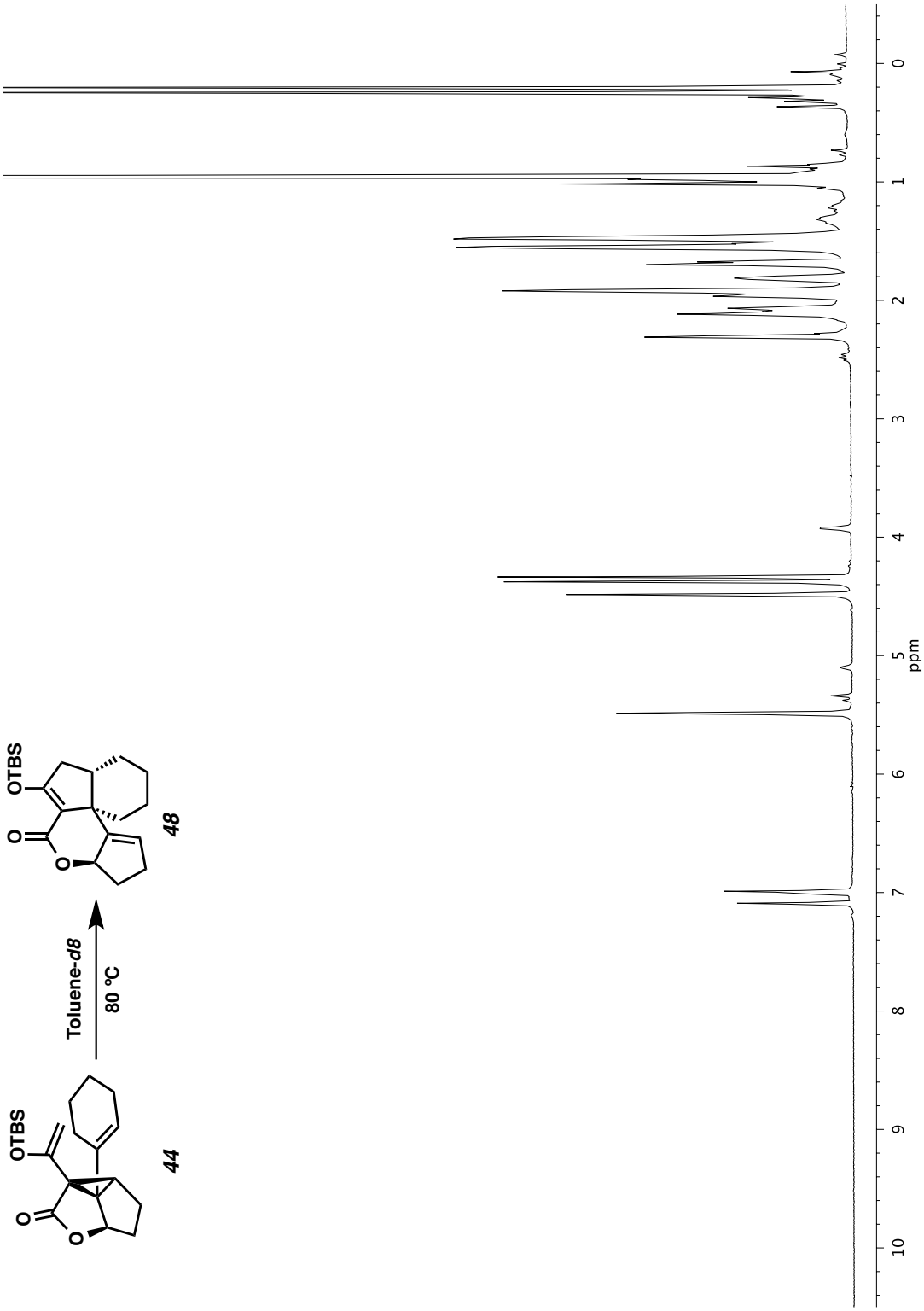

Figure A6.7 ^{1}H NMR (600 MHz, Toluene-*d8* at 80 °C, reaction time: 5 min) of compound **44** to **48**

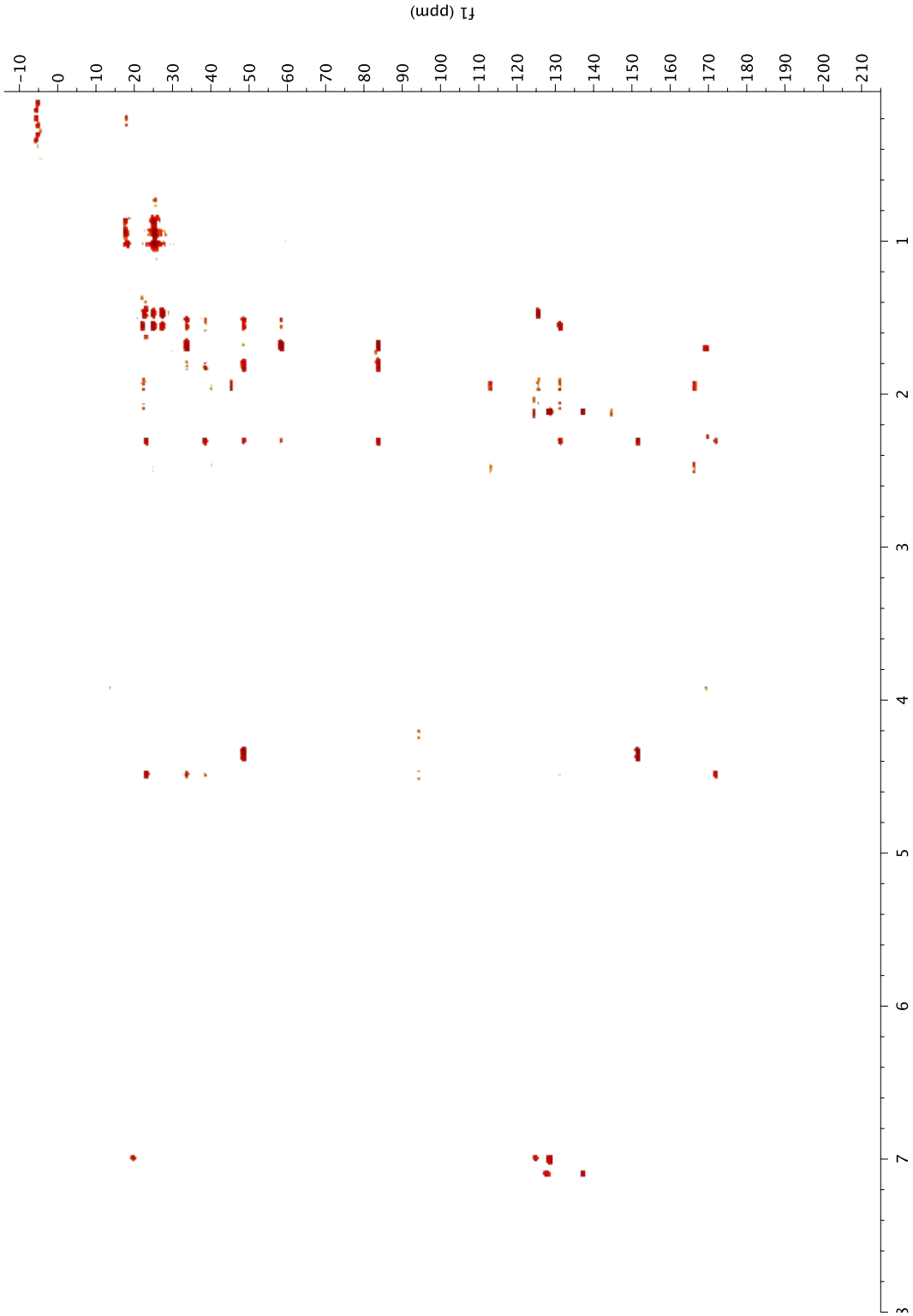

Figure A6.8 ^{1}H-^{13}C HMBC (600 MHz, Toluene-*d8* at 80 °C, reaction time: 10 min – 44 min) of compound **44** to **48**

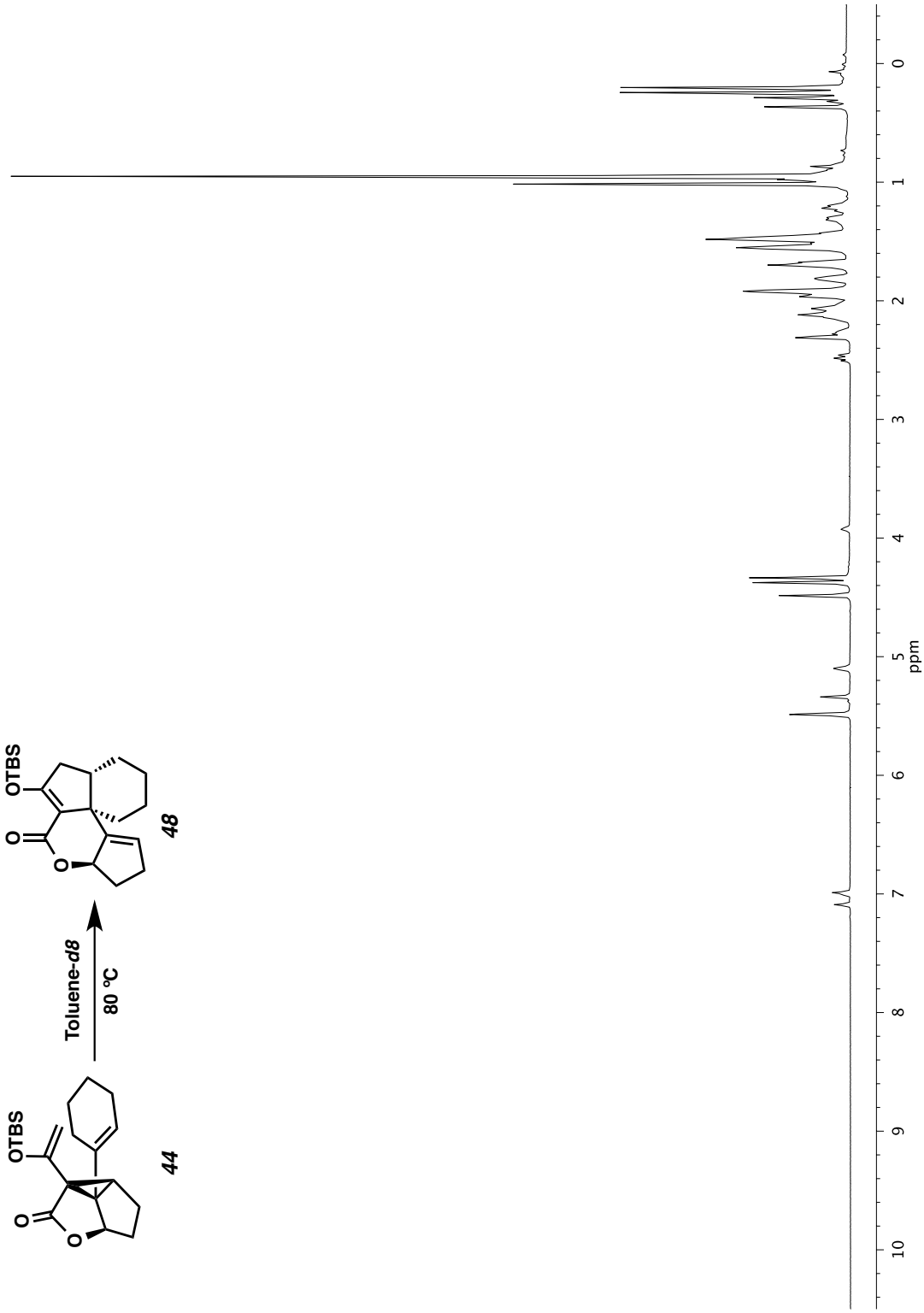

Figure A6.9 ^{1}H NMR (600 MHz, Toluene-*d8* at 80 °C, reaction time: 44 min) of compound **44** to **48**

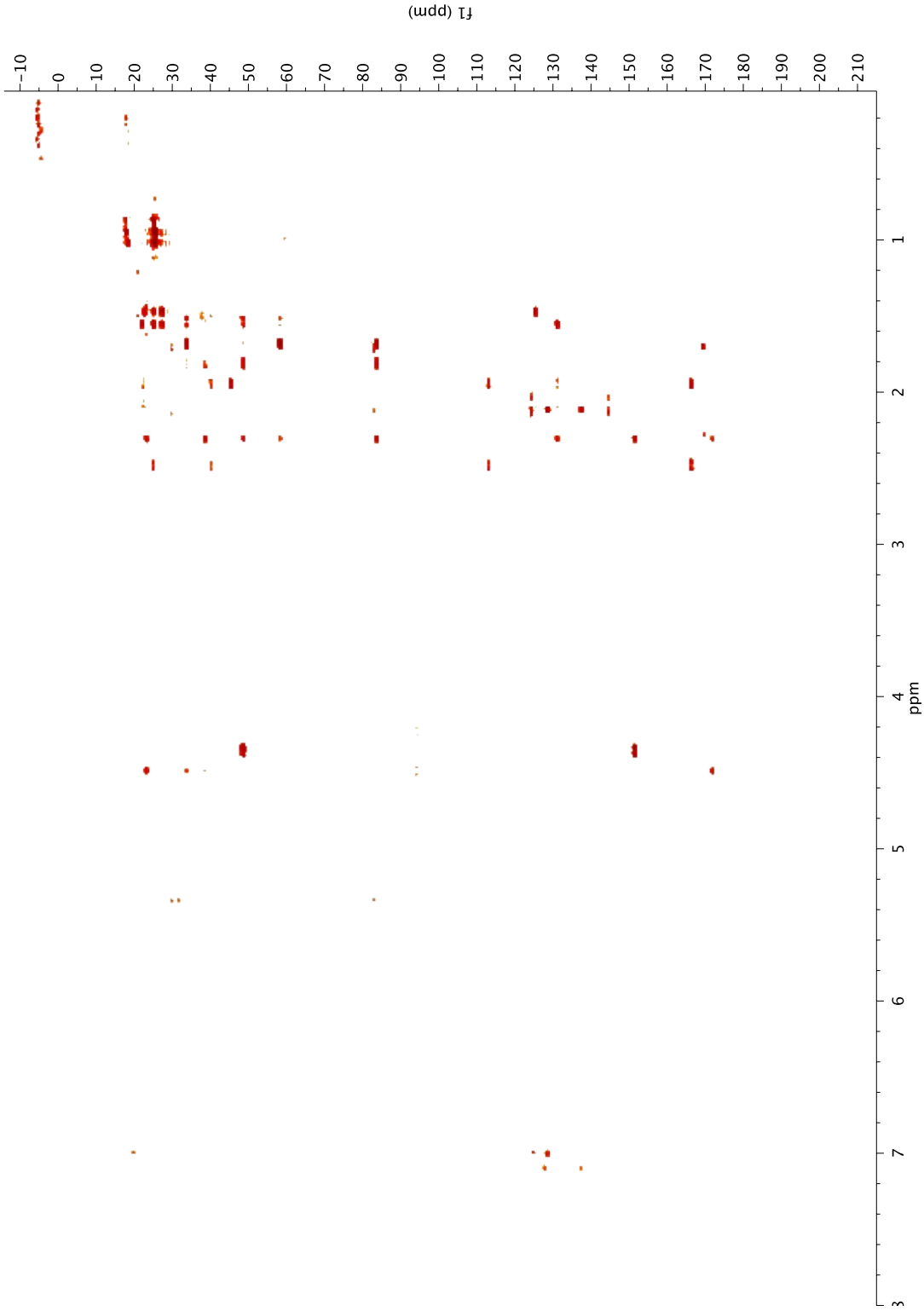

Figure A6.10 ^{1}H-^{13}C HMBC (600 MHz, Toluene-*d8* at 80 ºC, reaction time: 44 min–78 min) of compound **44** to **48**

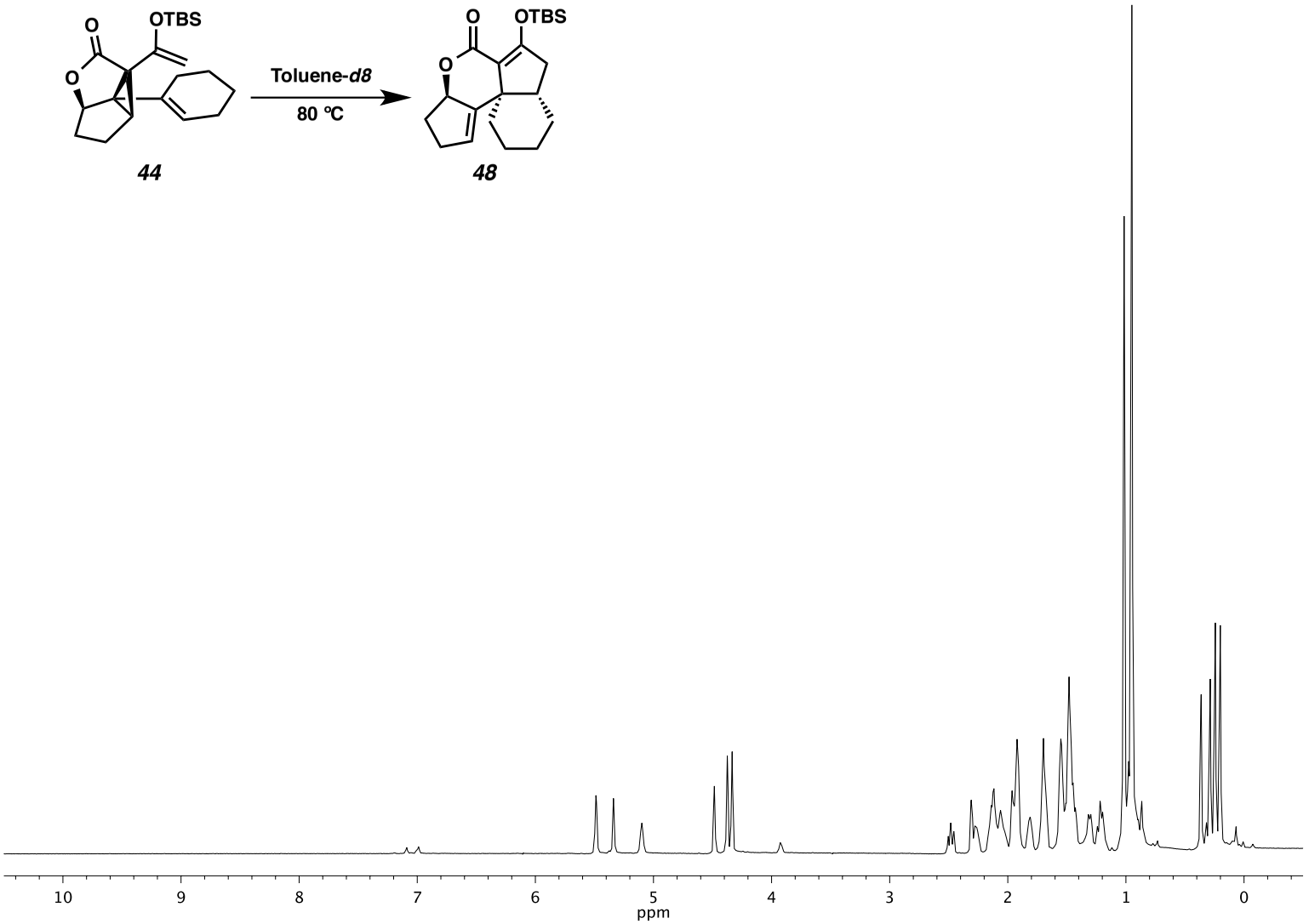

Figure A6.11 ^{1}H NMR (600 MHz, Toluene-*d8* at 80 °C, reaction time: 78 min) of compound **44** to **48**

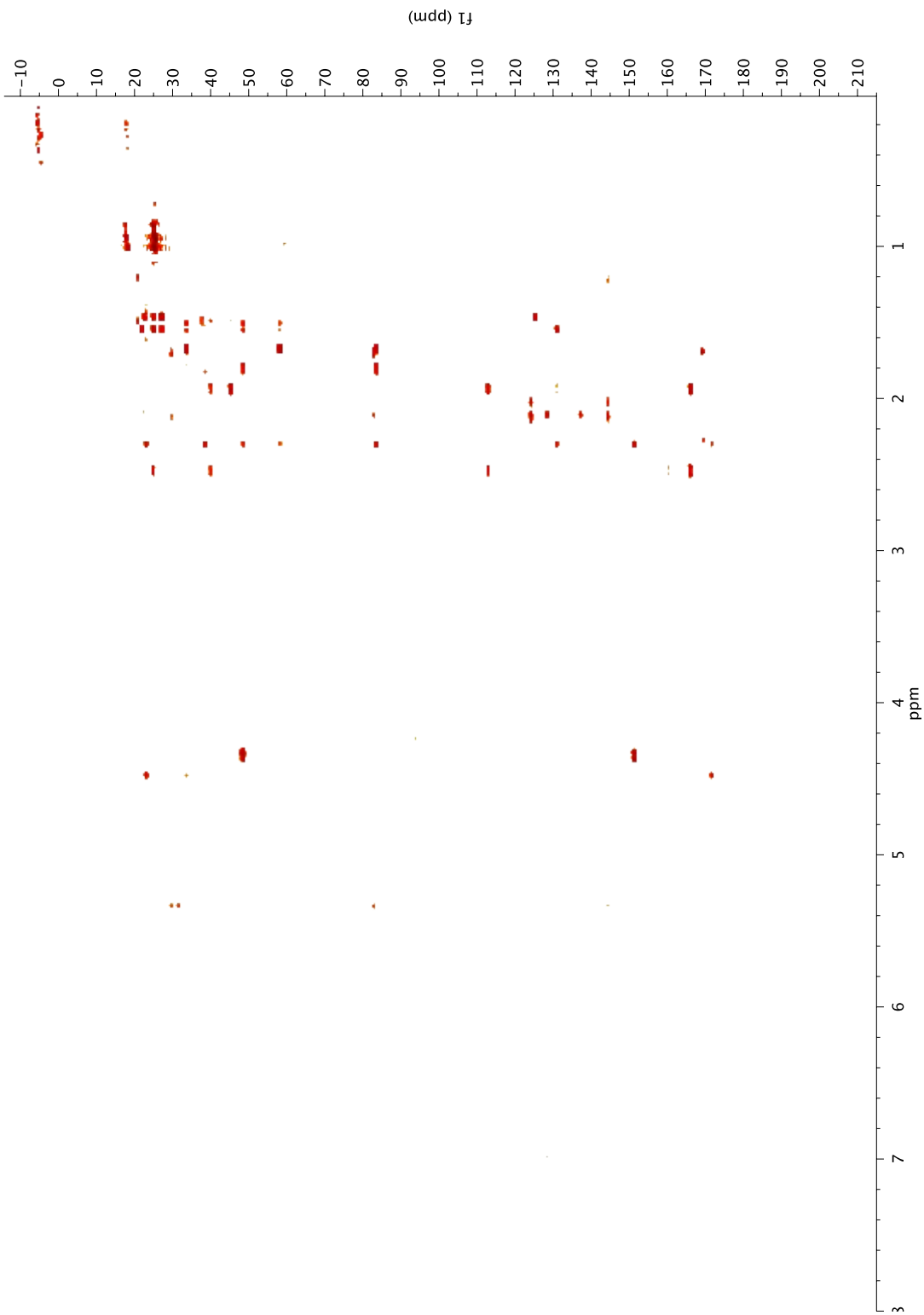

Figure A6.12 ^{1}H-^{13}C HMBC (600 MHz, Toluene-*d8* at 80 °C, reaction time: 78 min–112 min) of compound **44** to **48**

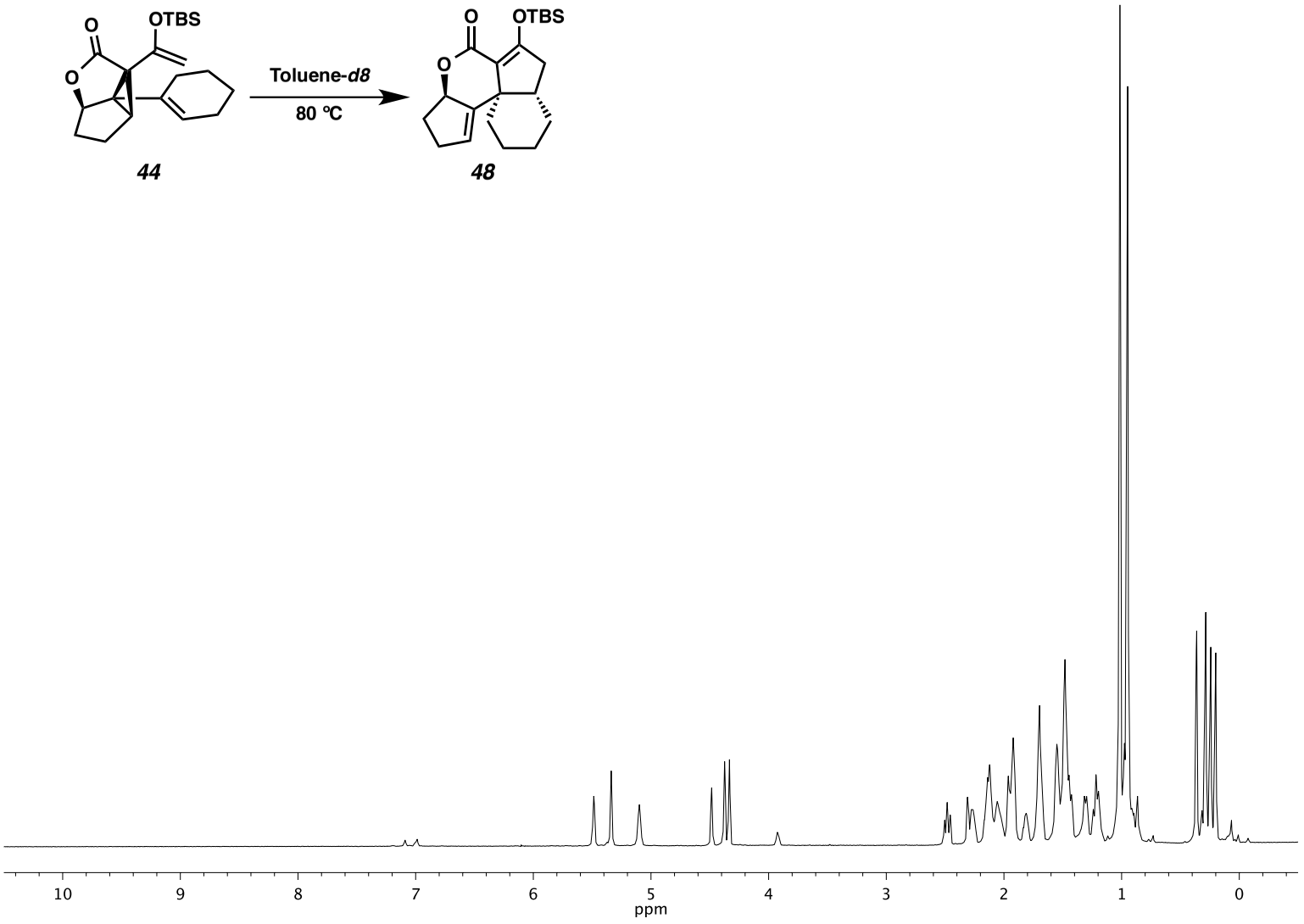

Figure A6.13 ^{1}H NMR (600 MHz, Toluene-*d8* at 80 ºC, reaction time: 112 min) of compound **44** to **48**

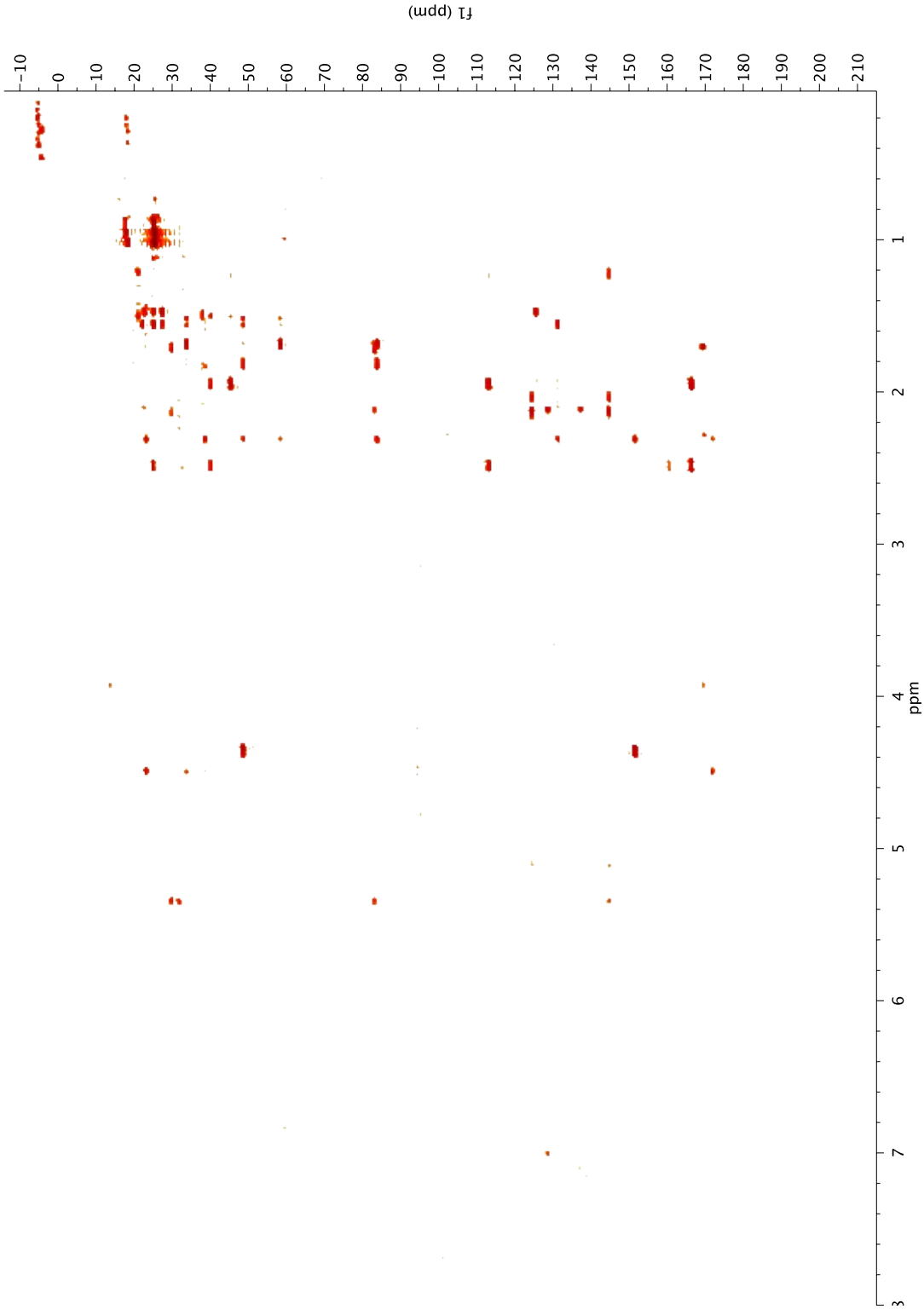

Figure A6.14 ^{1}H-^{13}C HMBC (600 MHz, Toluene-*d8* at 80 °C, reaction time: 112 min–146 min) of compound **44** to **48**

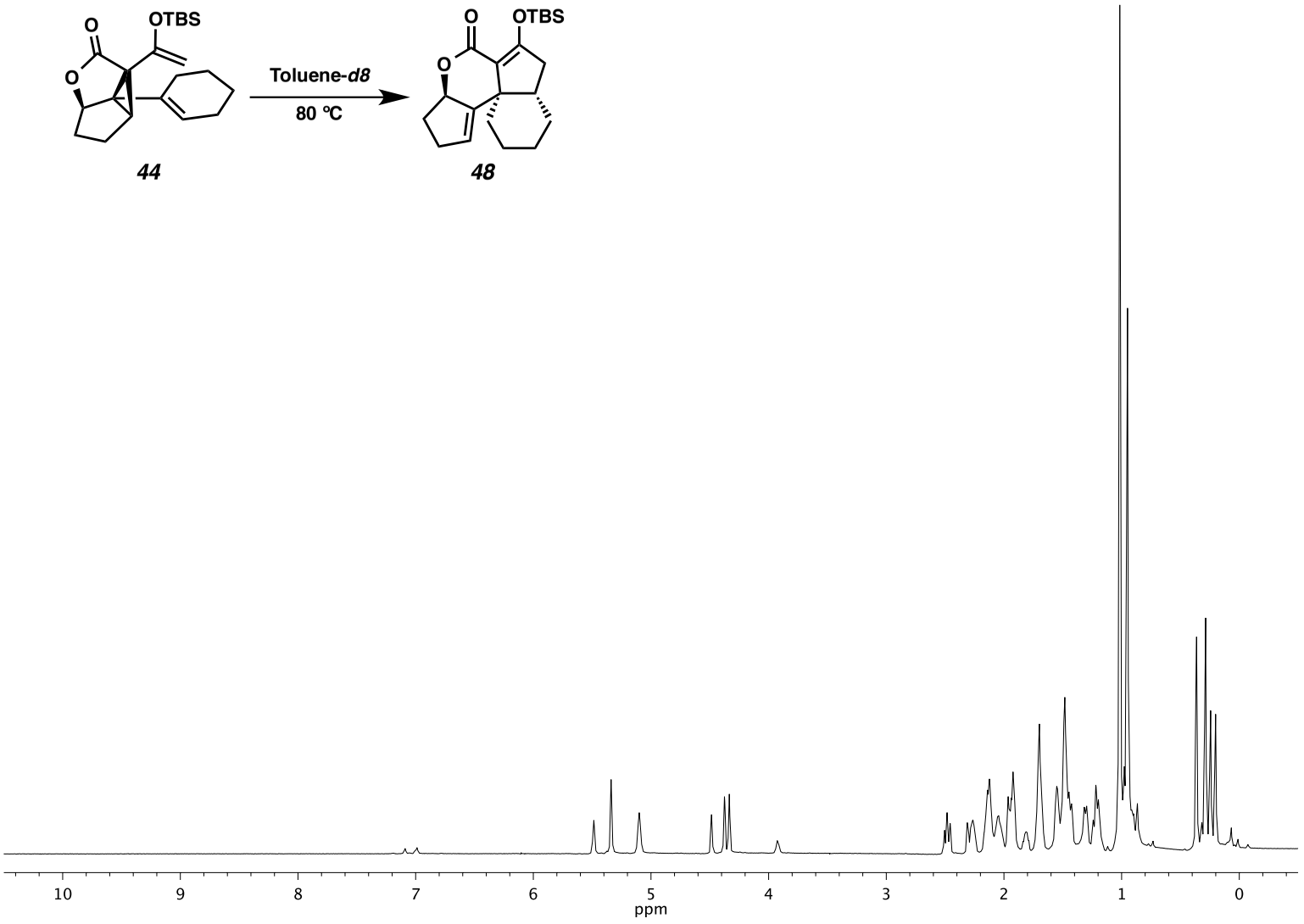

Figure A6.15 ^{1}H NMR (600 MHz, Toluene-*d8* at 80 ºC, reaction time: 146 min) of compound **44** to **48**

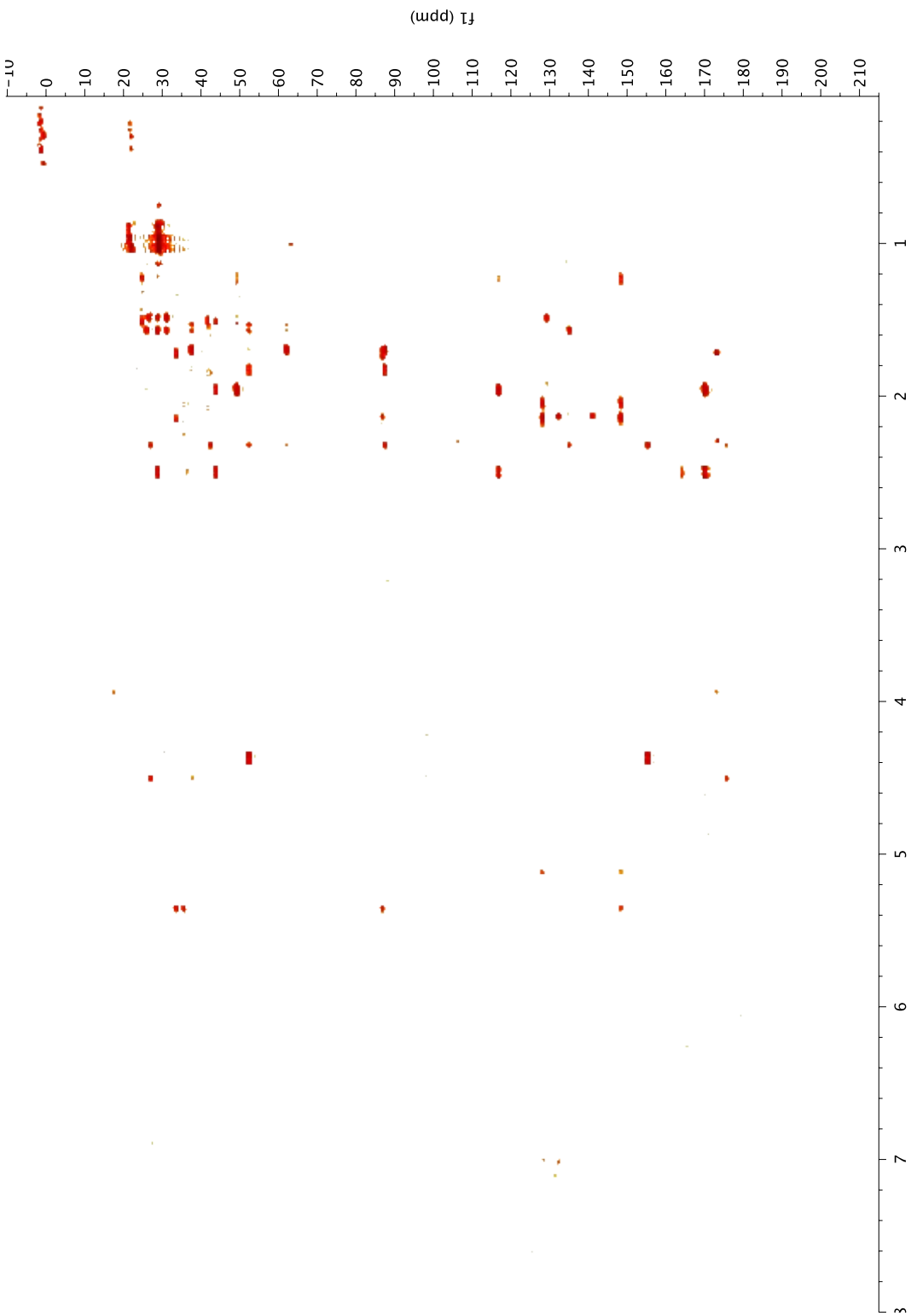

Figure A6.16 ^{1}H-^{13}C HMBC (600 MHz, Toluene-*d8* at 80 °C, reaction time: 146 min – 180 min) of compound **44** to **48**

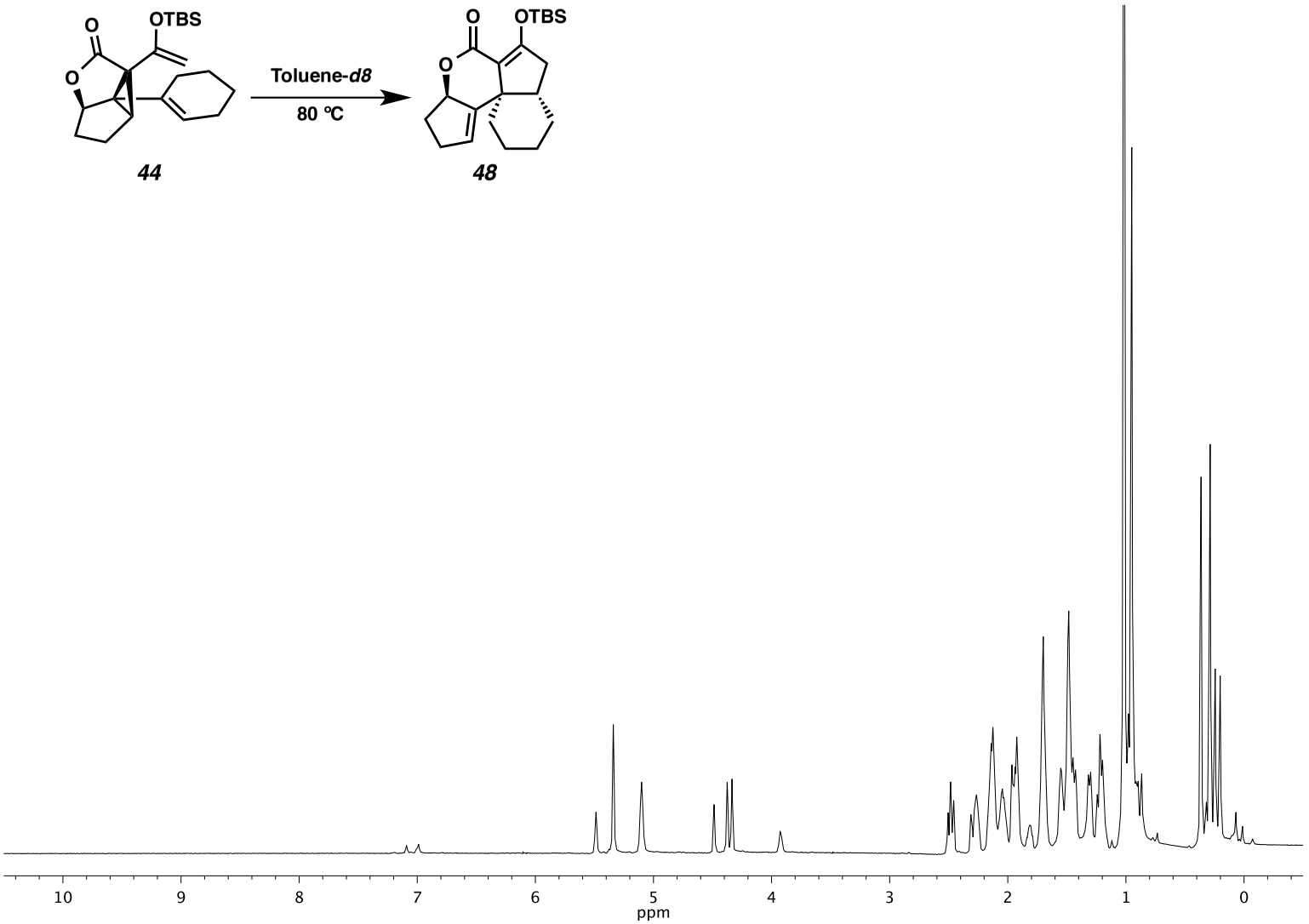

Figure A6.17 ^{1}H NMR (600 MHz, Toluene-*d8* at 80 ºC, reaction time: 180 min) of compound **44** to **48**

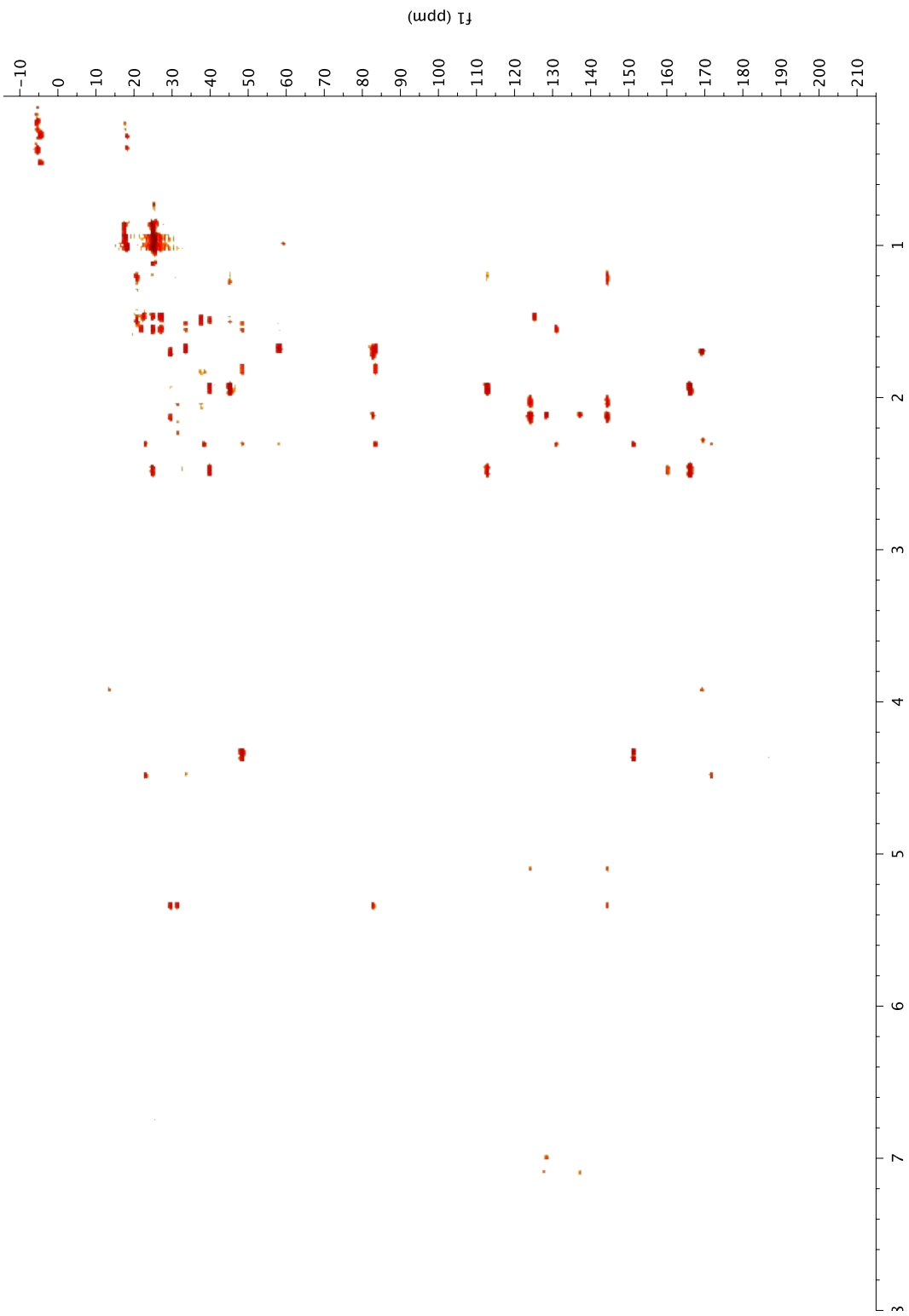

Figure A6.18 ^{1}H-^{13}C HMBC (600 MHz, Toluene-*d8* at 80 °C, reaction time: 180 min – 214 min) of compound **44** to **48**

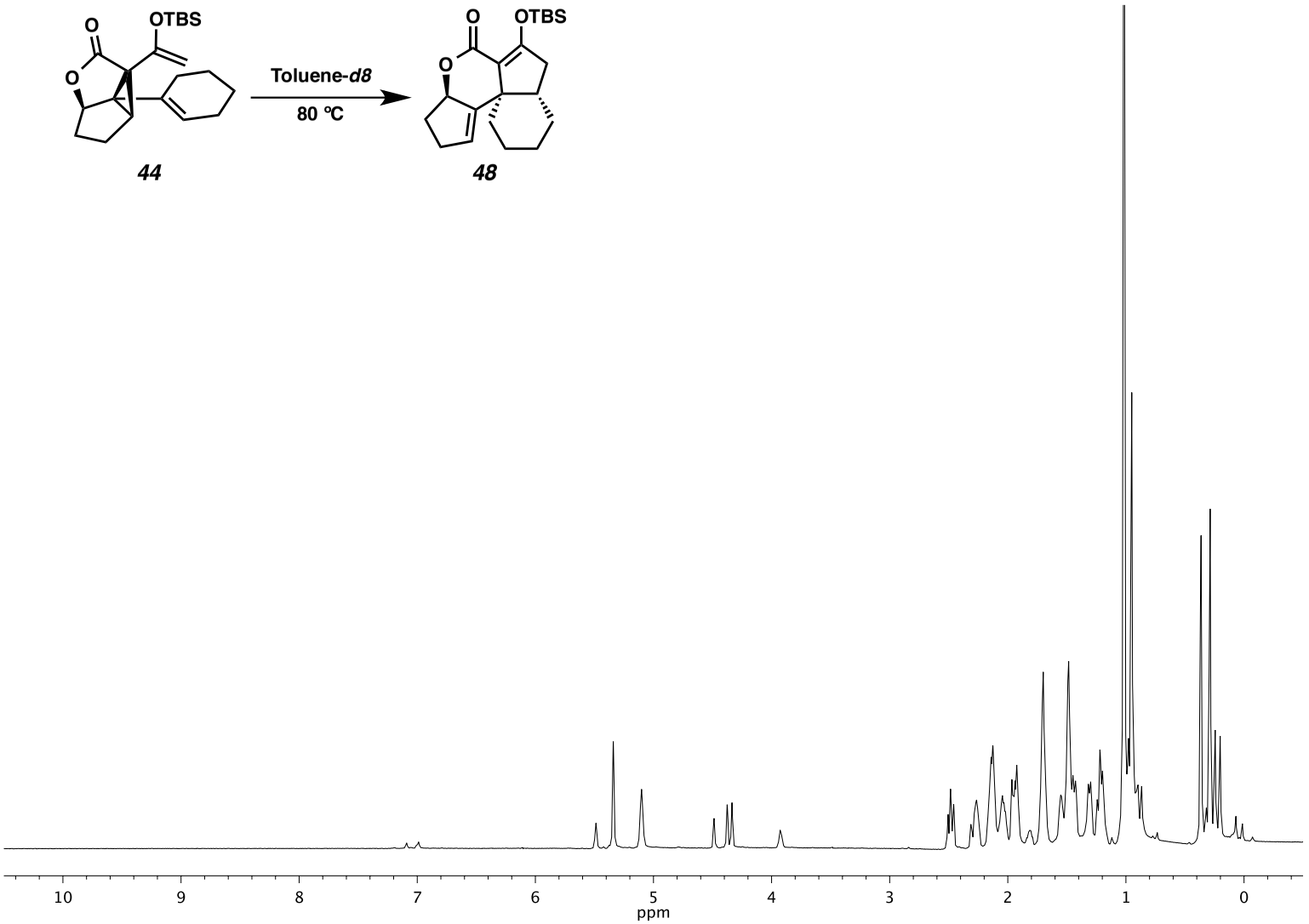

Figure A6.19 ^{1}H NMR (600 MHz, Toluene-*d8* at 80 ºC, reaction time: 214 min) of compound **44** to **48**

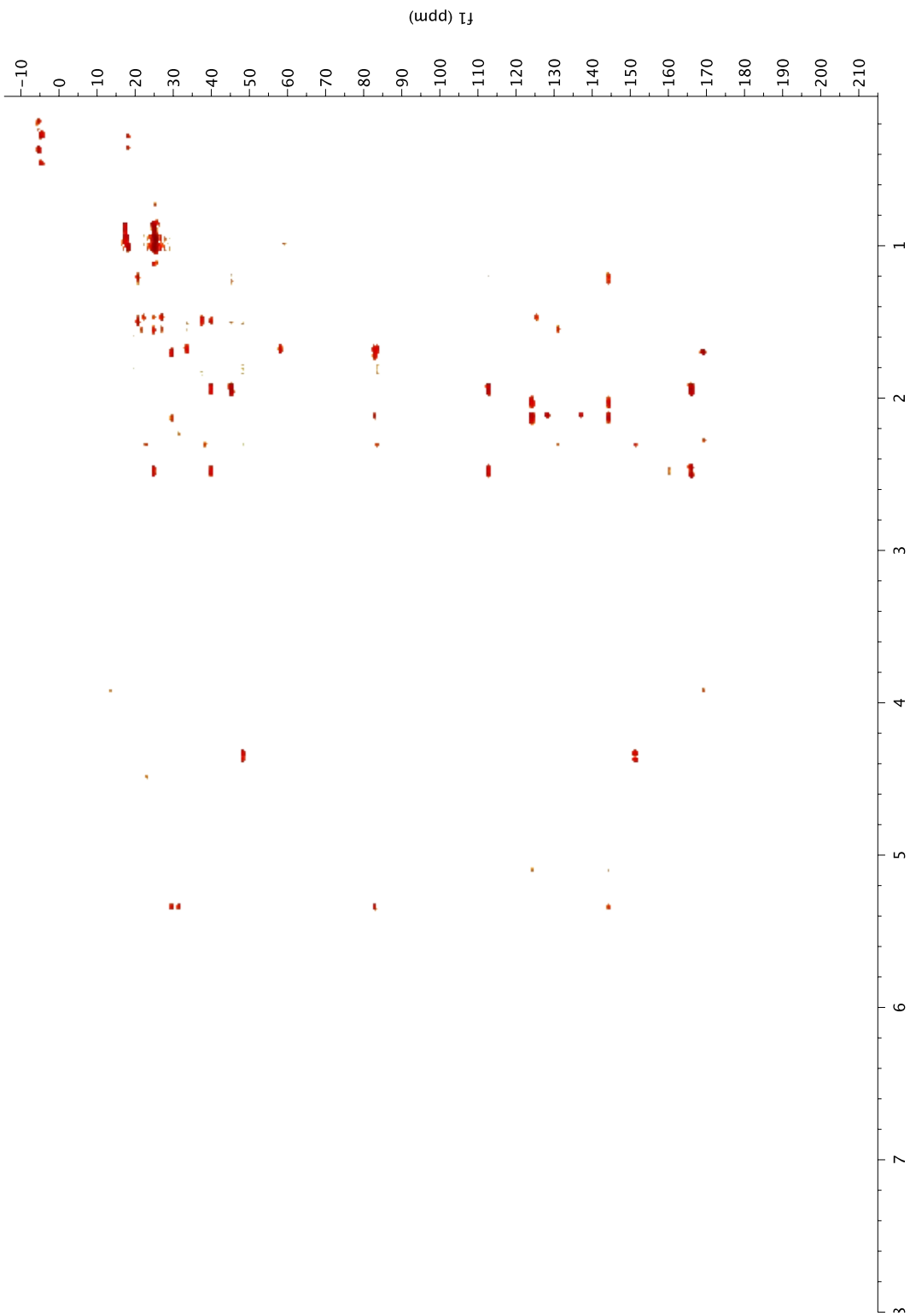

Figure A6.20 ^{1}H-^{13}C HMBC (600 MHz, Toluene-*d8* at 80 °C, reaction time: 214 min – 244 min) of compound **44** to **48**

CHAPTER 3

Stereochemical Evaluation of Bis(phosphine) Copper Catalysts for the Alkylation of 3-Bromooxindoles with α-Arylated Malonate Esters[†]

3.1 INTRODUCTION AND SYNTHETIC STRATEGY

3.1.1 INTRODUCTION

3,3-Disubstituted oxindole moieties are present in a wide variety of natural products and pharmaceutical agents.[1] Accordingly, methods for the asymmetric construction of 3,3-disubstituted oxindoles have attracted considerable attention from the synthetic community, and a number of catalytic stereoselective approaches to provide C3 quaternary stereocenters on oxindoles have been reported.[2,3] In 2007, we discovered that 3,3-disubstituted oxidoles **180** were furnished efficiently by base-mediated alkylation of reactive electrophilic *o*-azaxylyxene **179**, generated from 3-halooxindole **178**, with nucleophilic malonate esters (Scheme 1a).[4] Additionally, we developed a method for the

[†] This work was performed in collaboration with Seo-Jung Han and Scott C. Vilgil. Additionally, this work has been pubilished and adapted with permission from Lee, C. W.; Han, S.-J.; Virgil, S. C.; Stoltz, B. M. *Tetrahedron* **2014** doi:10.1016/j.tet.2014.10.065.

enantioselective alkylation of racemic 3-bromooxindoles by using a [Cu((*R*)-Ph-BOX)$(SbF_6)_2$] complex (Scheme 3.1.1).[5]

Scheme 3.1.1. Construction of 3,3-Disubstituted Oxindoles by Alkylation of 3-Halooxindoles

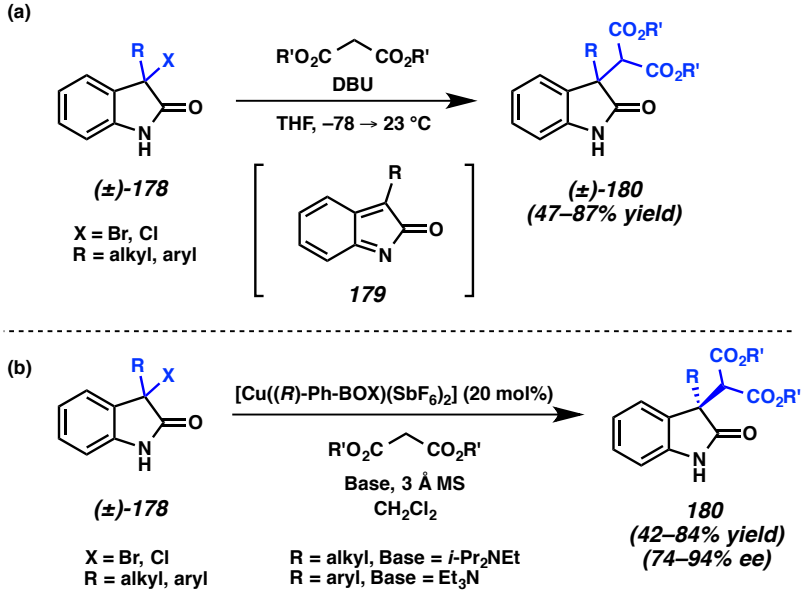

Following our development of these methods, our attention turned to the syntheses of the polycyclic alkaloids communesin F and perophoramidine.[6,7] We envisioned that the stereochemistry at the vicinal quaternary centers on communesin F and perophoramidine could be installed utilizing the conditions described in Scheme 1b. However, attempts to produce diesters **185** and **186** via copper(II) bisoxazoline catalyzed enantioselective alkylation of 3-bromooxindoles **181** and **182** with α-arylated malonate esters **183** and **184** were unsuccessful (Scheme 3.1.2). It was unsurprising since nucleophiles, α-arylated malonate esters **183** and **184**, were highly stabilized by *o*-nitrophenyl substituent and sterically demanding. Therefore, we pursued the development of an alternative catalytic system.

Scheme 3.1.2. Attempts for Alkylation of 3-Bromooxindoels with α-Arylated Malonate Esters

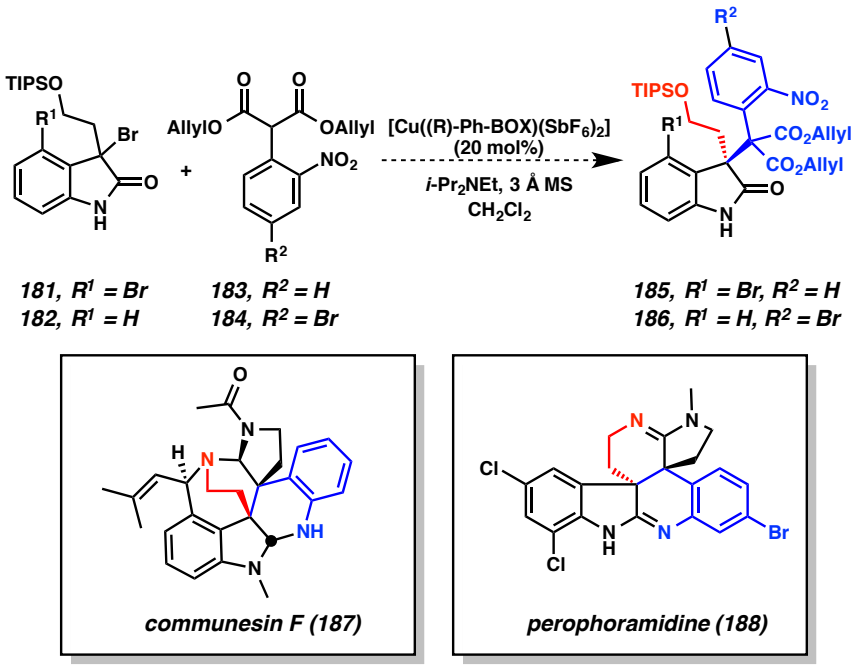

In our previous studies, we tested a variety of metal catalysts (e.g. Cu^{II}, Mg^{II}, La^{III}, and Ni^{II}) and discovered that the combination of Cu^{II} and a chiral bisoxazoline ligand effectively promoted the catalytic reaction.[4,5] Chiral Cu(II) bis(phosphine) complexes have also found use in stereoselective synthesis.[8] Since the catalytic system can be formed with a number of different chiral bis(phosphine) ligands, multiple options would be available for developing a stereoselective reaction. Herein, we describe several screening studies designed and undertaken to optimize the reaction conditions for the alkylation of 3-bromooxindoles with α-arylated malonate esters using a copper(II) bis(phosphine) catalyst.

3.2 RESULTS AND DISSCUSION

3.2.1 INITIAL SCREENING

To develop a stereoselective alkylation method, we chose simple substrates for optimization studies; specifically, we used bromooxindole **182** without a substituent on the aromatic ring and *o*-nitrophenyl dimethylmalonate **190** as a coupling partner. Bromooxindole **182**, easily prepared from indole in four steps by a known sequence,[6] was added to *o*-nitrophenyl dimethylmalonate **190** and cesium carbonate in THF solvent to afford a racemic product **191** in good yield (Scheme 3.2.1).

Scheme 3.2.1. Synthesis of the Racemic Product

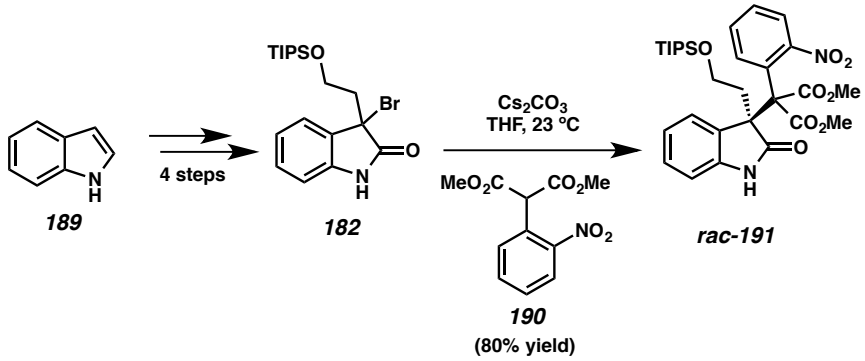

Choosing (*R*)-BINAP as a chiral ligand, we began our research by screening various copper sources, bases, and solvents. For instance we attempted the following variations of copper ions: Copper(II) triflate, copper(II) chloride with silver hexafluoroantimonate, copper(II) isobutyrate, copper(II) *tert*-butoxide (generated in situ by adding lithium *tert*-butoxide to copper(II) isobutyrate and ligand mixture), copper(II) ethylhexanoate, and copper(II) trifluoroacetylacetonate. We explored both organic and inorganic bases, including diisopropylethylamine, pyridine, tetramethylethylenediamine (TMEDA), triethylamine, diisopropylamine, 1,8-diazabicyclo[5,4,0]undec-7-ene (DBU), sodium

carbonate, potassium acetate, sodium ethylhexanoate and cesium carbonate. The various reactions combinations were attempted in the following solvents: dichloromethane, tetrahydrofuran, benzene, acetonitrile, and dioxane. Evaluating the 93 reactions that were explored (Table 3.2.1), we found that copper(II) *tert*-butoxide and the ligand complex generated in THF, which was similar to Fandrick's conditions for asymmetric propargylation,[8] exhibited the best conversion without generation of side products for the coupling of the arylated malonate **12** and bromooxindole **5** in CH_2Cl_2 (high conversion, 20% ee).

Table 3.2.1. Initial Screening Results

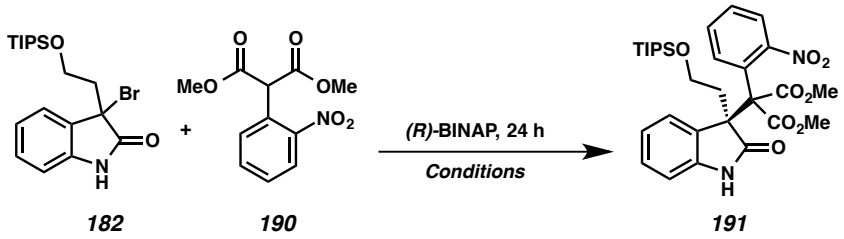

182 ***190*** ***191***

entry	metal	solvent	additives	base	temp	ee[a]
1	$Cu(OTf)_2$	CH_2Cl_2		Et_3N	23 ºC	25%
2	$Cu(OTf)_2$	CH_2Cl_2		*i*-Pr_2NEt	23 ºC	-
3	$Cu(OTf)_2$	CH_2Cl_2		*i*-Pr_2NH	23 ºC	-
4	$Cu(OTf)_2$	CH_2Cl_2		Pyridine	23 ºC	-
5	$Cu(OTf)_2$	CH_2Cl_2		DBU	23 ºC	10%
6	$Cu(OTf)_2$	CH_2Cl_2		TMEDA	23 ºC	-
7	$Cu(OTf)_2$	CH_2Cl_2		KOAc	23 ºC	Mix
8	$Cu(OTf)_2$	CH_2Cl_2		Na_2CO_3	23 ºC	Mix
9	$Cu(OTf)_2$	CH_2Cl_2		Cs_2CO_3	23 ºC	Mix
10	$Cu(OTf)_2$	CH_2Cl_2		DBU	–20 ºC	7%
11	$Cu(OTf)_2$	CH_2Cl_2		KOAc	–20 ºC	Mix
12	$Cu(OTf)_2$	CH_2Cl_2		Na_2CO_3	–20 ºC	trace
13	$Cu(OTf)_2$	CH_2Cl_2		Cs_2CO_3	–20 ºC	Mix
14	$Cu(OTf)_2$	C_6H_6		DBU	–20 ºC	-
15	$Cu(OTf)_2$	C_6H_6		KOAc	23 ºC	trace
16	$Cu(OTf)_2$	C_6H_6		Na_2CO_3	23 ºC	trace

Table 4.2.1. Initial Screening Results - Continued

entry	metal	solvent	additives	base	temp	ee[a]
17	$Cu(OTf)_2$	C_6H_6		Cs_2CO_3	23 ºC	15%
18	$CuCl_2$	CH_2Cl_2	$AgSbF_6$	DBU	23 ºC	5%
19	$CuCl_2$	CH_2Cl_2	$AgSbF_6$	KOAc	23 ºC	mix
20	$CuCl_2$	CH_2Cl_2	$AgSbF_6$	Na_2CO_3	23 ºC	mix
21	$CuCl_2$	CH_2Cl_2	$AgSbF_6$	Cs_2CO_3	23 ºC	mix
22	$CuCl_2$	CH_2Cl_2	$AgSbF_6$	Et_3N	23 ºC	-
23	$CuCl_2$	CH_2Cl_2	$AgSbF_6$	*i*-Pr_2NEt	23 ºC	-
24	$CuCl_2$	CH_2Cl_2	$AgSbF_6$	*i*-Pr_2NH	23 ºC	-
25	$CuCl_2$	CH_2Cl_2	$AgSbF_6$	Pyridine	23 ºC	trace
26	$CuCl_2$	CH_2Cl_2	$AgSbF_6$	DBU	-30 ºC	-
27	$CuCl_2$	CH_2Cl_2	$AgSbF_6$	Cs_2CO_3	-30 ºC	20%
28	$Cu(OTf)_2$	CH_2Cl_2	$AgNO_3$	Et_3N	23 ºC	trace
29	$Cu(OTf)_2$	CH_2Cl_2	$AgNO_3$	*i*-Pr_2NEt	23 ºC	30%
30	$Cu(OTf)_2$	CH_2Cl_2		Cs_2CO_3	–50 ºC	trace
31	$Cu(OTf)_2$	CH_2Cl_2		DBU	–50 ºC	-
32	$Cu(OTf)_2$	THF		Cs_2CO_3	–50 ºC	mix
33	$Cu(OTf)_2$	CH_2Cl_2	$AgNO_3$[a]	Cs_2CO_3	–50 ºC	mix
34	$Cu(OTf)_2$	CH_2Cl_2	$AgNO_3$	DBU	–50 ºC	-
35	$Cu(OTf)_2$	THF	$AgNO_3$	DBU	–50 ºC	-
36	$Cu(OTf)_2$	THF	$AgNO_3$	Et_3N	23 ºC	10%
37	$Cu(OTf)_2$	THF	$AgNO_3$	*i*-Pr_2NEt	23 ºC	10%
38	$Cu(isobutyrate)_2$	CH_2Cl_2	LiO*t*-Bu	Et_3N	23 ºC	6%
39	$Cu(isobutyrate)_2$	CH_2Cl_2	LiO*t*-Bu	*i*-Pr_2NEt	23 ºC	20%
40	$Cu(isobutyrate)_2$	CH_2Cl_2	LiO*t*-Bu	Cs_2CO_3	–30 ºC	25%
41	$Cu(isobutyrate)_2$	CH_2Cl_2	LiO*t*-Bu	KOAc	23 ºC	trace
42	$Cu(isobutyrate)_2$	CH_2Cl_2	LiO*t*-Bu	Na_2CO_3	23 ºC	mix
43	$Cu(isobutyrate)_2$	CH_2Cl_2	$AgNO_3$, LiO*t*-Bu	Et_3N	23 ºC	10%
44	$Cu(isobutyrate)_2$	CH_2Cl_2	$AgNO_3$, LiO*t*-Bu	*i*-Pr_2NEt	23 ºC	7%
45	$Cu(isobutyrate)_2$	CH_2Cl_2	$AgNO_3$, LiO*t*-Bu	Et_3N	–30 ºC	18%
46	$Cu(isobutyrate)_2$	CH_2Cl_2	$AgNO_3$, LiO*t*-Bu	*i*-Pr_2NEt	–30 ºC	10%
47	$Cu(isobutyrate)_2$	CH_2Cl_2	LiO*t*-Bu	*i*-Pr_2NEt	–45 ºC	8%
48	$Cu(isobutyrate)_2$	CH_2Cl_2	LiO*t*-Bu	Et_3N	–45 ºC	10%
49	$Cu(isobutyrate)_2$	CH_2Cl_2	$AgNO_3$, LiO*t*-Bu	*i*-Pr_2NEt	–45 ºC	20%
50	$Cu(isobutyrate)_2$	CH_2Cl_2	$AgNO_3$, LiO*t*-Bu	Et_3N	–45 ºC	20%
51	$Cu(isobutyrate)_2$	CH_2Cl_2		*i*-Pr_2NEt	23 ºC	-

Table 4.2.1. Initial Screening Results - Continued

entry	metal	solvent	additives	base	temp	ee[a]
52	$Cu(isobutyrate)_2$	CH_2Cl_2	Li*O*t-Bu	Et_3N	23 ºC	-
53	$Cu(isobutyrate)_2$	CH_2Cl_2	$AgNO_3$, Li*O*t-Bu	Cs_2CO_3	–45 ºC	mix
54	$Cu(isobutyrate)_2$	C_6H_6	Li*O*t-Bu	Cs_2CO_3	23 ºC	-
55	$Cu(isobutyrate)_2$	C_6H_6	Li*O*t-Bu	*i*-Pr_2NEt	23 ºC	trace
56	$Cu(isobutyrate)_2$	C_6H_6	$AgNO_3$, Li*O*t-Bu	Cs_2CO_3	23 ºC	racemic
57	$Cu(OTf)_2$	Dioxane	$AgNO_3$	*i*-Pr_2NEt	23 ºC	7%
58	$Cu(OTf)_2$	Dioxane	$AgNO_3$	Et_3N	23 ºC	15%
59	$Cu(OTf)_2$	Dioxane		Cs_2CO_3	-30 ºC	mix
60	$Cu(OTf)_2$	Dioxane		Na_2CO_3	23 ºC	10%
61	$Cu(OTf)_2$	Dioxane		KOAc	23 ºC	Mix
62	$Cu(OTf)_2$	CH_3CN	$AgNO_3$	*i*-Pr_2NEt	23 ºC	15%
63	$Cu(OTf)_2$	CH_3CN	$AgNO_3$	Et_3N	23 ºC	15%
64	$Cu(OTf)_2$	CH_3CN		Cs_2CO_3	–30 ºC	trace
65	$Cu(OTf)_2$	CH_3CN		Na_2CO_3	23 ºC	mix
66	$Cu(OTf)_2$	CH_3CN		KOAc	23 ºC	mix
67	$Cu(isobutyrate)_2$	THF	Li*O*t-Bu	*i*-Pr_2NEt	–50 ºC	-
68	$Cu(isobutyrate)_2$	CH_2Cl_2	$AgNO_3$, Li*O*t-Bu	*i*-Pr_2NEt	–50 ºC	20%
69	$Cu(isobutyrate)_2$	CH_2Cl_2	$AgNO_3$	Cs_2CO_3	–50 ºC	trace
70	$Cu(isobutyrate)_2$	CH_2Cl_2	$AgNO_3$	Cs_2CO_3	23 ºC	trace
71	$Cu(isobutyrate)_2$	CH_2Cl_2	$AgNO_3$, Li*O*t-Bu	Cs_2CO_3	–50 ºC	mix
72	$Cu(isobutyrate)_2$	CH_2Cl_2	$AgNO_3$, Li*O*t-Bu (1 mol %)	*i*-Pr_2NEt	–50 ºC	mix
73	$Cu(isobutyrate)_2$	CH_2Cl_2	$AgNO_3$, Li*O*t-Bu (2 mol %)	*i*-Pr_2NEt	–50 ºC	17%
74	$Cu(isobutyrate)_2$	CH_2Cl_2	$AgNO_3$, Li*O*t-Bu (4 mol %)	*i*-Pr_2NEt	–50 ºC	19%
75	$Cu(isobutyrate)_2$	CH_2Cl_2	$AgNO_3$, Li*O*t-Bu (8 mol %)	*i*-Pr_2NEt	–50 ºC	20%
76	$Cu(isobutyrate)_2$	CH_2Cl_2	$AgNO_3$, Li*O*t-Bu, NaEH	*i*-Pr_2NEt	–50 ºC	mix
77	$Cu(isobutyrate)_2$	CH_2Cl_2	$AgNO_3$, NaEH (ex)		23 ºC	racemic
78	$Cu(isobutyrate)_2$	CH_2Cl_2	$AgNO_3$	Cs_2CO_3	–50 ºC	mix
79	$Cu(EH)_2$	CH_2Cl_2		*i*-Pr_2NEt	–50 ºC	9%
80	$Cu(EH)_2$	CH_2Cl_2		Et_3N	–50 ºC	-
81	$Cu(EH)_2$	CH_2Cl_2		Cs_2CO_3	–50 ºC	-
82	$Cu(EH)_2$	CH_2Cl_2	$AgNO_3$	*i*-Pr_2NEt	–50 ºC	20%
83	$Cu(EH)_2$	CH_2Cl_2	$AgNO_3$	Et_3N	–50 ºC	15%
84	$Cu(EH)_2$	CH_2Cl_2	$AgNO_3$	Cs_2CO_3	–50 ºC	-
85	$Cu(EH)_2$	CH_2Cl_2	$AgNO_3$, Li*O*t-Bu	*i*-Pr_2NEt	–50 ºC	10%
86	$Cu(EH)_2$	CH_2Cl_2	$AgNO_3$, Li*O*t-Bu	Et_3N	–50 ºC	-
87	$Cu(EH)_2$	CH_2Cl_2	Li*O*t-Bu	NaEH	23 ºC	-

Table 4.2.1. Initial Screening Results - Continued

entry	metal	solvent	additives	base	temp	ee[a]
88	$Cu(tfacac)_2$	CH_2Cl_2		Et_3N	–50 ºC	-
89	$Cu(tfacac)_2$	CH_2Cl_2		*i*-Pr_2NEt	–50 ºC	-
90	$Cu(tfacac)_2$	CH_2Cl_2		Cs_2CO_3	–50 ºC	-
91	$Cu(tfacac)_2$	CH_2Cl_2		NaEH	–50 ºC	-
92	$Cu(tfacac)_2$	THF		Et_3N	–50 ºC	7%
93	$Cu(tfacac)_2$	THF		*i*-Pr_2NEt	–50 ºC	-

$Cu(hfacac)_2$: copper(II) hexafluoroacetylacetonate, $Cu(EH)_2$: copper(II) ethylhexanoate, $Cu(tfacac)_2$: copper(II) trifluoroacetylacetonate, -: Desired product was not observed. [a] enantiomeric excess was measured by chiral SFC. [b] 44 mol % of ligand was used. mix: complex mixtures

3.2.2 LIGAND SCREENING AND OPTIMIZATION STUDIES

Based on previous studies (Table 3.2.1, entries 39 and 68), we selected copper(II) *iso*-butyrate, lithium *tert*-butoxide and THF solvent for generation of the catalytic species with chiral ligands, diisopropylamine as the base and CH_2Cl_2 as solvent. We have screened 69 chiral bis(phosphine) ligands (Figure 3.2.1) under similar condition, finding DiazaPHOS (W2, –50% ee) and WALPHOS (N1, N2 27% ee) to give the best enantioselectivities (Table 3.2.2).

Figure 3.2.1. Ligand List

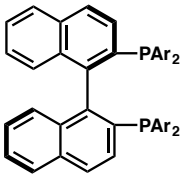

A1 : Ar = Ph
A2 : Ar = Tol
A3 : Ar = Xyl
BINAP

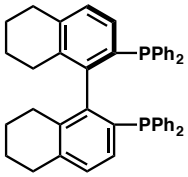

A4

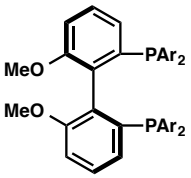

B1 : Ar = Xyl
B2 : Ar = 3,5-*t*-BuPh
B3 : Ar = 3,5-*t*-Bu-4-MeOPh
B4 : Ar = 3,5-*i*-Pr-4-Me$_2$NPh
MEOBIPHEP

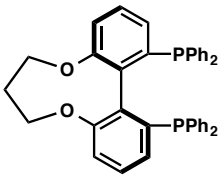

C1
TUNEPHOS

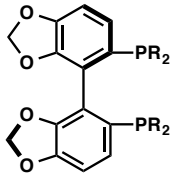

D1 : R = Ph
D2 : R = 3,5-Me$_2$Ph
D3 : R = 3.5-*t*-Bu$_2$-4-MeOPh
D4 : R = *i*-Pr
SEGPHOS

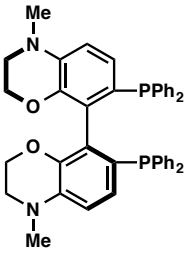

E1
SOLOPHOS

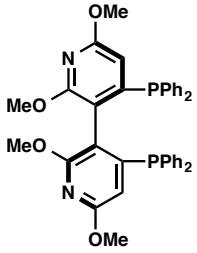

F1
P-Phos

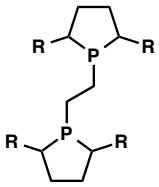

G1 : R = (*S,S*)-Me
G2 : R = (*R,R*)-Et
G3 : R = (*R,R*)-*i*-Pr
BPE

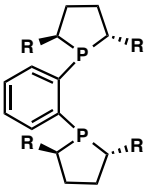

H1 : R = Me
H2 : R = Et
H3 : R = *i*-Pr
DUPHOS

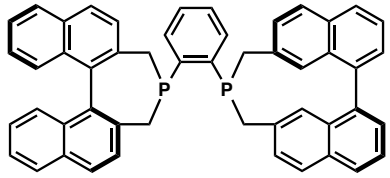

I1
BINAPHANE

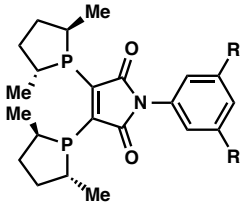

J1 : R = Me
J2 : R = CF$_3$

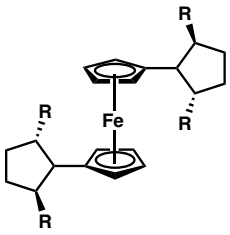

K1 : R = Me
K2 : R = Et
K3 : R = *i*-Pr
Ferrocelane

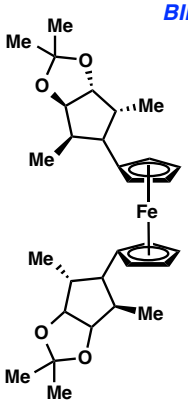

L1
KetalPhos

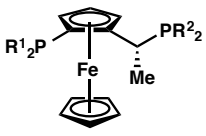

JOSIPHOS

M1 : R^1,R^2 = Ph, Cy
M2 : R^1,R^2 = Ph, *t*-Bu
M3 : R^1,R^2 = Ph, Xyl
M4 : R^1,R^2 = aNp, *t*Bu
M5 : R^1,R^2 = aNp, Cy
M6 : R^1,R^2 = 3,5-(CF$_3$)$_2$-Ph, Cy
M7 : R^1,R^2 = 3,5-(CF$_3$)$_2$-Ph, Xyl
M8 : R^1,R^2 = 3,5-Me$_2$-4-MeOPh, Cy
M9 : R^1,R^2 = 3,5-Me$_2$-4-MeOPh, *t*Bu
M10 : R^1,R^2 = 3,5-Me$_2$-4-MeOPh, Xyl
M11 : R^1,R^2 = 2-Furyl, *t*Bu
M12 : R^1,R^2 = 2-Furyl, Xyl
M13 : R^1,R^2 = Cy, Cy
M14 : R^1,R^2 = Cy, *t*-Bu
M15 : R^1,R^2 = Cy, Ph
M16 : R^1,R^2 = *t*-Bu, Ph
M17 : R^1,R^2 = *t*Bu, 2-Tol

Figure 3.2.1. Ligand List - Continued

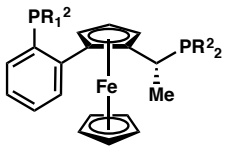

N1 : R^1,R^2 = Ph, Ph
N2 : R^1,R^2 = Ph, Xyl
N3 : R^1,R^2 = Ph, Xyl^F
N4 : R^1,R^2 = 3,5-Me_2-4-MeOPh, Xyl^F
N5 : R^1,R^2 = Ph, Cy
N6 : R^1,R^2 = Cy, Xyl^F
N7 : R^1,R^2 = Xyl, Xyl
N8 : R^1,R^2 = Ph, Norbonyl

WALPHOS

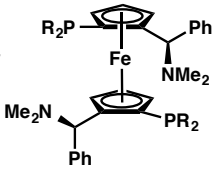

O1 : R = Ph
O2 : R = 2-Tol
O3 : R = Xyl
O4 : R = Xyl^F
O5 : R = 3,5-Me_2-4-MeOPh
O6 : R = Cy (opposite stereochemistry)

MANDYPHOS

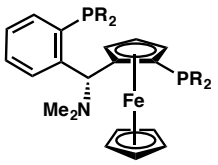

P1 : R = Ph
P2 : R = Cy

TANIAPHOS

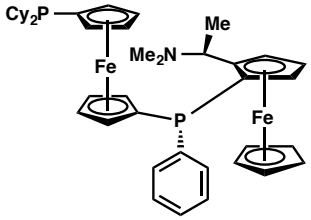

Q1

CHENPHOS

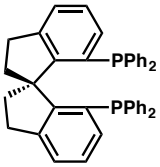

R1

***R*-SDP**

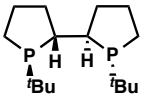

S1

TANGPHOS

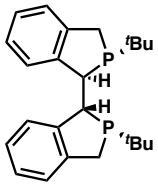

T1

DUANPHOS

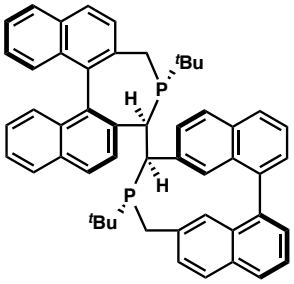

U1

Binapine

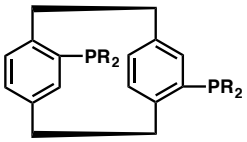

V1 : R = Ph
V2 : R = Xyl

PHANEPHOS

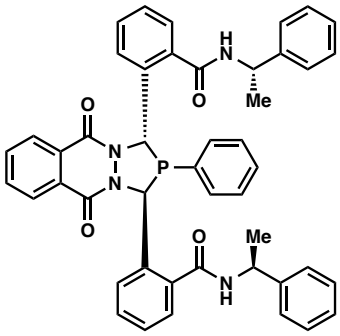

W1 : ***(S,S,S)*-DiazaPHOS-PPE**
W2 : ***(R,R,S)*-DiazaPHOS-PPE**
W3 : Bis[***(R,R,S)*-DiazaPHOS-SPE]**
W4 : Bis[***(S,S,S)*-DiazaPHOS-SPE]**

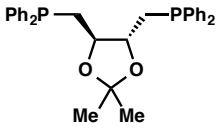

X1

DIOP

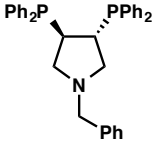

Y1

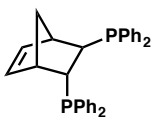

Z1

NORPHOS

Table 3.2.2. Ligand Screening Results

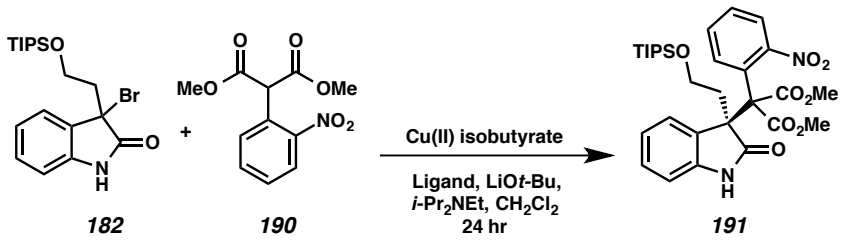

182 ***190*** ***191***

entry	ligand	temp	ee[a]	entry	ligand	temp	ee[a]
1	**A1**	0 ºC	10%	36	**M12**	23 ºC	20%
2	**A2**	0 ºC	14%	37	**M13**	23 ºC	mix
3	**A3**	0 ºC	20%	38	**M14**	23 ºC	–10%
4	**A4**	0 ºC	-	39	**M15**	23 ºC	-
5	**B1**	0 ºC	11%	40	**M16**	23 ºC	10%
6	**B2**	0 ºC	10%	41	**M17**	23 ºC	racemic
7	**B3**	0 ºC	9%	42	**N1**	23 ºC	27%
8	**B4**	0 ºC	12%	43	**N2**	23 ºC	27%
9	**C1**	0 ºC	-	44	**N3**	23 ºC	racemic
10	**D1**	0 ºC	17%	45	**N4**	23 ºC	trace
11	**D2**	0 ºC	10%	46	**N5**	23 ºC	-
12	**D3**	0 ºC	racemic	47	**N6**	23 ºC	trace
13	**D4**	0 ºC	8%	48	**N7**	23 ºC	-
14	**E1**	0 ºC	NR	49	**N8**	23 ºC	-
15	**F1**	0 ºC	10%	50	**O1**	23 ºC	-
16	**G1**	0 ºC	16%	51	**O2**	23 ºC	-
17	**G2**	0 ºC	racemic	52	**O3**	23 ºC	20%
18	**G3**	0 ºC	8%	53	**O4**	23 ºC	10%
19	**H1**	0 ºC	14%	54	**O5**	23 ºC	20%
20	**H2**	0 ºC	10%	55	**O6**	23 ºC	-
21	**H3**	23 ºC	-	56	**P1**	23 ºC	10%
22	**J2**	23 ºC	27%	57	**P2**	23 ºC	–5%
23	**K1**	23 ºC	17%	58	**Q1**	23 ºC	-
24	**K2**	23 ºC	22%	59	**R1**	23 ºC	-
25	**K3**	23 ºC	-	60	**S1**	23 ºC	-
26	**M1**	23 ºC	-	61	**T1**	23 ºC	-
27	**M2**	23 ºC	trace	62	**V1**	23 ºC	-
28	**M3**	23 ºC	mix	63	**V2**	23 ºC	-

Table 4.2.2. Ligand Screening Results - Continued

entry	ligand	temp	ee[a]	entry	ligand	temp	ee[a]
29	**M4**	–50 ºC	-	64	**W1**	23 ºC	40%
30	**M5**	–50 ºC	6%	65	**W2**	23 ºC	–50%
31	**M6**	23 ºC	-	66	**W3**	23 ºC	10%
32	**M7**	–50 ºC	16%	67	**X1**	23 ºC	-
33	**M8**	23 ºC	-	68	**Y1**	23 ºC	-
34	**M10**	–50 ºC	14%	69	**Z1**	23 ºC	-
35	**M11**	–50 ºC	10%				

-: Desired product was not observed. [a] enantiomeric excess was measured by chiral SFC. [b] 44 mol % of ligand was used. mix: complex mixtures.

Having identified the most effective ligands, we next screened several copper sources under lower temperatures. Although none of these sources exhibited better results than the combination of copper(II) isobutyrate and lithium *tert*-butoxide for WALPHOS (**N1** and **N2**), we were able to observe better stereoselectivity at low temperature (Table 3.2.3, entries 6 and 16). With DiazaPHOS (**W1**), copper(II) triflate showed better selectivity at 0 ºC (Table 3.2.3, entries 22 and 23).

Table 3.2.3. Further Investigations using WALPHOS and DiazaPHOS in the alkylation reaction

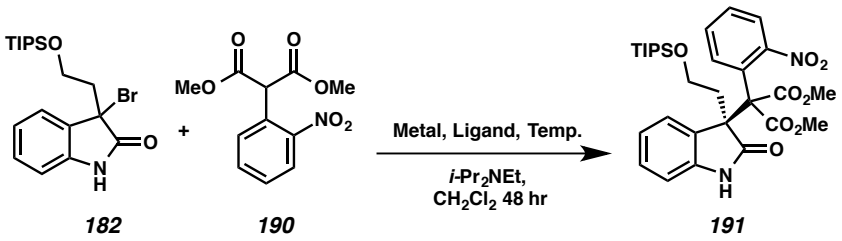

182 ***190*** ***191***

entry	metal	ligand	additive	temp	ee[a]
1	$CuCl_2$	**N1**	$AgBF_4$	–45 ºC	-
2	$CuCl_2$	**N1**	$AgNTf_2$	–45 ºC	-
3	$CuCl_2$	**N1**	$AgPF_6$	–45 ºC	-
4	$CuCl_2$	**N1**	$AgSbF_6$	–45 ºC	-
5	$CuCl_2$	**N1**	LiO*t*-Bu	–45 ºC	-
6	Cu(isobutyrate)$_2$	**N1**	LiO*t*-Bu	–45 ºC	44%
7	Cu(isobutyrate)$_2$	**N1**	$AgSbF_6$	–45 ºC	-
8	Cu(hfacac)$_2$	**N1**		–45 ºC	trace
9	Cu(OTf)$_2$	**N1**		–45 ºC	trace
10	Cu(OTf)$_2$	**N1**	LiO*t*-Bu	–45 ºC	23%
11	Cu(EH)$_2$	**N1**		–45 ºC	trace
12	$CuCl_2$	**N2**	$AgBF_4$	–45 ºC	-
13	$CuCl_2$	**N2**	$AgNTf_2$	–45 ºC	-
14	$CuCl_2$	**N2**	$AgPF_6$	–45 ºC	-
15	$CuCl_2$	**N2**	$AgSbF_6$	–45 ºC	-
16	Cu(isobutyrate)$_2$	**N2**	LiO*t*-Bu	–45 ºC	54%
17	Cu(hfacac)$_2$	**N2**		–45 ºC	30%
18	Cu(OTf)$_2$	**N2**		–45 ºC	45%
19	Cu(EH)$_2$	**N2**		–45 ºC	trace
20	Cu(isobutyrate)$_2$	**W1**	LiO*t*-Bu	–45 ºC	trace
21	Cu(isobutyrate)$_2$	**W1**[b]	LiO*t*-Bu	–45 ºC	trace
22	Cu(OTf)$_2$	**W1**		–45 ºC	40%
23	Cu(OTf)$_2$	**W1**[b]		–45 ºC	50%

Conditions: 0.0049 mmol **182**, 0.0145 mmol **190**, Cu (20 mol %), Ligand (22 mol %), Additive (20 mol %), *i*-Pr_2NEt (3 equiv.), 0.1 mL CH_2Cl_2 (0.049 M). Metal catalyst, ligand and additives were mixed in THF. THF was removed in *vacuo*, and the resultant was diluted with the reaction solvent. The reaction was initiated by addition of base. Cu(hfacac)$_2$: copper(II) hexafluoroacetylacetonate, Cu(EH)$_2$: copper(II) ethylhexanoate. [a] enantiomeric excess was measured by chiral SFC. -: Desired product was not observed. [b] 44 mol % of ligand was used.

With a suitable bis(phosphine) ligand in hand (N1), we tested multiple solvents and bases. However, amine bases weaker than Hünig's base (Table 3.2.4, entries 1-12) could not initiate the reaction, whereas stronger base (entries 13-18) decreased the stereoselectivity. The copper bis(phosphine) complex demonstrated similar selectivity in dichloromethane (entry 19), THF (entry 20), and chloroform (entry 22), however it showed worse selectivity in acetonitrile (entry 21) and failed to proceed at all in toluene and 1,2-dimethoxyethane (DME).

Table 3.2.4. Investigation of reaction solvents and bases with WALPHOS in the alkylation reaction

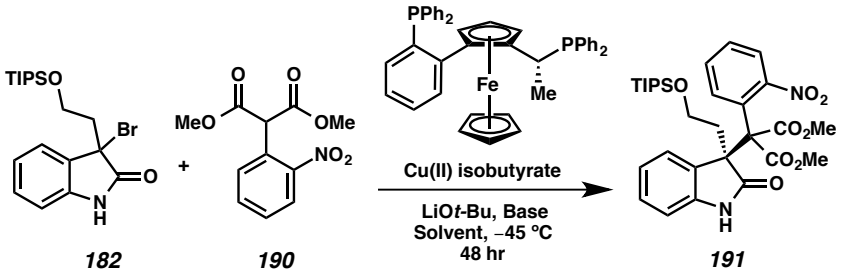

entry	solvent	base	ee[a]
1	CH_2Cl_2	DABCO	-
2	THF	DABCO	-
3	CH_3CN	DABCO	-
4	$CHCl_3$	DABCO	-
5	Toluene	DABCO	-
6	DME	DABCO	-
7	CH_2Cl_2	DMAP	-
8	THF	DMAP	-
9	CH_3CN	DMAP	-
10	$CHCl_3$	DMAP	-
11	Toluene	DMAP	-
12	DME	DMAP	-
13	CH_2Cl_2	Cs_2CO_3	35%
14	THF	Cs_2CO_3	15%
15	CH_3CN	Cs_2CO_3	20%
16	$CHCl_3$	Cs_2CO_3	20%
17	Toluene	Cs_2CO_3	-
18	DME	Cs_2CO_3	10%
19	CH_2Cl_2	*i*-Pr_2NEt	40%
20	THF	*i*-Pr_2NEt	50%
21	CH_3CN	*i*-Pr_2NEt	30%
22	$CHCl_3$	*i*-Pr_2NEt	40%
23	Toluene	*i*-Pr_2NEt	-
24	DME	*i*-Pr_2NEt	-

Conditions: 0.0024 mmol **182**, 0.0072 mmol **190**, Cu (20 mol %), Ligand (22 mol %), LiO*t*-Bu (20 mol %), Base (3 equiv), 0.06 mL Solvent (0.04 M). [a] enantiomeric excess was measured by chiral SFC. -: Desired product was not observed.

In addition to these studies, we examined the effect of the catalyst and ligand loading on the stereoselectivity of our alkylation reaction. Unsatisfactory results were produced with low catalyst or ligand loading (Table 3.2.5, entries 1,2 and 4), but 20 mol % of copper(II) isobutyrate and 40 mol % of the ligand gave the product in 56% ee (Table 3, entry 3). Stoichiometric amounts of the copper precursor and ligand produced only a slight increase in ee (Table 3.2.5, entry 5). Additionally, we investigated the impact of the equivalents of Hünig's base on the selectivity of the reaction. Results showed the amount of Hünig's base had little effect on the stereoselectivity of the product (Table 3.2.5, entries 6-13). Subsequent examination of concentration effects showed lowering the concentration of the reaction mixture from 0.05 M to 0.02 M resulted in increase stereoselectivity (Table 3.2.6).

Table 3.2.5. Examination of the Amount of Catalyst and Ligand Loading in the Alkylation Reaction

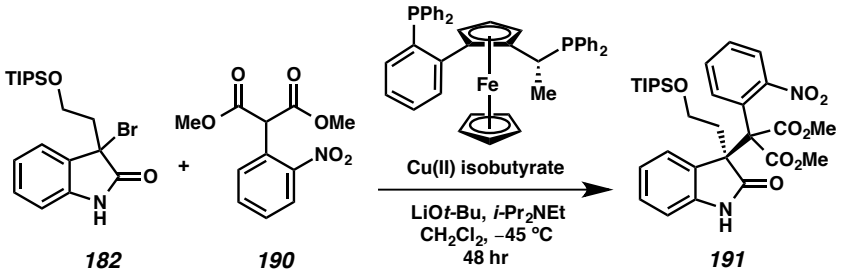

entry	$Cu(isobutyrate)_2$	ligand	*i*-Pr_2NEt	ee[a]
1	10 mol %	10 mol %	3.0 equiv	25%
2	10 mol %	20 mol %	3.0 equiv	28%
3	20 mol %	40 mol %	3.0 equiv	56%
4	20 mol %	10 mol %	3.0 equiv	35%
5	1 equiv	1 equiv	3.0 equiv	60%
6	20 mol %	20 mol %	1.0 equiv	33%
7	20 mol %	20 mol %	1.5 equiv	35%
8	20 mol %	20 mol %	2.0 equiv	38%
9	20 mol %	20 mol %	2.5 equiv	37%
10	20 mol %	20 mol %	4.0 equiv	36%
11	20 mol %	20 mol %	5.0 equiv	37%
12	20 mol %	20 mol %	6.0 equiv	36%
13	20 mol %	20 mol %	20 equiv	36%

Conditions: 0.0049 mmol **182**, 0.0145 mmol **190**, LiO*t*-Bu (10 mol %), 0.1 mL CH_2Cl_2 (0.049 M).

[a] enantiomeric excess was measured by chiral SFC.

Table 3.2.6. Examination of Concentration in the Malonate Addidion Reaction

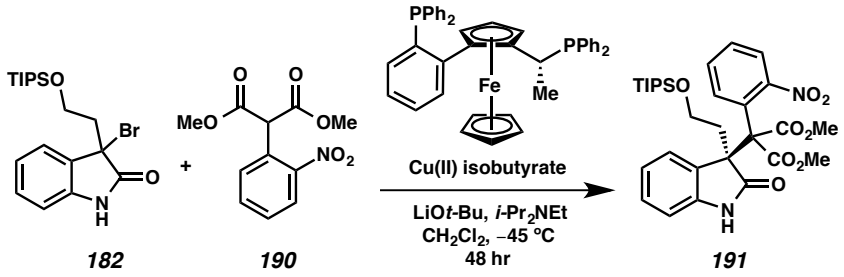

entry	concentration	ee[a]
1	0.005 M	53%
2	0.01 M	63%
3	0.02 M	64%
4	0.05 M	55%
5	0.25 M	40%

Conditions: 0.0049 mmol **182**, 0.0145 mmol **191**, Cu (20 mol %), Ligand (40 mol %), LiO*t*-Bu (20 mol %), *i*-Pr_2NEt (3 equiv). [a] enantiomeric excess was measured by chiral SFC.

Finally, we explored a set of WALPHOS ligands (**N1** – **N8**) under our optimized conditions. Gratifyingly, we observed improved ee by using (Ph,Cy)-WALPHOS (Table 3.2.7, entry 5), leading to product formation in 70% ee with moderate conversion, whereas other ligands showed diminished selectivity. To date, this is the best result we have, which is a great improvement over the starting point.

Table 3.2.7. The Effect of WALPHOS Substituent under Optimized Condition in the Alkylation Reaction

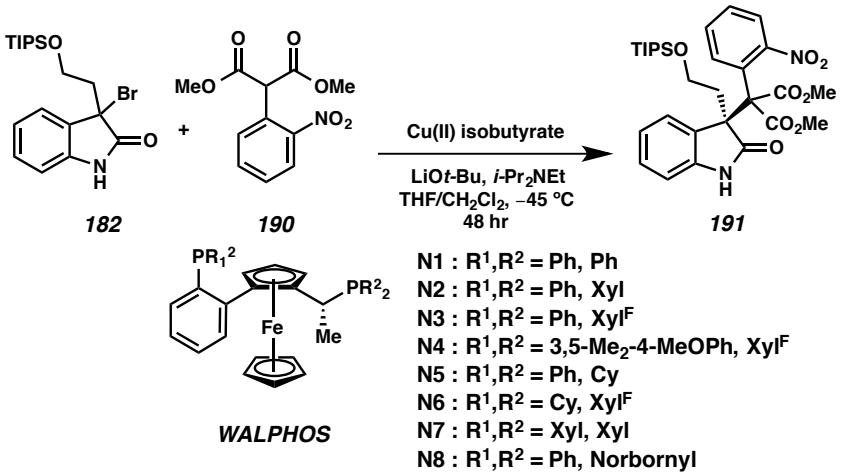

entry	ligand	ee
1	**N1**	60%
2	**N2**	trace
3	**N3**	25%
4	**N4**	25%
5	**N5**	70%
6	**N6**	-
7	**N7**	-
8	**N8**	-

Conditions: 0.0049 mmol **182**, 0.0145 mmol **190**, Cu (20 mol %), Ligand (40 mol %), LiO*t*-Bu (20 mol %), *i*-Pr_2NEt (3 equiv), 0.25 mL CH_2Cl_2 (0.02 M). -: Desired product was not observed. [a] enantiomeric excess was measured by chiral SFC.

3.3 CONCLUSION

Asymmetric alkylation of 3-halooxindoles with malonate esters is an effective method to construct 3,3,-disubstituted oxindole moieties. Herein, we have reported that copper(II) chiral bis(phosphine) complex demonstrated reactivity with an highly stabilized and sterically hindered α-arylated malonate ester, which were unreactive substrates in previously developed conditions. This method could be applied to the

installation of vicinal quaternary centers on the communesin F and perophoramidine scaffolds and could be useful in the synthesis of a variety of other natural products.

3.4 EXPERIMENTAL SECTION

3.4.1 MATERIALS AND METHODS

Unless stated otherwise, reactions were performed under an argon or nitrogen atmosphere using dry, deoxygenated solvents (distilled or passed over a column of activated alumina).[9] Commercially obtained reagents were used as received unless otherwise stated. Thin-layer chromatography (TLC) was performed using E. Merck silica gel 60 F254 precoated plates (0.25 mm) and visualized by UV fluorescence quenching, or potassium permanganate, iodine, or anisaldehyde staining. Silia*Flash* P60 Academic Silica gel (particle size 0.040-0.063 mm) was used for flash chromatography. ^{1}H and ^{13}C NMR spectra were recorded on a Varian Inova 500 (at 500 MHz and 126 MHz respectively), and are reported relative to $CHCl_3$ (δ 7.26 & 77.16 respectively). Data for ^{1}H NMR spectra are reported as follows: chemical shift (δ ppm) (multiplicity, coupling constant (Hz), integration). IR spectra were recorded on a Perkin Elmer Paragon 1000 Spectrometer and are reported in frequency of absorption (cm^{-1}). HRMS were acquired using an Agilent 6200 Series TOF with an Agilent G1978A Multimode source in mixed (MM) ionization mode.

3.4.2 PREPARATIVE PROCEDURES

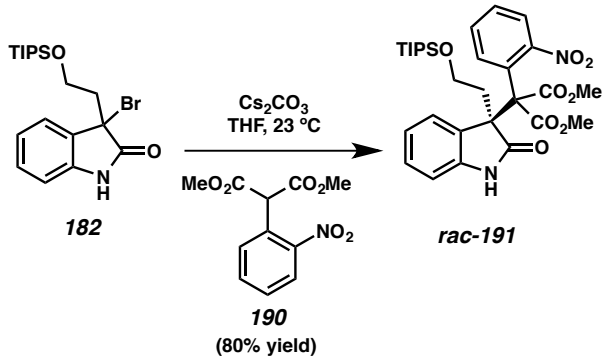

Oxindole *rac*-191: To a flame-dried round-bottomed flask equipped with a stirbar, was added bromooxindole **182** (20 mg, 0.045 mmol), *o*-nitrophenyl dimethylmalonate **190** (37 mg, 0.135 mmol) and THF (0.5 mL). To the mixture was added cesium carbonate (47.4 mg, 0.045 mmol) at ambient temperature and the reaction mixture was then stirred for 3 hr. The reaction mixture was then treated with saturated NH_4Cl aqueous solution, extracted with EtOAc, washed with brine and dried over $MgSO_4$. After concentration *in vacuo*, the crude product was obtained. Chromatography (6:1 hexanes : ethyl acetate) on silica gel afforded the title compound **191** (23 mg, 80% yield) as colorless oil: ^{1}H NMR (500 MHz, $CDCl_3$) δ 8.0 (d, *J* = 8.1 Hz, 1H), 7.85 (s, 1H), 7.74 (dd, *J* = 7.9, 1.7 Hz, 1H), 7.40 (dtd, *J* = 26.6, 7.4, 1.5 Hz, 2H), 7.30 (d, *J* = 7.8 Hz, 1H), 7.14 (td, *J* = 7.7, 1.3 Hz, 1H), 6.90 (td, *J* = 7.7, 1.2 Hz ,1H), 6.75 (dd, *J* = 7.8, 1.1 Hz, 1H), 3.74 (s, 3H), 3.65 (s, 3H), 3.35 (ddd, *J* = 9.5, 8.4, 6.9 Hz, 1H), 3.06 (td, *J* = 9.3, 4.5, 1H), 2.93 (ddd, *J* = 12.6, 8.8, 6.7 Hz, 1H), 2.54 (ddd, *J* = 12.8, 8.4, 4.4 Hz, 1H), 0.89 (s, 21H). ^{13}C NMR (126 MHz, $CDCl_3$) δ 177.86, 167.63, 167.27, 150.34, 140.67, 132.46, 131.12, 129.49, 129.23, 128.63, 128.61, 126.73, 125.39, 122.45, 109.98, 109.12, 59.52, 56.71, 52.81, 52.80, 38.34, 29.70, 17.85, 17,84, 11.80. IR (Neat Film, NaCl) 2923, 2852,

1722, 1617, 1532, 1463, 1353, 1259, 1097, 992, 799, 753 cm^{-1}; HRMS (MM) *m/z* calc'd for $C_{30}H_{40}N_2O_8Si$ $[M+H]^+$: 585.2627, found 585.2636.

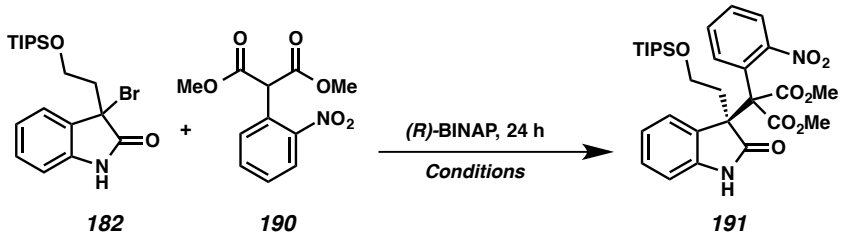

182 ***190*** ***191***

Initial Screening procedure

To an oven-dried vials equipped with stirbar was charged with copper source (20 mol %), BINAP (20 mol %) and 3 Å molecular sieve in THF. The heterogeneous solution was agitated at ambient temperature for 10-20 min until clear homogeneous solution was generated. To the reaction mixture was charged additive (20 mol % unless specified in table) Reaction mixture was allowed to stir for 5 min and concentrated under reduced pressure. Mixture of bromooxindole **5** (10 mg, 0.024 mmol) and malonate **12** (18.5 mg, 0.073 mmol) in reaction solvent (0.15 ml, 0.2 M) was added to the mixture and allowed to stir for 10 minutes. After setting reaction temperature, base (2 equiv) was added to initiate the reaction. Upon completion of the reaction, saturated aqueous ammonium chloride solution (0.1 mL) was added, and the mixture was filtered through silica gel. Each filtrate was diluted by 1 mL of solvent (ethyl acetate or isopropanol) and analyzed by chiral SFC. The mixture was separated by an AD-H column with 20% isopropanol as eluent.

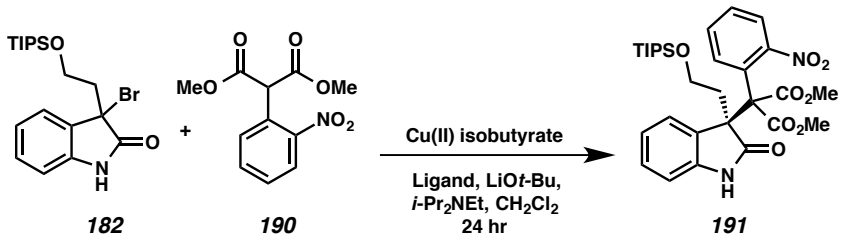

Ligand Screening procedure

Every step was performed in a nitrogen-filled glove box. Solutions of copper(II) isoburtyrate (8 mg, 0.034 mmol) in THF (3.5 mL), lithium *tert*-butoxide (2.72 mg, 0.034 mmol) in THF (3.5 mL), bromooxindole **5** (70 mg, 0.17 mmol) and malonate **12** (129 mg, 0.51 mmol) in CH_2Cl_2 (1.75 mL), *i*-Pr_2NEt (0.1 ml, 0.57 mmol) in CH_2Cl_2 (2 mL) were prepared in 2 dram vials prior to reaction setup. To 1 dram vials equipped with stirbars, and ligand (1.1 μmol, 22 mol %) were distributed copper(II) isobutyrate in THF (0.1 mL, 0.97 μmol, 20 mol %). The heterogeneous solution was agitated at room temperature for 10-20 min until a clear homogeneous solution was generated. The reaction mixtures were charged with lithium *tert*-butoxide in THF (0.1 mL, 0.97 μmol, 20 mol %). Reaction mixtures were allowed to stir for 5 min and concentrated under reduced pressure. A mixture of bromooxindole **5** and malonate **12** in CH_2Cl_2 (0.05 mL, 4.85 μmol, 14.55 μmol) was dispensed to each vial and allowed to stir for 10 min. After setting the reaction temperature, *i*-Pr_2NEt in CH_2Cl_2 (0.05 mL, 14.55 μmol, 3 equiv) was added to the reaction vials and allowed to stir for 48 h. Upon completion, sat. aq. ammonium chloride solution (0.1 mL) was added, and the mixture was filtered through silica gel. Each filtrate was diluted by 1 mL of solvent (ethyl acetate or isopropanol) and analyzed by chiral SFC. The mixture was separated by an AD-H column with 20% isopropanol as eluent.

3.5 NOTES AND REFERENCES

(1) (a) Tokunaga, T.; Hume, W. E.; Umezome, T.; Okazaki, K.; Ueki, Y.; Kumagai, K.; Hourai, S.; Nagamine, J.; Seki, H.; Taiji, M.; Noguchi, H.; Nagata, R. *J. Med. Chem.* **2001**, *44*, 4641–4649. (b) Woodward, C.; L.; Li, Z.; Kathcart, A. K.; Terrell, J.; Gerena, L.; Lopez-Sanchez, M.; Kyle, D. E.; Bhattacharjee, A. K.; Nichols, D. A.; Ellis, W.; Prigge, S. T.; Geyer, J. A.; Waters, N. C. *J. Med. Chem.* **2003**, *46*, 3877–3882. (c) Galliford, C. V.; Scheidt, K. A. *Angew. Chem., Int. Ed.* **2007**, *46*, 8748–8758. (d) Marti, C.; Carreira, E. M. *Eur. J. Org. Chem.* **2003**, 2209–2219. (e) Lin, H.; Danishefsky, S. J. *Angew. Chem., Int. Ed.* **2003**, 42, 36–51. (f) Trost, B. M.; Brennan, M. K. *Synthesis*, **2009**, 3003–3025. (g) Ding, K.; Lu, Y.; Nikolovska-Coleska, Z.; Wang, G.; Qiu, S.; Shangary, S.; Gao, W.; Qin, D.; Stuckey, J.; Krajewski, K.; Roller, P. P.; Wang, S. *J. Med. Chem.* **2006**, *49*, 3432–3435.

(2) Reviews: (a) Zhou, F.; Liu, Y.-L.; Zhou, J. *Adv. Synth. Catal.,* **2010**, *352*, 1381–1407. (b) Klein, J. E. M. N.; Taylor, R. J. K. *Eur. J. Org. Chem.* **2011**, 6821–6841. (c) Dalpozzo, R.; Bartoli, G.; Bencivenni, G. *Chem. Soc. Rev.* **2012**, *41*, 7247–7290. (d) Singh, G. S.; Desta, Z. Y. *Chem. Rev.* **2012**, *112*, 6104–6155.

(3) Recent examples: (a) Holmquist, M.; Blay, G.; Pedro, J. R. *Chem. Commun.* **2014**, *50*, 9309–9312. (b) Hu, F.-L.; Wei, Y.; Shi, M. *Chem. Commun.* **2014**, *50*, 8912–8914. (c) Chen, D.; Xu, M.-H. *J. Org. Chem.* **2014**, *79*, 7746–7751. (d) Li, C.; Guo, F.; Xu, K.; Zhang, S.; Hu, Y.; Zha, Z.; Wang, Z. *Org. Lett.* **2014**, *16*, 3192–3195. (e) Zhu, X.-L.; Xu, J.-H.; Cheng, D.-J.; Zhao, L.-J.; Liu, X.-Y. Tan, B. *Org. Lett.* **2014**, *16*, 2192–2195. (f) Liu, Z.-M.; Li, N.-K.; Huang, X.-F.; Wu, B.; Li, N.; Kwok, C.-Y.; Wang, Y.; Wang, X.-W. *Tetrahedron*, **2014**, *70*, 2406–2415. (g) Cao, Z.-Y.; Wang, Y.-H.; Zeng, X.-P.; Zhou, J. *Tetrahedron Lett.* **2014**,

55, 2571–2584. (h) Trost, B. M.; Osipov, M. *Angew. Chem., Int. Ed.* **2013**, *52*, 9176–9181. (i) Zhou, F.; Zeng, X.-P.; Wang, C.; Zhao, X.-L.; Zhou, J. *Chem. Commun.* **2013**, *49*, 2022–2024. (j) Katayev, D.; Jia, Y.-X. Sharma, A. K.; Banerjee, D.; Besnard, C.; Sunoj, R. B.; Kündig, E. P. *Chem. Eur. J.* **2013**, *19* 11916–11927. (k) Zhing, F.; Dou, X.; Han, X.; Yao, W.; Zhu, Q.; Meng, Y.; Lu, Y. *Angew. Chem., Int. Ed.* **2013**, *52*, 943–947. (l) Shen, K.; Liu, X.; Feng, X. *Chem. Sci.* **2012**, *3*, 327–334. (m) Uraguchi, D.; Koshimoto, K.; Ooi, T. *J. Am. Chem. Soc.* **2012**, *134*, 6972–6975. (n) Trost, B. M.; Xie, J.; Sieber, J. D. *J. Am. Chem. Soc.* **2011**, *133*, 20611–20622. (o*)* Ding, M.; Zhou, F.; Qian, Z.-Q.; Zhou, J. *Org. Biomol. Chem.* **2010**, *8*, 2912–2914. (p) Trost, B. M.; Zhang, Y. *Chem. Eur. J.* **2010**, *16,* 296–303. (q) Trost, B. M.; Czabaniuk, L. C. *J. Am. Chem. Soc.* **2010**, *132*, 15534–15536. (r) Tian, X.; Jiang, K.; Peng, J.; Du, W.; Chen, Y.-C. *Org. Lett.* **2008,** *10*, 3583–3586. (s) Trost, B. M.; Frederiken, M. U. *Angew. Chem., Int. Ed.* **2005**. *44*, 308–310.

(4) Krishnan, S.; Stoltz, B. M. *Tetrahedron Lett.* **2007**, *48*, 7571–7573.

(5) Ma, S.; Han, X.; Krishnan, S.; Virgil, S. C.; Stoltz, B. M. *Angew. Chem., Int. Ed.* **2009**, *48*, 8037–8041.

(6) Han, S.-J. Vogt, F.; Krishnan, S.; May, J. A.; Gatti, M.; Virgil, S. C. Stoltz, B. M. *Org. Lett.* **2014**, *16*, 3316–3319.

(7) Other efforts toward total syntheses of communesins and perophoramidine; (a) May, J. A.; Zeidan, R. K.; Stoltz, B. M. *Tetrahedron Lett.* **2003**, *44*, 1203–1205. (b) Crawley, S. L.; Funk, R. L. *Org. Lett.* **2003**, *5*, 3169–3171. (c) May, J. A.; Stoltz, B. M. *Tetrahedron* **2006**, *62*, 5262–5271. (d) Yang, J.; Song, H.; Xiao, X.;

Wang, J.; Qin, Y. *Org. Lett.* **2006**, *8*, 2187–2190. (e) Crawley, S. L.; Funk, R. L. *Org. Lett.* **2006**, *8*, 3995–3998. (f) Seo, J. H.; Artman, G. D., III; Weinreb, S. M. *J. Org. Chem.* **2006**, *71*, 8891–8900. (g) Yang, J.; Wu, H.; Shen, L.; Qin, Y. *J. Am. Chem. Soc.* **2007**, *129*, 13794–13795. (h) George, J. H.; Adlington, R. M. *Synlett* **2008**, 2093–2096. (i) Siengalewicz, P.; Gaich, T.; Mulzer, J. *Angew. Chem., Int. Ed.* **2008**, *47*, 8170–8176. (j) Liu, P.; Seo, J. H.; Weinreb, S. M. *Angew. Chem., Int. Ed.* **2010**, *49*, 2000–2003. (k) Zuo, Z.; Xie, W.; Ma, D. *J. Am. Chem. Soc.* **2010**, *132*, 13226–13228. (l) Zuo, Z.; Ma, D. *Angew. Chem., Int. Ed.* **2011**, *50*, 12008–12011. (m) Belmar, J.; Funk, R. L. *J. Am. Chem. Soc.* **2012**, *134*, 16941–16943. (n) Artman, G. D., III; Weinreb, S. M. *Org. Lett.* **2003**, *5*, 1523–1526. (o) Fuchs, J. R.; Funk, R. L. *J. Am. Chem. Soc.* **2004**, *126*, 5068–5069. (p) Sabahi, A.; Novikov, A.; Rainier, J. D. *Angew. Chem., Int. Ed.* **2006**, *45*, 4317–4320. (q) Evans, M. A.; Sacher, J. R.; Weinreb, S. M. *Tetrahedron* **2009**, *65*, 6712–6719. (r) Wu, H.; Xue, F.; Xiao, X.; Qin, Y. *J. Am. Chem. Soc.* **2010**, *132*, 14052–14054. (s) Schammel, A. W.; Chiou, G.; Garg, N. K. *Org. Lett.* **2012**, *14*, 4556–4559. (t) Ishida, T.; Takemoto, Y. *Tetrahedron* **2013**, *69*, 4517–4523. (u) Ishida, T.; Ikota, H.; Kurahashi, K.; Tsukano, C.; Takemoto, Y. *Angew. Chem., Int. Ed.* **2013**, *52*, 10204–10207. (v) Zhang, H.; Hong, L.; Kang, H.; Wang, R. *J. Am. Chem. Soc.* **2013**, *135*, 14098–14101. (w) Trost, B. M.; Osipov, M.; Krüger, S.; Zhang, Y. *Chem. Sci.* **2015**, *6*, 349-353.

(8) (a) Fandrick, D. R., Fandrick, K. R.; Reeves, J. T.; Tan, Z.; Tang, W.; Capacci, A. G.; Rodriguez, S.; Song, J. J.; Lee, H.; Yee, N. K.; Senanayake, C. H. *J. Am. Chem. Soc.* **2010**, *132*, 7600–7601. (b) Fandrick, K. R.; Fandrick, D. R.; Reeves, J. T.; Ma, S.; Li, W.; Lee, H.; Grinberg, N.; Lu, B.; Senanayake, C. H. *J. Am. Chem. Soc.* **2011**, *133*, 10332–10335. (c) Fandrick, K. R.; Ogikubo, J.; Fandrick, D. R.;

Patel, N. D.; Saha, J.; Lee, H.; Ma, S.; Grinberg, N.; Busacca, C. A.; Senanayake, C. H. *Org. Lett.* **2013**, *15*, 1214–1217.

(9) Pangborn, A. B.; Giardello, M. A.; Grubbs, R. H.; Rosen, R. K.; Timmers, F. J. *Organometallics* **1996**, *15*, 1518–1520.

APPENDIX 7

Spectra Relevant to Chapter 3:

Stereochemical Evaluation of Bis(phosphine) Copper Catalysts for the Alkylation of 3-Bromooxindoels with α-Arylated Malonate Esters

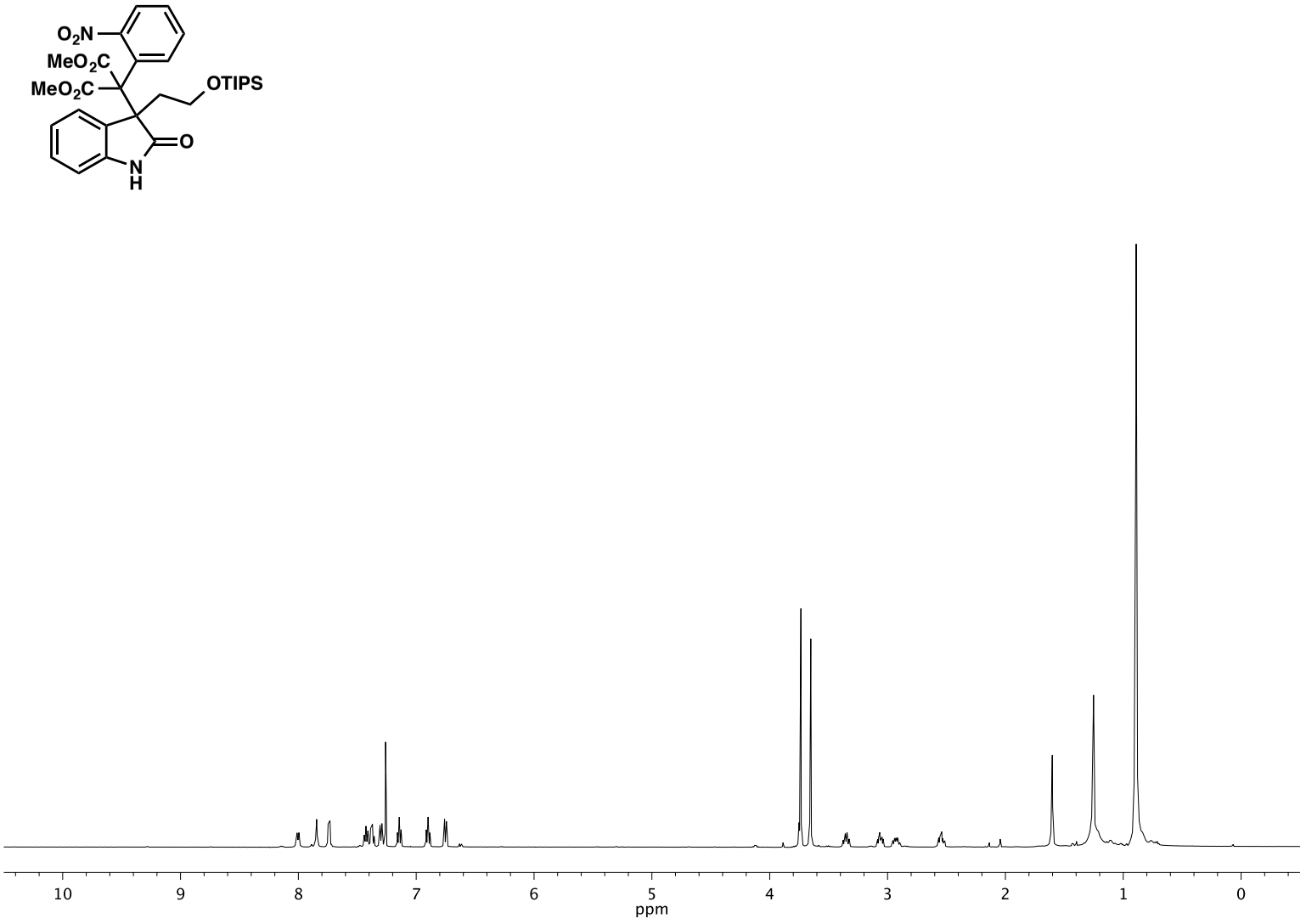

Figure A7.1 ^{1}H NMR (500 MHz, $CDCl_3$) of compound *rac*-**191**

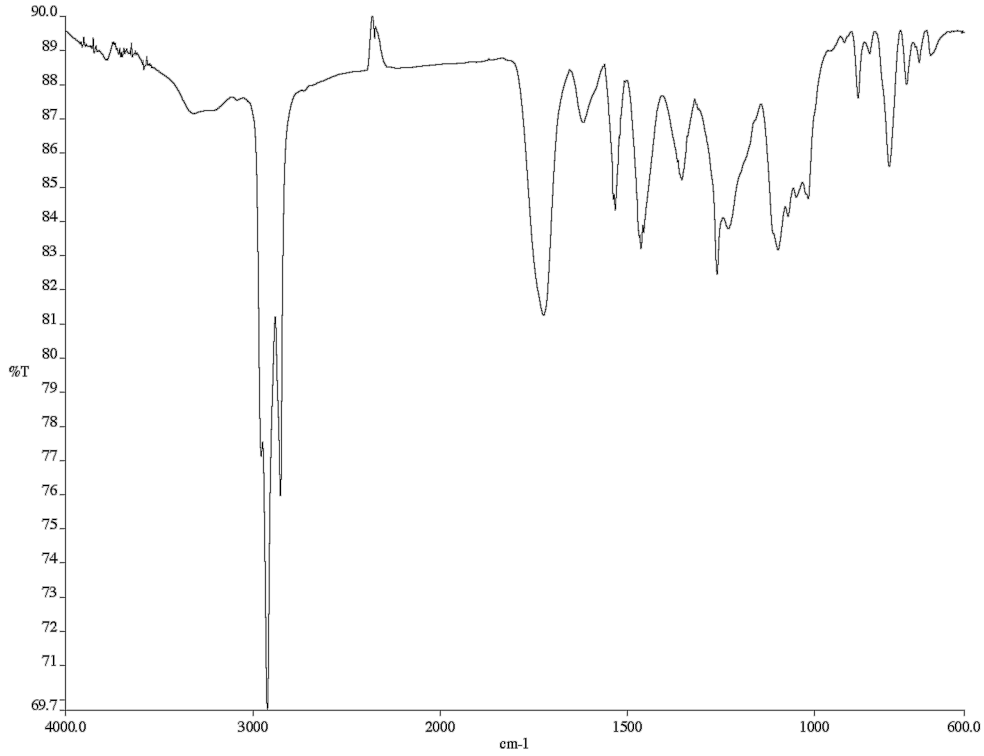

Figure A7.2 Infrared spectrum (thin film/NaCl) of compound *rac*-**191**

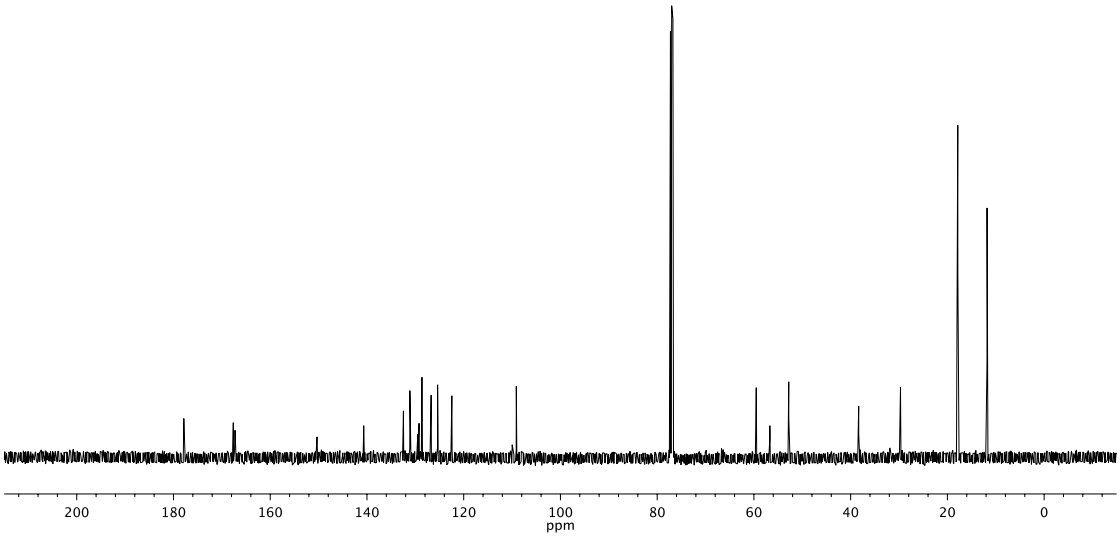

Figure A7.3 ^{13}C NMR (126 MHz, $CDCl_3$) of compound *rac*-**191**

APPENDIX 8

Notebook Cross-Reference

The following notebook cross-reference has been included to facilitate access to the original spectroscopic data obtained for the compounds within this thesis. The information is organized by chapter and electronic characterization folders have been created which contain copies of the original 1H NMR, 13C NMM, two-dimensional NMR, and IR spectra. A hard copy of spectra has been provided with this text. All notebooks are stored in the Stoltz group archive. All electronic data can be found on the Stoltz group server.

Table 8.1. Notebook Cross-Reference for Compounds in Chapter 1.2

Compound	Structure	Notebook reference	NMR and IR data files
25	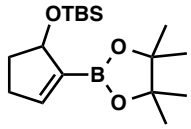	**CWL-II-283**	**CWL-IV-61**
33	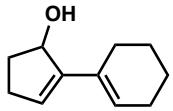	**CWL-II-73**	**CWL-II-73**
35	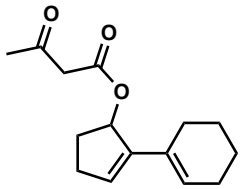	**CWL-II-293**	**CWL-IV-11**
36	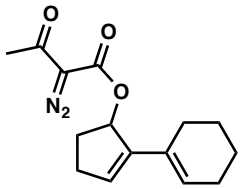	**CWL-II-295**	**CWL-IV-13** **CWL-II-295**
37	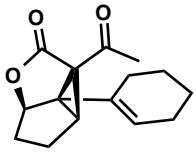	**CWL-III-47**	**CWL-III-41** **CWL-IV-15**
38	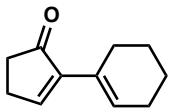	**CWL-III-47**	**CWL-VII-61**
42	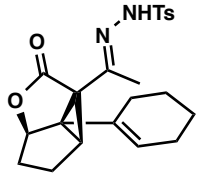	**CWL-III-263**	**CWL-III-263**

Table 8.1. Notebook Cross-Reference for Compounds in Chapter 1.2-Continued

Compound	Structure	Notebook reference	NMR and IR data files
43	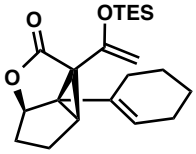	**CWL-IV-17**	**CWL-IV-17**
44	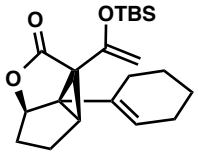	**CWL-VI-217**	**CWL-VI-241** **CWL-III-63**
47	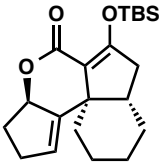	**CWL-III-69**	**CWL-VI-243** **CWL-III-69**
48	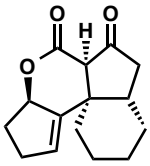	**CWL-III-91** **CWL-III-103**	**CWL-III-79** **CWL-III-91**
51	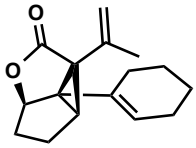	**CWL-III-267**	**CWL-II-87**
53	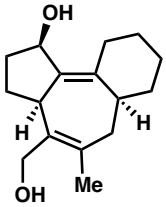	**CWL-VI-43**	**CWL-V-209** **CWL-IV-43** **CWL-IV-35**

Table 8.2. Notebook Cross-Reference for Compounds in Chapter 1.3

Compound	Structure	Notebook reference	NMR and IR data files
27	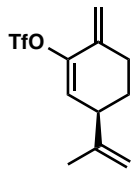	**CWL-IV-153**	**CWL-VI-129** **CWL-IV-169**
59	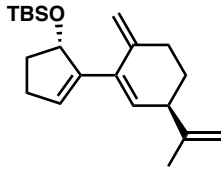	**CWL-IV-171**	**CWL-VII-41**
60	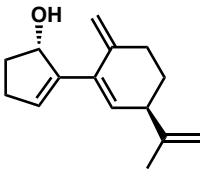	**CWL-IV-173**	**CWL-VII-37-OH**
61	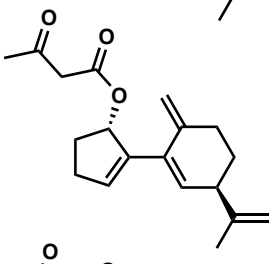	**CWL-VII-175**	**CWL-VII-39**
24	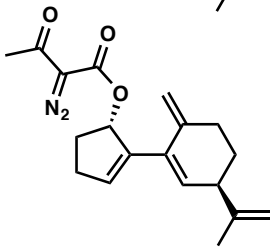	**CWL-VII-177**	**CWL-VII-37-N2**
ent-64	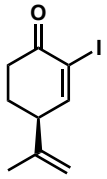	**CWL-V-63**	**CWL-VII-49**
69	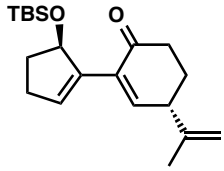	**CWL-V-49**	**CWL-VII-51**

Table 8.2. Notebook Cross-Reference for Compounds in Chapter 1.3-Continued

Compound	Structure	Notebook reference	NMR and IR data files
70	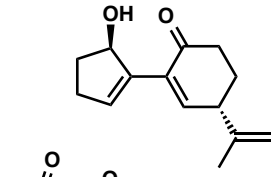	**CWL-V-95**	**CWL-VII-53**
71	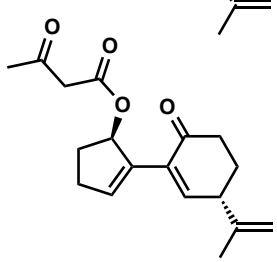	**CWL-V-133**	**CWL-VII-55**
72	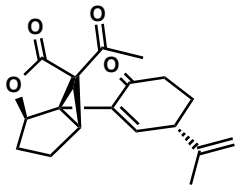	**CWL-V-113**	**CWL-V-111C**
73	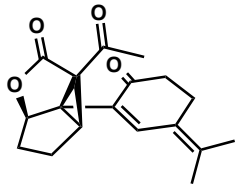	**CWL-V-113**	**CWL-V-111D**
76	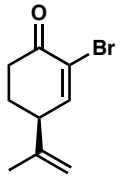	**CWL-VI-97**	**CWL-VI-97**
77	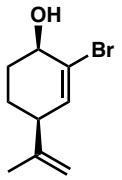	**CWL-VI-161**	**CWL-VI-99** **CWL-VI-143**
78	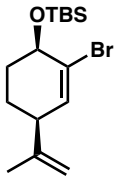	**CWL-VI-65**	**CWL-VI-101**

Table 8.2. Notebook Cross-Reference for Compounds in Chapter 1.3-Continued

Compound	Structure	Notebook reference	NMR and IR data files
79	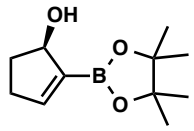	**CWL-VI-147**	**CWL-VII-15**
80	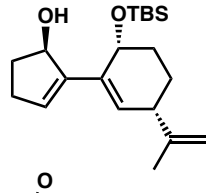	**CWL-VI-105**	**CWL-VI-105**
81	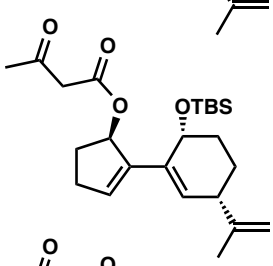	**CWL-VI-47**	**CWL-VI-107**
75	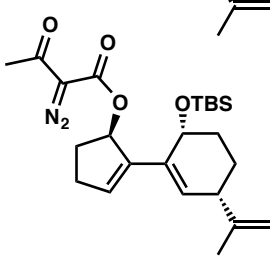	**CWL-VI-49**	**CWL-VI-109**
82	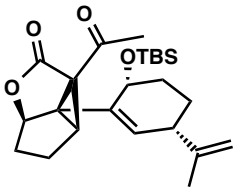	**CWL-VI-51**	**CWL-VI-111**
83	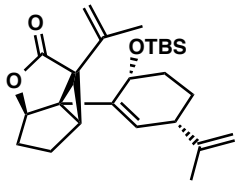	**CWL-VI-183**	**CWL-VI-113**
85	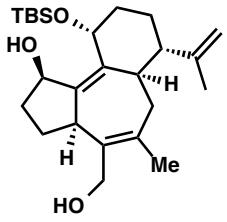	**CWL-VI-185**	**CWL-VI-115** **CWL-VI-185**

Table 8.3. Notebook Cross-Reference for Compounds in Chapter 2

Compound	Structure	Notebook reference	NMR and IR data files
140	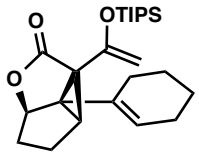	**CWL-VI-249**	**CWL-VI-249**
142	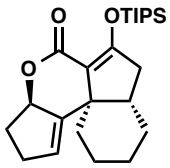	**CWL-VI-251**	**CWL-VI-251**

Table 8.4. Notebook Cross-Reference for Compounds in Chapter 3

Compound	Structure	Notebook reference	NMR and IR data files
rac-191	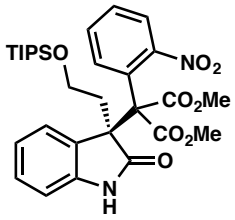	**CWL-II-85**	**CWL-VI-141**

COMPREHENSIVE BILBLIOGRAPHY

Abe, H.; Sato, A.; Kobayashi, T.; Ito, H. *Org. Lett.* **2013**, *15*, 1298–1301.

Achenbach, H.; Benirschke, G. *Phytochemistry* **1997**, *45*, 149–157.

Aiyelaagbe, O. O. H., A. A.; Fattorusso, E.; Taglialatela-Scafati, O.; Schroder, H. C.; Muller, W. E. G. *Evid-Based Compl. Alt.* **2011**, *Article ID 134954*, 7 pages.

Artman, G. D., III; Weinreb, S. M. *Org. Lett.* **2003**, *5*, 1523–1526.

Becke, A. D. *J. Chem. Phys.* **1993**, *98*, 5648.

Belmar, J.; Funk, R. L. *J. Am. Chem. Soc.* **2012**, *134*, 16941–16943.

Bennett, N. B.; Stoltz. B. M. *Chem. Eur. J.* **2013**, *52*, 17745.

Bernauer, K.; Englert, G.; Vetter, W. *Experientia* **1965**, *21*, 374–375.

Bernauer, K.; Englert, G.; Vetter, W.; Weiss, E. *Helv. Chim. Acta.* **1969**, *52*, 1886–1905.

Branca, S. J.; Smith, A. B. III *J. Am. Chem. Soc.* **1978**, *100*, 7767–7768.

Cances, E.; Mennucci, B.; Tomasi, J. *J. Chem. Phys.* **1997**, *107*, 3032.

Cannon, J. R.; Croft, K. D.; Matsuki, Y.; Patrick, V. A.; Toia, R. F.; White, A. H. *Aust. J. Chem.* **1982**, *35*, 1655–1664.

Cao, Z.-Y.; Wang, Y.-H.; Zeng, X.-P.; Zhou, J. *Tetrahedron Lett*. **2014**, *55*, 2571–2584.

Chai, J.-D.; Head-Gordon, M. *Phys. Chem. Chem. Phys*. **2008**, *10*, 6615.

Charles, R. G. *J. Org. Chem*. **1957**, *22*, 677–679.

Chen, B.-C.; Zhou, P.; Davis, F. A.; Ciganek, E. *Org. React*. **2003**, *62*, 1–356.

Chen, D.; Xu, M.-H. *J. Org. Chem*. **2014**, *79*, 7746–7751.

Chianese, G.; Fattorusso, E.; Aiyelaagbe, O. O.; Luciano, P.; Schröder, H. C.; Müller, W. E. G.; Taglialatela-Scafati, O. *Org. Lett*. **2011**, *13*, 316–319.

Choi, C.; Elber, R. *J. Chem. Phys*. **1991**, *94*, 751.

Clive, D. L.; Daigneault, S. *K. Chem. Soc., Chem. Commun*. **1989**, 332–335.

Collman, J. P.; Winter, S. R.; Clark, D. R. *J. Am. Chem. Soc*. **1972**, *94*, 1788–1789.

Cooke, M. P., Jr.; Parlman, R. M. *J. Am. Chem. Soc*. **1977**, *99*, 5222–5224.

Cope A. C.; Hardy, E. M. *J. Am. Chem. Soc*. **1940**, *62*, 441–444.

Corey, E. J.; Hegedus, L. S. *J. Am. Chem. Soc*. **1969**, *91*, 4926–4928.

Crawley, S. L.; Funk, R. L. *Org. Lett*. **2003**, *5*, 3169–3171.

Crawley, S. L.; Funk, R. L. *Org. Lett*. **2006**, *8*, 3995–3998.

Dalpozzo, R.; Bartoli, G.; Bencivenni, G. *Chem. Soc. Rev.* **2012**, *41*, 7247–7290.

Davies, M. L. H.; Cantrell, R. W.; Jr.; Romines, R. K.; and Baum, S. J.; *Org. Synth.* **1992**, 70, 93-100; *Coll. Vol. IX* **1998**, 422-426.

Davies, H. M. L.; Calvo, R.; Ahmed, G. *Tetrahedron Lett.* **1997**, *38*, 1737–1740.

Davies, H. M. L.; Calvo, R.; Townsend, R. J.; Ren, P.; Churchill, R. M. *J. Org. Chem.* **2000**, *65*, 4261–4268.

De Luca, L.; Giacomelli, G.; Porcheddu, A. *Org. Lett.* **2001**, *3*, 3041–3043.

Devappa, R. K. M., H. P. S.; Becker, K. *J. Toxicol. Environ. Health* **2010**, *13*, 476–507.

Devappa, R.; Maes, J.; Makkar, H.; De Greyt, W.; Becker, K. *J. Am. Oil Chem. Soc.* **2010**, *87*, 697–704.

Devappa, R.; Makkar, H.; Becker, K. *J. Am. Oil Chem. Soc.* **2011**, *88*, 301-322.

Ding, K.; Lu, Y.; Nikolovska-Coleska, Z.; Wang, G.; Qiu, S.; Shangary, S.; Gao, W.; Qin, D.; Stuckey, J.; Krajewski, K.; Roller, P. P.; Wang, S. *J. Med. Chem.* **2006**, *49*, 3432–3435.

Ding, M.; Zhou, F.; Qian, Z.-Q.; Zhou, J. *Org. Biomol. Chem.* **2010**, *8*, 2912–2914.

Doyle, M. P.; Dyatkin, A. B.; Kalinin, A. V.; Ruppar, D. A. *J. Am. Chem. Soc.* **1995**, *117*, 11021–11022.

Doyle, M. P.; Dyatkin, A. B.; Autry, C. L. *J. Chem. Soc. Perkin Trans.* **1995**, 619–621

Enquist. J. A.l Stoltz, B. M. *Nature* **2008,** *453*, 1228–1231.

Evans, M. A.; Sacher, J. R.; Weinreb, S. M. *Tetrahedron* **2009**, *65*, 6712–6719.

Fairless, D. *Nature* **2007**, *449*, 652.

Fandrick, D. R., Fandrick, K. R.; Reeves, J. T.; Tan, Z.; Tang, W.; Capacci, A. G.; Rodriguez, S.; Song, J. J.; Lee, H.; Yee, N. K.; Senanayake, C. H. *J. Am. Chem. Soc*. **2010**, *132*, 7600–7601.

Fandrick, K. R.; Fandrick, D. R.; Reeves, J. T.; Ma, S.; Li, W.; Lee, H.; Grinberg, N.; Lu, B.; Senanayake, C. H. *J. Am. Chem. Soc*. **2011**, *133*, 10332–10335.

Fandrick, K. R.; Ogikubo, J.; Fandrick, D. R.; Patel, N. D.; Saha, J.; Lee, H.; Ma, S.; Grinberg, N.; Busacca, C. A.; Senanayake, C. H. *Org. Lett*. **2013**, *15*, 1214–1217.

Fuchs, J. R.; Funk, R. L. *J. Am. Chem. Soc*. **2004**, *126*, 5068–5069.

Fukui, K. *Acc. Chem. Res*. **1981**, *14*, 363.

Fukuyama, T.; Chen, X. *J. Am. Chem. Soc*. 1994, *116*, 3125–3126.

Galliford, C. V.; Scheidt, K. A. *Angew. Chem., Int. Ed*. **2007**, *46*, 8748–8758.

George, J. H.; Adlington, R. M. *Synlett* **2008**, 2093–2096.

Goel, G. M., H. P. S.; Francis, G.; Becker, K. *Int. J. Toxicol.* **2007**, *26*, 279–288.

Greene, A. E.; Luche, M. J.; Serra, A. A. *J. Org. Chem.* **1985**, *50*, 3957–3962.

Grimme, S.; Ehrlich S.; Goerigk, L. *J. Comput. Chem.* **2011**, *32*, 1456.

Haas, W.; Sterk, H.; Mittelbach, M. *J. Nat. Prod.* **2002**, *65*, 1434–1440.

Han, S.-J. Vogt, F.; Krishnan, S.; May, J. A.; Gatti, M.; Virgil, S. C. Stoltz, B. M. *Org. Lett.* **2014**, *16*, 3316–3319.

Hanzawa, Y.; Narita, K.; Yabe, M.; Taguchi, T.; *Tetrahedron* **2002,** *58*, 10429–10435.

Hanzawa, Y.; Tabuchi, N.; Narita, K.; Kakuuchi, A.; Yabe M.; Taguchi, T.; *Tetrahedron* **2002**, *58*, 7559–7571.

Hashimoto, T.; Naganawa, Y.; Maruoka, K.; *J. Am. Chem. Soc.* **2011**, *133*, 8834–8837.

Hegedus, L. S.; Inoue, Y. *J. Am. Chem. Soc.* **1982**, *104*, 4917–4921.

Hegedus, L. S.; Perry, R. J. *J. Org. Chem.* **1985**, *50*, 4955–4960.

Hegedus, L. S.; Tamura, R. *Organometallics* **1982**, 1, 1188–1194.

Hermanson, J. R.; Hershberger, J. W.; Pinhas, A. R. *Organometallics* **1995**, *14*, 5426–5437.

Herrmann, W. A.; Fischer, R. W.; Correia, J. D. G. *J. Mol. Catal.* **1994**, *94*, 213–223.

Holmquist, M.; Blay, G.; Pedro, J. R. *Chem. Commun.* **2014**, *50*, 9309–9312.

Hoover, J. M.; Stahl, S. S. *J. Am. Chem. Soc.* **2011**, *133*, 16901–16910.

Hoye, T. R.; Jefferey, C. S.; Shao, F. *Nat. Protoc.* **2007**, *2*, 2451–2458.

Hratchian, H. P.; Schlegel, H. B. *J. Chem. Theory Comput.* **2005**, *1*, 61.

Hu, F.-L.; Wei, Y.; Shi, M. *Chem. Commun.* **2014**, *50*, 8912–8914.

Ide, W. S.; Buck, J. S. *In Organic Reactions*; Adams, R., Ed.; Wiley: New York, **1948**, 4, 269.

Isegawa, M.; Maeda, S.; Tantillo, D. J.; Morokuma, K. *Chem. Sci.* **2014**, *5*, 1555.

Ishida, T.; Ikota, H.; Kurahashi, K.; Tsukano, C.; Takemoto, Y. *Angew. Chem., Int. Ed.* **2013**, *52*, 10204–10207.

Ishida, T.; Takemoto, Y. *Tetrahedron* **2013**, *69*, 4517–4523.

James, N. C.; Um, J. M.; Padias, A. B.; Hall Jr., H. K.; Houk, K. N. *J. Org. Chem.* **2013**, *78*, 6582–6592.

Jing, L. F., Y.; Ying, X.; Wenxing, H.; Meng, X.; Syed, M. N.; Mang, C. *J. Appl. Entomol.* **2005**, *129*, 98–104.

Katayev, D.; Jia, Y.-X. Sharma, A. K.; Banerjee, D.; Besnard, C.; Sunoj, R. B.; Kündig, E. P. *Chem. Eur. J.* **2013**, *19* 11916–11927.

Kauffmann, T.; Ennen, B.; Sander, J.; Wieschollek, R. *Angew. Chem.* **1983**, *95*, 237–238; *Angew. Chem., Int. Ed. Engl.* **1983**, *22*, 244–245.

Kauffmann, T.; Abel, T.; Beirich, C.; Kieper, G.; Pahde, C.; Schreer, M.; Toliopoulos, E.; Wiescholiek, R. *Tetrahedron Lett.* **1986**, *27*, 5355–5358.

Kauffmann, T.; Fiegenbaum, P.; Wieschollek, R. *Angew. Chem.* **1984**, *96*, 500–501; *Angew. Chem., Int. Ed. Engl.* **1984**, *23*, 531–532.

Kauffmann, T.; Mçller, T.; Rennefeld, H.; Welke, S.; Wieschollek, R. *Angew. Chem.* **1985**, *97*, 351 –352; *Angew. Chem., Int. Ed. Engl.* **1985**, *24*, 348–350.

Khan, S.; Nobuki, K.; Masahiro, H. *Synlett* **2000**, 1494–1496.

Kimbu, S. F.; Keumedjio, F.; Sondengam, L. B.; Connolly, J. D. *Phytochemistry* **1991**, *30*, 619–621.

Klein, J. E. M. N.; Taylor, R. J. K. *Eur. J. Org. Chem.* **2011**, 6821–6841.

Krishnan, S.; Stoltz, B. M. *Tetrahedron Lett.* **2007**, *48*, 7571–7573.

Lebel, H.; Paquet. V. *J. Am. Chem. Soc.* **2004**, *126*, 320–326.

Lee, C.; Yang, W.; Parr, R. G. *Phys. Rev. B* **1988**, *37*, 785.

Li, C.-Y.; Devappa, R. K.; Liu, J.-X.; Lv, J.-M.; Makkar, H. P. S.; Becker, K. *Food Chem. Toxicol.* **2010**, *48*, 620–625.

Li, C.; Guo, F.; Xu, K.; Zhang, S.; Hu, Y.; Zha, Z.; Wang, Z. *Org. Lett.* **2014**, *16*, 3192–3195.

Li, P.; Yamamoto, H. *J. Am. Chem. Soc.* **2009**, *131*, 16628–16629.

Lin, H.; Danishefsky, S. J. *Angew. Chem., Int. Ed.* **2003**, 42, 36–51.

Liu, J.-Q.; Yang, Y.-F.; Li, X.-Y.; Liu, E.-Q.; Li, Z.-R.; Zhou, L.; Li, Y.; Qiu, M.-H. *Phytochemistry* **2013**, *96*, 265–272.

Liu, P.; Seo, J. H.; Weinreb, S. M. *Angew. Chem., Int. Ed.* **2010**, *49*, 2000–2003.

Liu, Z.-M.; Li, N.-K.; Huang, X.-F.; Wu, B.; Li, N.; Kwok, C.-Y.; Wang, Y.; Wang, X.-W. *Tetrahedron*, **2014**, *70*, 2406–2415.

Lucio Anelli, P.; Biffi, C.; Montanari, F.; Quici, S. *J. Org. Chem.* **1987**, *52*, 2559–2562.

Ma, S.; Han, X.; Krishnan, S.; Virgil, S. C.; Stoltz, B. M. *Angew. Chem., Int. Ed.* **2009**, *48*, 8037–8041.

MacDougall, J. M.; Santora, V. J.; Verma, S. K.; Turnbull, P.; Hernandez, C. R.; Moore, H. W. *J. Org. Chem.* **1998**, *63*, 6905–6913.

Maeda, S., Morokuma, K. *J. Chem. Theo. Comp.* **2011**, *7*, 2335–2345.

Maeda, S., Ohno, K., Morokuma, K. *Phys. Chem. Chem. Phys.* **2013**, *15*, 3683–3701.

Maeda, S., Saito, R., Morokuma, K. *J. Chem. Phys.* **2010**, *24*, 241102/1–4.

Maeda, S., Taketsugu, T., Morokuma, K. *J. Comp. Chem.* **2014**, *35*, 166–173.

Marti, C.; Carreira, E. M. *Eur. J. Org. Chem.* **2003**, 2209–2219.

Matsumoto, K.; Koyachi, K.; Shindo, M. *Tetrahedron* **2013**, *69*, 1043–1049.

Matthies, S.; Stallforth, P.; Seeberger, P. H. *J. Am. Chem. Soc.* **2015**, *137*, 2848–2851.

May, J. A.; Stoltz, B. M. *Tetrahedron* **2006**, *62*, 5262–5271.

May, J. A.; Zeidan, R. K.; Stoltz, B. M. *Tetrahedron Lett.* **2003**, *44*, 1203–1205.

Mayasundari, A.; Young, D. G. J. *Tetrahedron Lett.* **2001**, *42*, 203-206.

McMurry, J. E.; Andrus, A. *Tetrahedron Lett.* **1980**, *21*, 4687–4690.

McUliffe, C. A.; Hosseiny, A.; McCullough, F. P. *Inorg. Chim. Acta* **1979,** *33*, 5–10.

Meyer, M. E.; Phillips, J. H.; Ferreira, E. M.; Stoltz B. M. *Tetrahedron* **2003**, *69*, 7626–7635.

Min, S.-J.; Danishefsky, S. J. *Tetrahedron Lett.* **2008**, *49*, 3496–2399.

Muangman, S. T., M.; Tohtong, R. *In Vivo* **2005**, *19*, 265–268.

Müller, P.; Bernardinelli, G.; Nury, P. *Tetrahedron Asymmetry* **2002**, *13*, 551–558.

Murakami, M.; Amii, H.; Shigeto, K.; Ito, Y. *J. Am. Chem. Soc.* **1996**, *118*, 8285–8290.

Naengchomnong, W.; Thebtaranonth, Y.; Wiriyachitra, P.; Okamoto, K. T.; Clardy, J. *Tetrahedron Lett*. **1986**, *27*, 2439–2442.

Naengchomnong, W.; Thebtaranonth, Y.; Wiriyachitra, P.; Okamoto, K. T.; Clardy, J. *Tetrahedron Lett*. **1986**, *27*, 5675–5678.

Naengchomnong, W. T., B.; Thebtaranonth, Y. *J. Sci. Soc. Thailand* **1994**, *20*, 73–83.

Nakano, T. T., T.; Ishii, Y.; Ogawa, M. *Synthesis* **1986**, 774–776.

Newhouse, T. R.; Kaib, P. S. J.; Gross, A. W.; Corey, E. J. *Org. Lett*. **2013**, *15*, 1591–1593.

Ochoa, M. E.; Arias, M. S.; Aguilar, R.; Delagade, F.; Tamariz, J. *Tetrahedron* **1999**, *55*, 14535–14546.

Openshaw, K. *Biomass Bioenergy* **2000**, *19*, 1-15.

Pangborn, A. B.; Giardello, M. A.; Grubbs, R. H.; Rosen, R. K.; Timmers, F. J. *Organometallics* **1996**, *15*, 1518–1520.

Peverati, R.; Truhlar, D. G. *J. Phys. Chem. Lett*. **2011**, *3*, 117.

Phillips, A. M. F.; Romao, C. *Eur. J. Org. Chem*. **1999**, 1767–1770.

Picha, P. N., W.; Promratanapongse, P.; Kano, E.; Hayashi, S.; Ohtsubo,; T.; Zhang, S. W. S., H.; Kitai, R. *J. Exp. Clin. Cancer Res*. **1996**, *15*, 177–183.

Pieniazek, S. N.; Clemente, F. R.; Houk, K. N. *Angew. Chem. Int. Ed.* **2008**, *47*, 7746–7749.

Plettner, E. Mohle, A.; Mwangi, M. T.; Griscti, J.; Patrick, B. O.; Nair, R.; Batchelor, R. J.; Einstein, F. *Tetrahedron Aymmetry* **2005**, *16*, 2754–2763.

Ravindranath, N. R., M. R.; Ramesh, C.; Ramu, R.; Prabhakar, A.; Jagadeesh, B.; Das, B. *Chem. Pharm. Bull.* **2004**, *52*, 608–611.

Ravindranath, N.; Ramesh, C.; Das, B. *Biochem. Syst. and Ecol.* **2003**, *31*, 431–432.

Ravindranath, N.; Ravinder Reddy, M.; Mahender, G.; Ramu, R.; Ravi Kumar, K.; Das, B. *Phytochemistry* **2004**, *65*, 2387–2390.

Reeder, L. M.; Hegedus, L. S. *J. Org. Chem.* **1999**, *64*, 3306–3311.

Ribeiro, R. F.; Marenich, A. V.; Cramer, C. J.; Truhlar, D. G. *J. Phys. Chem. B* **2011**, *115*, 14556.

Sabahi, A.; Novikov, A.; Rainier, J. D. *Angew. Chem., Int. Ed.* **2006**, *45*, 4317–4320.

Sawa, Y.; Hashimoto, I.; Ryang, M.; Tsutsumi, S. *J. Org. Chem.* **1968**, *33*, 2159–2161.

Schammel, A. W.; Chiou, G.; Garg, N. K. *Org. Lett.* **2012**, *14*, 4556–4559.

Seo, J. H.; Artman, G. D., III; Weinreb, S. M. *J. Org. Chem.* **2006**, *71*, 8891–8900.

Shen, K.; Liu, X.; Feng, X. *Chem. Sci.* **2012**, *3*, 327–334.

Siengalewicz, P.; Gaich, T.; Mulzer, J. *Angew. Chem., Int. Ed.* **2008**, *47*, 8170–8176.

Singh, G. S.; Desta, Z. Y. *Chem. Rev.* **2012**, *112*, 6104–6155.

Smith, M. B.; March, J. March's *Advanced Organic Chemistry: Reactions, Mechanisms, and Structure,* 5th ed.; Wiley-Interscience: New York, 2001; pp 1514–1517.

Stetter, H. *Angew. Chem., Int. Ed. Engl.* **1976**, *15*, 639–647.

Stetter, H.; Kuhlmann, H. *Chem. Ber.* **1976**, *109*, 2890–2896.

Stetter, H.; Kuhlmann, H. *In Organic Reactions*; Paquette, L. A., Ed.; Wiley: New York, **1991**, *40*, 407.

Subbaraju, G. V.; Manhas, M. S.; Bose, A. K. *Synthesis* **1991**, 816–818.

Szabó, L. F. *ARKIVOC* **2007**, 280–290.

Thippornwong, M.; Tohtong, R. *AACR Meeting Abstracts* **2006**, A112.

Tian, X.; Jiang, K.; Peng, J.; Du, W.; Chen, Y.-C. *Org. Lett.* **2008,** *10*, 3583–3586.

Tokunaga, T.; Hume, W. E.; Umezome, T.; Okazaki, K.; Ueki, Y.; Kumagai, K.; Hourai, S.; Nagamine, J.; Seki, H.; Taiji, M.; Noguchi, H.; Nagata, R. *J. Med. Chem.* **2001**, *44*, 4641–4649.

Trost, B. M.; Brennan, M. K. *Synthesis*, **2009**, 3003–3025.

Trost, B. M.; Czabaniuk, L. C. *J. Am. Chem. Soc.* **2010**, *132*, 15534–15536.

Trost, B. M.; Frederiken, M. U. *Angew. Chem., Int. Ed.* **2005**. *44*, 308–310.

Trost, B. M.; Mikhail, G. K. *J. Am. Chem. Soc.* **1987***, 109,* 4124–4127.

Trost, B. M.; Osipov, M. *Angew. Chem., Int. Ed.* **2013**, *52*, 9176–9181.

Trost, B. M.; Osipov, M.; Krüger, S.; Zhang, Y. *Chem. Sci.* **2015**, *6*, 349–353.

Trost, B. M.; Xie, J.; Sieber, J. D. *J. Am. Chem. Soc.* **2011**, *133*, 20611–20622.

Trost, B. M.; Zhang, Y. *Chem. Eur. J.* **2010**, *16,* 296–303.

Ulitsky, A.; Elber, R. *J. Chem. Phys.* **1990**, *92*, 1510.

Uraguchi, D.; Koshimoto, K.; Ooi, T. *J. Am. Chem. Soc.* **2012**, *134*, 6972–6975.

Wang, Q.; Fan, S. Y.; Wong, H. N. C. *Tetrahedron* **1993**, *49*, 619–638.

Wang, X.-C.; Zheng, Z.-P.; Gan, X.-W.; Hu, L.-H. *Org. Lett.* **2009**, *11*, 5522–5524.

Wen, X.; Norling, H.; Hegedus, L. S. *J. Org. Chem.* **2000**, *65*, 2096–2103.

Woodward, C.; L.; Li, Z.; Kathcart, A. K.; Terrell, J.; Gerena, L.; Lopez-Sanchez, M.; Kyle, D. E.; Bhattacharjee, A. K.; Nichols, D. A.; Ellis, W.; Prigge, S. T.; Geyer, J. A.; Waters, N. C. *J. Med. Chem.* **2003**, *46*, 3877–3882.

Wu, H.; Xue, F.; Xiao, X.; Qin, Y. *J. Am. Chem. Soc.* **2010**, *132*, 14052–14054.

Yadav, J. S.; Mallikarjuna Reddy, N.; Ataur Rahman, M.; Mallikarjuna Reddy, A.; Prasad, A. R. *Helv. Chim. Acta* **2014**, *97*, 491–498.

Yang, J.; Song, H.; Xiao, X.; Wang, J.; Qin, Y. *Org. Lett.* **2006**, *8*, 2187–2190.

Yang, J.; Wu, H.; Shen, L.; Qin, Y. *J. Am. Chem. Soc.* **2007**, *129*, 13794–13795.

Yoshikai, K.; Hayama, T.; Nishimura, K.; Yamada, K.; Tomioka, K. *J. Org. Chem.* **2005,** *70*, 681–683.

Zhang, J. L; Che, C.-M. *Org. Lett.* **2002**, *4*, 1911–1914.

Zhang, H.; Hong, L.; Kang, H.; Wang, R. *J. Am. Chem. Soc.* **2013**, *135*, 14098–14101.

Zhang, X.-Q.; Li, F.; Zhao, Z.-G.; Liu, X.-L.; Tang, Y.-X.; Wang, M.-K. *Phytochemistry Lett.* **2012**, *5*, 721–724.

Zhao, Y.; Truhlar, D. G. *J. Chem. Phys.* **2006**, *125*, 194101.

Zhao, Y.; Truhlar, D. G. *Phys. Chem. Chem. Phys.* **2008**, *10*, 2813.

Zhao, Y.; Truhlar, D. *Theor. Chem. Acc.* **2008**, *120*, 215.

Zhing, F.; Dou, X.; Han, X.; Yao, W.; Zhu, Q.; Meng, Y.; Lu, Y. *Angew. Chem., Int. Ed.* **2013**, *52*, 943–947.

Zhou, F.; Liu, Y.-L.; Zhou, J. *Adv. Synth. Catal.,* **2010**, *352*, 1381–1407.

Zhou, F.; Zeng, X.-P.; Wang, C.; Zhao, X.-L.; Zhou, J. *Chem. Commun.* **2013**, *49*, 2022–2024.

Zhu, Q. A., J.; Li, F.; Wang, M.; Wu, J.; Tang, Y. *Chin. J. Appl. Environ. Biol.* **2013**, *19*, 956–959.

Zhu, X.-L.; Xu, J.-H.; Cheng, D.-J.; Zhao, L.-J.; Liu, X.-Y. Tan, B. *Org. Lett.* **2014**, *16*, 2192–2195.

Ziegler, F. E.; Kover, R. X.; Yee, N. N. K. *Tetrahedron Lett.* **2000**, *41,* 5155–5159.

Zuo, Z.; Ma, D. *Angew. Chem., Int. Ed.* **2011**, *50*, 12008–12011.

Zuo, Z.; Xie, W.; Ma, D. *J. Am. Chem. Soc.* **2010**, *132*, 13226–13228.

INDEX

A

B

C

D

E

G

I

J

K

L

M

N

O

P

R

S

ß

S

T

U

W

X

Z

ABOUT THE AUTHOR

Chung Whan Lee was born in Seoul, Korea on 27 February 1987. He is the only child of Myung Kap Lee and Dong Shin Seo. Chung Whan spent his formative years in Gyeonggi province, where he spent most of his time at a childeren's playground. He was first exposed to chemistry at Gyeonggi Science High School where he studied advanced chemistry.

After finishing high school in two years, he was accepted into the Department of Chemistry at Seoul National University and begain his undergraduate studies in 2004. He was led to organic synthesis in the winter of 2005 by a conversation with Professor Eun Lee, who offered aportunity to experience modern research. His first research topic was the total synthesis of (–)-blepharocalyxin D. He became skilled in doing research in synthetic chemistry and came to realize that organic synthesis was the most interesting area for him. He achieved a B.S. degree in 2007, graduating Summa Cum Laude, and continued to study in the Eun Lee group in the graduate school of SNU. In graduate school, he finished the total synthesis of (–)-amphidinolide K with other graduate students. It was great achievement for him and he continued doing research with Professor Chulbom Lee, where developed synthetic methodology with ruthenium catalyzed three-component coupling. He learned the beauty of transition metal catalysis with this project. In 2009, he received a M.S. degree and received a research staff appointment from SNU with Professor Chulbom Lee. He spent his time for the synthesis of Exiguamine A until 2010.

In the fall of 2010, Chung Whan moved to Pasadena, California, where he began doctoral research with Professor Brian M. Stoltz at the California Institute of Technology. His doctoral research involves the total synthesis of curcusone C and the development of alkylation of halooxindoles with malonate esters. During investigations of the synthesis of the natural product, he discovered an unexpected outcome, which led him to focus on mechanistic elucidation. This training in synthetic chemistry will serve as an outstanding background for his research in industry. He will return to Seoul, Korea, in July 2015 and begin an industrial career with LG Chemistry.